

## ***Advanced Characterisation and Operando Spectroscopies***

FEZA21-PO-002

### **Understanding the impact of zeolite hierarchization on their textural properties**

A. Sachse<sup>1</sup>, T. Aumond<sup>1,\*</sup>, I. Batonneau-Gener<sup>1</sup>

<sup>1</sup>IC2MP, Poitiers, France

**Abstract Text:** Zeolites are microporous solids of great importance in catalysis. Due to the extended microporous channel and/or cage systems in zeolites very long diffusion path lengths arise that lead to low efficiency factors. In order to increase zeolite efficiency the shortening of the diffusion path length through the development of secondary, larger porosity within the zeolite crystals has been put forward as sound solution. Indeed, a great variety of synthetic and post-synthetic strategies have been developed to reach this goal.[1]

With the aim to rationalize catalytic behaviors of hierarchical zeolites, their catalytic activity, selectivity and stability are compared to those of pristine zeolites. The often times improved catalytic properties of hierarchical zeolites are related to their superior textural properties. Yet, the determination of the microporous volume, the BET surface area and the amount of occluded mesopores in hierarchical zeolites is far from being evident through standard gas physisorption techniques (N<sub>2</sub>, Ar). Indeed, the strong sorbent-surface interactions do not allow to distinguish the micropore filling from the formation of monolayers, which is at the origin of the mesopore filling. As underlined by several authors, the usually employed t-plot procedure is not suitable to determine accurately the micropore volume since its value varies significantly with the pressure range arbitrarily chosen to set the linear regressions.[2-3] All these issues lead to strong misinterpretations of the real microporous volume. Similarly, it is difficult to determine the exact BET surface area from nitrogen (or argon) adsorption in hierarchical zeolites, as the adsorption on the microporous surface does not lead to multilayer formation.[4]

In this contribution we present a strategy based on the comparison of the nitrogen physisorption isotherms at 77 K of hierarchical zeolite samples with those of their *n*-nonane retaining counterparts. The strategy allowed for ZSM-5 the determination of the exact microporous volume by simply comparing the nitrogen adsorption and desorption isotherms at 77 K before and after the *n*-nonane preadsorption (Figure 1a).[5] This strategy further permitted for calculating the exact monolayer capacity (and hence the exact BET surface area) and to quantify the amount of occluded mesopores (*i.e.* mesopores only accessible via the micropores).

This approach was further applied for determining the textural properties of hierarchical zeolites of the MCM-22 family.[6] Through characterizing hierarchical MCM-22 based materials and comparing their properties with those of the *n*-nonane retaining counterparts important evidence on the impact of the hierarchization treatment on the accessible micropore volume was evidenced (Figure 1b). The latter is related to the amount of hemicages on the crystal surface and allows hence to deduce the impact of hierarchization on the different pore systems.

As such, it was proved that though substantial growth of BET surface area and interlayer-mesopore volume in MCM-36 the accessible micropore volume fraction hardly increases compared to calcined MCM-22. This indicates that the pillaring only marginally allows to increase accessibility to hemicages. As far as desilication treatments are concerned, most lead to a reduced accessible micropore volume fraction, indicating that desilication preferentially destroys hemicages on the crystal surface. For the swollen MCM-22(P) precursor desilication yet allows for a substantial increase in the accessible micropore volume fraction, which is probably related to the presence of the cationic surfactant in the interlayer volume that hence allows to induce surfactant-templating from the inside of the crystal.

Image 1:

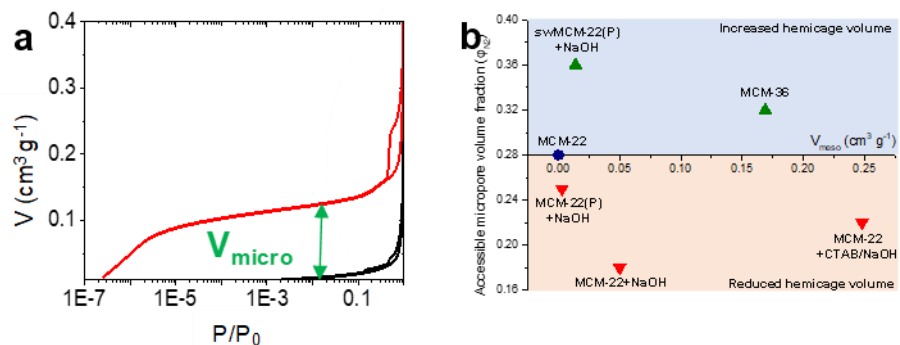


**Figure 1.** a) Nitrogen adsorption and desorption isotherm at 77 K of ZSM-5 nanoboxes before (red) and after (black)  $n$ -nonane preadsorption. b) The accessible micropore volume fraction as a function of hierarchical MCM-22 based zeolites.

- References:** 1. A. Sachse, J. Garcia-Martinez, Chem. Mater. 2017, 29, 3827-3853.  
2. C. Buttersack, J. Möllmer, J. Hofmann, R. Gläser, Microporous Mesoporous Mater. 2006, 236, 63-70.  
3. A. Galarneau, F. Villemot, J. Rodriguez, F. Fajula, B. Coasne, Langmuir 2014, 30, 13266-13274.  
4. J. Rouquerol, P. Llewellyn, F. Rouquerol, Stud. Surf. Sci. Catal. 2007, 160, 49-56.  
5. I. Batonneau-Gener, A. Sachse, J. Phys. Chem. C 2019, 123, 4235-4242.  
6. A. Sachse, T. Aumond, J. Rousseau, I. Batonneau-Gener, Adv. Mater. Interfaces 2021, DOI : 10.1002/admi.202100356.

## **Advanced Characterisation and Operando Spectroscopies**

FEZA21-PO-003

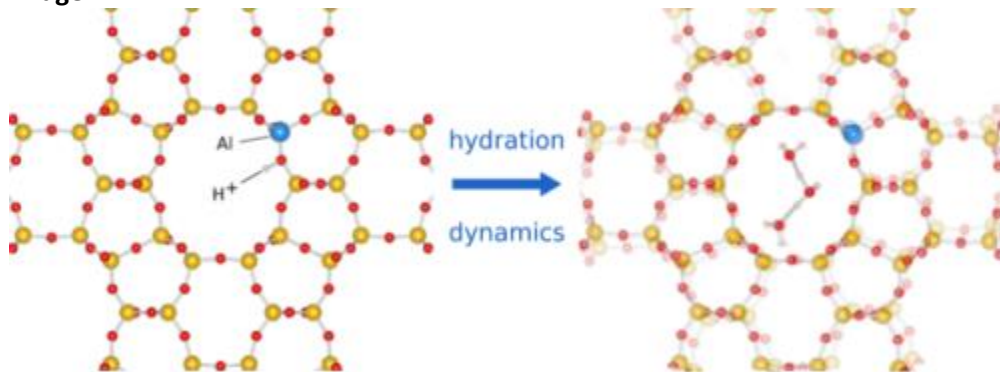
### **Characterization of the effect of hydration on nuclear magnetic resonance properties in zeolites**

S. Vanlommel<sup>1,\*</sup>, A. E. J. Hoffman<sup>1</sup>, S. Smet<sup>2</sup>, S. Radhakrishnan<sup>2</sup>, C. V. Chandran<sup>2</sup>, J. A. Martens<sup>2</sup>, E. Breyneert<sup>2</sup>, V. Van Speybroeck<sup>1</sup>

<sup>1</sup>Center for Molecular Modeling, Ghent University, Ghent, <sup>2</sup>Center for Surface Chemistry and Catalysis, KU Leuven, Leuven, Belgium

**Abstract Text:** Zeolites are crystalline aluminosilicates that are used for a broad range of industrial applications such as gas separation and capture and as highly efficient catalysts. Their structure consists of tetrahedrally coordinated  $\text{SiO}_4$  units connected in a network of pores and channels. Catalytic activity results from substitution of silicon for aluminum which requires the presence of countercharges that act as active centers. The local environment of the aluminum sites can strongly influence the catalytic activity of the acid sites [1]. Therefore, to be able to tune the framework for specific applications, it is crucial to characterize the aluminum distribution in the material, which requires techniques sensitive on short ranges. Nuclear magnetic resonance (NMR) spectroscopy has already been used to characterize the aluminum distribution in ZSM-5 [2]. However, zeolites typically operate under hydrous conditions, which can affect the local geometry of the material and therefore the NMR properties. Especially in the case of protic zeolites, water molecules can strongly change the nature of the acid sites through the solvation of protons [3, 4]. In supporting the interpretation of experimental data, it is crucial for computational techniques to explicitly take into account the presence of water. Furthermore, dynamic effects such as the rapid reorientation of the chemical shielding tensor due to molecular motion [5] cannot always be accounted for by solely using a static approach. Therefore we are interested in operando modeling techniques, as to mimic the real world operating conditions of the zeolite as closely as possible, by including both hydration and dynamics. The validity of the methodology is verified through comparison to experimental NMR results on a JBW zeolite.

#### **Image 1:**



**References:** [1] Wang et al., *Curr. Opin. Chem. Eng.*, 2019, 23, 146–154.

[2] Dib et al., *J. Phys. Chem. Lett.*, 2018, 9, 19–24.

[3] Vener et al., *Phys. Chem. Chem. Phys.*, 2009, 11, 1702.

[4] Wang et al., *J. Am. Chem. Soc.* 2019, 141, 3444–3455.

[5] Dračinský et al., *CrystEngComm*, 2013,15, 8705-8712.

## **Advanced Characterisation and Operando Spectroscopies**

FEZA21-PO-004

### **Mapping the reaction landscape for partial methane activation by Cu-modified zeolites**

E. Khramenkova<sup>1,\*</sup>, M. Medvedev<sup>2</sup>, E. Pidko<sup>1</sup>

<sup>1</sup>Chemical Engineering, TU Delft, Delft, Netherlands, <sup>2</sup>Laboratory for X-Ray Diffraction Studies, Zelinsky Institute of Organic Chemistry RAS, Moscow, Russian Federation

**Abstract Text:** Zeolites modified with the transition metals (TM) are promising materials for one-step low-temperature methane oxidation to methanol. Such catalysts often combine the benefits of being stable and recyclable and having well-defined geometry.<sup>1</sup> Their unique reactivity stems from the presence of extraframework TM cationic complexes electrostatically stabilized in the micropores by a negatively charged zeolitic framework. Earlier studies pointed to the high mobility of such cationic species allowing for the dynamic diffusion and change of nuclearity under the reaction conditions.<sup>2</sup> Nevertheless, the structural proposals for the active sites are still dominated either by the single-populated configurations determined within the 0K/UHV (ultra-high vacuum) approximation of the first-principles calculations or by the structural interpretations of the ensemble-average signals from the spectroscopic characterization studies. In this work, we demonstrate that such approximations do fail to adequately represent the configurational space of the active site populated under the actual catalytic conditions. We introduce a practical computational method to efficiently scan the different intrazeolite active site configurations to identify the reactive ensembles responsible for the catalytic properties of the zeolite materials.

Ab initio molecular dynamic (aiMD) simulations were carried out to sample the neighbouring regions of the potential energy surface around the  $[\text{Cu}_3\text{O}_3]^{2+}$  site in MOR zeolite earlier proposed as the active site for methane oxidation based on the detailed EXAFS analysis.<sup>3</sup> To enable the exhaustive configurational search, we made use of the initial velocity filtration to drag the system along the low modes in aiMD simulations. A novel clustering algorithm was introduced to identify the structurally distinct clusters in the trajectories, which were found to be more stable than the alternative  $[\text{Cu}_3\text{O}_3]^{2+}$  configurations considered in previous experimental and theoretical studies. Among the low-lying configurations are the diverse peroxo- and oxo-clusters. Many of these highly diverse configurations show comparable thermodynamic stabilities and their interconversion proceeds with relatively low barriers. Our results point to the simultaneous presence and rapid interconversion of such clusters in the zeolite pores under the reactive conditions giving rise to highly dynamic and diverse reactive ensembles defining the catalytic properties and behaviour of the cation-exchanged zeolites.

#### **References:**

1. Li, G. & Pidko, E. A. The Nature and Catalytic Function of Cation Sites in Zeolites: a Computational Perspective. *ChemCatChem* (2019) doi:10.1002/cctc.201801493.
2. Paolucci, C. et al. Dynamic multinuclear sites formed by mobilized copper ions in NO<sub>x</sub> selective catalytic reduction. *Science* (80-. ). (2017) doi:10.1126/science.aan5630.
3. Grundner, S. et al. Single-site trinuclear copper oxygen clusters in mordenite for selective conversion of methane to methanol. *Nat. Commun.* 6, 1–9 (2015).

## ***Advanced Characterisation and Operando Spectroscopies***

FEZA21-PO-006

### **The effect of chemical and redox environment on Cu proximity in Cu-mordenite**

G. Deplano<sup>1,\*</sup>, M. Signorile<sup>1</sup>, A. Martini<sup>1</sup>, E. Borfecchia<sup>1</sup>, V. Crocellà<sup>1</sup>, S. Svelle<sup>2</sup>, S. Bordiga<sup>1</sup>

<sup>1</sup>Department of Chemistry, NIS and INSTM Reference Centre, University of Turin, Via G. Quarello 15, I-10135 and Via P. Giuria 7, I-10125, Turin, Italy, <sup>2</sup>Department of Chemistry, SMN Centre for Materials Science and Nanotechnology, University of Oslo, N-0315 Oslo, Oslo, Norway

**Abstract Text:** Since the first observation in 2005 by Schoonheydt's group<sup>1</sup>, Cu-exchanged zeolites have been extensively studied for the direct conversion of methane-to-methanol. Along the years, many different topologies, Al and Cu contents and preparation methods have been explored with the aim to improve substantially the activity and preserving the selectivity of these materials. Several techniques, both experimental and theoretical, have been applied<sup>2</sup> hoping to find direct correlations between the structural properties and the catalytic performances of the materials under study. Nonetheless, the exact nature of the active species is far from well understood and a plethora of different mechanisms and candidates have emerged in the years. Notwithstanding the significant variability arising from different structure and composition of these materials, as well as the possibility of different reaction conditions, two key features lie at the core of this process: the Cu(I)/Cu(II) redox cycle and the local coordination environment of the Cu sites. Apart from leading the mechanisms underlying this reaction, redox and coordination properties of these Cu sites influence the average Cu-Cu distance, and thus the ability of the metal to form complexes and multimetric cores inside the zeolite framework<sup>3</sup>. Furthermore, it has been shown that certain gas-phase reactants that are used to reduce and coordinate the Cu possess the ability to mobilize the metal atoms inside the structure of the zeolite to some extent: it is the case of NH<sub>3</sub>, which is able to form stable complexes with the Cu atoms, that are mobile enough to move to different positions depending on the properties of the host material<sup>4</sup>.

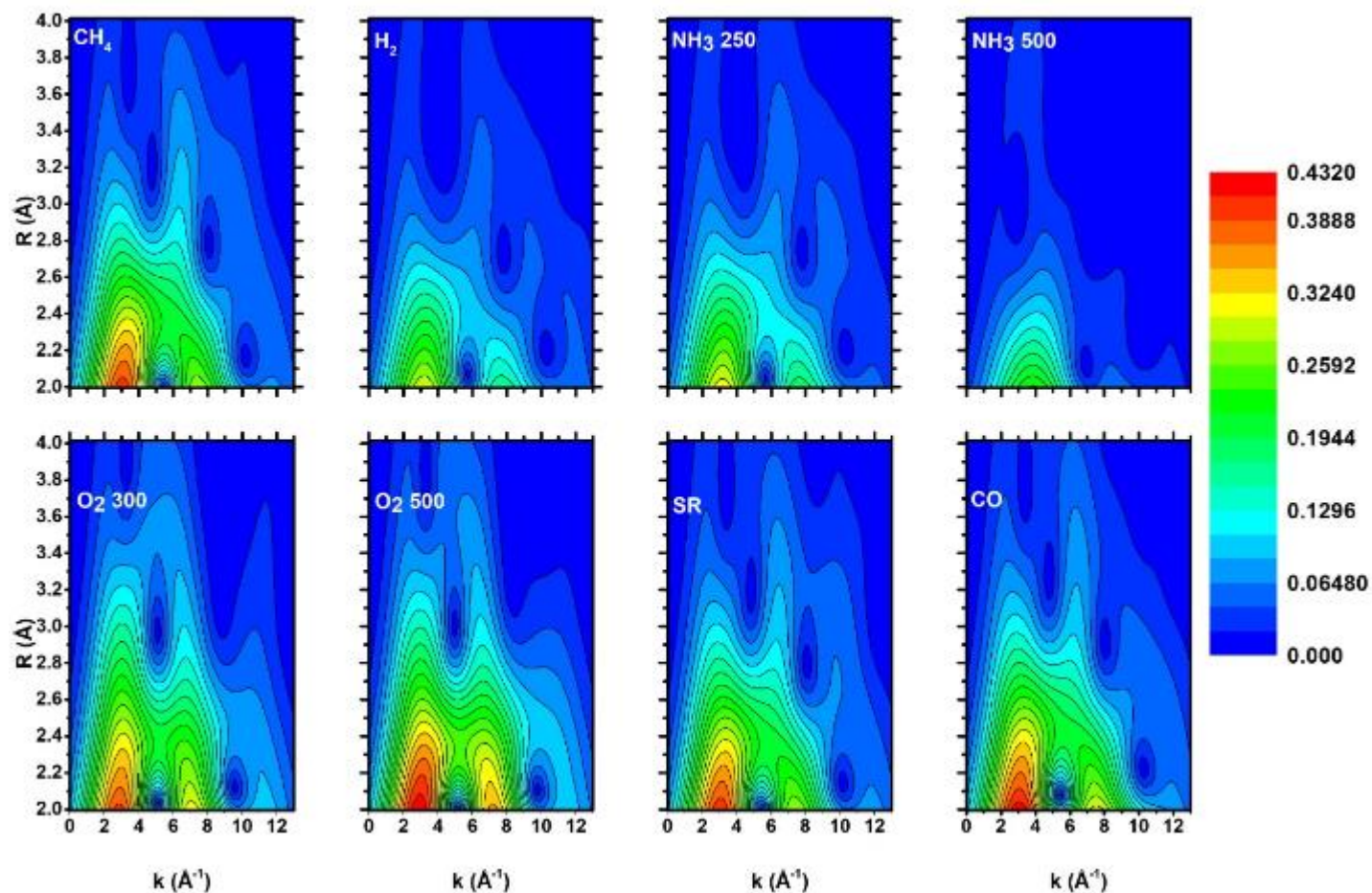
In this study, we treated a Cu mordenite sample (Si/Al=8.22, Cu/Al=0.27) with a series of reducing agents in order to assess their different effect with respect to the Cu species, both in term of reducibility and final location. In addition, two samples were treated in O<sub>2</sub> at different temperatures to have a reference for the oxidized states. All the samples were studied by Cu K-edge X-ray Absorption Spectroscopy (XAS) at the Elettra Synchrotron facility (Trieste). Both X-ray Absorption Near Edge Structure (XANES) and Extended X-ray Absorption Fine Structure (EXAFS) spectra were analysed, providing important, element-selective information on the redox behaviour and on the local coordination environment of the Cu sites. Furthermore, to obtain specific information on the possible multimetric Cu sites and distinguish their signal contribution from the lighter framework elements, we employed Wavelet Transform Analysis (WTA) on the collected EXAFS data. This novel approach allows to obtain a 2D representation of the EXAFS signal in k and R space simultaneously, making it possible to single out the contributions arising from scattering atoms with different atomic number, which are of ambiguous identification using the classic Fourier Transform analysis.

The WTA reported in Image 1 show how a "lobe" forms at high k and R values for some selected samples. This 2D contribution is mainly due to Cu-Cu neighbouring interactions and demonstrates how it is possible to prove the existence of multimetric Cu sites in a selective manner<sup>5</sup>.

#### **Acknowledgements**

Dr. Angelo Bellia is acknowledged for providing MOR samples. The work was financially supported by the European Research Council (ERC), under the Horizon 2020 research and innovation program: CuBE ERC-Synergy project (Grant agreement n° 856446).

Image 1:



References:

- 1 M. H. Groothaert et al., *J. Am. Chem. Soc.*, 2005, 127, 1394–1395.
- 2 M. A. Newton et al., *Chem. Soc. Rev.*, 2020.
- 3 E. Borfecchia et al., *Chem. Soc. Rev.*, 2018, 47, 8097–8133.
- 4 C. Paolucci et al., *Science*, 2017, 357, 898 LP – 903.
- 5 A. Martini et al., *Phys. Chem. Chem. Phys.*, 2020, 22, 18950–18963.

## **Advanced Characterisation and Operando Spectroscopies**

FEZA21-PO-007

### **Inelastic Neutron Scattering Study of Aluminum and Brønsted Site Location in Si/Al LTA Zeolite**

T. Lemishko, M. Jiménez-Ruiz, A. Vidal-Moya, S. Valencia, T. Blasco, F. Rey, G. Sastre\*

**Abstract Text:** LTA zeolite has three types of protons O1H, O2H and O3H (structural effect). But, is the acidity of each of these sites (O<sub>x</sub>H, x=1-3) the same regardless the Al-distribution of the zeolite?. As the Si/Al ratio decreases, the number of Brønsted site neighbours of an acid site increases, and this will also affect the acidity (chemical effect). Both factors (structural and chemical) need to be analyzed to assess and understand acidity. This can be done using models and appropriate techniques from a computational chemistry viewpoint, but, how can these models be compared to experiments if the real Al-distribution is unknown?. In the present work we propose a model to find Al-distributions in LTA zeolite by using Inelastic Neutron Scattering, <sup>29</sup>Si NMR spectra and periodic DFT calculations. It is yet to be seen whether this approach can be successfully used with more complex zeolites.

We study two LTA samples with Si/Al ratios of 40 and 5, whose corresponding models are Si<sub>47</sub>AlO<sub>96</sub>H and Si<sub>40</sub>Al<sub>8</sub>O<sub>96</sub>H<sub>8</sub> unit cells (2×1×1 from the smallest cell). The structure of LTA zeolite contains micropores consisting of large (α) and small (sodalite) cavities, in which O1H and O3H point to a 8-ring at the intersection between two α-cages, while O2H points to a 6-ring at the intersection between α-cage and sodalite.

The first sample (LTA-40) [1] contains, arguably, isolated Brønsted sites, and only three different sites (O1H, O2H, O3H) with no 'chemical effect' meaning only one Al-distribution consisting on 47 Si(0Al) and 1 Si(1Al). Either O1H, O2H, or O3H (or a mixture of them), all isolated sites, must be present. With exhaustive testing, O2H was found to give the best agreement with the experimental INS data (Figure 1, top).

The second sample (LTA-5) [2] is much more complex since the three structurally different sites (O1H, O2H, O3H) can be affected differently depending on the Al-distribution (chemical effect). By generating 100 randomly different Al-distributions, their calculated <sup>29</sup>Si NMR spectra was compared to the experimental and 9 of them were selected as similar to the NMR data. One of them, more in agreement with the experimental INS spectrum, was selected as the most probable Al distribution for LTA-5 (Figure 1, bottom).

Inelastic neutron scattering (INS) has been used to study the acid sites of the LTA zeolite with different Si/Al ratios. It is not possible to measure bending modes of the acid sites with IR spectroscopy since these bands overlap with the strong bands from the zeolite framework. The combination of an extremely high quality of the samples and the sensitivity of the instrument allows to detect with high precision the acid sites of both high-silica and low-silica zeolites and obtain information about their position.

#### **Acknowledgements**

We thank MICINN of Spain for funding through projects RTI2018-101784-B-I00, RTI2018-101033-B-I00 and SEV-2016-0683.

Image 1:

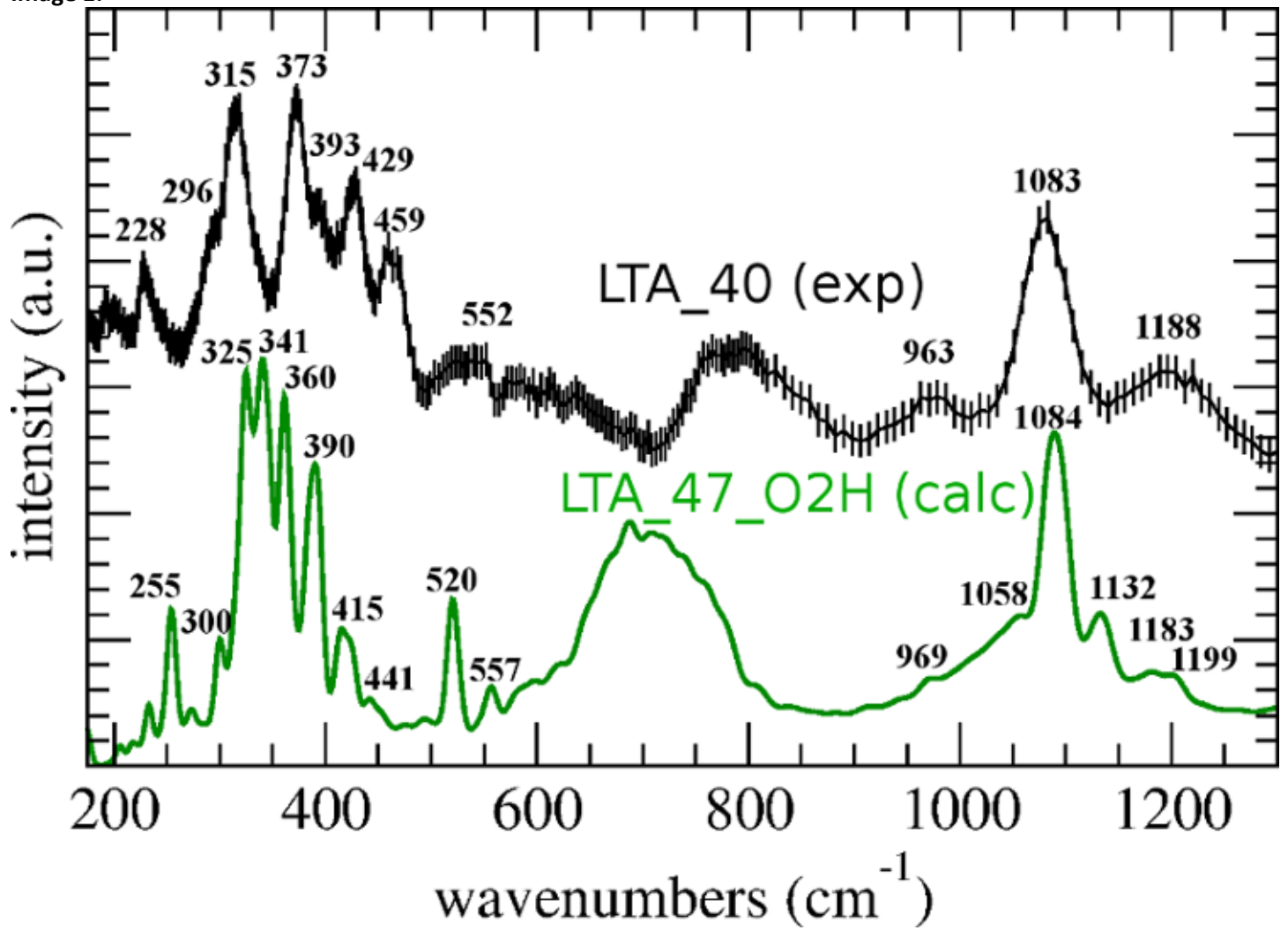
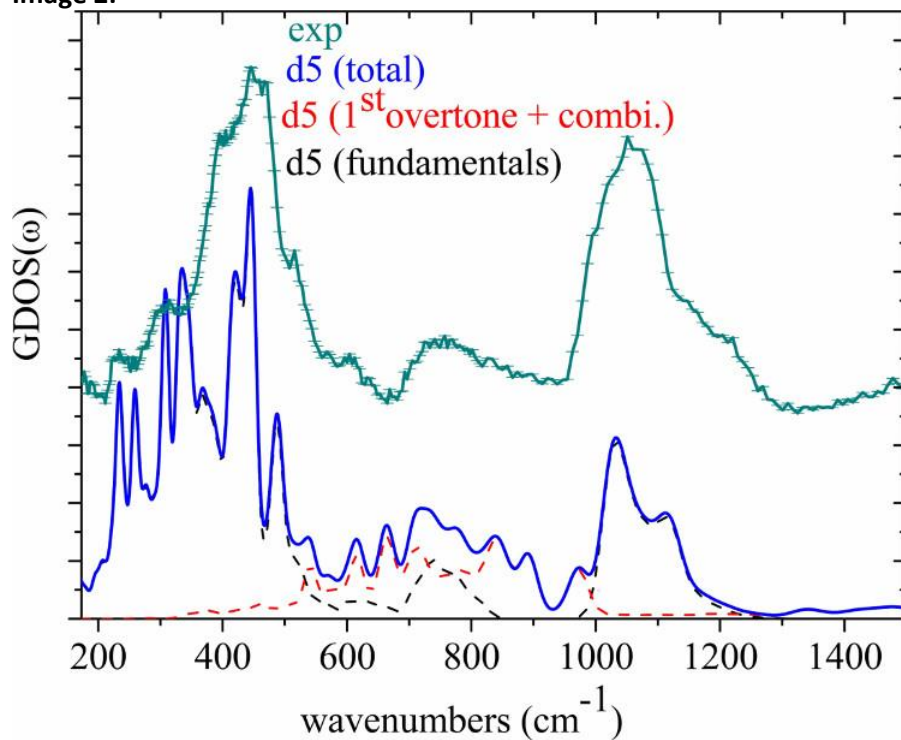


Image 2:



**References:** 1 T. Lemishko, S. Valencia, F. Rey, M. Jiménez-Ruiz, G. Sastre; “Inelastic Neutron Scattering Study on the Location of Brønsted Acid Sites in High Silica LTA Zeolite”; *J. Phys. Chem. C* 2016, 120, 24904–24909.

2 T. Lemishko, M. Jiménez-Ruiz, F. Rey, S. Valencia, T. Blasco, A. Vidal-Moya, G. Sastre; “Inelastic Neutron Scattering Study of Aluminum and Brønsted Site Location in Si/Al LTA Zeolite”; *J. Phys. Chem. C* 2018, 122, 11450-11454.

## Advanced Characterisation and Operando Spectroscopies

FEZA21-PO-009

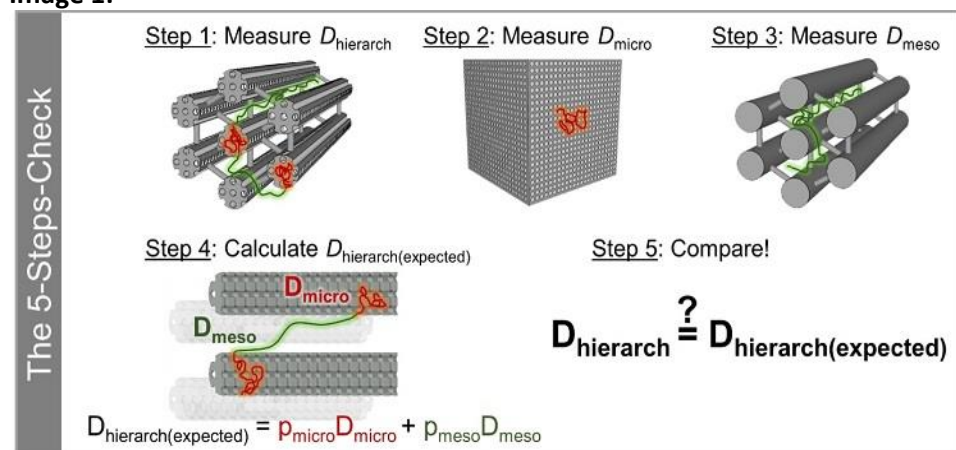
### Determination of the Rate-Limiting Step in the Dis(charging) Process of Supercapacitors by Coupling Ionic Diffusion in Porous Carbons at Micro- and Macroscales

M. Dvoyashkin<sup>1,\*</sup>, L. Borchardt<sup>2</sup>

<sup>1</sup>Institute of Chemical Technology, Universität Leipzig, Leipzig, <sup>2</sup>Institute of Inorganic Chemistry, Ruhr-Universität Bochum, Bochum, Germany

**Abstract Text:** In supercapacitors, the rate of charging depends on how quickly ions can reach and accommodate the surface of electrodes. The latter are often made of pelletized porous carbons being electrically conductive and offering high tunability of porosity for efficient ion accommodation. The diffusion of ions inside pores of carbon, a parameter reflecting the speed of their migration within individual carbon particles, is believed to be crucial in designing supercapacitor electrodes [1]. Herein, we discuss this belief by bridging the microscopic picture of diffusion seen by NMR with the macroscopic charging behavior of supercapacitors investigated by impedance spectroscopy. Quantification of the average residence time of ions within carbon particles showcases that the nanopore environment may not be the rate-limiting factor for the overall ion mobility and thus the performance of a supercapacitor cell – as commonly expected [2]. Combining direct diffusion studies performed with neat and solvated ionic liquids and those on organic electrolytes, we developed the so far lacking criteria for the rational selection of electrolyte-carbon systems and give recommendations for the preparation of transport-optimized materials for supercapacitors to minimize ionic diffusion limitations.

#### Image 1:



**References:** [1] L. Borchardt, D. Leistenschneider, J. Haase, and M. Dvoyashkin, *Adv. Energy Mater.* 111 (2018) 1800892; [2] M. Dvoyashkin, D. Leistenschneider, J. D. Evans, M. Sander, L. Borchardt, *Adv. Energy Mater.* (accepted).

**Structure-function relations in Fe-zeolite active sites for small molecule activation**

B. F. Sels<sup>1</sup>, E. I. Solomon<sup>2</sup>, M. L. Bols<sup>1,\*</sup>, R. A. Schoonheydt<sup>1</sup>, M. J. Dusselier<sup>1</sup>, J. Devos<sup>1</sup>, D. Plessers<sup>1</sup>, B. E. Snyder<sup>3</sup>, H. M. Rhoda<sup>2</sup>

<sup>1</sup>M2S, KU Leuven, Leuven, Belgium, <sup>2</sup>Chemistry Department, Stanford University, Stanford, <sup>3</sup>Chemistry Department, University of California, San Francisco, United States

**Abstract Text:** The highly reactive  $\alpha$ -O site in zeolites, capable of the low temperature activation of nitrous oxide, methane and benzene was recently defined as a high spin ( $S=2$ ) square pyramidal Fe(IV)=O species. The  $\alpha$ -O site can be formed by oxygen atom abstraction from  $N_2O$  by the  $\alpha$ -Fe(II) precursor, which can be hosted in extra-framework cation exchange sites of 6MR containing zeolites such as MFI, \*BEA, FER and CHA with specific positioning of aluminum-substituted T-atoms.

With the active site's geometry and electronic structure, as well as spectroscopic handles of active site through reaction cycles identified, detailed mechanistic studies can now be carried out. Key reaction intermediates have been spectroscopically identified for the oxygen atom abstraction from  $N_2O$ , the hydroxylation of benzene, and the hydroxylation of methane. Mechanistic insight reveals rate limiting steps and causes of reduced selectivity and catalyst turnover. The reaction profiles can be modified through active site manipulation, as demonstrated by a comparison between Fe-\*BEA and Fe-CHA. Three key catalyst characteristics are discussed: confinement, ligand field strength and geometry, and molecular sieving. All computational data are supported by experimental characterization and kinetic studies.

**Image 1:**

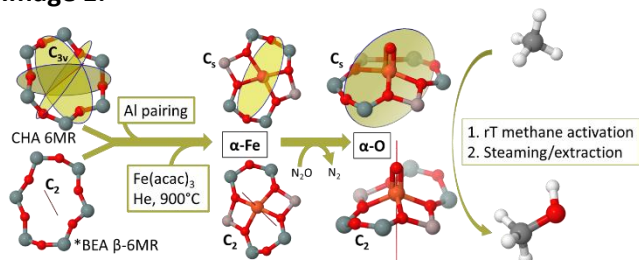
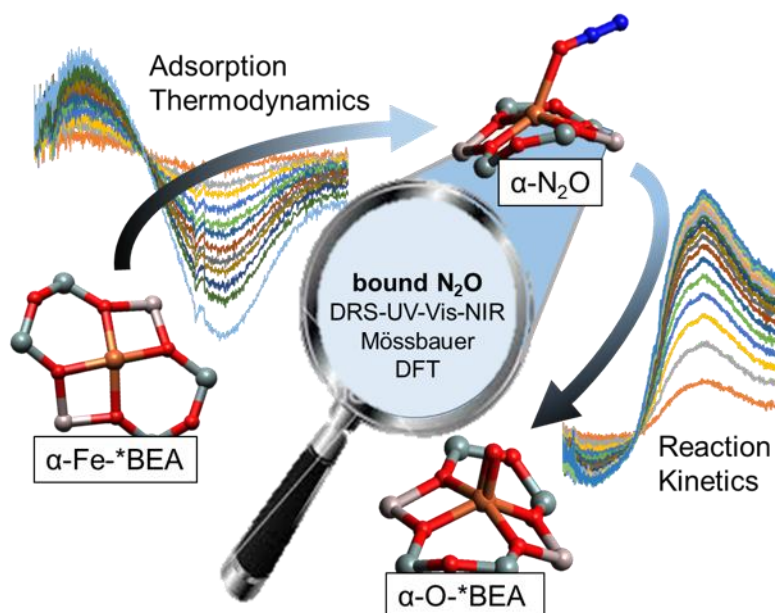


**Image 2:**



- References:** 1. B.E.R. Snyder, P. Vanelderen, M.L. Bols, S.D. Hallaert, L.H. Böttger, L. Ungur, K. Pierloot, R.A. Schoonheydt, B.F. Sels, E.I. Solomon. *Nature* 2016, 536, 317-321.
2. Snyder, B. E. R.; Böttger, L. H.; Bols, M. L.; Yan, J. J.; Rhoda, H. M.; Jacobs, A. B.; Hu, M. Y.; Zhao, J.; Alp, E. E.; Hedman, B.; Hodgson, K. O.; Schoonheydt, R. A.; Sels, B. F.; Solomon, E. I. Structural Characterization of a Non-Heme Iron Active Site in Zeolites That Hydroxylates Methane. *Proc. Natl. Acad. Sci.* 2018, 115, 4565–4570.
3. M.L Bols, S.D. Hallaert, B.E.R. Snyder, J. Devos, D. Plessers, H.M. Rhoda, M. Dusselier, R.A. Schoonheydt, K. Pierloot, E.I. Solomon, B.F. Sels. Spectroscopic Identification of the  $\alpha$ -Fe /  $\alpha$ -O Active Site in Fe-CHA Zeolite for the Low-Temperature Activation of the Methane C-H bond. *J. Am. Chem. Soc.* Just Accepted Manuscript.
4. Hallaert, S. D.; Bols, M. L.; Vanelderen, P.; Schoonheydt, R. A.; Sels, B. F.; Pierloot, K. Identification of  $\alpha$ -Fe in High-Silica Zeolites on the Basis of Ab Initio Electronic Structure Calculations. *Inorg. Chem.* 2017, 56, 10681–10690.
5. Snyder, B. E. R.; Bols, M. L.; Schoonheydt, R. A.; Sels, B. F.; Solomon, E. I. Iron and Copper Active Sites in Zeolites and Their Correlation to Metalloenzymes. *Chem. Rev.* 2018, 118, 2718–2768.

**The Use of Pair Distribution Function to Probe the ADOR Mechanism**

S. Russell<sup>1,\*</sup>, S. Henkelis<sup>2</sup>, S. Vornholt<sup>1</sup>, R. Morris<sup>1</sup>

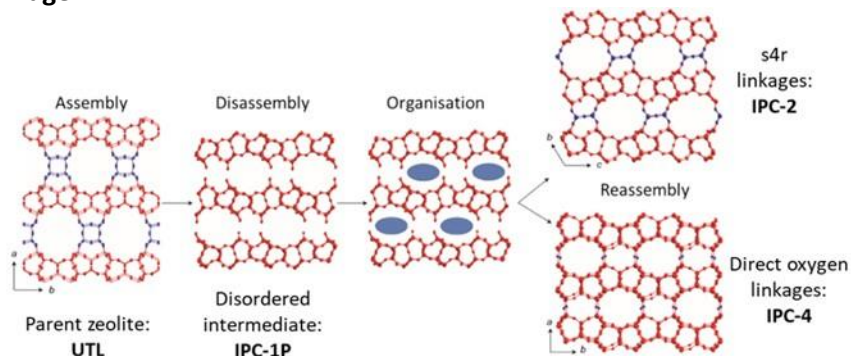
<sup>1</sup>School of Chemistry, University of St Andrews, St Andrews, United Kingdom, <sup>2</sup>Nanoscale Sciences Department, Sandia National Laboratories, Albuquerque, United States

**Abstract Text:**

The Assembly-Disassembly-Organisation-Reassembly (ADOR) process is a method of producing new zeolite frameworks, which may have been unfeasible from traditional hydrothermal methods, through the disassembly of an initial parent structure (Image 1).<sup>1</sup> An in-depth understanding of the mechanism behind the breakdown of the parent zeolite is useful to understand the control over the formation of the final products. The work presented here focusses on the disassembly stage of the process, attempting to understand the sequence of bond breakage and layer organisation prior to the formation of the final product.

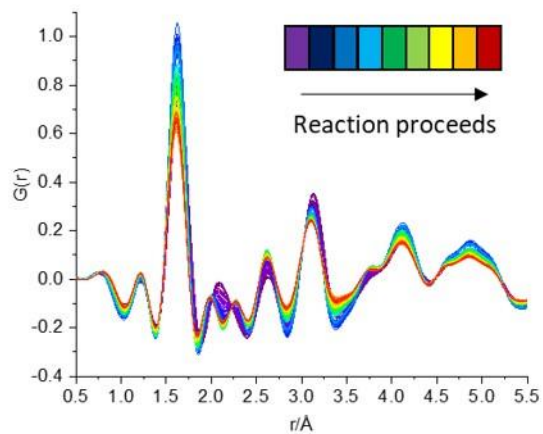
The disassembly of the parent zeolite results in a large degree of disorder within the framework. The consideration of both Bragg and diffuse scattering, known as total scattering, from pair distribution function (PDF) makes it an extremely useful tool for probing the local changes within the structure as the disassembly and organisation proceeds. The hydrolysis of UTL by 6 M acid was monitored by in-situ PDF measurements at the Advanced Photon Source (APS). The resulting data has provided interesting insights in to the mechanism of the ADOR process (Image 2).

**Image 1:**



A summary of the ADOR process as the parent zeolite UTL is disassembled, organised and reassembled to form new products.

**Image 2:**



The observed PDF data as the in-situ hydrolysis of the parent zeolite UTL proceeds.

**References:** 1. W. J. Roth, P. Nachtigall, R. E. Morris, P. S. Wheatley, V. R. Seymour, S. E. Ashbrook, P. Chlubná, L. Grajciar, M. Položij, A. Zuka, O. Shvets and J. Cejka, *Nat. Chem.*, 2013, 5, 628–33.

## **Advanced Characterisation and Operando Spectroscopies | Zeolites/Inorganic materials**

FEZA21-PO-013

### **Characterisation of the natural zeolite clinoptilolite**

V. Grill<sup>1,\*</sup>, J. M. Welch<sup>2</sup>, C. Strelt<sup>2</sup>, J. H. Sterba<sup>2</sup>, T. Bretschneider<sup>2</sup>, K. Hradil<sup>3</sup>, C. Knoll<sup>4</sup>

<sup>1</sup>Radiation Protection and Radiochemistry, AGES, <sup>2</sup>Atominstut, <sup>3</sup>X-ray Center, <sup>4</sup>Institute of Applied Synthetic Chemistry, TU Wien, Vienna, Austria

**Abstract Text:** Clinoptilolite samples were characterized by several quantitative and qualitative analytical methods [1]. The zeolites were first assessed by Infrared (IR) Spectroscopy to gather preliminary structural knowledge and to confirm their high clinoptilolite content. Their thermal stability (dehydration) was evaluated by combining Differential Scanning Calorimetry (DSC) and Thermogravimetry Analysis (TGA) (Simultaneous Thermal Analysis; STA). After these preliminary experiments, precise determination of elementary compositions of the zeolite samples was done by Neutron Activation Analysis (NAA) and Total Internal Reflection X-Ray Fluorescence (TXRF). Powder X-Ray Diffraction (PXRD) was used to investigate crystalline phase compositions. Furthermore, all the data collected were analysed together to clarify the zeolite type and elemental composition. The results were compared to elemental composition of clinoptilolites in the literature.

The company LITHOS Industrial Minerals GmbH provided the following information about the zeolite samples. Sample A and D have a grain size of 0-125 $\mu$ m, sample B of 0-100 $\mu$ m and sample C of 0.5-2mm. Sample C was milled for the analysis IR, STA, NAA, TXRF and PXRD. Sample A, B and C should contain 90% of clinoptilolite and sample D only less than 60%.

#### Analysis

The analysis of NAA and TXRF was done by comparison to NIST standard Coal Fly Ash (CFA). The Si content of the samples cannot be determined directly by combined NAA and  $\gamma$ -spectroscopy, because silicon does not have an easily detectable  $\gamma$ -peak. By detecting the  $\gamma$ -peak of <sup>29</sup>Al [2] the silicon content of the sample can be calculated the same way as the other element amounts were determined. For the TXRF analysis, the thin film approximation was used. The element silicon was set to the internal standard, which means the proportional constant of silicon was set to 1000. The software of the used instrument Atomika 8030C calculates the other element specific concentration proportional constants, which are used for the determination.

#### Results

The IR spectra of the samples confirmed that all four samples contain mostly clinoptilolite. However, the exact content cannot be determined by IR spectroscopy. It is clear from the STA data that the water content of the sample materials does not change drastically over the temperature range studied, and no further consideration is necessary for the following NAA and TXRF experiments.

The Si/Al ratio for samples A and B lies between 4.0 and 5.5 as is characteristic for clinoptilolite. For sample C the ratio is also in this range, if calculated from the NAA data. It can be concluded that sample A, B and C are mainly clinoptilolite. Sample D has a higher value for the Si/Al ratio, which indicates the presence of some additional non-clinoptilolite material. While NAA has been previously applied to the analysis of zeolitic materials, it has also been demonstrated that TXRF analyses of finely powdered zeolites are also possible using a very simple sampling method (Tab. 1). Nonetheless, TXRF seems to systematically underestimate the quantitative element content of the zeolites. This can be explained by absorption effects and the inadequacy of the thin film approximation to the sampling method applied.

PXRD verified that samples A, B and C have clinoptilolite-Na as the major phase and sample D contains an additional non-clinoptilolite phase.

#### Acknowledgements

Open access funding provided by TU Wien and AGES. The authors want to thank Lithos Natural for the provision of the samples. Special thanks to Prof. Dr. Georg Steinhauser of the Institute of Radioecology and Radiation Protection (IRS) of Leibniz Universität Hannover for assistance with the Si content determination of the samples via <sup>29</sup>Al detection.

#### **Image 1:**

Tab. 1 Comparison of the quantitative content of the elements determined with TXRF and NAA

A	TXRF		NAA		Difference
	wt %	$\sigma$	wt %	$\sigma$	
Al	4.29	0.15	6.00	0.12	28.41
Si	23.02	0.09	30.16	3.46	23.68
K	1.64	0.12	2.89	0.43	43.37
Ca	1.83	0.12	2.70	0.15	32.27
Ti	0.07	0.01	0.09	0.01	20.90
Fe	1.34	0.10			
<b>B</b>					
Al	4.15	0.09	5.73	0.11	27.46
Si	23.02	0.09	30.53	2.12	24.60
K	1.76	0.04	3.04	0.72	42.01
Ca	1.83	0.09	2.77	0.14	33.77
Ti	0.07	0.01	0.10	0.01	25.88
Fe	1.31	0.08			
<b>C</b>					
Al	3.75	0.10	5.69	0.12	34.02
Si	23.02	0.09	26.11	3.17	11.84
K	1.43	0.05	2.25	0.31	36.54
Ca	1.35	0.07	2.17	0.12	37.75
Ti	0.08	0.01	0.09	0.01	13.85
Fe	1.32	0.08			
<b>D</b>					
Al	3.81	0.08	6.78	0.14	43.80
Si	23.02	0.09	39.90	4.42	42.30
K	1.08	0.03	1.81	0.10	40.41
Ca	0.90	0.06	2.03	0.10	55.48
Ti	0.11	0.01	0.13	0.02	15.77
Fe	1.59	0.11			

- References:** [1] Grill V (2019) Characterization of Natural Clinoptilolite Material for Remediation of Sr-90 and Cs-137 in Seawater. TU Wien  
 [2] Alfassi ZB (1994) Determination of Trace Elements. VCH Verlagsgesellschaft, Weinheim

**Formation and reactivity of (di)alpha oxygen prepared by the dissociation of O<sub>2</sub> over Fe-FER; in situ spectroscopic studies**

J. E. Olszówka<sup>1,\*</sup>, E. Tabor<sup>1</sup>, K. Mlekodaj<sup>1</sup>, M. Lemishka<sup>1,2</sup>, S. Sklenak<sup>3</sup>, Z. Sobalik<sup>1</sup>, J. Dedecek<sup>1</sup>

<sup>1</sup>Department of Structure and Dynamics in Catalysis, J. Heyrovský Institute of Physical Chemistry Czech Academy of Sciences, Prague, <sup>2</sup>Faculty of Chemical Technology, University of Pardubice, Pardubice, <sup>3</sup>Department of Theoretical Chemistry, J. Heyrovský Institute of Physical Chemistry Czech Academy of Sciences, Prague, Czech Republic

**Abstract Text:**

**Introduction**

Oxyfunctionalization of hydrocarbons is highly required transformation in industrial chemistry. Recently, it was shown, that two Fe(II) ions of binuclear Fe(II) species stabilized in ferrierite (FER) can cooperate in facilitation of N<sub>2</sub>O decomposition and formation of active oxygen (called  $\alpha$ -oxygen) used subsequently for methane to methanol oxidation [1,2]. Application of such a route with more atom-efficient O<sub>2</sub> would be very interesting in selective oxidation of hydrocarbons. In this work the reactivity of  $\alpha$ -oxygen stabilized by binuclear Fe(II) species in FER for selective oxidation of CH<sub>4</sub> at ambient temperature to valuable oxygen containing products is studied by spectroscopic means.

**Materials & Methods**

Commercially available FER Si/Al 8.6 was exchanged with NH<sub>4</sub>NO<sub>3</sub> to NH<sub>4</sub>-form of FER. The Fe(II)-FER catalyst with Fe/Al 0.04, was prepared by impregnation with FeCl<sub>3</sub> dissolved in acetylacetone. For Mössbauer spectroscopy measurements sample was prepared by the same procedure using isotopically enriched <sup>57</sup>FeCl<sub>3</sub>. FTIR, Mössbauer and UV-Vis spectroscopy were used for determination of the redox properties of Fe species in FER. Recorded spectra were collected after evacuation (at 450 °C, 3h) and after following treatments: i) 30 min interaction with O<sub>2</sub> at RT (p<sub>O<sub>2</sub></sub>= 1 atm.), ii) O<sub>2</sub> desorption at RT/200°C, iii) interaction with CH<sub>4</sub> at RT/200°C (p<sub>CH<sub>4</sub></sub> = 1 atm.), iv) evacuation of CH<sub>4</sub> at RT/200°C.

**Results & Discussion**

Mössbauer spectroscopy revealed that evacuated Fe-FER contained exclusively atomically dispersed Fe(II) located in cationic sites ( $\alpha$  and  $\beta$  [2] IS > 0.9 and, QS 0.48-2.20 mm/s). The interaction of Fe-FER with O<sub>2</sub> at RT (followed by an evacuation) results in its oxidation and formation of the new doublet with the hyperfine parameters (IS = 0.38 and QS=0.78 mm/s) similar to previously established parameters of  $\alpha$ -oxygen [Fe(IV)O]<sup>2+</sup> (equivalent to [Fe(III)O•]<sup>2+</sup>) formed after interaction of Fe-zeolite with N<sub>2</sub>O. The interaction of the oxidized Fe-FER with CH<sub>4</sub> followed by an evacuation results in the presence of Fe(II), exclusively. FTIR spectrum of the dehydrated Fe-FER confirms the presence of the band at 938 and 918 cm<sup>-1</sup> assigned to bare Fe(II) ( $\alpha$  and  $\beta$  cationic sites, respectively). The interaction with O<sub>2</sub> at RT results in (i) disappearing the bands attributed to the bare Fe(II) cations and (ii) the formation of a new band at around 880 cm<sup>-1</sup>. This band stable at RT and 200°C is assigned to the  $\alpha$ -oxygen and reflects stronger perturbation of the T-O-T vibrations by the ligation of [Fe(IV)O]<sup>2+</sup> to the zeolite ring [2]. FTIR spectrum recorded after the subsequent interaction of the oxidized Fe-ferrierite with CH<sub>4</sub> at RT followed by an evacuation at 200°C exhibited the bands at 938 and 918 cm<sup>-1</sup>, which are assigned to Fe(II). Also UV-Vis-NIR spectroscopy evidence the oxidation of Fe(II) ions. A new band, identical as observed for Fe-beta [1] zeolite after oxidation by N<sub>2</sub>O, attributable to the formation of Fe(IV)=O at 30 000 cm<sup>-1</sup> was formed. Results from all used spectroscopies, confirm the interaction between CH<sub>4</sub> and  $\alpha$ -oxygen originating from O<sub>2</sub> dissociation. Moreover, the presence of Fe(II) after CH<sub>4</sub> treatment of oxidized Fe-FER suggested that the products of CH<sub>4</sub> oxidation are easily released.

**References:**

- [1] Solomon, E. I. et al., Nature, 536 (2016) 317-321
- [2] Tabor, E. et al., Commun. Chem., 2 (2019)

**Time-resolved FTIR Analysis of Ethanol Conversion over Medium-Pore Zeolites: a Mechanistic Study**

K. Pyra<sup>1</sup>, K. Tarach<sup>1</sup>, K. Gołębek<sup>1</sup>, K. Góra-Marek<sup>1,\*</sup>

<sup>1</sup>Faculty of Chemistry, Jagiellonian University in Kraków, Krakow, Poland

**Abstract Text:** The catalytic potential of zeolites is determined by their crystalline structure. The pore structure given by the zeolite framework defines the well-known concept of shape-selective catalysis. This is due to a strong stabilization of the transition states by the van der Waals interactions with the zeolite framework (confinement effect) as well by channels topology and size of the internal voids. In this work studies of ethanol transformation over 10-ring zeolites exhibiting similar acidic property were carried out to evidence the role of the size of internal cavities on the associative and dissociative pathways for ethanol dehydration. The difference of the internal void formed at the intersection of 10-ring (ZSM-5 and TNU-9) and 10- and 8-ring channels (TNU-10) determines the type of the chemisorbed adducts (blue spectrum in Fig. 1), their successive transformations and finally decides on the type of the product formed. For zeolites offering spacious internal cavities formed by 10-ring channels intersected (ZSM-5 and TNU-9) ethanol molecules are hydrogen-bonded to the Si(OH)Al groups. The intensities of the C component of ABC structure (1800-1500 cm<sup>-1</sup>) clearly indicate the significant difference in the cavity volume (500, vs. 1410 Å<sup>3</sup> for ZSM-5 and TNU-9, resp.) [1] being easily accessible to ethanol molecules. In TNU-10 the rapid transformation of ethanol molecules into intermediate species does not provide the interference of the spectra by the Fermi resonance is observed. This suggests that the reduced void volume (8- and 10-ring channels intersected) favors the immediate transformation of the chemisorbed ethanol to ethoxy intermediate species with the elimination of water molecule. Both hydrogen-bonded ethanol molecules and ethoxy species are consumed on time, nearly fully consumed within 5 min. at 220 °C (red spectrum in Fig. 1) providing ethene as the main product. Nevertheless, the more confined environment in TNU-10 ensures the rapid transformation of the ethoxy species directly to butenes (1630 cm<sup>-1</sup>) while the intermediate species detected in ZSM-5 and TNU-9 serve as the substrates in forming oligomeric species (a broad band at 1620 cm<sup>-1</sup>). Our preliminary results on the ethanol transformation over 10-ring zeolites evidence a highly selective production of ethylene in TNU-10; the structures with the larger cavities in the intersection of the 10-MR channels architecture (ZSM-5, TNU-9) yield in smaller ethylene selectivity. Such differentiated adsorption feature strongly supports the confinement effect. This can be tuned by the size of the internal cavities while the concentration and strength of the acid sites can be considered of a secondary importance. K.G.M. acknowledges the financial support from the National Science Centre, Poland (Grant No. 2015/18/E/ST4/00191 and No. 2017/27/B/ST5/00191).

**References:** 1. <http://www.iza-structure.org/databases>.

## **Advanced Characterisation and Operando Spectroscopies | Zeolites/Inorganic materials**

FEZA21-PO-021

### **Insight on a hierarchical zeolite: from structural arrangement to active sites**

A. Airi<sup>1,\*</sup>, M. Signorile<sup>1</sup>, F. Bonino<sup>1</sup>, P. Quagliotto<sup>1</sup>, S. Bordiga<sup>1</sup>, S. Radhakrishnan<sup>2</sup>, G. Vanbutsele<sup>2</sup>, S. P. Sree<sup>2</sup>, J. Martens<sup>2</sup>, V. Crocellà<sup>1</sup>

<sup>1</sup>Chemistry department, University of Turin, Turin, Italy, <sup>2</sup>Centre for Surface Chemistry and Catalysis: Characterisation and Application Team (COK-KAT), KU Leuven, Leuven, Belgium

**Abstract Text:** One of the most promising field in heterogeneous catalysis, increasingly oriented to realize materials with even higher selectivity and efficacy, is represented by the production of hierarchical zeolites, able to overcome the major drawbacks related to the dimensions of the zeolitic micropores by reducing the steric limitations and the rate of intracrystalline diffusion for reactants and products. Numerous different strategies for the synthesis of such materials have been studied. Among all, the approach developed by Ryoo and coworkers appears revolutionary.<sup>1</sup> It applies some bifunctional surfactants (poly-quaternary ammonium salts, presenting long alkylic chains) as templating agents, which should be able to drive the formation of a very thin layer of aluminum silicate over the surface of the micelle in aqueous media: the hydrophobic long tails would produce the mesopores, while the external ammonic heads lead to the formation of the microporous framework. Applying the synthetic route developed by Na et al.<sup>2</sup> the possibility of obtaining a hierarchical ZSM-5 through this soft templating approach is critically evaluated in the present work. We performed a series of tailored experiments with the aim to achieve a deep knowledge of the structural arrangement and how an effective zeolitic MFI lattice is disposed in the multi-level porous system. The latter in fact, is a nebulous topic in many cases of production of hierarchical zeolites, mainly because of the difficulties in synthesizing long range ordered materials, which hampers the structural determination by X-Ray diffraction. For this reason, a strategy based on the combination of surface physico-chemical analysis, vibrational and MAS-NMR spectroscopy and a targeted catalytic test has been applied, comparing the results with a classical microporous ZSM-5 and with a mesoporous MCM-41. First, 77K N<sub>2</sub> adsorption revealed the presence of two families of pores: the smaller one has the diameter of the typical MFI micropores, the second one, definable as mesoporous, is compatible with the hexagonally shaped cavities visible in the TEM micrographs (See Image 1). The *in situ* IR spectroscopy, in the presence of adsorbed probe molecules with proper proton affinity and steric hindrance, has been employed for describing the complex acidic population. The existence of both Brønsted and Lewis acidic sites is attested; they are mainly located at the pore mouths as probed by the adsorption of sterically hindered molecules<sup>3</sup> (See Image 2). The acidic form of the sample (as bifunctional catalyst in presence of platinum) has been also tested in the reaction of n-decane hydrocracking, analyzing the products of isomerization and cracking by gas chromatography.<sup>4</sup> The prevalence of terminal methyl isomers indicates the shape selectivity typical for ZSM-5, whereas the suppression of secondary cracking demonstrates the great increase of diffusion rate generated by the mesoporous framework. All the results converge in describing a mesoporous structure consisting of a thin layer of ZSM-5 zeolite capable of acting as a catalyst through the action of its acidic sites exposed at the surface of the channels.

Image 1:

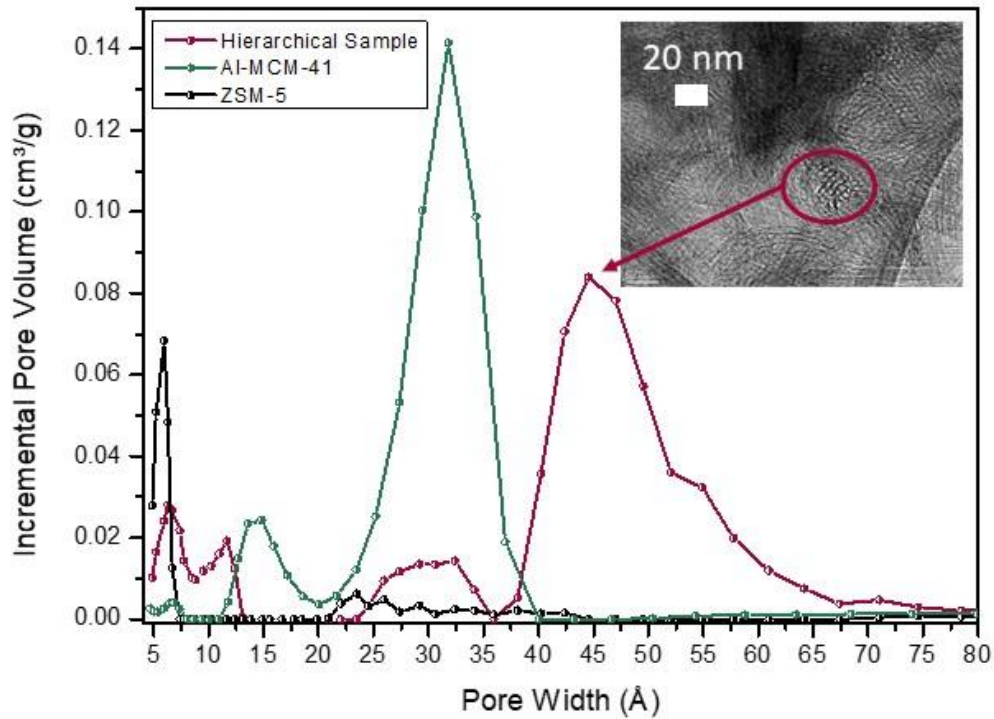
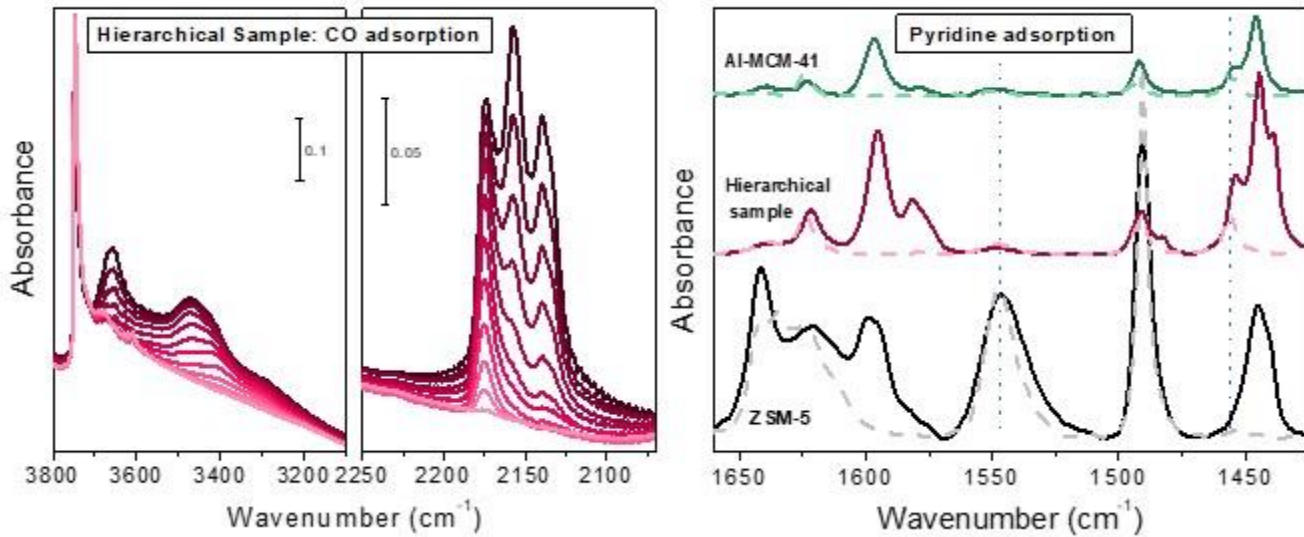


Image 2:



References:

- 1 K. Na, M. Choi and R. Ryoo, *Microporous Mesoporous Mater.*, 2013, 166, 3–19.
- 2 K. Na, C. Jo, J. Kim, K. Cho, J. Jung, Y. Seo, R. J. Messinger, B. F. Chmelka and R. Ryoo, *Science* (80-. ), 2011, 333, 328–332.
- 3 B.-T. Lønstad Bleken, L. Mino, F. Giordanino, P. Beato, S. Svelle, K. P. Lillerud and S. Bordiga, *Phys. Chem. Chem. Phys.*, 2013, 15, 13363.
- 4 J. A. Martens and P. A. Jacobs, *Zeolites*, 1986, 6, 334–348.

**Quantitative determination of acid sites content in BEA zeolites by  $^{31}\text{P}$  MAS NMR spectroscopy of adsorbed alkyl-substituted phosphine oxides**

D. S. Zasukhin<sup>1,\*</sup>, I. A. Kasyanov<sup>1</sup>, Y. G. Kolyagin<sup>1</sup>

<sup>1</sup>Department of Chemistry, Lomonosov Moscow State University, Moscow, Russian Federation

**Abstract Text:** NMR spectroscopy of adsorbed organophosphorus probe molecules is a promising method for studying the acid properties of zeolite catalysts. According to the literature data, a number of such molecules has already been tested: trimethylphosphine (TMP), oxides of trimethylphosphine (TMPO) and its homologues such as tri-*n*-butyl- (TBPO) and tri-*n*-octyl- (TOPO) phosphine [1]. However, most of the proposed techniques allow only a qualitative characterization of acidity in zeolites, as it is not possible to introduce a given number of probe molecules into the sample. Therefore, this study was aimed at developing an approach for the quantitative determination of acid sites in zeolites based on  $^{31}\text{P}$  MAS NMR spectroscopy.

For this study we used commercially available BEA zeolites CP814Q and CP811C (Zeolyst) with Si/Al ratio 25 and 150, which are further named AIBEA-25 and AIBEA-150, respectively. Also we used SiBEA and dealuminated DeAl-BEA zeolites, which were synthesized by ourselves. NMR experiments were executed using AVANCE-II 400WB Bruker NMR spectrometer with 4 mm double-channel MAS probe. For quantitative measurements 90-degree pulse (2.0  $\mu\text{s}$ ) with high-power  $^1\text{H}$  decoupling and preliminary  $^{31}\text{P}$  saturation was used. TMPO, TBPO and TOPO were used as probe molecules. For the correct quantitative assessment of acid sites, it was necessary to optimize the conditions of spectra acquisition, as  $^{31}\text{P}$  nuclei, depending on their location, can have different, e.g. too long, relaxation times. Application of a standard was necessary for quantitative correlation of the integrated intensity of various signals in the NMR spectra. Crystalline aluminum phosphate with the structure of tridymite ( $\text{AlPO}_4$ -tridymite) as the internal standard and gallium phosphide (GaP) as the external standard were chosen owing to their exact chemical composition and stability. Chemical shift in  $^{31}\text{P}$  NMR spectrum for  $\text{AlPO}_4$ -tridymite is observed at -30 ppm, and for GaP it is at -145 ppm.

The Image 1 shows the  $^{31}\text{P}$  NMR spectra of TBPO supported on BEA zeolites with  $\text{AlPO}_4$ -tridymite as an internal standard. The grey rectangles mark the regions corresponding to the following sites: "B + L" – the region with overlapping Brønsted and Lewis sites, "SiOH" – the region with signal attributed to TBPO on different silanol groups, "Phys. Ads." – physically adsorbed TBPO. The signals recorded on the samples studied are partly consistent with those presented in literature regions characteristic for zeolites of various structure [2], however further clarification in the attribution of signals to the sites different in nature, localization and strength is needed. The correlation of signal intensities corresponding to different sites with an internal or external standard signal along with the mass and amount of substances in the sample for NMR measurements makes it possible to quantify the content of various types of zeolite acid sites.

Comparison of the data obtained during the adsorption of probe molecules resulted in estimation of both the total acidity (when using TMPO or TBPO) and the number of external acid sites (when using TOPO) of BEA zeolites. It can be clearly seen from the Table that the amount of Brønsted and Lewis sites from the NMR spectra of adsorbed TBPO coincide with the amount of aluminum atoms much better than the data from IR spectroscopy of adsorbed pyridine (FTIR Py). Acid sites in AIBEA-25 seem to be rather close to each other, so that probe molecules (both Py and TBPO) cannot cover all the sites.

Thus, as a result of our work, we proposed a technique for the quantitative determination of acid sites in zeolites according to  $^{31}\text{P}$  NMR spectroscopy of adsorbed alkyl-substituted phosphine oxides. It allows one to estimate the amount of Brønsted and Lewis sites of different strength, as well as to determine their accessibility for probe molecules of different size.

The authors gratefully acknowledge Russian Science Foundation (project № 19-73-10160) for the financial support.

Image 1:

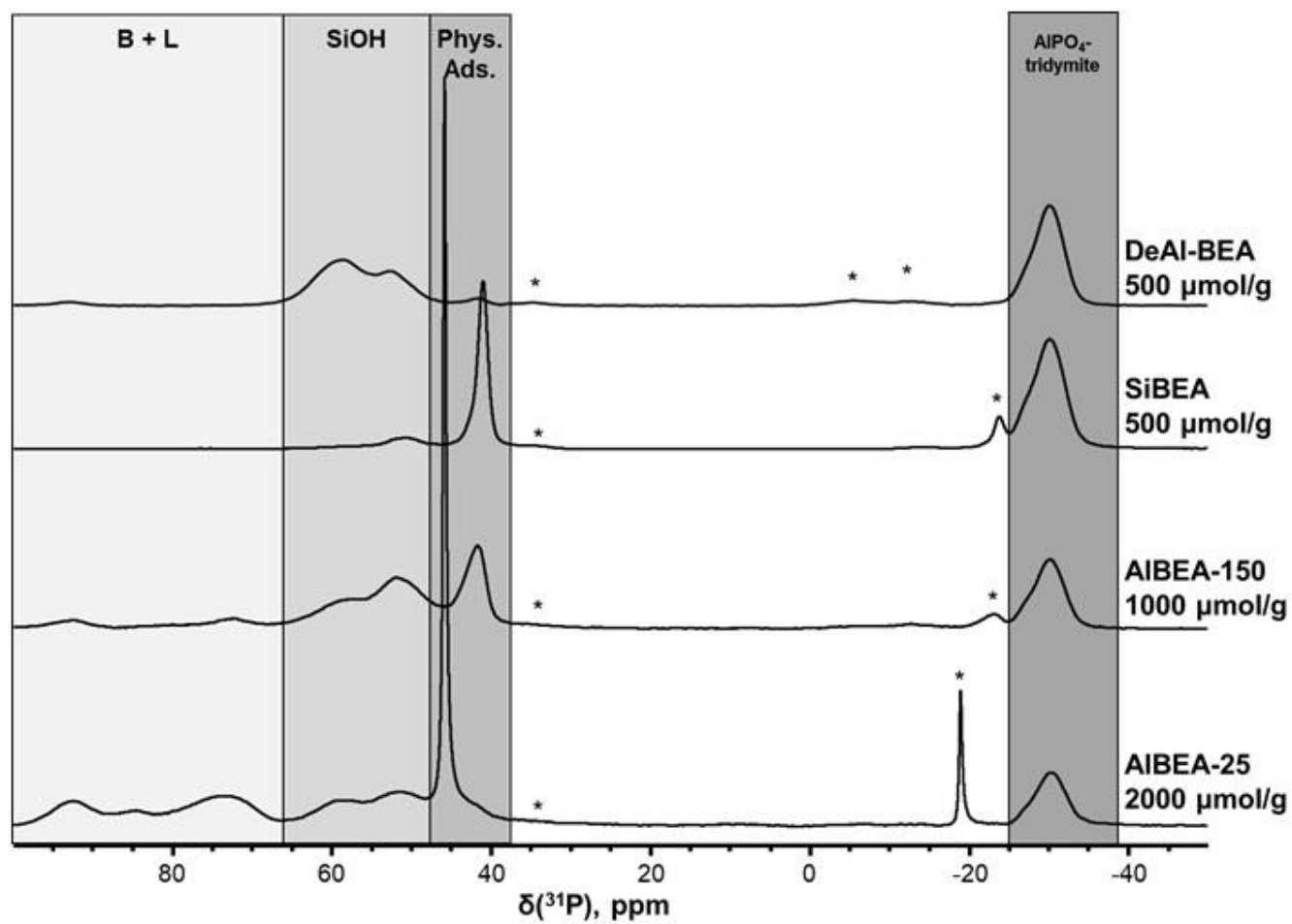


Image 2:

Quantitative data obtained from  $^{31}\text{P}$  MAS NMR spectra of adsorbed TBPO  
on different BEA zeolites

Sample	B + L, $\mu\text{mol/g}$	SiOH, $\mu\text{mol/g}$	Phys. Ads., $\mu\text{mol/g}$	Total adsorbed amount, $\mu\text{mol/g}$	FTIR Py, $\mu\text{mol/g}$	N(Al), $\mu\text{mol/g}$
SiBEA	0	150	350	500	0	0
DeAl-BEA	20	330	30	380	2	25
AIBEA-150	120	480	350	950	75	120
AIBEA-25	500	450	570	1520	425	600

**References:** [1] Zheng A., Deng F., Liu S. B. // Annual reports on NMR spectroscopy, 2020, 101, 65-149.

[2] Zhao Q., Chen W.-H., Huang S.-J., Wu Y.-C., Lee H.-K., Liu S.-B. // J. Phys. Chem. B, 2002, 106, 4462-4469.

**A Combined Quasi Elastic Neutron Scattering (QENS) and Molecular Dynamics (MD) Study of Diffusion of NH<sub>3</sub> in Zeolites**

M. Sarwar<sup>1,\*</sup>, A. O'Malley<sup>2</sup>, I. Silverwood<sup>3</sup>, I. Hitchcock<sup>1</sup>, J. Armstrong<sup>3</sup>, S. Hindocha<sup>1</sup>, A. York<sup>1</sup>, R. Catlow<sup>4</sup>, P. Collier<sup>1</sup>

<sup>1</sup>Clean Air Research, Johnson Matthey, Reading, <sup>2</sup>Chemistry, University of Bath, Bath, <sup>3</sup>ISIS, STFC, Oxfordshire,

<sup>4</sup>Chemistry, University College London, London, United Kingdom

**Abstract Text:** Zeolites are widely used as catalysts in a variety of reactions including the selective catalytic reduction of nitrous oxides which are a major component of diesel vehicle emissions. A number of studies recently have reported the high activity, stability and selectivity of Cu-SSZ-13 [1-4] which has the CHA framework topology. However, the nature of the active site and its location within the framework is subject to much debate in the literature. In addition, diffusion is a key step in the catalytic cycle within zeolites, as reactants must diffuse to the active site and the products formed diffuse out. An understanding of the nature and location of the active site within the framework, along with its accessibility will help guide the design of future catalysts with improved performance and efficiency.

In this presentation an overview of a combined theoretical and experimental approach to determine the ion location and accessibility of adsorbates such as NH<sub>3</sub> to the active site, will be presented. QM/MM calculations are used to assess the stability of the ion at different sites within the framework. The interaction of NO with the ion at each site is also modelled using the QM/MM approach to study how NO interacts with the ion and changes in ion geometry as a result. Vibrational frequencies are computed and compare well to values measured by DRIFTS.

Following on from this the accessibility of the active site is assessed using the diffusion of NH<sub>3</sub> in the CHA framework and LEV frameworks. Molecular Dynamics (MD) simulations have been widely used to study the diffusion of molecules within zeolites. There are a number of complimentary experimental techniques, such as Pulse Field Gradient (PFG)-NMR and Quasi Elastic Neutron Scattering (QENS) that can probe the same length and time-scales as MD simulations and therefore provide a direct comparison. Using both QENS and MD simulations, we investigate the effect of the Cu<sup>2+</sup> counter-ion on the diffusion of NH<sub>3</sub> by comparing to the brønsted acid form of the zeolite. We also investigate the effect of zeolite topology and dimensionality on diffusion properties by comparing diffusion of NH<sub>3</sub> in CHA(3D) and LEV(2D).

**References:** [1] Bull, I.; Xue, W. M.; Burk, P.; Boorse, R. S.; Jaglowski, W. M.; Kroemer, G. S.; Moini, A.; Patchett, J. A.; Dettling, J. C.; Caudle, M. T. Copper CHA Zeolite Catalysts. U.S. Patent 7 601 662 B2, 2009 to BASF.

[2] Kwak, J. H.; Varga, T.; Peden, H. F.; Gao, F.; Hanson, J.C; Szanyi, J., J. Catal. 2014, 314, 83–93.

[3]. Fickel, D.W.; Lobo, R.F; J Phys Chem C, 2010, 114, 1633 – 1640

[4] Beale A.M , Gao F, Lezcano-Gonzalez I, Peden C.H, Szanyi J, Chem Soc Rev, 2015, 44, 7371-7405

**Interpretation of  $^{27}\text{Al}$  MAS NMR results based on ab initio molecular dynamics: effects of temperature and water loading**

C. Lei<sup>1,\*</sup>, F. Brivio<sup>1</sup>, A. Erlebach<sup>1</sup>, P. Nachtigall<sup>1</sup>

<sup>1</sup>Department of Physical and Macromolecular Chemistry, Charles University, Praha 2, Czech Republic

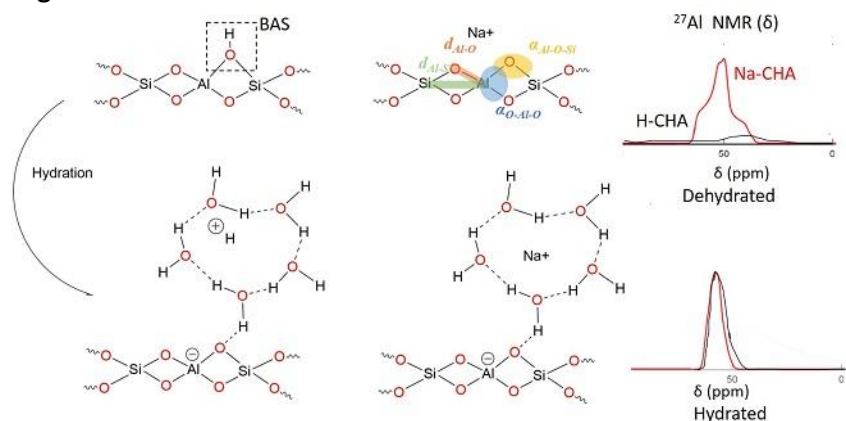
**Abstract Text:** Solid state NMR (ssNMR) is an important technique to the structural characterization of catalytic material zeolite with aluminum substitution. [1, 2] Together with computational modeling of NMR spectra it provides many details about the catalytic sites. [3, 4] Due to the cost of DFT ssNMR simulations, typically the interpretation of data relies only on the comparison with simple static models. Unfortunately, this approach neglects the material dynamic and overlooks some important aspects that can significantly affect the structure, such as the role of water, Si/Al ratio, temperature.

In this work we present a synergic method that includes *ab-initio* molecular dynamics(AIMD), DFT ssNMR simulations and machine learning analysis. In this way we aim to improve the interpretation of NMR spectra taking in account realistic conditions and to connect  $^{27}\text{Al}$  isotropic chemical shifts with geometrical descriptors.

Here we focused on how hydration, and the thermodynamic states affected the structure and NMR signals based on models of chabazite zeolite with counterions,  $\text{H}^+$  and  $\text{Na}^+$ . For each model, we generated a dataset of structures from thermodynamic ensembles obtained from AIMD trajectories. Consequently, for each structure in the dataset we calculated NMR tensors by using the GIPAW method. Once the dataset has been generated, we used machine learning to correlate the simulated-NMR response to the structural parameters.

We found that the  $^{27}\text{Al}$  isotropic chemical shifts can be easily described using a linear model that employs few structural descriptors of the local environment of Al. In light of this model, the theoretical chemical shift can be calculated bypassing the DFT-NMR calculations. Furthermore, the relation is general for all tetrahedrally coordinated Al in zeolites, which allows to scale up the size of system of interest if AIMD simulations are replaced with reliable classical simulations.

**Image 1:**



**References:**

- [1] J. Holzinger, P. Beato, L.F. Lundegaard, J. Skibsted, Distribution of Aluminum over the Tetrahedral Sites in ZSM-5 Zeolites and Their Evolution after Steam Treatment, *Journal of Physical Chemistry C*, 122 (2018) 15595-15613.
- [2] S.H. Li, F. Deng, Recent Advances of Solid-State NMR Studies on Zeolites, in: G.A. Webb (Ed.) *Annual Reports on Nmr Spectroscopy*, Vol 78/2013, pp. 1-54.
- [3] T. Helgaker, M. Jaszuński, K. Ruud, Ab Initio Methods for the Calculation of NMR Shielding and Indirect Spin-Spin Coupling Constants, *Chemical Reviews*, 99 (1999) 293-352.
- [4] G.N. Li, E.A. Pidko, The Nature and Catalytic Function of Cation Sites in Zeolites: a Computational Perspective, *Chemcatchem*, 11 (2019) 134-156.

**Probe-based MAS-NMR Characterization of Brønsted and Lewis acid sites in zeolite heterogeneous catalysts**

M. Carravetta<sup>1,\*</sup>, J. M. Le Brocq<sup>1</sup>, E. S. Goodier<sup>1</sup>, A. E. Oakley<sup>1</sup>, M. E. Potter<sup>1</sup>, M. E. Light<sup>1</sup>, R. Raja<sup>1</sup>, B. Vandegehucht<sup>2</sup>, M. Schreiber<sup>2</sup>

<sup>1</sup>Chemistry, University of Southampton, Southampton, United Kingdom, <sup>2</sup>Total Research & Technology, Total, Feluy, Belgium

**Abstract Text:**

We present an overview of methods for detecting acid sites in zeolites and AIPO-based frameworks by means of solid state NMR, and demonstrate them on a selected range of model systems: zeolite beta, mordenite, metal-doped AIPO-5, AIPO-34 and AIPO-37, with single metal substitution, including Mg, Sn, Si, Co, and Ni. Acid strength and nature (Brønsted and Lewis sites) in AIPOs can be tuned by careful choice metal substitution.

Moreover the choice of framework allows us to tune cavity size and accessibility, through the pore aperture and tortuosity offered by frameworks (see Figure 1).

NMR experiments will involve a comparison of a range of probes, including <sup>15</sup>N-pyridine, <sup>15</sup>N-acetonitrile, and <sup>15</sup>N-ammonia, trimethylphosphine and trimethylphosphine oxide. Isotopic enriched probe molecules will be used as appropriate to allow for effective signal detection without overloading the samples, as for the case of nitrogen-based probe molecule.

As an example, a selection of data obtained with two different probes is shown in Fig. 2. The possibility to study the acid catalyst-probe molecule interaction using the more abundant nitrogen isotope, nitrogen-14, will also be considered.

One-dimensional and two-dimensional NMR methods will be used as appropriate, in order to provide a clearer understanding of the acid sites where a superior resolution is required.

NMR data will be complemented by independent measurements performed with complementary techniques to fully characterise the materials, including XRD, BET and DRIFTS measurements.

The project leading to these findings was funded by TOTAL.

**Image 1:**

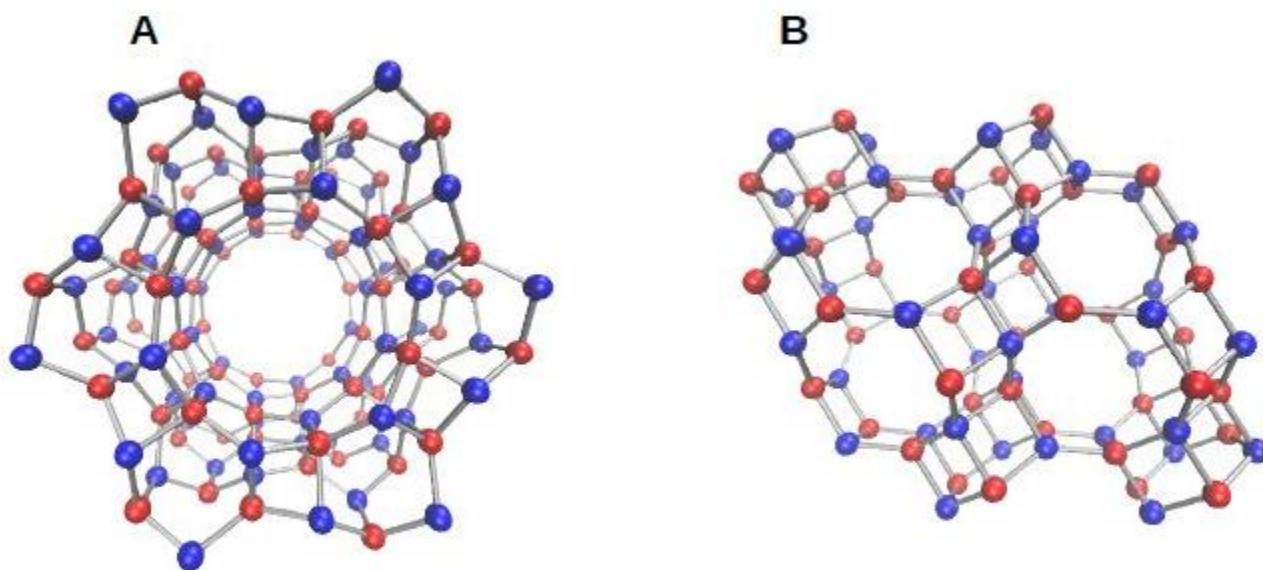


*Figure 1. (A) AIPO-5, 7.3 Å channel; (B) AIPO-34, 3.8 Å, cage.*

Image 2:

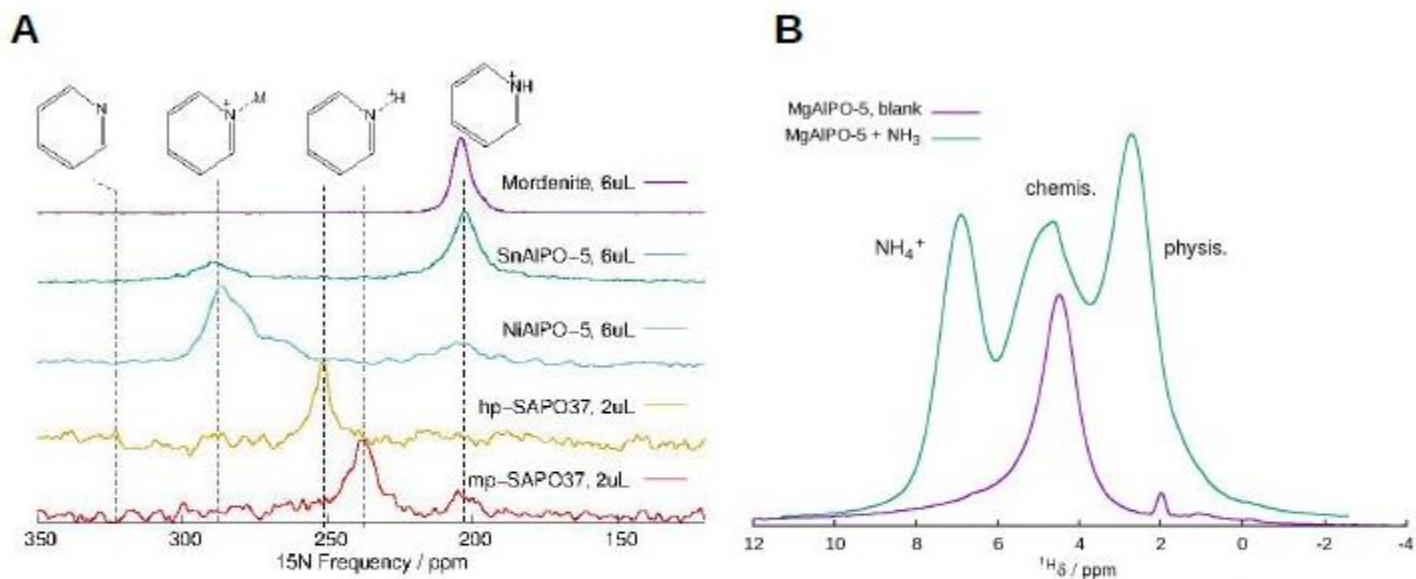


Figure 2: (A)  $^{15}\text{N}$  data obtained with cross polarization at 14.1 T and 13 kHz. Sample nature and dosing of  $^{15}\text{N}$ -pyridine are specified in the legend. A range of sites can be identified clearly for different compounds. (B)  $^1\text{H}$  NMR on MgAlPO-5 dosed with ammonia acquired at 20 T and 60 kHz, with peak assignment.

**A Kerr-gated Raman Probe into the Catalytic Fast Pyrolysis Reaction**

E. J. Campbell<sup>1,\*</sup>, I. Sazanovich<sup>2</sup>, M. Towrie<sup>2</sup>, A. Beale<sup>1</sup>, I. Lezcano-Gonzalez<sup>1</sup>, M. Watson<sup>3</sup>

<sup>1</sup>Chemistry, University College London, <sup>2</sup>ULTRA, Central Laser Facility, Science and Technology Facilities Council, Didcot, Oxfordshire, <sup>3</sup>Johnson Matthey, Johnson Matthey PLC, Billingham, United Kingdom

**Abstract Text:** Introduction

Raman Spectroscopy can be highly valuable to study catalytic mechanisms by revealing molecular vibrations that can identify important intermediate species. However, in many cases catalyst defects or emissive hydrocarbon species present cause intense fluorescence which saturates the detector, preventing collection of Raman signals (see Fig. 1). To avoid this, UV or near-IR probe wavelengths may help, though often at a compromise to sample damage or low scattering intensity, respectively [1]. This work uses a novel technique, employing a visible wavelength source (400 nm) with a Kerr-gated spectrometer that separates Raman signal from fluorescence due to their different lifetimes [2]. Using this unique technique, we have identified intermediate species in the reaction of furan and other oxygenated hydrocarbons over zeolite catalysts – as a model for the Catalytic Fast Pyrolysis reaction (CFP). Biomass transformation becomes increasingly important for the production of high value hydrocarbons from renewable resources, but the high oxygen content of raw bio-oils causes problems due to their acidity, instability and low heating values when compared with their crude oil counterparts [3]. In CFP, volatile vapours of biomass pyrolysis pass over the catalyst where they undergo decarbonylation, decarboxylation and dehydration processes, rejecting oxygenates and improving aromatic and olefinic yields. The current downfall of this reaction is the rapid catalyst deactivation caused by carbon laydown or “coke” making regeneration necessary [3]. Through studying the mechanism, we aim to understand the chemistry such that it can be manipulated to improve lifetime and therefore, process efficiency.

Results and Discussion

Fig. 2 illustrates some spectral changes throughout the experiment of H-ZSM-5 (Si/Al = 40). At low temperatures, furan oligomers form through reaction at zeolite acid sites. By increasing the temperature to 200 °C, oxygenates are detected by MS, whilst a growing band at 1542 cm<sup>-1</sup> indicates the evolution of a benzofuran intermediate [4] postulated to arise from the Diels-Alder coupling of two furan molecules [3]. With further increase in temperature this band grows and by 400 °C is consumed. At high temperature, growth at 1380 cm<sup>-1</sup> indicates that polyaromatic species formed [5]. Studies using alternative feeds such as acetic acid, acetaldehyde and dihydrofuran reveal dynamic chemistry.

The zeolite topologies studied (MFI, FER, FAU and BEA) impose spatial restrictions on the intermediates able to form which we have identified. Importantly at the end of each reaction - while faujasite, ferrierite and beta show D & G bands typical of coke, ZSM-5 exhibits distinct bands comparable to spectra obtained during reaction of ZSM-5 in the Methanol-to-Hydrocarbons reaction - supporting the idea that CFP proceeds via an analogous hydrocarbon pool mechanism [6].

Image 1:

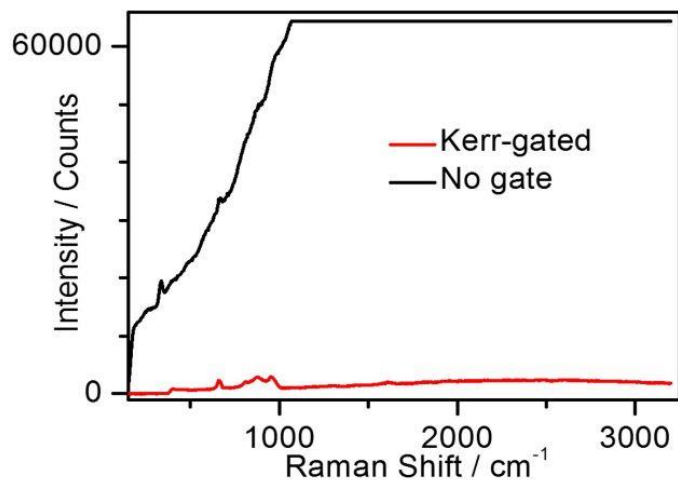
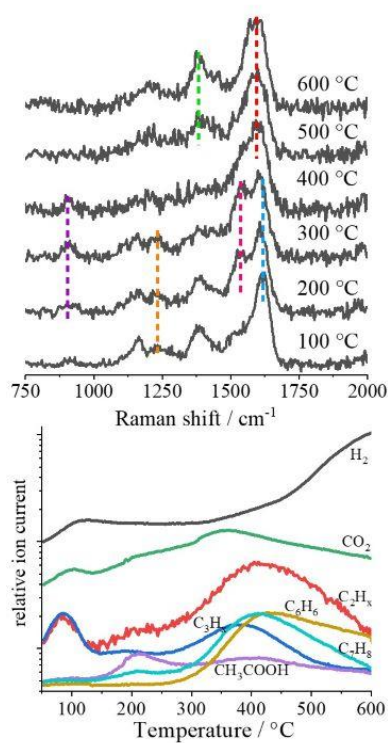


Image 2:



- References:**
1. P. C. Stair, *Advances in Catalysis*, vol. 51, pp. 75–98, Jan. 2007
  2. P. Matousek et al., *J. Raman Spectrosc.*, vol. 32, no. 12, pp. 983–988, Dec. 2001.
  3. C. Liu et al., *J. Phys. Chem. C*, vol. 119, no. 42, pp. 24025–24035, Oct. 2015.
  4. B. Singh, *Spectrochim. Acta A*, vol. 65, no. 5, pp. 1125–1130, Dec. 2006
  5. P. M. Allotta and P. C. Stair, *ACS Catal.*, vol. 2, no. 11, pp. 2424–2432, Nov. 2012
  6. C. Mukarakate et al., *Green Chem.*, vol. 17, no. 8, pp. 4217–4227, Aug. 2015

## Impact of spatial heterogeneity on diffusion in mesoporous $\gamma$ -alumina catalyst supports

A. Glowska<sup>1,2,\*</sup>, E. Jolimaître<sup>1</sup>, L. Catita<sup>1</sup>, M. Fleury<sup>3</sup>, T. Chevalier<sup>4</sup>, M.-O. Coppens<sup>2</sup>

<sup>1</sup>Physics & Analysis, IFPEN, SOLAIZE, France, <sup>2</sup>Centre for Nature Inspired Engineering (CNIE), University College London, London, United Kingdom, <sup>3</sup>Geoscience, <sup>4</sup>Physics & Analysis, IFPEN, Rueil-Malmaison, France

**Abstract Text:** Gamma-alumina ( $\gamma$ -Al<sub>2</sub>O<sub>3</sub>) is considered to be the most important transition alumina, due to its frequent use in the petroleum and automotive industries as a catalyst or catalyst support. Previous studies have revealed the high complexity of  $\gamma$ -alumina's spatial organization, which includes several aggregation levels of elementary boehmite nanoparticles, with a hierarchical pore network organization that ranges from the nanometer to the millimeter scale [1,2]. Furthermore, each organization level could be spatially heterogeneous and anisotropic [3]. All these pore network properties could have a profound impact on the kinetics of mass transfer in the catalyst. Therefore, their characterization is of great importance, and represents an opportunity to guide new catalyst designs and optimize catalytic processes. This work presents a multi-technique strategy to characterize  $\gamma$ -alumina, comprising of techniques that probe the geometry of the pore network (N<sub>2</sub> adsorption and mercury porosimetry) and the effective diffusivity of confined molecules at multiple scales by PFG (Pulsed-Field Gradient) NMR.

Two mesoporous  $\gamma$ -aluminas were synthesized, so as to produce a similar BET surface area, pore volume and pore size distribution (PSD), as determined by the NLDFT model applied to the N<sub>2</sub> isotherm adsorption branch, but different N<sub>2</sub> desorption isotherms, i.e. different pore blocking effects (Table 1 and Fig.1).

By comparing the results obtained from N<sub>2</sub> adsorption, Hg porosimetry and NMR cryoporometry with water, the effective PSD of each sample is evaluated and the percolation effects are highlighted. MEB pictures show that the samples are heterogeneous, i.e. contain grains of different density than that of the matrix. Diffusion in both aluminas was characterized by PFG-NMR experiments for a range of organic liquids (namely acetonitrile, n-heptane, and toluene, see Table 2) and tortuosity,  $\tau$ , was calculated from the ratio of the measured molecular diffusivity in the bulk and effective diffusivity in alumina, at a temperature of 32°C. As shown in Fig. 2, the same tortuosity values are obtained for molecules of different size and polarity, showing that liquid-surface interactions do not influence diffusion. Hence, the notably different  $\tau$  values obtained for the two supports ( $\tau = 2.8$  vs.  $\tau = 2.0$ , a 40% difference) are directly related to the distinct multi-level organization of their pore networks, as suggested by the difference in *apparent* PSD, obtained from the N<sub>2</sub> isotherm desorption branch.

The impact of the pore network organization on tortuosity will be discussed in detail and a global characterization strategy, applicable to any mesoporous solid, will be proposed.

Image 1:

TABLE 1. TEXTURAL PROPERTIES OF GAMMA-ALUMINA SUPPORTS			
ALUMINA SUPPORT	$S_{\text{BET}}$ [ $\text{m}^2/\text{g}$ ]	$V_p$ [ $\text{cm}^3/\text{g}$ ]	$\epsilon_p$
A	292	0.82	0.74
B	299	0.86	0.71

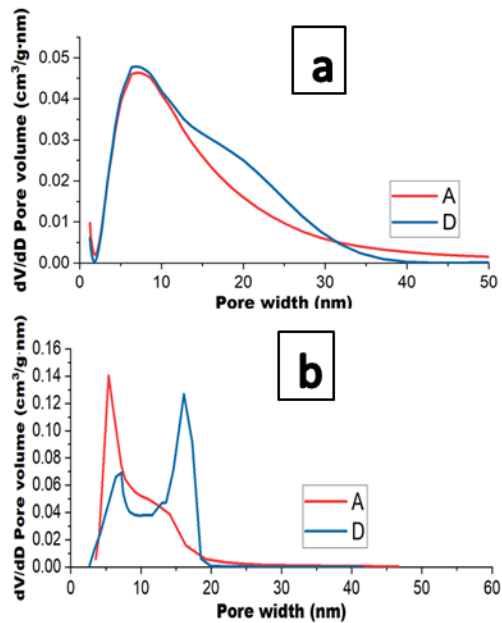


Figure 1. PSD estimated from  $\text{N}_2$  isotherms by the a) NLDFT model for slit pores from the adsorption branch, and b) BJH method from the desorption branch

Image 2:

TABLE 2. SIZES AND DIPOLE MOMENTS OF STUDIED MOLECULES		
ORGANIC MOLECULE	MOLECULAR RADIUS* [Å]	DIPOLE MOMENT [D]
Acetonitrile	2.76	3.92
Toluene	3.49	0.36
n-Heptane	3.89	0

\*Assumption of spherical molecular shape

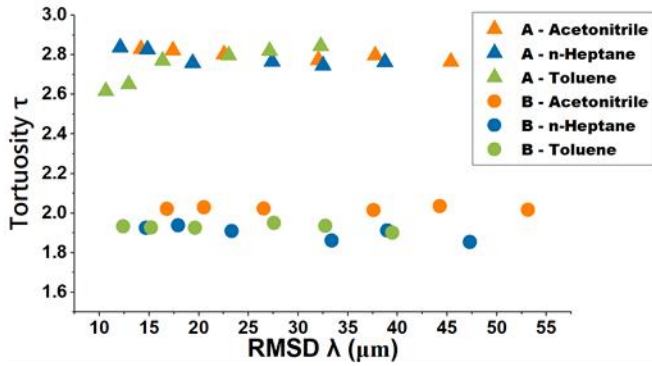


Figure 2. Tortuosity values obtained with different molecular tracers as a function of the RMSD ( $\lambda$ )

#### References:

1. Chiche, D., Digne, M., Revel, R., Chaneac, C., and Jolivet, J.P., J. Phys. Chem. C 112, 8524–8533 (2008)
2. Forman, E.M., Trujillo, M.A., Ziegler, K.J., Bradley, S.A., Wang, H., Prabhakar, S., and Vasenkov, S., Micropor. Mesopor. Mat. 229, 117–123 (2016)
3. Mange, F., Fauchadour, D., Barré, L., Normand, L., and Rouleau, L., Colloids and Surfaces A: Physicochemical and Engineering Aspects 155, 199–210 (1999)

**Understanding the deactivation mechanism in zeolites via a combination of theoretical and experimental operando Raman spectroscopy**

A. E. J. Hoffman<sup>1,\*</sup>, I. Lezcano-Gonzalez<sup>2</sup>, E. Campbell<sup>2</sup>, M. Bocus<sup>1</sup>, I. Sazanovich<sup>3</sup>, M. Towrie<sup>3</sup>, A. Beale<sup>2</sup>, V. Van Speybroeck<sup>1</sup>

<sup>1</sup>Center for Molecular Modeling, Ghent University, Zwijnaarde, Belgium, <sup>2</sup>Chemistry, University College London, <sup>3</sup>ULTRA, Central Laser Facility. STFC, Didcot, United Kingdom

**Abstract Text:** The methanol-to-olefin (MTO) process over acidic zeolites has attracted a lot of interest the last decades, both from academia and industry, as it forms a sustainable alternative to crude oil for the generation of hydrocarbons required for polymer production [1]. To date, there is consensus about the necessity of hydrocarbon pool species to act as co-catalysts for the conversion [1,2]. Nevertheless, the uncertainty on the actual catalytic cycles leading to olefin production remains. Insight in the evolution of hydrocarbon species during the MTO conversion is vital to be able to optimize the reaction process. This optimization is necessary, not only to tune the conditions towards desired products [2,3], but also to reduce the deactivation of the catalyst [4]. The build-up of spacious hydrocarbons during the conversion of methanol decreases the efficiency as they block the zeolite pores. Therefore, fully understanding the deactivation mechanism enables the development of performant MTO catalysts. To characterize the MTO process during operating conditions, multiple spectroscopic techniques have been developed. An attractive method to track the evolution of hydrocarbon species is Raman spectroscopy, as the resulting vibrational fingerprints are unique for each structure [5]. An important consideration in Raman measurements is the wavelength of the excitation source, which may result in a too weak signal (infrared) or a degraded sample (ultraviolet). Ideally, a visible excitation source can be applied, but this may result in fluorescence of the sample. However, to get rid of the fluorescence background a Kerr-gate spectrometer can be used [6]. The use of operando Kerr-gated Raman spectroscopy has now lead to the generation of high-quality spectra during the MTO process [7]. Although detailed experimental Raman spectra could be measured under operating conditions, the interpretation of the different fingerprints remains cumbersome due to the complexity of the reactions. In that regard, theoretical simulations are indispensable as they can make a distinction between the vibrational fingerprints of different hydrocarbons. The advance in computer power and methodological developments [8] have enabled the calculation of Raman spectra of complex nanoporous systems at experimental conditions [9]. We have developed a general theoretical procedure, based on ab initio molecular dynamics calculations, that allowed to identify the reaction intermediates present at all stages of the MTO process in SSZ-13 zeolite [7]. Our results pointed out that methanol conversion dropped once linear polyenes entered the scene, because their limited mobility inside the chabazite cages blocked the pores and deactivated the catalyst. Branched polyenes have not been observed as we found them to undergo immediate cyclization, which eventually led to polyaromatic species. This refutes earlier assumptions that deactivation was initiated by the latter.

**References:** [1] Yarulina, I., Chowdhury, A. D., Meirer, F., Weckhuysen, B. M. & Gascon, J. Recent trends and fundamental insights in the methanol-to-hydrocarbons process. *Nat. Catal.* 1, 398–411 (2018).

[2] Olsbye, U., Svelle, S., Bjørgen M., Beato, P., Janssens, T. V. W., Joensen, F., Bordiga, S. & Lillerud, K. P. Conversion of Methanol to Hydrocarbons: How Zeolite Cavity and Pore Size Controls Product Selectivity. *Angew. Chemie Int. Ed.* 51, 5810–5831 (2012).

[3] Yarulina, I., De Wispelaere, K., Bailleul, S., Goetze, J., Radersma, M., Abou-Hamad, E., Vollmer, I., Goesten, M., Mezari, B., Hensen, E. J. M., Martínez-Espín, J. S., Morten, M., Mitchell, S., Perez-Ramirez, J., Olsbye, U., Weckhuysen, B. M., Van Speybroeck, V. Kapteijn, F. & Gascon, J. Structure–performance descriptors and the role of Lewis acidity in the methanol-to-propylene process. *Nat. Chem.* 10, 804–812 (2018).

[4] Olsbye, U., Svelle, S., Lillerud, K. P., Wei, Z. H., Chen, Y. Y., Li, J. F., Wang, J. G. & Fan, W. B. The formation and degradation of active species during methanol conversion over protonated zeotype catalysts. *Chem. Soc. Rev.* 44, 7155–7176 (2015).

- [5] Signorile, M., Rojo-Gama, D., Bonino, F., Beato, P., Svelle, S. & Bordiga, S. Topology-dependent hydrocarbon transformations in the methanol-to-hydrocarbons reaction studied by operando UV-Raman spectroscopy. *Phys. Chem. Chem. Phys.* 20, 26580–26590 (2018).
- [6] Stanley, A., Parker, A. W., Towrie, M. & Matousek, P. Efficient Rejection of Fluorescence from Raman Spectra Using Picosecond Kerr Gating. *Appl. Spectrosc.* 53, 1485–1489 (1999).
- [7] Lezcano-Gonzalez, I., Campbell, E., Hoffman, A. E. J., Bocus, M., Sazanovich, I. V., Towrie, M., Agote-Aran, M., Gibson, E. K., Greenaway, A., De Wispelaere, K., Van Speybroeck, V. & Beale, A. M. Insight into the effects of confined hydrocarbon species on the lifetime of methanol conversion catalysts. *Nat. Mater.* 19, 1081–1087 (2020).
- [8] Thomas, M., Brehm, M., Fligg, R., Vöhringer, P. & Kirchner, B. Computing vibrational spectra from ab initio molecular dynamics. *Phys. Chem. Chem. Phys.* 15, 6608 (2013).
- [9] Hoffman, A. E. J., Vanduyfhuys, L., Nevjestic, I. Wieme, J., Rogge, S. M. J., Depauw, H., Van Der Voort, P., Vrielinck, H. & Van Speybroeck, V. Elucidating the vibrational fingerprint of the flexible metal-organic framework MIL-53(Al) using a combined experimental/computational approach. *J. Phys. Chem. C* 122, 2734 (2018).

**Electron crystallography methods for structure determination of low dimensional zeolitic materials**

T. Willhammar<sup>1,\*</sup>

<sup>1</sup>Department of Materials and Environmental Chemistry, Stockholm University, Stockholm, Sweden

**Abstract Text:** Two-dimensional (2D) zeolitic materials have the advantage of an enhanced access to catalytically active sites and shortened diffusion length in comparison with three-dimensional (3D) framework structures. The two dimensionality of the layered materials however imposes difficulties for the purposes of structure determination. Over the last decade methods for three-dimensional electron diffraction (3D ED) have opened up a more straightforward route for structure determination from sub-micrometer sized crystals.<sup>1</sup> Using the 3D ED methods the small crystals can now be considered to be single-crystals. Layered materials however still remain a challenge. Since they lack periodicity in one dimension, no periodic 3D reciprocal lattice is available. For these materials imaging methods are of utmost importance in order to retrieve structural information.

Recent developments of modern electron microscopes are now enabling several opportunities for real-space examination of porous solids. The aberration-correction makes it possible to obtain scanning transmission electron microscopy (STEM) images with sub atomic resolution. The recently developed integrated differential phase contrast (iDPC) technique opens up for imaging with electron beam doses an order of magnitude lower than before.

One example of an intrinsically layered material was found as an intermediate in the synthesis of EU-12.<sup>2</sup> The phase was first identified from powder X-ray diffraction and denoted as PST-9. Evaluation of the morphology TEM imaging revealed a layered morphology of PST-9, which later transformed to a 3D crystal of EU-12. 3D ED methods showed that the material indeed lacked a structural integrity in one dimension. Interestingly the curly PST-9 sheets showed to flatten out prior to the transformation to EU-12, which seems to occur in a folding manner. The structure of PST-9 however remained elusive. Using aberration-corrected STEM imaging images of single sheets, with a thickness of <2 nm, could be observed with atomic resolution. Based on the STEM images and the periodicities revealed by the 3D ED data it was possible to build a model for the structure of the layered PST-9. PST-9 is one example of a material where STEM imaging is a crucial technique for characterization of porous materials, providing information from the meso-scale all the way to the atomic level.

Image 1:

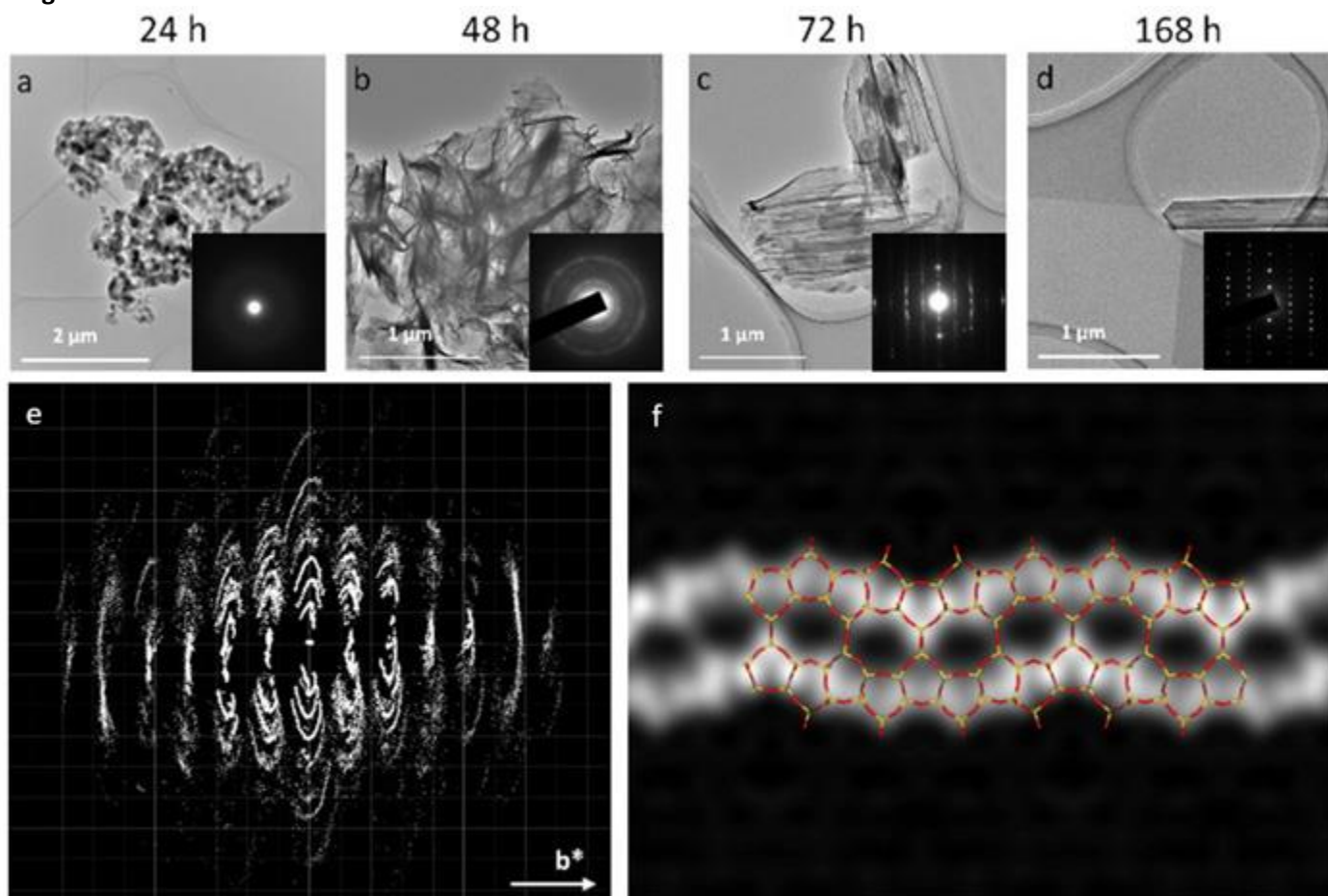


**Figure 1.** (a-d) The evolution of the synthesis from (a) amorphous over (b) the curly layers of PST-9 and (c) the folding intermediate to (d) the final 3D crystals of EU-12. The atomic scale ordering can be monitored in the electron diffraction patterns as insets. (e) 3D ED data from the folding intermediate shows a well-defined ordering in one dimension a lack of the same in the remaining two. (f) Average potential map constructed from a STEM image of a single layer of PST-9 reveals the atomic structure of the material.

**References:** 1 Transmission electron microscopy as an important tool for characterization of zeolite structures W Wan, J Su, XD Zou, T Willhammar *Inorganic Chemistry Frontiers* 2018, 5, 2836-2855, DOI: 10.1039/C8QI00806J  
2 Phase Transformation Behavior of a Two-Dimensional Zeolite J Bae, M O Cichocka, Y Zhang, Z Bacsik, S Bals, XD Zou, T Willhammar, and S B Hong *Angew. Chem. Int. Ed.* 2019, 131, 10336–10341, DOI: 10.1002/anie.201904825

**Capability of Flow MAS NMR for In Situ and In Operando Detection of Carbon Dioxide Capture- and Hydrogenation Processes by Nanoporous Solids**

M. Wenzel<sup>1,\*</sup>, J. Matysik<sup>1</sup>, R. Gläser<sup>2</sup>, M. Dvoyashkin<sup>2</sup>

<sup>1</sup>Institute of Analytical Chemistry, <sup>2</sup>Institute of Chemical Technology, Universität Leipzig, Leipzig, Germany

**Abstract Text: Capability of Flow MAS NMR for In Situ and In Operando Detection of Carbon Dioxide Capture- and Hydrogenation Processes by Nanoporous Solids**

*M. Wenzel<sup>1</sup>, J. Matysik<sup>1</sup>, R. Gläser<sup>2</sup>, M. Dvoyashkin<sup>2</sup>*

*<sup>1</sup>Institute of Analytical Chemistry, Universität Leipzig, 04103 Leipzig, Germany*

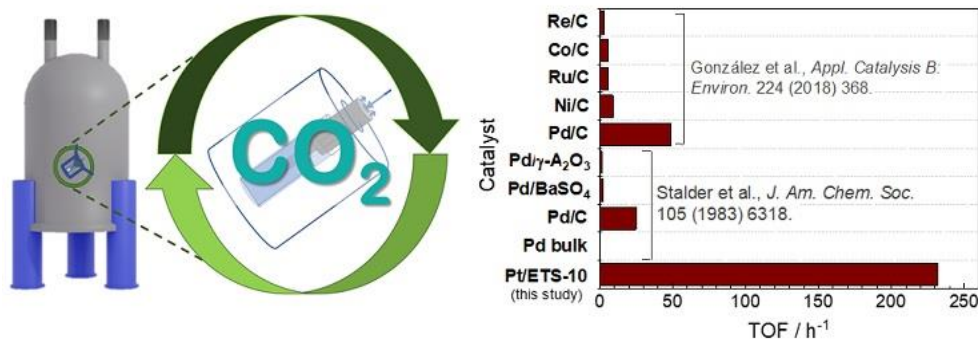
*<sup>2</sup>Institute of Chemical Technology, Universität Leipzig, 04103 Leipzig, Germany*

The depletion of fossil fuels and implications of a climate change resulting from their consumption stimulates society to implement sustainable solutions for the energy conversion, storage, and its efficient utilization. In this context, it is expected that renewable energies in combination with chemical energy conversion will play a crucial role in future energy scenarios.

One of the promising possibilities for conversion of the electrical energy into valuable chemicals is the heterogeneously-catalyzed CO<sub>2</sub>-hydrogenation reaction. It may result in production of chemicals, such as methanol or formic acid, depending on the type of catalyst used and reaction conditions. At that, one of reaction components that being consumed is CO<sub>2</sub> – a potent greenhouse gas contributing to the climate change.

In the present contribution, we report a successful application of continuous-flow magic angle spinning NMR for in situ and in operando observation of CO<sub>2</sub> -capture and -conversion by and over the nanoporous solids [1]. As case studies, we focused on the processes of CO<sub>2</sub>-sorption into the amine-functionalized silicas and its conversion over the Pt-containing titanosilicate catalyst Pt/ETS-10 [2]. The obtained results show that the CO<sub>2</sub> is stored on the surface of silica in the form of carbamate. In case of Pt-/ETS-10 catalyst, the CO<sub>2</sub> converts to formates as the product in the hydrogenation reaction with H<sub>2</sub>. In addition, it was possible to quantify the amount of product formed under the steady state conditions and calculate the turnover frequency (see figure) following the calibration procedure according to the quantitative NMR approach.

**Image 1:**



**References:** [1] M. Wenzel, M.A. Zaheer, D. Issayeva, D. Poppitz, J. Matysik, R. Gläser, and M. Dvoyashkin, *J. Phys. Chem. C* (under review).

[2] M. A. Zaheer, D. Poppitz, K. Feyzullayeva, M. Wenzel, J. Matysik, R. Ljupkovic, A. Zarubica, A. Karavaev, A. Pöpl, R. Gläser, and M. Dvoyashkin, *Beilstein J. Nanotechnol.* 10 (2019) 2039–2061.

**Investigating the nature of zeolites in an aqueous environment**

B. L. Griffiths<sup>1,\*</sup>, S. E. Ashbrook<sup>1</sup>

<sup>1</sup>School of Chemistry, EaStCHEM and Centre of Magnetic Resonance, University of St Andrews, St Andrews KY16 9ST, United Kingdom

**Abstract Text:**

Zeolites are a classification of microporous material known for their applications under conditions of high temperatures and low water-vapour. There has however been increasing incentive to understand the application of zeolites at milder, aqueous conditions, such as biomass conversion and low temperature catalysis.<sup>[1]</sup> Recent investigations into how zeolites behaved under such conditions using NMR spectroscopy found that the frameworks of a number of zeolites were dynamic and labile.<sup>[2]</sup> Investigations into the effect of aqueous conditions on the frameworks and establishing the mechanism(s) of bond breakage and reformation will help drive forward establishing new and exciting applications for zeolites.

The primary method of investigation has utilised adding <sup>17</sup>OH<sub>2(l)</sub> to the zeolite in question to generate a slurry, allowing us to follow isotopic exchange into the zeolite framework and to use <sup>17</sup>O NMR spectroscopy to investigate the dynamic nature of bonds. <sup>27</sup>Al and <sup>29</sup>Si NMR spectroscopy has also been utilised to attempt to fully understand the frameworks both before, during and after enrichment. The topologies that have been focused on are the Chabazite (CHA) and Mordenite (MOR) with varying distributions of Al, while different forms of the zeolites (e.g., H-, Na-) have also been considered.<sup>[1][2]</sup>

**References:**

1. C. J. Heard, L. Grajciar, C. M. Rice, S. M. Pugh, P. Nachtigall, S. E. Ashbrook and R. E. Morri, *Nat. Commun.*, 2019, 10, 4690
2. S. M. Pugh, P. A. Wright, D. J. Law, N. Thompson and S. E. Ashbrook, *J. Am. Chem. Soc.*, 2019 in press

**Direct probing of binuclear transition metal ion sites in FER by Zn<sup>2+</sup> laser-induced emission spectroscopy**

J. E. Olszówka\*, P. Kubat<sup>1</sup>, J. Dedecek<sup>2</sup>

<sup>1</sup>Department of Spectroscopy, <sup>2</sup>Department of Structure and Dynamics in Catalysis, J. Heyrovský Institute of Physical Chemistry Czech Academy of Sciences, Prague, Czech Republic

**Abstract Text:**

**Introduction**

Extending the knowledge about the nature of active sites is of key importance for understanding, predicting and even designing properties of catalytic materials in order to maximize their potential performance. Recently it was shown that binuclear transition metal ion (Fe, Co, Mn, Ni) species stabilized in the ferrierite (FER) matrix exhibit unique properties. They are able to facilitate N<sub>2</sub>O decomposition and, moreover, they can cooperate in decomposition of molecular oxygen and subsequent formation of highly active oxygen, used subsequently for methane oxidation [1,2]. However, although the unique activity of such binuclear sites was well documented, they were up to now evidenced only indirectly due to the long distance of the M(II) ions in these sites which is ca. 7 Å. Nevertheless, as shown for Cu-containing zeolites [4,5], emission spectroscopy of the luminescent transition metal ions introduced into the cationic sites in zeolites stands for an excellent tool to gather information on the vicinity of transition metal ions. In this work, quenching of the luminescent Zn<sup>2+</sup> cations was employed to monitor their proximity with Co<sup>2+</sup> cations.

**Materials & Methods**

A series of Zn and Zn/Co-containing samples was prepared from FER Si/Al 8.5 by ionic exchange and by impregnation method using aqueous solutions of zinc and cobalt nitrates and/or acetate. XRF, UV-Vis, FTIR and Zn(II) emission spectroscopies were used for characterization of the samples. Recorded spectra were collected after evacuation at 450 °C for 3h. Zn(II) time resolved luminescence spectra were measured using excitation by excimer laser (wavelength 308 nm, pulse width 28 ns, pulse energy ~ 100 mJ). A long pass filter (> 330 nm) was situated between cell and the monochromator.

**Results & Discussion**

Emission spectra of Zn and Zn/Co-containing zeolites revealed that the presence of divalent cobalt ions in the extraframework cationic sites result in enhanced quenching of the intrinsic Zn<sup>2+</sup> cations photoluminescence. The strongest interaction was observed for the sample in which the ratio between Zn/Co was closest to 1. The effect clearly evidences the proximity of the introduced transition metal ions, and represents the first direct experimental evidence of the formation of binuclear transition metal ion active site in silicon rich zeolites.

**References:**

1. Solomon, E. I. et al., Nature, 536 (2016) 317-321
2. Tabor, E. et al., Commun. Chem., 2 (2019)
3. Strome. D. H. and Klier, K, J. Phys. Chem., 84 (1980) 981
4. Wichterlova, B. et al., J. Catal., 169 (1997) 194

**Application of IR spectroscopy of substituted pyridines for the determination of acid sites accessibility in micro-mesoporous materials obtained by MWW zeolite recrystallization**

A. V. Shkuropatov<sup>1,\*</sup>, A. G. Popov<sup>1</sup>, I. V. Dobryakova<sup>1</sup>, I. I. Ivanova<sup>1</sup>

<sup>1</sup>Chemistry, Lomonosov Moscow State University, Moscow, Russian Federation

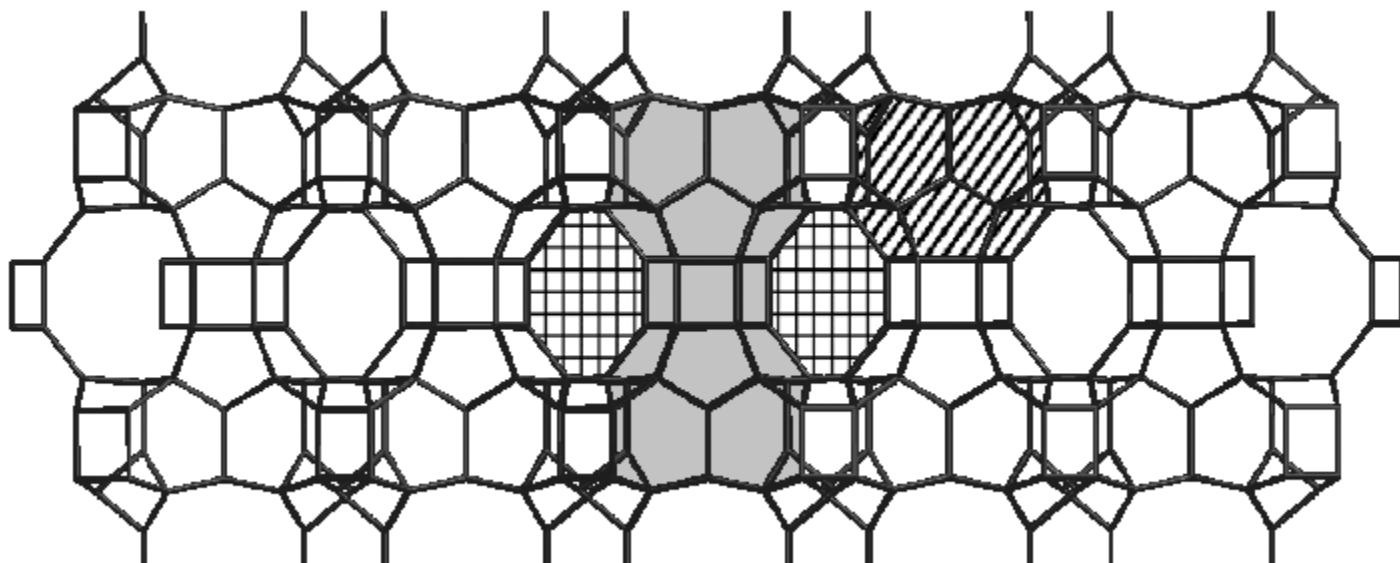
**Abstract Text:** The development of efficient zeolite catalysts requires thorough investigation of their acid properties. Infrared spectroscopy of adsorbed probe molecules is one of most utilized methods for studying acid sites of solid catalysts. Amongst convenient probe molecules pyridine is the most used one, however bulky pyridines are more compatible for characterization of acid sites on the outer surface. In this work, we consider the selection of a probe molecule for studying catalytically active sites of zeolites with MWW structure in the alkylation of benzene with propylene. Zeolite agglomerates are spherical beads formed by layered flat zeolite crystals, which consist of primary nanoplates of MWW structure having two independent pore systems. The first system passes in the plane of the plate and is limited to 10-membered rings (checkered area on the picture), the second has the form of an hourglass, which are perpendicular to the plane of the crystal, and has access to the surface of the crystal through 12-membered rings (grey area). According to published data [1], benzene alkylation with propylene proceeds at the Brønsted acid centers located in "cups" with 12-membered rings (striped area).

Recrystallization of MWW zeolite was carried out in a solution of alkali and CTAB, followed by pH adjustment with hydrochloric acid [2]. As a result of recrystallization, a partial destruction of the crystals occurred, followed by the formation of the mesoporous material MCM-41 on the surface of the modified zeolite. Infrared spectra were recorded on a Nicolet Protégé 460 FTIR spectrometer equipped with vacuum line applicable for heating the samples and adsorption of probe molecules. Pyridine, 2,6-ditertbutylpyridine, 2,3,6-trimethylpyridine, 2,6-dipropylpyridine, 2,4,6-trimethylpyridine were used as probe molecules. Porous characteristics of MWW zeolites were studied by low-temperature nitrogen adsorption. Alkylation of benzene with propylene was carried out in an automated catalytic unit with a flow-type reactor made of stainless steel. Analysis of the reaction products was carried out by gas chromatography.

Post-processing in an alkaline medium leads to the destruction of the spherical agglomerates, which should cause an increase in surface area. Nevertheless, according to low-temperature nitrogen adsorption data, recrystallization does not affect the specific surface area (calculated from BET), since mesopores are formed due to partial destruction of micropores. At the same time, the availability of acid sites for bulky probe molecules did not change, as evidenced by the preservation of the peak area of the vibrations of the Al-O(H)-Si group after the adsorption of 2,4,6-trimethylpyridine. Post-synthetic modification led to an increase in the catalytic activity of MWW in the reaction of benzene alkylation with propylene. This effect can be caused by an increase in the diffusion rate in crystalline zeolite agglomerates. The results show, the accessibility of acid sites on the outer surface changes depending on the size of substituted pyridines, which indicates that the most voluminous pyridine homologues do not fit in the "cups" of MWW zeolite. An important part of the work was the selection of a probe molecule for which acid sites in the "cups" are accessible, but acid sites that are not active in the alkylation of benzene with propylene are inaccessible. Based on the data obtained, a technique for determining the concentration of catalytically active sites in the alkylation of benzene with propylene by infrared spectroscopy of adsorbed probe molecules has been developed.

The authors gratefully acknowledge Russian Science Foundation (project № 19-73-10160) for the financial support.

Image 1:



**References:** [1] Corma, A., V. Martinez-Soria, and E. Schnoefeld. "Alkylation of benzene with short-chain olefins over MCM-22 zeolite: catalytic behaviour and kinetic mechanism." *Journal of catalysis* 192.1 (2000): 163-173.  
[2] Knyazeva, E. E., et al. "Synthesis and Physicochemical Properties of Hierarchical MWW Zeolites." *Russian Journal of Physical Chemistry A* 93.10 (2019): 1939-1945.

## **Biomedical Applications**

FEZA21-PO-039

### **UV filters Encapsulation in Zeolites**

R. Fantini<sup>1,\*</sup>, M. G. Vezzalini<sup>1</sup>, A. Zambon<sup>1</sup>, E. Ferrari<sup>1</sup>, F. Di Renzo<sup>2</sup>, M. Fabbiani<sup>2</sup>, R. Arletti<sup>1</sup>

<sup>1</sup>Department of Chemical and Geological Sciences, University of Modena and Reggio Emilia, Modena, Italy, <sup>2</sup>ICGM, ENSCM, CNRS, Université de Montpellier, Montpellier, France

**Abstract Text:** The number of annually diagnosed skin cancers is growing year after year, including both malignant melanoma (MM) and non-melanoma skin cancer (NMSC). Unprotected solar, and hence UV, exposure is the main recognized cause of skin carcinogenesis, and the general UV irradiance rise leads to growing health concerns.

Sunscreen products, and organic and inorganic UV filters (UVf), have become ubiquitous in personal-care products, packaging, plastics, dyes, and many other sectors. Unfortunately, organic UVfs have some stability and efficacy issues under UV exposure, whatever they are combined or not with inorganic UVfs. Concerning cosmetics, different UVfs and co-formulants are often combined to enhance the stability and efficacy of sunscreens, but photochemically incompatible ingredients must be avoided. Thus, it is important to find stable, safe, and broad-spectrum UV absorbers, that must be safe for human health.

In this work, we realized hybrid UV filters by the encapsulation of organic filters into zeolites, up to now marginally investigated by previous studies [1-3]. UV filters octinoxate (OMC) and avobenzone (AVO) were separately encapsulated into zeolites with different chemistry and framework type LTL, MOR, FAU, and MFI. The hybrids UV filters (hereafter ZEOfilters) are expected to overcome traditional UV filters issues thanks to their improved stability.

We carried out the optimization of the loading procedure for UV filters encapsulation and a deep ZEOfilters characterization, including UV filtering properties. Finally, as a proof of concept, ZEOfilters were formulated into a simple cosmetic formulation.

All loadings were performed with exceeding UV filter, and different washing techniques were tested to optimize the filter removal from ZEOfilters grain surface. TGA measurements were performed on pristine zeolites, pure UV filters, and ZEOfilters. The results on the hybrids indicate the incorporation of the filters in zeolite porosities and the observed losses are in good agreement with elemental analysis results.

To assess the UV absorption properties, UV-Vis spectra were collected on pristine zeolites, bare UVfs, and ZEOfilters. As demonstrated in Images 1-2, some ZEOfilters exhibit an enhanced UV absorbance also compared to pristine UV filters. Some of the realized ZEOfilters display a decrease of visible light transmittance, probably due to zeolite particle scattering, indicating that the zeolite particle size must be optimized. Overall, the encapsulation of UV filters resulted in an enhanced UV filtering capacity for cationic ZEOfilters, whereas, high silica ZEOfilters seem less effective but still able to absorb UV radiation.

The observed enhancement of UV filtering power is of paramount importance for the future development and exploitation of ZEOfilters. Indeed, a more effective UV filtering can be the key to reduce the amount of UVfs, stabilizers, and co-formulants employed in cosmetic formulations.

**Image 1-2.** UV-Vis spectra of ZEOfilters in vaseline: LTL, FAU-13X, High Silica-FAU, High Silica-MOR with OMC (1) and LTL, FAU-13X, High Silica-MOR with AVO (2). Spectra of free UV filters in vaseline are also shown.

**Image 1:**

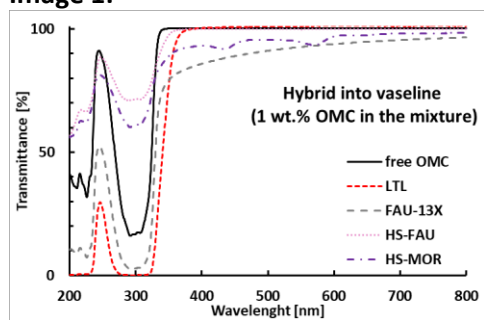
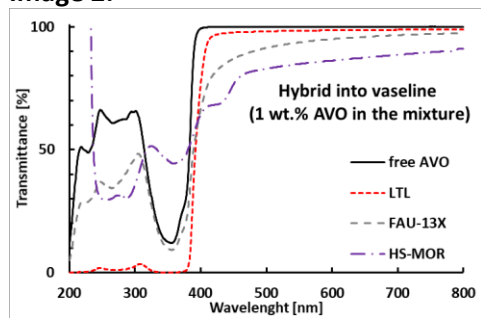


**Image 2:**



**References:**

- [1] Chretien M.N. Pure Appl. Chem. 2007, 79, 1.
- [2] Chretien M.N., Heafey E., Scaiano J.C. Photochem. Photobiol. 2010, 86, 153.
- [3] Chretien M.N., Migahed L., Scaiano J.C. Photochem. Photobiol., 2006, 82, 1606.

**Tuning the properties of nanosized faujasite zeolites for optimal delivery of O<sub>2</sub> and CO<sub>2</sub>**

A. Daouli<sup>1,2,\*</sup>, S. Komaty<sup>3</sup>, M. Badawi<sup>1</sup>, A. Hasnaoui<sup>2</sup>, C. Anfray<sup>4</sup>, M. Zaarour<sup>3</sup>, O. Touzani<sup>4</sup>, S. Valable<sup>4</sup>, S. Mintova<sup>3</sup>

<sup>1</sup>Laboratory of Theoretical Physics and Chemistry UMR 7019 CNRS, University of Lorraine, Nancy, France, <sup>2</sup>Research Laboratory in Materials Science, Mathematics and Modeling (LS3M), University of Sultan Moulay Slimane, Khouribga, Morocco, <sup>3</sup>UNICAEN, CNRS, ENSICAEN, Catalysis and Spectrochemistry Laboratory (LCS), Normandie Univ, Caen, France, <sup>4</sup>UNICAEN, CEA, CNRS, ISTCT/CERVOxy group, GIP Cyceon, Normandie Univ, Caen, France

**Abstract Text:**

Nanozeolites offer tunable priorities including crystal size and morphology, large external surface area, fast diffusion and high thermal stability, which open the possibility of using them in advanced applications (1,2). In the present work, we report on the preparation of customized nanozeolites for delivering oxygen and carbon dioxide under hypoxia conditions to improve the effectiveness of the conventional treatment of glioblastoma. The sorption properties of nanosized zeolite with faujasite type structure throughout an ionic exchange of sodium (Na<sup>+</sup>) by various cations (Ce<sup>3+</sup>, Gd<sup>3+</sup> and Fe<sup>3+</sup>) for O<sub>2</sub> and CO<sub>2</sub> have been investigated experimentally and by Density Functional Theory (DFT) calculations.

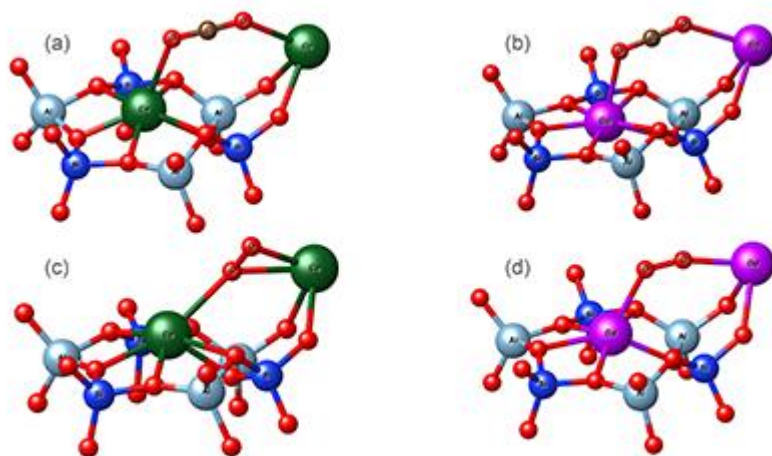
Indeed, it has been proven that adsorption enthalpies of various molecules within zeolites can now be accurately predicted by DFT (3-5). For example, DFT computations of the adsorption enthalpies of alkanes in different zeolite structures (FAU, ZSM-5, BEA, MOR, CHA) are in a good agreement with calorimetric experiments with an average error below 5 kJ/mol (4,5). Then DFT periodic approaches have been employed to perform cationic screening for selective capture of CO<sub>2</sub> (6) or iodine species from nuclear streams (7-9). In all the aforementioned studies, the effect of the cations has been highlighted. In this presentation, we will report on the influence of the monovalent cations (Cu<sup>+</sup>, Ag<sup>+</sup>, Na<sup>+</sup>...), divalent (Fe<sup>2+</sup>, Mn<sup>2+</sup>, Pd<sup>2+</sup>, Pt<sup>2+</sup>...) as well as trivalent cations (Ce<sup>3+</sup>, Gd<sup>3+</sup>...) on the adsorption properties of CO<sub>2</sub> and O<sub>2</sub> in the faujasite zeolite framework using dispersion-corrected density functional theory with periodic boundary conditions. The low-symmetry triclinic FAU unit cell was used as a model containing around 144 atoms (7). Isolated cations have been first considered, and the most promising cations have been then embedded in a more realistic zeolite with FAU structure (zeolite X, Si/Al ratio of 1.4).

DFT isolated cationic screening of a primitive cell of FAU type zeolite revealed that the Cu<sup>+</sup> alongside with Pt<sup>2+</sup> and Pd<sup>2+</sup> have the strongest affinity for O<sub>2</sub> compared to CO<sub>2</sub>. O<sub>2</sub> is more favorably absorbed than CO<sub>2</sub> by 85 kJ/mol over the Pt<sup>2+</sup> isolated cations, followed by Cu<sup>2+</sup> and Pd<sup>2+</sup> with a difference adsorption energy of 40 kJ/mol. More realistic FAU zeolite structure was used for further characterizations; the most promising cations were Gd<sup>3+</sup> and Ce<sup>3+</sup>. Pure Gd-X zeolite is expected to adsorb O<sub>2</sub> more strongly than CO<sub>2</sub> by 40 kJ/mol, while the pure Ce-X zeolite is expected to adsorb O<sub>2</sub> more strongly than CO<sub>2</sub> by 50 kJ/mol.

The O<sub>2</sub> and CO<sub>2</sub> sorption properties of the faujasite nanocrystals were studied experimentally by FTIR. The experimental and theoretical results show that samples bearing trivalent cations have stronger affinity towards O<sub>2</sub> in presence of CO<sub>2</sub>, which would be important in promoting the O<sub>2</sub> delivery through the blood stream where CO<sub>2</sub> is generally present. The nanozeolites are non-toxic on cells as demonstrated by cytotoxicity tests performed at various concentrations.

*Figure: DFT computed adsorption modes of CO<sub>2</sub> in (a) Ce-X, (b) Gd-X, and O<sub>2</sub> in (c) Ce-X, (d) Gd-X zeolites*

Image 1:



### References:

1. V. Georgieva, C. Anfray, R. Retoux, V. Valtchev, S. Valable, S. Mintova, Iron loaded EMT nanosized zeolite with high affinity towards CO<sub>2</sub> and NO, *Microporous and Mesoporous Materials*. 232 (2016) 256–263. <https://doi.org/10.1016/j.micromeso.2016.06.015>.
2. C. Anfray, B. Dong, S. Komaty, S. Mintova, S. Valable, Acute Toxicity of Silver Free and Encapsulated in Nanosized Zeolite for Eukaryotic Cells, *ACS Appl. Mater. Interfaces*. 9 (2017) 13849–13854. <https://doi.org/10.1021/acsami.7b00265>.
3. Rocca, D.; Dixit, A.; Badawi, M.; Lebègue, S.; Gould, T.; Bučko, T. Bridging Molecular Dynamics and Correlated Wave-Function Methods for Accurate Finite-Temperature Properties. *Phys. Rev. Materials* 2019, 3 (4), 040801. <https://doi.org/10.1103/PhysRevMaterials.3.040801>.
4. Göltl F, Grüneis A, Bucko T, Hafner J (2012) Van der Waals interactions between hydrocarbon molecules and zeolites: Periodic calculations at different levels of theory, from density functional theory to the random phase approximation and Møller-Plesset perturbation theory. *J Chem Phys* 137:114111
5. Piccini G, Alessio M, Sauer J, Zhi Y, Liu Y, Kolvenbach R, Jentys A, Lercher JA, (2015) Accurate Adsorption Thermodynamics of Small Alkanes in Zeolites. Ab initio Theory and Experiment for H-Chabazite. *J Phys Chem C* 119:6128–6137
6. Pirngruber GD, Raybaud P, Belmabkhout Y, Čejka J, Zúcal A (2010) The role of the extra-framework cations in the adsorption of CO<sub>2</sub> on faujasite Y. *Phys. Chem. Chem. Phys.* 12:13534–13546. doi:10.1039/B927476F
7. Chebbi M, Chibani S, Paul J-F, Cantrel L, Badawi M (2017) Evaluation of volatile iodine trapping in presence of contaminants: A periodic DFT study on cation exchanged-faujasite. *Microporous Mesoporous Mater* 239:111–122. doi:10.1016/j.micromeso.2016.09.047
8. Chibani S, Chebbi M, Lebègue S, Bučko T, Badawi M (2016) A DFT investigation of the adsorption of iodine compounds and water in H-, Na-, Ag-, and Cu- mordenite. *J Chem Phys* 144(24):244705. doi:10.1063/1.4954659
9. Chibani S, Medlej I, Lebègue S, Ángyán JG, Cantrel L, Badawi M (2017) Performance of CuII-, PbII-, and HgII-Exchanged Mordenite in the Adsorption of I<sub>2</sub>, ICH<sub>3</sub>, H<sub>2</sub>O, CO, ClCH<sub>3</sub>, and Cl<sub>2</sub>: A Density Functional Study. *ChemPhysChem* 18(12):1642–1652. doi: 10.1002/cphc.201700104

**Prolonged Release of Atenolol from Zeolites: A Theoretical and Experimental Investigation**

J. Wise<sup>1</sup>, J. Sefy<sup>1</sup>, E. Barbu<sup>1</sup>, M. van der Merwe<sup>1</sup>, S. McHugh<sup>2</sup>, A. O'Malley<sup>2</sup>, P. Cox<sup>1,\*</sup>

<sup>1</sup>School of Pharmacy, University of Portsmouth, Portsmouth, <sup>2</sup>Department of Chemistry, University of Bath, Bath, United Kingdom

**Abstract Text:** Introduction

A combination of experiment and theory has been used to investigate the controlled release of atenolol from FAU and BEA structures with different Si/Al ratios. The drug atenolol is a beta-blocker, widely used in the treatment of angina and hypertension. It is also used to prevent heart attacks. Being able to carefully control the release of the drug would improve its bioavailability as well as reducing both dosing frequency and unwanted side-effects. Another interesting feature of the atenolol molecule is its distinct hydrophobic and hydrophilic regions which make it difficult to predict the effect that adjustments made to the Si/Al ratio of the host will have on the release rate of the drug.

Experimental

Experimental drug release rates from loaded zeolite samples of FAU and BEA with different Si/Al ratios were measured using USP/Ph.Eur paddle dissolution apparatus. All release studies were carried out under sink conditions in triplicate. Molecular dynamics (MD) simulations were performed using the program Materials Studio. Simulations were carried out at 310 K with a time-step of  $1 \times 10^{-5}$  s and total simulation time of 20 ns.

Results and Discussion

The observed release rates for atenolol from two different FAU samples are shown in Figure 1. While both samples demonstrate prolonged release, the release from the H-FAU ( $\text{SiO}_2/\text{Al}_2\text{O}_3 = 80:1$ ) sample is considerably extended compared with the H-FAU ( $\text{SiO}_2/\text{Al}_2\text{O}_3 = 5.1:1$ ) sample. This is a particularly interesting observation because the H-FAU ( $\text{SiO}_2/\text{Al}_2\text{O}_3 = 80:1$ ) sample has a decreased number of Brønsted acid sites (associated with a higher Si/Al ratio) and therefore less opportunity for H-bonding between the sorbate and zeolite; something which might be expected to lead to greater mobility and hence faster release of the atenolol. Moreover, the release from FAU ( $\text{SiO}_2/\text{Al}_2\text{O}_3=80:1$ ) is quite remarkable considering the simplicity of the drug delivery system, with linear ( $R^2=0.9959$ ) release for 24 hours and prolonged release continuing for over 72 hours. It may therefore be possible to formulate a dosage form for routes other than oral delivery, such as transdermal delivery via a patch that lasts for 72 hours.

The MD simulations yield complementary information about the motion of the atenolol molecule within the host structure. In FAU, the molecules move around within a sodalite cage until they adopt an orientation that will allow them to pass to an adjacent cage. In contrast, molecules in BEA move from adjacent intersections via a distinct hopping mechanism (Figure 2).

Conclusions

The results of the dissolution tests demonstrate the potential of FAU to produce prolonged release drug delivery systems, notably using samples with a high Si/Al ratio. Interaction of the drug with Brønsted acid sites is not the dominant interaction in terms of prolonging release rate in this system. Distinct diffusion mechanisms are identified in BEA and FAU.

Image 1:

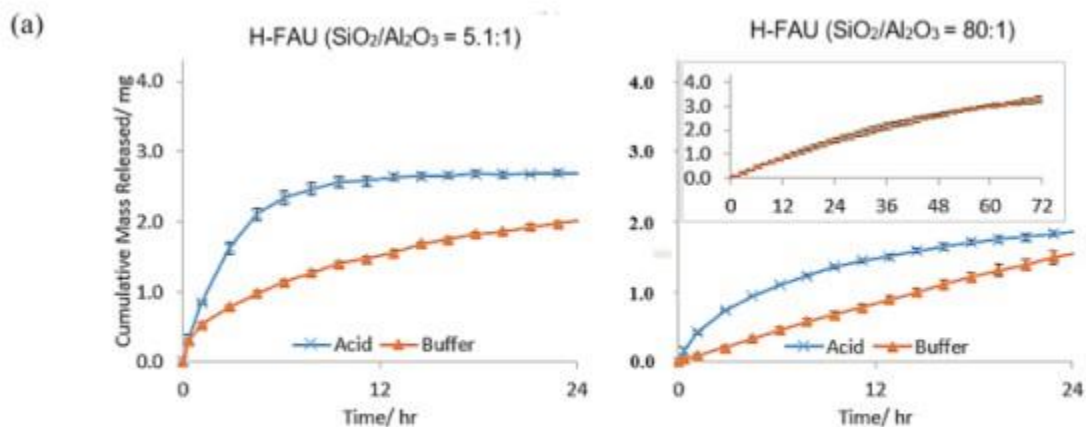


Figure 1: A comparison of cumulative release from the FAU framework in acid and buffer (a)  $\text{SiO}_2/\text{Al}_2\text{O}_3 = 5.1:1$  and (b)  $\text{SiO}_2/\text{Al}_2\text{O}_3 = 80:1$ . Figure 1(b) inset shows the dissolution profile from H-FAU over 72 hours in buffer.

Image 2:

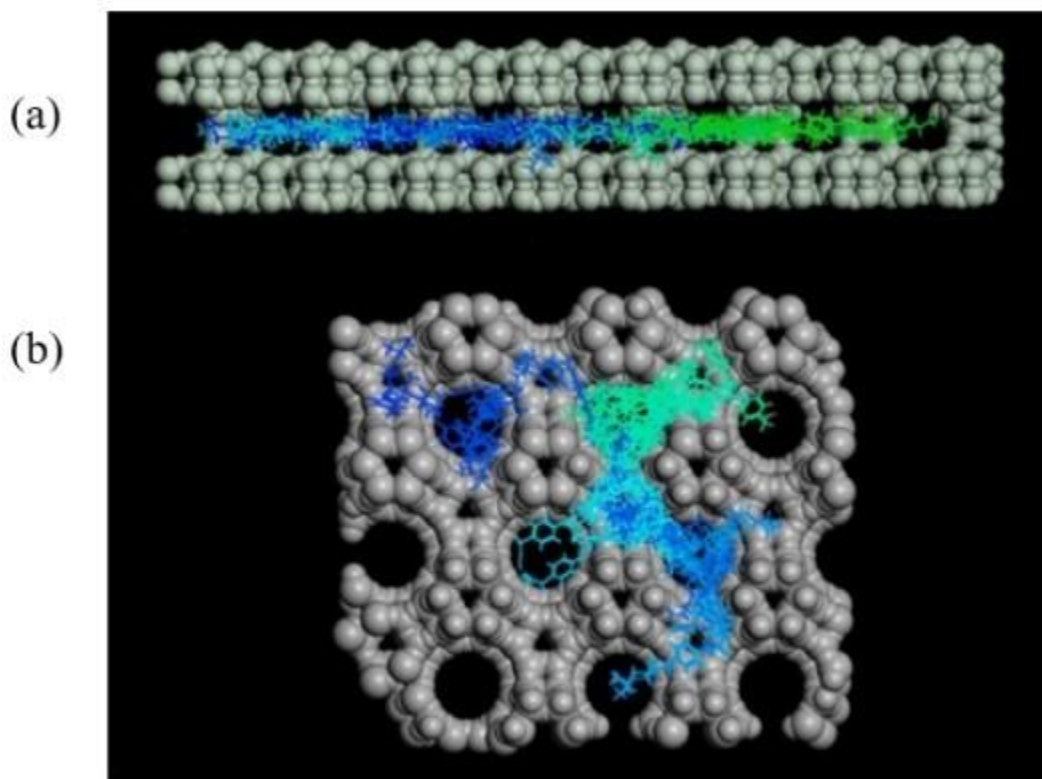


Figure 2: The diffusion pathway of atenolol molecules within (a) the BEA structure and (b) FAU.

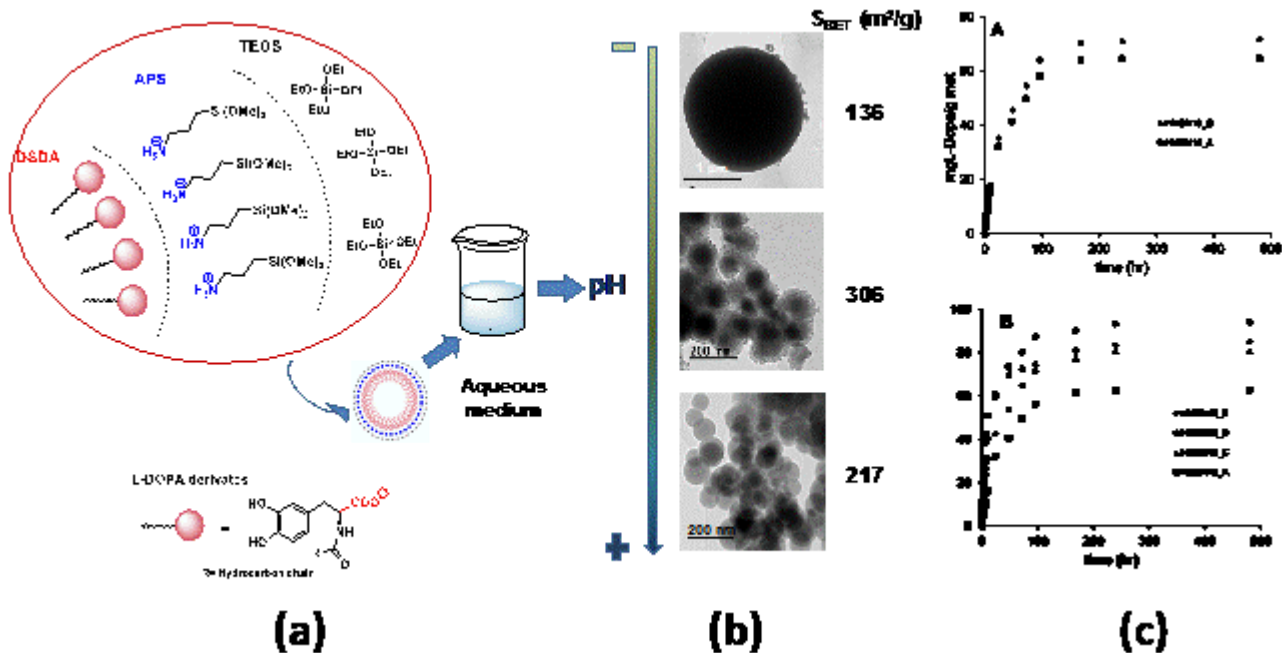
**Mesoporous silica nanoparticles template by L-Dopa derivatives as alternative therapy for Parkinson disease**

S. Martinez-Erro <sup>1,\*</sup>, E. Romani-Cubells <sup>1</sup>, F. Navas <sup>1</sup>, V. Morales <sup>1</sup>, R. A. García-Muñoz <sup>1</sup>, R. Sanz <sup>1</sup>

<sup>1</sup>Department of Chemical and Environmental Technology, Rey Juan Carlos University, Móstoles, Spain

**Abstract Text:** Parkinson is one of the most common neurodegenerative diseases (PD) among elderly people [1]. It is a progressive disorder that is characterized for the impairment of the motor and nonmotor functions of the human body. The treatment of the disease is generally performed with the precursor L-Dopa, which is transported to the brain and converted then to dopamine in the neurons. Nowadays, the administration of L-Dopa is intermittent with the consequent fluctuation of the drug concentration in the body. Therefore, it is highly desirable to develop drug delivery systems (DDS) of L-Dopa to obtain a more sustained and controlled release of this drug. In this context, mesoporous silica nanoparticles (MSNs) have emerged as very promising cargos for the delivery of several drugs due to their high surface area, large pore volumes and good bioavailability. Based on our previous studies, we envisioned the synthesis of L-Dopa derivatives that could act as director-structure-directing agents (DSDAs) in the synthesis of MSNs [2]. The present work describes the synthesis of hollow-shell mesoporous silica nanoparticles (HMSNs) using L-Dopa derivatives as templates for the micellar system that also provides an inherent therapeutic role against Parkinson's disease. The variation of the synthetic conditions of the HMSNs has allowed the tailoring of the morphological and textural properties, especially the size, from diameters of 1.5  $\mu\text{m}$  to 100 nm. Finally, the controlled released of L-Dopa in these materials has been tested in two different physiological fluids at different pH (acidic and neutral). Under gastric conditions at pH 1.2, the HMSNs with L-Dopa barely showed any release, which would avoid the unwanted release of the drug in the stomach. On the other hand, L-Dopa was released in a sustained and control manner for intestinal conditions at pH 7.4, making these nanomaterials suitable as oral delivery systems of L-Dopa against Parkinson's disease.

**Image 1:**



**References:** [1] L. V. Kalia, A. E. Lang, Parkinson's Disease. Lancet 2015, 386, 896–912.

[2] V. Morales, M. Gutiérrez-Salmerón, M. Balabasquer, J. Ortiz-Bustos, A. Chocarro-Calvo, C. García-Jiménez, R. A. García-Muñoz, Adv. Funct. Mater. 2016, 26, 7291–7303.

**The effect of framework structure and composition on molecular behaviour in controlled 5-Fluorouracil release by zeolites.**

S. Mchugh<sup>1,\*</sup>, A. O'Malley<sup>1</sup>, P. Cox<sup>2</sup>, J. Wise<sup>2</sup>

<sup>1</sup>Chemistry, University of Bath, Bath, <sup>2</sup>Pharmacy, University of Portsmouth, Portsmouth, United Kingdom

**Abstract Text:** The development and selection of materials for drug delivery systems (DDS) is an important area of research for the pharmaceutical sector. An ideal DDS would improve drug bioavailability and help to prevent its premature degradation whilst potentiating the effect of the drug. Zeolites are favourable for this use as they are crystalline and have tuneable porous channels of molecular dimensions suitable for the accommodation of different drug molecules. This study aims to determine the effect of material characteristics, such as pore size and topology, composition (Si/Al ratio), presence of difference extra-framework cations or any defects, on drug release from zeolites. Such insight would allow for the design and optimisation of affordable and precisely controlled release dosage forms of drugs, e.g. anticancer drugs.

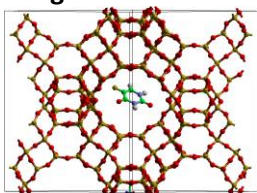
The anticancer drug 5-Fluorouracil (5-FU) - which is conventionally given intravenously and topically - has low oral bioavailability, numerous unpleasant side effects and a short biological half-life requiring multiple doses daily. 5-FU has been selected as a model drug for application in zeolite drug release in this study. The above issues make this drug an excellent target for sustained release formulations.

5-FU will be encapsulated into the zeolite host. The drug, zeolite host and the DDS (drug encapsulated within the zeolite host) will all be characterised using Fourier Transform Infrared Spectroscopy (FTIR), X-Ray Diffraction (XRD), Thermogravimetric Analysis (TGA), Nuclear Magnetic Resonance (NMR) and Scanning Electron Microscopy (SEM) to determine whether the drug and/or zeolite host is damaged or dramatically altered in the encapsulation procedure. Additionally, characterisation of the DDS using quasielastic neutron scattering (QENS) experiments will be carried out to investigate the mobility of 5-FU in the zeolite host as well as INS vibrational spectroscopy which will probe the interactions of 5-FU with the zeolite host. Classical molecular dynamics simulations will be run alongside the laboratory experiments with the aim of complementing the results found experimentally. Good agreement has been reported in other studies between simulations and observed release profiles of 5-FU from faujasite.<sup>1</sup>

The poster will present quasielastic neutron scattering results, carried out at the ISIS Neutron and Muon Source, alongside complementary classical molecular dynamics simulation data probing the diffusion rates and mechanisms through the zeolite host.

Image shows 5-Fluorouracil molecule confined within the supercage of a fully siliceous Faujasite zeolite.

**Image 1:**



**References:** 1. M. Spanakis, N. Bouropoulos, D. Theodoropoulos, L. Sygellou, S. Ewart, A. M. Moschovi, A. Siokou, I. Niopas, K. Kachrimanis, V. Nikolakis, P. A. Cox, I. S. Vizirianakis and D. G. Fatouros, *Nanomedicine Nanotechnology, Biol. Med.*, 2014, 10, 197–205.

## Biomedical Applications

FEZA21-PO-044A

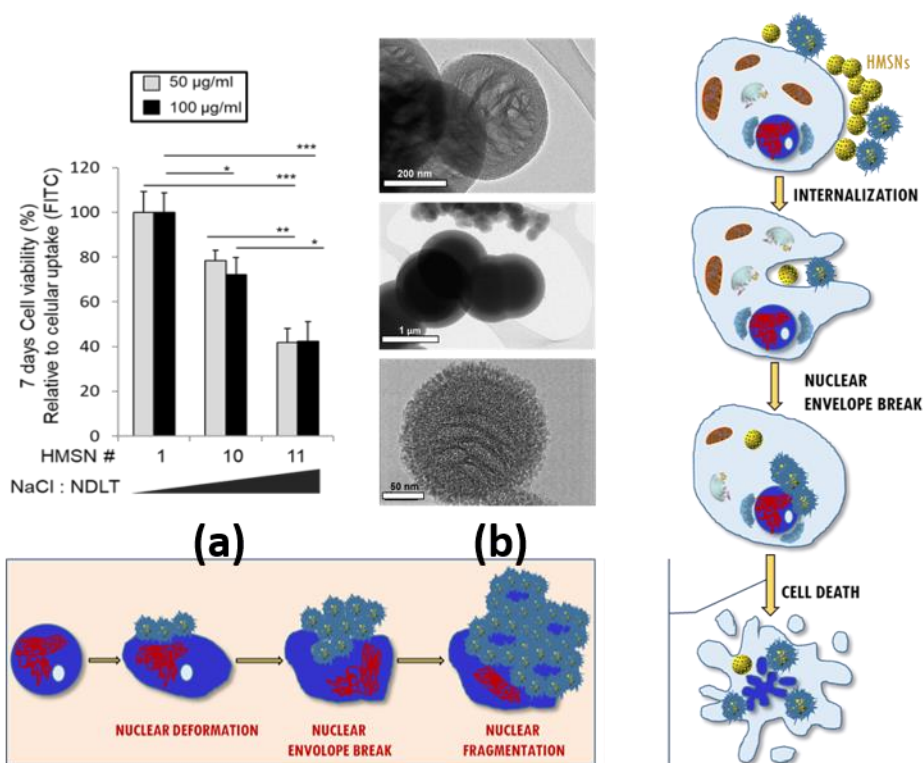
### TAILORING HOLLOW MESOPOROUS SILICA NANOPARTICLES TO INCREASE THEIR ANTICANCER POTENTIAL

F. Navas<sup>1,\*</sup>, E. Romani-Cubells<sup>1</sup>, S. Martinez-Erro<sup>1</sup>, V. Morales<sup>1</sup>, M. Gutierrez-Salmeron<sup>2</sup>, A. Chocarro-Calvo<sup>2</sup>, C. García-Jimenez<sup>2</sup>, R. Sanz<sup>1</sup>, R. A. García-Muñoz<sup>1</sup>

<sup>1</sup>Department of Chemical and Environmental Technology, <sup>2</sup>Department of Basic Health Sciences, Rey Juan Carlos University, Móstoles, Spain

**Abstract Text:** Hollow-shell mesostructured silica nanoparticles (HMSNs) are structures with internal hollows or voids surrounded by mesoporous shells of different dimensions allowing an easy diffusion of guest molecules, which make them potential and promising pharmaceutical carriers [1][2]. Their specific structure provides nanoparticles with low density and high surface/volume ratio, which optimizes load and diffusion of bioactive compounds over conventional methods. In this kind of nanoparticles, the election of the surfactant is critical. Recently, it has been reported the concept of drug-structure-directing agents, based on the use of N-acyl amino acid-based anionic surfactants [3]. It is necessary to design and optimize the nanocarrier parameters so as to overcome the different biological barriers. In this work, it is presented the impact of changing physicochemical properties of HMSNs (by tuning the synthesis conditions) on their interactions with human colon healthy and cancer cells at the level of cellular uptake and viability. The synthesis of these HMSNs also combined the use of an anionic DSDA, the N-decanoyl-L-tryptophan (NLDT), which is used as both a surfactant template for mesopores and an oil phase for hollow or voids formation to produce the final materials. Additionally, 3-(aminopropyl)trimethoxysilane (APS) is used as co-surfactant and TEOS as silica source. We have identified how several changes in the synthesis conditions control can regulate the size, morphology, surface charge and density or degree of compaction of HMSNs and modify their capacity to induce cellular uptake and cytotoxicity in cancer cells. This strategy may open new avenues to design HMSNs nanoarchitectures for biomedical applications, without the incorporation of external active pharmaceutical ingredient, but themselves acting as therapeutic agents.

#### Image 1:



**References:** [1] Y. Li, N. Li, W. Pan, Z. Yu, L. Yang, B. Tang, ACS Appl. Mater. Interfaces, 2017, 9, 2123–2129.

[2] Y. Wang, Q. Zhao, N. Han, L. Bai, J. Li, J. Liu, E. Che, L. Hu, Q. Zhang, T. Jiang, S. Wang, *Nanomed. Nanotechnol. Biol. Med.* 2015, 11, 313–327.

[3] V. Morales, M. Gutierrez-Salmeron, M. Balabasquer, J. Ortiz-Bustos, A. Chocarro-Calvo, C. Garcia-Jimenez, R.A. Garcia-Munoz, *Adv. Funct. Mater.* 2016, 26, 7291–7303.

## **Catalytic Properties**

FEZA21-PO-045

### **Highly selective production of ethylene by fine-tuning the chemical state and acidity of ceria incorporated in hierarchical zeolites**

M. Ketkaew<sup>1,\*</sup>, S. Klinyod<sup>1</sup>, K. Saenluang<sup>1</sup>, C. Rodaum<sup>1</sup>, A. Thivasasith<sup>1</sup>, P. Kidkhunthod<sup>2</sup>, C. Wattanakit<sup>1</sup>

<sup>1</sup>Chemical and Biomolecular Engineering, Vidyasirimedhi Institute of Science and Technology (VISTEC), Rayong,

<sup>2</sup>Synchrotron Light Research Institute (Public Organization), Nakhon Ratchasima, Thailand

**Abstract Text:** Ethanol is a potentially promising platform molecule to produce various high value-added chemicals such as light olefins and aromatics. Among them, ethylene is one of the most interesting compounds, which can be widely used in the production of polyethylene, ethylene oxide, ethylene dichloride, and so on.<sup>1</sup> The conventional ethylene production can be observed via steam cracking, which indeed often suffers from high energy consumption and an intensive CO<sub>2</sub> emission. Over the past decades, the catalytic ethanol dehydration to ethylene has been considered as an environmentally friendly pathway that could be achieved at a significantly lower reaction temperature.<sup>2</sup>

In the present study, the incorporation of cerium oxide (CeO<sub>2</sub>) with hierarchical zeolites for ethanol dehydration was systematically investigated. The synthesis of CeO<sub>2</sub> modified catalysts can be categorized into two main processes to determine the effect of support materials and loading methods on the catalytic performance. Various types of zeolites, which are hierarchical silicalite-1, hierarchical ZSM-5, and conventional ZSM-5, were employed as support materials by using impregnation, and ion-exchange methods for the addition of CeO<sub>2</sub> nanoparticles. Interestingly, CeO<sub>2</sub> is well dispersed on hierarchical zeolites, especially on hierarchical ZSM-5 prepared by the ion-exchange method. Furthermore, aluminum sites in the zeolite framework can enhance the catalytic performance in both ethanol conversion and ethylene selectivity. Moreover, CeO<sub>2</sub> loading by the ion-exchange method can further improve the catalytic performance, eventually providing a high yield of ethylene almost 100%, which is much higher than that of using an impregnation method. Additionally, the acid distribution of these catalysts can be considered as a great influence on the catalytic performance for ethanol dehydration due to an improvement of the moderate acid strength from CeO<sub>2</sub> insertion. Besides, a low ethanol conversion over the CeO<sub>2</sub> modified conventional zeolite can again confirm the beneficial effect of hierarchical zeolites possessed the outstanding external surface area.<sup>3</sup> Therefore, the chemical state, metal-support interaction, and acidity of catalysts can be fine-tuned by using the hierarchical zeolite and using an ion-exchange method, eventually facilitating ethanol dehydration to ethylene.<sup>4</sup>

**References:** 1. J. Ouyang, F. Kong, G. Su, Y. Hu and Q. Song, *Catalysis Letters*, 2009, 132, 64-74.

2. S. Shetsiri, A. Thivasasith, K. Saenluang, W. Wannapakdee, S. Salakhum, P. Wetchasat, S. Nokbin, J. Limtrakul and C. Wattanakit, *Sustainable Energy & Fuels*, 2019, 3, 115-126.

3. P. Iadrat, N. Horii, T. Atitthep and C. Wattanakit, *ACS Applied Materials & Interfaces*, 2021, 13, 8294-8305.

4. M. Ketkaew, S. Klinyod, K. Saenluang, C. Rodaum, A. Thivasasith, P. Kidkhunthod and C. Wattanakit, *Chemical Communications*, 2020, 56, 11394-11397.

## **Catalytic Properties**

FEZA21-PO-046

### **Synthesis and application of core-shell FAU@AMO-LDHs composites for one-pot synthesis of ethyl trans- $\alpha$ -cyanocinnamate**

C. Rodaum<sup>1,\*</sup>, D. Suttipat<sup>1</sup>, J. Morey<sup>2</sup>, T. Witoon<sup>3</sup>, C. Wattanakit<sup>1</sup>

<sup>1</sup>Chemical and Biomolecular Engineering, Vidyasirimedhi Institute of Science and Technology, Rayong, Thailand, <sup>2</sup>Ecole Nationale Supérieure de Chimie, de Biologie et de Physique (ENSCBP), University of Bordeaux, Pessac, France, <sup>3</sup>Chemical Engineering, Kasetsart University, Bangkok, Thailand

**Abstract Text:** Recently, ethyl trans- $\alpha$ -cyanocinnamate has been used as a raw material in many petrochemical industries, such as plastics, cosmetics, and pharmaceuticals. Typically, it can be produced from the one-pot deacetalization-Knoevenagel cascade reaction by using a multifunctional acid-base catalyst. However, the development of a bifunctional catalyst with tunable acid-base properties for this reaction is still a challenging task. In terms of acid part, one of the most promising catalysts is an acidic faujasite (FAU) zeolite containing a high acid density, which has been used as an acid catalyst in various potential applications, such as bio-oil catalytic upgrading, and acid-base reactions.<sup>[1]</sup> Apart from this perspective, the interesting material for basic sites is aqueous miscible organic-layered double hydroxides (AMO-LDHs), well-known as solid-base catalysts with unique versatile properties including high specific surface area, and ability of tunable basicity.<sup>[2]</sup> Therefore, the combination of the benefits between zeolites and AMO-LDHs, such as adjustable acid-base properties, high surface area, and dispersion of active sites would enhance the catalytic performance for one-pot deacetalization-Knoevenagel cascade reaction.

Herein, we report the fabrication of the acid-base bifunctional catalyst prepared by the growth of layered double hydroxides (LDH) precursors on Faujasite zeolite surfaces (FAU) called core-shell FAU@AMO-LDHs composites. This composite contains faujasite zeolite (FAU) as a core and LDH as a shell for acid and base parts, respectively. Moreover, it can be adjustable acid-base sites by controlling the amount of LDH in order to achieve the high yield of ethyl trans- $\alpha$ -cyanocinnamate. Interestingly, the core-shell FAU@AMO-LDHs catalyst can achieve up to 90% yield of ethyl trans- $\alpha$ -cyanocinnamate obtained via a one-pot deacetalization-Knoevenagel cascade reaction. To investigate the synergistic effect between acid and base functions, the physical mixing between FAU and LDHs catalysts was applied to test and compare the catalytic performance under the same reaction condition. Compared to the composite one (90 % yield of ethyl trans- $\alpha$ -cyanocinnamate), it was found that the physical mixture as a catalyst showed a considerably lower yield of designed product (62.3%). This is attributed to the synergistic effects between acid and base functions in which basic sites are close to Brønsted acid sites in the composite catalyst, which can promote the transfer of benzaldehyde intermediate to basic sites for the production of the final product. This opens up a new perspective of the development of a tunable acid-base composite catalyst in an acid-base cascade reaction (deacetalization-Knoevenagel reaction).<sup>[3]</sup>

**References:** [1] D. Suttipat, T. Yuthalekha, W. Wannapakdee, P. Dugkhuntod, P. Wetchasat, P. Kidkhunthod, C. Wattanakit, *ChemPlusChem* 2019, 84, 1503-1507.

[2] C. Rodaum, A. Thivasasith, D. Suttipat, T. Witoon, S. Pengpanich, C. Wattanakit, *ChemCatChem* 2020, 12, 4288-4296.

[3] C. Rodaum, D. Suttipat, J. Morey, T. Atitthep, T. Witoon, C. Wattanakit, *Adv. Mater. Interfaces*, 2021, doi: 10.1002/admi.202002259.

## **Catalytic Properties**

FEZA21-PO-047

### **The effect of calcium dopant in Au-SBA-15 and Au-Nb/SBA-15 on the catalytic activity and selectivity in methanol oxidation**

J. Wisniewska<sup>1</sup>, I. Sobczak<sup>1,\*</sup>, M. Ziolk<sup>1</sup>

<sup>1</sup>Faculty of Chemistry, Adam Mickiewicz University in Poznan, Poznan, Poland

#### **Abstract Text:**

##### **Introduction**

Methanol transformations to other chemicals via oxidation or oxidative dehydrogenation have been the subjects of intense research and interest [1]. Oxidation of methanol is a process needed for production of important target products like formaldehyde (FA), methyl formate (MF) or dimethoxy methane (DMM). The product distribution depends on the redox and/or acid-base centres on the catalyst surface.

The aim of this study was to prepare redox (gold) - basic (calcium species) SBA-15 catalysts with different compositions and to estimate the role of calcium species and composition of the support in the mechanism of methanol oxidation.

##### **Experimental**

SBA-15, NbSBA-15 and Nb<sub>2</sub>O<sub>5</sub>/SBA-15 supports were modified with calcium (7 wt.%) and gold (2 wt.%). All catalysts were calcined at 973 K. The materials prepared were characterized by XRD, TEM, UV-Vis, FT-IR, XP spectroscopy and the test reaction of 2-propanol decomposition. The catalytic MeOH oxidation was performed in gas phase (Ar/O<sub>2</sub>/CH<sub>3</sub>OH = 88/8/4 mol %) at 373-573 K.

##### **Results and discussion**

Three different supports were applied for gold and/or calcium loading, namely mesoporous silica SBA-15, niobiosilicate (NbSBA-15) and Nb<sub>2</sub>O<sub>5</sub>/SBA-15 (i.e. SBA-15 impregnated with niobium precursor transformed to niobium(V) oxide).

Negatively charged metallic gold species were found on all samples and their presence was confirmed by XPS studies. The crystal phases on the surface of the supports were identified by XRD analysis. The formation of the CaCO<sub>3</sub> phase in all calcium containing samples was verified. The lack of reflections characteristic of CaO in the XRD patterns suggests very high dispersion of CaO species on silica surface. The presence of Nb<sub>2</sub>O<sub>5</sub> crystallites was observed only for Au-CaNbO<sub>x</sub>/SBA-15. The composition of the support had an impact on the material basicity, estimated by 2-propanol decomposition reaction. It is clear that introduction of calcium decreased the acidic properties of Au-SBA-15, Au/NbSBA-15 and Au/Nb<sub>2</sub>O<sub>5</sub>/SBA-15 catalysts (decrease in the activity) and generated basicity (increase in the selectivity to acetone).

The results of methanol oxidation indicated that the activity of gold catalysts doped with calcium considerably increased in comparison with that of the catalyst without calcium. Gold-calcium catalysts were active in MeOH oxidation even at a low temperature of 423 K, at which the following order of activity was observed: Au/Ca/NbSBA-15 (4 % MeOH conversion) < Au/Ca/SBA-15 (13 % MeOH conversion) < Au/CaNbO<sub>x</sub>/SBA-15 (25 % MeOH conversion). The latter catalyst is especially attractive because of 93 % selectivity to MF, which allows us to propose this catalyst for low temperature MF production. On the other hand, Au/Ca/SBA-15 is promising for neutralization of methanol wastes, as at 523 K in its presence 100 % yield of CO<sub>2</sub> was observed (total oxidation of MeOH).

It was concluded [2] that the composition of the support for gold determines the methanol oxidation pathways. In the presence of Au/SBA-15, silanol groups from the support, combined with negatively charged gold NPs, took part in the dissociative chemisorption of methanol towards methoxy species chemisorbed on gold NPs. It was followed by oxidative dehydrogenation towards formate species. The latter were strongly bound to the catalyst surface and therefore, partially inhibited the following reaction steps. For Au/Ca/SBA-15, Au/Ca/NbSBA-15 and Au/CaNbO<sub>x</sub>/SBA-15 it was evidenced that synergistic interaction between gold and calcium species was responsible for weak chemisorption of methoxy and formate species and in this way accelerated the interaction between them leading to MF product. On the

other hand, the methanol total oxidation to CO<sub>2</sub> was enhanced as a result of dissociative adsorption of molecular oxygen on Ca species followed by spillover of atomic oxygen to Au NPs.

*Acknowledgement:* We are grateful to the National Science Centre in Poland (Project no. 2018/29/B/ST5/00137) for financial support.

**References:**

[1] C. H. Bartholomew, R. J. Farrauto, *Fundam. Ind. Catal. Process.*, 2006, 578–597.

[2] J. Wiśniewska, I. Sobczak, M. Ziolek, *Catalysis Science & Technology*, 11, 2021, 2242-2260.

## **Catalytic Properties**

FEZA21-PO-048

### **The impact of Au deposition method on the catalytic performance of Beta zeolite-based gold catalysts in base-free glucose oxidation**

A. Walkowiak<sup>1,\*</sup>, J. Wolska<sup>1</sup>, I. Sobczak<sup>1</sup>, L. Wolski<sup>1</sup>, M. Ziolek<sup>1</sup>

<sup>1</sup>Faculty of Chemistry, Adam Mickiewicz University, Poznan, Poznań, Poland

#### **Abstract Text:**

Growing depletion of fossil fuel resources and the increasing awareness of climate change have driven recent research activities towards more environment-friendly areas [1]. One of the examples of such an approach is the use of biomass as a renewable feedstock for the production of fuels and chemicals. Among the vast array of products of biomass conversion, sugars draw the particular attention of scientists. The most abundant one – glucose – can be transformed into a wide range of valuable chemicals. Oxidation of glucose leads towards the formation of sugar acids (e.g. gluconic and glucuronic acids) that are applied in the food, cosmetics, and pharmaceutical industries [2].

Hitherto, it has been documented [1,2] that heterogeneous gold catalysts are attractive materials dedicated to base-free catalytic oxidation of glucose. This approach overcomes some disadvantages of conventionally employed methods such as biochemical oxidation processes or catalytic oxidation in basic media (e.g. problems with the separation of final product from post-reaction mixture). The main goal of this study was the preparation of a series of new Beta zeolite-based gold bifunctional catalysts (providing redox and acidic sites) using four different synthesis procedures, i.e. ion-exchange (**IE**), impregnation (**IM**), deposition-reduction (**DR**), grafting with organosilane ((3-aminopropyl)trimethoxysilane, APTMS; **AP**) and the evaluation of their activity and selectivity in the base-free glucose oxidation.

The prepared catalysts were characterized with the use of different complementary techniques such as XRD, N<sub>2</sub> adsorption-desorption, UV-Vis, TEM, FTIR, ICP-OES in order to examine the composition, structure/texture, and gold phase properties. Pyridine adsorption combined with FTIR was conducted for acidity measurements. The catalytic activity of selected catalysts was investigated in aerobic oxidation of glucose without any pH adjustment.

The results obtained in this study have shown that the efficiency of gold introduction, the size of supported gold nanoparticles as well as acidic properties of zeolite support were strongly affected by the catalysts synthesis procedure. The smallest and uniformly dispersed gold particles were obtained when following the procedure of grafting with APTMS for Au deposition (**AP**) (gold particle size estimated from XRD ca. 8 nm). In contrast, the largest ones were present in the sample obtained by **IM** method (ca. 88 nm). It has been estimated that Au particles sizes for materials prepared via **DR** and **IE** methods were ca. 52 and 32 nm, respectively.

The results of aerobic glucose oxidation (reaction conditions: 20 mL of 0.2 M glucose solution, glucose/Au (molar ratio) = 1970/1; mixing: 600 rpm, T = 383 K, pO<sub>2</sub>: 0.5 MPa, time: 2 h) have shown that the most active catalyst was the material with the finest Au particles – Au-HBeta(**AP**). The degree of glucose conversion in the presence of the catalysts studied decreased in the sequence **AP** > **IE** > **DR** > **IM**, i.e. with the increasing Au particle sizes. Such an observation is indeed in line with foregoing literature data [3,4]. Moreover, the selectivity, in general, was consistent for all the examined materials and the main product was gluconic acid. However, it has been documented that the highest TOF number (expressing the activity of a single gold atom on the surface of Au particle) was reached, surprisingly, for the material obtained via the **IE** method (Au particle size ~32 nm). This phenomenon will be discussed. As concerns the stability of the catalysts, the most stable was Au-HBeta(**AP**) whilst the drop in catalytic activity in subsequent cycles (possibly related to the leaching of the active phase) was observed for Au-HBeta(**DR**) and Au-Beta(**IE**) samples.

National Science Centre in Poland (projects no. 2018/29/B/ST5/00137 and 2018/28/C/ST5/00255) and Ministry of Education and Science (project “Diamentowy Grant” no. DI2018 002248) are acknowledged for the financial support of this work.

**References:**

- [1] R. Wojcieszak, C. Ferraz, J. Sha, S. Houda, L. Rossi, S. Paul, *Catalysts* 7 (2017) 352.
- [2] X. Meng, Z. Li, D. Li, Y. Huang, J. Ma, C. Liu, X. Peng, *Green Chem.* 22 (2020) 2588–2597.
- [3] L. Prati, A. Villa, A. R. Lupini, G. M. Veith, *Phys. Chem. Chem. Phys.* 14 (2012) 2969.
- [4] C. Megías-Sayago, J. L. Santos, F. Ammari, M. Chenouf, S. Ivanova, M. A. Centeno, J. A. Odriozola, *Catal. Today* 306 (2018) 183–190.

## Catalytic Properties

FEZA21-PO-049

### Tuning Nb-zeolite based catalysts for the oxidation of glucose and 5-hydroxymethylfurfural

M. A. El Fergani<sup>1,\*</sup>, N. Candu<sup>1</sup>, P. Granger<sup>2</sup>, V. I. Parvulescu<sup>1</sup>, S. M. Coman<sup>1</sup>

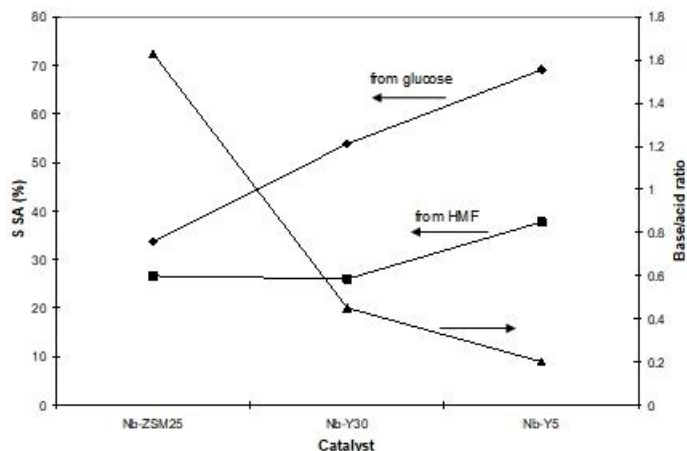
<sup>1</sup>Organic chemistry, Biochemistry and catalysis, University of Bucharest, Bucharest, Romania, <sup>2</sup>Sciences and Technologies kinetics and catalysis, university of Lille , Lille , France

**Abstract Text:** Nowadays, the catalytic transformation of renewable raw materials into high-value molecules represents one of the most attractive and challenging topics in heterogeneous catalysis. Among others these include mono- or dicarboxylic acids. In this context, glucose can be oxidized to succinic acid (SA) which is largely used as an important monomer for the production of bio-plastics [1]. Then, hydroxymethylfurfural (HMF) can be transformed into 2,5-furandicarboxylic acid (FDCA) that is utilized as a substitute of terephthalic acid for the production of polyesters [2]. The noble metal catalysts generally show high catalytic performances towards these products but due to their high prices hamper a large-scale production [3,4].

To overcome these drawbacks we focused our efforts to design an innovative cheap alternative to the noble metals-based catalysts. Here, we report the synthesis of two types of catalysts, namely Nb@(0.05 moles%)- and MO<sub>x</sub>(M = Mn, Co and Fe)@Nb@(0.05 moles%)@zeolite (ZSM25, Y5, Y30, Beta12, and Beta18, where the number denote the Si/Al ratio) materials. The catalysts were exhaustively characterized using XRD, TG-DTA, XPS, SS-NMR, CO<sub>2</sub>/NH<sub>3</sub>-TPD and IR spectroscopy.

Indeed, catalytic experiments with Nb@zeolite catalysts showed a better efficiency for the selective oxidation (in aqueous medium and air) of glucose (instead of HMF) to SA. This behavior has been directly correlated to the base/acid site ratio in the investigated samples (Figure 1). In contrast, MO<sub>x</sub>@Nb@@zeolite provided high-efficiency towards the FDCA production by the HMF oxidation in organic medium and organic peroxides as source of oxygen. Besides the catalytic efficiency the new proposed free of noble metal catalysts showed a very good recyclability.

#### Image 1:



**References:** [1] M. E. Fergani, N. Candu, M. Tudorache, P. Granger, V. I. Parvulescu and S. M. Coman. *Molecules* 25 (2020) 4885

[2] R. J. v. Putten, J. C. v. d. Waal, E. d. Jong, C. B. Rasrendr, H. J. Heeres and J. G. d. Vries. *Chem. Rev.*, 113 (2013) 1499-1597

[3] L. Bui, H. Luo, W. R. Gunther and Y. R. Leshkov. *Angew. Chem. Int. Ed.* 52 (2013) 8022–8025

[4] Y. R. Leshkov and M. E. Davis. *ACS Catal.* 1 (2011) 1566–1580

## Catalytic Properties

FEZA21-PO-050

### Mechanistic investigation of allyl chloride epoxidation with hydrogen peroxide over TS-1.

Z. Y. Pastukhova<sup>1,\*</sup>, L. G. Bruk<sup>1</sup>

<sup>1</sup>Department of General Chemical Technology, Lomonosov Institute of Fine Chemical Technologies RTU MIREA, Moscow, Russian Federation

**Abstract Text:** The most effective and preferred method for producing epoxides from an environmental and technological point of view is the oxidation of alkenes with hydrogen peroxide over TS-1 [1-4]. Among the studies, there are practically no systematic kinetic studies aimed at a detailed study of the mechanism [3-6]. The kinetics of allyl chloride epoxidation with hydrogen peroxide was studied in the presence of a titanium-containing TS-1 zeolite catalyst. The aim of this study was to try to obtain information about the mechanism of participation of an alkene in the process of its epoxidation by considering a fairly wide set of hypothetical mechanisms and identifying them based on the results of a targeted kinetic experiment [7].

The results of the kinetic study allow us to conclude: a necessary condition for an adequate description of the kinetic dependences of the epoxidation process is to take into account the inhibition of the process rate by the product (epichlorohydrin). It is established that both the Eli-Ridyl-type mechanism (Image 1) and the Langmuir-Hinshelwood-type mechanism (Image 2) with the activation of allyl chloride and hydrogen peroxide in various catalytic centers allow us to describe the kinetic regularities within the experimental error. Further research is needed to distinguish further.

#### Image 1:

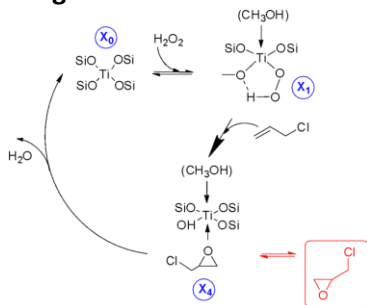
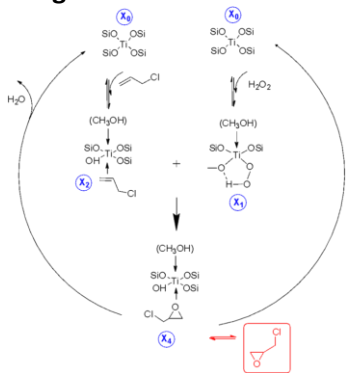


#### Image 2:



**References:** [1] L. Ding, J. Yin, W. Tong, R. Peng, J. Jiang, H. Xu and P. Wu/ *New J. Chem.* 45 (2021) 331.

[2] S. Bordiga, S. Coluccia, C. Lamberti, L. Marchese, A. Zecchina, F. Boscherini, F. Buffa, F. Genoni, G. Leofanti, G. Petrini, G. Vlaic/ *J. Phys. Chem.* 98 (1994) 4125.

[3] X. Liu, X. Wang, X. Guo, G. Li/ *Catal. Today.* 93-95 (2004) 505.

[4] Q. Guo, K. Sun, Z. Feng, G. Li, M. Guo, F. Fan, C. Li/ *Chem. Eur. J.* 18 (43) (2012) 13854.

[5] H. Salavati, A. Teimouri/ *Int. J. Electrochem. Sci.* 12 (2017) 7829.

[6] Zh.Yu. Pastukhova, F.D. Nasybulin, A.V. Sulimov, V.R. Flid, L.G. Bruk/ *Fine chemical technologies.* 11 (4) (2016) 26.

[7] O.N. Temkin, L.G. Bruk, A.V. Zeigarnik/ *Kinetics and catalysis.* 34 (1993) 445.

## Catalytic Properties

FEZA21-PO-051

### The Property-Activity Correlations of the Bifunctional Ni/ZSM-5 Catalysts in the Vapor-Phase Hydrogenation of Levulinic Acid in Packed-Bed Reactor

H. T. Vu<sup>1,\*</sup>, A. Kostyniuk<sup>1</sup>, P. Djinović<sup>1</sup>, M. Grilc<sup>1,2</sup>, B. Likozar<sup>1</sup>, N. Novak Tušar<sup>1,2</sup>

<sup>1</sup>National Institute of Chemistry, Ljubljana, Slovenia, Ljubljana, <sup>2</sup>University of Nova Gorica, Nova Gorica, Slovenia

#### Abstract Text:

$\gamma$ -valerolactone (GVL) is considered as a platform chemical and can be found in a plethora of industrial applications [1]. The synthesis of GVL, particularly, from biomass-derived levulinic acid (LA) has been the focus of many studies [2]. The conversion of LA to GVL requires both the acid and redox functionalities of the catalysts. Zeolite ZSM-5 functionalized with Ni is therefore a potential catalyst. Understanding the relations between the properties and catalytic activity of the bifunctional Ni/ZSM-5 catalyst can enable tailoring of products selectivity and thus obtain the desired products while maintaining high productivity. Moreover, ZSM-5 zeolites are also known for the high (hydro)thermal stability, which is beneficial for continuous heterogeneously-catalyzed processes in vapor phase. Therefore, in this study, a series of ZSM-5 zeolites with different  $n_{\text{Si}}/n_{\text{Al}}$  ratios, denoted as ZSM-5- $x$  ( $x = n_{\text{Si}}/n_{\text{Al}} = 13, 21$  and  $28$ ) were synthesized using a template-free hydrothermal method published in our previous work [3]. Obtained zeolites were impregnated with Ni (Ni content of 5 wt.%) denoted as Ni/ZSM-5- $x$ . To unveil the correlations of the properties and activity, the bifunctional Ni/ZSM-5 catalysts were characterized and tested in the vapor-phase hydrogenation of LA in a packed-bed reactor.

All catalysts exhibit MFI framework structure according to XRD results and comparable specific surface area ( $400 \text{ m}^2 \text{ g}^{-1}$ ) determined by  $\text{N}_2$  sorption. The preliminary catalytic results of the hydrogenation of LA with *iso*-propanol ( $T = 250 \text{ }^\circ\text{C}$ ,  $c_{\text{LA}} = 1 \text{ wt.}\%$ ,  $Q_{\text{LA}} = 0.03 \text{ g min}^{-1}$  and  $Q_{\text{H}_2} = 30 \text{ ml min}^{-1}$ ) show good agreement with available literature. The conversion of LA into GVL underwent via angelica lactone (AL) formation as suggested by the detection of AL in all catalytic experiments, i.e.,  $Y_{\text{AL}} = 1 - 7\%$ . Based on the components of reaction mixtures, a reaction pathway is proposed and displayed in Fig. 1.

With increasing  $n_{\text{Si}}/n_{\text{Al}}$ , LA conversion slightly increased from 54% to 78%. The selectivity of products, i.e., GVL and PL, is considerably affected. GVL yield increased from 1% through 42% and further to 61%. This is accompanied with a gradual decrease in PL yield, i.e., from 47% to 21% and to 13%, respectively, indicating the highest hydrogenation activity for the Ni/ZSM-5-28 catalyst. This is further confirmed by the detection of PA ( $Y_{\text{PA}} = 1\%$ ), a hydrogenated product of GVL. Considering the analogous Ni content and textural properties, the higher activity observed for Ni/ZSM-5-28 might be associated to the high  $n_{\text{Si}}/n_{\text{Al}}$  ratio. Thus, Ni/ZSM-5-750, i.e., Ni supported on a commercial Si-rich ZSM-5 zeolite with  $n_{\text{Si}}/n_{\text{Al}} = 750$ , was further investigated under identical conditions. A higher PA yield, i.e.,  $Y_{\text{PA}} = 13\%$ , was recorded. Hence, it is concluded that the catalytic activity of Ni/ZSM-5 catalysts is proportional to  $n_{\text{Si}}/n_{\text{Al}}$  ratio in the hydrogenation of LA under investigated conditions. Further investigation focusing on both acid and redox properties of the catalysts will be conducted to disclose its relations with the catalytic activity in the vapor-phase hydrogenation of LA.

Image 1:

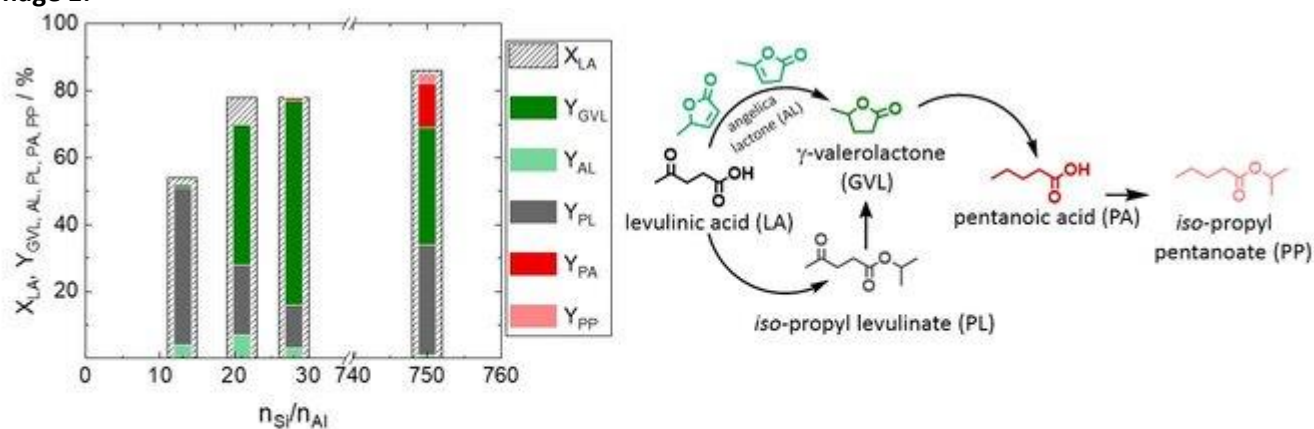


**Fig. 1:** LA conversion ( $X_{LA}$ ), yield (Y) of products (GVL, AL, PL, PA and PP) over the bifunctional Ni/ZSM-5 catalysts with various  $n_{Si}/n_{Al}$  (13, 21, 28 and 750) (left) and proposed reaction pathway (right) of the hydrogenation of LA ( $m_{cat} = 100$  mg,  $Q_{H_2} = 30$  ml min<sup>-1</sup>,  $c_{LA} = 1$  wt.-%,  $Q_{LA} = 0.03$  g min<sup>-1</sup>, 250 °C, 4 h).

**References:**

- [1] S.G. Wettstein et al., Curr. Opin. Chem. Eng. 1 (2012) 218 – 224.
- [2] R. Xu et al., ChemSusChem 13 (2020) 6461 – 6476.
- [3] M. Popova et al., Front. Chem. 6 (2018) 285 – 297.

## **Catalytic Properties**

FEZA21-PO-052

### **Anti-coke behaviour of silylated Nb/SBA-15 catalysts for glycerol dehydration**

K. Stawicka<sup>1,\*</sup>, M. Trejda<sup>1</sup>, M. Ziolk<sup>1</sup>

<sup>1</sup>Faculty of Chemistry, Adam Mickiewicz University, Poznań, Poland

**Abstract Text:** Glycerol is the main side-product obtained in the synthesis of biodiesel. Increasing production of biodiesel and thus increasing availability of glycerol have stimulated the search for ways of its use for the synthesis of other valuable products. One of the possible catalytic routes for glycerol transformation is its dehydration to acrolein<sup>1</sup> and oxidehydration to acrylic acid<sup>2</sup>. Glycerol dehydration is a typical acid-catalysed reaction. Brønsted acid sites (BAS) take part in glycerol dehydration to acrolein, whereas Lewis acid sites (LAS) favour the formation of hydroxyacetone. It is worth noting that effectiveness of glycerol dehydration depends not only on the presence of acid sites, but also on the textural properties of the catalyst. Different solid acid catalysts have been investigated up to now in the dehydration of glycerol to acrolein. Among them are zeolites, metal oxides and heteropolyacids<sup>2</sup>. One of the most significant reasons for catalysts deactivation in glycerol dehydration is formation of coke deposit by strong BAS. Thus, new synthesis routes for catalysts preparation or different reaction conditions have been proposed to overcome this problem.

The goal of this work was the application of mesoporous SBA-15 silica as a support for niobium species and to get a deeper insight into the character of active centres formed by applying of different methods for niobosilicas synthesis. The niobosilicas were synthesized by two strategies: i) SBA-15 modification with ammonium niobate(V) oxalate by impregnation method or ii) SBA-15 mixing with amorphous Nb<sub>2</sub>O<sub>5</sub>. The niobosilicas surface was also modified by silylation strategy (with using 3-aminopropyltrimethoxysilane (APTMS) as a silylating agent) towards minimization of carbon deposits. The research hypothesis was that both, the use of the support with large mesopores and large surface area together with silylation of niobium containing SBA-15, lead to a decrease in coke formation and enhance the acrolein selectivity.

The results obtained showed that the acid-base properties of the synthesized niobosilicas depend on the metal location in the SBA-15 support. The catalysts containing only Nb<sub>2</sub>O<sub>5</sub> on the surface showed the presence of only weak BAS and LAS centres. Stronger BAS and LAS were observed in the samples in which niobium species were located not only in extra lattice positions but also in silica framework. The niobium species in the framework position played a crucial role as active centres in glycerol dehydration to acrolein. However, too high concentration of such niobium species reduces the acrolein yield. Thus, the optimum choice was a low concentration of BAS with high strength together with the possible proximity of LAS and BAS on the surface of niobosilicas, which were responsible for the highest activity and selectivity to acrolein. Silylation of niobium containing SBA-15, in which niobium was located in the silica framework, resulted in catalysts showing some decrease in glycerol conversion. However, a significant increase in acrolein selectivity was observed which was accompanied by considerable decrease in coke deposition. Thus, anti-coke behaviour of silylated niobosilicas in glycerol dehydration was postulated.

*Acknowledgments: National Science Centre in Poland (Grant No. 2018/29/B/ST5/00137) is acknowledged for the financial support.*

**References:** 1 J. A. Cecilia, C. García-Sancho, C. P. Jiménez-Gómez, R. Moreno-Tost and P. Maireles-Torres, *Materials (Basel)*, 2018, 11, 1–19.

2 S. T. Wu, Q. M. She, R. Tesser, M. Di Serio and C. H. Zhou, *Catal. Rev. - Sci. Eng.*, 2020, 62, 481–523.

## **Catalytic Properties**

FEZA21-PO-053

### **Gas-phase continuous-flow ketonization of propionic acid over Al, Zr, La phosphates and related oxides**

J. De Maron<sup>1,\*</sup>, L. Bellotti<sup>1</sup>, A. Baldelli<sup>1</sup>, T. Tabanelli<sup>1</sup>, C. Lucarelli<sup>2</sup>, N. Dimitratos<sup>1</sup>, F. Cavani<sup>1</sup>

<sup>1</sup>Dipartimento di Chimica Industriale "Toso Montanari", Unibo, Bologna, <sup>2</sup>Dipartimento di Scienza e Alta Tecnologia, Uninsubria, Como, Italy

#### **Abstract Text:**

In recent years, the pyrolysis of lignocellulosics materials and the upgrading of the resulting bio-oils to bio-fuels and/or bio-chemicals have emerged as frontier research domains<sup>1</sup>. In particular, the catalytic ketonization of carboxylic acids is now widely recognized as a promising strategy to remove acidity from bio-oils and increase calorific power by reducing oxygen content and creating new C-C bonds at the same time<sup>2</sup>.

In this context, propionic acid (PA) ketonization has been extensively investigated over metal oxides<sup>3</sup>; however, to the best of our knowledge, the activity of metal phosphates is unknown for this reaction. In this work, the continuous-flow ketonization of PA to yield 3-pentanone (3-Pa) was investigated in the gas-phase over metal phosphates of Al, Zr and La. These materials were synthesized by means of precipitation using aqueous NH<sub>3</sub> as the base and their physico-chemical properties and morphology were thoroughly characterized by means of X-ray diffraction on powder, X-ray fluorescence, N<sub>2</sub> porosimetry with the BET method and temperature programmed desorption of CO<sub>2</sub> and NH<sub>3</sub>. The corresponding metal oxides (Al<sub>2</sub>O<sub>3</sub>, ZrO<sub>2</sub>, La<sub>2</sub>O<sub>3</sub>) have been synthesized adapting the precipitation techniques used to prepare the phosphates and tested for comparison. The obtained metal phosphates were amorphous while metal oxides were poorly crystalline.

It is generally accepted that ketonization proceeds faster over catalysts possessing a strong amphoteric character: this behaviour is confirmed by the higher activity of metal oxides in respect to the respective phosphates (which completely lacks any basicity) and by the activity order ZrO<sub>2</sub> > La<sub>2</sub>O<sub>3</sub> > Al<sub>2</sub>O<sub>3</sub> (Image 1a). However, despite their lack of basicity metal phosphates were nonetheless able to catalyse to a certain extent PA ketonization and their activity increased with their acidity (i.e., Al/P/O > Zr/P/O > La/P/O) (Image 1b). Interestingly, Al/P/O was slightly more active than the respective oxide.

Starting from these results, a hydrothermal synthetic technique involving urea decomposition as *in situ* source of NH<sub>3</sub> was developed and optimized allowing to obtain a ZrO<sub>2</sub> catalyst with enhanced physico-chemical properties such as much higher specific surface area and stronger Lewis surface acid/base pairs (as demonstrated by N<sub>2</sub> porosimetry and NH<sub>3</sub> and CO<sub>2</sub> TPD characterizations).

The catalytic activity of this material was then investigated in reaction conditions similar to those used industrially for the synthesis of 3-Pa (e.g. high reactant concentration, conversion and selectivity as high as possible to avoid recycle). Results obtained as a function of time on stream by feeding 20 mol % PA diluted in N<sub>2</sub> at T = 400 °C obtaining a stable 100 % PA conversion and 98 % 3-Pa yield during the first 10 hours of reaction. PA conversion slowly decreased down to 80 % during the following 10 hours of reaction suggesting the occurrence of a deactivation phenomenon, but a very high 3-Pa selectivity (98 %) was maintained. Finally, regeneration at 450 °C for 3 hours with 20 mL/min of air allowed to recover most of the catalytic activity and selectivity.

The obtained 3-Pa productivity of 7.5 h<sup>-1</sup> (calculated as the mL of 3-Pa produced in 1 hour divided by the mL of catalyst used) is higher than most of those reported for the same reaction in the academic and patent literature<sup>3-7</sup> (Image 2).

#### **Image 1:**

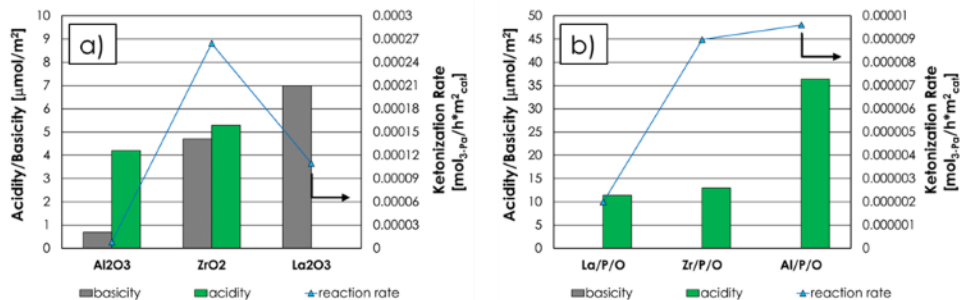


**Image 2:**

Catalyst	$\tau$ [sec]	T [°C]	% PA feed	X <sub>PA</sub>	Y <sub>3-P</sub>	P <sub>M</sub> [h <sup>-1</sup> ]	P <sub>V</sub> [h <sup>-1</sup> ]	Ref.
m-ZrO <sub>2</sub> -HT	0,1	400	20	99	98	5,7	7,5	This work
19 wt. % MnO <sub>2</sub> /Al <sub>2</sub> O <sub>3</sub>	4	370	85	99	98	/	0,75	4
TiO <sub>2</sub>	7	360	60	100	99	/	0,31	5
Zr/Ce/Mn/O (Mn 40 mol %)	/	350	/	/	/	1,9	/	6
Mn/Ce/O (Mn 60 mol %)	0,3*	350	35	93	91	3,6	/	7
52 wt. % U <sub>2</sub> O <sub>5</sub> /SiO <sub>2</sub>	0,3	425	9,9	100	97	/	0,98	3

### References:

- (1) G. Wang et al, A Review of recent advances in biomass pyrolysis, *Energy Fuels* 34 (2020) 15557–15578.
- (2) T. N. Pham et al, Ketonization of carboxylic acids: mechanisms, catalysts, and implications for biomass conversion, *ACS Catalysis* 3 (2013), 2456–2473.
- (3) M. Glinski et al, Catalytic ketonization over metal oxide catalysts. XIII. Comparative measurements of activity of oxides of 32 chemical elements in ketonization of propanoic acid, *Applied Catalysis A: General* 470 (2013) 278–284.
- (4) G. P. Hussmann, US4754074, Preparation of dialkyl ketones from aliphatic carboxylic acids, 1988.
- (5) C. Schommer et al, US4950763, Preparation of ketones, 1990.
- (6) H. Dou et al, US8748670B1, Highly active oxide catalysts for the catalytic ketonization of carboxylic acids, 2014.
- (7) O. Nagashima et al, Ketonization of carboxylic acids over CeO<sub>2</sub>-based composite oxides, *Journal of Molecular Catalysis A: Chemical* 227 (2004) 231–239.

## Catalytic Properties

FEZA21-PO-054

### Effect of mesoporous in zeolites for the selective conversion of carbohydrates into methyl lactate.

A. Sacchetti\*, I. Tosi<sup>1</sup>, T. Tabanelli<sup>2</sup>, F. Cavani<sup>2</sup>, A. Riisager<sup>3</sup>

<sup>1</sup>Technical University of Denmark, Department of Chemistry Kemitorvet, Lyngby, Denmark, <sup>2</sup>Industrial Chemistry, Alma Mater Studiorum- Università di Bologna, Bologna, Italy, <sup>3</sup>Technical University of Denmark, Department of Chemistry Kemitorvet, Lyngby, Denmark

**Abstract Text:** The depletion of fossil fuels and the need to find eco-friendly alternative resources has pushed the academic and industrial research to find renewable and more sustainable alternatives for every-day use goods like plastics. A well-known example is given by lactic acid (LA) and its esters (e.g. methyl lactate, ML) which represent promising bio-building blocks: they derive from renewable biomass like sugarcane and corn, and are used for the production of polylactic acid (PLA) which is a biodegradable thermoplastic polyester. With an industrial production of 206 Ktons<sup>[1]</sup> per year, PLA finds a wide range of applications ranging from plastic bottles, textiles and food packages. The production of ML from glucose had already shown great efficiency when using a Sn-beta zeolite (Sn-BEA) as catalyst due to the synergistic effect of Lewis acid sites and crystalline structure<sup>[2]</sup>. However, the microcrystalline structure present in the zeolite can lead to some limitations (i.e. diffusional) when dealing with bulky substrates, limiting the range of choice among substrates. Therefore, we decided to investigate different synthetic routes for the controlled formation of mesopores in two zeolites frameworks (FAU and BEA) and test their activity and selectivity towards bulky molecules, which are easily found in unprocessed biomass substrates.

After proper characterization, these new catalysts (Sn-BEA<sub>meso</sub> and Sn-USY<sub>meso</sub>) were tested not only with glucose, but with inulin and sucrose, which are oligomers of fructose and glucose, respectively. This permits a direct comparison between the well-known microporous system and the new mesoporous ones. <sup>1</sup>H-<sup>13</sup>C HSQC allowed the distinction of the different sugars and methyl glycosides. Quantification of products was performed relative to internal quantification standards using <sup>13</sup>C NMR.

The contemporary presence of micro and meso pores inside the zeolite allowed the full substrate conversion with unaffected yield into ML (Y<sub>ML</sub>=20% after 2 hours), confirming the selectivity of these newly synthesized materials toward the target product in standard reactions conditions (Microwave reaction, substrate 3 wt%, 5 mL MeOH, catalyst 1 wt%, 80  $\mu$ L DMSO as internal standard, 160 °C, 2-4 hours). A determinant step for the ML production is the formation of methyl fructosides, which are intermediates formed from fructose in the early stage of the reaction. Therefore, we performed short time reaction (5-15 minutes), to evaluate their formation rates. Comparing with the microporous systems, improvement towards methyl fructosides yields were reached for both mesoporous catalysts, increasing from 4% to 8,5% in case of Sn-BEA<sub>meso</sub> and from 3% to 6% for Sn-USY<sub>meso</sub>. The same trend of improvement was maintained for longer reaction time (4 hours), leading to an increase in methyl fructosides yields of 10% compared to the results obtained with microporous systems. A higher amount of ML was a direct consequence of higher and faster formation of the intermediates. This was explained by the presence of mesopores that avoid diffusional limitations, speeding up the reaction rate and the substrate solvolysis<sup>[3]</sup>. The obtained results evidenced the key role of the internal pore distribution of the catalyst for the occurrence of the target reaction and the importance of shape selectivity towards reagents.

**Image 1:**

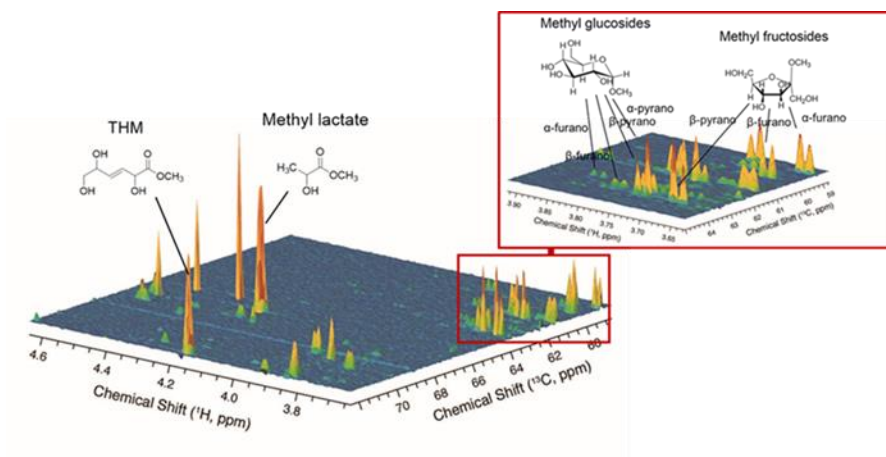
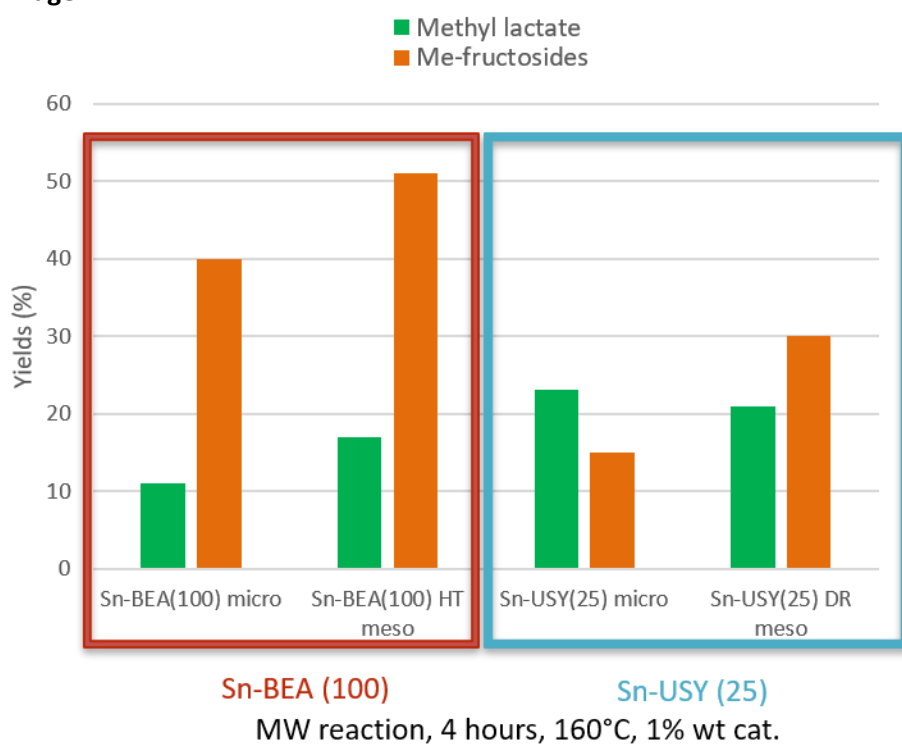


Image 2:



References: [1] European Bioplastics, nova-Institute (2017)

[2] Holm, M.S., S. Saravanamurugan, and E. Taarning, Science, 2010. 328(5978): p. 602-605.

[3] I. Tosi, A. Sacchetti, J. S. Martinez-Espin, S. Meier and A. Riisager, Topics in Catalysis volume 62, pages 628–638 (2019)

## **Catalytic Properties**

FEZA21-PO-055

### **Application of Nanostructured Silicas with Different Pores as Support Materials for Plasmonic Nanocatalysts**

Y. Yamazaki<sup>1,\*</sup>, Y. Kuwahara<sup>1,2,3</sup>, K. Mori<sup>1,2</sup>, H. Yamashita<sup>1,2</sup>

<sup>1</sup>Graduate School of Engineering, Osaka University, Osaka, <sup>2</sup>Elements Strategy Initiative for Catalysts and Batteries (ESICB), Kyoto University, Kyoto, <sup>3</sup>PRESTO, Japan Science and Technology Agency (JST), Saitama, Japan

**Abstract Text:** Metal nanoparticles, such as silver, gold, and copper are efficient materials for harvesting solar energy for chemical processes due to surface plasmon resonance (SPR). Because silver nanoparticles (Ag NPs) exhibit the highest SPR efficiency among the plasmonic metals, they have been intensively studied for surface enhanced Raman scattering, bioanalysis, and catalysis. However, the catalytic activity observed on Ag NPs by SPR is still low. For enhancement of the catalytic activity, combination of Ag NPs with a functional material as a support is an attractive approach. As the support of the composite catalyst, porous silica can be a promising candidate due to its unique structure, tunability, interesting properties, and versatile application. Macroporous structure, which is composed of hierarchically ordered macropores, exhibits light scattering properties. Mesoporous silica exhibits efficient molecules diffusion and high surface area, which are fascinating as a desirable support material for catalysts. Combining both features, macromesoporous silica composed of hierarchically ordered macropores and mesopores in the silica wall is expected to be an attractive support. Mesoporous frameworks allow to increase its surface area and enhance the efficiency of mass transfer in neighboring macropores, and macropores are expected to allow efficient scattering of incident light.

In this study, the effect of porous structure of silica supports to plasmonic Ag catalyst was investigated.

Macromesoporous silica (MMS), which is composed of hierarchically ordered macropores and mesopores with the short channels, hierarchically ordered macroporous silica (Macro), mesoporous silica (Meso), and bulk silica without porous structure (SiO<sub>2</sub>) were synthesized by a previously reported template method [1]. Ag NPs were deposited on these prepared silica supports by a microwave assisted alcohol reduction method [2]. The characteristics of four types of the prepared silica supports before and after Ag NPs deposition were investigated by SEM, TEM, XRD, N<sub>2</sub> adsorption/desorption measurement, and UV-vis spectroscopy. TEM observation revealed that Ag NPs were highly dispersed within macropores of MMS and Macro, whereas Ag NPs were deposited on the surface of Meso and SiO<sub>2</sub>. The catalytic activity was tested for 4-nitrophenol (4-NP) reduction in the presence of sodium borohydride as a reducing agent under the dark condition and visible light irradiation ( $\lambda > 420$  nm). Ag/MMS showed the highest catalytic activity under dark due to efficient mass transfer (Figure 1). Furthermore, Ag/MMS exhibited the highest activity enhancement by SPR under visible light irradiation.

**Image 1:**

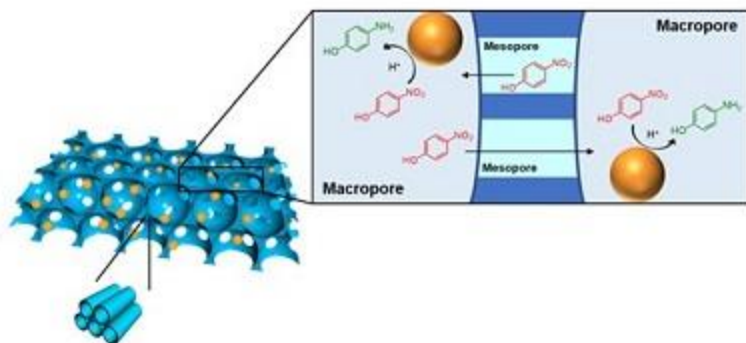


**Figure 1.** Application of Ag NPs supported on MMS for 4-NP reduction.

- References:** [1] T. Kamegawa, Y. Ishiguro, H. Seto, H. Yamashita, *J. Mater. Chem. A* 3 (2015) 2323-2330.  
[2] K. Fuku, R. Hayashi, S. Takakura, T. Kamegawa, K. Mori, H. Yamashita, *Angew. Chem. Int. Ed.* 52 (2013) 7446-7450.

## **Catalytic Properties**

FEZA21-PO-057

### **Identification of new templates for the synthesis of BEA, BEC and ISV zeolites using artificial intelligence and pattern recognition techniques**

M. Galvez-Llompart<sup>1,2,\*</sup>, J. Galvez<sup>2</sup>, F. Rey<sup>1</sup>, G. Sastre<sup>1</sup>

<sup>1</sup>Instituto de Tecnología Química, UPV-CSIC, Universidad Politecnica de Valencia, <sup>2</sup>Dept. Physical Chemistry, University of Valencia-Faculty of Chemistry, Valencia, Spain

**Abstract Text:** The presence of organic structure directing agents (templates) in the synthesis of zeolites allows the synthesis to be directed, in many cases, towards structures in which there is a large stabilisation between the template and the zeolite micropore due to dispersion interactions.<sup>1-2</sup>

Although other factors are also important (temperature, pH, Si/Al ratio, etc), systems with strong zeolite-template interactions are good candidates for an application of new computational algorithms, for instance those based in molecular topology (MT), that can be used in combination with large databases of organic molecules. Computational design of new templates allows the synthesis of existing and new zeolites to be expanded and refined.

Three zeolites with similar 3-D large pore system, BEA, BEC and ISV were selected with the aim of finding new templates for their selective synthesis. Using a training set of active and inactive templates (obtained from literature) for the synthesis of target zeolites it was possible to select chemical descriptors related to activity, meaning a good candidate template. With a discriminant function defined upon MT, the screening through a database of organic molecules led to a small subset (preselection) of candidate templates for the synthesis of BEA, BEC and ISV. As far as we know, this is the first time that topological/topochemical descriptors, which do not consider 3-D information of the molecules, have been used to predict the activity of zeolite structure directing agents (SDA).<sup>3</sup>

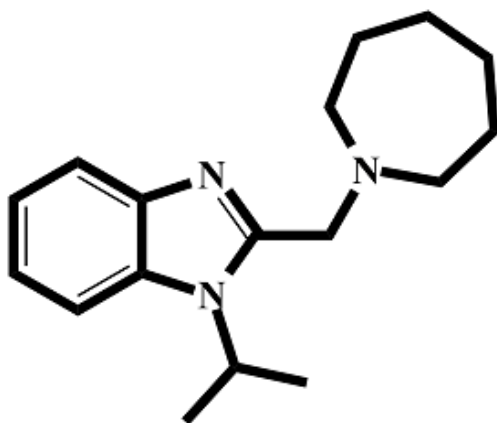
Following the prediction of SDAs using MT, an automated approach of sequential template filling of micropores based on a combination of Monte Carlo and lattice energy minimization was applied for all the candidate templates in the three zeolites. Two results can be obtained from this: an evaluation of the quality of the molecular topology Quantitative structure-activity relationship (QSAR) models leading to the preselection of templates, and, a final selection of candidate templates for the selective synthesis of BEA, BEC and ISV. Regarding the latter, a good template will be that which maximizes the zeolite-template dispersion interactions with one, and only one, of the three zeolites. The presented methodology can be used to find alternative (maybe cheaper or perhaps more selective) templates than those already known.<sup>3</sup>

An example of one of the SDAs identified as selective for the synthesis of BEC zeolite (SDA20) is presented in figure 1. An optimized location of SDA20 in BEC zeolite (4 molecules per unit cell) can be seen in figure 2.

Figure 1. Chemical representation of SDA20 (selective SDA for the synthesis of BEC zeolite).

Figure 2. Optimized location of SDA20 in BEC zeolite with a loading of 4 molecules per unit cell. BEC micropore system is shadowed and partially transparent.

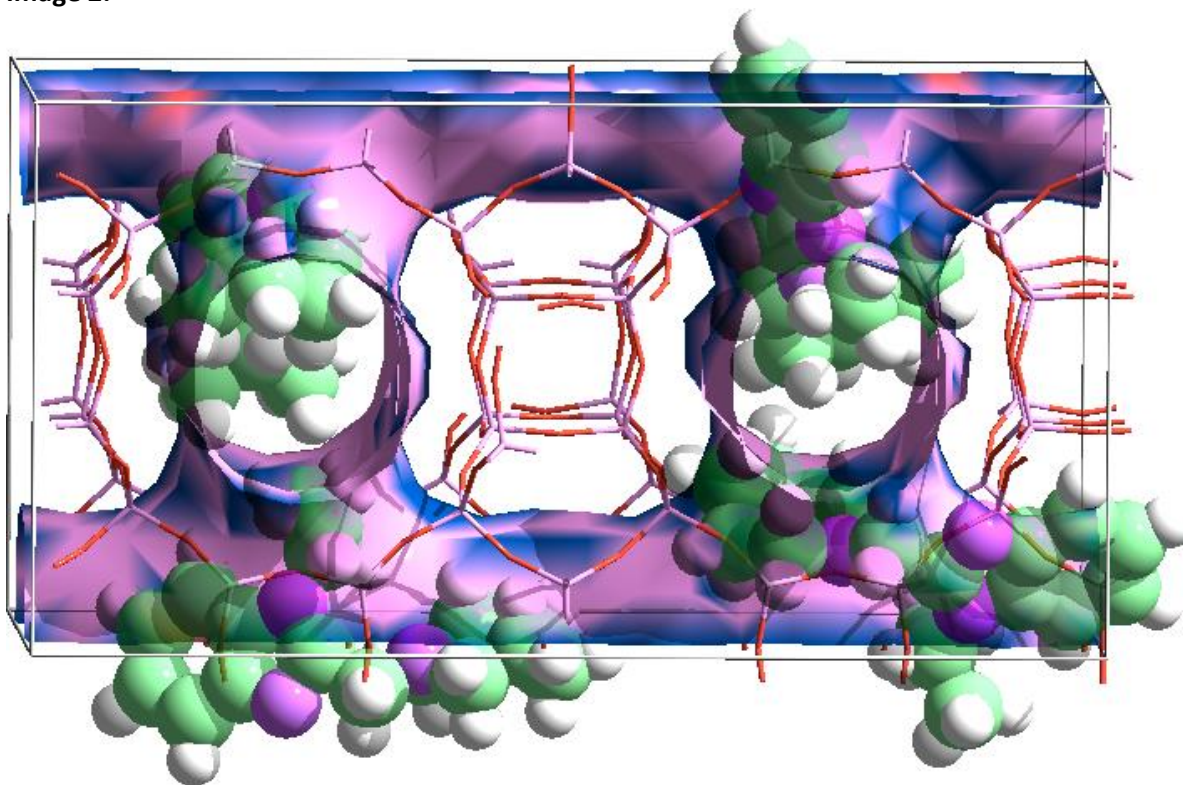
Image 1:



2-(azepan-1-ylmethyl)-1-isopropyl-1*H*-benzo[*d*]imidazole

SDA20

Image 2:



#### References:

- 1.- Moliner, M.; Rey, F.; Corma, A. Towards the Rational Design of Efficient Organic Structure-directing Agents for Zeolite Synthesis. *Angew. Chem., Int. Ed. Engl.* 2013, 52,13880-13889.
- 2.- Gálvez-Llompart, M.; Cantín, A.; Rey, F.; Sastre, G. Computational Screening of Structure Directing Agents for the Synthesis of Zeolites. A Simplified Model. *Z. Kristallogr. -Cryst. Mater.* 2019, 234, 451-460.
- 3.- Gálvez-Llompart, M.; Gálvez, J.; Rey, F.; Sastre, G. Identification of New Templates for the Synthesis of BEA, BEC and ISV Zeolites Using Molecular Topology and Monte Carlo Techniques. *J. Chem. Inf. Model.* 2020 60, 2819-2829.

## Catalytic Properties

FEZA21-PO-058

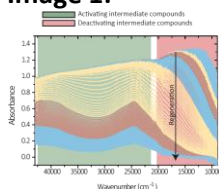
### Regeneration as an Alternative Approach to Discover Mechanistic Insights in the Methanol-to-Olefins Process Studied with Operando Spectroscopy

S. H. Van Vreeswijk<sup>1,\*</sup>, R. Oord<sup>1</sup>, B. M. Weckhuysen<sup>1</sup>

<sup>1</sup>Inorganic Chemistry and Catalysis, Utrecht University, Utrecht, Netherlands

**Abstract Text:** In methanol-to-olefins (MTO) process, methanol is converted to the more valuable molecules ethylene and propylene, which can serve as feedstocks for plastics. This process is of great commercial interest as the used methanol can be obtained from conventional as well as more renewable sources such as natural gas, biomass, carbon containing waste and CO<sub>2</sub>. [1][2] A key step in this MTO process is the formation of a so-called hydrocarbon pool, in which hydrocarbons act as active intermediates as well as deactivating compounds. The nature of the hydrocarbon pool is different for different zeolite catalysts and strongly influence the product distribution. With *operando* spectroscopy, the formation of the aromatic intermediate products and the deactivating coke molecules can be followed (*operando* UV-vis spectroscopy) and structural changes (*operando* X-ray diffraction) due to the reaction or the formation of coke can be analyzed with time-on-stream and linked to the actual reaction intermediates. [3][4] It was found that our *operando* UV-vis experiments do not only provide information on the active MTO process phase, but also on the regeneration process. Polyaromatic molecules are removed first, leaving the active aromatic intermediate molecules inside the cages of the SSZ-13 structure (**Figure 1**). The deactivating compounds could thereby selectively be removed from the catalyst. In this way we were able to establish an alternative approach to study the MTO mechanism, in which the zeolite was partially regenerated and analyzed with different (*operando* and in-situ) experiments. The lifetime of the partially regenerated samples was decreased compared to the fresh sample, but the optimum in selectivity to ethylene is reached much earlier. The lifetime and the ethylene selectivity are linear related to the carbon content and the lattice expansion, which proved that the coke is formed within the zeolite cages causing lattice expansion and that the ethylene selectivity is related to the abundance of carbon molecules. By correlating all the (*operando*) catalytic performance data and (spent) catalyst characterization, evidence for transition state selectivity and the appearance of two parallel reaction mechanisms (dual cycle mechanism) in the chabazite structure were found.

#### Image 1:



#### References: (1)

Vogt, C.; Monai, M.; Kramer, G. J.; Weckhuysen, B. M. The Renaissance of the Sabatier Reaction and Its Applications on Earth and in Space. *Nat. Catal.* 2019, 2, 188–197.

<https://doi.org/10.1038/s41929-019-0244-4>.

(2)

Kamarudin, S. K.; Shamsul, N. S.; Ghani, J. A.; Chia, S. K.; Liew, H. S.; Samsudin, A. S. Production of Methanol from Biomass Waste via Pyrolysis. *Bioresour. Technol.* 2013, 129, 463–468.

<https://doi.org/10.1016/j.biortech.2012.11.016>.

(3)

Goetze, J.; Meirer, F.; Yarulina, I.; Gascon, J.; Kapteijn, F.; Ruiz-Martínez, J.; Weckhuysen, B. M. Insights into the Activity and Deactivation of the Methanol-to-Olefins Process over Different Small-Pore Zeolites As Studied with Operando UV-Vis Spectroscopy. *ACS Catal.* 2017, 7, 4033–4046.

<https://doi.org/10.1021/acscatal.6b03677>.

(4)

Goetze, J.; Yarulina, I.; Gascon, J.; Kapteijn, F.; Weckhuysen, B. M. Revealing Lattice Expansion of Small-Pore Zeolite Catalysts during the Methanol-to-Olefins Process Using Combined Operando X-Ray Diffraction and UV-Vis Spectroscopy. *ACS Catal.* 2018, 8, 2060–2070.

<https://doi.org/10.1021/acscatal.7b04129>.

**FORMATION OF HIERARCHICAL SAPO-5 & SAPO-34 MATERIALS VIA POST-SYNTHETIC ALKALI TREATMENT AND THEIR ENHANCED CATALYTIC PERFORMANCE IN TRANSESTERIFICATION OF TRIACETIN**

D. T. Jadav<sup>1,\*</sup>

<sup>1</sup>Chemistry, IITRAM, Ahmedabad, India

**Abstract Text: Formation of hierarchical SAPO-5 & SAPO-34 materials via post-synthetic alkali treatment and their enhanced catalytic performance in transesterification of triacetin**

Divya Jadav<sup>1</sup>, Mahuya Bandyopadhyay<sup>1\*</sup>

<sup>1</sup>Institute of Infrastructure Technology Research and Management, Near Khokhara circle, Maninagar east, Ahmedabad, Gujarat 380026, India

E-mail: divya.jadav.17pc@iitram.ac.in, mahuyabandyopadhyay@iitram.ac.in

SAPO-5 and SAPO-34 materials were treated via post-synthetic alkali treatment which leads to the formation of mesoporosity. Hierarchical SAPO-5 and SAPO-34 materials found to be promising catalysts with their enhanced catalytic application in transesterification of triacetin reaction.

SAPO-5 and SAPO-34 materials were synthesized according to literature procedure [1]. Synthesized materials were modified via post-synthetic alkali treatment using mixture of NaOH and TPAOH solution. Alkali treatment leads to the formation of mesoporosity by desilication in the microporous framework. Generation of mesoporosity was identified through powder XRD, SEM, N<sub>2</sub> adsorption/desorption isotherm and ICP-OES analyses. Low angle XRD patterns in the range of 1.5° to 10° 2θ shows mesoporous peaks for alkali treated materials. Pore diameter and pore volume increases after alkali treatment again indicating the formation of mesopore to the microporous materials. Moreover, from ICP-OES analysis the decrease in Si wt% after alkali treatment confirms that desilication occurs to generate the mesoporosity, which in good agreement with literature report [2]. Prepared Hierarchical SAPO-5 and SAPO-34 materials were tested in transesterification of triacetin reaction. After thorough optimization, 90% triacetin conversion was achieved using alkali treated SAPO-5 material and 68% conversion was achieved using alkali treated SAPO-34 material. Alkali treated SAPO-5 catalyst was recyclable up to 4<sup>th</sup> cycle.

**Image 1:**

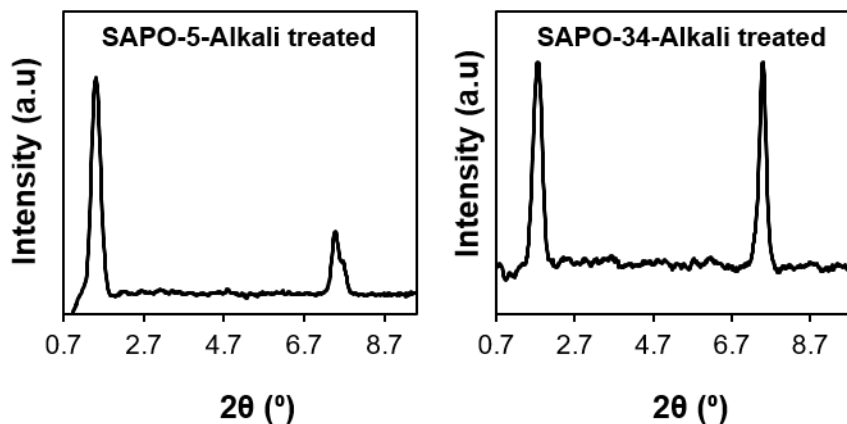
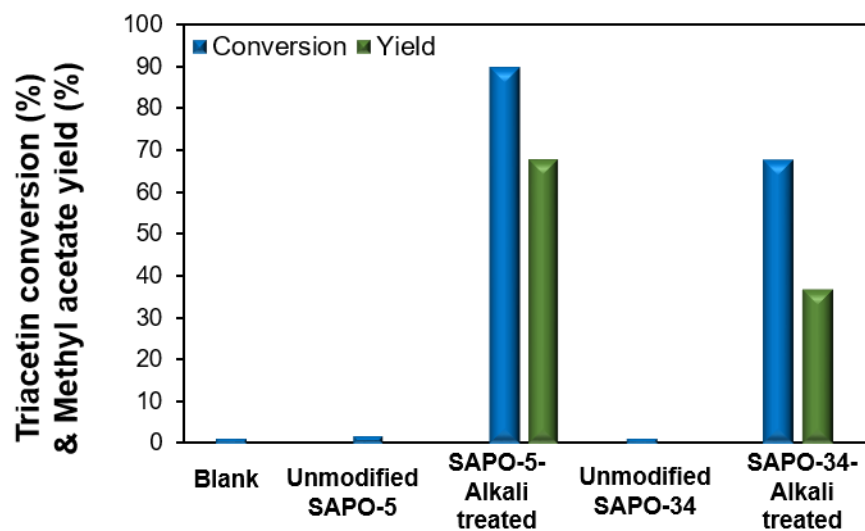


Image 2:



**References:** (1) Bandyopadhyay, M.; Bandyopadhyay, R.; Tawada, S.; Kubota, Y.; and Sugi, Y. *Appl. Catal. A Gen.* 2002, 225, 51-62.

(2) Verboekend, D.; Vilé, G.; Pérez-Ramírez, J. *Adv. Funct. Mater.* 2012, 22, 916-928.

**Encapsulation of Ni nanoparticles in Silicalite-1 for high activity and thermal stability for dry reforming of methane**

H. Fujitsuka<sup>1,\*</sup>, T. Kobayashi<sup>1</sup>, T. Tago<sup>1</sup>

<sup>1</sup>Department of Chemical Science and Engineering, Tokyo Institute of Technology, Tokyo, Japan

**Abstract Text:** Dry reforming of methane (DRM;  $\text{CH}_4 + \text{CO}_2 \rightarrow 2\text{CO} + 2\text{H}_2$ ) is one of the most promising reactions for conversion of  $\text{CO}_2$  to chemical feedstock. It has been reported that novel metals, Pt, Rh, and Pd, and base metals like Ni exhibit high activity for DRM [1]. Though Ni catalyst is desired for an industrial application, it is necessary to suppress coke formation during DRM and improve thermal stability because DRM requires high reaction temperature operation due to the highly endothermic reaction. Thus, the encapsulation structure of Ni nanoparticles in zeolite particles can be effective in high activity and thermal stability of Ni catalyst in DRM. We have succeeded in the preparation of Pt nanoparticles encapsulated in Silicalite-1 zeolite (Pt@Silicalite-1) by combining the methods for Pt nanoparticles encapsulated in amorphous silica (Pt@SiO<sub>2</sub>) in water-in-oil microemulsion solution and that for nanocrystalline zeolite in water-in-oil microemulsion solution [2]. In this study, Ni@Silicalite-1 was synthesized as a similar manner to Pt@Silicalite-1 synthesis and the activity and thermal stability of Ni@Silicalite-1 was investigated by DRM at 850 °C. For Ni@Silicalite-1 synthesis, Ni nanoparticles encapsulated in amorphous silica (Ni@SiO<sub>2</sub>) were prepared in the microemulsion solution and were added into an aqueous solution mixture containing tetraethyl orthosilicate as additional Si source and tetraethylammonium hydroxide as an organic structure-directing agent. Then, the solution was transferred into a Teflon-sealed autoclave. The hydrothermal synthesis was carried out for 3 days at 100 °C. The obtained sample was washed with isopropanol, dried overnight at 110 °C in an oven, and calcined at 550 °C for 12 h. For comparison, an incipient wetness impregnation was applied to prepare Ni loaded Silicalite-1 catalyst (Ni/Silicalite-1). Nitrogen adsorption isotherm, XRD, TEM and H<sub>2</sub> temperature-programmed reduction (H<sub>2</sub>-TPR) were used for the characterization of the prepared catalysts. The DRM reaction was performed by using a fixed bed reactor. The reaction gas composition was CH<sub>4</sub>:CO<sub>2</sub>:Ar:He = 2:2:4:1 and GHSV was varied from 108,000 to 1,080,000 mL-STP/(g-cat·h). The product gas was analyzed by an on-line gas chromatograph.

N<sub>2</sub> adsorption isotherm and the XRD pattern indicated the formation of MFI type zeolite for both catalysts. As shown in Figure 1, TEM image of the as-prepared Ni@Silicalite-1 showed a needle-shaped material of Ni and 2–6 nm of Ni nanoparticles were observed inside the zeolite particles after the reduction at 850 °C. This result suggests that Ni phyllosilicate, a sheet silicate material consisting of NiO and SiO<sub>2</sub> [3], was formed during hydrothermal synthesis. To elucidate the formation of Ni phyllosilicate during the synthesis of Ni@Silicalite-1, H<sub>2</sub>-TPR was conducted. The reduction peak of Ni species in Ni@Silicalite-1 was observed above 700 °C, which was consistent with the reduction temperature of Ni phyllosilicate in literature [3]. On the other hand, around 30 nm of Ni nanoparticles were observed by TEM after reduction of Ni/Silicalite-1 at 850 °C and the reduction peak of Ni species in Ni/Silicalite-1 was observed around 500 °C. Therefore, we concluded that Ni@Silicalite-1, which encapsulates Ni nanoparticles inside the zeolite, was successfully prepared by using Ni@SiO<sub>2</sub> due to the formation of Ni phyllosilicate inside zeolite.

Finally, the DRM of the prepared catalysts was tested at 850 °C to check their activity and thermal stability. The initial conversions of CH<sub>4</sub> and CO<sub>2</sub> of Ni@Silicalite-1 were higher than those of Ni/Silicalite-1 at all GHSVs tested as shown in Figure 2, which was attributed to Ni particle sizes. After the DRM, the Ni particle size of Ni@Silicalite-1 was maintained at 2–6 nm. In conclusion, the encapsulation structure of Ni nanoparticles inside zeolite particles successfully enhanced the activity and thermal stability because Ni nanoparticles were physically immobilized inside the zeolite.

### Image 1:

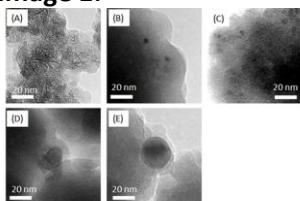


Figure 1. The TEM images of Ni@Silicalite-1 (A) as-prepared, (B) after reduction at 850 °C, and (C) after DRM at 850 °C for 5 h, and Ni/Silicalite-1 (D) as-prepared and (E) after reduction at 850 °C.

### Image 2:

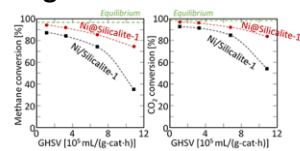


Figure 2. The CH<sub>4</sub> and CO<sub>2</sub> conversions in DRM over the prepared catalysts at 850 °C and various GHSV

**References:** [1] S. Arora, R. Prasad, RSC Adv. 6 (2016) 108668-108688.

[2] T. Kobayashi, T. Furuya, H. Fujitsuka, T. Tago, Chem. Eng. J. 377 (2019) 120203-120210.

[3] Z. Bian, S. Kawi, ChemCatChem 9 (2001) 29-35.

## Catalytic Properties/Zeolites/Inorganic materials

FEZA21-PO-066

### Study of Coke Formation in 1,3-butanediol Dehydration Reaction.

A. C. Rodriguez<sup>1,\*</sup>, M. E. Sad<sup>1</sup>, A. Astafan<sup>2</sup>, M. Tarighi<sup>2</sup>, C. L. Padró<sup>1</sup>, L. Pinard<sup>2</sup>

<sup>1</sup>Instituto de Investigaciones en Catálisis y Petroquímica, Facultad de Ingeniería Química-UNL, Santa Fe, Argentina,

<sup>2</sup>Institut de Chimie des Milieux et des Matériaux de Poitiers, Université de Poitiers, Poitiers, France

#### Abstract Text:

##### Introduction

1,3-butadiene (BD) is an important intermediate used for synthetic rubber, elastomers and polymeric resins manufacture [1]. BD is mainly obtained as a by-product of steam cracking of naphtha and gas oil for ethylene production. However, in recent years this way of production of ethylene has been partly replaced by lighter raw materials coming from shale gas and consequently the butadiene from non-renewable resources has decreased. Therefore, it is highly desirable to find an alternative route starting from renewable feedstock. Between the alternative routes proposed, the dehydration of 1,3 butanediol (1,3BDOL) using acid catalysts is becoming attractive for bio-BD production with high yields [2]. However, the main drawback is the formation of carbonaceous deposits that deactivate the catalysts. Therefore, the objective of this work was to study the coke formed during the 1,3-BDOL dehydration and how this affects the catalytic performance.

##### Experimental

The catalysts used in this work were zeolite HZSM5, SiO<sub>2</sub>/Al<sub>2</sub>O<sub>3</sub>, Al<sub>2</sub>O<sub>3</sub> and HPA (Tungstophosphoric acid)/SiO<sub>2</sub>. The gas phase 1,3-BDOL dehydration was carried out in a fixed bed reactor at 523 K and 101.3 kPa. The effluent gases from the reactor were analyzed using an Agilent 6850 chromatograph. The coke retained on the outer surface of the spent catalysts was extracted with CH<sub>2</sub>Cl<sub>2</sub> and the soluble coke was analyzed by MALDI-TOF MS. The fresh, spent and washed catalysts were characterized by N<sub>2</sub> physisorption, and FTIR of pyridine. The amount of coke (%C) was determined by TGA-DTA. Also the spent catalyst was dissolved in HF solution and the residue was extracted by CH<sub>2</sub>Cl<sub>2</sub>. Insoluble coke was recovered and weighted. The soluble coke fraction was analyzed by GC-MS.

##### Results

Table 1 compares the catalytic results obtained at the same conversion ( $X_{t=0}=60\%$ ) and shows the deactivation as variation in conversion between  $t=0$  and  $t=3h$  ( $\Delta X/X^0$ ). Al<sub>2</sub>O<sub>3</sub>, which has only Lewis acid sites, showed a well differentiated behavior. It practically did not form BD but the main products formed were propene (P), formaldehyde (F), 2,4-methyl 1,3-dioxane (MD) and others (products from condensation and dehydrogenation). On the rest of the catalysts the main reaction path was dehydration with formation of unsaturated alcohol (3B1OL) and BD with a selectivity ( $S_{BD}$ ) between 41% (HZSM5) and 60% (on HPA/SiO<sub>2</sub>).

Fig. 1 a) and b) depict the characterization of fresh, spent and washed catalysts. The decrease in  $S_{BET}$  after coke deposition (%C of spent catalysts ranged 9-14%) was close to 50% on all the catalyst except HZSM5 which showed a dramatic loss of surface area exposed, and therefore of catalytic sites, probably by blocking its microporous structure. The results of FTIR using pyridine reveal a decrease of the acid sites concentration after 3 h of reaction, being particularly significant on HZSM5. Although the extraction with CH<sub>2</sub>Cl<sub>2</sub> was more effective on Al<sub>2</sub>O<sub>3</sub> (% of coke solubilized), the recovery of the acid sites was almost complete on SiO<sub>2</sub>/Al<sub>2</sub>O<sub>3</sub> (FTIR results). The extraction process produced leaching of part of HPA and as a consequence a decrease in the number of acid sites. The analysis by MALDI-TOF MS of the extracted coke (Fig. 1 c) shows significant differences in the nature of carbonaceous compounds. The deposits extracted from HPA and HZSM5 were similar and clearly heavier than those formed on SiO<sub>2</sub>/Al<sub>2</sub>O<sub>3</sub>. Moreover, the coke on SiO<sub>2</sub>/Al<sub>2</sub>O<sub>3</sub> is less toxic causing less deactivation.

In addition, after dissolution with HF, it was observed that all the catalysts had only soluble coke, except for HPA which presented 7% insoluble coke. Unlike the case of mesoporous materials, the GC-MS spectra showed the presence of aromatic compounds on the zeolite due to a shape selectivity mechanism of coke formation.

## Conclusion

The coke formed during BD production was fully characterized using different techniques revealing that its nature is strongly influenced by the structure and acidity of the catalysts.

## Image 1:

Table 1. Catalytic results

Catalyst	Selectivity at X=60 % (T=523 K, P <sub>T</sub> =1 atm, P <sub>1,3BDOL</sub> =0.018 atm)					$\frac{\Delta X}{X^0} \cdot 100$	% C	
	S <sub>BD</sub>	S <sub>P+F</sub>	S <sub>3B1OL</sub>	S <sub>MD</sub>	S <sub>Others</sub>		Spent	Washed
Al <sub>2</sub> O <sub>3</sub>	2	48	7	30	13	22	13	9
SiO <sub>2</sub> /Al <sub>2</sub> O <sub>3</sub>	44	14	14	12	16	37	14	12
HZSM5	41	9	24	11	15	67	12	9
HPA/SiO <sub>2</sub>	60	6	20	6	8	67	9	8

## Image 2:

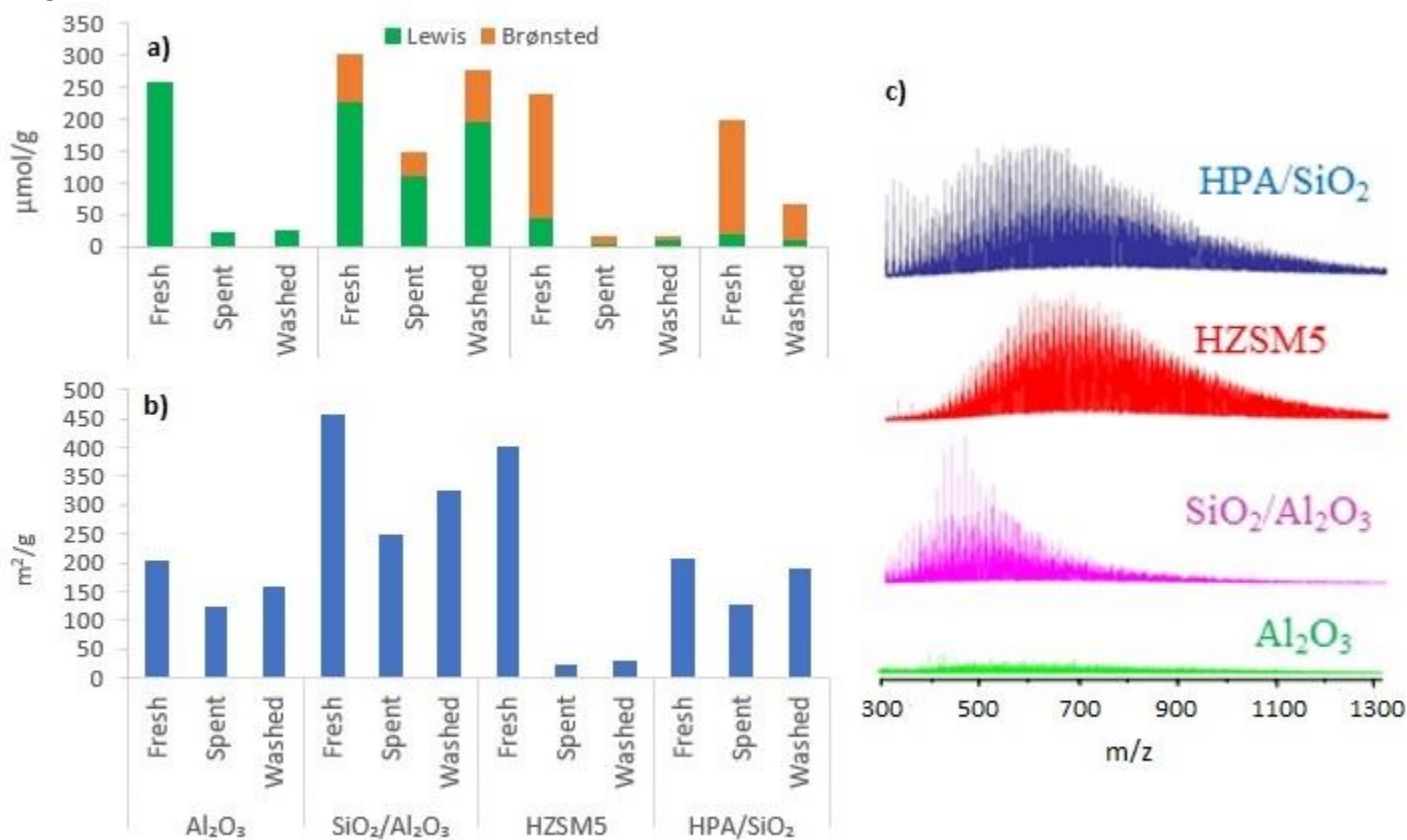


Figure 1. a) Brønsted and Lewis acidity measure. b) Specific Surface Area. c) MALDITOF-MS

## References:

1. White, W.M.C. Chem. Biol. Interface 166, 10 (2007)
2. Ichikawa, N. Sato, S. Takahashi, R. Sodesawa, T J. Mol. Catal. A: Chem. 256, 106(2006)

**Structure-activity relationship in selective oxidation of terpenes over titanasilicate catalysts**

J. Přeč 1,\*

<sup>1</sup>Dept. of Physical and Macromolecular Chemistry, Faculty Of Science, Charles University, Prague 2, Czech Republic

**Abstract Text:** Epoxides are key reactive intermediates used in chemical industry. Their production by organic synthesis requires using either chlorine and a strong base or oxidation with organic peroxides or peracids. These processes raise safety, environmental and economic issues (e.g., stoichiometric amounts of by-products must be recycled or disposed of). Titanosilicates activate hydrogen peroxide for the epoxidation of C=C double bonds. In this direct epoxidation, the only side product is water; however, to perform the reaction, particularly using a larger substrate, many catalyst variables, such as hydrophilicity, active site local environment, and accessibility, must be tuned. Accordingly, we report here investigation of such variables in titanosilicate catalysed epoxidation of terpenes, terpenoids and cyclic olefins with hydrogen peroxide as oxidant.

We followed the structure-activity relationship between the catalyst and the reaction in epoxidation of linalool, citronellol, citral, humulene, cyclodecene and cyclododecene using a set of titanosilicate catalysts with different morphology and textural properties: conventional titanium silicalite 1 (TS-1) zeolite, mesoporous TS-1, layered TS-1, pillared TS-1, and nanosponge TS-1, all having the MFI zeolite crystalline structure. The mentioned catalysts differ mostly in the morphology (conventional vs. layered) and external surface area and pore volume. In addition, mesoporous TS-1, layered TS-1, and pillared TS-1 were prepared with Ti introduced in both hydrothermal synthesis as well as post-synthesis. The reactions were performed in acetonitrile, methanol and 2-propanol as solvents at 60°C with 0.5 molar equivalent of hydrogen peroxide in respect to number of C=C double bonds.

All substrates are sterically demanding, albeit particularly citronellol, linalool and citral are somewhat flexible.

Conversions were found independent on Ti content (Si/Ti molar ratio was in range 30 – 100 for all the catalysts) but they were proportional to external surface area and mesopore volume. The more open was the structure, the higher was the conversion. Way of titanium incorporation (direct hydrothermal synthesis vs. post-synthesis incorporation), linked to the character of the active sites, influenced selectivity of linalool and citronellol epoxidation when acetonitrile was used as solvent (e.g. linalool epoxidation: linalool oxide furanoid selectivity in range 0-25% conversion was 35% over hydrothermally synthesized Ti catalysts vs. 26% silica-titania pillared TS-1 (containing both directly introduced and post-synthesis introduced titanium) vs. 21% Ti impregnated nanosponge TS-1 catalyst. When methanol is used as solvent, the difference vanished and particularly citronellol epoxide is very prone to ring opening reaction with the solvent.

Cyclodecene and cyclododecene are not well soluble in acetonitrile or methanol and thus 2-propanol was used as solvent. Conversion of these bulky substrates is defined by active site accessibility and the epoxides are stable under the reaction conditions. Thus selectivity above 90% was achieved at 10% conversion using all the layered TS-1, pillared TS-1 and nanosponge TS-1. On the other hand, expectably, conventional TS-1 and mesoporous TS-1 were almost inactive in this reaction due to diffusion restrictions.

In conclusion, all the studied epoxidation reactions were diffusion-driven. Way of Ti incorporation appears to have a slight influence on selectivity of terpenoids epoxidation under particular conditions but it is linked to the solvent effect. In contrast, no such influence was observed for epoxidation of large cyclic olefins.

## ***Catalytic Properties/Zeolites/Inorganic materials***

FEZA21-PO-070

### **Zeolite catalyst design for heat neutral NTO and MTO reaction**

Y.-K. Park<sup>1,\*</sup>, N. Y. Kang<sup>1</sup>, Y. J. Lee<sup>1</sup>, J. Shin<sup>1</sup>

<sup>1</sup>Research Center for Convergent Chemical Process, Korea Research Institute of Chemical Technology, Daejeon, Korea, Republic Of

**Abstract Text:** Light olefins (ethylene, propylene) have been produced by conventional thermal cracking which is energy intensive (endothermic, 800-900 °C) and relatively high in by-product formation [1]. Recently, as an alternative, two new fluidized-bed processes were suggested by KBR and DICI to produce propylene-rich light olefins: one is the catalytic naphtha cracking process (K-COT<sup>TM</sup>) and the other is the methanol to propylene process (DMTP<sup>TM</sup>).

As shown in Table 1, naphtha-to-olefin (NTO) and methanol-to-olefin (MTO) reactions have the opposite characteristics in heat of reaction: 890 kcal/kg-ethylene of heat energy is required for NTO (endothermic) while 199 kcal/kg-ethylene of heat energy is generated during reaction (exothermic). If these two reactions are carried out together, it is possible to produce the light olefins in heat neutral condition [2]. However, due to the differences of reaction temperature and reaction mechanism, the catalyst should be designed carefully for the selective production of light olefins.

To carry out the NTO and MTO reactions simultaneously, relatively high reaction temperature is required. However, if the catalyst is not prepared properly, a lot of low-valued by-product such as CO and CH<sub>4</sub> are produced. According to our recent study, the controlling of physical and chemical properties of catalyst is quite important to hybridize the NTO and MTO reactions successfully: the control of pore size and acidity of zeolite catalyst is quite critical to suppress these by-product formation during the reaction.

The formation of by-products is mainly induced in the MTO reaction: the thermally unstable dimethyl ether (DME) is formed very rapidly from MeOH by dehydration and the formed DME is transformed into CO and CH<sub>4</sub> through auto-thermal decomposition if it is not managed well by the catalyst. To prevent this auto-thermal decomposition of DME in the external site of zeolite and to induce only MTO reaction, it is necessary to control external acid site and pore size distribution of zeolites. If the acidity and porosity of zeolite are controlled well, the level of by-product formation could be reduced to less than 5.0 wt% even in the hybridized NTO and MTO reaction.

For commercial application, the catalyst should be prepared in micro-spherical form having the size of 100 micron.

When preparing the micro-spherical catalyst, the control of the porosity is also important. If mass transfer limit exists in the catalyst, it is difficult to expect high light olefin yield due to secondary reaction such as an olefin interconversion, oligomerization, cyclization and hydrogen transfer. To minimize mass transfer limit, it is necessary to prepare the catalyst with a hierarchical pore structure. To make a catalyst with the inter-connected micro-, meso- and macro-porosity, it is efficient to introduce different size of porogens to the catalyst.

Not only the hierarchical pore structure of catalyst but also the inter-connectivity of pores is important. To measure the inter-connectivity of pores, dynamic adsorption experiments were carried out by the Intelligent Gravimetric Analyser (IGA) and Accelerated Surface Area and Porosimetry System (ASAP). It provides the efficient tools to correlate cracking selectivity and inter-connectivity of catalyst pore. The porosity and inter-connectivity controlled catalyst revealed 15 wt% increase in light olefin yield than that of K-COT<sup>TM</sup>.

**Image 1:**

**Table 1**

Key issues in the hybridization of NTO and MTO.

	Naphtha to olefin (NTO)	Methanol to olefin (MTO)	Naphtha and Methanol to olefin (NMTO)
Process	K-COT™	DMTO™	NMTO
ΔH	890 kcal/kg-C <sub>2</sub> = (Endothermic)	-199 kcal/kg-C <sub>2</sub> = (Exothermic)	128 kcal/kg-C <sub>2</sub> = (Heat Neutral)
Catalyst	PZSM-5 (pore size = 5.5 Å)	SAPO-34 (pore size = 3.8 Å)	Modified Zeolite
Temp. (°C) & reactor type	~700, CFB reactor	350~500, CFB reactor	~650, CFB reactor
WHSV (h <sup>-1</sup> )	20	3	28
E+P (wt%)	34	78	52

**References:** [1] Y. Yoshimura, N. Kijima, T. Hayakawa, K. Murata, K. Suzuki, F. Mizukami, K. Matano, T. Konishi, T. Oikawa, M. Saito, T. Shiojima, K. Shiozawa, K. Wakui, G. Sawada, K. Sato, S. Matsuo, N. Yamaoka, *Catal. Surveys Jpn.* 4 (2001) 157.

[2] F. Chang, Y. Wei, X. Liu, Y. Qi, D. Zhang, Y. He, Z. Liu, *Catal. Lett.* 106 (2006) 3.

### **Catalytic Properties|Zeolites/Inorganic materials**

FEZA21-PO-071

#### **AFX synthesized by use of TEBOP as OSDA providing a better performance for NH<sub>3</sub>-SCR**

M. Ogura<sup>1,\*</sup>, M. Ehara, Y. Kubota, K. Shimizu, N. Tsunoji, T. Yokoi<sup>1</sup>Institute of Industrial Science, The University of Tokyo, Tokyo, Japan

**Abstract Text:** We have mined a specific zeolite which shows unique catalytic properties for selective catalytic reduction (SCR) of nitric oxide (NO) by use of ammonia (NH<sub>3</sub>) as the reducing agent [1]. The All-Japan project has been conducted via a collaborative study with all Japanese automobile companies under a support of consortium named AICE, where the companies get together to build up specific clean diesel technologies for low CO<sub>2</sub> emission. Among tested, some zeolite candidates were designated to study for a further step toward social implementation. Zeolite AFX having the same topology of SSZ-16, is one of the zeolites. This zeolite can be synthesized by using 1,1'-tetramethylenebis(1-azonia-4-azabicyclo[2.2.2]octane; Dab-4, resulting in the formation of Al-rich AFX with Si/Al below 5 [2]. As well as such a textbook method to be crystallized, Kubota and his coworkers have found originally that *N,N,N',N'*-tetraethylbicyclo[2.2.2]oct-7-ene-2,3:5,6-dipyrrolidinium ion, called TEBOP here, could have a function to crystallize the same analog with a bit high silica with Si/Al=6~9 having a smaller particle size [3]. The latter properties would be expected for utilization of it as the zeolitic support to load a divalent Cu ionic species showing high activity for NH<sub>3</sub>-SCR. Here we would perform to prepare an AFX-based SCR catalyst and compare its catalytic performance with the analogous SSZ-16 synthesized with Dab-4 as well as a worldwidely-used zeolite SSZ-13 having CHA structure.

The synthesis of AFX type zeolite was carried out according to the literature [3]. Characterization of the product with Cu ion exchange was conducted by XRD, ICP, NMR, TG-DTA, N<sub>2</sub> adsorption, and UV-VIS. Catalytic performance was evaluated by a flow-type reactor having the test gas composed of 300 ppmNO-300 ppmNH<sub>3</sub>-2%O<sub>2</sub>-5%H<sub>2</sub>O that was flown to 30mg Cu-containing zeolites, and the resultant gas mixture was introduced to gas analyzers which could detect the concentrations of NO/NO<sub>2</sub>, NH<sub>3</sub>, and N<sub>2</sub>O. Those tested zeolites were also treated under hydrothermal conditions using O<sub>2</sub>/H<sub>2</sub>O at most 800°C, then the physicochemical stability was investigated.

Figure 1 shows the typical catalytic NO conversions on fresh and aged AFX. Even at 800°C pretreatment under hydrothermal conditions, high conversion and a wide temperature window for NO removal were attained. Compared with conventional SSZ-13, AFX possessed a large amount of Al in the framework, which means a higher capacity for Cu ionic species active for SCR. More Cu ionic species could be maintained on AFX, nevertheless extra-framework Cu oxide species might exist to catalyze NH<sub>3</sub> oxidation with oxygen coexisted in the reactant stream. On SSZ-13, the selectivity of NH<sub>3</sub> for SCR was worse, and thus the activity window became narrower in particular at high temperatures, while AFX demonstrated a wide active window for SCR.

It is quite interesting to note that SSZ-16 synthesized with Dab-4 demonstrated the comparable NO abatement activity in its fresh form, but much less activity was confirmed on the aged sample. Silicon-29 MASNMR suggests that Al distribution in their frameworks seems quite different between AFX by TEBOP and SSZ-16 by Dab-4, which might contribute to a better performance on the aged media even it has still a quantity of Al in the framework. This feature derives from the rigidity and accommodation of one TEBOP molecule that fits well in one *qft* cage of AFX structure. Moreover, the distance of negatively-charged N atoms in the identical molecule of TEBOP brings forth the highly distributed location of Al in the framework as well as highly dispersed Cu ionic species.

As a conclusion, we could find a unique property of AFX which derives from the nature of OSDA used for the synthesis, leading to fine control of Al distribution and thus hydrothermal stability.

**References:** [1] Vishnupriya, et al., Bull. Chem. Soc. Jpn., 91, 355 (2018).

[2] Lobo, Zones, Medrud, Chem. Mater., 8, 2409 (1996).

[3] Nakazawa, Inagaki, Kubota, Adv. Porous Mater., 4, 219 (2016).

## Catalytic Properties|Zeolites/Inorganic materials

FEZA21-PO-075

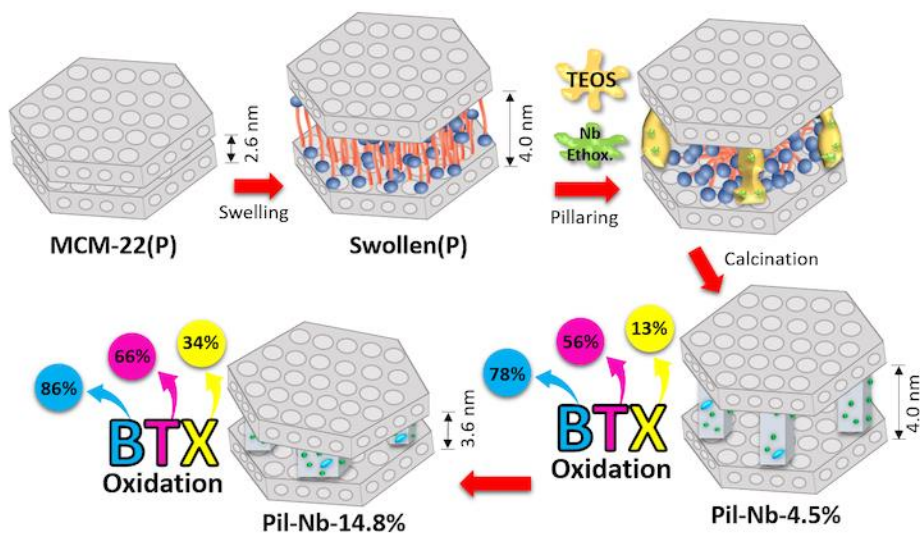
### Pillared lamellar MWW zeolite with silicon and niobium oxides: Active catalyst for the oxidation of volatile organic compounds

A. J. Schwanke<sup>1</sup>, R. Balzer<sup>2</sup>, C. W. Lopes<sup>1</sup>, D. M. Meira<sup>3</sup>, U. Diaz<sup>4</sup>, A. Corma<sup>4</sup>, S. Pergher<sup>5,\*</sup>

<sup>1</sup>Chemistry, UFRGS, Porto Alegre, <sup>2</sup>Chemistry, UFPR, Palotina, Brazil, <sup>3</sup>CLS@APS setor 20, Argonne National Laboratory, Argonne, United States, <sup>4</sup>Chemistry, ITQ/UPV, Valencia, Spain, <sup>5</sup>Chemistry, UFRN, Natal, Brazil

**Abstract Text:** In this work, an MWW-type zeolite with pillars containing silicon and niobium oxide was synthesized to obtain a hierarchical zeolite. The obtained materials were characterized by: Powder X-ray diffraction (XRD); Nitrogen adsorption isotherms at -196 °C; Inductively coupled plasma optical emission spectrometry (ICP-OES); Field-emission scanning electron microscopy (FESEM); Transmission electron microscopy (TEM); Fourier transform infrared (FTIR) spectrometry with adsorption-desorption of pyridine; Diffuse reflectance UV-Vis (DR UV-Vis) spectroscopy; X-ray Absorption Spectroscopy experiments were carried out at Nb K-edge (18986 eV) at the 20 BM beamline of Argonne National Laboratory and EXAFS. The effect of niobium insertion in the pillaring process was determined by combining a controllable acidity and accessibility in the final material. All pillared materials had niobium occupying framework positions in pillars and extra-framework positions. The pillared material, Pil-Nb-4.5 with 4.5 wt% niobium, did not compromise the mesoporosity formed by pillaring, while the increase of niobium in the structure gradually decreased the mesoporosity and ordering of lamellar stacking. The morphology of the pillared zeolites and the niobium content were found to directly affect the catalytic activity. Specifically, we report on the activity of the MWW-type zeolites with niobium catalyzing the gas-phase oxidation of volatile organic compounds (VOCs), which is an important reaction for environmental remediation. All produced MWW-type zeolites with niobium were catalytically active, even at low temperatures and low niobium loading, and provided excellent conversion efficiencies.

#### Image 1:



**References:** [1] M. Misono, in M. Makoto (Editor), *Stud. Surf. Sci. Catal.*, Vol. Volume 176, Elsevier, 2013, p. 1.

[2] X. Zhang, J. Guo, P. Guan, C. Liu, H. Huang, F. Xue, X. Dong, S.J. Pennycook and M.F. Chisholm, *Nature Commun.*, 4 (2013) 1924.

[3] W. Yan, G. Zhang, H. Yan, Y. Liu, X. Chen, X. Feng, X. Jin and C. Yang, *ACS Sus. Chem. Eng.*, 6 (2018) 4423.

[4] H. Sasai and S. Takizawa, *Sustainable Catalysis: With Non-endangered Metals, Part 1*, The Royal Society of Chemistry, 2016, p. 216.

[5] M. Ziolk and I. Sobczak, *Catal. Today*, 285 (2017) 211.

[6] K. Tanabe, *Catal. Today*, 78 (2003) 65.

- [7] K. Nakajima, Y. Baba, R. Noma, M. Kitano, J. N. Kondo, S. Hayashi and M. Hara, *J. Am. Chem. Soc.*, 133 (2011) 4224.
- [8] I. Nowak and M. Ziolek, *Chem. Rev.*, 99 (1999) 3603.
- [9] M.E. Davis, *Nature*, 417 (2002) 813.
- [10] K. Li, J. Valla and J. Garcia-Martinez, *ChemCatChem*, 6 (2014) 46.
- [11] J. Perez-Ramirez, C.H. Christensen, K. Egeblad, C.H. Christensen and J.C. Groen, *Chem. Soc. Rev.*, 37 (2008) 2530.
- [12] W. Schwieger, A.G. Machoke, T. Weissenberger, A. Inayat, T. Selvam, M. Klumpp and A. Inayat, *Chem. Soc. Rev.*, 45 (2016) 3353.
- [13] U. Diaz and A. Corma, *Dalton Trans.*, 43 (2014) 10292.
- [14] S. Maheshwari, C. Martínez, M. Teresa Portilla, F.J. Llopis, A. Corma and M. Tsapatsis, *J. Catal.*, 272 (2010) 298.
- [15] E. Dumitriu, F. Secundo, J. Patarin and I. Fechete, *J. Mol. Catal. B: Enzym.*, 22 (2003) 119.
- [16] W. J. Roth, J. C. Vartuli and C. T. Kresge, in S. Abdelhamid and J. Mietek (Editors), *Stud. Surf. Sci. Catal.*, Vol. Volume 129, Elsevier, 2000, p. 501.
- [17] J.-O. Barth, J. Kornatowski and J.A. Lercher\*, *J. Mater. Chem.*, 12 (2002) 369.
- [18] J.-O. Barth, A. Jentys, E.F. Iliopoulou, I.A. Vasalos and J.A. Lercher, *J. Catal.*, 227 (2004) 117.
- [19] F. Jin, S. Huang, S. Cheng, Y. Wu, C.-C. Chang and Y.-W. Huang, *Catal. Sci. Technol.*, 5 (2015) 3007.
- [20] A. Wojtaszek-Gurdak, M. Zielinska and M. Ziolek, *Catal. Today*, (2018).
- [21] T. Ushikubo, *Catal. Today*, 57 (2000) 331.
- [22] G. Sberveglieri, V. Ferrari, A. Bertuna, E. Comini, N. Poli, D. Zappa and G. Sberveglieri, *Procedia Engineering*, 87 (2014) 807.
- [23] G. Zhen, V. Egli, J. Vörös, P. Zammaretti, M. Textor, R. Glockshuber and E. Kuennemann, *Langmuir*, 20 (2004) 10464.
- [24] A. Corma, F.X. Llabrés i Xamena, C. Prestipino, M. Renz and S. Valencia, *J. Phys. Chem. C*, 113 (2009) 11306.
- [25] M. Trejda, A. Wojtaszek, A. Floch, R. Wojcieszak, E.M. Gaigneaux and M. Ziolek, *Catal. Today*, 158 (2010) 170.
- [26] A. Wojtaszek, M. Ziolek, S. Dzwigaj and F. Tielens, *Chem. Phys. Lett.*, 514 (2011) 70.
- [27] M. Hartmann, A.M. Prakash and L. Kevan, *Catal. Today*, 78 (2003) 467.
- [28] F. Tielens, T. Shishido and S. Dzwigaj, *J. Phys. Chem. C*, 114 (2010) 3140.
- [29] I. Sobczak, N. Kieronczyk, M. Trejda and M. Ziolek, *Catal. Today*, 139 (2008) 188.
- [30] M. Trejda, A. Tuel, J. Kujawa, B. Kilos and M. Ziolek, *Microporous Mesoporous Mater.*, 110 (2008) 271.
- [31] B. Kilos, A. Tuel, M. Ziolek and J.-C. Volta, *Catal. Today*, 118 (2006) 416.
- [32] A.S. Dias, S. Lima, D. Carriazo, V. Rives, M. Pillinger and A.A. Valente, *J. Catal.*, 244 (2006) 230.
- [33] A.M. Prakash and L. Kevan, *J. Am. Chem. Soc.*, 120 (1998) 13148.
- [34] A.G.M. da Silva, T.S. Rodrigues, E.G. Candido, I.C. de Freitas, A.H.M. da Silva, H.V. Fajardo, R. Balzer, J.F. Gomes, J.M. Assaf, D.C. de Oliveira, N. Oger, S. Paul, R. Wojcieszak and P.H.C. Camargo, *J. Colloid Interf. Sci.*, 530 (2018) 282.
- [35] R. Balzer, L.F.D. Probst, H.V. Fajardo, F.S. Teodoro, L.V.A. Gurgel and L.F. Gil, *Industrial Crops and Products*, 97 (2017) 649.
- [36] S. Brunauer, P.H. Emmett and E. Teller, *J. Am. Chem. Soc.*, 60 (1938) 309.
- [37] K.S.W. Sing, D.H. Everett, R.A.W. Haul, L. Moscou, R.A. Pierotti, J. Rouquerol, T. Siemieniowska and *Pure Appl. Chem*, 57 (1985) 603.
- [38] C.A. Emeis, *J. Catal.*, 141 (1993) 347.
- [39] B. Ravel and M. Newville, *J Synchrotron Radiat*, 12 (2005) 537.
- [40] M.A. Cambor, A. Corma, M.-J. Díaz-Cabañas and C. Baerlocher, *J. Phys. Chem. B*, 102 (1998) 44.

- [41] G.G. Juttu and R.F. Lobo, *Microporous Mesoporous Mater.*, 40 (2000) 9.
- [42] P. Chlubná, W.J. Roth, A. Zukal, M. Kubů and J. Pavlatová, *Catal. Today*, 179 (2012) 35.
- [43] A. Ramanathan, R. Maheswari and B. Subramaniam, *Top. Catal.*, 58 (2015) 314.
- [44] A. Wojtaszek-Gurdak and M. Ziolek, *RSC Adv.*, 5 (2015) 22326.
- [45] M.K. Bahl, *J. Phys. Chem. Solids*, 36 (1975) 485.
- [46] S.L. Fernandes, L.G.S. Albano, L.J. Affonço, J.H.D.d. Silva, E. Longo and C.F.d.O. Graeff, *Frontiers in Chemistry*, 7 (2019).
- [47] H. Yoshida, T. Tanaka, T. Yoshida, T. Funabiki and S. Yoshida, *Catal. Today*, 28 (1996) 79.
- [48] C. Tiozzo, C. Bisio, F. Carniato, A. Gallo, S.L. Scott, R. Psaro and M. Guidotti, *Phys. Chem. Chem. Phys.*, 15 (2013) 13354.
- [49] A. Corma, X. Labrés i Xamena, C. Prestipino, M. Renz and S. Valencia, *J. Phys. Chem. C*, 113 (2009) 11306.
- [50] P. Matias, J.M. Lopes, S. Laforge, P. Magnoux, P.A. Russo, M.M.L. Ribeiro Carrott, M. Guisnet and F. Ramôa Ribeiro, *J. Catal.*, 259 (2008) 190.
- [51] S. Laforge, P. Ayrault, D. Martin and M. Guisnet, *Applied Catalysis A: General*, 279 (2005) 79.
- [52] J.A. Cecilia, C. García-Sancho and F. Franco, *Microporous Mesoporous Mater.*, 176 (2013) 95.
- [53] M. Nolan, S.C. Parker and G.W. Watson, *Surf. Sci.*, 595 (2005) 223.
- [54] O.H. Laguna, A. Pérez, M.A. Centeno and J.A. Odriozola, *Appl. Catal. B.*, 176-177 (2015) 385.
- [55] N. Guillén-Hurtado, A. García-García and A. Bueno-López, *J. Catal.*, 299 (2013) 181.
- [56] A.G.M. da Silva, H.V. Fajardo, R. Balzer, L.F.D. Probst, A.S.P. Lovón, J.J. Lovón-Quintana, G.P. Valença, W.H. Schreine and P.A. Robles-Dutenhefner, *J. Power Sources*, 285 (2015) 460.
- [57] X. Tang, Y. Xu and W. Shen, *Chem. Eng. J.*, 144 (2008) 175.
- [58] B. Solsona, M. Pérez-Cabero, I. Vázquez, A. Dejoz, T. García, J. Álvarez-Rodríguez, J. El-Haskouri, D. Beltrán and P. Amorós, *Chem. Eng. J.*, 187 (2012) 391.
- [59] M. Ousmane, L.F. Liotta, G.D. Carlo, G. Pantaleo, A.M. Venezia, G. Deganello, L. Retailleau, A. Boreave and A. Giroir-Fendler, *Appl. Catal. B.*, 101 (2011) 629.
- [60] J.M. López, A.L. Gilbank, T. García, B. Solsona, S. Agouram and L. Torrente-Murciano, *Appl. Catal. B.*, 174-175 (2015) 403.
- [61] M. Hatanaka, N. Takahashi, T. Tanabe, Y. Nagai, K. Dohmae, Y. Aoki, T. Yoshida and H. Shinjoh, *Appl. Catal. B.*, 99 (2010) 336.
- [62] W.B. Li, J.X. Wang and H. Gong, *Catal. Today*, 148 (2009) 81.

## **Catalytic Properties|Zeolites/Inorganic materials**

FEZA21-PO-077

### **Distribution of International Reference Zeolite by Catalysis Commission**

N. Katada <sup>1,\*</sup>, M. Ogura <sup>2</sup>, M. Hartmann <sup>3</sup>, P. J. Kooyman <sup>4</sup>, J. Lercher <sup>5</sup>, K. Nakai <sup>6</sup>, S. Suganuma <sup>1</sup>, K. Tomishige <sup>7</sup>, F. Rey <sup>8</sup>

<sup>1</sup>Center for Research on Green Sustainable Chemistry, Tottori University, Tottori, <sup>2</sup>Institute of Industrial Science, The University of Tokyo, Tokyo, Japan, <sup>3</sup>Erlangen Catalysis Resource Center, FAU Erlangen-Nürnberg, Erlangen, Germany, <sup>4</sup>Department of Chemical Engineering, University of Cape Town, Rondebosch, South Africa, <sup>5</sup>Department of Chemistry, Technische Universität München, München, Germany, <sup>6</sup>Head Office, Microtrac BEL Corp., Osaka, <sup>7</sup>Department of Applied Chemistry, Tohoku University, Sendai, Japan, <sup>8</sup>Instituto de Tecnología Química, Universitat Politècnica de València, Valencia, Spain

#### **Abstract Text:** 1. Outline:

Since 1986, the Catalysis Commission of the International Zeolite Association has worked on standardization of catalytic model reactions based on reference samples of zeolite<sup>1,2</sup>. We here report on standardization of cracking of heptane and cumene studied since 2018. In addition, we will extend this study to establish a reference zeolite system for wide distribution of samples and collection of various data. This plan will be discussed.

#### 2. Properties of IRZ-MFI001 and IRZ-FAU001:

As the first part of this project, two samples from Tosoh Corp., IRZ-MFI001 (H-MFI) and IRZ-FAU001 (H-FAU) with Si/Al molar ratios 12 and 15, respectively, have been distributed to the members. Some physicochemical properties and catalytic results have been collected (Table 1). The reported results are reasonably consistent. TEM and SEM indicate aggregated small crystals for both samples. The particle size is up to ca. 2  $\mu\text{m}$ .  $\text{N}_2$  and Ar adsorption at 77 and 87 K, respectively, show the presence of ink-bottle type mesopores in addition to the micropores. The external surface areas of MFI and FAU are estimated to be high, 98 and 192  $\text{m}^2 \text{g}^{-1}$ , respectively, from the  $\text{N}_2$  adsorption. Laser diffraction / scattering in water reveals micrometric dimension of the particles (still more aggregates). IR of evacuated zeolites shows high density of SiOH. All these results show that the two samples are formed from aggregates of small crystallites, and the external surface area is FAU > MFI. <sup>27</sup>Al NMR (Figure 1) and other physicochemical properties tell us that both samples, even MFI, had extra-framework Al. The number of Brønsted acid sites is 0.8 times [Al], indicating that most of Al is in the framework of the MFI; in FAU, the number of Brønsted acid sites is 0.3 times [Al]. The estimated ammonia desorption enthalpy from Brønsted acid site (an index of Brønsted acid strength) is MFI > FAU, and the activities for cracking of linear alkanes and cumene are also MFI > FAU. In contrast, the activities for dealkylation of di- and tri-isopropylbenzenes are FAU > MFI, reflecting the external surface area.

#### 3. The next step:

Although not enough experimental results have been collected for standardization of the methods, we found that the collected experimental data were reasonably consistent. Based on these results, the Commission proposes an extended project. In addition to the already distributed samples, we have obtained more samples, 50 kg of each, in Japan, and are sending them to distribution bases in Belgium, Czech Republic, France, Germany, Spain, South Africa, and the United Kingdom. These samples will be distributed to scientists in those countries through face-to-face communications. In principle, the use of the reference zeolites is not limited to specific applications, and application to new subjects is encouraged. Direct reporting of the experimental results is not compulsory, but reporting the bibliographic information after publication of a paper involving the results on reference zeolite is.

The present samples, IRZ-MFI001 and IRZ-FAU001, are typical commercial zeolites, and therefore they have distorted structures. In order to clarify the influence of the distorted structure, we have obtained two new samples,  $\text{NH}_4$ -MFI with Si/Al 11.6 and H-MFI with Si/Al 50 from Tosoh and Mizusawa Chemical Industry, respectively. These samples have been distributed to a few countries already.

This plan is based on the experiences of the reference catalyst system in Japan. The Catalysis Society of Japan has a database in which one can search the papers showing the results of XRD, ICP, XRF, XPS, XAFS, NMR, etc., including catalytic reactions, on the reference samples<sup>3</sup>. Similar database on the international reference zeolite will be collected on a web site.

We call on scientists in academic and industrial community of zeolite research to participate this project by being the distributor for your country, using the reference samples, and supplying unique zeolite samples.

Image 1:

Table 1 Reported experimental results

Affiliation	Experiments
FAU Erlangen-Nürnberg	XRD, NMR ( $^1\text{H}$ , $^{27}\text{Al}$ and $^{29}\text{Si}$ )
Univ. Cape Town	HR-TEM
Tottori Univ.	Ammonia IRMS-TPD, Cumene cracking
Microtrac BEL Corp.	Gas adsorption, Particle size distribution
Tohoku Univ.	Heptane cracking
Univ. Polytechnica Valencia	Reactions

Image 2:

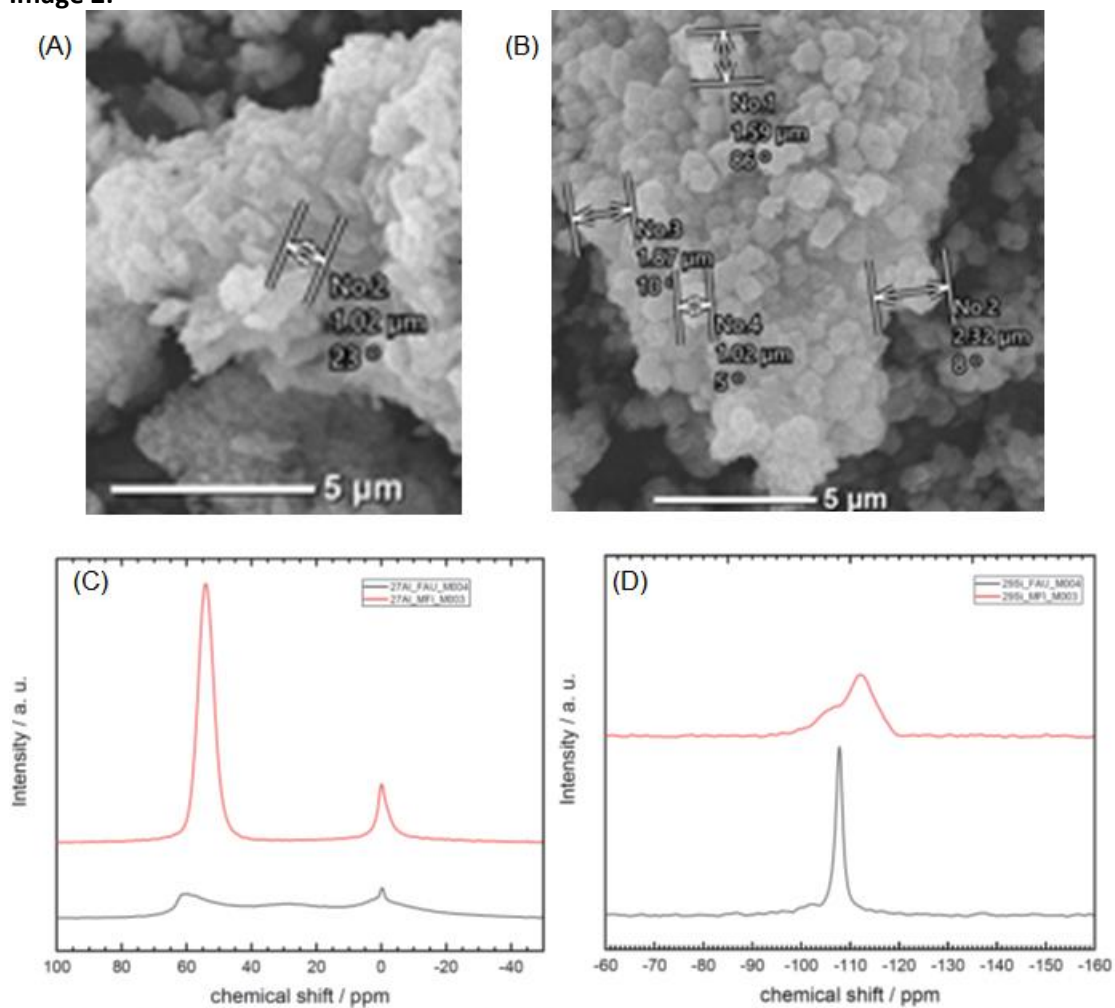


Figure 1 SEM of IRZ-MFI001 (A) and IRZ-FAU001 (B), and <sup>27</sup>Al NMR (C) and <sup>29</sup>Si NMR (D) of IRZ-MFI001 (upper) and IRZ-FAU001 (lower).

**References:** 1) <http://www.iza-online.org/catalysis/default.htm>, referred on 2020/1/14.

2) D.E. De Vos, S. Ernst, C. Perego, C.T. O'Connor and M. Stöcker, *Micropor. Mesopor. Mater.*, 56 (2002) 185.

3) N. Katada, *Shokubai (Catalysts & Catalysis)*, 53 (2011) 433.

## **Catalytic Properties|Zeolites/Inorganic materials**

FEZA21-PO-081

### **A stable extra-large pores IM-12 zeolite and its outstanding catalytic activity**

E. El Hayek<sup>1,2,\*</sup>, C. Chizallet<sup>1</sup>, B. Harbuzaru<sup>1</sup>, S. Radhakrishnan<sup>2</sup>, E. Breynaert<sup>2</sup>, G. Vanbutsele<sup>2</sup>, J. Martens<sup>2</sup>

<sup>1</sup>Catalysis, Biocatalyse and Separation Division, IFP Energies Nouvelles, Lyon, France, <sup>2</sup>Center for Surface Chemistry and Catalysis, KU Leuven, Leuven, Belgium

#### **Abstract Text:**

Zeolites are crystallized microporous aluminosilicates composed by three-dimensional arrangement of SiO<sub>4</sub> and AlO<sub>4</sub> tetrahedral. Adding Ge to the synthesis medium of these zeolites is a strategy for accessing new structures, sometimes with extra-large pores. From a structural point of view, this has a strong interest in catalysis. However, a major remaining challenge is the possibility of substituting Ge with Al to generate structures with compensation cations necessary for the reactivity of the zeolites. Also, microporous silicogermanates are often unstable in aqueous condition after calcination, which limits their application. To stabilize these silicogermanates, two experimental post treatment approaches are described in the literature. The first approach allowed the maintain of the initial structure of the parent zeolite through the direct substitution of Ge for another structural element such as Al (e.g. ITQ-17 zeolite)<sup>[1]</sup> while the second led to the creation of new stable structures. For example, the IM-12 is a zeolite (UTL structural type)<sup>[2]</sup> having pore openings with 12 and 14 tetrahedral atoms. To date, this zeolite could not be synthesized without Ge. Its post treatments led to the formation of zeolites with new structures and smaller pores<sup>[3;4]</sup> or to the partial maintain of the UTL structure with an important loss of microporous volume<sup>[5]</sup>. The aim of this work, is to stabilize the UTL structure and to maintain its high microporous volume responsible of attractive applications.

To reach this goal we developed a new post treatment unit using silicon tetrachloride. This treatment allowed the stabilization of the zeolite by the substitution of Ge for Si. This substitution was verified by XRF that indicated an increase of the Si/Ge molar ratio from 4.9 to 9.7. While the XRD proved the maintaining of the initial UTL structure even after water washing, figure 1. The N<sub>2</sub> physisorption indicated that the initial microporous volume was slightly affected (0.21 to 0.19 mL/g).

The obtained stable IM-12 was then functionalized by post-incorporation of Al through a series of polyaluminum chloride hydroxide treatments and HCl washing. The XRD and the N<sub>2</sub> physisorption confirmed the conservation, after the treatments, of the UTL type structure (figure 1) and of the microporous volume (0.184 mL/g). The Si/Ge molar ratio increased to 105. In addition, the pyridine adsorption and FTIR spectroscopy reflected that the obtained zeolite had small amounts of acid sites: 34 μmol/g of Bronsted acidity and 75 μmol/g of Lewis acidity. This low acidity was confirmed by the <sup>27</sup>Al MAS NMR quantification indicating a Si/Al (intraframework) ratio of 99. Furthermore, the <sup>27</sup>Al MAS NMR spectra in figure 2 shows a chemical shift around 6ppm that is characteristic of hexacoordinated Al in zeolites and a second dominant peak around 55 ppm. The latter is identified as tetra coordinated Al in zeolites.

To evaluate the activity of this material in bifunctional catalysis, it was then impregnated with an aqueous Pt(NH<sub>4</sub>)<sub>3</sub>Cl<sub>2</sub> solution to reach a loading of 0.3 wt.% Pt. The resulting bifunctional Pt/IM-12 catalyst was tested for the hydroisomerization of decane in a continuous-flow fixed bed reactor. The reaction products were analyzed using a GC. The results show that this catalyst of low acidity presents an outstanding activity. With a Si/Al (intraframework) ratio of 100 the isomers yield is around 40% while a nanosheet MFI with a Si/Al ratio of 50 has the similar isomerization yield<sup>[6]</sup> and an USY with a Si/Al ratio of 5.8 has an isomerization yield of 70%<sup>[7]</sup>.

Ongoing studies aim to identify the environment of Si, Ge and Al of the different materials using <sup>1</sup>H; <sup>27</sup>Al; <sup>29</sup>Si MAS NMR and 2D <sup>1</sup>H DQ-SQ MAS NMR combined with Ab initio NMR and IR simulations. This identification will help us understanding the activity of this catalyst, and identify the location of the acid sites. The results reflect a positive step toward silicogermanates stabilization which can lead to industrial valorization.

Image 1:

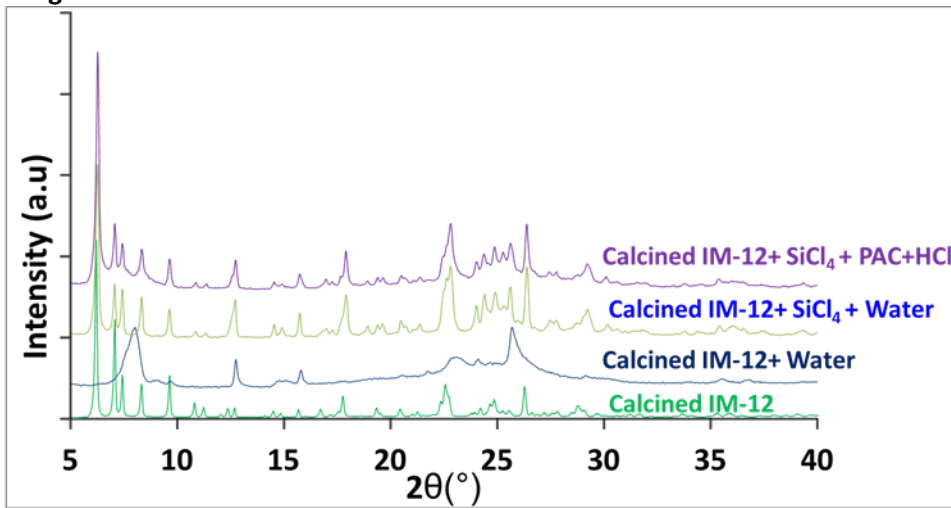
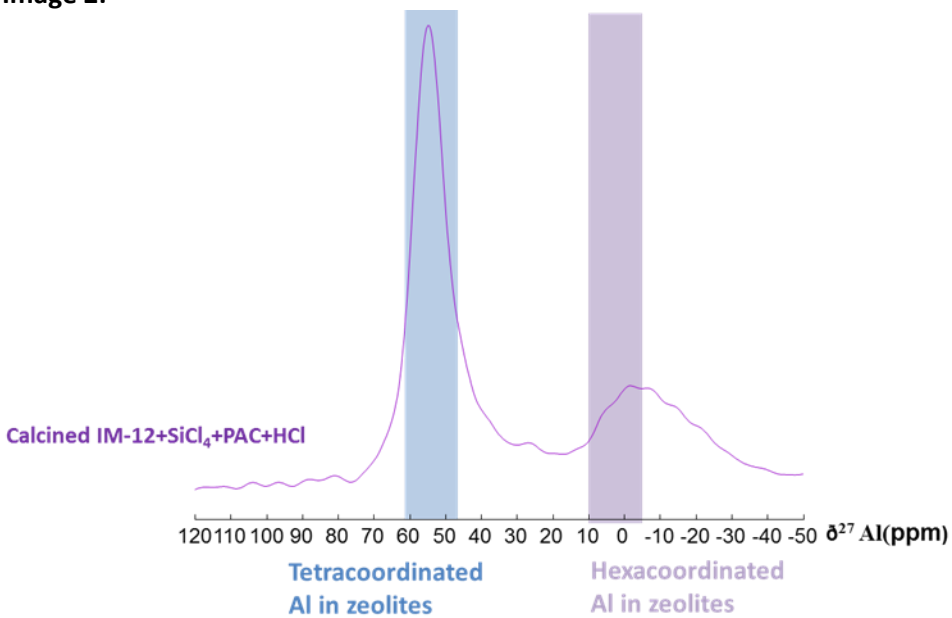


Image 2:



References: [1] F.Gao, M. Jaber, K. Bozhilov, A. Vicente, C. Fernandez and V. Vatchev, J. Am. Chem. Soc.,131, 16580 (2009).

[2] J.L Paillaud, B. Harbuzaru, J. Patarin and N. Bats, Science, 304, 990 (2004).

- [3] P.S.Wheatley, P. Chlubna-Eliasova, H. Greer, W. Zhou, V.R. Seymour, D.M. Dawson, S.E. Ashbrook, A.B. Pinar, L.B. McCusker, M. Opanasenko, J. Cejka and R.E. Morris, *Angew. Chem. Int. Ed.*, 53, 13210 (2014).
- [4] E. Verheyen, L. Joos, K. Van Havenbergh, E. Breynaert, N. Kasian, E. Gobechiya, K. Houthoofd, C. Martineau, M. Hinterstein, F. Taulelle, V. Van Speybroeck, M. Waroquier, S. Bals, G. Van Tendeloo, C.E.A. Kirschhock and J.A. Martens, *Nature Materials*, 11, 1059 (2012).
- [5] M.V. Shamzy, P. Eliasova, D. Vitvarova, M.V. Opanasenko, D.S. Firth and R.E. Morris, *Chem. Eur. J.*, 22, 17377 (2016).
- [6] E. Verheyen, C. Jo, M. Kurttepel, G. Vanbutsele, E. Gobechiya, T. I. Korányi, S. Bals, G. Van Tendeloo, R. Ryoo, C.E.A. Kirschhock and Johan A. Martens, *J. Catal.*, 300, 70 (2013).
- [7] J. A. Martens, E. Benazzi, J. Brendlé, S. Lacombe and R. Le Dred, *Stud. Surf. Sci. Catal.*, 130, 293 (2000).

### ***Catalytic Properties / Zeolites / Inorganic materials***

FEZA21-PO-085

#### **Heterogeneously catalysed formation of methylenedianiline on zeolites and alternative solid acids**

K. Y. Cheung<sup>1,\*</sup>, P. Tomkins<sup>1</sup>, D. De Vos<sup>1</sup>, T. De Baerdemaeker<sup>2</sup>, A. Gordillo<sup>3</sup>, A. Parvulescu<sup>2</sup>

<sup>1</sup>cMACS, KU Leuven, Leuven, Belgium, <sup>2</sup>Zeolite Catalysis Research, <sup>3</sup>Process Catalysis Research, BASF SE, Ludwigshafen, Germany

**Abstract Text:** Methylenedianiline (MDA) is one of the most important intermediates for the production of polyurethanes. MDA is industrially synthesised using aniline and formaldehyde, and the process is homogeneously catalysed by hydrochloric acid. The product mixture then requires a large amount of sodium hydroxide for acid neutralisation and further treatment to remove the unreacted aniline before waste discharge. The product mixture contains isomers (2,2'-MDA, 2,4'-MDA, and 4,4'-MDA) and oligomers of MDA (3 or more anilines bridged by methylene groups). The isomer and oligomer distribution can be adjusted by changing the aniline:formaldehyde molar ratio, acid content, water content, reaction temperature and time. Selectivity towards the 4,4'-MDA is expressed in the isomer ratio, defined as  $4,4'\text{-MDA}/(2,2'\text{-MDA}+2,4'\text{-MDA})$ .<sup>1</sup>

In light of the large amount of waste generated in the homogeneous process and the risk of corrosion associated with using hydrochloric acid as the catalyst, numerous solid acid catalysts have been tested as potential substitutes throughout the years. The heterogeneous process is split into two steps: the first step involves a neutral condensation of aniline and formaldehyde followed by phase separation to isolate the organic phase. In the second step, the neutral condensate in the organic layer is consumed in an acid-catalysed rearrangement to form MDA via aminobenzylaniline (ABA) intermediates (Image 1).

In this work, a porous Lewis acidic catalyst was used in the second step of MDA synthesis to reach high conversions and selectivity towards the 4,4'-isomer; side products, namely N-methyl, N-formyl, and quinazoline MDA derivatives were only formed in very small quantities. Compared with ITQ-18, a delaminated zeolite which was already more active due to improved accessibility to the acid sites,<sup>2</sup> our catalyst achieved the same MDA yield with a higher selectivity towards the 4,4'-isomer using less catalyst. The catalyst herein also retained more of its activity than the high-performing zeolite Y (Image 2).<sup>3</sup>

**Image 1:**

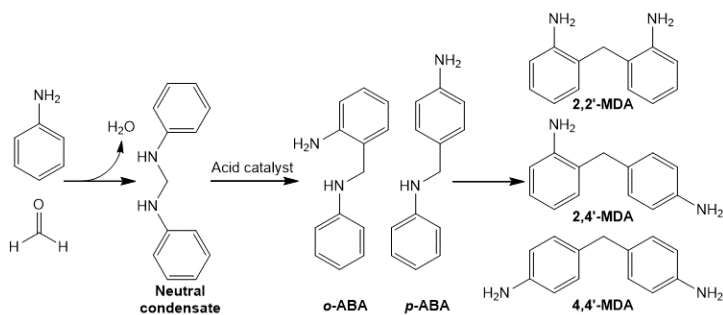
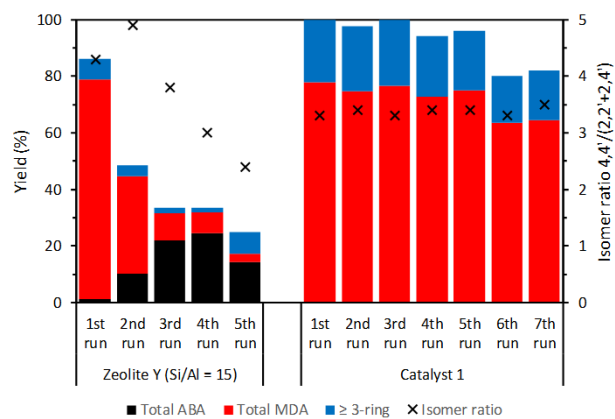


Image 2:



- References:** 1. S. Lowenkron, Amines, Aromatic, Methylenedianiline in Kirk-Othmer Encyclopedia of Chemical Technology, ed., 2000, DOI: 10.1002/0471238961.1305200812152305.a01  
 2. A. Corma, P. Botella and C. Mitchell, Chem. Commun., 2004, 17, 2008–2010, DOI: 10.1039/B406303A  
 3. T. C. Keller, J. Arras, S. Wershofen and J. Pérez-Ramírez, ACS Catal., 2015, 5, 734–743, DOI: 10.1021/cs5017694

## Influence of the location of Pt nanoparticles in Pt/ $\gamma$ -Al<sub>2</sub>O<sub>3</sub>/zeolite catalysts on the catalytic performance and kinetic parameters

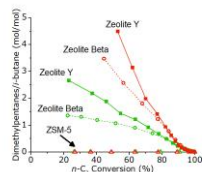
J. Oenema<sup>1,\*</sup>, A. Poursaeidesfahani<sup>2</sup>, T. Vlugt<sup>2</sup>, J. Zecevic<sup>1</sup>, K. de Jong<sup>1</sup>

<sup>1</sup>Department of Chemistry, Inorganic chemistry and catalysis, Utrecht University, Utrecht, <sup>2</sup>Process & Energy Department, Delft University of Technology, Delft, Netherlands

**Abstract Text:** Bifunctional metal-acid catalysts are crucial in current industrial processes for upgrading of hydrocarbon feedstocks towards transportation fuels and chemicals, whereas they also find use to enable routes for the production of renewable synthetic fuels. It is generally accepted that for optimal catalytic performance of these catalysts, a close intimacy between the metal sites and acid sites is desired.<sup>[1]</sup> However, recent studies report detrimental effects on selectivity when Pt nanoparticles are located inside zeolite micropores, in closest proximity with zeolite acid sites. Bifunctional catalysts with the metal function located outside the zeolite, at nanoscale distance from the zeolite acid sites, displayed a higher selectivity towards isomers and less secondary cracking.<sup>[2,3]</sup> Here, we performed a systematic study on impact of the location of Pt nanoparticles by using zeolite based catalysts with medium to large micropores: ZSM-5, zeolite Beta and zeolite Y. The location of Pt nanoparticles in zeolite/ $\gamma$ -Al<sub>2</sub>O<sub>3</sub> composite supports was controlled by using different Pt precursors: a cationic Pt(NH<sub>3</sub>)<sub>4</sub><sup>2+</sup> (aq) complex that exchanged with protons from the zeolite, or an anionic PtCl<sub>6</sub><sup>2-</sup> (aq) complex that adsorbed on positively charged  $\gamma$ -Al<sub>2</sub>O<sub>3</sub> in acidic conditions (pH ~ 3). Results of *n*-C<sub>7</sub> hydroisomerisation tests show a slight increase in catalytic activity for catalyst with the Pt nanoparticles located on the  $\gamma$ -Al<sub>2</sub>O<sub>3</sub> binder for all catalysts. For ZSM-5 based catalysts, selectivity towards monobranched products was identical for both catalysts, whereas no dibranched isomers were observed (Figure 1). The slow micropore diffusion of the branched heptane isomers within ZSM-5, results in an isomer product distribution dictated by shape selectivity and is not affected by the location of Pt nanoparticles.<sup>[4]</sup> For large pore zeolites (zeolite Beta, zeolite Y) locating Pt nanoparticles on the  $\gamma$ -Al<sub>2</sub>O<sub>3</sub> binder had a beneficial effect on isomer selectivity, especially towards desired dibranched C<sub>7</sub> isomers (Figure 1). The higher isomer selectivity for the large pore zeolites is tentatively attributed to the shorter diffusion pathway of olefinic intermediates through zeolite micropores, which is slower than their paraffinic counterparts due to adsorption on Brønsted acid sites. In order to provide more insight on the influence of the location of Pt nanoparticles on kinetic parameters, a kinetic study was performed on Pt/ $\gamma$ -Al<sub>2</sub>O<sub>3</sub>/zeolite Y catalysts over a broad range of reaction conditions and using several *n*-hydrocarbons, to obtain the apparent activation energies, and reactant reaction orders. The results thereof will be presented in the full paper.

**Figure 1:** The isomer selectivity plot shows the ratio of dibranched to cracked products as a function of conversion, with green symbols for catalyst with Pt nanoparticles located inside the zeolite and red symbols for catalysts with Pt nanoparticles located on the  $\gamma$ -Al<sub>2</sub>O<sub>3</sub> binder. *n*-C<sub>7</sub> hydroisomerisation experiments were conducted at: H<sub>2</sub>/*n*-C<sub>7</sub> of 10 mol/mol; WHSV of *n*-C<sub>7</sub> ~ 2 h<sup>-1</sup> and 10 bar of total pressure.

### Image 1:



**References:** [1]P. B. Weisz, Adv. Catal. 1962, 13, 137–190.

[2]O. Ben Moussa, L. Tinat, X. Jin, W. Baaziz, O. Durupthy, C. Sayag, J. Blanchard, ACS Catal. 2018, 8, 6071–6078.

[3]J. Zečević, G. Vanbutsele, K. P. de Jong, J. A. Martens, Nature 2015, 528, 245–248.

[4]A. Poursaeidesfahani, M. F. de Lange, F. Khodadadian, D. Dubbeldam, M. Rigutto, N. Nair, T. J. H. Vlugt, J. Catal. 2017, 353, 54–62.

## **Catalytic Properties|Zeolites/Inorganic materials**

FEZA21-PO-088

### **Insights into synergistic mechanisms between extra-framework aluminum species and Brønsted acid sites in HY zeolites**

J. Zheng<sup>1,2,\*</sup>, Y. Qin<sup>2</sup>, L. Song<sup>1,2</sup>

<sup>1</sup>College of Chemistry & Chemical Engineering, China University of Petroleum (East China), Qingdao, <sup>2</sup>Key Laboratory of Petrochemical Catalytic Science and Technology, Liaoning Shihua University, Fushun, China

#### **Abstract Text: 1 Introduction**

The properties of Brønsted acid sites (BAS) are the crucial factors for the application performance of Y zeolites. For decades, significant attentions have been paid to understand the impact of framework and extra-framework species on the properties of Brønsted acid sites.

The internal relation between the extra-framework aluminum (EFAl) species and the Brønsted acid sites (BAS) has always been a topic of concern, which has been widely studied both experimentally and theoretically [1,2]. From these reports, two models could be summarized as follows, (a) the presence of adjacent EFAl increase the acid strength of the BAS by polarization, and (b) the existence of EFAl species enhance the stabilization of the reactant molecules or the intermediate states in the zeolite lattice via dispersive interactions. By doing so, a positive effect could be drawn that the presence of the EFAl is associated with the rate enhancement in cracking of the BAS, but the specific role of what the EFAl played may not be confirmed.

The present contribution provides an additional explanation for the controversy of the various assignments of the specific role of EFAl. The impact of the adjacent and non-adjacent extra-framework aluminum species on acidity and adsorption properties of the BAS in zeolites has been explored using ammonia, pyridine and thiophene with different sizes and polarity as the model probe and HY as model zeolite by a periodic DFT study.

#### **2 Materials and Methods**

The primitive cell for FAU topology is a rhombohedral cell with the lattice parameters of  $a=b=c=17.2\text{\AA}$  and  $\alpha=\beta=\gamma=60.0^\circ$ , which contains complete a super cage and a sodalite cage with 48T atoms. The framework Si/Al ratio and the location of the hydrogen proton of BAS are chosen the same with the literature [3]. The EFAl-containing Y models used in this work were all established from the rhombohedral cell of Y zeolite mentioned above. The EFAl species, located in the SII site of faujasite, were chosen to simulate HY zeolites with typical EFAl species, which are shown in Image 1. Two kind of Al distribution contained both the isolated Al centers and the Al-O-(Si-O)<sub>2</sub>-Al sequences in the six-membered rings (SII sites) connecting the super cage and sodalite cage.

All calculations are performed using DMol3 and CASTEP software package, contained in the Materials Studio of Accelrys, based on DFT. The exchange-correlation energy is calculated within the generalized gradient approximation (GGA) using the form of the functional proposed by the Perdew-Burke-Ernzerhof (PBE).

#### **3 Results and Discussion**

The findings in this work are significant for the selection of the reasonable probe molecules to characterize the synergistic effect of the EFAl to the BAS, as well as for the development of the excellent adsorbents and catalysts in aspects of adsorption and reaction performances (Image 2).

#### **4 Conclusions**

A series of model probes with different sizes and polarity, such as ammonia, pyridine and thiophene, have been used to insight into the influence mechanisms of EFAl species on the properties of Brønsted acid sites in HY zeolites by periodic DFT calculation. EFAl species enhance the intrinsic strength of BAS in HY zeolites similar to the generally accepted results. However, the presence of EFAl species induce significant deviation of correlation between the adsorption energies of the probe molecules and the changes in intrinsic acidity characterized by DPE. These results demonstrate that EFAl species exert the additional forces (dispersion forces) on the probe molecules adsorbed on the BAS. In this work, a principal finding is using weaker polarity and right fit size molecule (that of thiophene in this work) as a probe can reveal the synergistic mechanisms between the EFAl species and the BAS.

Image 1:

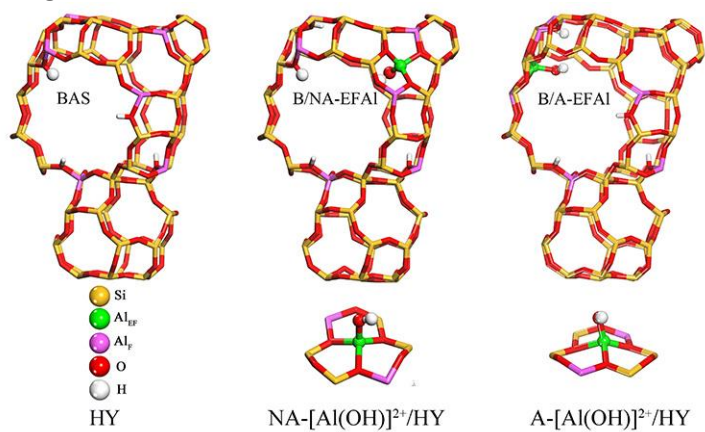
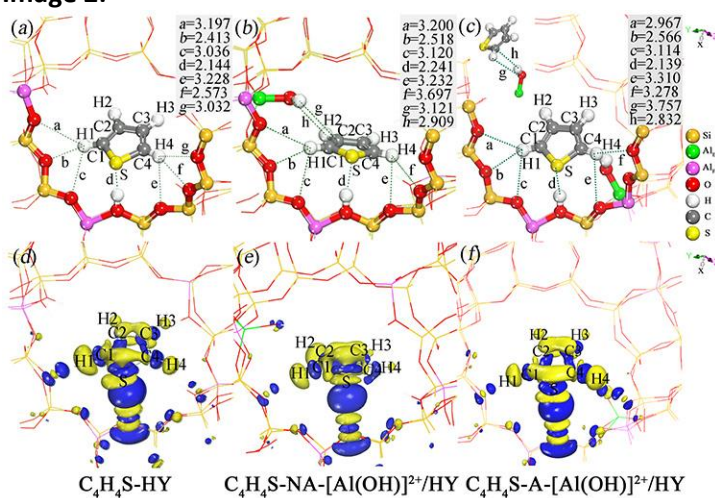


Image 2:



References: 1. Li, S., Zheng, A., Su, Deng, F. J. Am. Chem. Soc. 129 (2007)

2. Schallmoser, S., Ikuno, T., Lercher, J. A. J. Catal. 316 (2014).

3. Liu, C., Hensen, E.J.M., Pidko, E.A. ACS Catal. 5, 11 (2015).

## **Catalytic Properties/Zeolites/Inorganic materials**

FEZA21-PO-089

### **Effect of transition metal ion on the activity of binuclear cationic sites in zeolites in the selective oxidation of methane to methanol by molecular oxygen**

A. Kornas<sup>1,\*</sup>, M. Lemishka<sup>1,2</sup>, K. Mlekodaj<sup>1</sup>, H. Jirglová<sup>1</sup>, S. Sklenak<sup>3</sup>, J. Dědeček<sup>1</sup>, E. Tabor<sup>1</sup>

<sup>1</sup>Structure and Dynamics in Catalysis, Heyrovský Institute of Physical Chemistry Czech Academy of Sciences, Prague,

<sup>2</sup>Faculty of Chemical Technology, University of Pardubice, Pardubice, <sup>3</sup>Theoretical Chemistry, Heyrovský Institute of Physical Chemistry Czech Academy of Sciences, Prague, Czech Republic

#### **Abstract Text: Introduction**

Selective oxidation of methane to methanol represents highly required transformation for both academic research and industry. Recently, it was shown that transition metal ions (Me=Fe, Ni, Co or Mn) embedded in ferrierite (FER) structure effectively stabilized active oxygen ( $\alpha$ -oxygen) originating from  $N_2O$  and used it to oxidize methane to methanol at ambient temperature.<sup>1</sup> This exceptional behaviour was explained by the presence of binuclear cationic Me sites in FER collaborating in  $N_2O$  decomposition and stabilization of  $\alpha$ -oxygen on cation  $[Me(IV)O]^{2+}$ .<sup>2</sup> DFT calculation results indicate that binuclear Ni-, Co-, or Mn-species in FER can cooperate in molecular oxygen dissociation resulting in  $\alpha$ -oxygen formation. This work is targeted on preparation of binuclear Ni-, Co-, and Mn-species in FER and analysis of their redox properties in selective oxidation of methane by molecular oxygen at room temperature (RT) using in-situ FTIR spectroscopy and mass spectrometry (MS).

#### **Experimental part**

Commercial FER Si/Al 8.6 was ion exchanged to the  $NH_4$  form and further transferred to maximum loaded Mn and Co forms by ion exchange and to Ni form by impregnation procedure.<sup>2,3</sup> The presence of divalent cations (Ni, Co, and Mn) in cationic position of FER was confirmed by FTIR spectroscopy. In-situ FTIR spectra of Me-FER were collected at RT after evacuation (3h at 450 °C) and after following treatments performed at RT: i) 1h interaction with  $O_2$  (1 atm.), ii) 1h interaction with  $O_2$  (1 atm.) and 5 min  $O_2$  desorption, iii) 1h interaction with  $O_2$  (1 atm.) followed by 5 min  $O_2$  desorption and 1h interaction with  $CH_4$  (1 atm.). Mass spectrometry was used to characterize the products of methane oxidation. The sample placed in the quartz reactor was activated in Ar flow (20 mL/min) for 3 h at 450 °C. Subsequently, the sample was treated in a flow of  $O_2$  (40 mL/min) at RT for 1 h followed by a purging with Ar (20 mL/min) for 5 minutes. Finally, the oxidized sample was left to interact with  $CH_4$  (30 mL/min) at RT.

#### **Results and discussion**

FTIR spectra of all prepared Me-FER exhibited the intense bands around 918 and 940  $cm^{-1}$  indicating presence of bare Me(II), which are responsible for formation of binuclear Me(II) species.<sup>2,3</sup> The interaction of Me-FER with molecular oxygen at RT results in disappearing bands attributed to Me(II) and the formation of a new band at around 880  $cm^{-1}$ , assigned to the  $\alpha$ -oxygen stabilized on cation  $[Me(IV)O]^{2+}$ . The introduction of  $CH_4$  to Me-FER containing  $\alpha$ -oxygen caused a shift of the band from 880  $cm^{-1}$  to 918  $cm^{-1}$ . This result clearly confirms the complete reduction of the  $[Me(IV)O]^{2+}$  species by  $CH_4$  to Me(II). Moreover, in the FTIR spectra after  $CH_4$  treatment new bands at 2920 and 2832  $cm^{-1}$  describing methoxy species and at 2979 and 1371  $cm^{-1}$  characteristic for methanol vibrations were detected. Titration of  $\alpha$ -oxygen by methane was monitored by mass spectrometry. The signals typical for methanol ( $m/z = 31$ ),  $CO_2$  ( $m/z = 44$ ) and other (i.e., HCHO, HCOOH, or  $CH_3OCH_3$ ) possible oxidation products  $m/z = 29$  were detected. The quantitative analysis was based on the signal  $m/z = 31$ , exclusively representing methanol. MS results confirmed the RT methane oxidation by molecular oxygen, the protonation of methoxy groups and the release of oxidation products over all studied Me-FER.

#### **Conclusions**

FTIR and MS studies confirmed that binuclear transition metal (Ni, Co, and Mn) species in FER can split molecular oxygen at RT. For the first time, we showed that the  $\alpha$ -oxygen stabilized on metal cations (Ni, Co, or Mn) easily oxidizes methane to methanol at RT. The yield of methanol formation depend on the transition metal ion embedded to FER structure.

Image 1:

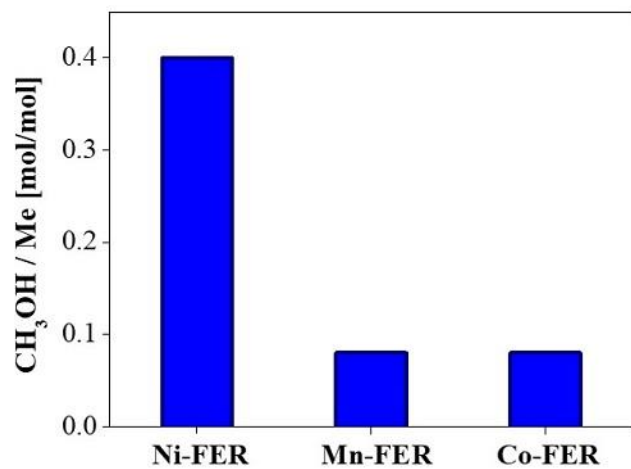


Fig.1. MS results of yields of methanol presented as CH<sub>3</sub>OH/Me.

- References:** 1. Sklenák, S. et al., *J. Catal.* 272 (2), 262-274, 2010.  
2. Tabor, E. et al., *Commun.Chem.* 2:71, 2019.  
3. Lemishka, M. et al., *Pure. Appl. Chem.* 91, 1721-1732(12), 2019.

**ZSM-5 based Catalyst for Cracking of Butenes to Propylene: Influence of zeolite Si/Al ratio, crystal size and morphology**

P. Del Campo<sup>1,\*</sup>, M. D. Khokhar<sup>2</sup>, F. Jumah<sup>2</sup>, H. Khunaizi<sup>2</sup>, M. T. Navarro<sup>1</sup>, C. Martínez<sup>1</sup>, S. K. Shaikh<sup>2</sup>, A. Corma<sup>1</sup>

<sup>1</sup>Instituto de Tecnología Química, Universitat Politècnica de València, Consejo Superior de Investigaciones Científicas (UPV-CSIC), Av de los Naranjos s/n, 46022, Valencia, Spain, <sup>2</sup>Research & Development Center, Saudi Aramco, Dhahran-31311, Saudi Arabia

**Abstract Text:** The synthesis of propylene via the cracking of raffinate butenes represents an attractive alternative to the conventional steam cracking of naphtha or fluid catalytic cracking. Among the on-purpose technologies, the upgrading of low value butenes fractions is gaining interest since it reduces process energy consumption while increasing propylene make<sup>1</sup>. ZSM-5 based catalyst with high Si/Al ratios (>150) and large crystal size (>10  $\mu\text{m}$ ), have been demonstrated as the most adequate in terms of propylene selectivity and catalyst lifetime for the butenes cracking reaction<sup>2-3</sup>. Although the low amount of acidic sites leads to low efficiency, a larger active site density increases the number of undesired consecutive reactions along the long diffusional paths and, consequently, aromatics formation and fast deactivation<sup>4</sup>. In recent years, there has been an increased effort in synthesizing zeolites with reduced acidity, by either lowering the amount of Brønsted acid sites, attenuating the acid strength via post-synthetic treatments, or by incorporating heteroatoms within the zeolite lattice<sup>5</sup>. Reducing the size of the zeolite crystal was shown to be beneficial for catalyst stability and proven to reduce deactivation<sup>6</sup>. However, the influence of morphology has scarcely been studied<sup>7</sup>. To derive the underlying structure-property relationships, a systematic study of the influence of crystal size, morphology and Si/Al ratio of high silica-ZSM-5 on the butenes cracking reaction is much desired.

In this work, we study the effect of crystal size, morphology and Si/Al ratio of differently synthesized ZSM-5 catalysts on the performance of butenes cracking. By synthesizing two sets of samples, under fluoride-free media, it has been possible to unravel independently the effect of the catalyst properties. The first type is composed of ZSM-5 zeolites with crystal sizes ranging from 20-35 to 1  $\mu\text{m}$  and coffin or square morphology, but similar Si/Al ratio. In the second, the Si/Al ratio has been varied from 150 up to 600, for samples with comparable square shaped crystallites of 1  $\mu\text{m}$  in size. All catalysts have been tested for cracking of 1-butene in a fixed-bed reactor at 550  $^{\circ}\text{C}$  and at atmospheric pressure.

The catalytic results demonstrate, primarily, that superior-performing large crystal ZSM-5 catalysts can be prepared under fluoride-free synthesis conditions. These would there resolve the issues associated with catalyst scale-up faced by typical F based catalyst. This catalyst, with coffin-like morphology, outperforms the initially more active reference ZSM-5 prepared under fluoride medium when comparing propylene yield at longer TOS, while minimizing the production of aromatics. Secondly, the results suggest that the guidelines for designing highly productive, propylene selective and stable ZSM-5 based catalyst for butenes cracking should be directed to reduce the crystal size to ca. 1  $\mu\text{m}$  while keeping the aspect ratio of the crystallite close to 1 and Si/Al around 300. The Si/Al ratio of ca. 300 leads to adequate cracking activity, which gets penalized at lower Al contents, and avoids the production of undesired aromatics, which is favoured at lower Si/Al ratios. A larger crystallite size or reduced aspect ratio of the zeolite crystal results in faster deactivation and yields more by-products such as isoamylenes, or aromatics, as compared to smaller sized catalysts. Moreover, the optimal 1  $\mu\text{m}$  sized catalyst with an intermediate amount of Al (Si/Al = 300) is more selective to ethylene as compared to other catalysts evaluated in the study.

A preliminary mechanistic study also revealed that paraffin formation via hydride transfer, which is generally associated with aromatization and coke formation, did not penalize the propylene selectivity for our optimal catalysts. This suggests that paraffins are preferentially involved in the formation of intermediate carbenium ions, which most likely follow the oligomerization-cracking route to produce propylene.

**References:** 1. Corma, A.; Corresa, E.; Mathieu, Y.; Sauvinaud, L.; Al-Bogami, S.; Al-Ghrami, M. S.; Bourane, A., Crude oil to chemicals: light olefins from crude oil. *Catal. Sci. Technol.* 2017, 7 (1), 12-46.

2. Al-Khattaf, S. S.; Palani, A.; Aitani, A. M., Catalytic hydrocracking of light olefins. US0217855A1 (2017).

3. Johnson, D. L.; Nariman, K. E.; Ware, R. A., Catalytic production of light olefins rich in propylene. US6222087B1 (2001).

4. Zhu, X.; Liu, S.; Song, Y.; Xu, L., Catalytic cracking of C4 alkenes to propene and ethene: influences of zeolites pore structures and Si/Al 2 ratios. *Applied Catalysis A: General* 2005, 288 (1), 134-142.
5. Blay, V.; Epelde, E.; Miravalles, R.; Perea, L. A., Converting olefins to propene: Ethene to propene and olefin cracking. *Catalysis Reviews* 2018, 1-58.
6. Zhao, G.-L.; Teng, J.-W.; Xie, Z.-K.; Yang, W.-M.; Chen, Q.-L.; Tang, Y., Catalytic cracking reactions of C 4-olefin over zeolites H-ZSM-5, H-mordenite and H-SAPO-34. *Studies in Surface Science and Catalysis* 2007, 170, 1307-1312.
7. Shi, J.; Zhao, G.; Teng, J.; Wang, Y.; Xie, Z., Morphology control of ZSM-5 zeolites and their application in Cracking reaction of C4 olefin. *Inorganic Chemistry Frontiers* 2018.

**Ce and Nb as dopants in Ca/MCF system for enhancement of basicity**

K. Grzelak<sup>1,\*</sup>, M. Trejda<sup>1</sup>, M. Ziolek<sup>1</sup>

<sup>1</sup>Chemistry Department, Adam Mickiewicz University, Poznan, Poland, Poznan, Poland

**Abstract Text: Introduction**

Catalysts having basic properties are of great importance for the production of biofuels, e.g. in the transesterification process of vegetable oils with methanol or ethanol. Although homogeneous catalysts such as sodium or potassium hydroxides are conventionally applied, the heterogenization of this process is desirable. In the liquid phase processes, the key factor is enabling the diffusion of substrates and products to/from the active centers. This can be realized by the application of catalysts having large and regular in size pores or cavities. Moreover, doping alkaline active phase with transition metals can boost basicity. Therefore, in this study, we applied siliceous calcium-modified MCF solid doped with niobium and cerium species in order to obtain effective basic catalysts.

**Experimental**

MCF materials were prepared using the procedure described in [1]. Niobium and cerium species were incorporated by one-pot wetness impregnation using niobium(V) ethoxide and cerium(III) nitrate, respectively. In the second step, calcium species were included by impregnation with an aqueous solution of calcium acetate monohydrate and calcined at 973 K for 5h. Materials obtained were characterized using: X-ray diffraction (XRD), N<sub>2</sub> adsorption/desorption, temperature programmed desorption of CO<sub>2</sub> (TPD-CO<sub>2</sub>), X-ray photoelectron spectroscopy (XPS) and UV-vis spectroscopy. Cyclization and dehydration of 2,5-hexanedione as a test reaction was examined at 623 K. The activity of catalysts was evaluated in the liquid phase transesterification of ethyl butyrate with methanol at 333 K.

**Results and discussion**

Three catalysts impregnated with 20 wt % of calcium and various wt % content of niobium and cerium (Ce/Nb = 1:1, 1:3, 3:1) were prepared. N<sub>2</sub> adsorption measurements confirmed the successful synthesis of MCF samples. Although the calcium loading was high the final materials remained mesoporous structure showing relatively large surface area in the range between 230-260 m<sup>2</sup>g<sup>-1</sup>. The crystal phases on the surface of the support were identified by XRD analysis. It was found that not only calcium oxide species were generated after calcination process. Calcium carbonates were also identified in XRD patterns. Basing on XPS and UV-vis data cerium evolved in the form of cerium oxide whereas niobium was incorporated into the MCF structure. Both, the number and a kind of surface species formed after impregnation and followed by calcination had an impact on material basicity estimated by TPD-CO<sub>2</sub> and the test reaction, i.e. 2,5-hexanedione cyclization and dehydration. The catalysts were applied in the model transesterification process, i.e. reaction of ethyl butyrate with methanol. XPS analysis showed that the catalytic activity was influenced by the ratio of Ce<sup>3+</sup>/Ce<sup>4+</sup> species in cerium oxide which varied depending on Ce/Nb ratio. Non-equivalent weight loading of niobium and cerium favoured evolution of Ce<sup>4+</sup> whose higher content enhanced the activity of calcium containing MCF samples. Impact of the above-mentioned parameters on catalytic performance will be presented and discussed in details.

*Acknowledgements:* We are grateful to the National Science Center in Poland (Project no. 2018/29/B/ST5/00137), the National Centre for Research and Development in Poland and European Union (Project no POWR.03.03.00-00-1026/16) for financial support.

**References:** 1. M. Trejda, K. Stawicka, M. Ziolek, *Catal. Today* 192 (2012) 130–135

## ***Catalytic Properties|Zeolites/Inorganic materials***

FEZA21-PO-095

### **Zeolite hosted Cu-oxo clusters for direct methane oxidation to methanol**

L. Tao<sup>1,\*</sup>, I. Lee<sup>1</sup>, J. A. Lercher<sup>1,2</sup>, M. Sanchez-Sanchez<sup>1</sup>

<sup>1</sup>Department of Chemistry, Technical University Munich, Garching, Germany, <sup>2</sup>Institute for Integrated Catalysis, Pacific Northwest National Laboratory, Richland, WA, United States

**Abstract Text:** High availability of methane in natural gas resources has driven the scientific interest towards converting methane to methanol via direct selective oxidation. However, it is very challenging to achieve a selective transformation to methanol at significant conversions. Prior studies have shown that Cu-zeolites are able to selectively convert methane into methanol at moderate temperatures [1]. Cu-exchanged on 8-MR frameworks are the materials showing the highest methanol yields [2], allegedly because of preferential formation of active Cu-oxo nanoclusters in 8-MR pores [2,3]. Here we study the impact of zeolite pore size and interconnectivity in the formation of Cu-oxo active species, by comparing a well-defined Cu-MOR reference material with activity of Cu ions exchanged in other selected zeolite frameworks.

Cu-zeolites were prepared following the method optimized for CuMOR [2, 4]. Catalytic tests are performed in three steps: thermal activation, reaction with CH<sub>4</sub> at 200 °C, and H<sub>2</sub>O steam treatment at 135 °C to strip the products from the zeolite. Characterization of the materials was performed by XAS, NMR, IR- and UV-VIS spectroscopies.

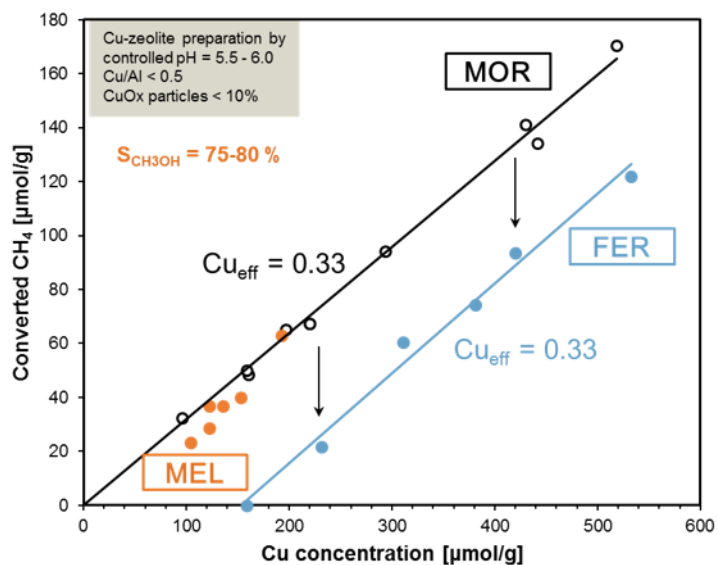
For this study, FER and MEL zeolites were selected, because their frameworks are built up with 8 and 10 membered-rings, similar to those known to host active Cu species for methane oxidation to methanol [1, 2]. The preparation protocol was adjusted for each zeolite system to avoid the presence of precipitated Cu oxide particles, following our previously published approach [2, 4].

Activity tests in methane oxidation showed a linear increase of activity with Cu loading, indicating the controlled speciation of Cu into formation of Cu-oxo active sites. Figure 1 shows the strong influence of framework in the Cu speciation in ion exchanged zeolites, and in particular in the formation of active Cu-oxo clusters. Cu-exchanged MEL achieves remarkably high Cu efficiency (defined as mol CH<sub>4</sub> activated per mol Cu), close to the benchmark values of well-defined CuMOR materials. Cu-FER shows an offset of activity indicating that the preferred Cu exchange positions at low loadings are inactive. The linear increase of activity for middle range a high Cu loading FER samples, however, points to the formation of Cu-oxo trimeric clusters similar to those spectroscopically identified on CuMOR [2]. This is further supported by the spectroscopic characterization of these CuMEL and CuFER materials, showing common features that are regarded as fingerprint of the active Cu-oxo clusters in CuMOR.

Results obtained here show that, by tuning the preparation protocol, other zeolite frameworks can selectively stabilize active Cu-oxo ions for the selective oxidation of methane to methanol. The interplay of synthesis and activation parameters with the thermodynamically preferred exchange positions of Cu, affected by local environment and zeolite properties, determines Cu ion speciation in zeolites. The understanding of these processes is key to develop rationally designed materials with homogeneous Cu speciation and high concentration of active sites.

**Image 1:**

### Increase of activity with Cu loading for the step-wise CH<sub>4</sub> oxidation at 200 °C



### References:

- [1] M. H. Groothaert, P. J. Smeets, B. F. Sels, P. A. Jacobs, R. A. Schoonheydt, *J. Am. Chem. Soc.* 127, 1394 (2005)
- [2] S. Grundner, M. A. Marcovits, G. Li, M. Tromp, E. A. Pidko, E. J. M. Hensen, A. Jentys, M. Sanchez-Sanchez, J. A. Lercher. *Nature Commun.* 6, 7546 (2015)
- [3] P. Vanelderem, B. E. R. Snyder, M.-L. Tsai, R. G. Hadt, J. Vancauwenbergh, O. Coussens, R. A. Schoonheydt, B. F. Sels, E. I. Solomon, *J. Am. Chem. Soc.* 137, 6383 (2015)
- [4] S. Grundner, W. Luo, M. Sanchez-Sanchez, J. A. Lercher. *Chem. Commun.* 52, 2553 (2016)

## ***Catalytic Properties|Zeolites/Inorganic materials***

FEZA21-PO-100

### **Key factors during the milling stage of the seed assisted and solvent-free synthesis of MFI and catalytic behavior in the alkylation of phenol with tert-butyl alcohol**

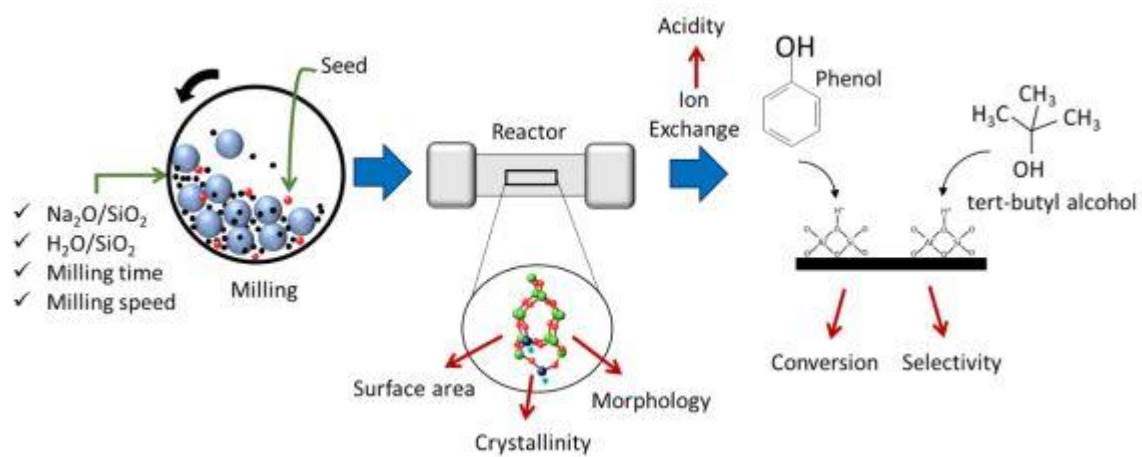
J. T. García Sánchez<sup>1,\*</sup>, I. D. Mora Vergara<sup>1</sup>, D. R. Molina Velasco<sup>2</sup>, J. A. Henao Martínez<sup>3</sup>, V. G. Baldovino Medrano<sup>1,4</sup>

<sup>1</sup>Centro de Investigaciones en Catálisis (CICAT), <sup>2</sup>Laboratorio de Resonancia Magnética Nuclear, <sup>3</sup>Laboratorio de Rayos-X,

<sup>4</sup>Laboratorio de Ciencia de Superficies (SurfLab), Universidad Industrial de Santander, Piedecuesta, Colombia

**Abstract Text:** The so-called mechanochemical method for the synthesis of zeolites reduces the generation of liquid residues and gaseous pollutants as compared to the conventional solvothermal method. Different types of zeolites have been synthesized at the laboratory scale with this method using mostly pestle and mortar. However, such an approach hinders both the systematic comprehension of the effects of the input variables of the milling process and its further scale-up towards the synthesis of the zeolites and their catalytic application. This work investigates the influence of key factors involved in the ball milling stage of the mechanochemical route for the synthesis of MFI done with the assistance of a commercial MFI seed and in the absence of solvents over the most salient physicochemical properties of this type of materials. The catalytic behavior of the thus produced materials during the alkylation of phenol with tert-butyl alcohol was also studied. The synthesis of the materials was planned and executed following a full 2<sup>4</sup> factorial experiment whose input variables were the Na<sub>2</sub>O/SiO<sub>2</sub> and H<sub>2</sub>O/SiO<sub>2</sub> molar ratios and the milling time and speed. The effects of both main and interaction factors over the recovery percentage, production cost, morphology, surface area and porosity, crystallinity, acidity of the protonated MFI, and catalytic behavior of the latter on the alkylation of phenol with tert-butyl alcohol were established within the explored sampling space. Results showed that the Na<sub>2</sub>O/SiO<sub>2</sub> molar ratio plays a key role for the mechanochemical synthesis of MFI. Namely, this input variable may make the synthesis either viable or unviable economically due to its strong influence over the recovery percentage. This variable may also direct the synthesis to the preferential production of MOR instead of MFI. On the other hand, it was found that the milling time and speed and their interactions markedly impact the textural properties of MFI. Furthermore, the triple interaction between the input variables affected the concentration of Lewis acid sites of the produced materials. These effects were rationalized by considering that: (i) sodium can act as a structure directing agent during the mechanochemical synthesis of MFI and also can promote the incorporation of aluminum to its structure. Indeed, all the synthesized zeolites had a higher aluminum concentration as compared to the MFI seed. (ii) The milling time and speed are non-linearly correlated to the milling energy required for forming the aluminosilicate precursor that crystallizes during the hydrothermal stage of the process. Overall, all the zeolites synthesized by the mechanochemical route were less crystalline than both the MFI used as seed and an MFI synthesized by sol-gel. This was associated to the formation of amorphous agglomerates around the zeolitic crystals. It was established that these agglomerates contributed to the formation of a certain fraction of mesopores and to the Lewis acidity of the zeolites. Finally, the catalytic behavior of the mechanochemical MFI zeolites in the studied reaction was found to be linearly and positively correlated with both the concentration of Brønsted sites and with the density of acid sites. The catalytic tendencies were consistent with the proposal of a stepwise Langmuir-Hinshelwood mechanism for the alkylation of phenol with tert-butyl alcohol.

Image 1:



## **Catalytic Properties|Zeolites/Inorganic materials**

FEZA21-PO-101

### **Towards rational catalyst design: Site-specific scaling relations observed during methanol-to-olefins conversion over ZSM-5 catalysts**

T. Omojola<sup>1,2,3,\*</sup>, A. van Veen<sup>3</sup>

<sup>1</sup>Inorganic Chemistry, Fritz Haber Institute of the Max Planck Society, Berlin, Germany, <sup>2</sup>Department of Chemical Engineering, University of Bath, Bath, <sup>3</sup>School of Engineering, University of Warwick, Coventry, United Kingdom

**Abstract Text:** Understanding the formation of the first C-C bond from methanol has been a fundamental challenge in catalysis since 1977. More than 20 mechanisms have been proposed. None has quantitatively considered the elementary steps leading from oxygenates to primary olefins. Temporal analysis of products (TAP) experimentation and neutron scattering techniques decouple for the first time, diffusion, adsorption, surface reaction and desorption of species involved in the formation of the first C-C bond from methanol. An integrated approach is compared to a reductionist approach with microkinetic models applied to temperature programmed desorption (TPD), temperature programmed surface reaction (TPSR), quasi-elastic neutron scattering (QENS) and step response studies. Site-specific scaling relations are unravelled, which allow computational catalyst screening.

10 mg of ZSM-5 catalysts of varying composition (Si/Al=25, 36 and 135) formed a 2 mm shallow catalyst layer in a 25 mm packed bed employed in TPD, TPSR, step response in a TAP reactor. Additional studies were conducted to probe the mobility of methanol and DME using the QENS technique. 5 vol% methanol or DME (balance argon) was fed over the ZSM-5 catalysts at a heating rate of 5, 15 and 30 K/min. Microkinetic models accounting for dispersion, convection, adsorption, desorption, and surface reactions were solved in MATLAB.

Six ensembles of sites are obtained from the TPSR profiles of methanol and dimethyl ether over the ZSM-5 catalysts of varying compositions. Three ensembles are spectator sites solely involved in adsorption and desorption.<sup>1</sup> In accordance with archived literature,<sup>2</sup> site ensembles are assigned to different local environments in the ZSM-5 catalysts, and species thereon occupy a minority (< 1%) of them.<sup>3</sup> Following recent spectroscopic evidence and density functional theory calculations,<sup>4</sup> the methoxy methyl mechanism was further investigated. Activation energies of desorption of DME were observed to scale linearly with the barriers of the formation of key intermediates such as methoxy methyl cation and methyl propenyl ether. The scaling relation suggests a similarity in the transition state during DME desorption and that during the formation of the quoted key intermediates. It is speculated that the adsorption of DME involves an interaction of an H atom with the concerned sorption site. It was further observed that sites active between 450 – 600 K have the highest density of rate sensitive steps. Consequently, we observe that the activation energies of DME desorption can serve as a descriptor for tuning catalyst activity during MTO catalysis.<sup>5</sup> For the first time, we provide site-specific information for tuning activity over ZSM-5 catalysts.

**References:** 1. Omojola, T.; Cherkasov, N.; McNab, A. I.; Lukyanov, D. B.; Anderson, J. A.; Rebrov, E. V.; van Veen, A. C., *Catal. Lett.* 2018, 148 (1), 474-488.

2. Svelle, S.; Tuma, C.; Rozanska, X.; Kerber, T.; Sauer, J., *Journal of the American Chemical Society* 2009, 131 (2), 816-825.

3. Taylor, H. S., *Proceedings of the Royal Society of London. Series A, Containing Papers of a Mathematical and Physical Character* 1925, 108 (745), 105-111.

4. Li, J.; Wei, Z.; Chen, Y.; Jing, B.; He, Y.; Dong, M.; Jiao, H.; Li, X.; Qin, Z.; Wang, J.; Fan, W., *J. Catal.* 2014, 317 (0), 277-283.

5. Omojola, T.; van Veen, A. C., Under review. 2021.



**THERMAL DECHLORINATION AND CATALYTIC PYROLYSIS OF WEEE PLASTIC OVER NANOCRYSTALLINE MFI-ZEOLITES: THE EFFECT OF PRETREATMENT ON PRODUCTS DISTRIBUTION AND PROPERTIES**

A. Marino<sup>1,\*</sup>, A. Aloise<sup>1</sup>, J. Feroso<sup>2</sup>, P. Pizarro<sup>2,3</sup>, D. Cozza<sup>1</sup>, M. Migliori<sup>1</sup>, G. Giordano<sup>1</sup>, D. Serrano<sup>2</sup>

<sup>1</sup>University of Calabria, Rende (Cs), Italy, <sup>2</sup>Imdea Energy Institute, <sup>3</sup>ESCET, Universidad Rey Juan Carlos, Mostoles (Madrid), Spain

**Abstract Text:** Halogens represent the main bottleneck for plastic residues conversion into valuable liquids via catalytic pyrolysis, as corrosive and toxic hydro-halogens acids and organohalides can form, contaminating the products and deactivating the catalyst. A thermal pretreatment can be a suitable option to reduce the chlorine content from waste plastic, resulting in a proper feedstock before the thermo-catalytic conversion<sup>[1]</sup>.

Pyrolysis products distribution and properties can be tailored by using zeolites as catalysts to upgrade the vapors formed in the primary thermal pyrolysis of plastic. Likewise, through the optimization of the operating conditions, it is possible to direct the production towards oils rich in aromatics which, once properly extracted, can be suitable as fuels or chemicals<sup>[2-4]</sup>.

In this work, the effect of (i) thermal de-chlorination pretreatment and (ii) zeolite catalyzed upgrading are discussed in terms of products distribution from catalytic pyrolysis of plastics of real Waste Electrical and Electronic Equipment (WEEE, supplied by R.ED.EL. Srl). For this purpose, commercial nanocrystalline H-ZSM-5 (Si/Al = 42) was used as catalyst to pyrolyze the waste plastic, under different conditions (temperature, catalyst/feedstock ratio, de-halogenation step). De-chlorination pretreatment consisted in heating the feedstock (grinded to a particle size of c.a. 1 mm) at 350°C for 30 min, under N<sub>2</sub> flow. Reactions were carried out at atmospheric pressure, in a downdraft fixed-bed stainless steel reactor, with the pyrolysis and catalytic zones independently heated. Both the feedstock and reaction products were characterized by different analytical techniques (GC, GC-MS, TGA, IC).

The physicochemical characterization of the raw material revealed a polymer mixture containing 5.1 %wt of PVC, with HDPE and LDPE as major components, and contaminated by inorganics, such as calcite and metals. The pretreatment of the feedstock at 350°C allowed the amount of chlorine to be sharply reduced (61%), whilst just 3.2 wt% of organics was lost.

Compared to thermal pyrolysis, the products distribution changed considerably when the pyrolysis vapors were contacted with nanocrystalline H-ZSM-5 zeolite. When the raw plastic was employed at thermal/catalytic temperatures of 600°C and 450°C, respectively, the increase in the catalyst/feedstock ratio provided progressively lower oil yields (Table 1), favoring the formation of gaseous products from cracking reactions.

Figure 1 reports the effect of de-chlorination pretreatment on the products distribution of the oil fraction obtained from catalytic pyrolysis in presence of H-ZSM-5. Even with a similar overall mass balance, the analysis of pyrolysis oil revealed significant amounts of monocyclic aromatics (i.e. xylene and toluene), denoting that ZSM-5 promotes the oligomerization/cyclization/aromatization pathway. However, an increase in olefins and naphthenes content was found pyrolyzing the pretreated feedstock, evidencing a change on the reaction mechanism. On the other hand, as a result of de-chlorination pretreatment, a 65% reduction of the coke deposited over the zeolite was observed, together with a significant reduction (down to 95.5%) of chlorine content in pyrolysis oil.

The catalytic cracking of real plastic wastes is considerably improved using MFI-type zeolites as catalyst, due to their acidic and surface properties. The dechlorination pretreatment allows the chlorine content in the pyrolysis oil to be drastically reduced, without significant losses of organics. Moreover, a rearrangement in polymers chain is assumed to take place during the pretreatment, leading to a significant change in both oil composition and coke deposition. In summary, the results attained evidence the high potential of coupling the thermal pretreatment with the thermo-catalytic valorization over MFI-zeolites of PVC-containing waste plastics to produce oils with low-chlorine content and high-added value as fuels or chemicals.

**Image 1:**

Table 1. Product yields in pyrolysis of WEEE using H-ZSM-5 (Si/Al = 42).

Catalyst/feedstock ratio	Product yield (wt.%)				
	Wax	Gas	Oil	Char	Coke
0 (thermal)	79.0	3.1	8.9	8.9	-
0.2	0.0	28.1	62.3	8.3	0.7
0.4	0.0	47.2	43.3	8.1	0.9

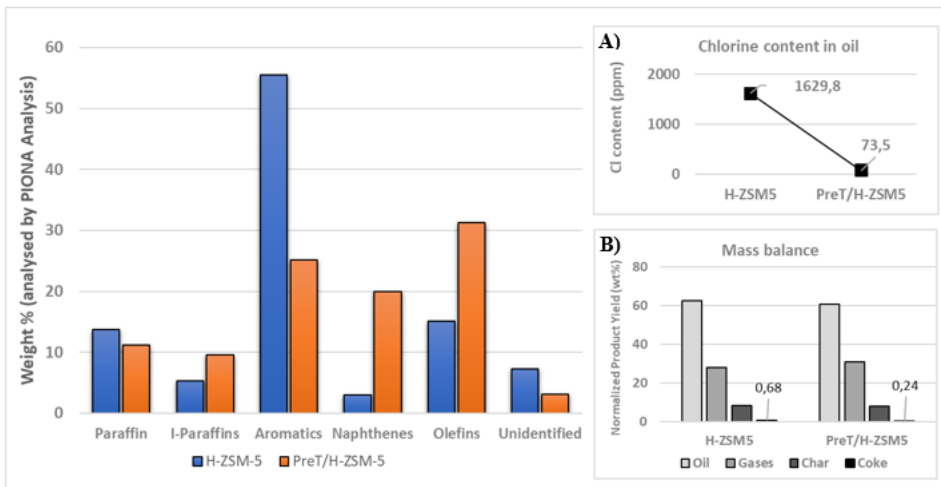
**Image 2:**

Figure 1. Products distribution, grouped in families, of the oil fraction obtained by catalytic pyrolysis of raw and pretreated WEEE plastic with H-ZSM-5 (Si/Al = 42, Cat./Feed. 0.2, thermal T = 600°C, catalytic T = 450°C). Inset A) Chlorine content of obtained pyrolysis oils. Inset B) Mass balances.

- References:** [1] Al-Salem, S.M.; Antelava, A.; Constantinou, A.; Manos, G.; Dutta, A. J. Environ. Manag. 2017, 197, 177-198.
- [2] Figueiredo A.L., Araujo A.S., Linares A., Peral A., García R.A., Serrano D.P., Fernandes Jr V.J. Journal of Analytical and Applied Pyrolysis, 2016, 117, 132-140.
- [3] Miandad, R.; Barakat, M.A.; Aburiazaiza, A.A.; Rehan, M.; Nizami, A.M. Process Safety and Environmental Protection. 2016, 102, 822-838.
- [4] Serrano D. P., Aguado J., Escola J. M.; ACS Catal. 2012, 2, 1924–1941.

## **Catalytic Properties/Zeolites/Inorganic materials**

FEZA21-PO-103

### **On the importance of molecular shape selectivity in catalytic fast pyrolysis on microporous and hierarchical Zeolites**

N. Pichot<sup>1,\*</sup>, L. Pinard<sup>1</sup>, A. Dufour<sup>2</sup>, A. Astafan<sup>1</sup>, F. Richard<sup>3</sup>, J. Liangyuan<sup>2</sup>

<sup>1</sup>E3, IC2MP, Poitiers, <sup>2</sup>LRGP, CNRS, Nancy, <sup>3</sup>E4, IC2MP, Poitiers, France

**Abstract Text:** Petrochemical products are an integral part of numerous industries and our daily lives, with plastics, packaging, clothing, digital devices, medical equipment, tires, etc. They provide substantial benefits to society, including a growing number of applications, in various cutting edge, clean technologies, which are critical to the sustainable energy system currently in development around the globe. These products are set to account for a third of the oil demand growth by 2030, and nearly half by 2050. On the other hand, oil demand for transportation fuels should decrease, owing to the generalization of public transport, alternative fuels, electrification, better fuel economy, etc. Hence, a shift in the oil, gas and petrochemical industries' landscape can be seen, going towards the development of high-value chemicals, such as BTX aromatics.

A majority of these BTX are currently produced from catalytic reforming and FCC units in refineries. These will eventually need to be replaced by more durable alternatives. One such option is the catalytic fast pyrolysis (CFP) of biomass. This process is interesting for its production of mostly green aromatics and olefins, copying the fluid catalytic cracking of crude oil. Pyrolysis is conducted under an N<sub>2</sub> atmosphere, and the gaseous emissions (oxygenated molecules derived from cellulose, hemicellulose and lignin) are upgraded on a dual fluidized bed of zeolite catalyst. They come into contact with the zeolite's acid sites, and form the aforementioned products (BTX, Olefins), along with some others, such as CO, CO<sub>2</sub> and coke. Despite growing interest for the process, CFP is still in relative infancy, when compared to some other processes, like gasification and combustion. While some processes are close to commercialisation (Anellotech/Axens, BioBTX ...), they require the development of more stable and BTX-selective catalysts.

One of the main issues with the current catalysts is their deactivation, owed to the formation of coke in their structure. In order to improve the selectivity and stability, understanding the effect of zeolite pore structure on the mechanism of coke deposition, and how these coke deposits poison the active sites (Brønsted acid sites).

A systemic comparison of various commercial (C), synthesized (S) and hierarchised (H) zeolites is provided:

- Mordenite (MOR), with a degree of hierarchisation ranging from 1.6 (C) to 4 (H<sub>A</sub>), Brønsted acidity ([PyH<sup>+</sup>], representing a concentration of Brønsted acid sites) ranging from 220 (H<sub>B</sub>) to 552 (C) μmol/g, and a mesoporous volume ranging from 0.11 (C) to 0.36 (H<sub>A</sub>) cm<sup>3</sup>/g.
- Beta (\*BEA), with a degree of hierarchisation ranging from 1.1 (S) to 4 (C), Brønsted acidity ranging from 334 (H<sub>A</sub>) to 523 (S) μmol/g, and a mesoporous volume ranging from 0.02 (S) to 0.75 (C) cm<sup>3</sup>/g.
- ZSM-5 (MFI) with a degree of hierarchisation ranging from 1.4(C) to 3.5(H<sub>A</sub>), Brønsted acidity ranging from 231(H<sub>A</sub>) to 304(C) μmol/g, and a mesoporous volume ranging from 0.07 (C) to 0.38 (H<sub>A</sub>) cm<sup>3</sup>/g.

(Characterisations given for fresh catalysts)

(Image 1)MFI appears to provide a better yield in monoaromatics HC (the target products), while producing a lesser amount of coke than MOR and \*BEA. An increase in DH produces largely better results with MFI than \*BEA and MOR. Finally, MFI, as it is or with hierarchisation, seems to be less susceptible to acid site deactivation from coke deposition.

(Image 2)A decrease in coke formation can be observed following the hierarchisation of MFI zeolite, while MOR and \*BEA's coke formations were inversely affected; while on first sight, stronger acidity seems to lead to higher coke contents for all zeolites, it appears that, through hierarchisation, it allows for less coke formation for MFI, while keeping with the supposed trend for \*BEA and MOR.

While MFI is the best so far, improvements need to be made to meet industry requirements and make it a viable option for HC production in the future.

Image 1:

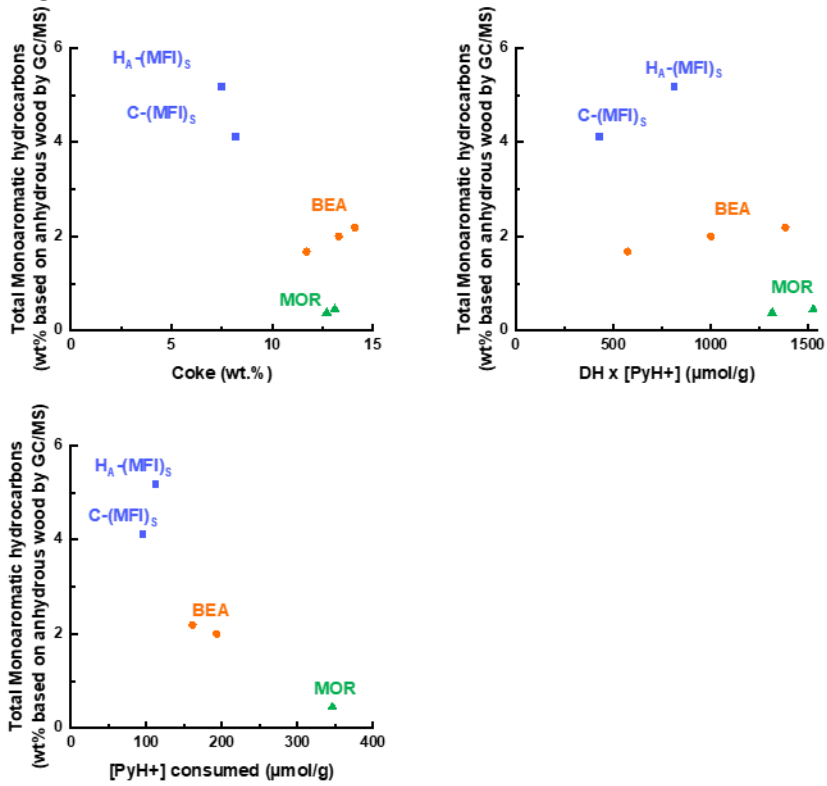
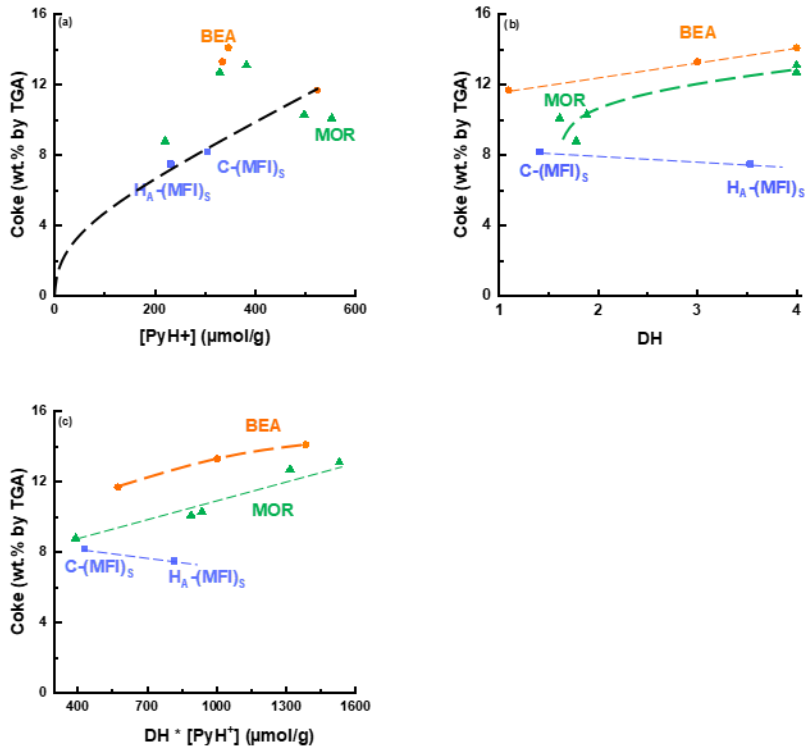


Image 2:



**Highly efficient titanosilicate catalyst Ti-MCM-68 for the oxidation of phenol with hydrogen peroxide**

S. Inagaki\*, S. Odagawa<sup>1</sup>, R. Ishizuka<sup>1</sup>, Y. Kubota<sup>1</sup>

<sup>1</sup>Division of Materials Science and Chemical Engineering, YOKOHAMA National University, Yokohama, Japan

**Abstract Text:** It is well documented that titanosilicates, which contain isolated tetrahedral Ti species in the zeolite framework, are highly efficient catalysts for the selective oxidation of a wide range of organic substrates using hydrogen peroxide (H<sub>2</sub>O<sub>2</sub>) as an oxidant [1, 2]. [Ti]-MCM-68 (**MSE** topology) has been developed as phenol oxidation catalyst showing high activity and selectivity toward *para*-isomer, hydroquinone [3, 4]. In this work, [Ti]-MCM-68 catalyst was prepared by a mild liquid-phase treatment starting from [Al]-MCM-68 for the first time. The key preparation procedures to excellent catalytic activity and high *para*-selectivity were the use of aqueous solutions of the Ti source and calcination at 650°C prior to catalytic use [5].

The hydrothermal synthesis of [Al]-MCM-68 was performed with the aid of *N,N,N',N'*-tetraethyl-bicyclo[2.2.2]oct-7-ene-2,3:5,6-dipyrrolidinium diiodide, TEBO<sup>2+</sup>(I<sup>-</sup>)<sub>2</sub> as a structure-directing agent. [Ti]-MCM-68 catalyst was obtained by the post-synthetic modification of framework Al of [Al]-MCM-68 into Ti via the acid treatment (dealumination) and the following mild liquid-phase treatment using titanium chloride hydrolysate. The Ti-modified sample, [Ti]-MCM-68\_Ti<sup>4+</sup>/H<sub>2</sub>O, was further calcined at 650°C for 4 h to give [Ti]-MCM-68\_Ti<sup>4+</sup>/H<sub>2</sub>O\_cal.

In UV-vis spectra, the as-prepared sample gave a clear peak at 210 nm, which corresponds to a 4-coordinated Ti species at closed sites, Ti(OSi)<sub>4</sub>, and a shoulder at 250 nm due to 4-coordinated Ti species at open sites, (OH)Ti(OSi)<sub>3</sub> [6], both of which are inside the framework. This reveals the successful incorporation of tetrahedral Ti into the silicate framework of dealuminated MCM-68 during the suitable treatment at room temperature. After thermal treatment at 650°C, the UV-vis peak at 210 nm increased slightly, while the UV-vis band at 250 nm remained almost unchanged, which indicates that the dehydration condensation of 4-coordinated Ti with an open site into one of the closed sites with an adjacent silanol proceeded at temperatures as high as 650°C.

Table 1 lists the results of phenol oxidation with H<sub>2</sub>O<sub>2</sub> over Ti-modified MCM-68 catalysts prepared in this work. [Ti]-MCM-68\_Ti<sup>4+</sup>/H<sub>2</sub>O (Table 1, run 1) exhibited a meaningful product yield (11.4%) with subtle *para*-selectivity (61.2%). This behaviour strongly supports the spectroscopic results suggesting the incorporation of 4-coordinated Ti species into the MSE framework with such a mild treatment. The reaction over [Ti]-MCM-68\_Ti<sup>4+</sup>/H<sub>2</sub>O\_cal obtained after thermal treatment (Table 1, run 2) gave significantly enhanced total yield (88.9%), turnover number (TON = 832) and *para*-selectivity (76.3%); the catalytic performance became much higher than that of a conventional [Ti]-MCM-68 prepared via gas-phase TiCl<sub>4</sub> treatment (Table 1, run 3). Such a thermal treatment played some role to increase the hydrophobicity of the titanosilicate catalyst, as proven by the H<sub>2</sub>O adsorption isotherm obtained at 25°C [5].

The effect of the alcoholic cosolvent was also examined. In the current catalytic system, ethanol (EtOH) was the most suitable cosolvent, which remarkably enhanced *para*-selectivity up to 94% [5]. The role of EtOH could be narrowing the space inside pores and deactivating the external active sites via hydrogen bonding between alcoholic OH and surface silanol groups [4, 5].

**Image 1:**

**Table 1.** Oxidation of phenol with H<sub>2</sub>O<sub>2</sub> over various titanasilicate catalysts<sup>a</sup>

Run	Catalyst	Temperature for Ti-introduction <sup>b</sup> / °C	Ti content <sup>c</sup> / mmol g <sup>-1</sup>	TON <sup>d</sup>	Yield <sup>e</sup> / %				para-selectivity <sup>f</sup> / %
					Total	HQ	CL	p-BQ	
1	[Ti]-MCM-68_Ti <sup>4+</sup> /H <sub>2</sub> O	25	0.206	121	11.4	5.1	4.4	1.8	61.2
2	[Ti]-MCM-68_Ti <sup>4+</sup> /H <sub>2</sub> O_cal	25	0.214	832	88.9	58.9	21.0	9.0	76.3
3	[Ti]-MCM-68_cal <sup>g</sup>	600	0.241	314	35.0	26.2	7.6	1.2	78.3

<sup>a</sup> Reaction conditions: catalyst, 20 mg; phenol, 21.25 mmol; H<sub>2</sub>O<sub>2</sub>, 4.25 mmol, H<sub>2</sub>O, 17.9 mmol; temperature, 100 °C; time, 10 min.

<sup>b</sup> The treatment with the liquid-phase titanium source was performed at predetermined temperature for 60 min.

<sup>c</sup> The Ti content per a gram-catalyst was determined by ICP-AES analysis.

<sup>d</sup> Turnover number = (moles of [HQ + CL + p-BQ] per mole of Ti site).

<sup>e</sup> Product yields based on added H<sub>2</sub>O<sub>2</sub>.

<sup>f</sup> Selectivity to *para*-isomers of dihydroxybenzenes and quinones (moles of [HQ + p-BQ] per moles of [HQ + CL + p-BQ]).

<sup>g</sup> The Ti-modification was performed using vapour-phase TiCl<sub>4</sub>.

## References:

- [1] B. Notari, *Adv. Catal.*, 41 (1996) 253.
- [2] P. Wu, T. Tatsumi, *Catal. Surv. Asia*, 8 (2004) 137.
- [3] Y. Kubota, Y. Koyama, T. Yamada, S. Inagaki, T. Tatsumi, *Chem. Commun.* (2008) 6224.
- [4] S. Inagaki, Y. Tsuboi, M. Sasaki, K. Mamiya, S. Park, Y. Kubota, *Green Chem.*, 18 (2016) 735.
- [5] S. Inagaki, R. Ishizuka, Y. Ikehara, S. Odagawa, K. Asanuma, S. Morimoto, Y. Kubota, *RSC Adv.*, 11 (2021) 3681.
- [6] M. Sasaki, Y. Sato, Y. Tsuboi, S. Inagaki, Y. Kubota, *ACS Catal.*, 4, (2014) 2653.

**Impact of proximity between Brønsted and metal sites on hydrogenation over bifunctional catalysts. Significant or Negligible?**

N. Batalha<sup>1</sup>, L. Pinard<sup>1,\*</sup>

<sup>1</sup>Institut de Chimie des Milieux et Matériaux de Poitiers (IC2MP), University of Poitiers, Poitiers, France

**Abstract Text:** Among the multiple alternatives for safe hydrogen transportation, Liquid Organic Hydrogen Carriers (LOHC) are promising technology compatible with the current infrastructure<sup>1</sup>. Hydrogen transportation via LOHC relies on the hydrogenation of aromatic hydrocarbons at the hydrogen production site, followed by their dehydrogenation at the destination point<sup>1</sup>.

The hydrogenation of aromatic compounds is promoted by supported metal catalysts, whose performance can be altered significantly by the nature of the support. Zeolites containing Brønsted sites, in specific, were demonstrated to enhance the activity of metal catalysts for the hydrogenation of aromatic hydrocarbons<sup>2</sup>. The positive effect of acid and metal sites proximity is essential for bifunctional reactions. However, hydrogenation does not follow a bifunctional mechanism, which makes the observed phenomenon more intriguing. Therefore, unraveling the mechanism behind the observed synergy can be the key to developing hydrogenation catalysts based on bifunctional catalysts.

The hydrogenation of pyridine molecules (Figure 1), at 220°C, on adsorbed on platinum promoted acid \*BEA zeolite (PtHBEA) and  $\gamma$ -Al<sub>2</sub>O<sub>3</sub> (PtAl<sub>2</sub>O<sub>3</sub>) at different proximity levels (Figure 1) to single out the mechanism behind the observed synergy. The hydrogenation reaction was followed by infrared spectroscopy as a function of hydrogen pressure, i.e.,  $0 < P(\text{H}_2) < 150$  mbar, permitting to evaluate pyridine transformation on Brønsted (PyH<sup>+</sup>) and Lewis sites (PyL) independently.

On Pt/Al<sub>2</sub>O<sub>3</sub>, piperidine formation was residual (Figure 2), even after the complete disappearance of the pyridine characteristic bands, indicating that pyridine desorption was the primary phenomenon. However, the addition of a small amount \*BEA into Pt/Al<sub>2</sub>O<sub>3</sub> (Figure 2 - PtA+HBEA (75-25)) significantly boosted piperidine formation. The increment of \*BEA in the mixture enabled higher amounts of piperidine to be formed, even if higher P(H<sub>2</sub>) was necessary (Figure 1 – PtA+HBEA (25-75)). Finally, of PtHBEA, piperidine formation was more intense and occurred at lower P(H<sub>2</sub>), clearly indicating Brønsted sites facilitate hydrogenation and the pyridinium ion (PyH<sup>+</sup>) is a reaction intermediate. Pure \*BEA could not promote pyridine hydrogenation, consequently suggesting PyH<sup>+</sup> can only be hydrogenated when in the vicinity of platinum sites.

The requirement for proximity between PyH<sup>+</sup> and platinum sites, linked to the active sites' static nature, indicates the hydrogenation occurs via hydrogenating species, often referred to as hydrogen spillover (H<sub>SP</sub>), which diffuse from the platinum sites to PyH<sup>+</sup>. The impact of hydrogen pressure in the formation of piperidine highlights this diffusion phenomenon since more P(H<sub>2</sub>) is required for complete hydrogenation to occur, i.e., attain plateau, when the PyH<sup>+</sup> and platinum are separated: PtHBEA > PtA+HBEA(75-25) >> PtA+HBEA (25-75). Additionally, no piperidine formation was observed when two non-touching wafers of PtAl<sub>2</sub>O<sub>3</sub> and HBEA were analyzed simultaneously (PtAl<sub>2</sub>O<sub>3</sub>|HBEA), suggesting hydrogenation to occur through surface diffusion.

Despite the long controversy around the existence of H<sub>SP</sub> on non-reducible supports, this has been demonstrated possible over short distances<sup>3</sup>, which would explain the synergy between Brønsted and platinum in hydrogenation to be affected by the distance between the site. Independently of the nature of H<sub>SP</sub>, the impact of the results show without a doubt that proximity between Brønsted and metal sites is significant for the hydrogenation over bifunctional catalysts. Only when these two active sites were close, significant conversion of pyridine into piperidine was observed. Hence, when Brønsted and platinum sites are close, the hydrogenation of pyridine occurred via a bifunctional mechanism with the PyH<sup>+</sup> working as a reaction intermediate.

Image 1:

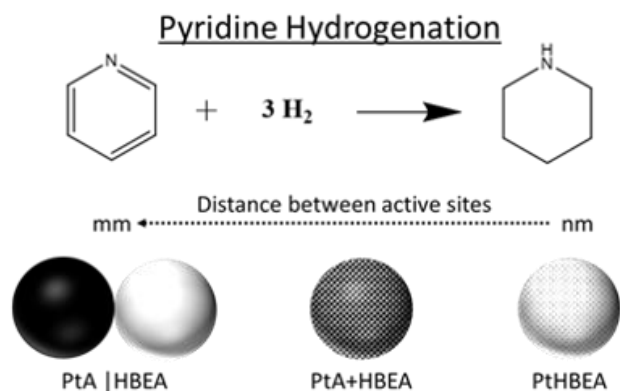


Figure 1. Scheme highlighting the distance between active sites among the different catalysts series to be used on pyridine hydrogenation to piperidine.

Image 2:

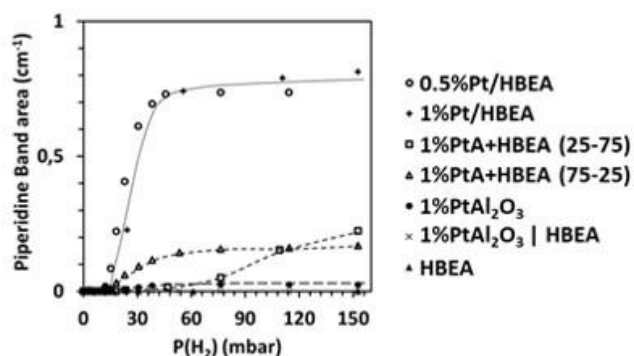


Figure 2. Piperidine formation as function of hydrogen pressure (P(H<sub>2</sub>)) for the different catalysts.

**References:** 1.

Modisha, P. M., Ouma, C. N. M., Garidzirai, R., Wasserscheid, P. & Bessarabov, D. The Prospect of Hydrogen Storage Using Liquid Organic Hydrogen Carriers. *Energy Fuels* 33, 2778–2796 (2019).

2. Chupin, J., Gnep, N. S., Lacombe, S. & Guisnet, M. Influence of the metal and of the support on the activity and stability of bifunctional catalysts for toluene hydrogenation. *Appl. Catal. Gen.* 206, 43–56 (2001).

3. Karim, W. et al. Catalyst support effects on hydrogen spillover. *Nature* 541, 68–71 (2017).

## **Catalytic Properties/Zeolites/Inorganic materials**

FEZA21-PO-106

### **On the true nature of deactivation mode in methane dehydroaromatization reaction**

A. Beuque\*, L. Pinard<sup>1</sup>, A. Sachse<sup>1</sup>, J.-F. Paul<sup>2</sup>, E. Berrier<sup>2</sup>, H. Hu<sup>2</sup>

<sup>1</sup>IC2MP, Poitiers, <sup>2</sup>UCCS, Lille, France

**Abstract Text:** Methane dehydroaromatization (MDA:  $6 \text{ CH}_4 \rightleftharpoons \text{C}_6\text{H}_6 + 9 \text{ H}_2$ ) under non oxidative condition has received great interests over the past three decades. This direct route allows to decarbonize methane into benzene while simultaneously producing sustainable hydrogen, which offers great potential as future energy resource. MDA yet faces two major hurdles: (i) low activity, as the one-pass conversion into benzene is thermodynamically limited (12% at 700 °C) and (ii) rapid catalyst deactivation, as coke formation catalysed by Brønsted sites is kinetically favoured. [1] Numerous methods have been developed in the quest to mitigate the deactivation based on new chemical engineering processes (dihydrogen permeable membrane [2], O<sub>2</sub> pulses, ...), catalyst preparation strategies (hierarchical zeolites [3]: dealumination, desilycation, templating approaches, etc...), and optimization of the operating conditions (co-reactants : CO, CO<sub>2</sub>, H<sub>2</sub>,...; precarburization nature: CH<sub>4</sub>, H<sub>2</sub>, butane,...). However, low catalytic stability still remains a major issue and is considered the major challenge to make the process viable.

In this communication, we firstly present a kinetic study of the reaction focussing on the typical deactivation period observed during the MDA reaction. From this two different phenomena could be established: (i) poisoning of molybdenum active sites by aromatics and (ii) the acting of hydrogen as scavenger, however H<sub>2</sub> excess would shift the reaction towards the reaction of methane.

Contact time was subsequently adjusted and MDA reaction was carried out at 700 °C with a reference catalyst constituted of 3wt% Mo on a commercial ZSM-5 zeolite (CBV 5020: Si/Al=25). Reaction products were analysed by gas chromatography. After 10 hours of reaction, the spent catalyst was recovered and characterized by thermogravimetric analysis. Surprisingly, rather unexpected results were obtained. Indeed, the carbon amount deposited on the recovered catalyst was higher at low contact time. Monitoring CO<sub>2</sub> intensity signals with the help of mass spectra allowed us to determine two different cokes:

- “soft” coke corresponding to the peak with lower oxidation temperature
- “hard” coke referring to higher oxidation temperature

It appeared that the “soft” coke develops independently of the contact time while the “hard” is inversely related to it (**Figure. 1**).

This observations arouse our curiosity on the real nature of deactivation in the MDA process. Further advanced characterizations and products distribution analysis revealed active sites inhibition by aromatics, which is attenuated in presence of hydrogen.

To support our assumption theoretical modelling was performed. Adsorption energy of benzene and naphthalene on molybdenum carbide was calculated and higher adsorption energy was revealed for aromatics with increasing number of cycles. . In the presence of hydrogen the adsorption energy is two times weaker demonstrating the scavenger effect of hydrogen (**Figure2**).

In conclusion, we elucidated molybdenum active sites poisoning, which allows to reason why the classical strategies based on improving diffusion properties of ZSM-5 do not yield improved catalyst stability. Indeed, improving deactivation issues in MDA process should rather be focused on active site processing.

Image 1:

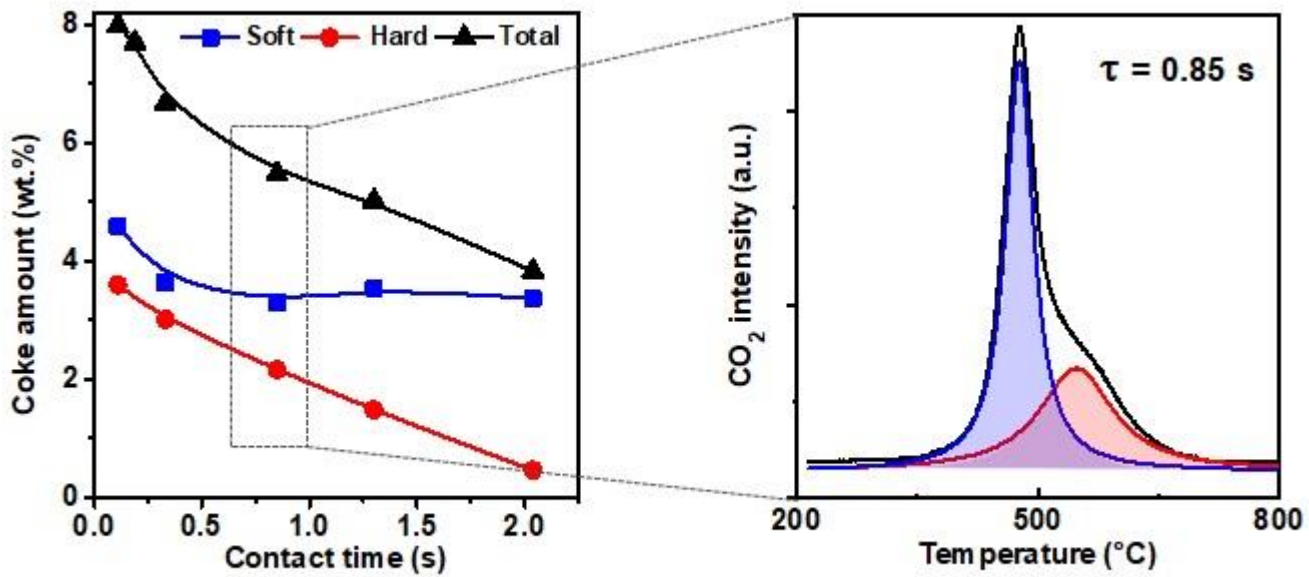


Figure.1: Coke content as function of contact time and TPO-CO<sub>2</sub> profile for one contact time : 0.85 s

Image 2:

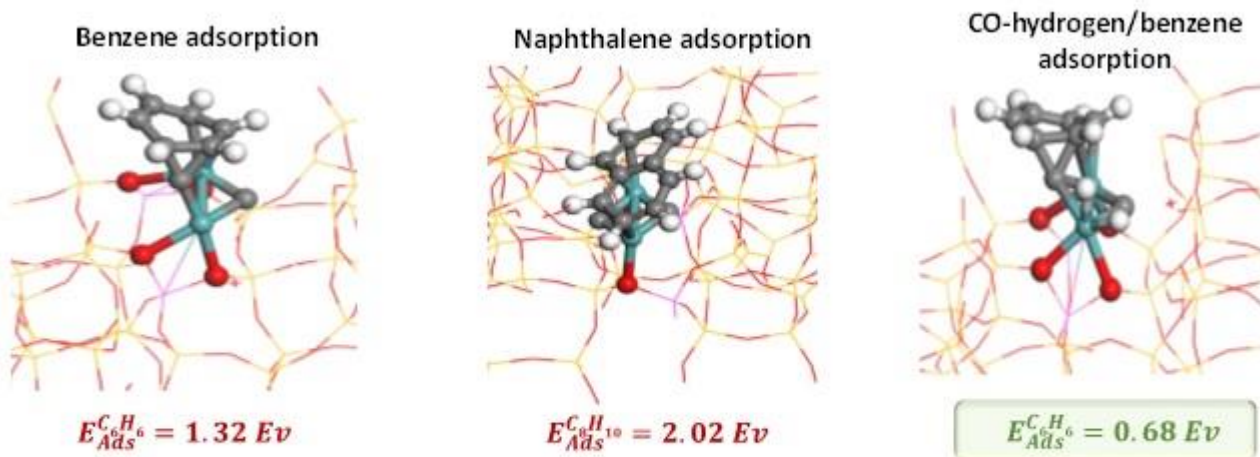


Figure. 2: DFT calculations of the adsorption energy of respectively benzene, naphthalene and benzene in presence of hydrogen on the active sites

- References: 1.Ma, S., Guo, X., Zhao, L., Susannah, S., and Bao, X. Journal of Energy Chemistry 22, 1 (2013).  
2.Natesalhawat, S., Means, N.C., and Morreale, B.D. Catal. Sci. Technol 5, 5023 (2015).  
3.Van Eck, E.R.H., and Hensen, E.J.M., Micropor. Mesopor. Mat 203, 259 (2015).

## ***Catalytic Properties/Zeolites/Inorganic materials***

FEZA21-PO-108

### **Alkylation of phenol with methanol by using zeolite catalysts**

S. R. Gajbhiye<sup>1</sup>, H. N. Pandya<sup>1,\*</sup>, V. K. Rathod<sup>1</sup>, L. K. Mannepalli<sup>1</sup>

<sup>1</sup>Department of Chemical Engineering, Institute of Chemical Technology, Mumbai, India

**Abstract Text:** Alkylation of phenol with methanol using  $\beta$ -zeolite, H- $\beta$ -zeolite, MCM-22 and H-MCM-22 was studied on a fixed bed reactor. The obtained products were anisole, 2,4-xylenol, *o*-cresol, *p*-cresol and 4-methyl anisole. Effect of various parameters such as mole ratio of reactants (phenol: methanol), temperature and weight hourly space velocity (WHSV) were studied to achieve highest phenol conversion and selectivity of the desired products. Phenol conversion decreased with increase of temperature over all the catalysts due to blocking of active sites by coke deposition. Selectivity to anisole decreased with increase of temperature due to its conversion to *p*-cresol and then to 2,4-xylenol. In addition, selectivity to anisole increases with increase of phenol to methanol feed ratio. Selectivity of 2,4-xylenol increases with increase in temperature which showed high activation energy required for the formation of 2,4-xylenol. The time on stream study showed preferential blocking of strong acid sites by coke deposition which reduces the formation of *p*-cresol and 2, 4-xylenol but weak acid sites dependent anisole formation increases. All the catalysts were analysed by different characterisation technique such as XRD, SEM-EDX, N<sub>2</sub> adsorption-desorption isotherm analysis and surface area.

**Keywords:** Zeolites, Alkylation, Phenol, Fixed bed reactor.

## ***Catalytic Properties/Zeolites/Inorganic materials***

FEZA21-PO-109

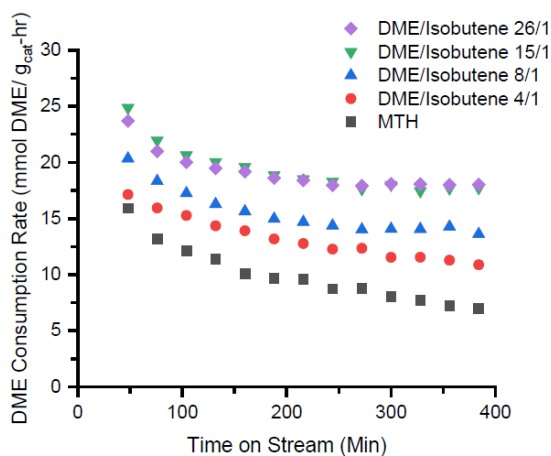
### **Olefin Methylation Reactions over Iron Zeolites: Increasing Reaction Rates at Lower Temperatures and Shifting the Selectivity Towards Desired Products**

M. LaFollette<sup>1,\*</sup>, R. Lobo<sup>1</sup>

<sup>1</sup>Chemical & Biomolecular Engineering, University of Delaware, Newark, United States

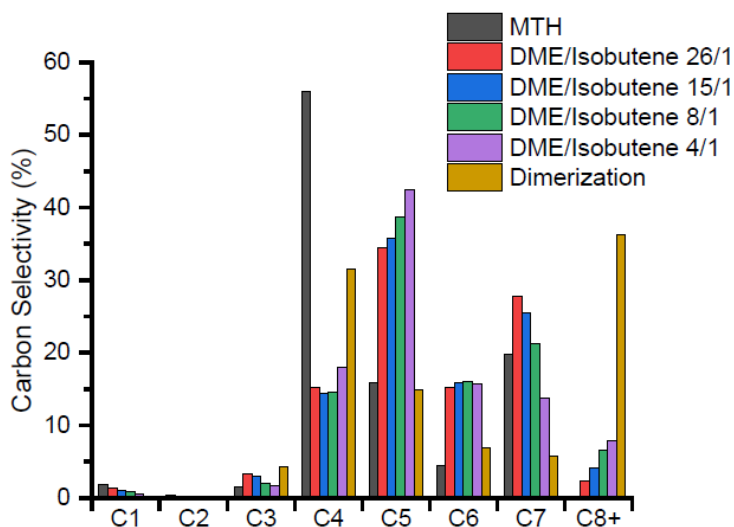
**Abstract Text:** The methanol to hydrocarbons (MTH) reaction is a pathway for converting methanol or dimethyl ether (DME) into fuels and chemicals. The reaction is catalyzed by a variety of acidic zeolites. With the large-pore zeolite H-[Al]Beta, the products are predominantly isobutane and triptane. The alkanes are formed via hydrogen transfer reactions of the isostructural olefins formed through successive methylation of small olefins in the olefin cycle of the MTH reaction. The hydride donors (other olefins) undergo further reactions to give aromatic products such as n-methylbenzenes; these side products are not valuable as a fuel and lead to catalyst deactivation. Zeolite catalysts containing framework iron reduce the rate of hydrogen transfer reactions due to their weaker Brønsted acid strength. At the same time, the methylation rates on Fe-zeolites are reduced thus, reaction temperature must be higher to get similar rates leading to rapid deactivation, for example at 400 °C and similar conditions the conversion for H-[Fe]ZSM-5 was 60% less than the for H-[Al]ZSM-5 (1). Alternatively, olefins can be added to the reactor feed to increase reaction rates at lower temperatures. This talk will describe research on understanding the kinetics and selectivity effects of olefin additives on Fe-zeolites. Over H-[Fe]Beta adding Isobutene at a DME:Isobutene ratio of 15:1 at 300 °C doubles the DME consumption rate while shifting the carbon selectivity towards C5, C6, and C7 olefins. These trends continue as the Isobutene loading is decreased; however, further addition of isobutene leads to reductions in DME consumption rates. When a medium pore zeolite H-[Fe]ZSM-5 is used, the DME consumption rate increases, and the selectivity to smaller olefin cracking products and C8 increases. Co-feeding isobutene overcomes low catalytic rates by increasing the DME consumption rate at lower reaction temperatures. The methylation of other molecules including C5-C8 olefins and cyclic alkenes over Fe-zeolites is also reported.

Image 1:



DME consumption rate over H-[Fe]Beta at 300 °C, 20 PSIG, and WHSV 6.12 g<sub>DME</sub>/g<sub>Catalyst</sub> hour<sup>-1</sup> with same total flow rate.

Image 2:



Carbon Selectivity Taken after 244 min time on stream. Reaction conditions of H-[Fe]Beta 300 °C, 20 PSIG, and WHSV of 6.12 g<sub>DME</sub>/g<sub>Catalyst</sub> hour<sup>-1</sup> with same total flow rate. Co-feed Isobutene not included in Carbon Selectivity.

Isobutene Dimerization run under similar conditions as in the DME/Isobutene ratio of 4/1 and the same total flowrate.

**References:** (1) Jin, Y.; Asaoka, S.; Zhang, S.; Li, P.; Zhao, S. Reexamination on Transition-Metal Substituted MFI Zeolites for Catalytic Conversion of Methanol into Light Olefins. *Fuel Process. Technol.* 2013, 115, 34–41. <https://doi.org/10.1016/j.fuproc.2013.03.047>.

## Catalytic Properties/Zeolites/Inorganic materials

FEZA21-PO-110

### Auto-reduction enhances low-temperature NH<sub>3</sub>-mediated NO<sub>x</sub> reduction over small-pore Cu-chabazite zeolites

D. Chen\*, V. Rizzotto, P. Chen, U. Simon

**Abstract Text: Keywords:** Cu-CHA; low-temperature NH<sub>3</sub>-SCR; auto-reduction; enhanced NO removal efficiency  
Small-pore Cu-chabazite (Cu-CHA) zeolites are the state-of-the-art catalysts for ammonia-assisted selective catalytic reduction (NH<sub>3</sub>-SCR) of automotive NO<sub>x</sub> emissions, owing to their excellent activity and hydrothermal stability.[1] However, the insufficient performance of Cu-CHA below 200 °C severely limits their practical applications.[2] Here, we demonstrated that Cu auto-reduction by non-oxidative thermal activation could enhance the low-temperature performance of Cu-CHA in NH<sub>3</sub>-SCR tests, in the presence or absence of water vapor. *In situ* impedance spectroscopy (IS) and *in situ* diffuse reflectance IR Fourier transform spectroscopy (DRIFTS) were combined to unravel the related promotion mechanisms. It was found that non-oxidative thermal activation led to an increased Cu mobility by weakening the Cu tethering to CHA framework. *In situ* DRIFTS evidenced that auto-reduction favored the activation of NO molecules to form highly reactive NO<sup>+</sup> species that are stabilized by the auto-reduced Cu sites. These mechanistic findings shed new light on tuning the condition-dependent speciation of Cu sites in small-pore zeolites to promote NH<sub>3</sub>-SCR catalysis and, more generally, selective redox catalysis for environmental and energy applications.

Image 1:

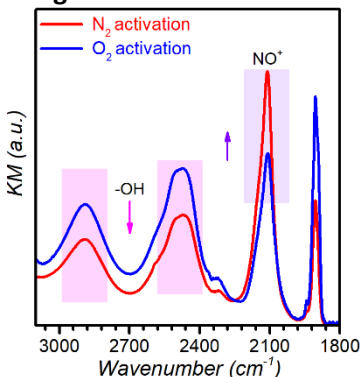
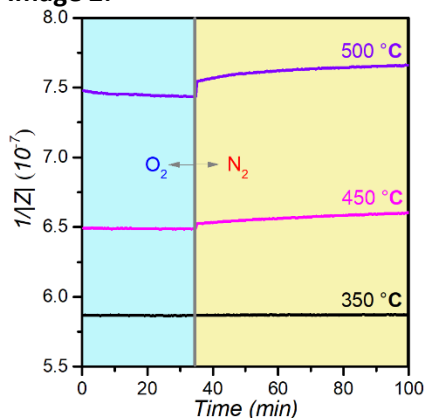


Image 2:



#### References: References

1. C. Paolucci, I. Khurana, et al. Science 2017, 357, 898-903.
2. A. Martini, E. Borfecchia, K, et al., Chem. Sci. 2017, 8, 6836-6851.

## ***Catalytic Properties/Zeolites/Inorganic materials***

FEZA21-PO-111

### **Effectiveness of 3D-printed hybrid metal-zeolite monoliths for the direct CO<sub>2</sub>-to-DME hydrogenation**

S. Todaro<sup>1,2,\*</sup>, C. Cannilla<sup>1</sup>, A. Mezzapica<sup>1</sup>, V. Middelkoop<sup>3</sup>, Y. De Vos<sup>3</sup>, F. Frusteri<sup>1</sup>, G. Bonura<sup>1</sup>

<sup>1</sup>Engineering, ICT and Technology for Energy and Transport, CNR-ITAE, Messina, <sup>2</sup>Department of Environmental Engineering, UNICAL, Rende, Italy, <sup>3</sup>Vlaamse Instelling voor Technologisch Onderzoek, VITO, Mol, Belgium

**Abstract Text:** With the aim to reduce greenhouse emissions, the recent perspectives of research are now focused not only on the development and optimization of technologies for carbon dioxide sequestration (CCS), but mainly on the conception and demonstration of new strategies for carbon dioxide utilisation (CCU) for the production of bulk chemicals or fuels [1]. In this context, particular attention has been paid on the direct catalytic hydrogenation of CO<sub>2</sub> into dimethyl ether (DME), an environmentally friendly fuel compatible with use in conventional diesel engines [2-3].

From a catalytic point of view, the direct DME synthesis is boosting an intense research effort in the development and application of novel multi-functional hybrid systems, wherein a mix of different active sites are in close interaction among them to facilitate the rate of mass transfer of a reaction intermediate towards the final product.

In this work, monolithic catalysts prepared by 3D printing are proposed as novel systems characterized by controllable and precise architectures that are unable to be made through conventional processes [1,4]. In particular, a series of CuZnZr-zeolite hybrid monoliths was prepared by a highly adaptable in-house 3D printing system that allows uniform and sufficient distribution of the active catalytic material [5,6]. This involves the direct (co)extrusion of a catalyst-containing paste and a co-catalyst through a syringe mounted on a x,y,z stage. Fine tuning of the preparation conditions also includes the selection of printing variables such as the nozzle opening (fibre thickness), the type of nozzle (fibre shape), the inter-fibre distance (pore size) and the stacking of the layers (architecture) followed by sintering.

The 3D printed monoliths were tested in the one-pot CO<sub>2</sub>-to-DME hydrogenation process (30 bar, 200-260°C), in a tubular fixed catalyst bed reactor (i.d., 14 mm; l., 250 mm), with cylinder of various compositions, diameter 9 mm, length 50 mm and porosity (voidage) 30%.

Figure 1 shows how the 3D-printed systems achieve an interesting catalytic performance, in terms of CO<sub>2</sub> conversion and DME yield, with values at 260 °C comparable to those reached on conventionally prepared systems (22% and 9% respectively).

Evidently, the operative conditions play a fundamental role in shifting the equilibrium towards the formation of MeOH/DME at expense of CO, due to a proper extent of metal-oxide interface for CO<sub>2</sub> activation induced by the preparation procedure, easy accessibility of acidic sites to drive MeOH dehydration and controlled Cu<sup>o</sup> particle size to depress the formation of side products.

These preliminary findings suggest the effectiveness of 3D-printing in the design of hybrid multi-site systems, owing to the capability of a full control of texture, structure, morphology and surface properties of the catalytic system necessary for scale-up and possible industrial exploitation.

This project has received funding from the European Union's Horizon 2020 research and innovation programme under grant agreement No. 838061. This document reflects only the authors' view and the Innovation and Networks Executive Agency (INEA) and the European Commission are not responsible for any use that may be made of the information it contains.

**Image 1:**

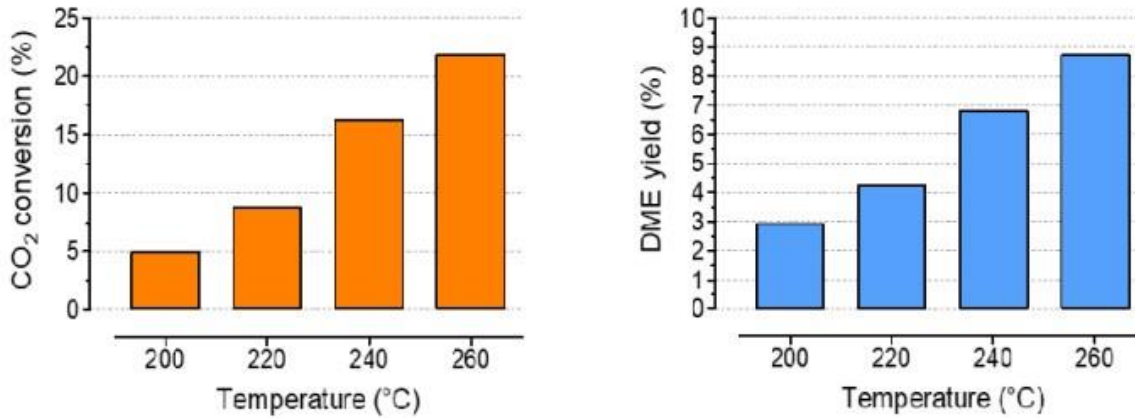


Fig. 1. CO<sub>2</sub> conversion (left) and DME yield (right) on a 3D-printed monolith. Experimental conditions. P<sub>R</sub>, 30 bar; GHSV: 1,000 NL/kg<sub>cat</sub>/h; CO<sub>2</sub>/H<sub>2</sub>/N<sub>2</sub>, 3/9/1 mol/mol.

**Image 2:**



**References:**

1. G.A. Olah, *Angew. Chem. Int. Ed.* 52 (2013) 104-107.
2. F. Frusteri, M. Cordaro, C. Cannilla, G. Bonura, *Appl. Catal., B* 162 (2015) 57-65.
3. G. Bonura, C. Cannilla, L. Frusteri, F. Frusteri, *Appl. Catal., A* 544 (2017) 21-29.
4. X. Jiang, X. Nie, X. Guo, C. Song, J.G. Chen, *Chem. Rev.* 120 (2020) 7984-8034.
5. E. Catizzone, C. Freda, G. Braccio, F. Frusteri, G. Bonura, *J. Energy Chem.* 58 (2021) 55.
6. V. Middelkoop, A. Vamvakeros, D. De Wit, S. Jacques, S. Danaci, C. Jacquot, Y. De Vos, D. Matras, S. Price, A. Beale, *J. CO<sub>2</sub> Util.* 33 (2019) 478-487.

## **Catalytic Properties/Zeilites/Inorganic materials**

FEZA21-PO-113

### **Fe, Co, Ni modified TiO<sub>2</sub> photocatalysts supported on zeolite Y with micro and hierarchical porous structure**

P. Gabriela\*, A. Elena Maria<sup>1</sup>, A. Irina<sup>1</sup>, C. Daniela Cristina<sup>1</sup>, B. Adriana<sup>1</sup>, P. Florica<sup>1</sup>, B. Jean-Luc, P. Viorica<sup>1</sup>

<sup>1</sup>Institute of Physical Chemistry "Ilie Murgulescu", Bucharest, Romania

### **Abstract Text: Fe, Co, Ni modified TiO<sub>2</sub> photocatalysts supported on zeolite Y with micro and hierarchical porous structure**

**G. Petcu<sup>1\*</sup>, E. M. Anghel<sup>1</sup>, I. Atkinson<sup>1</sup>, D. C. Culita<sup>1</sup>, A. Baran<sup>1</sup>, F. Papa<sup>1</sup>,  
J.-L. Blin<sup>2</sup> and V. Parvulescu<sup>1</sup>**

<sup>1</sup> Institute of Physical Chemistry "Ilie Murgulescu" of the Romanian Academy, Bucharest, Romania

<sup>2</sup> Faculté des sciences et technologies, Institut Jean Barriol, Université de Lorraine, Vandoeuvre lès Nancy cedex, France

#### **Introduction**

The activation of the zeolite framework by immobilization of heteroatoms (Ti and other transition metals) is a method used to obtain active photocatalysts [1]. Zeolite Y has been frequently used as support for dispersion of various metal oxides species in order to obtain highly photocatalytic active materials [2]. The supported TiO<sub>2</sub> materials were modified with different metals in order to enhance photocatalytic activity, especially under visible light irradiation. The aim of this work was to compare the effect of different 3d metallic species as Fe, Co and Ni on photocatalytic activity of Ti containing zeolite Y with microporous or hierarchical structure. The effects of support porosity and transition metal on TiO<sub>2</sub> photocatalytic properties were evaluated.

#### **Experimental**

Zeolite Y and hierarchical zeolite Y (hY) were obtained by hydrothermal method, as it was reported by our group [3]. The supports were impregnated with 5% TiO<sub>2</sub>, samples named YT5 and hYT5. The materials thus obtained have been further modified by impregnation with Fe (1 and 5%), Co or Ni (5%) using aqueous solutions of Fe(NO<sub>3</sub>)<sub>3</sub>, Co(NO<sub>3</sub>)<sub>2</sub> or Ni(NO<sub>3</sub>)<sub>2</sub>. The samples were suggestively named YT5F1, YT5F, YT5C, YT5N, hYT5F1, hYT5F, hYT5C and hYT5N. The catalysts were characterized by X-ray diffraction, SEM microscopy, N<sub>2</sub> sorption, UV-Vis, XPS, Raman spectroscopy and H<sub>2</sub>-TPR. Photocatalytic activity was evaluated in degradation of amoxicillin (AMX) under UV and visible light. The photocatalytic mechanism was investigated using scavengers. Formation of ·OH radical on the samples surface under irradiation was investigated by fluorescence technique.

The aim of this work was to compare the effect of porous support properties on photocatalytic activity and the interaction between supported gold and titanium oxides.

#### **Results and discussion**

Zeolite Y has a typical octahedral morphology (Fig. 1) with smooth surface, before and after Ti and transition metals immobilization. Change of morphology and formation of aggregates was evidenced for hierarchical samples. The wide angle X-ray diffraction patterns (Fig. 2) evidenced the preservation of zeolite Y crystallinity after immobilization of Ti and Fe, excepting the samples with higher Co and Ni oxide concentrations. In agreement with Raman results, XPS spectra of samples YT5F and hYT5F suggest formation of a non-stoichiometric Fe<sub>3</sub>O<sub>4-δ</sub> with a mixture of 2+ and 3+ oxidation states. For samples with Co and Ni was evidenced the presence of bulk oxides and some metal sites incorporated into the zeolite framework.

Fig. 1 SEM Images of zeolite Y (sample YT) and hierarchical zeolite Y (sample hYT) modified with TiO<sub>2</sub>

Fig. 2. Wide angle XRD patterns of modified zeolite Y and hY

The support properties and type of secondary immobilized metallic species influenced both the dispersion and metal-titania interaction, leading to formation of different reactive species responsible for the photocatalytic degradation of AMX. By using of scavengers it was showed a variation of the mechanisms for AMX degradation depending on metal nature. Thus, for samples with the best result (Ti-Ni modified zeolite Y), the main active species varied as follows: h<sup>+</sup>>O<sup>2-</sup>>·OH.

#### **Conclusions**

New active photocatalysts were obtained by dispersion of TiO<sub>2</sub> and different 3d transition metal (Fe, Co, Ni) oxides on zeolite Y with microporous or hierarchical structure. The higher efficiency in AMX degradation was obtained under visible light for all the samples with hierarchical zeolite.

Image 1:

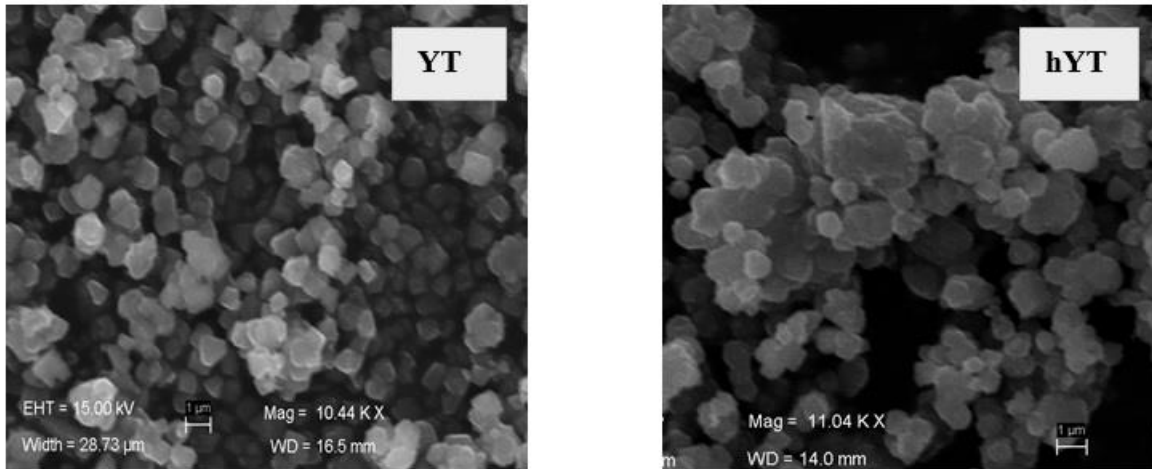
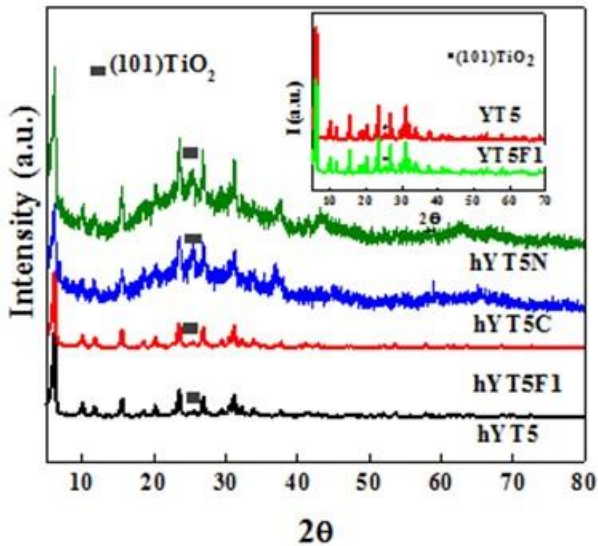


Image 2:



**References:** References

- [1] H. Wang, B. Yang, W. Zhang, *Advanced Materials Research* 129-131 (2010) 733-737.
- [2] T. Kamegawa, Y. Ishiguro, R. Kido, H. Yamashita, *Molecules* 19 (2014) 16477-16488.
- [3] G. Petcu, E. M. Anghel, S. Somacescu, S. Preda, D. Culita, S. Mocanu, M. Ciobanu, V. Parvulescu, *Journal of Nanosci Nanotechnol* 20 (2020) 1158-1169.

**Aqueous phase isomerization of saccharides over modified versions of AM-4**

A. A. Valente<sup>1,\*</sup>, M. M. Antunes<sup>1</sup>, A. Fernandes<sup>2</sup>, F. Ribeiro<sup>2</sup>, Z. Lin<sup>1</sup>

<sup>1</sup>CICECO - Aveiro Institute of Materials, Department of Chemistry, University of Aveiro, CICECO - Aveiro Institute of Materials, Department of Chemistry, University of Aveiro, Aveiro, <sup>2</sup>Centro de Química Estrutural, Instituto Superior Técnico, Universidade de Lisboa, Centro de Química Estrutural, Instituto Superior Técnico, Universidade de Lisboa, Lisbon, Portugal

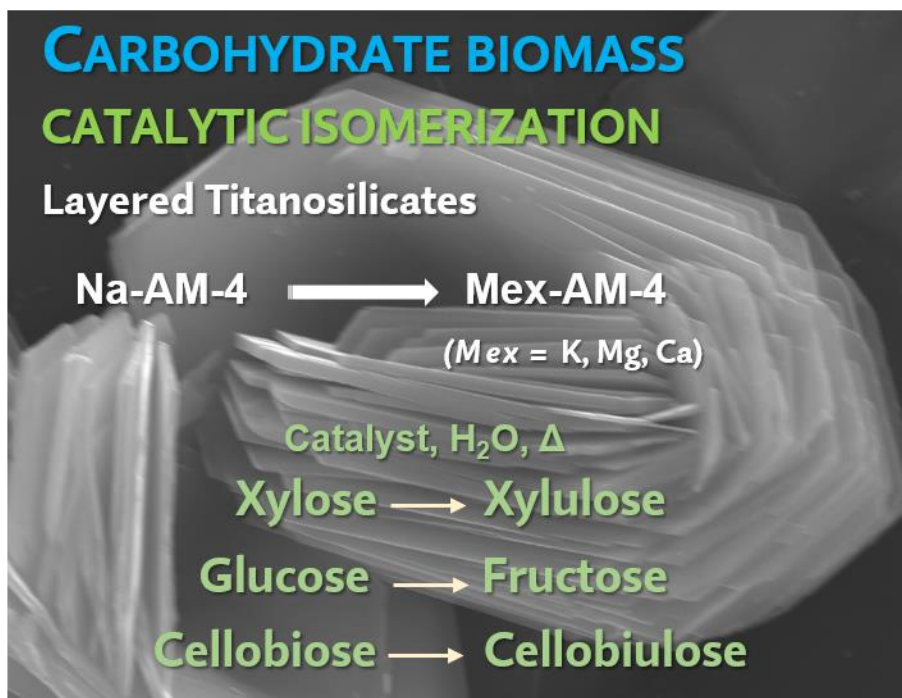
**Abstract Text:** The main organic components of vegetable biomass are carbohydrates such as, cellulose and hemicelluloses which may be hydrolyzed to the most abundant aldo-saccharides. The isomerization of aldoses to ketoses is an important transformation in biomass conversion processes, since it may allow the production in higher yields of platform and more specific bio-based products.<sup>1</sup>

The present work is focused on the heterogeneous catalytic isomerization of the saccharides D-glucose to fructose, D-xylose to xylulose, and D-cellobiose to cellobiulose, in water, at 100 °C (Figure 1). The titanosilicate Aveiro-Manchester material number 4, AM-4 ( $\text{Na}_3(\text{Na,H})\text{Ti}_2\text{O}_2[\text{SiO}_6]_2 \cdot 2\text{H}_2\text{O}$ ) has a unique layered structure and ion exchange ability, allowing to tune its properties for different applications.<sup>2</sup> Very few catalytic applications were reported to date for the AM-4 family, and were focused on the hydrothermally as-synthesized material. We set out to modify AM-4 by introducing potassium, magnesium and calcium in order to meet superior performances for the base-catalyzed isomerization of the aldo-saccharides, using water as solvent, at 100 °C. Special attention was given to aspects of catalyst stability. All materials prepared possessed isomerization activity. Although the as-synthesized AM-4 material was active for D-glucose isomerization, it was poorly stable.<sup>3</sup> The modified versions prepared in this work were more stable catalysts, with the magnesium-containing material being the most stable.

**Figure 1.** Modified AM-4 type catalysts for the aqueous phase isomerization of saccharides.

**Acknowledgements:** We acknowledge the support of CICECO-Aveiro Institute of Materials, project UIDB/50011/2020 & UIDP/50011/2020, financed by national funds through the FCT/MEC [FCT (Fundação para a Ciência e a Tecnologia)] and when appropriate co-financed by FEDER under the PT2020 Partnership Agreement. The positions held by M. M. A. and A.F. were funded by national funds (OE), through FCT, I.P., in the scope of the framework contract foreseen in the numbers 4, 5 and 6 of article 23 of the Decree-Law 57/2016 of 29 August, changed by Law 57/2017 of 19 July. The NMR spectrometers are part of the National NMR Network (PTNMR) and are partially supported by Infrastructure Project Nº 022161 (co-financed by FEDER through COMPETE 2020, POCI and PORL and FCT through PIDDAC).

Image 1:



**References:** [1] B. Li, P. Reluea, S. Varanasi, *Green Chem.* 14 (2012) 2436-2444. [2] M.S. Dadachov, A. Ferreira, J. Rocha, M.W. Anderson, *Chem. Commun.* (1997) 2371–2372. [3] S. Lima, A.S. Dias, Z. Lin, P. Brandao, P. Ferreira, M. Pillinger, J. Rocha, V. Calvino-Casilda, A.A. Valente, *Appl. Catal. A Gen.* 339 (2008) 21–27.

**Hydrodeoxygenation of levulinic acid over Pd/ZrO<sub>2</sub> catalysts**

E. G. Gioria<sup>1</sup>, G. Novodárszki<sup>2</sup>, L. Gutierrez<sup>1</sup>, Á. Szegedi<sup>2</sup>, J. Valyon<sup>2</sup>, M. R. Mihályi<sup>2,\*</sup>, D. Dekac<sup>3</sup>

<sup>1</sup>Research on Catalysis and Petrochemistry, INCAPE—(FIQ, UNL-CONICET), Santa Fe, Argentina, <sup>2</sup>Institute of Materials and Environmental Chemistry, Research Centre for Natural Sciences, Budapest, Hungary, <sup>3</sup>Tezpur University, Tezpur, India

**Abstract Text:** Lignocellulosic biomass represents a huge source of renewable carbon. Its processing into biofuels and chemicals is in the focus of global research. Acidic hydrolysis of its polymeric carbohydrate components, such as cellulose and hemicellulose, gives C<sub>6</sub> and C<sub>5</sub> sugars, respectively. Chemocatalytic transformation of sugars can be directed to give levulinic acid (LA) as main product. Large-scale production of LA has already been realized from waste cellulosic materials. In consecutive catalytic hydrogenation and dehydration reactions LA can be converted to  $\gamma$ -valerolactone (GVL).

Catalytic hydroconversion of LA gives GVL. Efficient production of GVL was demonstrated over both homogeneous and heterogeneous noble metal (mainly Ru) and non-noble metal (Cu, Ni) catalysts using either molecular H<sub>2</sub> or formic acid as hydrogen source. Pd supported on carbon, silica or niobia were also investigated as catalysts. Only few papers have been published about utilizing Pd/ZrO<sub>2</sub> catalyst in the reaction. In the present work, zirconia-supported palladium catalysts were prepared and tested.

Palladium chloride is a widely used precursor for the preparation of oxide supported Pd catalysts. Thermal decomposition of Pd precursor impregnated on the support results in a catalyst that retains chloride ions and thus accelerates or suppresses reactions in certain cases. We applied a novel preparation method to avoid the unfavorable catalytic activities. Physical mixture of commercial zirconia (MEI Inc.) and PdCl<sub>2</sub> was simply immersed and stirred in aqueous solution of ammonia. The thus formed Pd-tetraammine complex was reduced with hydrazine, depositing metallic Pd nanoparticles on the zirconia surface. By washing out the formed NH<sub>4</sub>Cl, the catalyst became totally chloride free. The catalyst was denoted as Pd/ZrO<sub>2</sub>(NH<sub>4</sub>). For comparison a catalyst was prepared by calcining H<sub>2</sub>PdCl<sub>4</sub>-impregnated zirconia (Pd/ZrO<sub>2</sub>(Cl) catalyst). The catalysts were characterized by chemical and thermogravimetric analysis, *in-situ* and *ex-situ* XRD, N<sub>2</sub> physisorption, FT-IR spectroscopy, TEM, and Raman spectroscopy. Dispersion of palladium was determined by the CO-chemisorption method. The Pd content of both catalysts was 5 m/m %. Their XRD patterns revealed that zirconia was in monoclinic phase. PdClO<sub>x</sub> species were identified by Raman spectroscopy in the Pd/ZrO<sub>2</sub>(Cl) catalyst, indicating that that catalyst contains chloride, bound to the zirconia support and/or to the metal. No chloride-containing species were detected in Pd/ZrO<sub>2</sub>(NH<sub>4</sub>) catalyst.

The activity, selectivity, and stability of the two catalysts were compared in the gas-phase hydrodeoxygenation of levulinic acid at atmospheric pressure in the temperature range of 260-320 °C. A continuous flow-through fixed-bed microreactor was used, and molecular hydrogen was applied as reducing agent. GVL was the main LA hydroconversion product over both catalysts. Angelica lactones ( $\alpha$ -AL, and  $\beta$ -AL) and 2-butanone appeared as side products. Results suggested that levulinic acid was first dehydrated to  $\alpha$ -AL and then the hydrogenation of its C=C double bond led to GVL. A fraction of  $\alpha$ -AL intermediate was isomerized to  $\beta$ -AL. Formation of a low amount of 2-butanone indicated that decarboxylation of levulinic acid also occurred to a small extent.

Although the Pd dispersion was higher in Pd/ZrO<sub>2</sub>(Cl) than in Pd/ZrO<sub>2</sub>(NH<sub>4</sub>), the latter catalyst showed better catalytic performance in LA hydrodeoxygenation. Higher LA conversion, higher selectivity to GVL, and higher stability were achieved over the chloride-free catalyst than over the chloride-containing one.

**Acknowledgments** The authors thank the financial support of the National Research, Development and Innovation Office of Hungary (Indo-Hungarian project, 2019-2.1.13-TET\_IN-2020-00043).

## A comparative study of methylamines synthesis over zeolites rho and PST-29

J. Shin<sup>1,\*</sup>, H. Lee<sup>2</sup>, K. Lee<sup>2</sup>, S. B. Hong<sup>2</sup><sup>1</sup>Research Center for Convergent Chemical Process, Korea Research Institute of Chemical Technology, Daejeon, <sup>2</sup>Center for Ordered Nanoporous Materials Synthesis, Division of Environmental Science and Engineering, POSTECH, Pohang, Korea, Republic Of

**Abstract Text:** Methylamines (MAs) synthesis is a technologically important process due to their main uses as intermediates in the solvent, pesticide, and water treatment industries [1]. The formation of trimethylamine (TMA,  $3.9 \times 5.4 \times 6.1 \text{ \AA}$ ) is thermodynamically more favourable than that of monomethylamine (MMA,  $3.7 \times 3.9 \times 4.4 \text{ \AA}$ ) or dimethylamine (DMA,  $3.9 \times 4.7 \times 6.0 \text{ \AA}$ ), industrially the most widely used product among the MAs. To enhance the selectivities to MMA and DMA, therefore, considerable effort has been devoted to the continuous testing of a number of small-pore zeolites with different framework structures and compositions [2].

Very recently, we have been able to synthesize the second generation of the RHO family named PST-29 (framework type PWN) using *N,N'*-dimethyl-1,4-diazabicyclo[2,2,2]octane as an organic structure-directing agent via a multiple inorganic cation approach [3]. Unlike its higher generation members of this family of zeolites, in addition, PST-29 when synthesized using a seeding technique can be converted into the proton form without severe loss of structural integrity. Here we compare the catalytic properties of H-rho and H-PST-29 and their steam-dealuminated analogues for MAs synthesis [4].

Figure 1a and 1b show methanol conversion and yields in the sum of MMA plus DMA as a function of time on stream (TOS) in MAs synthesis over H-rho, H-PST-29, and their steam analogues. An initial MeOH conversion close to 100% was observed for H-rho and H-PST-29. The same result was obtained from their steamed analogues at 600 °C (denoted as H-rho-600 and H-PST-29-600, respectively) with higher framework Si/Al ratios. Furthermore, H-PST-29 showed a comparable yield (81 vs 85%) in MMA plus DMA to that of H-rho, the most widely studied catalyst for this reaction. The same trend can be drawn from the catalytic results of their steamed analogues. Figure 1c shows the long-term performance of H-rho, H-PST-29, their steamed analogues, and H-mordenite at 400 °C but a higher WHSV ( $4.3 \text{ h}^{-1}$ ).

Interestingly, steam treatment at 600 °C gave H-rho and H-PST-29 an increase in catalyst lifetime, but which is much more apparent in H-PST-29, probably due to a larger decrease in strength of medium and strong acid sites, together with the mesopore generation. Another interesting result is that while the MeOH conversion of H-PST-29-600 is almost identical to that of H-mordenite, a formerly used commercial catalyst for this reaction, a fairly higher yield in MMA plus DMA is always observed for the former zeolite. The amount of organic deposited during MAs synthesis at 400 °C is higher in the order H-mordenite  $\sim$  H-PST-29-600 < H-PST-29 < H-rho-600 < H-rho. We note that this order is essentially opposite to that of yield in two smaller MAs observed after MAs synthesis at 400 °C and  $4.3 \text{ h}^{-1}$  WHSV for 50 h on stream. Therefore, we believe that the acidic properties of small-pore zeolites, especially the concentration and strength of their Brønsted acid sites, appear to be more important in achieving high stability during this reaction than their 8-ring dimensions and/or cage structure.

## Image 1:

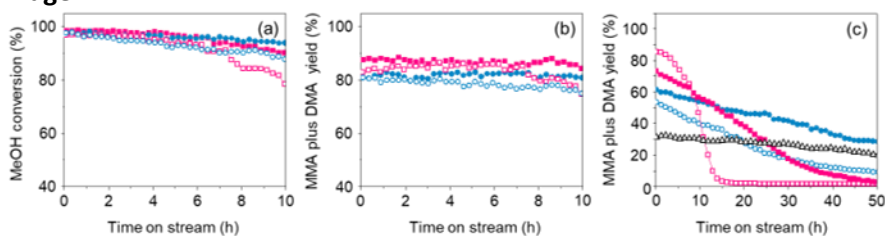


**Fig. 1.** (a) MeOH conversion and yields in (b) MMA plus DMA and (c) long-term MMA plus DMA as a function of TOS in MAs synthesis over H-rho (□), H-PST-29 (○), H-rho-600 (■), H-PST-29-600 (●), and H-mordenite (△) at 400 °C, 1.7 or  $4.3 \text{ h}^{-1}$  WHSV, and 10.1 kPa of both  $\text{NH}_3$  and MeOH.

**References:** [1] K. S. Hayes, Appl. Catal. A 221 (2001) 187.

[2] H. -Y. Jeon, C.-H. Shin, H. J. Jung, S. B. Hong, Appl. Catal. A 305 (2006) 70.

[3] H. Lee, J. Shin, W. Choi, H. J. Choi, T. Yang, X. Zou, S. B. Hong, Chem. Mater. 30 (2018) 6619.

[4] H. Lee, K. Lee, J. Shin, S. B. Hong, in preparation.

**Knoevenagel condensation catalyzed by amine-functionalized zeolite A at different crystallization degree**

I. W. Zapelini<sup>1,\*</sup>, D. Cardoso

<sup>1</sup>Chemical Engineering, Federal University of São Carlos, São Carlos, Brazil

**Abstract Text:** Zeolites may have basicity or acidity, depending on the procedures adopted during their preparation. Also, the silanols present in these materials allow exploring the functionalization of zeolites through reactions with various functional groups, which may be acidic, basic or multifunctional.

Anchoring amines to zeolites is a strategy for generating basic sites that can be used for catalysis or adsorption [1]. This functionalization occurs through the reaction of orthosilicates that contain the aminosilane group, by condensation with the superficial zeolite silanols. During functionalization, the presence of functional groups may clog the pores, generating diffusional restrictions that reduce the catalytic activity of these materials.

This study aimed to evaluate the effect of zeolite A crystallization degree on its ability to be functionalized with propylaminesilane groups. Synthesis of zeolite A in sodium form was performed via the hydrothermal method following the procedure described in [2], with a Si/ Al molar ratio of the reaction mixture equal to 0.963. The hydrothermal treatment of the mixture was performed at 100 ° C at different times (0, 60, 75, 90 and 120 min). Propylaminesilane groups were then anchored to the zeolites (250 mg) using aminopropyltrimethoxysilane (2 mL) under reflux of toluene (5 mL) for 48h at 80 ° C. The catalysts were named NH-A-x (where x = 0; 60; 75; 90; 120 is the zeolite crystallization time).

The materials were tested as catalysts in the Knoevenagel condensation between ethyl cyanoacetate and benzaldehyde in stoichiometric proportions using ethanol as a solvent (85% w/w). The reactions were carried out in a batch reactor with a 3 mL reaction mixture volume for 30 min at 40 °C, with an analysis of the reaction mixture by gas chromatography.

It is observed in Figure 1 that the onset of zeolite crystallization is detectable by X-ray diffraction in 75 min of hydrothermal treatment, and at 120 min the zeolite of pure LTA structure is obtained. Therefore, one has a completely amorphous aluminosilicate in 0 min and a completely crystalline aluminosilicate in 120 min.

**Figure 1.** XRD patterns Na-A at different times of crystallization.

**Figure 2.** Benzaldehyde conversion using amine-functionalized Na-A at different stages.

The catalytic results (Figure 2) show that the least crystallized aluminosilicates are the most active. From the beginning of crystallization, the catalytic activity drops considerably, with the activity of the catalyst NH-A-120 only 15% of the activity of the completely amorphous one (NH-A-0). These results can be attributed to two effects: (1) in less crystallized aluminosilicates, the amount of silanol defects in the solid is higher [3], which leads to a greater possibility of anchoring the amines via silane hydrolysis reactions with surface silanols; and (2) the greater activity in less crystallized materials may also be a result of greater accessibility to catalytic sites in these solids, as increased crystallization degree decreases exposure of catalytic sites [4].

These results show that the degree of crystallization of zeolite is an important variable in its catalytic activity when applied in reactions involving bulky molecules, such as the Knoevenagel condensation product studied in this work.

**Image 1:**

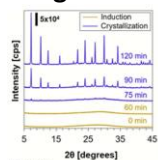


**Image 2:**

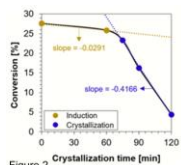


Figure 2

**References:** [1] Kalbasi, R. J.; Mansouri, S.; Mazaheri, O., *Res Chem Intermed*, v. 44, p. 3279-3291, 2018.

[2] Mintova, S., Barrier, N. *Verified Syntheses of Zeolitic Materials*, Elsevier, 2016.

[3] Chang, C. D.; Bell, A. T., *Catalysis Letters*, v. 8, p. 305-316, 1991.

[4] Haw, K.; Goupil, J.; Gilson, J.; Nesterenko, N.; Minoux, D.; Dath, J.; Valtchev, V., *New Journal of Chemistry*, v. 40, p. 4307-4313, 2016.

**Catalytic Properties/Zeolites/Inorganic materials/Poster**

FEZA21-PO-118

**LDPE Cracking over Zeolites: the role of pore size**

K. Pyra<sup>1,\*</sup>, K. Tarach<sup>1</sup>, D. Majda<sup>1</sup>, K. Góra-Marek<sup>1</sup>

<sup>1</sup>Faculty of Chemistry, Jagiellonian University in Kraków, Kraków, Poland

**Abstract Text:** Among the various methods of plastic waste recycling, the catalytic conversion realized via syn-gas into diesel or by direct catalytic conversion into valuable gas and liquid products (as a precursor to fuels or chemicals) seem the most promising method. Low-density polyethylene is of the highest demand polymer thus we focused on its catalytic degradation under operando conditions [1,2]. Zeolites are the most known acidic catalysts applied in refinery and petrochemistry processes. Their outstanding acidic properties corroborated with the presence of strictly defined internal voids are key properties ruling their catalytic behaviour.

The main purpose of this study was to determine the role of the pore size and channels topology on the catalytic cracking of LDPE. Both 10-ring (ZSM-5, TNU-9, IM-5) and 12-ring zeolites (Beta, Y, mordenite) were widely characterized (ICP EOS, XRD, TEM, low-temperature nitrogen sorption, IR spectroscopic studies of probes sorption) in order to obtain information on their textural, structural and acidity properties. The catalytic activity was evaluated in the cracking of LDPE followed by TGA analysis and *operando* IR studies. Among many interesting correlations derived from the catalytic tests, the special attention has been paid on the rate of coke precursors formation. In the 12-ring zeolites (zeolite Y) coke species appeared just after the reaction started while the 10-ring structure of ZSM-5 prevented the production of these compounds during LDPE cracking. The presence of 12-MR zeolites as the catalysts benefited in the decrease the 50 % conversion temperature ca. 150 °C in comparison to thermal cracking. For 10-MR zeolites, the observed effect was less significant.

*Acknowledgement: The work was financed from the National Science Centre, Poland under Grant No. 2017/27/B/ST5/00191 and POB Anthropocene student mini-grants Talent Management.*

**References:** [1] Association of Plastics Manufacturers, „Plastics – the Facts 2019: An analysis of European plastics production, demand and waste data”, PlasticsEurope 2019, 1–42.

[2] K. Tarach, K. Pyra, S. Siles, I. Melián-Cabrera, K. Góra-Marek, ChemSusChem, 2019, 12, 633-638.

**Mild liquid phase oxidation of benzyl alcohol in the presence of microporous framework copper silicates**

P. Neves<sup>1</sup>, A. Valente<sup>1</sup>, Z. Lin\*

<sup>1</sup>Department of Chemistry, CICECO and University of Aveiro, Aveiro, Portugal

**Abstract Text:** Benzaldehyde and benzoic acid are industrially produced chemicals with commercial importance due to their broad markets, which still continuously growing up. The most important industrial processes for these compounds involve liquid phase air oxidation of toluene. Few studies were reported on the synthesis of benzaldehyde and benzoic acid via partial oxidation of benzyl alcohol over heterogenous catalysts based on copper, which is an earth-abundant, relatively cheap transition metal capable of conferring versatile catalytic properties to materials for organic reactions involving one or two-electron mechanisms. In this work, the copper silicates  $(\text{Na,K})_4\text{Cu}_2\text{Si}_{12}\text{O}_{27}(\text{OH})_2 \cdot x(\text{Na,K})\text{OH} \cdot y\text{H}_2\text{O}$  (**1**) and  $(\text{Na,K})_2\text{CuSi}_5\text{O}_{12} \cdot x\text{H}_2\text{O}$  (**2**) were studied as heterogenous catalysts for producing benzaldehyde and benzoic acid via mild partial oxidation of benzyl alcohol, with the attention given to the influence of the type of oxidant and solvent on the reaction, mechanistic insights and catalyst stability. Both copper catalysts were prepared under hydrothermal conditions. They are, for the first time, used for the benzyl alcohol reaction. The materials were characterized by powder XRD, scanning electron microscopy, energy dispersive X-ray spectrometry, thermogravimetry, Nitrogen adsorption-desorption.

The results indicated that both materials are effective heterogeneous oxidation catalysts for producing benzaldehyde and benzoic acid from benzyl alcohol, under mild reaction conditions (approximately atmospheric pressure and 70 °C). The reaction of benzyl alcohol using tert-butyl hydroperoxide as oxidant and acetonitrile as solvent, led to 72-83% conversion at 24 h, and up to 82% total selectivity to benzaldehyde and benzoic acid. On the other hand, benzoic acid was obtainable in 94% yield from benzaldehyde. Both materials acted as heterogeneous catalysts promoting benzyl alcohol oxidation via a radical reaction mechanism where copper sites may activate the oxidant molecules. The type of oxidant and solvent influenced the catalytic performances.

**Acknowledgements:** we acknowledge the support of CICECO-Aveiro Institute of Materials, project UIDB/50011/2020 & UIDP/50011/2020, financed by national funds through the FCT/MEC [FCT (Fundação para a Ciência e a Tecnologia)] and when appropriate co-financed by FEDER under the PT2020 Partnership Agreement. The position held by P.N. was funded by national funds (OE), through FCT, I.P., in the scope of the framework contract foreseen in the numbers 4, 5 and 6 of article 23 of the Decree-Law 57/2016 of 29 August, changed by Law 57/2017 of 19 July.

**Polyester Monomer Production by Heterogeneous Zeolite Catalysts**

S. Meacham<sup>1,\*</sup>, R. Taylor<sup>1</sup>

<sup>1</sup>Department of Chemistry, Durham University, Durham, United Kingdom

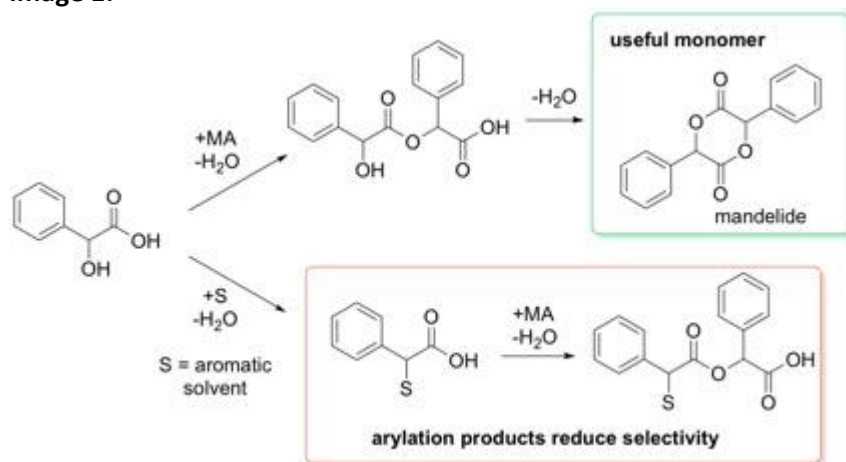
**Abstract Text:**

Cyclic esters such as lactones and lactides are key monomers for the synthesis of biodegradable polymers. Poly(lactic acid) (PLA) is the most common example, synthesised by ring opening polymerisation of lactide, the cyclic diester of lactic acid. PLA production is hampered by the energy intensive, multi-step process for synthesising lactide, as well as the resultant polymer's relatively low glass transition temperature (~55 °C). Heterogeneous zeolite catalysts can selectively produce lactide from lactic acid in a single step.<sup>1</sup> However, the use of zeolites in synthesis of monomers from alpha-hydroxy acids with greater functionality than lactic acid, such as 2-hydroxy-but-3-enoic acid, are reported to be less selective.

In this work, the cyclisation of a phenyl-substituted alpha-hydroxy acid, mandelic acid (MA), to its cyclic diester dimer, mandelide, has been investigated over a range of commercial Bronsted-acidic zeolites. Poly(mandelic acid), the polyester synthesised by ring opening polymerisation of mandelide, has been shown to have higher glass transition temperature than PLA, and is proposed as a polyester analogue of poly(styrene).<sup>2</sup>

Initial screening of commercial H-zeolites with various Si/Al ratios and framework type showed that H-Beta and H-Y were the most active for mandelic acid conversion. However, over H-Beta and H-Y, a significant amount of mandelic acid is arylated by the aromatic xylene reaction solvent used. This undesired substitution reaction renders mandelic acid unreactive towards cyclisation and significantly reduces selectivity towards mandelide compared with lactic acid to lactide over similar catalysts.<sup>1</sup> The formation of these byproducts has been further investigated in various solvents, in both batch and flow reactions. It has been found that the nature of the solvent can influence the selectivity of reactions similar to conventional aromatic substitutions. The substituents on the aromatic ring control the amount of arylation product formed and through solvent choice it is possible to increase mandelide yield above that of the initial reaction in xylene.

**Image 1:**



**References:**

1. M. Dusselier, P. Van Wouwe, A. Dewaele, P. A. Jacobs and B. F. Sels, *Science*, 2015, 349, 78-80.
2. T. Q. Liu, T. L. Simmons, D. A. Bohnsack, M. E. Mackay, M. R. Smith and G. L. Baker, *Macromolecules*, 2007, 40, 6040-6047.

**Comparative study of the catalytic performance in the 1,3,5-triisopropylbenzene conversion of embryonic, nano-sized and nanosheet-like ZSM-5**

M. Akouche<sup>1,\*</sup>, N. Nesterenko<sup>2</sup>, J.-P. Gilson<sup>1</sup>, J.-P. Dath<sup>2</sup>, V. Valtchev<sup>1</sup>

<sup>1</sup>Normandie Univ. ENSICAEN, CNRS, Laboratoire de Catalyse & Spectrochimie, Caen, France, <sup>2</sup>Total Research and Technology Feluy (TRTF), Zone industriel C, Feluy, Belgium

**Abstract Text:** Zeolites are the most efficient light oil cracking catalysts thanks to the presence of strong acid sites within their uniform micropore structure that enables shape-selective catalytic transformations. However, the tendency toward heavier fossil oils and biomass conversion requires new heterogeneous catalysts. More precisely, the pores of conventional zeolites are limited to 0.8 nm, which limits their uses to relatively small molecules. Therefore, there is an urgent need for extra-large zeolitic catalysts able to convert bulky molecules. In recent years, several zeolitic materials with extra-large pores were obtained, but none of these structures offer an industrial perspective because of limited (hydro)thermal stability.

In order to address this handicap, our team developed an advanced material consisting of more open zeolitic structures having all their active sites accessible. The material, which is semi-formed zeolite units, denoted as Embryonic Zeolites (EZ).<sup>1</sup> Their micropores are highly accessible and resistive to high temperatures (up to 700°C) and mechanical (up to 20 tons) treatments. The EZ exhibits moderate acidity, which is weaker than the conventional zeolites, yet strong enough to convert hydrocarbons.<sup>2</sup> These features give them superior catalytic performance in the conversion of bulky molecules. In order to highlight the performance of these advanced catalysts, we compared their physicochemical properties and their catalytic activity with a nano-sheet like (s-ZSM-5) and conventional nano-sized (n-ZSM-5) exhibiting high external surface area and short diffusion path.

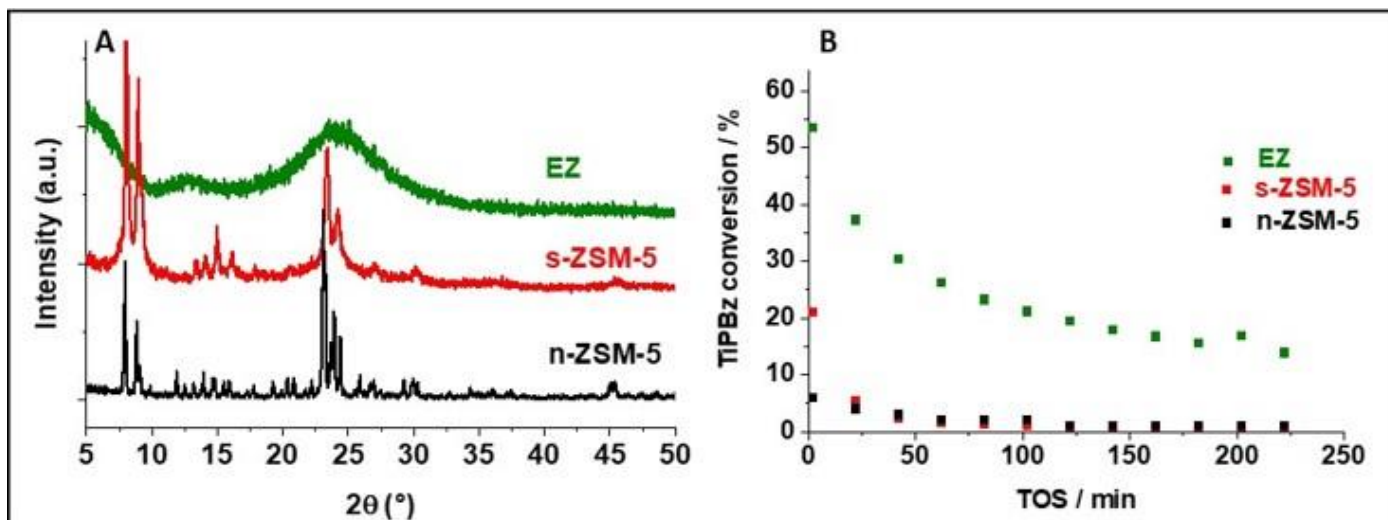
The physicochemical characterization of the EZ sample highlights the presence of some structural organization and a well-defined pore structure with a pore size below 2.5 nm. The major part of Al is tetrahedrally coordinated and as mentioned exhibits zeolite-like acidity. The micropore volume and  $S_{\text{BET}}$  area of the material are  $0.28 \text{ cm}^3 \cdot \text{g}^{-1}$  and  $658 \text{ m}^2 \cdot \text{g}^{-1}$ , respectively. On the other side, nanosheet-like ( $0.14 \text{ cm}^3 \cdot \text{g}^{-1}$ ;  $409 \text{ m}^2 \cdot \text{g}^{-1}$ ) and conventional ( $0.17 \text{ cm}^3 \cdot \text{g}^{-1}$ ;  $378 \text{ m}^2 \cdot \text{g}^{-1}$ ) ZSM-5 present lower micropore volume and specific surface area, but substantially higher acidity. Amongst these parameters, access to the active sites seems to be a key factor for processing bulky molecules. The EZ showed much higher catalytic performance in the conversion of TiPBz compared to nanosheet-like and nano-sized ZSM-5 (**Figure 1**). Also, the deactivation rate of the embryonic zeolites is much slower with respect to highly crystalline counterparts. These findings open the route to the preparation of advanced catalytic materials for bulky molecules conversion.

**Acknowledgments:**

The financial support from TOTAL Research and Technology Feluy, Belgium (TRTF) and the Industrial Chair ANR-TOTAL "Nanoclean Energy" is highly appreciated.

**Figure 1:** (A) XRD patterns and (B) 1,3,5-TiPBz conversion (conditions:  $T_{\text{reaction}}=300^\circ\text{C}$  and  $\text{WHSV}=8 \text{ h}^{-1}$ ) of nano-sized, nanosheets like and embryonic ZSM-5.

**Image 2:**



#### References:

- [1] Haw, K. G.; Goupil, J. M.; Gilson, J. P.; Nesterenko, N.; Minoux, D.; Dath, J. P.; Valtchev, V. Embryonic ZSM-5 zeolites: zeolitic materials with superior catalytic activity in 1, 3, 5-triisopropylbenzene dealkylation. *New Journal of Chemistry*, 2016, 40, 4307-4313.
- [2] Haw, K.-G.; Gilson, J.-P.; Nesterenko, N.; Akouche, M.; El Siblani, H.; Goupil, J.-M.; Rigaud, B.; Minoux, D.; Dath, J.-P.; Valtchev, V., Supported Embryonic Zeolites and their Use to Process Bulky Molecules. *ACS Catalysis* 2018, 8 (9), 8199-8212.

**Hierarchical structured materials: characterization and application**

M. Hornacek\*, K. Kupcova<sup>1</sup>, V. Jorik<sup>2</sup>, P. Hudec<sup>1</sup>

<sup>1</sup>Organic technology, catalysis and petroleum technology, <sup>2</sup>Inorganic chemistry, Faculty of Chemical and Food Technology, Slovak University of Technology, Bratislava, Slovakia

**Abstract Text:** Zeolites, which are classified as microporous materials, are crystalline aluminosilicates of alkaline elements, rare earth elements or other monovalent or multivalent metals [1]. These materials display a number of unique properties, due to which they are applied in catalysis. Despite their numerous advantages, zeolites also display diffusion limitations for branched molecules and transport of reagents with size similar to the size of the micropores is difficult. This leads to a situation in which only the external part of zeolite grain takes part in catalytic reaction while the interior remain catalytically inactive. Therefore, works have begun on the synthesis of zeolites with hierarchical porous structure which display secondary porosity i.e. show the presence of at least one additional pore system, mainly in the mesopore range (pore size according to IUPAC from 2 to 50 nm). Such solution aims to facilitate access of larger reagent molecules to active centers of the material while simultaneously maintaining acidity and crystallinity of zeolites. Shortening the length of diffusion path due to the reduction of crystal size (obtaining both nanocrystals and nanolayered zeolites) causes increase in catalyst life-span. Introducing additional porosity (meso-, macro-) also shortens the diffusion path, thus minimizing the possibility of catalyst deactivation [2]. Hierarchical zeolites have already found application in, among other things, catalysis, in such reactions as: alkylation, isomerization, transformation of methanol to hydrocarbons (MTH), aromatization, condensation, or catalytic cracking [3]. This work focuses on the synthesis and characterization of hierarchical zeolites ZSM-5 and their application in an aromatization of propane and n-hexane.

Recrystallization was realized with zeolite ZSM-5 (Si/Al=20.9) with different NaOH concentration, with different surfactant concentration under hydrothermal conditions at 110°C with and without pH change. Gallium and zinc was loaded after calcination to prepared zeolites. Prepared samples were characterized by: XRD, adsorption measurement, TPD of ammonia, FTIR pyridine adsorption, SEM and catalytic activity was tested by aromatization of propane and n-hexane at the temperature of 350-500°C. Adsorption of nitrogen confirmed the formation of secondary mesoporous structure due to the recrystallization of zeolite. Surface area, mesoporous surface area and total pore volume increased with increasing NaOH solution concentration. The  $S_{\text{t}}/S_{\text{BET}}$  ratio is linearly dependent on the concentration of NaOH in the recrystallization, and the conversion of propane and n-hexane increased with this ratio. The conversion of propane and n-hexane increased more than two times over the parent zeolite ZSM-5, after the treatment by recrystallization. The propane and n-hexane conversion values were almost unchanged with the reaction time, so the recrystallization also affected the coking of the catalyst.

**Acknowledgment:**

This research has been financially supported by the Slovak Research and Development Agency under No. APVV-18-0255.

**References:** [1] J. Weitkamp, Solid State Ionics 131 (2000) 175.

[2] M. Hartmann, et al. Chem. Soc. Rev. 45 (2016) 3313.

[3] J.M. Müller, et al. Microporous Mesoporous Mater 204 (2015) 50.

**Theoretical and Experimental evidence of Cu migration during the NH<sub>3</sub>-SCR-NO<sub>x</sub> reaction catalyzed by Cu-CHA catalysts**

R. Millán<sup>1</sup>, P. Cnudde<sup>2</sup>, P. Concepción<sup>1</sup>, A. Hoffman<sup>2</sup>, V. Van Speybroeck<sup>2</sup>, M. Boronat\*

<sup>1</sup>Instituto de Tecnología Química, UPV-CSIC, Instituto de Tecnología Química, UPV-CSIC, Valencia, Spain, <sup>2</sup>Center for Molecular Modeling, Ghent University, Ghent, Belgium

**Abstract Text:** The removal of nitrogen oxides (NO<sub>x</sub>) from exhaust gases in diesel vehicles is currently achieved through the NH<sub>3</sub>-SCR-NO<sub>x</sub> reaction, using copper exchanged zeolites with the CHA structure as catalysts.[1,2] The mechanism of the NH<sub>3</sub>-SCR-NO<sub>x</sub> reaction catalyzed by Cu-CHA materials comprises two half-cycles, oxidation and reduction, according to the changes in the oxidation state of Cu. In the reduction half-cycle, NO and NH<sub>3</sub> coordinate to Cu<sup>2+</sup> cations enabling the N–N coupling through the formation of H<sub>2</sub>NNO or NH<sub>4</sub>NO<sub>2</sub> as reaction intermediates, which subsequently decompose into N<sub>2</sub> and H<sub>2</sub>O while Cu<sup>2+</sup> is reduced to Cu<sup>+</sup>. In the oxidation half-cycle, Cu<sup>+</sup> is oxidized to Cu<sup>2+</sup> by adsorption of NO<sub>2</sub> or by reaction of NO with O<sub>2</sub> to form adsorbed nitrites or nitrates.[3-6] All these steps can take place on Cu<sup>+</sup> and Cu<sup>2+</sup> cations directly attached to framework oxygen atoms, as demonstrated both theoretically and experimentally.[6] But it has also been proposed that, at low temperature, NH<sub>3</sub> molecules can coordinate Cu<sup>+</sup> cations and release them from their positions to form mobile Cu<sup>+</sup>(NH<sub>3</sub>)<sub>2</sub> complexes, and that O<sub>2</sub> activation occurs on transient dimeric species that are formed when one Cu<sup>+</sup>(NH<sub>3</sub>)<sub>2</sub> monomer diffuses to an adjacent cavity containing another Cu<sup>+</sup>(NH<sub>3</sub>)<sub>2</sub> monomer, facilitating the formation of reactive Cu<sup>+</sup>(NH<sub>3</sub>)<sub>2</sub>-O-O-Cu<sup>+</sup>(NH<sub>3</sub>)<sub>2</sub> species. [7, 8] However, up to the moment there is no direct experimental evidence of this migration of Cu ions from the rings to the cavity.

In this contribution we combine molecular dynamics (MD) simulations and DFT calculated vibrational frequencies with a detailed analysis of the IR spectra of Cu-SAPO-34 in contact with the NH<sub>3</sub>-SCR-NO<sub>x</sub> reactants, either separately (NO, O<sub>2</sub>, NH<sub>3</sub>) and in mixtures (NO+O<sub>2</sub>, NO+NH<sub>3</sub>, NO+O<sub>2</sub>+NH<sub>3</sub>). Analysis of the IR spectra in the 800 – 1000 cm<sup>-1</sup> range shows that two NH<sub>3</sub> molecules are necessary to mobilize a Cu<sup>+</sup> cation, and that this is only experimentally observed when there is an excess of NH<sub>3</sub> in the reaction media.

**References:** [1] Beale, A. M.; Gao, F.; Lezcano-Gonzalez, I.; Peden, C. H. F.; Szanyi, J. Chem. Soc. Rev. 2015, 44, 7371.

[2] Zhang, R.; Liu, N.; Lei, Z.; Chen, B. Chem. Rev. 2016, 116, 3658.

[3] Lomachenko, K. A.; Borfecchia, E.; Negri, C.; Berlier, G.; Lamberti, C.; Beato, P.; Falsig, H.; Bordiga, S. J. Am. Chem. Soc. 2016, 138, 12025.

[4] Janssens, T. V. W.; Falsig, H.; Lundegaard, L. F.; Vennestrøm, P. N. R.; Rasmussen, S. B.; Moses, P. G.; Giordanino, F.; Borfecchia, E.; Lomachenko, K. A.; Lamberti, C.; Bordiga, S.; Godiksen, A.; Mossin, S.; Beato, P. ACS Catal. 2015, 5, 2832.

[5] Di Iorio, J. R.; Bates, S. A.; Verma, A. A.; Delgass, W. N.; Ribeiro, F. H.; Miller, J. T.; Gounder, R. Top. Catal. 2015, 58, 424.

[6] Moreno-Gonzalez, M.; Millan, R.; Concepción, P.; Blasco, T.; Boronat, M. ACS Catal. 2019, 9, 2725.

[7] Gao, F.; Mei, D.; Wang, Y.; Szanyi, J.; Peden, C. H. F. J. Am. Chem. Soc. 2017, 139, 4935.

[8] Paolucci, C.; Khurana, I.; Parekh, A. A.; Li, S.; Shih, A. J.; Li, H.; Di Iorio, J. R.; Albarracin-Caballero, J. D.; Yezerets, A.; Miller, J. T.; Delgass, W. N.; Ribeiro, F. H.; Schneider, W. F.; Gounder, R. Science 2017, 357, 898.

**Synthetic calcium aluminates as catalysts for the oxidation of chlorinated VOCs**

J. Martinez Triguero<sup>1,\*</sup>, A. E. Palomares<sup>1</sup>, A. Intiso<sup>1</sup>

<sup>1</sup>Instituto de Tecnologia Quimica UPV-CSIC, Valencia, Spain

**Abstract Text:** Catalytic oxidation is considered an efficient and sustainable technology for the abatement of Cl-VOCs in industrial emissions (1). Recently, synthetic calcium aluminates (mayenites) have been studied as catalysts due to their low cost and the special properties of their superoxide oxygen anions (2-4). They are able to oxidize hydrocarbons and also to be exchanged by other anions as in the case of chlorides. However, their activity is low compared with catalyst based on transition metals supported on alumina or zeolites which present higher surface area and therefore higher dispersion of the active phase. In this work, we will show that the activity of mayenites for the catalytic oxidation of trichloroethylene can be greatly improved by modifying synthesis conditions, addition of polymethylmethacrylate beads or doping with transition metal as iron.

The synthesis of calcium aluminates have been performed by hydrothermal, ceramic and sol-gel methods.

Polymethylmethacrylate (PMMA) beads and iron oxide were added to the gel before thermal treatment.

Trichloroethylene (1700 ppm) in air was fed through a fixed bed at increasing temperatures for obtaining the light-off curves. CO, CO<sub>2</sub> and hydrocarbons were analyzed by gas chromatography with TCD/FID detectors.

The analysis of light-off curves show that the samples synthesized by the hydrothermal method convert TCE at lower temperature. It has been attributed to their larger surface area and amount of superoxide anions. The addition of PMMA also increased the area and the amount of superoxide anions of oxygen confirming its direct relationship. By performing stability tests at 500°C of reaction, deactivation was observed in parallel with the decrease in the amount of superoxide oxygen anions and the appearance of chlorides as determined by Raman analysis (Fig. 1). The deactivation was suppressed by the addition of small amounts of iron oxide (1.5-2%Fe) that increased the activity at different temperatures and improved the stability (Fig. 2).

In summary, modified calcium aluminates present interesting properties as catalyst for oxidation of chlorinated VOCs due to their low cost and high efficiency.

**Image 1:**

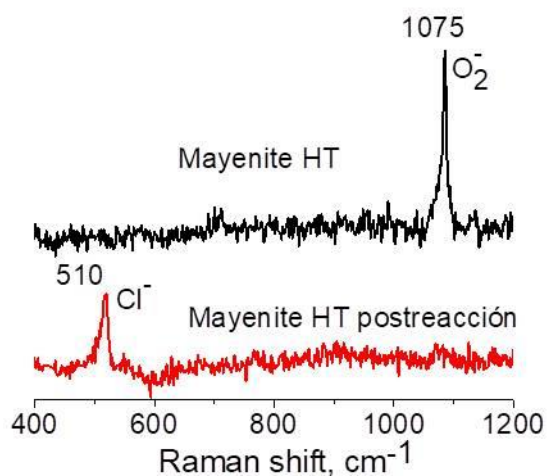
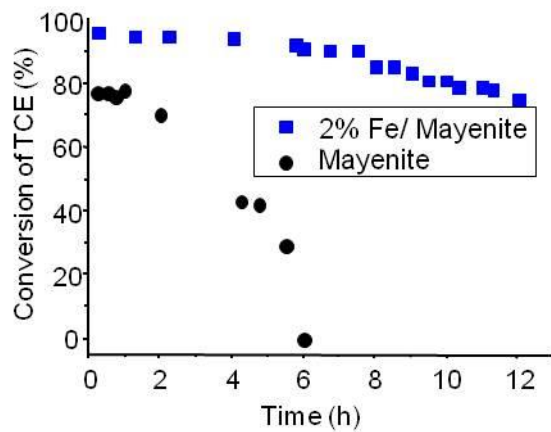


**Image 2:**



**References:** [1] Aranzabal, A., Pereda-Ayo, B., González-Marcos, M. P., González-Marcos, J. A., López-Fonseca, R., González-Velasco, J. R., Chem. Pap. 68 (9), 1169, 2014.

[2] Intiso, A., Martínez-Triguero, J., Cucciniello, R., Rossi, F., Palomares, A. E. Sci. Rep. 9, 425, 2019.

[3] Intiso, A., Martínez-Triguero, J., Cucciniello, R., Proto, A., Palomares, A. E., Rossi, F. Catalysts 9, 27, 2019.

[4] Cucciniello, R., Intiso, A., Siciliano, T., Palomares, A. E., Martínez-Triguero, J., Cerrillo, J. L., Proto, A., Rossi, F., Catalysts 9, 747, 2019

**Rational design of zeolite-based catalyst for Fries rearrangement**

O. Veselý<sup>1,\*</sup>, J. Přečh<sup>1</sup>, J. Čejka<sup>1</sup>

<sup>1</sup>Faculty of Sciences, Charles University, Prague, Czech Republic

**Abstract Text:** Fries rearrangement is an acid catalysed reaction used for preparation of aromatic ketones from aryl esters. Low substrate conversions, low selectivity for the desired products and rapid catalyst deactivation were always important issues when using zeolites as catalyst and thus they were never applied in large scale for this reaction, although they could replace currently used corrosive catalysts such as AlCl<sub>3</sub> and TiCl<sub>4</sub>.<sup>1,2</sup> Hierarchical zeolites are more resistant to deactivation and provide increased reaction rates in many reactions, including isomerization of 1,2,4-trimethylbenzene or Friedel–Crafts alkylation.<sup>3,4</sup> Thus, we revised the acid catalysed Fries rearrangement using the hierarchical zeolites and compared their performance with the conventional ones.

Zeolites with varying pore size and connectivity (MFI, \*BEA, MTW, FAU, CON, MWW) in their both bulk and hierarchical form were investigated in the Fries rearrangement of phenyl acetate (PhOAc). Unexpectedly, the bulk zeolite catalysts provided higher conversions and yields of products (2- and 4-hydroxyacetophenone – denoted as 2-HAP and 4-HAP, respectively) than their hierarchical counterparts (E.g. bulk \*BEA provided 24.7% conversion of PhOAc and 4.1% yield of 2-HAP after 24h, compared to hierarchical “nanosponge” \*BEA reaching only 16.0% conversion of PhOAc and 0.8% yield of 2-HAP). Thus, we hypothesized the rearrangement mainly occurs on the active centres located inside the micropores, whereas, the active centres on the external surface only cause decomposition of the reactant to phenol and acetic acid. As a result, the hierarchical zeolites are not superior to their bulk counterparts in Fries rearrangement, since their increased external surface only promotes the decomposition. Reducing the number of active sites on the external surface of the catalyst may suppress the decomposition and thereby increase the selectivity for desired products. Based on this hypothesis, a set of catalysts with reduced number of active sites on the external surface was prepared. Samples of commercial zeolite \*BEA were modified by surface silylation, poisoning of external surface sites with bulky amines and surface dealumination. The unmodified \*BEA provided 21.6% conversion of PhOAc, 18.1% selectivity towards 2-HAP, 5.3% towards 4-HAP and 31.3% towards phenol. After the dealumination the selectivity towards 4-HAP decreased to 0.6%, while the other values stayed virtually unchanged. The silylated sample provided slightly higher conversion 24%, while the selectivity towards the undesired product – phenol – decreased to 23.7%. On the other hand, the poisoning by amines caused a drop of conversion to 5.8% and consequent decrease of yields of products. Therefore, the poisoning was deemed unsuitable.

In summary, reducing the number of active sites on the external surface of the zeolite by post-synthetic modifications improves the selectivity of the catalyst in the Fries rearrangement towards the desired products. The approach presents a route to tune the selectivity of the catalyst between different products as well as lower the selectivity towards undesired side-products.

**References:** 1 Vogt, A.; Kouwenhoven, H.W.; Prins, R., *Appl. Catal.*, A 1995 123 37-49

2 Freese, U.; Heinrich, F.; Roessner, F., *Catal. Today* 1999 49 237-244

3 Přečh, J.; Pizarro, P.; Serrano, D.P.; Čejka, J., *Chem. Soc. Rev.* 2018 47 8263-8306

4 Kim, J. C.; Cho, K.; Ryoo, R., *Appl. Catal. A-Gen* 2014 470 420-426

***Catalytic Properties / Zeolites / Inorganic materials / Poster***

FEZA21-PO-129

**CATALYTIC DECOMPOSITION OF LIGNIN OVER ZEOLITE CATALYST**

P. Hudec<sup>1,\*</sup>, M. Horňáček<sup>2</sup>, J. Mikulec<sup>3</sup>, J. BLAŠKO<sup>4</sup>, R. KUBINEC<sup>4</sup>, V. Jorík<sup>5</sup>

<sup>1</sup>Faculty of Chemical and Food Technology SUT, <sup>2</sup>Organic Technology, Catalysis and Petroleum, Slovak University of Technology, <sup>3</sup>Research and Development, Research Institute for Petroleum and Hydrocarbon Gases, <sup>4</sup>Faculty of Natural sciences, Comenius University, <sup>5</sup>Inorganic Chemistry, Slovak University of Technology, Bratislava, Slovakia

**Abstract Text:** In the process of steam explosion (explosive defibrillation) of phytomass and subsequent enzymatic hydrolysis, the cellulose and hemicellulose are transformed into fermentable sugars and the lignin side stream is separated from the mixture. Lignin is a heterogenous crosslinked amorphous polymer produced during biosynthesis process within the plant by radical polymerization of p-coumaryl, coniferyl and sinapyl alcohols. Lignin side stream can be burned in fluid bed boiler where the heat energy is released in form of steam that represents a source of heat and subsequently also the electricity. Another, more valuable option of lignin utilization is catalytic conversion into a bio-aromatic hydrocarbons mixture, bio-phenols or the high-octane components of gasoline. Bifunctional catalysts based on metals/zeolites (Y, ZSM-5, SAPO, MCM-41, SBA-15) are the most suitable heterogeneous catalyst for this purposes. In this work, catalyst for lignin decomposition was prepared from SAPO-11 and USY zeolite. After repeated ion-exchange by ammonium ions, zeolite were impregnated by Cu (3 % wt.) and Ni (15 % wt.). 20 g of fine-milled lignin obtained from steam explosive decomposition of wheat-straw and 1g of activated catalyst were mixed with 100 mL of tetraline. Catalytic decomposition was carried out in 1000 mL autoclave (Parr Instruments) at pressure of hydrogen of 4 MPa and temperature 310 °C during 90 min. In gaseous products, small amount of methane, CO and CO<sub>2</sub> was detected. Liquid phase was separated from solid-phase by centrifuge; solid residue was washed by acetone and solution was added to tetraline phase. Material balance of lignin decomposition was calculated on the base of solid-phase product extraction by THF. Products of lignin decomposition in tetraline phase were analysed by GC-MS. At above-mentioned reaction conditions, about 55% conversion of lignin was achieved, In liquid products, wide spectrum of different oxygen-containing species was detected. Acknowledgement: This work was supported by the Slovak Research and Development Agency under the contract No. APVV-18-0255

### Framework Effects on Silver-Mediated Methane Upgrading

R. Kerrigan\*, R. A. Taylor<sup>1</sup>

<sup>1</sup>Chemistry, University of Durham, Durham, United Kingdom

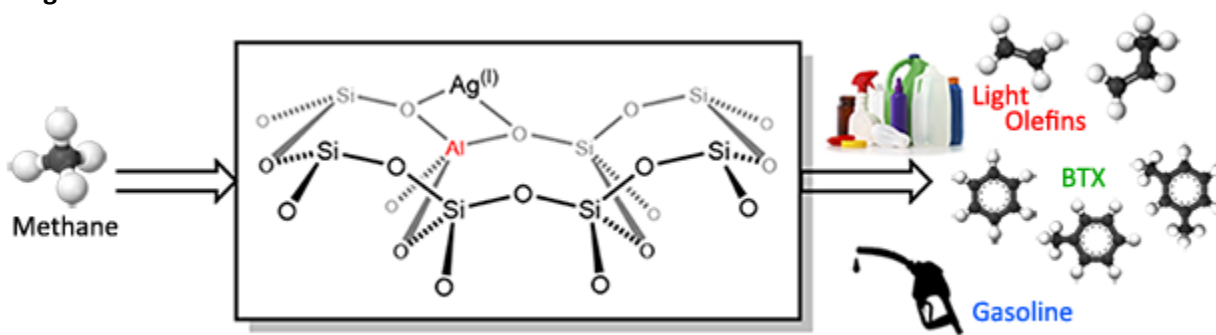
#### Abstract Text:

Utilising methane as a carbon feedstock for upgrading hydrocarbon streams presents a great opportunity to valorise an incredibly cheap and abundant material, whilst also avoiding the energy intensive process of producing synthesis gas. For this reason, direct conversion of methane has been a topic of major interest since the early 20<sup>th</sup> century.<sup>1,2</sup>

It has been shown that methane is activated over silver-exchanged ZSM-5 by both Stepanov *et al.*<sup>3</sup> and Baba *et al.*,<sup>4</sup> with the latter also demonstrating methane activation over silver-exchanged zeolite Y.<sup>5</sup> These materials have been shown to produce a silver hydride ( $\text{Ag}_n\text{-H}$ ) species and a framework methoxy  $[(\text{SiO}(\text{CH}_3)\text{Al}]$  group. This reactivity is the opposite to that of zinc, which produces a zinc-methyl  $[\text{Zn-CH}_3]^+$  species and a framework Brønsted acid site (BAS).<sup>6,7</sup>

The stoichiometric activation of methane by silver cations in frameworks other than zeolite Y and ZSM-5 has been little explored. In this contribution we aim to explore the influence of the zeolite framework on methane activation and functionalisation by silver cations. Using synthetic techniques such as ion-exchange and incipient wetness impregnation, we have produced numerous zeolite frameworks with varying silver-loading levels. Stoichiometric methane activation reactions using <sup>13</sup>C-methane, in conjunction with quantitative MAS NMR spectroscopy have shown which frameworks support a greater fraction of active silver species. The materials produced have been characterised using various analytical methods such as XRF, pXRD, solid-state NMR and SEM. Additional catalytic studies on methane upgrading using the most active silver-exchanged frameworks, tested on a fixed-bed reactor with on-line GCMS analysis, will be reported.

#### Image 1:



#### References:

1. W. A. Bone and R. V. Wheeler, *J. Chem. Soc., Trans.*, 1902, 81, 535–549.
2. S. Raynes, M. A. Shah and R. A. Taylor, *Dalton Trans.*, 2019, 48, 10364-10384
3. S. S. Arzuanov, D. I. Kolokolov, D. Freude and A. G. Stepanov, *J. Phys. Chem. C*, 2015, 119(32), 18481-18486
4. T. Baba, H. Sawada and Y. Abe, *Appl. Catal. A, General*, 2002, 231, 55.
5. T. Baba, N. Komatsu, H. Sawada, Y. Yamaguchi, T. Takahashi, H. Sugisawa and Y. Ono, *Langmuir*, 1999, 15(23), 7894-7896
6. Y. G. Kolyagin, I. I. Ivanova and Y. A. Pirogov, *Solid State Nucl. Magn. Reson.*, 2009, 35, 104-112
7. A. A. Gabrienko, S. S. Arzumanov, M. V. Lugzin, A. G. Stepanov and V. N. Parmon, *J. Phys. Chem. C*, 2015, 119(44), 24910-24918

**Removal of ibuprofen, naproxen and atenolol from aqueous solution using TiO<sub>2</sub> nanotubes/zeolite composites under visible light irradiation**

S. Stojanovic<sup>1</sup>, M. Vranjes<sup>2</sup>, V. Rac<sup>3</sup>, D. Krajisnik<sup>4</sup>, Z. Saponjic<sup>2</sup>, V. Rakic<sup>3,\*</sup>, L. Damjanovic-Vasilic<sup>1</sup>

<sup>1</sup>University of Belgrade - Faculty of Physical Chemistry, <sup>2</sup>University of Belgrade - "Vinča" Institute of Nuclear Science, Belgrade, <sup>3</sup>University of Belgrade - Faculty of Agriculture, Zemun, <sup>4</sup>University of Belgrade - Faculty of Pharmacy, Belgrade, Serbia

**Abstract Text: Introduction**

Pharmaceutically active compounds (ibuprofen (IBF), naproxen (NPX) and atenolol (ATL)) have been considered as emerging pollutants because of their widespread use and incomplete elimination by traditional wastewater treatments [1]. In recent years, titanium dioxide nanotubes (TNT) gained significant attention for catalytic degradation of various pollutants due to large specific surface area and high activity. Furthermore, depositing TiO<sub>2</sub> nanoparticles on zeolites (high surface area) can resolve TiO<sub>2</sub> agglomeration and costly filtration process following water treatments. The aim of this study was to evaluate photocatalytic degradation of IBF, NPX and ATL by composites based on TNT and different zeolites (HEU, FAU and MFI) in order to develop efficient photocatalyst.

**Experimental**

Natural zeolite clinoptilolite (Cli) from Zlatokop mine, Serbia, 13X (Si/Al = 1,2) from Union Carbide and ZSM-5 (Si/Al = 40) from Zeolyst were used as supports for hydrothermally synthesised TNT [2] (calcinated at 500 °C). TNT in amounts of 20 wt% were thoroughly mixed with zeolites using ethanol in a 10:1 ratio (ethanol ml/solid powder g); sonicated for 4 h at 80 °C; dried and calcinated in air at 500 °C for 5 h. The obtained materials were labelled as nTcli-20, nTZSM5-20 and nT13X-20 where nT stands for TNT; Cli, 13X and ZSM5 indicate the type of starting zeolite and the number represent wt% of used TNT. The composites were characterized by X-ray powder diffraction (XRPD), UV-Vis diffuse reflectance (DR) spectroscopy, Fourier transform infrared (FTIR) spectroscopy and scanning electron microscopy with energy-dispersive spectroscopy (SEM-EDS). The photocatalytic tests were performed with aqueous solution of IBF (30 mgL<sup>-1</sup>), NPX (5 mgL<sup>-1</sup>) and ATL (50 mgL<sup>-1</sup>) containing 1 gL<sup>-1</sup> of catalyst at room temperature under constant stirring and irradiation (lamp: Osram Vitalux 300 W). The IBF ( $\lambda_{\max} = 221$  nm), NPX ( $\lambda_{\max} = 230$  nm) and ATL ( $\lambda_{\max} = 224$  nm) concentrations were measured using UV-vis spectrophotometer.

**Results and discussion**

TNT loading and preservation of starting zeolitic structures in all synthesized composites were confirmed by the XRPD analysis (Fig. 1a). The IBF and ATL were stable in aqueous solution without photocatalysts under applied conditions, whereas NPX concentration decreased (~30 %) through photolysis process.

Figure 1. a) XRPD patterns of TNT (◆ refers to reflections of anatase phase), bare zeolites and composites; Photodegradation in the presence of TNT (TNT used in the experiment was 20 wt% of the catalyst loading (denoted as TNT-20)), bare zeolites and composites of b) IBF, c) NPX and d) ATL.

The composite based on ZSM-5 zeolite exhibited the highest removal rate toward IBF (Fig. 1b), NPX (Fig. 1c) and ATL (Fig. 1d) compared to the pure TNT and all other investigated composites. The enhanced removal of contaminants was obtained through two processes: adsorption and photocatalytic degradation. nTcli-20 showed better photocatalytic activity than nT13X-20 in the case of IBF and ATL, while in the case of NPX nT13X-20 was more efficient than nTcli-20.

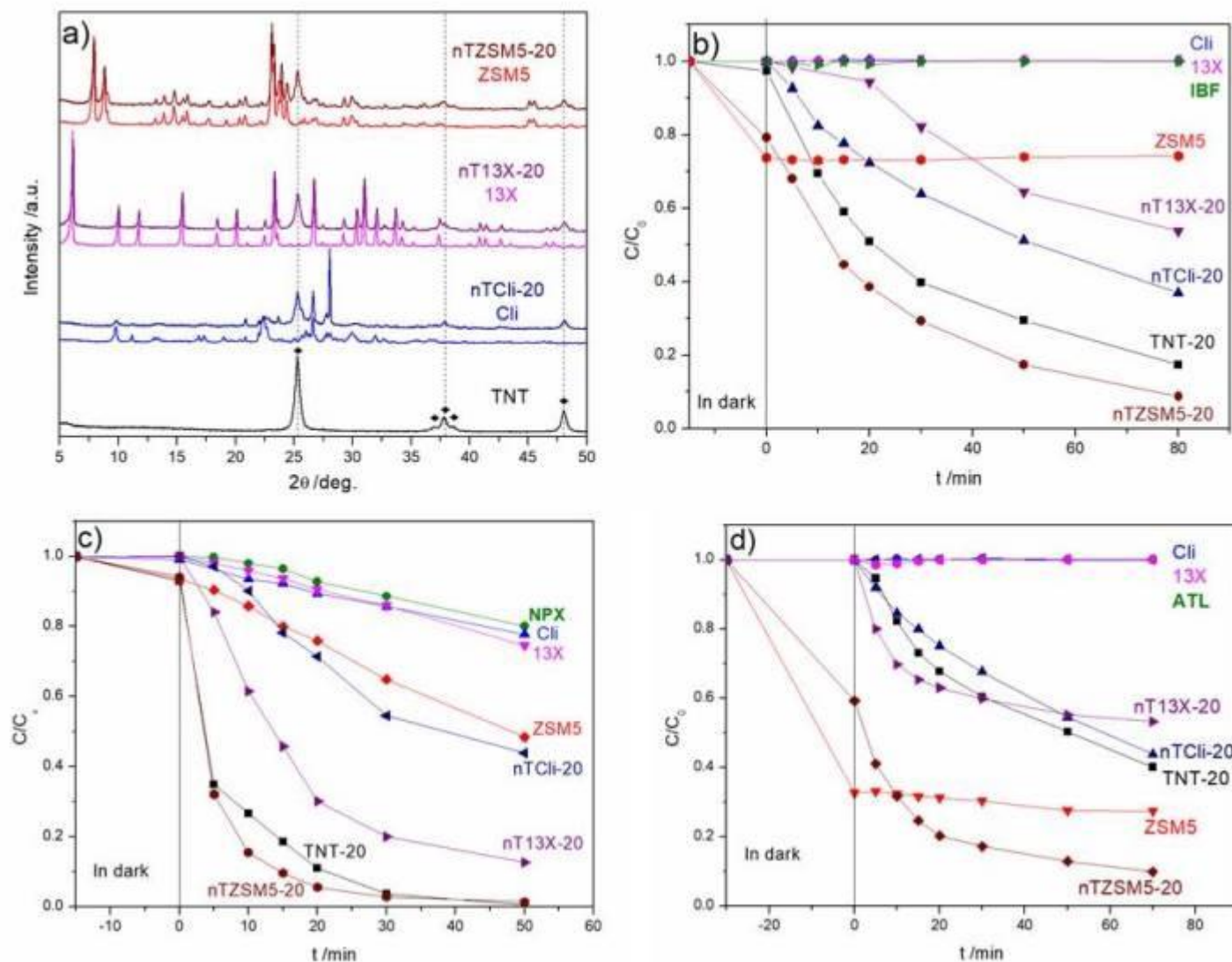
**Conclusions**

This study showed successful removal of IBF, NPX and ATL from aqueous solutions by all prepared composite materials, and the most efficient was the composite based on ZSM-5 zeolite and elongated titania nanostructures (TNT).

**Acknowledgements**

The authors acknowledge support from the Ministry of Education, Science and Technological Development, Republic of Serbia (Contract numbers: 451-03-9/2021-14/200146 and 451-03-9/2021-14/ 200116).

Image 1:



**References:** [1]. J. J. Rueda-Marquez, C. Palacios-Villarreal, M. Manzano, E. Blanco, M. Ramirez de Sol, I. Levchuk, Sol. Energy, 2020, 208, 480-492.

[2] M. Vranješ, Z.V. Šaponjić, Lj.S. Živković, V.N. Despotović, D.V. Šojić, B.F. Abramović, M.I. Čomor, Appl. Catal. B: Environ. 2014, 160–161(1), 589–96.

**Nickel-modified beta zeolite catalysts for the production of high value chemicals by pyrolysis of spent coffee grounds**

F. M. Mayer<sup>1,2</sup>, A. P. S. de Oliveira<sup>1</sup>, D. L. de Oliveira Júnior<sup>3</sup>, E. H. Tanabe<sup>3</sup>, C. A. Zini<sup>1</sup>, M. D. C. Rangel<sup>1,2,\*</sup>

<sup>1</sup>Institute of Chemistry, Federal University of Rio Grande do Sul, Porto Alegre, <sup>2</sup>Instituto Nacional de Ciência, Tecnologia e Inovação em Materiais Complexos Funcionais (Inomat), Campinas, <sup>3</sup>Chemical Engineering Department, Federal University of Santa Maria, Santa Maria, Brazil

**Abstract Text:** Currently,  $6 \cdot 10^6$  tonnes per year of spent coffee grounds are produced in the world. These wastes are produced in several places, including industries, offices, coffee shops, home environments and others. The improper disposal of these residues can be harmful to the environment because of some toxic components, such as tannin, polyphenol and caffeine. This damage can be avoided by changing these wastes into high value chemicals or fuels by fast pyrolysis. By using a catalyst, during this process, one can favour desirable reactions to produce specific classes of compounds, thus enabling the production of high-quality bio-oil, as well as high-value chemicals. Among several catalysts, zeolites are especially promising for pyrolysis, due to their acidity and high specific surface areas. These catalysts allow to obtain bio-oil rich in aromatic hydrocarbon especially benzene, toluene, ethylbenzene, and xylenes (BTEX). However, there is still some drawbacks which motivate the continuous research for finding more selective catalysts. Aiming to find catalysts able to process spent coffee grounds, nickel-modified beta zeolite catalysts were studied in this work. The catalysts were prepared by wet impregnation of nickel nitrate on beta zeolites, previously prepared to obtain 3 and 5 wt.% of nickel in the final solids (Ni3B and Ni5B). Samples were characterized by X-ray diffraction, ammonia temperature-programmed desorption, infrared spectroscopy of adsorbed pyridine, nitrogen adsorption/desorption and <sup>29</sup>Si and <sup>27</sup>Al NMR. The catalysts were evaluated by analytical pyrolysis (500 °C) of spent coffee grounds in a PY equipment (Multi-Shot Pyrolyzer EGA/Py-3030D), using a catalyst/biomass ratio of 5/1. The gaseous products were analysed by GC/MS coupled to the pyrolyzer. All diffractograms presented the pattern of beta zeolite, regardless nickel impregnation. The solids showed high specific surface areas (547-618 m<sup>2</sup> g<sup>-1</sup>). After nickel addition, the acid properties were changed, an increase of Lewis acid sites and a decrease of Bronsted acid sites being noted. Nickel-containing catalysts showed stronger acidic sites than pure zeolite, a fact that can be explained by the higher amount of octahedral aluminum in the framework when compared to pure zeolite, according to <sup>27</sup>Al NMR spectra. All catalysts were active in the pyrolysis of spent coffee grounds and showed different selectivity. Zeolites were active in desoxygenation reactions, being able of removing up 85.6 to 93.4% of oxygenated compounds, as compared to conventional pyrolysis (without catalyst). In the last case, the products were made mainly by 73.5% of oxygenated compounds (acid, ketone, ester, phenol and others) and nitrogen compounds (9.1%), mainly caffeine (6.4%). All nickel-modified catalysts produced bio-oil with monoaromatic and polyaromatic hydrocarbons. They were more efficient for BTEX production: 38.5 and 39.4% over Ni3B and Ni5B, respectively, while the conventional pyrolysis produced only 1.22%. In addition, nickel decreased the production of the highly toxic polyaromatic hydrocarbons (18.1 and 19.7% for Ni3B and Ni5B, respectively) as compared to beta zeolite (33.7%). These results can be related to changes in aluminium crystallographic sites and the formation of strong acid sites after impregnation of nickel, changing the kinds and the amount of acid sites as well as the electronic state of nickel. The catalyst with 3% of nickel showed the best performance, since it combined the lowest production of polyaromatics and the BTEX production close to Ni5B, besides having the lowest amount of metal.

**“Ru catalysts supported on zeolites and mesoporous silicas for CO<sub>2</sub> methanation”**

D. Aceto<sup>1,\*</sup>, C. M. Bacariza Rey<sup>1</sup>, C. Henriques<sup>1</sup>, F. Azzolina-Jury<sup>2</sup>

<sup>1</sup>CQE-DEQ, Instituto Superior Técnico, Universidade de Lisboa, Lisboa, Portugal, <sup>2</sup>Laboratoire Catalyse et Spectrochimie, Normandie Université, ENSICAEN, UNICAEN, CNRS, Caen, France

**Abstract Text:** The environmental concerns regarding the expansion of renewable sources for electricity production are partially related with the characteristic intermittency of these sources. In this way, valorising the excess of renewable electricity produced during low demand periods through the production of green H<sub>2</sub>, from water electrolysis, constitutes a promising alternative. Furthermore, CO<sub>2</sub> can be successfully converted into synthetic natural gas by using renewable H<sub>2</sub>. Overall, this strategy, promising for several industrial sectors, presents important benefits since renewable electricity surplus can be stored in the natural gas grid.

CO<sub>2</sub> methanation requires the use of catalysts due to the well-known stability of carbon dioxide molecules. In this way, active metals such as Ni, Ru or Rh and supports such as Al<sub>2</sub>O<sub>3</sub>, SiO<sub>2</sub>, zeolites, hydrotalcites, ZrO<sub>2</sub>, CeO<sub>2</sub>, SBA-15 or even MOFs have been widely analysed in the literature. Among them, the utilization of zeolite-based catalysts has been gaining attention in the last years, mainly due to their easily tuneable properties such as the presence of basic sites on the surface, additional active sites for CO<sub>2</sub> activation, improved metallic phase dispersion, hydrophobicity/hydrophilicity character, porosity and resistance to water.

Consequently, in the present work zeolites and mesoporous silicas were used as supports for Ru-catalysts to be applied in CO<sub>2</sub> methanation, with the aim of evaluating the influence of the support nature in the performances. Catalysts were prepared by incipient wetness impregnation dispersing 3 wt.% of Ru over four zeolites (BEA, MOR, ZSM-5 and USY; all containing the same compensating cation and similar Si/Al global ratio) and two mesoporous silicas (SBA-15 and MCM-41). Several characterization techniques were used for assessing catalysts' physicochemical properties, such as XRD, TGA, H<sub>2</sub>-TPR and CO<sub>2</sub>-TPD. Finally, CO<sub>2</sub> methanation tests (86100 mL g<sub>cat</sub><sup>-1</sup> h<sup>-1</sup>, P<sub>CO<sub>2</sub></sub> = 0.16 bar, H<sub>2</sub>/CO<sub>2</sub> = 4:1, 200-450 °C) were performed in a laboratory-scale unit.

Results indicated that the introduction of Ru on the supports did not induce structural changes in the supports, even after catalytic tests (XRD). All the prepared catalysts were found to be hydrophobic (TGA), being Ru present as RuO<sub>2</sub> after impregnation and calcination (XRD, H<sub>2</sub>-TPR). In terms of reducibility, RuO<sub>2</sub> was found to be fully reduced below 200 °C in most samples. Furthermore, the interactions of the catalysts with CO<sub>2</sub> varied significantly with the different supports used (CO<sub>2</sub>-TPD). In particular, intermediate and strong basic sites as well as a higher CO<sub>2</sub> adsorption capacity were observed in catalysts prepared using supports presenting mesopores (SBA-15, MCM-41, USY and BEA), whereas those supported on MOR and ZSM-5 zeolites showed a prevalence of weak basic sites and a very low CO<sub>2</sub> adsorption. In terms of performances, the catalytic tests showed encouraging results when coupled with an optimal pre-reduction temperature (200 °C). Among all, the use of zeolites led to the highest CO<sub>2</sub> conversion, whereas mesoporous materials presented the best CH<sub>4</sub> selectivity.

To sum up, in the present study the influence of the support nature (zeolites and mesoporous silicas) on the properties and performances of Ru-based catalysts for CO<sub>2</sub> methanation reaction was explored. Overall, hydrophobic properties, the presence a sufficient number of basic sites and the combination of micro- and mesoporosity on the support material seem to be key factors for obtaining an active and selective CO<sub>2</sub> methanation catalyst.

**References:** Blanco and Faaij, *Renew. Sustain. Energy Rev.* 81 (2018) 1049–1086;

Quindimil et al., *Appl. Catal. B Environ.* 238 (2018) 393-403;

Bacariza et al., *ChemCatChem.* 11 (2019) 2388–2400;

Bacariza et al., *Processes* 8(12) (2020) 1646.

## Gas Adsorption, Separation and Storage

FEZA21-PO-134

### Temperature regulated gas adsorption of K-ZSM-25 for nitrogen/methane separation

S. H. Mousavi<sup>1,\*</sup>, J. Zhao<sup>1</sup>, P. Webley<sup>2</sup>, G. Li<sup>1</sup>

<sup>1</sup>Department of Chemical Engineering, The University of Melbourne, <sup>2</sup>Department of Chemical Engineering, Monash University, Melbourne, Australia

**Abstract Text:** Specific small-pore zeolites exhibit a temperature-regulated adsorption phenomenon, in which the thermal oscillation of "door-keeping" cations controls gas molecules' diffusion. Different admission-trigger temperatures thus separate molecules.

Since methane (CH<sub>4</sub>) has a lower carbon footprint and higher heating efficiency than other fossil fuels, demand for CH<sub>4</sub>-based energy sources is growing worldwide. Natural gas, the main source of CH<sub>4</sub>, often contains 0.2-5% nitrogen (N<sub>2</sub>). Hence, purifying natural gas is required to meet pipeline and liquefied natural gas requirements. Since their close physical-chemical properties, separating N<sub>2</sub> from CH<sub>4</sub> is the most difficult step in gas processing. Efforts to produce a sorbent that can selectively adsorb N<sub>2</sub> have been unsuccessful for decades.

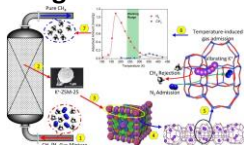
Here, we synthesized K-ZSM-25, a molecular "trapdoor" zeolite capable of capturing N<sub>2</sub> over CH<sub>4</sub> with a selectivity of up to 34. Exclusive temperature-regulated adsorption effect was detected in our experiments through adding potassium as a "door-keeping" cation. N<sub>2</sub> gas molecules were able to penetrate the internal pores of K-ZSM-25 at a moderate working temperature range of 240-300 K, while CH<sub>4</sub> was rejected.

In the atomic level, molecular dynamics (MD) and ab initio density functional theory (DFT) successfully unveiled the temperature-regulated adsorption mechanism. MD results demonstrated that a single N<sub>2</sub> molecule was free to travel to any position within the unit cell, resulting in multitude gas diffusion pathways into the depths of the zeolite crystal. In the case of K-ZSM-25, however, the entire unit cell was divided into different sections, each with K<sup>+</sup> at their borders, preventing the gas molecule from passing through the blocked pores. However, experimental gas uptakes at ambient temperatures revealed that rising the temperature enhances pore accessibility. Furthermore, the synchrotron PXRD spectrums in gas atmospheres were similar to that in vacuum, indicating no structural alteration in the zeolite. As a result, the thermal oscillation of door-keeping cations was the only possible way for the observed substantial gas adsorption as temperature increased.

DFT resulted energy barriers for forwards and reversed diffusion of CH<sub>4</sub> in the main pores of the unit cell were 1.16 and 1.05 eV, respectively, both far higher than those for N<sub>2</sub>, which were 0.99 and 0.81 eV, respectively. Since CH<sub>4</sub> has a higher energy barrier than N<sub>2</sub>, it must take more kinetic energy to push/pull away the door-keeping cations and diffuse through it. Consequently, N<sub>2</sub> diffusion into the particle depth should be possible at lower temperatures, as evidenced experimentally.

The temperature-regulated adsorption of K-ZSM-25 "trapdoor" zeolites opens up a new way to reject N<sub>2</sub> from CH<sub>4</sub> in the gas industry without requiring to use energy-intensive cryogenic distillations around 100 K. K-ZSM-25 also offers a reasonable strategy for the separation of gas pairs that are physically alike but have different gate-opening temperatures.

#### Image 1:



## **Gas Adsorption, Separation and Storage**

FEZA21-PO-135

### **Green synthesis of AlPO<sub>4</sub>-34 as a water adsorbent for solar sorption heat storage**

A. Ristić<sup>1,\*</sup>, A. Golobič<sup>2</sup>, N. Zabukovec Logar<sup>1,3</sup>

<sup>1</sup>Department for Inorganic Chemistry and Technology, National Institute of Chemistry Slovenia, <sup>2</sup>Faculty of Chemistry and Chemical Technology, University of Ljubljana, Ljubljana, <sup>3</sup>University of Nova Gorica, Nova Gorica, Slovenia

**Abstract Text:** Microporous AlPO<sub>4</sub>-34 serves as an excellent water adsorbent<sup>1</sup> in thermal energy storage, especially for solar thermochemical energy storage, which is becoming a critical technology to enable more efficient use of renewable energy and help reduce our dependence on fossil fuels. The main advantages of aluminophosphate adsorbents are their high thermal energy storage density, low regeneration temperature (90 °C) due to their hydrophobic-hydrophilic character evident in a Type V water adsorption isotherm, and excellent stability in repeated adsorption-desorption processes. The increase of the water adsorption capacity of the thermochemical material leads to a higher thermal energy storage density and thus to an improved performance of the adsorbent. On the other hand, the main drawback limiting their use in thermochemical energy storage applications is the significant preparation cost, especially when expensive templates or structure directing agents such as tetraethylammonium hydroxide are used. The use of ionic liquids as low-cost solvents with a structure directing role can increase the availability of these water adsorbents for thermochemical energy storage applications.

Here, we present an environmentally friendly template-free synthesis route of AlPO<sub>4</sub>-34 at ambient and elevated pressure by using 1-ethyl-3-methylimidazolium bromide ionic liquid as a low-cost solvent. Large 200 μm crystals were obtained at 200 °C after 6 days at elevated pressure, while 10 times smaller hexagonal prisms were crystallized at 200 °C after 3 days at ambient pressure. The crystal structure of the large AlPO<sub>4</sub>-34 crystal, determined by single crystal XRD at room temperature and 150 K, showed a chabazite structure with triclinic symmetry and the presence of 1,3-dimethylimidazolium cations in the pores.

The water adsorption capacity of AlPO<sub>4</sub>-34-IL, prepared by ionothermal synthesis and determined at 0.4 relative pressure, increased compared to the material obtained by hydrothermal synthesis, indicating the introduction of the additional defects in the structure after calcination. The textural properties of the sample prepared from the ionogel showed a higher specific surface area (778 m<sup>2</sup>/g), compared with the sample prepared from the hydrogel with a specific surface area of 422 m<sup>2</sup>/g. The AlPO<sub>4</sub>-34-IL showed a Type I water isotherm with less steep uptake, indicating a more hydrophilic character, while the hydrothermally prepared AlPO<sub>4</sub>-34 showed a typical Type V water isotherm with hydrophobic-hydrophilic character.

The ionothermal synthesis approach could be a breakthrough in the cost-effective industrial production of the aluminophosphate water adsorbents for solar thermochemical energy storage.

**References:** 1. A. Ristić, N. Zabukovec Logar, S. K. Henninger, V. Kaučič. The performance of small-pore microporous aluminophosphates in low-temperature solar energy storage: the structure-property relationship. *Advanced functional materials*, 2012, 22, 9, 1952-1957.

## Gas Adsorption, Separation and Storage

FEZA21-PO-136

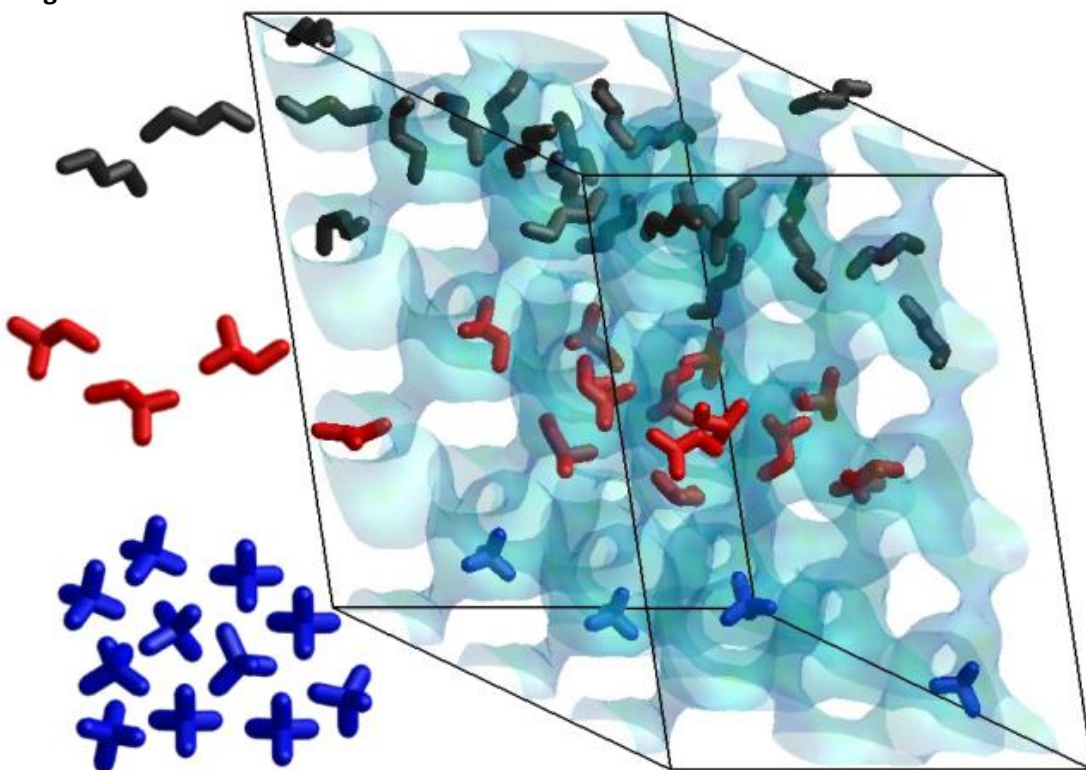
### Adsorption of linear, monobranched and dibranched alkanes on pure silica STW zeolite as a promising material for their separation

E. Pérez-Botella\*, A. Misturini<sup>1</sup>, A. Sala<sup>1</sup>, M. Palomino<sup>1</sup>, A. Corma<sup>1</sup>, G. Sastre<sup>1</sup>, S. Valencia<sup>1</sup>, F. Rey<sup>1</sup>

<sup>1</sup>Instituto de Tecnología Química, Universitat Politècnica de València - Consejo Superior de Investigaciones Científicas, Valencia, Spain

**Abstract Text:** Gasoline is a liquid mixture mainly consisting of hydrocarbons in the C<sub>4</sub>–C<sub>12</sub> fractions and is one of the most used fuels worldwide. Its performance is evaluated in terms of the octane number (ON). Hydroisomerization of linear short chain paraffins is an effective method of obtaining higher-octane components for the gasoline blend, i.e. multibranched products. The linear components are separated from the effluent and recycled by means of an adsorption process that uses zeolite 5A as the adsorbent.<sup>1</sup> The ideal target, however, is the separation and recycling of both linear and monobranched hydrocarbons, as the latter ones also present low ON. Medium pore materials with several structures and compositions have been proposed for this separation, out of which silicalite-1 (Si-MFI) is most frequently addressed.<sup>2</sup> Here, we present pure silica STW zeolite (Si-STW) as a material which is superior to Si-MFI for the said separation. The adsorption of linear, monobranched and dibranched saturated hydrocarbons in the gasoline range has been studied on Si-STW by using pentane, hexane, and heptane isomers as model adsorbates. Significant differences in both the equilibrium adsorption and especially the adsorption kinetics were found. The diffusivity increases in the order dibranched quaternary  $\ll$  dibranched- $\alpha$  < dibranched- $\beta$  < monobranched  $\approx$  linear. Size exclusion of quaternary carbon dibranched isomers is demonstrated, with monobranched and linear isomers being preferentially adsorbed on this material. The adsorption capacities and selectivities surpass those of Si-MFI in a factor of ca. 1.5. Altogether, Si-STW is presented as a promising adsorbent for increasing the ON of the hydroisomerization product by selectively excluding quaternary carbon dibranched hydrocarbons.

Image 1:



**References:** [1]

Ruthven, D. M. *Chemie-Ingenieur-Technik*, 83 (2011) 44–52

[2]

Laredo, G. C.; Trejo-Zarraga, F.; Jimenez-Cruz, F.; Garcia-Gutierrez, J. L., *Recent Patents Chem. Eng.*, 5 (2012) 153–173

## **Gas Adsorption, Separation and Storage**

FEZA21-PO-137

### **Aspen adsorption simulation of pressure swing adsorption process for CF<sub>4</sub>/N<sub>2</sub>**

D. Wang<sup>1,\*</sup>, L. Liu, G. Li

<sup>1</sup>School of Metallurgy, Northeastern University, Shenyang city, Liaoning province, China

#### **Abstract Text: Aspen adsorption simulation of pressure swing adsorption process for CF<sub>4</sub>/N<sub>2</sub>**

*Di Wang<sup>1</sup>, Liying Liu<sup>1,\*</sup>, Gang Li<sup>2,\*</sup>, Weijie Liu<sup>1</sup>, Ningyuan Zhang<sup>1</sup>, Simeng Xu<sup>1</sup>*

*(<sup>1</sup> State Environmental Protection Key Laboratory of Eco-Industry, Northeastern University, Shenyang, 110819, China; <sup>2</sup>*

*Department of Chemical Engineering, The University of Melbourne, VIC3010, Australia)*

*Corresponding authors: Liying Liu, liuly@smm.neu.edu.cn; Gang Li, li.g@unimelb.edu.au*

In the past half-century, due to the continuous increase in industrial demand and production activities, especially the expansion of aluminum production capacity in developing countries, the emission of CF<sub>4</sub> is increasing day by day. At present, the world's recognized gases with high greenhouse warming potential include CF<sub>4</sub>, has a destructive impact on the ozone layer. As a result, it is urgent to find an economical and reasonable CF<sub>4</sub> adsorption technology. Molecular sieve ETS-10 has a unique microporous framework structure, which has good adsorption, ion exchange, and catalytic properties. This multifunctional nature makes it useful in organic synthesis, catalysis, adsorption and separation, dehydration, denitration and desulfurization. According to the characteristics and advantages of molecular sieves, it can be used to study methods to increase the capacity of CF<sub>4</sub> adsorption.

Combined with the actual CF<sub>4</sub> adsorption and separation process, on the basis of experimental research, the Aspen Adsorption software is used to discuss the separation of CF<sub>4</sub>/N<sub>2</sub> mixed gas, and to explore the feasibility of using molecular sieve to separate CF<sub>4</sub>/N<sub>2</sub>. The main research idea is to establish a mathematical model, use a variety of equations to complete this model, and then apply this model to simulate, explore the impact of different designs on the simulation results, and the reaction mechanism of the adsorption process.

Firstly, process the data to get the adsorption isotherm. When the pressure is 120KPa, the maximum adsorption capacity of molecular sieve for CF<sub>4</sub> gas at 0°C, 30°C and 60°C is 1.40mmol/g, 1.12 mmol/g and 0.94 mmol/g. Then, according to the experimental data of the adsorption isotherm, the software fitting tool is used to fit the adsorption isotherm model parameters, and the applicability of the fitting results is discussed. The isotherm model was used to calculate the selective adsorption of molecular sieve to CF<sub>4</sub>/N<sub>2</sub>. Based on thermodynamics, fluid mechanics, heat and mass transfer, a model of multi-component gas in the adsorbent bed is established, the initial and boundary conditions of the model are given.

Finally, a mathematical model is used to establish a flow chart, and the auxiliary design of the adsorption process can be computed by Aspen Adsorption. The penetration curve diagram, the axial temperature distribution diagram, the axial gas-phase concentration diagram, and the temperature-time diagram in the tower can be gotten. Through the research of the breakthrough curve, the influence of pressure, mass transfer coefficient, temperature and other variables on the outflow curve can be observed, and the optimal conditions for improving the adsorption performance can be found; at the same time, we can utilize the curve to explore the reaction mechanism and mass transfer process of the adsorption process.

**Kinetics and adsorption equilibria on cation exchange LTA zeolites for Propane / Propylene Adsorptive Separation**

M. -E. A. Benchaabane<sup>1,\*</sup>, G. Chaplais<sup>2</sup>, E. Bloch<sup>1</sup>, P. Llewellyn<sup>1</sup>, J. Daou<sup>2</sup>, S. Bourrelly<sup>1</sup>

<sup>1</sup>Aix-Marseille Université CNRS-UMR7246, Laboratoire MADIREL, Marseille, <sup>2</sup>ENSCMu - Université de Haute-Alsace, Institut de Science des Matériaux de Mulhouse, UMR-7361, Mulhouse, France

**Abstract Text:** Separation of propane/propylene mixtures is of great commercial importance in petrochemical industries. Currently, this separation is accomplished by cryogenic distillation under complex conditions which make one of the highest capital and high energy-intensive separations process today. For this purpose, adsorption separation techniques based on porous materials have attracted an extensive interest due to the potential for tremendous energy savings. In this context, zeolites, often described as molecular sieves, are the widely used adsorbents in the area of separation and purification, due to their inherent ability to separate molecules depending on differences in size and polarity [1]. In the literature, many studies have been conducted on Linde Type A (LTA) zeolites [2]–[5], however, studies dealing with the effect of partially substituted cations in cationic zeolite on the propane/propylene separation-effectiveness are scarce [6].

In our present work, four LTA zeolites have been synthesized, namely, pure silica zeolite (Si-LTA) whose framework is neutral and some cationic zeolites: Na-LTA, MgNa-LTA and LiNa-LTA. The two last-mentioned zeolites are obtained by cation exchange process of the sodium zeolite (Na-LTA) with well-defined molar ratios. Textural and structural characterizations were performed using various techniques such as nitrogen (N<sub>2</sub>), water (H<sub>2</sub>O) and carbon dioxide (CO<sub>2</sub>) sorption measurements at 77K, 298K and 273K respectively, X-ray diffraction (XRD) and thermal analysis (TGA). Further, to study the usefulness of the four adsorbents for an efficient separation of propylene from propane, kinetics and adsorption equilibria were carried out, and for the first time the pseudo differential enthalpies of adsorption were measured for both gases at 303 K and up to 5 bar utilizing an accurate and simple home-made manometer apparatus coupled with calorimeter. Afterwards, various models have been adopted to correlate isotherm data, with the view to estimate the IAST (Ideal Adsorbed Solution Theory) selectivity of the aforementioned adsorbents towards propylene. Also, in order to predict the viability of the use of these sieves for cyclic adsorptive separation, i.e., pressure swing adsorption (PSA), both the reusability and the irreversible adsorbed amount of C<sub>3</sub>H<sub>6</sub> were assessed by gravimetric adsorption at temperatures ranging from 323 to 473 K. Finally, the separation mechanisms as well as the effect of the presence of monovalent and bivalent cations (Mg<sup>2+</sup> and Li<sup>+</sup>) in the structure of the four synthesized LTA zeolites were highlighted for the target separation (C<sub>3</sub>H<sub>6</sub> / C<sub>3</sub>H<sub>8</sub>).

**References:** [1] M. W. Ackley, S. U. Rege, and H. Saxena, "Application of natural zeolites in the purification and separation of gases," *Microporous Mesoporous Mater.*, vol. 61, no. 1–3, pp. 25–42, 2003, doi: 10.1016/S1387-1811(03)00353-6.

[2] C. A. Grande, S. Cavenati, and F. A. Da Silva, "Adsorption," pp. 7218–7227, 2005.

[3] C. A. Grande and A. E. Rodrigues, "Adsorption kinetics of propane and propylene in zeolite 4A," *Chem. Eng. Res. Des.*, vol. 82, no. 12, pp. 1604–1612, 2004, doi: 10.1205/cerd.82.12.1604.58029.

[4] C. A. Grande, C. Gigola, and A. E. Rodrigues, "Propane-Propylene Binary Adsorption on Zeolite 4A," *Adsorption*, vol. 9, no. 4, pp. 321–329, 2003, doi: 10.1023/A:1026223914143.

[5] C. A. Grande, C. Gigola, and A. E. Rodrigues, "Adsorption of propane and propylene in pellets and crystals of 5A zeolite," *Ind. Eng. Chem. Res.*, vol. 41, no. 1, pp. 85–92, 2002, doi: 10.1021/ie010494o.

[6] J. Padin, S. U. Rege, R. T. Yang, and L. S. Cheng, "Molecular sieve sorbents for kinetic separation of propane/propylene," *Chem. Eng. Sci.*, vol. 55, no. 20, pp. 4525–4535, 2000, doi: 10.1016/S0009-2509(00)00099-3.

## **Gas Adsorption, Separation and Storage**

FEZA21-PO-140

### **Study of the industrially relevant ethylene/ethane separation by Ag-Zeolites through Inelastic Neutron Scattering**

G. M. Almeida<sup>1,\*</sup>, A. de Marcos-Galan<sup>2</sup>, J. A. Vidal-Moya<sup>2</sup>, J. Martinez-Ortigosa<sup>2</sup>, G. Sastre<sup>3</sup>, F. Rey<sup>3</sup>, M. J. Ruiz<sup>1</sup>, T. Blasco<sup>3</sup>

<sup>1</sup>Spectroscopy Group, ILL, Grenoble, France, <sup>2</sup>ITQ, UPV-CSIC, <sup>3</sup>ITQ, UPV, Valencia, Spain

**Abstract Text:** Ethylene and propene are a crucial petrochemical feedstock, being the start chemical units for the most manufactured synthetic plastics in the world (polyethylene and polypropylene), among other materials<sup>1</sup>. During steam cracking, ethylene and propene are produced alongside with other hydrocarbons, such as ethane and propane, which requires a removal treatment. The separation of hydrocarbons with similar structures, sizes and physicochemical properties is still a challenge, being currently performed by cryogenic distillation, one of the most energy demanding processes in industry<sup>2</sup>.

Therefore, there is a real interest in developing an alternative method for these separations. The most promising are processes based on the application of porous solid adsorbents, such as metal-organic frameworks (MOFs) and zeolites<sup>1</sup>. Some MOFs (which are constructed by metal ions/clusters and multidentate organic linkers via coordination bonds), however, may present a rather poor stability, which could limit their practical applications<sup>3</sup>. Zeolites, microporous crystalline aluminosilicates containing orderly distributed micropores at molecular length scales, by the other hand, are widely known as stable materials, used as adsorbents since 1930's. Indeed, they have shown unique selectivity in ethylene/ethane<sup>1,4,5</sup> separations at ambient temperature. This selectivity may rely on mechanisms such as molecular sieving and a thermodynamic driven separation due to the  $\pi$ -complexation effect between unsaturated hydrocarbons of ethylene and metal ions contained in the adsorbent, specially Cu(I) and Ag(I), even though the exact adsorption of ethylene on Ag(I), for example, is still a matter of debate<sup>1,3</sup>.

In this work, we aim characterizing the interaction of adsorbed ethylene molecules on silver cations by the modification of the vibrational states of ethylene using Inelastic Neutron Scattering alongside with Multinuclear NMR and Ag K-edge X-ray absorption in zeolites CHA, LTA and RHO, with different Ag and ethylene loadings. First results of <sup>13</sup>C-Solid State NMR show that ethylene is modified upon adsorption in Ag-CHA (Si/Al =40) and Ag-CHA (Si/Al =5) as indicated by the shift towards high frequencies from 120.7 ppm to 122.8 ppm at very low ethylene loading. This shift is followed by the formation of polymers by increasing the temperature of adsorption, and/or the concentration of ethylene filling the zeolites, suggesting that proton transfer occurs from the zeolite to the adsorbed ethylene. INS spectra show significant modifications in ethylene vibrational states when comparing ethylene molecule database signals with the ones of ethylene absorbed within Ag-CHA-5. This information from the experimental data is being currently analyzed and rationalized by accurate Density-Functional Theory calculations.

**References:** 1.Wu, Y., Weckhuysen, B.M. *Angew. Chem. Int. Ed.* 10.1002/anie.202104318

2.Anson, A.; Wang, Y.; Lin, C. C. H.; Kuznicki, T. M.; Kuznicki, S. M. *Chem. Eng. Sci.* 63 (2008) 4171.

3.Ding, M., Cai, X., Jiang, H. *Chem. Sci.*, 2019, 10, 10209

4.Bericiartua, P. et al *Science* 358 (2017) 1068.

5.Horvatits C., Li D., Dupuis M., Kyriakidou, E. A., Walker J, E.A. *Phys. Chem. C* (2020), 124, 7295–7306.

**D<sub>2</sub>/H<sub>2</sub> adsorption selectivity in LTA and CHA zeolites: role of sorbent composition and temperature**

I. Bezverkhyy<sup>1,\*</sup>, M. Giraudet<sup>1,2</sup>, Q. Pujol<sup>1</sup>, C. Dirand<sup>1</sup>, M. Macaud<sup>2</sup>, J.-P. Bellat<sup>1</sup>

<sup>1</sup>ICB, CNRS, Dijon, <sup>2</sup>Centre Valduc, CEA, Is-sur-Tille, France

**Abstract Text:**

Small pore zeolites containing 8MR windows have been intensively studied as molecular sieves in separation of various gas mixtures. Recently a novel application for these materials has appeared which aims at the separation of hydrogen isotopes in the context of heavy isotopes production and recycling. This separation is based on the phenomenon of “quantum sieving” [1] observed at cryogenic temperatures ( $T < 77$  K). It results in the preferential adsorption of the heavier isotopes in pores whose size is comparable with the kinetic diameter of hydrogen molecules ( $\sim 0.29$  nm). Since this value is close to the pore size of 8MR windows in zeolites ( $\sim 0.38$  nm), they can exhibit a good selectivity in hydrogen isotope separation. Indeed, preliminary studies of commercial zeolites 4A [2] and 5A [3] confirmed their promising properties in D<sub>2</sub>/H<sub>2</sub> separation. In order to better understand the phenomenon and enhance the selectivity of small pore zeolites it is important to widen the scope of these studies to other framework types and cationic compositions.

We will present new results concerning the properties of several LTA and CHA zeolites in single gas adsorption and in D<sub>2</sub>/H<sub>2</sub> mixture coadsorption. In the case of LTA zeolite pure Na and Na-K containing materials were studied. For CHA framework, both Si/Al ratio and cationic composition (Li, Na, K) were varied. First, single gas D<sub>2</sub> and H<sub>2</sub> adsorption isotherms at 77 K were measured on all prepared materials using ASAP2020 sorptometer. Then for selected zeolites the equilibrium D<sub>2</sub>/H<sub>2</sub> selectivities were determined by coadsorption at 40 – 77 K for different D<sub>2</sub>/H<sub>2</sub> ratios (0.1 - 9) and mixture pressures (1 – 650 hPa). The coadsorption measurements were done using a home built setup based on the manometry coupled with mass spectrometry.

The impact of the zeolite composition and temperature on D<sub>2</sub>/H<sub>2</sub> selectivity will be discussed in our talk. Use of CHA zeolites with different Si/Al ratio showed that the best performances in terms of adsorbed amount and selectivity are observed for cation-rich materials. In the case of LTA we found that adjusting Na-K ratio in LTA structure allows to enhance the selectivity at 77 K. Concerning the role of temperature, D<sub>2</sub>/H<sub>2</sub> selectivity increases exponentially with lowering temperature as predicted by “quantum sieving” models. Moreover, the observed trend can be described by a simple model based on a spherical particle in a potential well [1]. Use of low temperature and optimal composition allowed to achieve high value of D<sub>2</sub>/H<sub>2</sub> selectivity. Thus, for Na<sub>3.9</sub>Al<sub>3.9</sub>Si<sub>8.1</sub>O<sub>24</sub> chabazite the value of 13 was found at 40 K and loading of 12 mmol.g<sup>-1</sup>. Another important conclusion concerns the applicability of IAST (Ideal Adsorbed Solution Theory) to D<sub>2</sub>/H<sub>2</sub> mixtures. We found that the behavior of the mixture strongly deviates from the ideal one at temperatures below 77 K despite the similar physico-chemical properties of H<sub>2</sub> and D<sub>2</sub>.

**References:**

1. J.J.M. Beenakker, V.D. Borman, S.Y. Krylov, Chem. Phys. Lett. 232 (1995) 379.
2. K. Kotoh, S. Takashima, T. Sakamoto, T. Tsuge, Fusion Eng. Des. 85 (2010) 1928.
3. R. Xiong, R. Balderas Xicohtencatl, L. Zhang, P. Li, Y. Yao, G. Sang, C. Chen, T. Tang, D. Luo, M. Hirscher, Microporous Mesoporous Mater. 264 (2018) 22.

**Cu-exchanged hydrophobic Sn-BEA zeolite utilised as a sensor for CO, CO<sub>2</sub>, NO and NO<sub>2</sub>**

M. Jendrlin<sup>1,\*</sup>, J. Grand<sup>2</sup>, S. Mintova<sup>2</sup>, V. Zholobenko<sup>1</sup>

<sup>1</sup>School of Chemical and Physical Sciences, University of Keele, Newcastle under Lyme, United Kingdom, <sup>2</sup>Laboratoire Catalyse et Spectrochimie, Normandie Univ., ENSICAEN, UNICAEN, CNRS, Caen, France

**Abstract Text: 1. Introduction**

Monitoring carbon and nitrogen oxides levels is linked to the greenhouse effect and air pollution. Higher levels of the related carbonate and nitrate species present in seas and rivers greatly affect natural habitats and in human blood these are vital health indicators. Recently, nano-crystals of MFI zeolites have been utilised in novel robust sensors for the detection of NO<sub>2</sub> at a ppm level in the atmosphere and in exhaust fumes<sup>[1]</sup>. The aim of this work is to explore the potential of hydrophobic Sn-BEA zeolite as a selective sensor in atmospheric conditions for carbon and nitrogen oxides at a low detection limit (<10 ppm).

**2. Experimental**

The hydrophobic Sn-BEA was prepared following a procedure from the literature<sup>[2]</sup>, while the preparation of zeolite-based sensors was conducted according to Ref<sup>[1]</sup>. Calcined zeolites were stirred with 0.1M solution of Cu(NO<sub>3</sub>)<sub>2</sub> (Figure 1) and then mounted as thin films on silicon wafers by spin coating. Zeolite samples were characterised by X-ray powder diffraction (Bruker D8 Advance diffractometer, Cu K $\alpha$  at 40 kV and 40 mA, 2 $\theta$ =5–60°), scanning electron microscopy (Hitachi TM 3000 with Bruker EDX analytical system at 500x magnification, 300s EDX exposition time), thermogravimetric analysis (Rheometric Scientific STA 1500, 20-800 °C, 10°C/min, 40 mL/min N<sub>2</sub> flow), and FTIR spectroscopy (Thermo iS10 spectrometer with a custom-made cell, 6000–1000 cm<sup>-1</sup>, 64 scans, 4 cm<sup>-1</sup> resolution, transmission mode).

**3. Results and Discussion**

The EDX and ICP-OES analysis of the Cu/Sn-BEA zeolites demonstrate that the Si/Al ratio is >1500 and Si/Sn ratio is 60, while the Cu loading is ~1 wt.%. Following the copper introduction into the calcined nano-sized Sn-BEA crystals, adsorption of CO, CO<sub>2</sub>, NO and NO<sub>2</sub> on the samples activated under a flow of argon has been examined by FTIR spectroscopy. The obtained peak positions of gas-phase molecules and the ones interacting with copper are in agreement with those reported in the literature<sup>[1], [3]</sup>. Our data demonstrated that CO can be detected in ppm quantities using the peak at ~2150 cm<sup>-1</sup> (Figure 2). In order to simulate the atmospheric conditions, the effect of water on the sensor responses was studied using an in situ cell in a concentration range of CO, CO<sub>2</sub>, NO and NO<sub>2</sub> from 0 to 5000 ppm.

**4. Conclusions**

This study demonstrates that thin films of a hydrophobic Sn-BEA ion-exchanged with copper can be utilised as a sensor for carbon and nitrogen oxides at low ppm values in a flow system. Monitoring of carbon and nitrogen oxides and the effect of water on sensing properties, which is necessary for potential practical applications under atmospheric conditions, have been investigated.

**Image 1:**

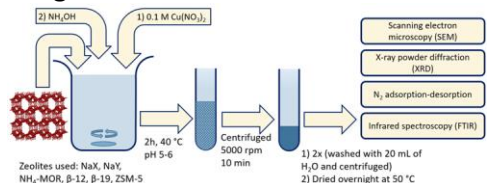
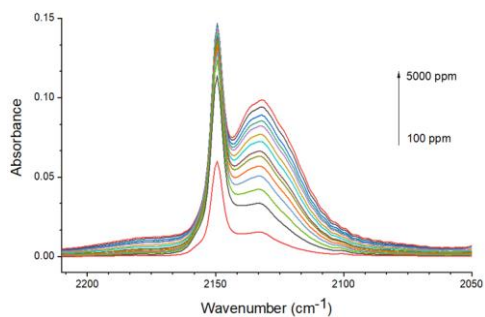


**Image 2:**



- References:** 1. S. N. Talapaneni, J. Grand, S. Thomas, H. Ali Ahmad, S. Mintova, *Materials and Design*, 99, 574–580 (2016)  
2. J. W. Harris, M. J. Cordon, J. R. Di Iorio, J. C. Vega-Vila, F.H. Ribeiro, R. Gounder, *Journal of Catalysis*, 335, 141–154 (2016)  
3. K. I. Hadjiivanov, G. N. Vayssilov, *Adv. Catal.*, 47, 307-511 (2002)

**FRAMEWORK FLEXIBILITY-DRIVEN CO<sub>2</sub> ADSORPTION ON A ZEOLITE**

H. J. Choi<sup>1,\*</sup>, J. G. Min<sup>1</sup>, S. H. Ahn<sup>1</sup>, J. Shin<sup>1</sup>, S. Radhakrishnan<sup>2</sup>, C. V. Chandran<sup>2</sup>, R. G. Bell<sup>3</sup>, E. Breynaert<sup>2</sup>, C. E. A. Kirschhock<sup>2</sup>, S. B. Hong<sup>1</sup>

<sup>1</sup>Division of Environmental Science and Engineering, POSTECH, Pohang, Korea, Republic Of, <sup>2</sup>Characterisation and Application Team (COK-kat), KU Leuven, Leuven, Belgium, <sup>3</sup>Department of Chemistry, University College London, London, United Kingdom

**Abstract Text:** Adsorption of the greenhouse gas CO<sub>2</sub> by ordered porous materials, although potentially cost-efficient and eco-friendly in reducing its concentration in the atmosphere, has not yet achieved large-scale practical application. Here, we report that K<sup>+</sup> and Rb<sup>+</sup> forms of the small-pore zeolite gismondine with a Si/Al ratio of 3.0 show marked hysteresis in their CO<sub>2</sub> isotherms, with very high CO<sub>2</sub> working capacities (2.8 and 3.0 mmol g<sup>-1</sup>) for a 50:50 CO<sub>2</sub>/CH<sub>4</sub> mixture under mild temperature swing conditions (25 - 100 °C at 1.0 bar), as well as high CO<sub>2</sub>/CH<sub>4</sub> selectivities (36 and 28) at 25 °C. This exceptional behavior is a consequence of the remarkable flexibility of the GIS framework caused by a subtle interplay between extra-framework cation-framework oxygen and extra-framework cation-adsorbate (CO<sub>2</sub>) interactions.

## ***Gas Adsorption, Separation and Storage | Zeolites/Inorganic materials***

FEZA21-PO-150

### **Measuring binary gas adsorption equilibria using the Integral Mass Balance (IMB) method**

D. P. Broom<sup>1,\*</sup>, O. Talu<sup>2</sup>, M. J. Benham<sup>1</sup>

<sup>1</sup>Hidden Isochema Ltd, Warrington, United Kingdom, <sup>2</sup>Chemical and Biomedical Engineering, Ohio State University, Cleveland, United States

**Abstract Text:** Measuring multicomponent gas adsorption equilibria is important when characterising the properties of nanoporous materials, such as zeolites, for gas separations.<sup>1,2</sup> However, most of the traditional techniques used for this purpose are either time-consuming or inaccurate,<sup>1</sup> with the most accurate methods requiring at least a day of experimental time and effort per data point. Large samples are also often required. We have recently introduced a new approach, called the *Integral Mass Balance* (IMB) method, which requires only a few grams of sample and can determine a ten point binary gas adsorption isotherm in a matter of hours.<sup>3</sup> To validate the technique we chose to measure N<sub>2</sub>/O<sub>2</sub> adsorption on a commercial zeolite 5A sample (Tosoh 5A). Such measurements are of industrial interest, due to the use of this material to produce oxygen from air, but thermodynamically consistent experimental data were also available in the literature for comparison.<sup>4</sup> In this presentation, we describe the technique and present binary N<sub>2</sub>/O<sub>2</sub> adsorption data and calculated selectivities for the Tosoh 5A sample at a pressure of 9.15 bar (915 kPa) and a temperature of 23°C (296 K). Excellent agreement with the previously measured data was found.

**References:** [1] O. Talu, Needs, status, techniques and problems with binary gas adsorption experiments. *Adv. Colloid Interface Sci.* 1998, 76-77, 227.

[2] D. P. Broom, K. M. Thomas, Gas adsorption by nanoporous materials: Future applications and experimental challenges. *MRS Bull.* 2013, 38(5), 412.

[3] O. Talu, D. P. Broom, and M. J. Benham, A new technique to measure multicomponent adsorption equilibrium: Integral Mass Balance (IMB), AIChE Annual Meeting, 10-15th November, Orlando, USA (2019).

[4] O. Talu, J. Li, R. Kumar, P. M. Mathias, J. D. Moyer, J. M. Schork, Measurement and analysis of oxygen/nitrogen/5A-zeolite adsorption equilibria for air separation. *Gas Sep. Purif.* 1996, 10(3), 149.

**Dynamic Sorption of CO<sub>2</sub> on Amine Functionalized Mesoporous Silica: Influence of Pore Structure and Pd Loading**

D. Issayeva<sup>1,\*</sup>, J. Pazdera<sup>2</sup>, H. Becker<sup>1</sup>, J. Titus<sup>1</sup>, A. Jentys<sup>2</sup>, R. Gläser<sup>1</sup>

<sup>1</sup>Institute of Chemical Technology, Universität Leipzig, Leipzig, <sup>2</sup>Chair of Chemical Technology II, Technische Universität München, Garching, Germany

**Abstract Text:**

**Introduction**

Amine-functionalized silica-based adsorbents are attractive for efficient and selective CO<sub>2</sub> capture. These materials offer high CO<sub>2</sub> adsorption capacity and tolerance to moisture in the feed [1,2]. The captured CO<sub>2</sub> can be potentially used for the conversion of CO<sub>2</sub>, e.g., by hydrogenation, if the material additionally contains a suitable catalytic functionality. Nevertheless, this functionality should not hinder CO<sub>2</sub> capturing ability of the amine groups. Thus, we investigate the adsorption behavior of amine-functionalized silica (AFS) and the impact of Pd nanoparticles on their dynamic sorption properties. Further, the influence of the pore width and structure of the AFS (based on SiO<sub>2</sub>, MCM-41 and SBA-15) on CO<sub>2</sub> sorption characteristics are studied.

**Experimental Part**

Silica functionalized with 3-aminopropyl groups (NH<sub>2</sub>-Si) was prepared by a base-catalyzed condensation reported by Hahn et al. [3]. To introduce Pd nanoparticles, Pd(II) acetylacetonate was added during the condensation reaction. To make up for the loss of amine groups during calcination (723 K in N<sub>2</sub>), the Pd-containing materials were post-synthetically treated with 3-aminopropyl trimethoxysilane (APTMS) at room temperature. Besides the materials obtained via condensation, functionalization with APTMS was also performed on SiO<sub>2</sub> spheres (Fuji Silysia® Chromatorex MB70-75/200) as well as on spherical beads of MCM-41 obtained via pseudomorphic transformation [4] and on SBA-15 prepared via sol-gel synthesis [5]. CO<sub>2</sub> sorption experiments at atmospheric pressure using 200 mg of adsorbent, a CO<sub>2</sub> partial pressure of 60-200 Pa and at 323-403 K. CO<sub>2</sub> loading as a function of time was fitted to the Avrami fractional-order kinetic model. Surface species formed upon CO<sub>2</sub> exposure were studied via FTIR spectroscopy under a flow of 10 vol.% CO<sub>2</sub> in He (20 ml min<sup>-1</sup> total flow rate) at atmospheric pressure.

**Results and Discussion**

The loading of CO<sub>2</sub> on both NH<sub>2</sub>-Si and Pd-NH<sub>2</sub>-Si expectedly decreases with increasing temperature from 343 to 373 K and increases with higher CO<sub>2</sub> partial pressures (Image 1). Even though both functionalized silica materials show the same trends, the adsorption capacity of NH<sub>2</sub>-Si is higher than that of Pd-NH<sub>2</sub>-Si. This is likely due to the different amine loadings on NH<sub>2</sub>-Si (4.9 mmol g<sup>-1</sup>) and Pd-NH<sub>2</sub>-Si (2.2 mmol g<sup>-1</sup>) resulting from the post-synthetic grafting procedure. The kinetic parameters were derived by fitting the CO<sub>2</sub> adsorption data as a function of time to the Avrami kinetic model [6,7]. This fits the data better than the widely used pseudo-first or pseudo-second order kinetic models. Further, the activation energy of CO<sub>2</sub> adsorption was calculated using the Arrhenius plot, which for NH<sub>2</sub>-Si and Pd-NH<sub>2</sub>-Si was found to be 39±5 kJ mol<sup>-1</sup>. This suggests that CO<sub>2</sub> adsorption sites are the same for both samples, while CO<sub>2</sub> adsorption capacity depends on the density of amine groups on the materials. The IR difference spectrum (Image 2) shows the formation of carbamates stabilized by adjacent ammonium ion and carbamic acid, which is in equilibrium with the carbamates, thus confirming the chemisorption of CO<sub>2</sub> on amine groups. The influence of pore structure on CO<sub>2</sub> loading is shown via CO<sub>2</sub> sorption isotherms for APTMS functionalized SiO<sub>2</sub>, MCM-41 and SBA-15 spheres. Besides the pore structure, the silanol group density (~2.0 nm<sup>-2</sup> for SiO<sub>2</sub> and ~0.7 nm<sup>-2</sup> for MCM-41), is shown to affect the CO<sub>2</sub> loading on the amine-functionalized silica spheres.

Image 1:

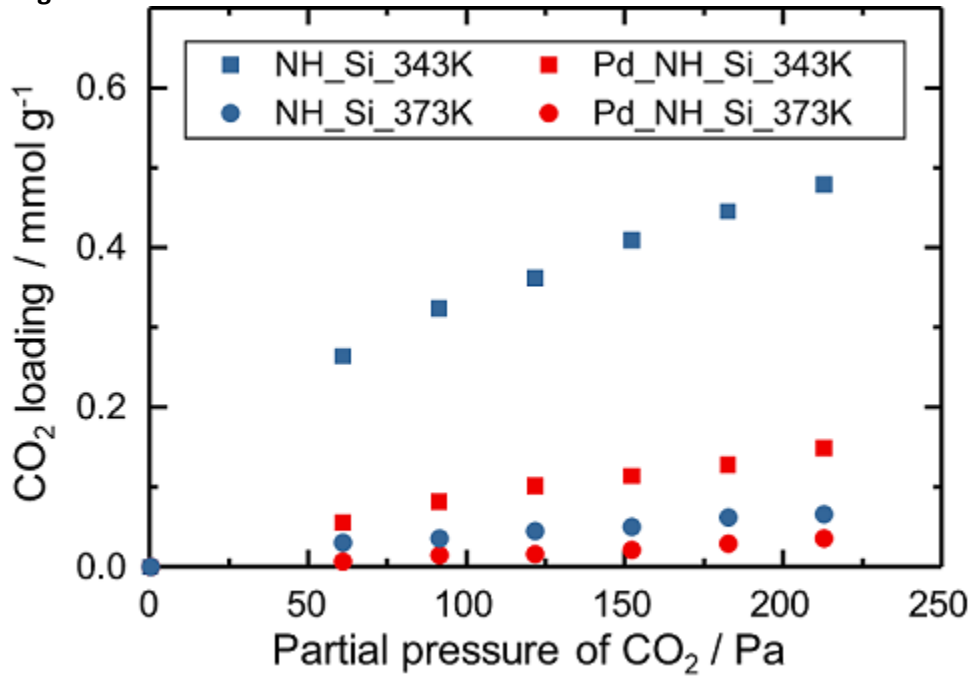
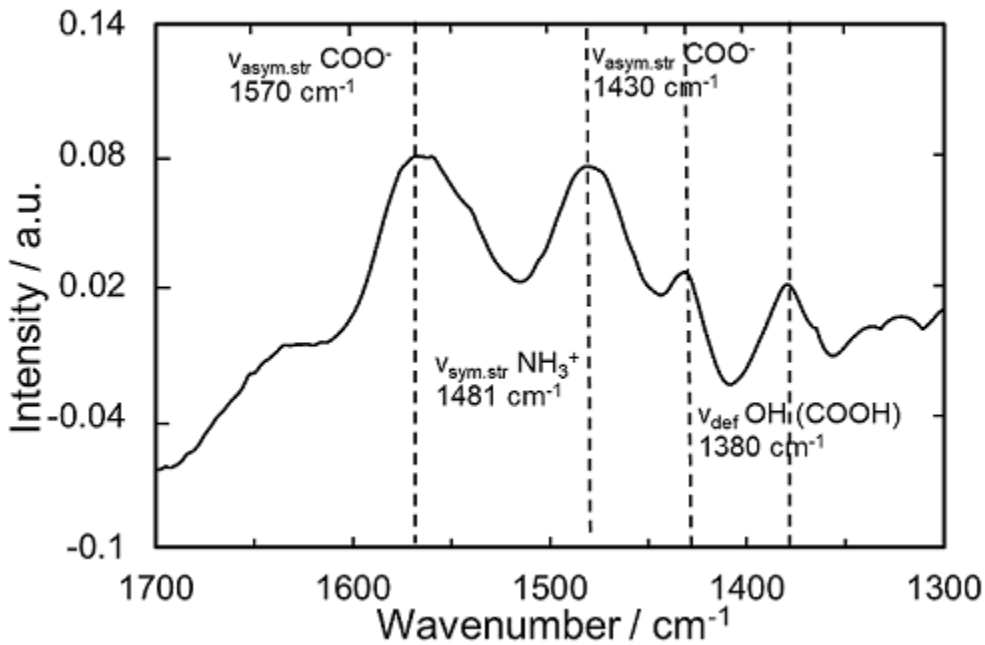


Image 2:



**References:**

- [1] M.W. Hahn, J. Jelic, E. Berger, K. Reuter, A. Jentys, J.A. Lercher, *J. Phys. Chem. B* 120 (2016) 1988-1995.
- [2] R. Dey, R. Gupta, A. Samanta, *Sep. Sci. Technol.* 53 (2018) 2683-2694.
- [3] M.W. Hahn, M. Steib, A. Jentys, J.A. Lercher, *J. Mater. Chem. A* 2 (2014) 13624-13634.
- [4] W.-D. Einicke, D. Enke, M. Dvoyashkin, R. Valiullin, R. Gläser, *Materials* 6 (2013) 3688-3709.
- [5] V. Meynen, P. Cool, E.F. Vansant, *Microporous and Mesoporous Mater.* 125 (2009) 170-223.
- [6] Q. Liu, J. Shi, S. Zheng, M. Tao, Y. He, Y. Shi, *Ind. Eng. Chem. Res.* 53 (2014) 11677-11683.
- [7] B. Ohs, M. Krödel, M. Wessling, *Sep. Purif. Technol.* 204 (2018) 13-20.

**Development of hybrid materials with activated carbon and zeolite 13X for CO<sub>2</sub> capture: Effect of electrification in regeneration**

M. J. Regufe<sup>1,\*</sup>, A. Ferreira<sup>1</sup>, J. M. Loureiro<sup>1</sup>, A. E. Rodrigues<sup>1</sup>, A. M. Ribeiro<sup>1</sup>

<sup>1</sup>Chemical Engineering, FEUP, Porto, Portugal

**Abstract Text:** Carbon dioxide is the major gas emitted by human activities and is the best-known greenhouse gas contributing to global warming. To address this problem, several technologies have been extensively studied to reduce CO<sub>2</sub> emissions, such as carbon capture and storage (CCS). Adsorption processes have been considered as one of the most promising technologies for CCS. Known since 1970, Electric Swing Adsorption (ESA) is an adsorption process where the adsorbent is regenerated by increasing temperature, but the heat is generated by applying an electric current directly in the adsorbent, and the temperature increases through the Joule effect. The viability of the ESA process was already tested, and several studies demonstrated its application for CO<sub>2</sub> capture [1-3], with advantages, such as, higher efficiency, minimization of the lost heat, smaller systems needed, among others. However, the difficulty in developing a material with the ideal characteristics for ESA application, i.e., high CO<sub>2</sub> adsorption capacity and excellent electric conductivity, is evident. In this context, new hybrid materials, shaped by extrusion, suitable to be used in the ESA process for CO<sub>2</sub> capture were developed. Pellets were produced with four different activated carbon/zeolite 13X ratio: pellets containing only activated carbon (100%AC), pellets with 70% of activated carbon and 30% of zeolite 13X (70%AC-30%13X), pellets containing 50% of activated carbon and 50% of zeolite 13X (50%AC-50%13X), and pellets with 30% of activated carbon and 70% of zeolite 13X (30%AC-70%13X). To produce these pellets, CMC was used as binder, and its quantity was about 5% (%w/w) of the total mixture.

An extensive characterization of the pellets using a variety of conventional techniques was done, including N<sub>2</sub> adsorption at 77 K, CO<sub>2</sub> adsorption at 273 K, mercury intrusion porosimetry, thermogravimetric analysis, SEM/EDS analysis, and mechanical strength tests. Additionally, adsorption equilibrium isotherms of CO<sub>2</sub> and N<sub>2</sub> were measured at three different temperatures (303, 333 and 373 K) up to 1.5 bar for all produced pellets, using a magnetic suspension microbalance (MSB, Rubotherm<sup>®</sup>, Bochum, Germany).

As expected, the results demonstrated that CO<sub>2</sub> is the most adsorbed component, when compared with N<sub>2</sub>. Besides, it was possible to verify the increase of the CO<sub>2</sub> adsorbed amount in line with the increase of the zeolite amount in the sample. The opposite occurs for N<sub>2</sub>, because the affinity of this gas in zeolite 13X is less than in activated carbon. The CO<sub>2</sub>/N<sub>2</sub> equilibrium selectivity of the pellets was estimated and values of 62.8, 41.9, 24.6, 12.2 at 1.5 bar, and 298 K, respectively for the 30%AC-70%13X, 50%AC-50%13X, 70%AC-30%13X, and 100%AC pellets were obtained, considering multicomponent adsorption of 20% of CO<sub>2</sub> in N<sub>2</sub>.

The pellets were subjected to an electric current, under helium, to evaluate the capability of these materials to heat by the Joule effect. According to the results, the most suitable pellets to be used in ESA, considering the adsorption capacity and the capacity to heat using electrification (heated until 315 K in 900 seconds), were the 50%AC-50%13X pellets.

Taking into account the results of the heating experiments, binary CO<sub>2</sub>/N<sub>2</sub> breakthrough experiments with and without electrification were carried out in a lab-scale fixed-bed unit to evaluate the fixed-bed dynamic behavior of the column packed with 50%AC-50%13X pellets, in order to compare the effect of the heating by Joule effect.

A mathematical model, including mass, energy and momentum balance was proposed and implemented in gProms software. Simulations results were validated with the experimental breakthrough results.

The results demonstrated that 50%AC-50%13X pellets revealed a good capacity for CO<sub>2</sub> adsorption and an intermediate performance in the electrification step and therefore are the most feasible ones to be employed in the ESA process.

**References:** 1.

Grande, C.A. and A.E. Rodrigues, Electric Swing Adsorption for CO<sub>2</sub> removal from flue gases. International Journal of Greenhouse Gas Control, 2008. 2(2): p. 194-202.

2. An, H. and B. Feng, Desorption of CO<sub>2</sub> from activated carbon fibre–phenolic resin composite by electrothermal effect. *International Journal of Greenhouse Gas Control*, 2010. 4(1): p. 57-63.
3. Ribeiro, R.P.P.L., C.A. Grande, and A.E. Rodrigues, Activated carbon honeycomb monolith – Zeolite 13X hybrid system to capture CO<sub>2</sub> from flue gases employing Electric Swing Adsorption. *Chemical Engineering Science*, 2013. 104(0): p. 304-318.

**Adsorption behavior of chitosan-zeolite composite aerogels**

E. Luzzi<sup>1,\*</sup>, P. Aprea<sup>1</sup>, M. Salzano de Luna<sup>1</sup>, D. Caputo<sup>1</sup>, G. Filippone<sup>1</sup>

<sup>1</sup>Dipartimento di Ingegneria Chimica, dei Materiali e della Produzione Industriale, Università degli Studi di Napoli Federico II, Napoli, Italy

**Abstract Text:**

CO<sub>2</sub> increasing concentration in the atmosphere is worldwide recognized as a critical concern, severely impacting the environment and human health.<sup>1</sup> Adsorption based processes are commonly regarded as a viable solution for CO<sub>2</sub> removal,<sup>2</sup> so great efforts are directed towards the identification of cost-effective and environmentally friendly materials with superior adsorption capacity.<sup>3</sup>

High specific surface area and good selectivity through the pollutant make zeolite 13X a natural candidate for this purpose,<sup>4</sup> but its powdery form usually prevents its use in many practical applications. Binding agents, often used to obtain compact zeolite-based adsorbents, induce a partial occlusion of the porosity that usually lower the adsorption capacity.<sup>5</sup>

In this work, we fully exploited the attractive CO<sub>2</sub> adsorption properties of zeolite 13X by embedding the powder (from 50 wt.% up to 90 wt.%) in a chitosan framework to obtain millimetric aerogel beads (see Fig. 1a) via a phase-inversion method followed by freeze-drying. Chitosan is crucial to the realization of highly porous aerogels provided with mechanical coherence and strength yet preserving the zeolite performances. Its peculiar microstructure (see Fig. 1b) resulted in a coherent system possessing high specific surface area and excellent CO<sub>2</sub> uptake capacity (561 m<sup>2</sup> g<sup>-1</sup> and 4.23 mmol g<sup>-1</sup>, respectively, for zeolite fraction  $\phi_{zX}=0.90$ ). Interestingly, a small positive deviation from the mixing rule is observed in specific surface area evaluation (see Fig. 2b), indicating that dispersing the zeolite powder in the chitosan phase leads to an optimized surface exposure, thus enhancing the adsorption performance (see Fig.2a).

Moreover, being the adsorption process reversible, the obtained aerogel beads are easily regenerable by means of a pressure swing process at room temperature, still preserving their performance unaltered over several adsorption/desorption cycles.

### Image 1:

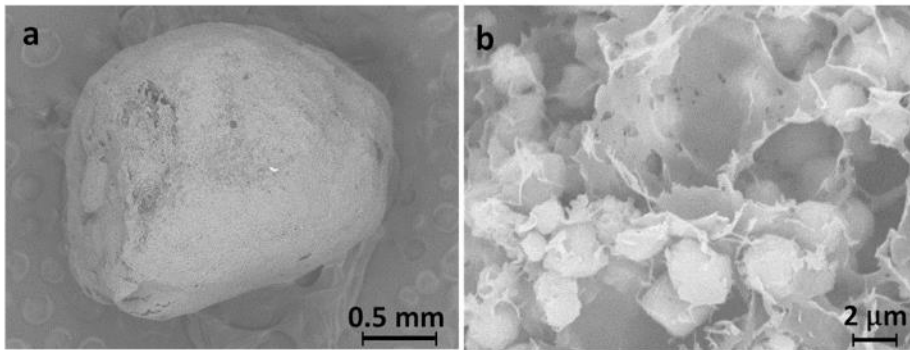


**Figure 1.** SEM micrographs of chitosan-zeolite13X aerogel beads ( $\phi_{ZX}=0.90$ ) a) external surface and b) inner morphology.

### Image 2:

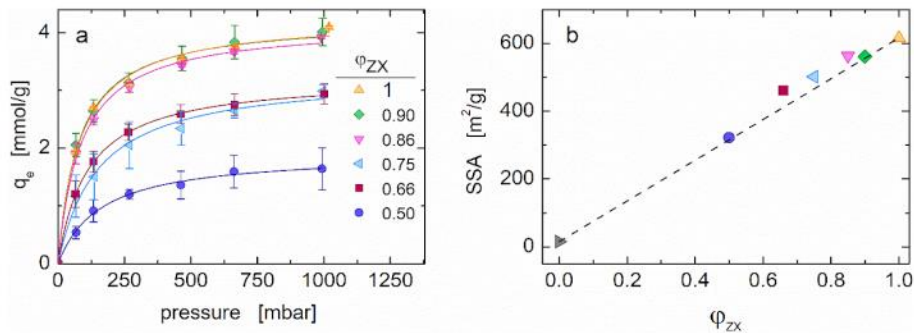


**Figure 2.** a) CO<sub>2</sub> adsorption isotherms of chitosan-zeolite13X aerogel beads. Solid lines represent the best fitting of the Langmuir model to experimental data. b) Specific surface area measured with BET method. Dashed line shows the expectations of the mixing rule.

### References:

- (1) Jacobson, T. A.; Kler, J. S.; Hernke, M. T.; Braun, R. K.; Meyer, K. C.; Funk, W. E. Direct Human Health Risks of Increased Atmospheric Carbon Dioxide. *Nat. Sustain.* 2019, 2 (8), 691–701. <https://doi.org/10.1038/s41893-019-0323-1>.
- (2) Riboldi, L.; Bolland, O. Overview on Pressure Swing Adsorption (PSA) as CO<sub>2</sub> Capture Technology: State-of-the-Art, Limits and Potentials. *Energy Procedia* 2017, 114 (1876), 2390–2400. <https://doi.org/10.1016/j.egypro.2017.03.1385>.
- (3) Choi, S.; Drese, J. H.; Jones, C. W. Adsorbent Materials for Carbon Dioxide Capture from Large Anthropogenic Point Sources. *ChemSusChem* 2009, 2 (9), 796–854. <https://doi.org/10.1002/cssc.200900036>.
- (4) Harlick, P. J. E.; Tezel, F. H. An Experimental Adsorbent Screening Study for CO<sub>2</sub> Removal from N<sub>2</sub>. *Microporous Mesoporous Mater.* 2004, 76 (1–3), 71–79. <https://doi.org/10.1016/j.micromeso.2004.07.035>.
- (5) Aranzabal, A.; Iturbe, D.; Romero-Sáez, M.; González-Marcos, M. P.; González-Velasco, J. R.; González-Marcos, J. A. Optimization of Process Parameters on the Extrusion of Honeycomb Shaped Monolith of H-ZSM-5 Zeolite. *Chem. Eng. J.* 2010, 162 (1), 415–423. <https://doi.org/10.1016/j.cej.2010.05.043>.

**Flow membrane reactor for the esterification of acetic acid using MOR-type zeolite membrane**

M. Sakai<sup>1,\*</sup>, Y. Nonaka<sup>2</sup>, M. Matsukata<sup>1,2,3</sup>

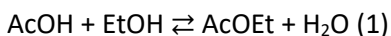
<sup>1</sup>Research Organization for Nano & Life Innovation, <sup>2</sup>Applied Chemistry, <sup>3</sup>Advanced Research Institute for Science and Engineering, Waseda University, Tokyo, Japan

**Abstract Text:** Esterification is an important process for chemical production, but the attainable level of conversion is always thermodynamically limited. Currently, esterification is carried out in batch reactors by using an excess amount of alcohol to increase acid conversion. Thus, huge energy is consumed for the purification of ester from alcohol and water. Dehydration membrane reactor has been drawn attention as a novel energy-saving process for esterification for recent decades. Employing dehydration membranes to remove water from the reaction system increases the level of conversion achievable beyond that thermodynamic limits without the use of excess alcohol. Consequently, one can expect that energy consumption for purification process after reaction is reduced as well as the improvement of one-path yield of products.

We previously reported MOR-type zeolite membrane for dehydration and pointed out that the MOR membrane had high chemical resistance for organic acid [1]. In this study, we applied the MOR membrane to a plug flow reactor for the esterification of acetic acid.

MOR membranes were synthesized by a seed-assisted crystallization method on the outer surface of porous tubular  $\alpha$ -alumina support (Noritake, i.d. = 7 mm, o.d. = 10 mm) of which the average pore size of top layer was ca. 150 nm. The outer surface of support was seeded by a dip-coating method using a colloidal suspension of MOR seed crystals. MOR membranes were obtained by hydrothermal treatment of this seeded support.

Acetic acid esterification shown in eq. (1) was carried out in a plug flow membrane reactor equipped with MOR membrane.



An equimolar mixture of acetic acid and ethanol was used as feed for the reaction. Temperature and pressure were adjusted at 403K and 1.0 MPa, respectively. Amberlyst-15, a catalyst for esterification, was packed on the outer side of tubular membrane. The permeate was analyzed for its composition by using GC-TCD. The yields of ethyl acetate produced in the plug flow reactor (PFR) without membrane and the plug flow membrane reactor (PFMR) were compared.

The level of acetic acid conversion in PFR was about 67%, which was almost the same as equilibrium conversion. In contrast, the conversion level in PFMR exceeded the equilibrium limitation and reached >88%. The concentration of water that permeated MOR membrane was >90%, indicating that MOR membrane selectively removed water from reaction side. These results clearly showed that selective removal of water by using MOR membrane contributed to the enhancement of acetic acid conversion in PFMR. In addition, separation and permeation performance were stable at least up to 7 h, suggesting that MOR zeolite is one of the feasible membrane materials for dehydration under acidic conditions.

(1) G. Li, E. Kikuchi and M. Matsukata, "The control of phase and orientation in zeolite membranes by the secondary growth method" *Microporous Mesoporous Mater.* 62 (2003) 211-220.

**Ethylene/Ethane Separation by Gas-Phase SMB in Binderfree Zeolite 13X Monoliths**

R. A. Seabra\*, V. Martins, A. Ferreira, A. M. Ribeiro, A. Rodrigues

**Abstract Text:** Petrochemicals play an important role in the chemical and petroleum industries due to their utilization as starters/intermediates to create a diversity of products, from pharmaceuticals to all kinds of plastics and textiles<sup>1</sup>. One of the basic petrochemicals is light olefins as ethylene, whose production exceeds that of any other organic compound. The most extensively used process to produce ethylene is steam-cracking of hydrocarbons. Still, since the required polymer grade purity is above 99.9%, for ethane/ethylene separation, an effective distillation column is required. This step is frequently performed at extreme operating conditions, making this one of the most cost-intensive separation processes in the petrochemical industry. Several technologies have been studied, and among the alternatives, adsorption-based separations, such as gas-phase simulated moving bed (gas-SMB), appear to be one of the most promising energy-effective options.

Our research group explored olefin/paraffin separation by the SMB technology, first by phenomenological model-based simulations<sup>2-3</sup>, and later by experiments in the gas-phase SMB bench unit, home built<sup>4,5</sup>. In this study, enhanced binder-free 13X zeolite monoliths were used as adsorbents and propane as desorbent. This work<sup>6</sup> makes evident the efficiency of the gas-phase SMB for olefin/paraffin separations.

The adsorbent studied was binderfree zeolite 13X monolith provided by Chemiewerk Bad Köstritz GmbH. To test the potential of the monolith as adsorbent and propane as desorbent, several SMB cycles were proposed for the production of polymer-grade ethylene from 0.48/0.52 feed mixtures. The operating conditions are summarized in **Table 1**.

**Table 1.** Experimental conditions for the SMB cycles.

**Figure 1a** shows the composition of the three components for the eight SMB monoliths of Run 2, at cyclic steady-state. It can be found that the high desorbent flow rate, high contact time between adsorbent and desorbent, and three columns in the zone I allow almost complete adsorbent regeneration. The feed mixture is introduced in the node between zone II and III. In zone II the molar fraction of ethane is almost constant, and a stream with a 97.7% purity of ethylene is collected in the extract port. In zone III the molar fraction of ethylene decreases and a stream with 97.5% purity of ethane is collected in the raffinate port.

In section IV, the molar fraction of ethane also decreases and a pure propane stream is obtained at the end of the section.

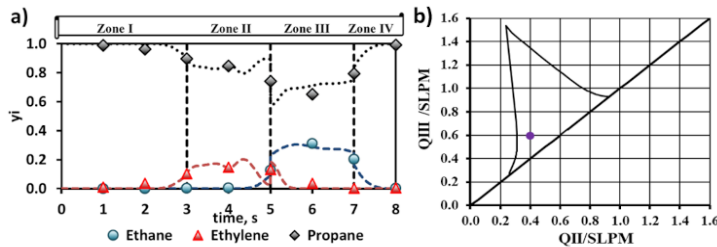
**Figure 1.** –a) Internal profile as function of column number, sample collected at step half time; Dashed lines represent the simulation results. b) Separation region determined with the complete model for C2 separation on binderfree zeolite 13X monoliths with a 3-2-2-1 configuration, switching time of 250 s, temperature of 373 K, and extract purity (ethylene) over 99.9% and recovery of at least 98%. Run 2 operating point.

A productivity of  $16.9 \text{ kg}_{\text{C}_2\text{H}_4} \cdot \text{h}^{-1} \cdot \text{m}_{\text{bed}}^{-3}$ , and  $14.5 \text{ kg}_{\text{C}_2\text{H}_6} \cdot \text{h}^{-1} \cdot \text{m}_{\text{bed}}^{-3}$  were obtained for ethylene and ethane respectively. As the experimental data allowed the global model validation (Figure 1a), it was possible to determine the separation region. The separation region was evaluated, taking into account the purity of extract (ethylene) higher than 99.9% and purity of raffinate (ethane) higher than 97%. As can be seen, the separation zone is quite large, allowing the treatment of up to 1.2 SLPM of an 0.48/0.52 (molar based) ethane/ethylene feed composition.

This work experimentally demonstrated that the combination of gas-phase SMB with structured zeolitic adsorbents can be an efficient technology for olefin/paraffin separations. It is possible to produce polymer grade ethylene with a high recovery using binder-free 13X zeolite monoliths as adsorbent and propane as desorbent.

**Image 1:**

Run	T, K	P, bar	t, s	Config.	Feed flow rate, SLPM	Desorbent flow rate, SLPM	Extract flow rate, SLPM	Raffinate flow rate, SLPM
1	373	2.5 – 1.6	250	4-2-2	0.09 C <sub>2</sub> H <sub>6</sub> 0.10 C <sub>2</sub> H <sub>4</sub>	1.51	1.12	0.64
2	373	2.3 – 1.5	250	3-2-2-1	0.09 C <sub>2</sub> H <sub>6</sub> 0.10 C <sub>2</sub> H <sub>4</sub>	1.51	1.08	0.46

**Image 2:****References: 1.**

- Martins, V. F.; Ribeiro, A. M.; Chang, J.-S.; Loureiro, J. M.; Ferreira, A.; Rodrigues, A. E., Towards polymer grade ethylene production with Cu-BTC: gas-phase SMB versus PSA. *Adsorption* 2018, 1-17.
- Campo, M. C.; Baptista, M. C.; Ribeiro, A. M.; Ferreira, A.; Santos, J. C.; Lutz, C.; Loureiro, J. M.; Rodrigues, A. E., Gas phase SMB for propane/propylene separation using enhanced 13X zeolite beads. *Adsorption* 2014, 20 (1), 61-75.
- Sá Gomes, P.; Lamia, N.; Rodrigues, A. E., Design of a gas phase simulated moving bed for propane/propylene separation. *Chemical Engineering Science* 2009, 64 (6), 1336-1357.
- Martins, V. F. D.; Ribeiro, A. M.; Plaza, M. G.; Santos, J. C.; Loureiro, J. M.; Ferreira, A. F. P.; Rodrigues, A. E., Gas-phase simulated moving bed: Propane/propylene separation on 13X zeolite. *Journal of Chromatography A* 2015, 1423, 136-148.
- Martins, V. F. D.; Ribeiro, A. M.; Santos, J. C.; Loureiro, J. M.; Gleichmann, K.; Ferreira, A.; Rodrigues, A. E., Development of gas-phase SMB technology for light olefin/paraffin separations. *AIChE Journal* 2016, 62 (7), 2490-2500.
- Seabra, R.; Martins, V. F.; Ribeiro, A. M.; Rodrigues, A. E.; Ferreira, A. P., Ethylene/ethane separation by gas-phase SMB in binderfree zeolite 13X monoliths. *Chemical Engineering Science* 2021, 229, 116006.

**ADSORPTION OF PCDD/F BY ZEOLITES**

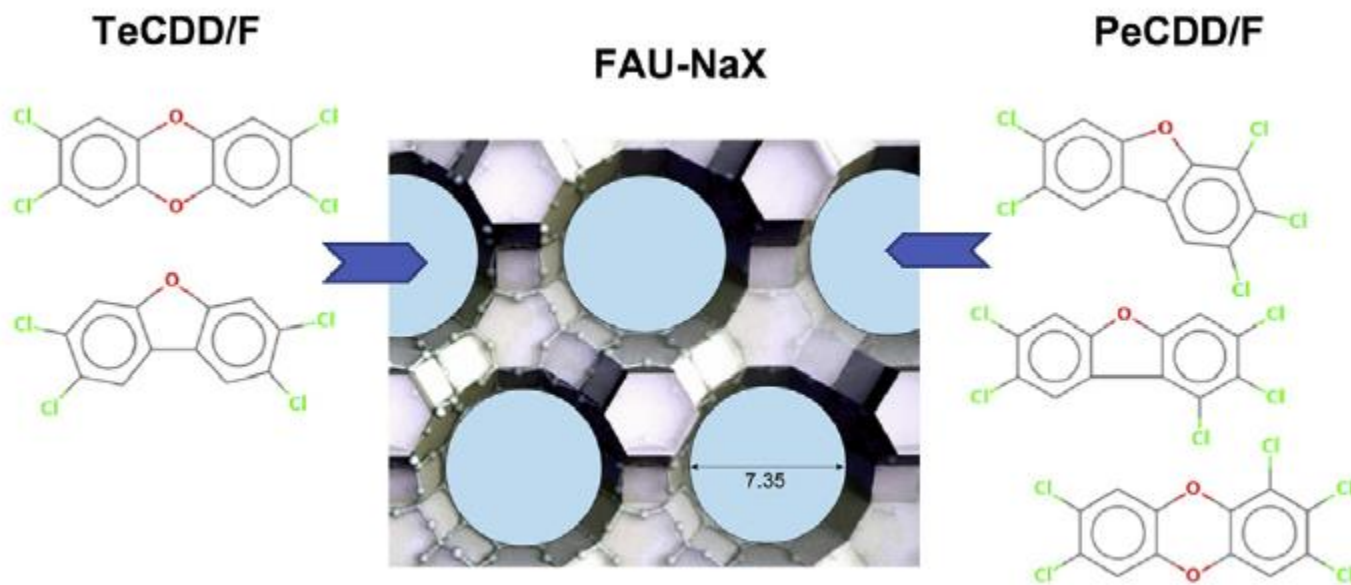
A. Simon-Masseron\*, O. Schäf, L. Tortet, S. Defour, C. Coste, Y. Zerega

**Abstract Text:** Polychlorinated dibenzo-p-dioxins and polychlorinated dibenzofurans (PCDD/F) monitoring at stationary sources is compliant with EN1948 standard. In long-term sampling method, XAD-2 resin adsorbent is exposed to gas stream for 3-4 weeks, and subsequently analysed in an accredited laboratory for 2 weeks. Selective adsorbents could preferentially accumulate toxic dioxin congeners prior to mass analysis with the aim of developing an on-line mass spectrometer device. Zeolites possess micropores for adsorbing molecules specifically in addition to non-specific surface area adsorption.<sup>[1]</sup>

Beads of zeolites<sup>[2]</sup> allowing adsorption in the micropores of only tetra- and penta-chlorinated toxic congeners (TeCDD/F, PeCDD/F) have been exposed to the gas flow of a waste incinerator within the methods compliant with EN1948 standard. As the extraction method of the standard does not allow us to discern the two types of adsorption, the sampling point have been located before the last filter. With high congener concentrations, it is expected that the dynamic adsorption properties of the zeolites can be deduced from the breakthrough of some congeners.

The electronic interactions between zeolite surface area and PCDD/F involve the polarizability of the molecules.<sup>[3]</sup> Thanks to the congener breakthrough comparing two zeolite structure types, it has been deduced that toxic TeCDD/F and PeCDD/F were adsorbed in the micropores of FAU-NaX zeolite due to steric compatibility of these congeners. Moreover, the partition of congeners between the condensate and gas phase was elucidated by considering the polarizability of PCDD/F molecules.

**Image 1:**



**References:** 1. Ben Abda, M. ; Schäf, O.; Ziarelli, F.; Pizzala, H.; Denoyel, R.; Viel, S.; Zerega, Y., *Microporous Mesoporous Mater.* 2016, 234, 200-206.

2. Rioland, G.; Bullot, L.; Daou, T.J.; Simon-Masseron, A.; Chaplais, G.; D. Faye, Fiani, E.; Patarin, J., *RSC Adv.* 2016, 6, 2470-2478.

3. Schäf, O.; Tortet, L.; Simon-Masseron, A.; Patarin, J.; Defour, S.; Blanc, R.; Coste, C.; Zerega, Y., *Chemosphere* 2020, 259, 127457.

**Adsorption of hydrogen sulfide from thermal water by natural zeolite**

L. G. Akhalbedashvili\*, C. Beruashvili<sup>1</sup>, N. Janashvili<sup>1</sup>, S. Jalaghania<sup>1</sup>

<sup>1</sup>Ivane Javakhishvili Tbilisi State University, Ivane Javakhishvili Tbilisi State University, Тбилиси, Georgia

**Abstract Text: Adsorption of hydrogen sulfide from thermal water by natural zeolite**

*L. Akhalbedashvili, C. Beruashvili, N. Janashvili, S. Jalaghania*

Iv. Javakhishvili Tbilisi State University, Georgia

**Abstract**

Hydrogen sulfide is strong poisonous to the human organism, because it binds to iron in the mitochondrial cytochrome enzymes, and thus interfering cellular respiration and especially damaging the nervous system.

H<sub>2</sub>S very weakly dissolves in water at ambient conditions and only in small degree dissociates according to equation  $H_2S + H_2O \rightarrow HS^- + H^+$ , forming a weak acid areas (pH=6.8). According to recent investigations by Raman spectroscopy, in aqueous solutions only hydrosulfide (HS<sup>-</sup>) anions are present and no sulfide (S<sub>2</sub><sup>-</sup>). At pressures above 18 bar H<sub>2</sub>S remains dissolved in water. The hydrogen sulfide can further react with aqueous metal ions to produce hardly soluble, black-colored sulfides such as ferrous and copper sulfides (FeS, FeS<sub>2</sub>, CuS).

Different methods have been tested to remove hydrogen sulfide from drinking water such as chlorination, aeration, or nitrate addition. Currently, many different types of materials are used as adsorbents for the removal of H<sub>2</sub>S, such as modified zeolites.

Being a successful adsorbent for removal of hydrogen sulfide, zeolites should have high capacity regard to sulfur, good regenerability and saving structure. These are natural zeolites having high adsorption capacity compared to synthetic zeolites. They can be modified by metals or metal oxides in order to increase their adsorption capacity. Removal of H<sub>2</sub>S is an essential process because it causes to corrosion in transport lines, equipment and poisoning of many catalysts even in low levels.

This study offered the purification method of geothermal water, containing toxic hydrogen sulfide, using modified natural zeolite- clinoptilolite (CL) as adsorbent. The underlying assumption of this adsorption process is that introduced Fe<sup>3+</sup> will be reduced to Fe<sup>2+</sup> and the sulfide precipitates as iron sulfide (FeS or FeS<sub>2</sub>) or oxidizes further to less-toxic sulfate anions (SO<sub>4</sub><sup>2-</sup>).

The specific objectives of this study were to determine flow rate of water, pH of areas, time of working of adsorbent till skip, optimal ratio adsorbent : water; to calculate the dynamic exchange capacity (DEC), adsorption degree and some kinetic parameters.

Experimental studies were performed by using natural zeolite, CL, taken from Dzegvi region of Georgia in initial and modified forms and compared with activated carbon (AC), modified with 1 M potassium hydroxide (KOH). Cation-exchanged zeolitic samples were obtained by treating of natural CL with ferric and copper salts using wet milling method. The second type of processing included preliminary treatment of zeolite with hot solution of KMnO<sub>4</sub>. The quantity of exchanged metal was determined by AAS method. The pH of the solutions was measured using a pH meter.

The adsorption capacity of studied materials regards to the H<sub>2</sub>S was performed using a laboratory-designed test at room temperature and atmospheric pressure in a flow and circular regimes. The surface properties and structure of all samples were characterized using pH, X-ray and IR-spectroscopy analysis.

The results obtained demonstrate that all studied samples were effective in H<sub>2</sub>S sorption, but in different degree: the best were AC and Fe-exchanged CL. The sorption capacity ranged from 0.28 mg/g to 8.17 mg/g. pH of thermal water before sorption was 8.97 and in filtrates changed in very wide ranges – from 10.44 till 3.55 depending on type of modification.

H<sub>2</sub>S adsorption on the thermally treated at different temperatures Fe-exchanged CL occurs via both physical sorption and chemisorption. The first-order adsorption kinetics showed a relatively good fit to the experimental data for the H<sub>2</sub>S adsorption process, which adsorbed coordinatively on the cations via the sulfur atom.

**CO<sub>2</sub> ADSORPTION ON MODIFIED MESOPOROUS SILICAS: THE ROLE OF THE ADSORPTION SITES**

M. Popova\*, H. Lazarova, M. Ravutsov, S. Simeonov, P. Shestakova

**Abstract Text:** CO<sub>2</sub> is considered the main greenhouse gas because it is emitted in enormous amounts from anthropogenic activities [1-3]. Recently, the targets for limiting CO<sub>2</sub> emissions into the atmosphere have driven the intensive development of innovative technological solutions. Carbon capture, utilization and storage (CCUS) technologies are among the most important environmental protection issues aimed at mitigation of the environmental impact of greenhouse gases. CO<sub>2</sub> separation *via* adsorption has gained considerable attention as a viable alternative to the currently used technologies, because of the higher energy efficiency and environmental compatibility. In recent years, the adsorption of CO<sub>2</sub> on porous solid materials with a high specific surface area has been the subject of extensive research. The physical characteristics and surface chemical properties of porous materials determine their CO<sub>2</sub> adsorption capacity, as well as their selectivity and stability in the presence of other contaminants and water vapor. Sorption materials must meet a number of important criteria, both operational and economic, in order to be suitable for CO<sub>2</sub> capture from flue gases.

**In the present study** the morpholine and 1-methylpiperazine modified mesoporous MCM-48 and SBA-15 silicas were developed and studied as efficient adsorbents of CO<sub>2</sub>.

MCM-48 and SBA-15 silicas were modified by post-synthesis procedure with cyclic amines, morpholine and 1-methylpiperazine. The initial and modified materials were characterized by XRD, N<sub>2</sub> physisorption, thermal analysis and solid state NMR. A high specific surface area of the modified materials was registered due to the preservation of their structure during the modification procedure. The CO<sub>2</sub> adsorption was tested under dynamic and equilibrium conditions and revealed high capacity for all the modified materials with some alterations depending on the functional groups and the support peculiarities. The formation of different CO<sub>2</sub> adsorbed forms was observed and studied by NMR spectroscopy. The 1-methylpiperazine modified mesoporous MCM-48 and SBA-15 silicas show higher adsorption capacity in comparison to their morpholine-modified analogs. The materials exhibited high stability and in all cases only a minor decrease in CO<sub>2</sub> adsorption was observed over three subsequent adsorption/desorption cycles. Our studies revealed that the obtained new modified silica materials exhibited superior properties for CO<sub>2</sub> capture, thus are promising candidates for the development of carbon capture and storage (CCS) and carbon capture and utilization (CCU) technologies.

**Acknowledgements:** This work is supported by the Bulgarian Ministry of Education and Science under the National Research Programme E<sup>+</sup>: Low Carbon Energy for the Transport and Households, grant agreement D01-214/2018, D01-321/18.12.2019 and D01-361/17.12.2020. Research equipment of distributed research infrastructure INFRAMAT (part of the Bulgarian National Roadmap for Research Infrastructures) supported by the Bulgarian Ministry of Education and Science under contracts D01-155/28.08.2018 and D01-284/17.12.2019 was used in this investigation.

**References:**

1. D. M. D'Alessandro, B. Smit, J. R. Long, *Angew. Chem. Int. Ed.*, 49 (2010) 6058.
2. G. T. Rochelle, *Science*, 325 (2009) 1652.
3. P.J.E. Harlick, A. Sayari, *Ind. Eng. Chem. Res.*, 45 (9) (2006) 3248.

**Effect of operation conditions on water flux through ZSM-5 membrane in forward osmosis operation**

M. Sakai<sup>1</sup>, Y. Nomura<sup>2,\*</sup>, M. Matsukata<sup>1,2,3</sup>

<sup>1</sup>Research Organization for Nano & Life Innovation, <sup>2</sup>Applied Chemistry, <sup>3</sup>Advanced Research Institute for Science and Engineering, Waseda University, Tokyo, Japan

**Abstract Text:** Forward osmosis (FO) is a promising membrane separation process in wastewater reclamation, osmotic membrane bioreactor, food processing and power generation. In these applications, FO has advantages with low energy consumption and less membrane fouling compared with reverse osmosis, nanofiltration and ultrafiltration. Previously, various types of polymeric membranes and mixed matrix membranes were studied for FO operations.

Zeolite membrane has advantages of thermal and chemical resistance as characteristics of inorganic material in comparison with polymeric membranes. We recently found that ZSM-5 was able to play as FO membrane for the first time<sup>1)</sup>. In this study, we shed light on the water flux through the ZSM-5 membrane in the FO operation.

ZSM-5 membrane was prepared on the outer surface of  $\alpha$ -alumina tubular support by a secondary growth method. The outer diameter and length of the support were 10 and 30 mm, respectively. The effective membrane area,  $A$ , was  $6.28 \times 10^{-4} \text{ m}^2$ . To characterize membrane, the water permeance and reverse salt flux were evaluated in FO operation. NaCl aqueous solution and distilled water were used as the draw solution (DS) and the feed solution (FS), respectively.

The effects of the membrane temperature and DS concentration on the water flux were investigated. The water flux linearly increased with increasing membrane temperature due to the decrease in the viscosity of water. The water flux also increased with increasing DS concentration, the flux reached a plateau at higher concentrations. These results indicated that the bulk osmotic pressure difference did not work as driving force at all, since concentration polarization is more likely to occur at higher NaCl concentrations in DS. The reverse salt flux through ZSM-5 membrane was very small under all tested conditions, indicating that ZSM-5 membrane exhibited the potential for FO based on the molecular sieving effect.

We will represent the effect of an effect of chemical engineering factors such as the Re number and the structural parameter of membrane support on the performance of FO operation.

1) Motomu Sakai, Masahiro Seshimo, Masahiko Matsukata, Hydrophilic ZSM-5 membrane for forward osmosis operation, J. Water Proc. Eng. 32 (2019) 100864.

**Removal of Persistent Organic Pollutants by cationic zeolites under humid conditions**

T. AMMOULI<sup>1,\*</sup>, I. Deroche<sup>1</sup>, P. Sonnet<sup>1</sup>, R. Stephan<sup>1</sup>, M.-C. Hanf<sup>1</sup>, J.-L. Paillaud<sup>1</sup>

<sup>1</sup>Haut-Rhin, University of Haute Alsace, MULHOUSE, France

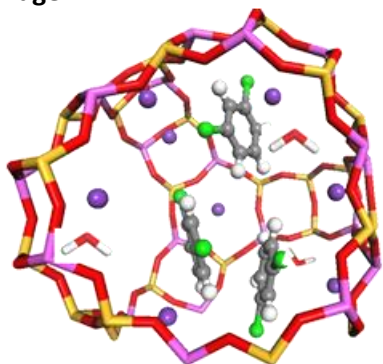
**Abstract Text:** Although according to the World Health Organization (WHO), POPs are carcinogens and teratogens species, they're still implied in pesticides, herbicides...manufacturing processes [1] wherefrom they become airborne. Among possible removal solutions, cationic zeolites are considered as promising host-candidates to remove these compounds by selective adsorption process. Nevertheless, the inescapable hydrated framework of these minerals under normal thermodynamic conditions could constraint their performances.

Through this work we aim to bring to light the mechanism of POPs adsorption within cationic faujasite type framework when varying both, the humidity rate and the nature of the charge compensating cation. For that purpose we combine several molecular simulation techniques to experimental tools. Moreover, a development of new force field that describes specifically the cation-framework interaction, based on ab-initio calculations is in progress. Subsequently, it will be implemented in classical molecular simulation, in order to reproduce experimental data.

We demonstrate that a residual amount of water has no significant effect on POPs adsorption properties, but, they are remarkably impacted beyond (3%wt). Thus, we could save considerable time and energy wasted on expensive regeneration cost. Besides, cations within the framework increase notably the affinity of faujasite toward POPs, but decrease its uptake capacity comparing to pure silica faujasite [2].

**Key word :** zeolithe, adsorption, extra-framework cation, molecular simulation.

**Image 1:**



**References:** [1]: Rossberg, Manfred, et al. "Chlorinated hydrocarbons." Ullmann's encyclopedia of industrial chemistry (2000): 105-108

[2]: Randrianandraina, J., et al. "Bis-chlorinated aromatics adsorption in Faujasites investigated by molecular simulation-influence of Na<sup>+</sup> cation." Microporous and Mesoporous Materials 251 (2017): 83-93

**On the textural properties' investigation of ion-exchanged embryonic zeolites**

R. Guillet-Nicolas<sup>1,\*</sup>, M. Akouche<sup>1</sup>, V. Valtchev<sup>1</sup>

<sup>1</sup>LCS, CNRS, Caen, France

**Abstract Text:** X-ray amorphous zeolite precursors, embryonic zeolites (EZ), were prepared using tetrapropylammonium (TPA+) hydroxide as a structure-directing agent. The EZs belong to the family of extra-large microporous (1 – 2.5 nm) materials and were recently proposed as highly active heterogeneous catalysts for processing and converting bulky and/or very polar molecules such as heavy oil and bio-sourced feedstocks.<sup>1,2</sup> Of major interest is the very open and accessible structure of EZs originating from the cage-like arrangement between the organic structuredirecting agent (OSDA) and the (alumino)silicate species. To investigate in more details the peculiarities of these novel materials, a series of EZs was ion-exchanged in water at different temperatures with sodium, ammonium and cesium. The resulting materials were thoroughly characterized before and after template elimination via high-temperature combustion of the residual OSDA. Analyses of N<sub>2</sub> and Ar adsorption at 77 and 87 K, respectively, coupled with the application of state-of-the-art NLDFT data reduction methods, revealed unusual physicochemical properties. While a reduced microporosity was obtained as compared to their pristine counterparts, ion-exchanged EZs exhibit very homogeneous and tailored mesopore size distribution, echoing the ones found in ordered mesoporous silicas. Aiming at an exhaustive understanding and rationalization of processes leading to such unique texture and pore architecture, the present study proposes an advanced physico-chemical investigation of these materials based on a modern methodology combining, among others, high-resolution hysteresis desorption scanning experiments, electron microscopy and XRD. Our data provide new insights into the correlation between the relation synthesis/pore structure and shed some light on important questions concerning the applied potential of embryonic zeolites in catalysis.

**References:** [1] K.-G. Haw, J.-P. Gilson, N. Nesterenko, M. Akouche, H. El Siblani, J.-M. Goupil, B. Rigaud, D. Minoux, J.-P. Dath, V. Valtchev, *ACS Catal.* 2018, 8, 8199-8212.

[2] M. Akouche, J.-P. Gilson, N. Nesterenko, S. Moldovan, D. Chateigner, H. El Siblani, D. Minoux, J.-P. Dath, V. Valtchev, *Chem. Mater.* 2020, 32, 2123-2132.

**Halloysite Nanotube Synthesis of Zeolite-X and Application in CO<sub>2</sub> Capture**

X. Lu<sup>\*</sup>, L. Liu<sup>1</sup>, G. Li

<sup>1</sup>School of metallurgy, Northeastern University, Shen yang, China

**Abstract Text: Halloysite Nanotube Synthesis of Zeolite-X and Application in CO<sub>2</sub> Capture**

*Xinmei Lu<sup>1</sup>, Liying Liu<sup>1,\*</sup>, Gang Li<sup>2,\*</sup>*

*(<sup>1</sup> State Environmental Protection Key Laboratory of Eco-Industry, Northeastern University, Shenyang, 110819, China; <sup>2</sup>*

*Department of Chemical Engineering, The University of Melbourne, VIC3010, Australia)*

*Corresponding authors: Liying Liu, liuly@smm.neu.edu.cn; Gang Li, li.g@unimelb.edu.au*

Zeolite-X has good selective adsorption, ion exchange and hydrophilic properties, and has been widely studied and applied in chemical industry, medical treatment and environmental protection. Halloysite nanotubes (HNTs) with a unique tubular microstructure, natural availability, and low cost, have been widely applied in ceramics, drug sustained release system, catalysis, and adsorption. In this paper, natural HNTs from different origins (A, B, C, D) were studied, and the performance of the synthesized zeolite-X was evaluated under the same conditions. Zeolite-X with high crystallinity and large specific surface area were synthesized by purifying HNTs, calcining HNTs and hydrothermal synthesis. The influence of calcination temperature, calcination time, aging temperature, aging time, crystallization temperature, crystallization time and NaOH concentration on the crystal phase and static saturated water absorption of Zeolite-X were investigated. The structure, shape and thermal stability of the synthesized Zeolite-X were characterized by XRD, ICP, SEM, and FT-IR techniques and analysis methods. At the same time, the adsorption properties of CO<sub>2</sub> at different temperatures were measured. The results showed that the optimal conditions for the preparation of Zeolite-X were as follows: calcination at 650°C for 3 h, aging in 2 mol/L sodium hydroxide solution for 1 h (at 40°C), and crystallization at 90°C for 24 h. The CO<sub>2</sub> equilibrium adsorption capacity of samples (HNTs produced in A) reaches up to 6.12 mmol/g (between 0 and 1 bar at 273 K), which is the highest among other samples. In short, the Zeolite-X synthesized by this method has high crystallinity, cubic octahedron, uniform particle size and similar thermal stability to industrial zeolite.

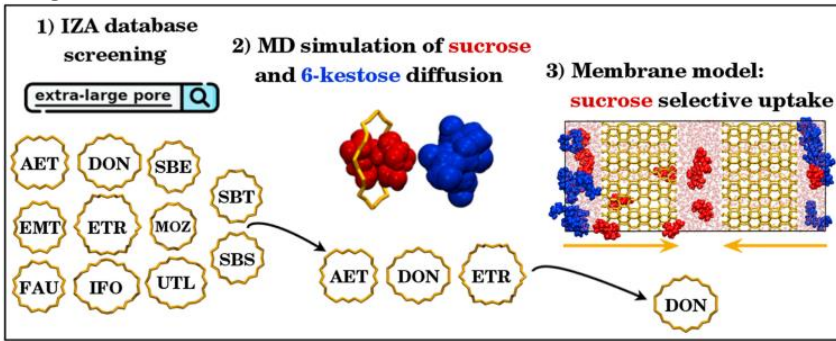
**Separation of an aqueous mixture of 6-kestose/sucrose using extra-large pore zeolites: A molecular dynamics simulation**

I. Bolaño Losada<sup>1</sup>, P. Grobas-Illobre<sup>1</sup>, A. Misturini<sup>1,\*</sup>, J. Polaina<sup>2</sup>, Y. Seminovski<sup>1</sup>, G. Sastre<sup>1</sup>

<sup>1</sup>Instituto de Tecnología Química - UPV, CSIC, Universidad Politécnica de Valencia, <sup>2</sup>Instituto de Agroquímica y Tecnología de Alimentos, CSIC, Valencia, Spain

**Abstract Text:** Zeolites are well-known for their adsorption properties, arising from the wide surface area and high porosity. The topology of zeolite micropores also play an important role in mixture separation, due to the “shape selectivity” phenomena, where molecules with shapes similar to that of the micropore are preferably adsorbed. The discovery of new low-glycemic sugars is very attractive as new healthy additives in the food field. 6-Kestose is an oligosaccharide of industrial interest because of its prebiotic and other functional properties. A significant technical problem of the production procedure is the need to purify 6-kestose from sucrose [1]. Exploring the large variety of pore sizes in zeolites, we search for suitable candidates for the separation of 6-kestose and sucrose in aqueous solution. A first selection, between all 253 zeolites in the IZA (International Zeolite Association) database, has been made by comparing sugar dimensions with micropore size. As a result, 11 extra-large pore zeolites, whose pore size is, roughly, between 6.8×7.0 and 10.1×10.1 Å (AET, DON, EMT, ETR, FAU, IFO, MOZ, SBE, SBS, SBT, and UTL) fulfill this criterion (left part of Image 1), and (in principle) may preclude 6-kestose diffusion (with approximate size of 11.4×9.1×6.7 Å), allowing only the diffusion of sucrose (with approximate size of 9.4×7.5×6.3 Å). Molecular dynamics simulations with this small set of candidates containing one sugar molecule inside the micropore were performed during 10 ns. The usual 3-D zeolite periodic model was considered, with all atoms of the system allowed to relax and without external surface. By analyzing the mobility of both sugars in the selected zeolites during the simulations, 3 frameworks could be selected for further evaluation by presenting clearly larger mobility for sucrose than for 6-kestose: AET, ETR, and DON (central part of Image 1). Thus, an in-depth analysis through a molecular dynamics study of aqueous systems, considering zeolite external surface, was performed with AET, DON and ETR frameworks. The simulation boxes (right part of Image 1) contained two zeolite layers terminated by silanol groups, and separated by 20 Å, producing two reservoirs. Some zeolite atoms were kept fixed during the simulation, to keep the zeolite layer separation, while silanol groups were allowed to relax. Sugar molecules were initially located outside the zeolite layers (in reservoir 1), and 20 ns simulations were carried out with low (4 sucrose and 4 6-kestose) and high (9 sucrose and 9 6-kestose for ETR; 12 sucrose and 12 6-kestose for AET and DON) sugar loading. At low loading none of the membranes shows significant uptake after 20 ns, illustrating the so called ‘surface barrier’ effect [2]. In these simulations, sugar molecules stayed attached to the zeolite external surface due to its strong interaction, reducing the probability of ‘jump’ into the zeolite channel. Therefore, sugar adsorption over the zeolite surface is more energetically accessible rather than the sugar flow through the zeolite cavity. On the other hand, at increased loadings, the external surface becomes quickly saturated with a monolayer of sugar molecules, after which the incoming molecules will interact less strongly with the zeolite external surface and hence diffusion into the channel will become more probable. This phenomenon could be seen in the simulations containing high loading of sugar, where sucrose molecules were preferentially adsorbed in all three frameworks (AET, DON, ETR), while 6-kestose remained in the reservoir 1. In addition, DON membrane showed not only a selective uptake of sucrose but also a very high molecular flux, with sucrose molecules reaching, or being very close to, reservoir 2. The results show that DON presents the most promising theoretical results for a selective sucrose/6-kestose separation [3].

Image 1:



**References:** [1] J. Marín-Navarro, D. Talens-Perales, J. Polaina, One-pot production of fructooligosaccharides by a *Saccharomyces cerevisiae* strain expressing an engineered invertase, *Appl. Microbiol. Biotechnol.* 99 (2015) 2549–2555, <https://doi.org/10.1007/s00253-014-6312-4>.

[2] G. Sastre, J. Kärger, D.M. Ruthven, Molecular dynamics study of diffusion and surface permeation of benzene in silicalite, *J. Phys. Chem. C* 122 (2018) 7217–7225, <https://doi.org/10.1021/acs.jpcc.8b00520>.

[3] Losada, I. B., Grobas-Illobre, P., Misturini, A., Polaina, J., Seminovski, Y., Sastre, G. Separation of an aqueous mixture of 6-kestose/sucrose with zeolites: A molecular dynamics simulation. *Microporous and Mesoporous Materials* 319 (2021) 111031, <https://doi.org/10.1016/j.micromeso.2021.111031>.

**Adsorption behavior of methyl iodide on silver ion-exchanged zeolites**

M. B. Park<sup>1,\*</sup>, H. An<sup>1</sup>, S. J. Kweon<sup>1</sup>, M. H. Kim<sup>1</sup>

<sup>1</sup>Department of Energy and Chemical Engineering, Incheon National University, Incheon, Korea, Republic Of

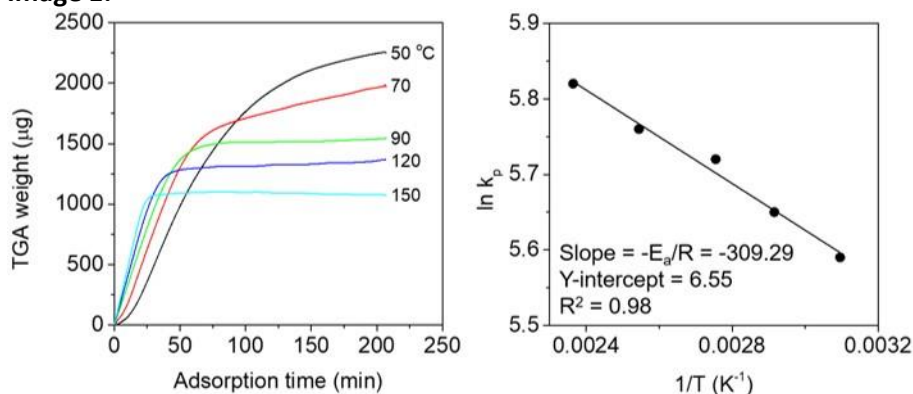
**Abstract Text:** An organic iodide, especially methyl iodide (CH<sub>3</sub>I), is one of the most safety concerns against a nuclear power plant severe accident because it is highly toxic and easily inhaled. In order to prevent its environmental release, it should be required to decontaminate using a filtration system. A wet-type filtration method using a pool scrubbing is not ideal due to a high re-volatile characteristic of CH<sub>3</sub>I. It easily becomes volatile after leaving a water pool and forms gas phase again at the surface of water pool. Therefore, a dry filtration using adsorbents like a zeolite should be installed to effectively capture the gas phase of CH<sub>3</sub>I and makes it immobile within the dry filter. Although it is important to accurately assess the performance of dry filter in a postulated severe accident situation, no sufficiently accurate adsorption kinetic behaviors have been reported yet.

A silver ion-exchanged zeolite (Ag-zeolite) has been recognized as an effective adsorbent for the removal of CH<sub>3</sub>I due to its ordered microporous structure inside, and chemical binding of iodine with a silver ion for the immobilization [1,2]. The performance of Ag-zeolite filter is usually explained by a breakthrough curve which contains a record of the concentration of CH<sub>3</sub>I in the off-gas with time using a GC or FT-IR. The breakthrough curves provide the important performance specifications of filter such as an adsorption capacity and a saturation time. However, the breakthrough curves provide no information to draw the kinetic parameters (e.g., adsorption reaction rate, activation energy, etc.). To quantify the adsorption kinetic parameters, the real time adsorption behaviors should be recorded with a high accurate measurement system.

In this study, we designed the highly accurate experimental set-up, TGA-GC coupled system, which can allow to accurately measuring the weight change of adsorbent in real time and also successively monitoring the off-gas contents, and performed the CH<sub>3</sub>I adsorption tests on Ag-ZSM-5 zeolites at a wide temperature range (50 – 150 °C) under the postulated severe accident condition. The Ag-ZSM-5 was prepared by ion-exchange method refluxing twice in 0.1 M AgNO<sub>3</sub> aqueous solutions and the Ag-loaded sample was calcined in air at 550 °C for 2 h before the adsorption experiment. The adsorption behaviors of weight change rate and the trend of adsorbed concentration of CH<sub>3</sub>I determined by TGA and GC, respectively, were well matched each other. Furthermore the CH<sub>3</sub>I adsorption content was almost identical to the conventional system.

The fresh and adsorbed Ag-ZSM-5 samples were characterized by powder XRD, elemental analysis, and SEM-EDS, and the further CH<sub>3</sub>I adsorption behaviors were discussed in depth. By using the parabolic Arrhenius theory and the initial adsorption rates determined from the TGA weight change curves at different adsorption temperatures, the activation energy for the formation of Ag-I on the ZSM-5 adsorbent was successfully calculated as 2.57 kJ/mol (Figure attached). From the overall characterization results, it has been confirmed that the Ag<sup>+</sup> ions were well dispersed in the fresh Ag-ZSM-5, and the chemisorbed AgI molecules were formed after the CH<sub>3</sub>I adsorption. The amount of chemisorbed I<sup>-</sup> at 150 °C was estimated as 962 μg, which is only 3.4% different from the calculated value. Our findings provide the useful fundamentals for a model development of dry filter performance assessment.

Image 1:



**References:** [1] T. Pham, S. Docao, I. C. Hwang, M. K. Song, D. Y. Choi, D. Moon, P. Oleynikov, K. B. Yoon, *Energy Environ. Sci.* 9 (2016) 1050.

[2] B. Azambre, M. Chebbi, *ACS Appl. Mater. Interfaces* 9 (2017) 25194.

### **Gas Adsorption, Separation and Storage | Zeolites/Inorganic materials | Poster**

FEZA21-PO-167

#### **Exploring Adsorption Properties of ADOR Materials**

M. Trachta<sup>1,\*</sup>, M. Rubes<sup>1</sup>, O. Bludsky<sup>1</sup>, R. Bulanek<sup>2</sup>, E. Koudelkova<sup>2</sup>, M. Shamzhy<sup>3</sup>

<sup>1</sup>Computational Chemistry, Institute of Organic Chemistry and Biochemistry, AS CR, Prague, <sup>2</sup>Physical Chemistry, Faculty of Chemical Technology, University of Pardubice, Pardubice, <sup>3</sup>Physical and Macromolecular Chemistry, Faculty of Science, Charles University, Prague, Czech Republic

**Abstract Text:** The ADOR (assembly - disassembly - organization - reassembly) strategy led to synthesis of numerous new materials.<sup>1</sup> Some of them exhibit unusual properties, violating criteria based on framework energy - density correlation and therefore being considered as unfeasible synthesis targets (in terms of the traditional solvothermal route).<sup>2-3</sup> These new materials and new structural motives may certainly be helpful in improving performance of current technological applications. We employed periodic density functional theory (DFT) calculations using the DFT/CC approach and also an ab initio empirical potential to investigate the adsorption properties of the mentioned materials. Both these methods were parameterized by us solely for the purpose of this study. The developed methodology may be used for a screening of adsorption properties of hypothetical zeolites accessible via the ADOR synthetic route<sup>4</sup> and consequent identification of synthesis targets with optimal features for a given application.

The adsorption of three different gasses (CH<sub>4</sub>, N<sub>2</sub>, CO<sub>2</sub>) was investigated by means of molecular dynamics and Monte Carlo simulations. In the case of CH<sub>4</sub> and N<sub>2</sub>, the heats of adsorption estimated by theory should be very accurate (r.m.s.d. on a set of individual structures of about 1.5 kJ·mol<sup>-1</sup>). The large discrepancy with respect to experiment in case of CH<sub>4</sub> in **UTL** (2.0 kJ·mol<sup>-1</sup>) may be plausibly explained by structural defects of the measured material.<sup>5</sup> Modeling CO<sub>2</sub> adsorption is much more demanding. Some of the investigated zeolites contain small cavities, where the adsorbate molecule fits very tightly. This puts very high demands on the accuracy of the potential. We therefore used an importance sampling technique and calculate the heats using DFT instead of using ab initio force field. The resulting heats of adsorption are in good agreement with experimental values.

A recently published discovery of a new synthesis pathway has opened up the possibility of a step increase in the number of zeolite frameworks available, many of them with uncommon features. We have examined the properties of synthesized ADOR zeolites, both theoretically and experimentally. Although the investigated materials have the same layer topology as the corresponding parent material, their channel structure and diffusion characteristics are significantly different. Some of the investigated zeolites possess small window openings, and therefore the diffusion

limitations through 7-, 8-, and 9-membered rings were determined for several probe molecules (CH<sub>4</sub>, N<sub>2</sub>, CO<sub>2</sub>). These findings may lead to the optimal design and improved functions for future applications.

**References:** (1) P. Eliasova, M. Opanasenko, P.S. Wheatley, M. Shamzhy, M. Mazur, P. Nachtigall, J.W. Roth, R.E. Morris, J. Cejka, *J. Chem. Soc. Rev.* **44**, 7177 (2015). (2) D. Majda, F.A.A. Paz, O.D. Friedrichs, M.D. Foster, A. Simperler, R.G. Bell, J. Klinowski, *J. Phys. Chem. C* **112**, 1040 (2008). (3) M. Mazur, P.S. Wheatley, M. Navarro, W.J. Roth, M. Polozij, A. Mayoral, P. Eliasova, P. Nachtigall, J. Cejka, R.E. Morris, *Nat. Chem.* **8**, 58 (2016). (4) M. Trachta, P. Nachtigall, O. Bludsky, *Catal. Today* **243**, 32 (2015). (5) M. Rubes, M. Trachta, E. Koudelkova, R. Bulanek, V. Kasneryk, O. Bludsky, *Phys. Chem. Chem. Phys.* **19**, 16533 (2017).

**The Structural Response of Merlinoite to CO<sub>2</sub> Adsorption**

E. L. Bruce<sup>1,\*</sup>, V. M. Georgieva<sup>1,2</sup>, M. Verbraeken<sup>3</sup>, S. Brandani<sup>3</sup>, P. A. Wright<sup>1</sup>

<sup>1</sup>EaStCHEM School of Chemistry, University of St Andrews, St Andrews, <sup>2</sup>Johnson Matthey Technology Centre, Chilton, Billingham, <sup>3</sup>School of Engineering, University of Edinburgh, Edinburgh, United Kingdom

**Abstract Text:** Flexible small pore zeolites are of interest in CO<sub>2</sub> adsorption, especially those which adapt to extra-framework cations upon dehydration. Such zeolites can possess extremely high selectivity to CO<sub>2</sub> over less polar molecules (such as CH<sub>4</sub> and N<sub>2</sub>) and their adsorption properties may be tailored through ion exchange. This was the case for zeolite Rho, with cation content determining window size and altering adsorption behaviour.<sup>1</sup> Another promising candidate for such behaviour is zeolite merlinoite (framework type MER).

As for Rho, MER has a 3-D connected 8-membered ring (8R) channel system and is a low Si/Al zeolite, with a relatively high cation content and the unit cell shrinks upon dehydration. Whilst Rho has only 1 crystallographically unique window site, MER has 3 (in highest symmetry), making a detailed understanding of the structure more challenging. We recently reported the structures and gas adsorption properties of a MER material with Si/Al = 3.8 in pure alkali metal cation forms.<sup>2</sup> Smaller cations Li and Na adopted the *Immm* space group, whilst K and Cs occupied *P4<sub>2</sub>/nmc*. Larger cation sizes lead to smaller structural distortions upon dehydration.

Materials exhibited a “breathing” transition from narrow to wide pore forms with increasing pCO<sub>2</sub>. Additionally, K-MER shows a “triggered” opening, with very low pCO<sub>2</sub> causing a rapid transition to the wide pore form. The low pCO<sub>2</sub> at which this occurs suggests that the 2 structures are very finely energetically balanced. Na- and Cs-MER underwent transitions at higher pCO<sub>2</sub> whilst the Li material was unstable. It was suggested that access for CO<sub>2</sub> to the double 8R (D8R) site was important, as this led to the widening of the structure. As Cs<sup>+</sup> is large, access is hindered, and the cations do not readily accommodate CO<sub>2</sub> molecules. Whilst Na<sup>+</sup> is much smaller, the D8R site is highly occupied, impeding CO<sub>2</sub> diffusion. The Na-MER structure is also extremely distorted and so it was suggested that this gave greater cation-framework interactions, obstructing cation migration.

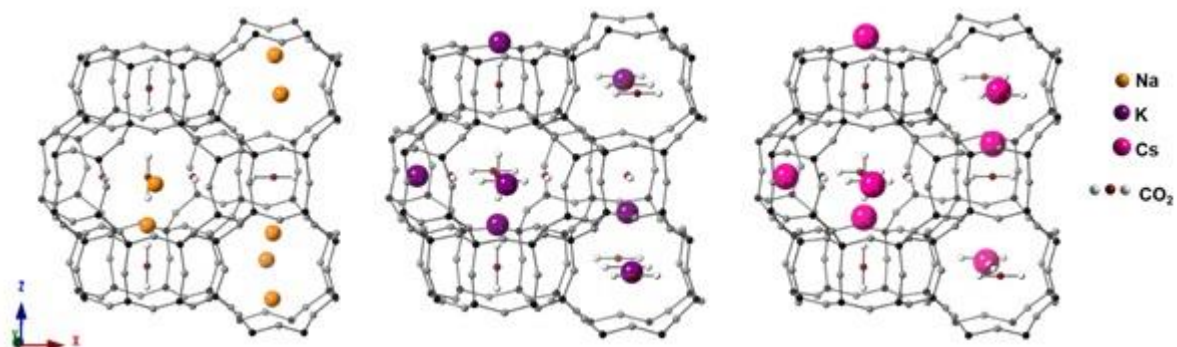
Materials with a higher Si/Al of 4.2 have since been synthesised and initial results show that despite a small change in Si/Al, there are some significant differences in gas adsorption properties and crystal structures. Work is required to understand these differences, but it can already be seen that the properties of MER can be greatly influenced with minor cation alterations.

**Acknowledgements**

The authors acknowledge the financial support provided by EPSRC (an NPIF Ph.D. scholarship for E.L.B.; EP/R512199/1), Cation-Controlled Gating for Selective Gas Adsorption over Adaptable Zeolites (EPSRC EP/ N032942 (VG, PAW); EP/N033329/1 (MV, SB)). Professor Tina Düren (Bath University) and Drs. Carole A. Morrison and Claire L. Hobday (Edinburgh University) are thanked for their helpful suggestions.

Figure 1: From left to right, the wide pore structures of Na-, K- and Cs-MER upon CO<sub>2</sub> adsorption.

Image 1:



**References: 1.**

M. M. Lozinska, J. P. S. Mowat, P. A. Wright, S. P. Thompson, J. L. Jorda, M. Palomino, S. Valencia and F. Rey, *Chem. Mater.*, 2014, 26, 2052–2061.

2.

V. M. Georgieva, E. L. Bruce, M. C. Verbraeken, A. R. Scott, W. J. Casteel, S. Brandani and P. A. Wright, *J. Am. Chem. Soc.*, 2019, 141, 12744–12759.

**Carbon dioxide capture by lanthanum-modified MCM-41**

T. R. S. Ribeiro<sup>1</sup>, D. P. D. S. Da Silva<sup>2</sup>, J. D. R. S. Solano<sup>2</sup>, A. O. S. Da Silva<sup>2</sup>, M. D. C. Rangel<sup>1,3,\*</sup>

<sup>1</sup>Federal University of Bahia, Salvador, <sup>2</sup>Federal University of Alagoas, Maceió, <sup>3</sup>Institute of Chemistry, Federal University of Rio Grande do Sul, Porto Alegre, Brazil

**Abstract Text:** The gases from anthropogenic activities, responsible for the greenhouse effect, absorb the infrared radiation reflected by the Earth surface, causing the global warming, one of the most crucial problems faced by mankind, in last decades. Carbon dioxide is one of the main greenhouse gases, requiring its removal from the atmosphere. Among the several methods for the removal of carbon dioxide, adsorption is recognized as one of the most efficient option, being included in the used technologies. However, the development of efficient adsorbents still needs to be improved in order to increase the efficiency of the process. The combination of MCM-41 and lanthanum oxide is expected to result in a promising adsorbent, because of the large pores and the high specific surface area of MCM-41 as well as the basic character of lanthanum oxide, which results in high chemical affinity to carbon dioxide. Aiming to get efficient adsorbents for carbon dioxide capture, mesoporous MCM-41 samples modified with different amounts of lanthanum (xMCM-41; x = 5; 10; 20 and 30% La) were studied in this work. The samples were prepared by incorporating the lanthanum precursor during the synthesis of MCM-41. The adsorbents were characterized by X-ray diffraction and nitrogen adsorption/desorption and evaluated by thermoprogrammed desorption. All samples showed typical X-ray diffractograms of MCM-41 ordered mesoporous hexagonal structure, regardless lanthanum incorporation. However, different hysteresis loops were found: H1 type for pure MCM-41 and 5MCM-41 and H4 for the other solids. The samples showed narrow unimodal pore distribution curves (2-4 nm). In the case of MCM-41 and 5MCM-41 samples, 86% and 73% of the pores were in the range of 2 to 3 nm respectively. For the other samples, 42% (10MCM-41), 33% (20MCM-41) and 29% (30MCM-41) of the pores were in the range of 2 to 4 nm. Therefore, the increase of lanthanum amount led to a decrease in the quantity of mesopores, being the 30MCM-41 the least mesoporous. The average diameter of the mesopores was also increased by lanthanum. This suggests that some mesopores collapsed and/or were occupied by bulky La<sup>3+</sup> ions, explaining the decrease in specific surface area. However, the average mesoporous volume was almost not changed, indicating that some mesopores did not collapse and/or were not occupied by lanthanum. The sample with 30% La showed the highest percentage of collapsed and/or blocked pore explaining its lowest specific surface area. This probably hindered the carbon dioxide diffusion into the pores and then this sample exhibited the least adsorptive capacity for carbon dioxide. The other samples showed specific surface areas and similar adsorptive capacities, indicating that the lowest content of lanthanum (5%) is enough to obtain an efficient adsorbent for carbon dioxide. This was assigned to the generation of well dispersed active sites of lanthanum oxide for adsorption and to the large pores, allowing the diffusion of carbon dioxide molecules towards the active sites. This solid is the most promising adsorbent, with the advantage of having lower cost due to the lower lanthanum amount.

## ***Ion Exchange and Other Applications***

FEZA21-PO-177

### **A novel zeolite-based adsorbent for ciprofloxacin removal from water media**

B. Kalebic\*, J. Pavlovic, J. Dikic, A. Recnik, S. Gyergyek, N. Rajic

**Abstract Text:** A novel adsorbent based on natural zeolite-clinoptilolite and nano-oxide particles of magnetite was prepared for removal of the antibiotic ciprofloxacin (CIP) from water media. The adsorbent efficiently removes CIP for initial concentration 15-75 mg dm<sup>-3</sup> at 283-293 K at pH=5 following the Lagergren's pseudo-second-order equation. For all studied temperatures and initial concentrations more than 80% of CIP is removed within the first 10 min. The adsorption mechanism includes electrostatic interactions between negatively charged aluminosilicate lattice and cationic form of CIP accompanied by an ion-exchange reaction. The leaching test showed that less than 5% of the adsorbed CIP is desorbed during 24 h suggesting strong interactions between CIP and the adsorbent not only due to electrostatic interactions between CIP and the clinoptilolite lattice but also due to interaction of the carboxylic groups of the CIP and magnetite nano particles. It seems that magnetite coverage not only induces magnetism to the zeolite but also protects the CIP from desorption. The CIP-containing adsorbent exhibits a strong antibacterial activity towards pathogenic bacteria suggesting its applicability in a tertiary stage of a water treatment.

## ***Ion Exchange and Other Applications***

FEZA21-PO-178

### **Cerium recovery from very diluted solution using NH<sub>4</sub>-exchanged LTL zeolite**

G. Confalonieri\*, G. Vezzalini, F. Di Renzo, V. Gozzoli, R. Arletti

**Abstract Text:** Nowadays the interest in technologies to recover Rare Earth Elements (REE) from wastes is increasingly growing. Indeed, in one hand, Europe presents scarcity of natural resources for these elements, and, on the other one, this process would promote the development of circular and green economy good practices. Among the different methods to separate and recover REE from leached liquids obtained by wastes, the ionic exchange is one of the most promising. So far MOFs or ion exchangeable resins have been applied, however, efficient recycling can be achieved using other porous materials such as zeolites. Despite the well-known ion-exchange properties of these materials, just a few preliminary works investigated their application for REE separation and recycle<sup>1 2 3 4</sup>. Thus, their potential use to recover these elements from acid-leached liquors of industrial waste should be better investigated. In this work, we present a double ion-exchange experiment to recover cerium from a very diluted solution ( $[Ce^{3+}] = 0.002$  M) using a *NH<sub>4</sub>-LTL* zeolite. This concentration was chosen to test the zeolite in a very extreme condition representative of the real concentration of leached liquids obtained from spent fluid catalytic cracking (FCC) catalysts. In the first ion exchange experiment the zeolite was put in contact with the very diluted solution for 72 h at room temperature, testing different liquid/solid ratio (*i.e.* 30, 60, 90, 180, 270, 750 mL/g). The aim of this test is to define the best working conditions, meeting the industrial requirements such as low energy consumption and fast recover. ICP analysis were performed monitoring daily the cerium concentration into the solution and the obtained exchanged zeolite were fully chemically characterized. From the results obtained, the liquid/solid ratio equal to 90 mL/g shows the best compromise for the cerium ion exchange. Indeed, the 100% of cerium was recovered from the solution in the first 24 h, incorporating in LTL porosities 0.55 Ce ions p.u.c.. Once cerium is trapped into the zeolite porosities, A second ion exchange experiment, using NH<sub>4</sub> solution, was successfully performed on the Ce-exchanged samples with the aim to recover Ce for further exploiting.

**References:** 1. Mosai, A. K.; Chimuka, L.; Cukrowska, E. M.; Kotze, I. A.; Tutu, H., The Recovery of Rare Earth Elements (Rees) from Aqueous Solutions Using Natural Zeolite and Bentonite. *Water Air and Soil Pollution* 2019, 230.

2. Faghihian, H.; Amini, M. K.; Nezamzadeh, A. R., Cerium Uptake by Zeolite a Synthesized from Natural Clinoptilolite Tuffs. *JRNC* 2005, 264, 577-582.

3. Duploux, L. Preliminary Investigation of Rare Earth Elements Ion Exchange on Zeolites. University of Helsinki, Université de Lille, 2016.

4. Barros, O.; Costa, L.; Costa, F.; Lago, A.; Rocha, V.; Vipotnik, Z.; Silva, B.; Tavares, T., Recovery of Rare Earth Elements from Wastewater Towards a Circular Economy. *Molecules* 2019, 24.

## ***Ion Exchange and Other Applications***

FEZA21-PO-179

### **Generation of Brønsted acid sites by ion-exchange in 8- and 12-rings of YNU-5 zeolite**

M. Fukui<sup>1,\*</sup>, S. Suganuma<sup>1</sup>, E. Tsuji<sup>1</sup>, N. Katada<sup>1</sup>

<sup>1</sup>Center for Research on Green Sustainable Chemistry, Tottori University, Tottori, Japan

**Abstract Text:** Pore size of zeolite is classified into, in most cases, 8-, 10- and 12-rings. Zeolites with large pores and strong Brønsted acidity are demanded for catalysts activating large molecules. However, strong Brønsted acid sites tend to be found in small pores<sup>1</sup>. YNU-5 type zeolite (framework: YFI)<sup>2</sup>, which was synthesized by Nakazawa and Kubota et al., has straight channel consisting of single 8-ring, and a 2-dimensional network of twin 8-ring and 12-ring. The single 8-ring is separated from the 12-ring by a silicate wall with one atomic layer thickness. We have found strong Brønsted acid sites accessible from 12-ring on the YNU-5. In this study, change in the acidic property of YNU-5 with ion exchange was analyzed mainly from a view of locations of sites.

The YNU-5 zeolite was synthesized as previous reports<sup>2</sup>. NaOH aq., KOH aq., colloidal silica and Me<sub>2</sub>Pr<sub>2</sub>NOH were stirred in a Teflon beaker for 2 h with heating. After cooling to the ambient temperature, an FAU type zeolite was added and stirred for 10 min. This mixture was put in a Teflon-lined autoclave and maintained at 433 K for 5 days in a convection oven. After cooling to the room temperature, the solid was filtered, washed three times with de-ionized water, dried overnight at 383 K, and heated at 1.5 K min<sup>-1</sup> and calcined at 823 K for 2 h in a muffle furnace to remove OSDA (Me<sub>2</sub>Pr<sub>2</sub>NOH). The zeolite synthesis was performed twice, and the calcined Na+K-form YNU-5 samples are denoted as Na+K-YFI#1 and Na+K-YFI#2. They were ion-exchanged by stirring in NH<sub>4</sub>NO<sub>3</sub> aq. with various concentrations to adjust the NH<sub>4</sub><sup>+</sup>/Al ratio for 4 h at 343 K. After cooling to the room temperature, the obtained solid was filtered, washed three times with de-ionized water and dried overnight at 383 K. The acidic property was analyzed with an ammonia IRMS-TPD method<sup>3</sup>, where the above Na+K+NH<sub>4</sub>-YFI zeolite was pre-treated at 823 K in oxygen without exposure to the atmosphere before the measurement, and thus NH<sub>4</sub> was removed to form in-situ Na+K+H-YFI. Therefore, the YNU-5 sample was denoted as in-situ Na+K+H (x) where x shows (amount of NH<sub>4</sub> in the solution) / (amount of Al in the zeolite) employed for the ion-exchange. Repetition of the ion-exchange procedure gave the lowest Na and K contents, and the obtained sample is denoted as in-situ H-YFI.

The ammonia desorption enthalpy (*DH*) of Brønsted acid site, as an index of acid strength, was distributed over a wide range (110~160 kJ mol<sup>-1</sup>) on YNU-5 zeolites as shown in Figure 1. Hereafter we will discuss the numbers of weak (*DH* < 140 kJ mol<sup>-1</sup>) and strong (> 140 kJ mol<sup>-1</sup>) Brønsted acid sites. On the Na+K form YNU-5 (as-calcined ones), *DH* was widely distributed; the counter cations were mainly Na<sup>+</sup> and K<sup>+</sup> on these samples, while a part of ion-exchange sites which had been occupied by Me<sub>2</sub>Pr<sub>2</sub>NOH acted as acid sites after calcination. From NH<sub>4</sub>/Al = 10 to 70 %, the ion-exchange increased both of weak and strong Brønsted acid sites. From NH<sub>4</sub>/Al = 70 % to in-situ H form, the number of weak Brønsted acid sites were approximately saturated, and the strong Brønsted acid sites increased. Very strong Brønsted acid sites (*DH* > 170 kJ mol<sup>-1</sup>) was generated by the final stage of ion-exchange to form the in-situ H-YNU-5. Quantum calculations have clarified that the strong Brønsted acid sites are the protons in the single 8-ring, and the weak ones are those in 12-ring in most cases, as shown in Figure 2<sup>4</sup>. These findings indicate that the ion-exchange among Na<sup>+</sup>, K<sup>+</sup> and NH<sub>4</sub><sup>+</sup> took place preferentially in the 12-ring to form strong Brønsted acid sites, and then the cations in the single 8-ring were exchanged in high NH<sub>4</sub><sup>+</sup> concentration.

Acknowledgement: This study was partly supported by JST, CREST (JPMJCR17P1) and JSPS, KAKENHI (21H01717).

Image 1:

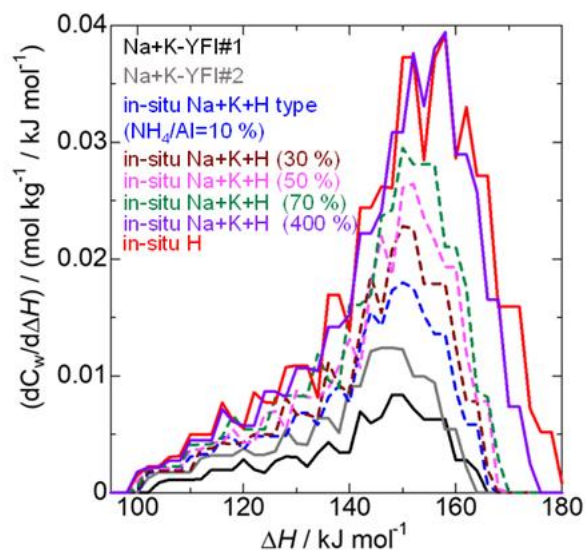


Figure 1 Observed distributions of strength ( $\Delta H$ , standard molar enthalpy of ammonia desorption) of Brønsted acid sites.

Image 2:

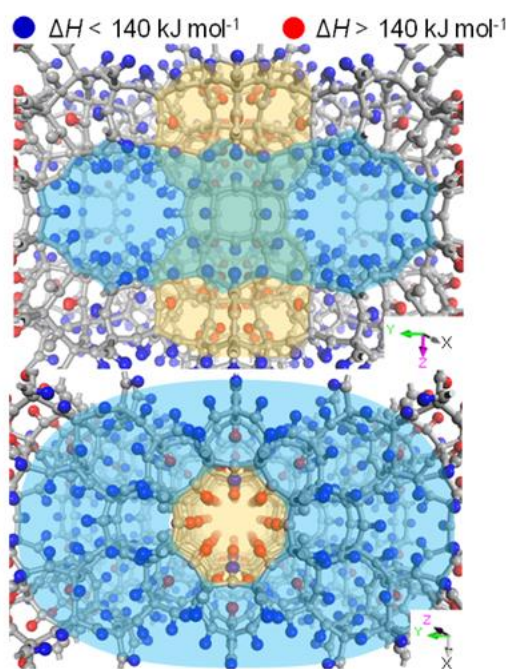


Figure 2 Calculated positions of protons showing strong (red) and weak Brønsted acidity (blue) in YFI type framework.

- References:** 1) N. Katada, *Mol. Catal.*, 458 (2018) 116.  
2) N. Nakazawa et al., *J. Am. Chem. Soc.*, 139, 7989 (2017).  
3) S. Suganuma et al., *Mol. Catal.*, 435, 110 (2017).  
4) M. Fukui et al., 36th Zeolite Research Presentation Meeting, Japan, B17 (2021).

## ***Ion Exchange and Other Applications***

FEZA21-PO-180

### **Structural evidence of perfluorooctanoic acid (PFOA) and perfluorooctane sulfonate (PFOS) adsorption from water by Y and silver-Y exchanged zeolites.**

M. Mancinelli<sup>1,\*</sup>, F. Colombo<sup>1</sup>, M. Ardit<sup>1</sup>, A. Martucci<sup>1</sup>

<sup>1</sup>Department of Physics and Earth Sciences, University of Ferrara, Via Saragat 1, I-44121, Ferrara, Italy

#### **Abstract Text:**

Perfluorooctanoic acid (PFOA) and perfluorooctane sulfonate (PFOS) are two highly representative per- and polyfluoroalkyl substances (PFAS) recognized as environmental persistent organic contaminants [1-2]. Adsorption on zeolites is a reliable alternative to eliminate these compounds from water and wastewaters because of their framework flexibility, high organic contaminant selectivity, high specific capacity, rapid kinetics, excellent resistance to chemical, biological, mechanical or thermal stress [3-4]. Ag-exchanged zeolites show unique physical, chemical, and antibacterial properties along with strong absorption property and good stability thus working synergistically in removal of PFAS from water. Consequently, a deep investigation of these materials with exceptional performances must be explored beside their effectiveness for PFAS removal. In this work, the interactions between PFOA and PFOS and Y zeolites (FAU-topology) with different SiO<sub>2</sub>/AlO<sub>2</sub> (SAR) were systematically investigated for the first time, in order to evaluate the role of hydrophobic and electrostatic forces in the interaction between polyfluoroalkyl substances and the adsorbents. A careful characterization of Y zeolites (with SAR= 30, 60 and 500, respectively) loaded with PFOA and PFOS, respectively, was carried out before and after silver functionalization in order to: i) investigate the effectiveness of synthetic Y and Ag-Y zeolites with a different SAR ratio towards PFAS, ii) characterize their structure; iii) localize the host species in the zeolites channel system, iv) investigate the thermal stability and their crystallinity degree, v) probe the interaction between PFAS molecules, water molecules, Ag ions and framework oxygen atoms. X-ray powder diffraction patterns (XRD) of the as-synthesized and Ag-loaded Y samples before and after PFAS adsorption, were collected at room temperature by using Bruker D8 Advance Diffractometer with a Sol-X detector, Cu K $\alpha$ 1,  $\alpha$ 2 radiation. Rietveld structure refinements were performed using the GSAS package with EXPGUI graphical interface in the Fd-3m space group. The zeolites crystallite sizes were achieved by both the Scherrer and Williamson-Hall approaches. TG and DTA measurements of all samples were performed in constant air flux conditions from room temperature up to 900 °C using an STA 409 PC LUX<sup>®</sup> - Netzsch (10 °C/min heating rate). After PFOS and PFOA adsorption, the selected materials maintain a high crystallinity degree. PFASs adsorption on Y and AgY samples was evidenced by differences in both the positions and intensities of the powders diffraction peaks, which are indicative of structural variations in terms of nature and concentration of the extraframework species, unit cell dimensions and framework geometry. The PFOA and PFOS adsorption was accompanied by deformations of the framework, evidenced by the value of the crystallographic free area of the zeolites channel systems. In all samples, PFOA and PFOS molecules were localized at the centre of Y-supercage, thus assuming six different orientations. The bond distances indicated strong interactions mediated via water molecules between zeolite framework and PFASs reactive carboxylic and sulfonyl functional groups. The structure refinements gave an extraframework content corresponding to ~7.0 and 14% wt. of PFOA and PFOS, respectively, in good agreement with the weight loss given by the thermogravimetric analyses. Our results highlighted that Ag-exchanged zeolites with high SAR were the most efficient adsorbents thus representing selective tools for PFOS and PFOA abatement as environmentally friendly, bactericidal and low-cost materials.

**References:** [1] Sinclair, G.M., Long, S.M., Jones, O.A.H. (2020). What are the effects of PFAS exposure at environmentally relevant concentrations? *Chemosphere*, 258, 127-340

[2] Pan, C., Liu, Y., and Ying, G. (2016). Perfluoroalkyl substances (PFASs) in wastewater treatment plants and drinking water treatment plants: removal efficiency and exposure risk. *Water Research*. 106, 562-570.

[3] Gagliano, E., Sgroi, M., Falciglia, P.P., Vagliasindi, F.G.A., Roccaro, P. (2020). Removal of poly- and perfluoroalkyl substances (PFAS) from water by adsorption: Role of PFAS chain length, effect of organic matter and challenges in adsorbent regeneration. *Water Res.* 171, 115-381.

[4] Mingshu, L., Yujie, R., Ji, W., Yuanhui, W., Jieyu, C., Xinrong, L. and Xiaoyan, Z. (2020). Effect of cations on the structure, physico-chemical properties and photocatalytic behaviors of silver-doped zeolite Y. *Microporous and Mesoporous Materials*, 293, 109-800.

## ***Ion Exchange and Other Applications / Zeolites / Inorganic materials***

FEZA21-PO-182

### **Capacity of the natural zeolite material clinoptilolite for strontium and caesium**

V. Grill<sup>1,\*</sup>, J. M. Welch<sup>2</sup>, C. Strelt<sup>2</sup>, J. H. Sterba<sup>2</sup>

<sup>1</sup>Radiation Protection and Radiochemistry, AGES, <sup>2</sup>Atominstytut, TU Wien, Vienna, Austria

**Abstract Text:** The zeolite clinoptilolite can be used to remove caesium and strontium radioisotopes from aqueous nuclear wastes.

In previous work, the adsorption capacity of four different zeolite products (LithoFill 100 "T", LithoFill 100, LithoGran 2 and "Extern I" designated A, B, C and D, respectively) from the Austrian company LITHOS Industrial Minerals GmbH was investigated [1]. To better understand and compare the information gathered, detailed knowledge of the composition and structure of the zeolites used is essential. This characterisation was achieved by applying several different quantitative and qualitative analytical methods [2]. The knowledge of the elemental composition was used to design an experiment to determine the maximal capacity of the materials for caesium and strontium ions using the radiotracers <sup>134</sup>Cs and <sup>85</sup>Sr.

#### Capacity Analysis with Radiotracers Dilution Experiment

Dilution experiments utilising radiotracers are a simple and effective tool for the study of ion-exchange capacity and to acquire information about the nature of ion-exchange processes. Such experiments utilise the simple proportionality between readily measurable tracer activity and analyte concentration to assess the distribution of material between two phases. Radiotracers are readily applicable to dilution studies and can be easily produced (e.g. by neutron capture in a nuclear reactor) and detected (e.g. by  $\gamma$ -spectroscopy if their decay is associated with a gamma emission).

The strontium or caesium capacity of the zeolite samples were of interest. Both Sr and Cs are available as readily soluble nitrate salts Sr(NO<sub>3</sub>)<sub>2</sub> and CsNO<sub>3</sub>. For a dilution experiment typically, a suitable tracer is prepared, tracer-containing analyte solutions are created, and the solutions are then applied to the material under study followed by homogenisation. The phases are subsequently separated, the radionuclide distribution quantified and the resulting data analysed (Fig. 1). Two different stock solutions were prepared for the Sr and for the Cs capacity experiment. The second stock solution had a concentration ten-fold higher than the first one.

The results are summarized in Tab. 1. For strontium, an uptake limit of 13 mg Sr per 500 mg zeolite powder was found for samples A and B. For caesium, sample B has a slightly higher capacity with 82 mg Cs per 500 mg zeolite than sample A. The milled version of sample C (C\_2) has an even larger capacity. It was shown that the grain size is important for the ion adsorption [3]. The external sample D has the lowest capacity for Sr and Cs as expected from previous studies [1].

#### Acknowledgements

Open access funding provided by TU Wien and AGES. The authors want to thank LITHOS Industrial Minerals GmbH for the provision of the samples. We also want to express our thanks to our lab assistant Michaela Foster for her general support in the radiochemistry laboratory.

**Image 1:**

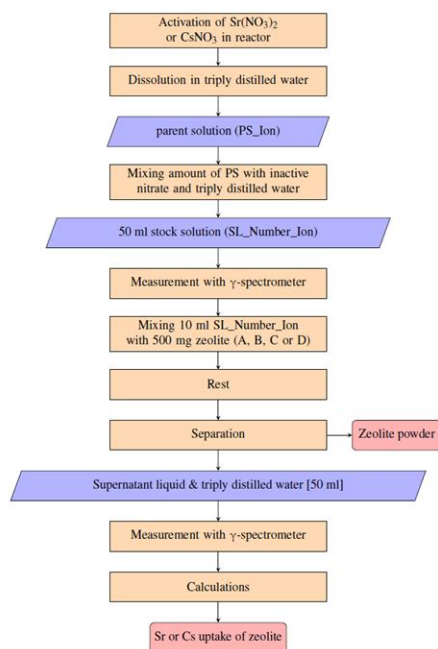


Fig. 1 Flow chart describing the experimental procedure for capacity determination. Two different stock solutions (Number = 1, 2) for each radiotracer (Ion = Sr, Cs) were prepared (labelled "SL\_Number\_Ion"). The second stock solution had a ten-fold higher concentration than the first stock solution.

## Image 2:

Tab. 1 Uptake of Sr or Cs for stock solution 1 and stock solution 2

Sample_solution	Sr Uptake in mg	$\sigma$	Cs Uptake in mg	$\sigma$
A_1	13.39	1.71	47.55	0.79
B_1	13.41	1.71	59.36	0.73
C_1	12.97	1.73	56.35	0.76
D_1	7.03	2.02	26.62	0.94
A_2	33.14	22.73	69.53	8.93
B_2	39.25	22.43	82.10	8.89
C_2	16.42	23.57	83.91	8.83
D_2	12.48	23.76	52.07	8.85

- References:** [1] Sterba JH, Sperrer H, Wallenko F, Welch JM (2018) Adsorption characteristics of a clinoptilolite-rich zeolite compound for Sr and Cs. *Journal of Radioanalytical and Nuclear Chemistry* 318:267–270
- [2] Grill V (2019) Characterization of Natural Clinoptilolite Material for Remediation of Sr-90 and Cs-137 in Seawater. TU Wien
- [3] He Q, Walling DE (1996) Interpreting Particle Size Effects in the Adsorption of <sup>137</sup>Cs and Unsupported <sup>210</sup>Pb by Mineral Soils and Sediments. *J Environ Radioactivity* 30, No. 2:117–137

***Ion Exchange and Other Applications / Zeolites / Inorganic materials***

FEZA21-PO-183

**Metal removal process optimization of zeolites obtained from fly ash and its characterization**

L. Martinez Maldonado<sup>1,\*</sup>, F. Trejo Zarraga<sup>1</sup>, G. Peña Rodriguez<sup>2</sup>

<sup>1</sup>Centro de Investigación en Ciencia Aplicada y Tecnología Avanzada, Instituto Politécnico Nacional, Ciudad de Mexico, Mexico, <sup>2</sup>Grupo de Investigación en investigación y física de la materia condensada, Universidad Francisco de Paula Santander, Cucuta, Colombia

**Abstract Text:** Zeolites were synthesized from coal combustion fly ashes through hydrothermal synthesis varying temperature and using sodium hydroxide at two different molar concentrations. Removal efficiency of As, Cr, Pb, Cd, Ni, Hg and Cu in contaminated water was evaluated using two concentration of zeolites and the full factorial experiment design was used to find the optimal conditions for synthesizing the material with the highest metal removal. Optimal synthesis conditions were NaOH 1.5 M and  $150 \pm 5$  °C using 0.6 g of material to obtain mainly zeolite P. Conversion of fly ash to zeolite was 71.1% with a correlation coefficient of 0.98. At these conditions, efficiency of metal removal was 79% having the highest elimination for As, Hg, Cr, Pb, Cd and Cu. Zeolite was characterized by XRD, SEM, XRF, XPS and FTIR and it was stated that metal removal was carried out by ion exchanging.

## ***Ion Exchange and Other Applications / Zeolites / Inorganic materials***

FEZA21-PO-186

### **Ag-zeolites as bactericidal agent for polymers**

J. L. Cerrillo Olmo<sup>1,2,\*</sup>, A. E. Palomares Gimeno<sup>2</sup>, F. Rey Garcia<sup>2</sup>

<sup>1</sup>KAUST Catalysis Center, King Abdullah University Science and Technology, Thuwal, Saudi Arabia, <sup>2</sup>Instituto de Tecnología Química de Valencia, Instituto de Tecnología Química de Valencia - Universitat Politècnica de València (UPV-CSIC), Valencia, Spain

**Abstract Text:** Healthcare-Associated Infections (HAIs) are some of the most common infections in hospital care units, producing 37000 deaths per year just in Europe [1]. This problem is mostly related to microorganism contamination on the surface of medical devices. The incorporation of biocide properties in materials such as polymers is a crucial strategy to overcome this problem [2]. Silver is one of the most recognized and used antimicrobial substance, although its biocide effects are short in time. Several studies reported that in order to prolong the biocide activity, incorporating silver in carrier materials is a promising option [3,4]. In this work we studied zeolites as a carrier material for Ag not only due to their ion-exchange properties but also, due to their physical and chemical stability that permit the incorporation of these Ag-zeolites in other materials. Therefore, this work focuses on the biocidal activity of Ag-zeolites with different topologies and Si/Al ratio under both in vitro and realistic conditions against two bacteria. Furthermore, lixiviation and physico-chemical properties of the Ag-zeolites are studied.

LTA and FAU zeolites were ion-exchanged with AgNO<sub>3</sub> solutions for 16 hours at 298 K in darkness [4]. Afterwards, the Ag-zeolite was recovered by filtration and dried at 353 K, providing Ag-zeolites with approximately 2 wt% of Ag loading. XRD, FESEM-EDS, ICP-OES, TPR or GFAAS were used to characterize the prepared Ag-zeolites. The Ag-zeolites were evaluated as biocidal materials against *S.aureus* and *E.coli* as Gram(-) and Gram(+) bacteria in Tryptic Soy Broth (TSB) at *in vitro* experiments (MIC values). Finally, the best performing Ag-zeolites were incorporated in a polypropylene matrix and flat plates were prepared to study the biocidal activity using ISO-standard 22196:2011.

Chemical composition of Ag-zeolites was studied by both ICP-OES and FESEM-EDS techniques. The Ag amount in each zeolite was as expected and both techniques revealed similar results, indicating a homogeneous dispersion of Ag on the zeolites. The zeolite morphology remained unchanged after the incorporation of Ag. These outcomes demonstrate that Ag-exchange method is adequate and a proper for obtaining homogeneous and stable Ag-zeolites. XRD did not show any peak related to Ag(0) or Ag<sub>2</sub>O indicating that Ag is presented in its cationic form. Moreover, UV-Vis analysis only present bands related to Ag<sup>+</sup>, corroborating the previous deduction.

Regarding in vitro experiments (**Fig.1**), FAU with a Si/Al ratio of 2.4 presents the best biocidal effects against both bacteria. The more open framework of FAU (12-MR) compared with LTA (8-MR) seems to improve the bactericidal activity, probably due to an easy release of Ag<sup>+</sup>. Comparing same zeolitic structures but with diverse Si/Al ratio, the best results are obtained with zeolites with Si/Al ratio close to 2. These results are probably related to the relative position of Ag<sup>+</sup> when the Si/Al ratio is close to 2, which probably improves the release of Ag<sup>+</sup> to the media. To corroborate these suppositions, lixiviation studies were performed demonstrating that the FAU sample releases higher amounts of Ag than LTA and the zeolites with Si/Al ratios of 2 lixiviate more Ag to the media, thus presenting better biocidal activity.

Finally, different polymeric plates were synthesized mixing polypropylene and different amounts of Ag-zeolites with optimal Si/Al ratio. The best results were obtained with FAU zeolite, being consistent with in vitro tests. However, some visual modifications (darkening) were observed when Ag-zeolites were incorporated, probably due to the presence of reduced silver species during the preparation of the polymeric plates. To solve this problem, some photo-stabilizing substances (HALS) were incorporated into the functionalized polymer. This new formulation solved the darkening problem (**Fig.2**) without affecting the polymer properties and obtaining better bactericide activity when HALS was incorporated.

Image 1:

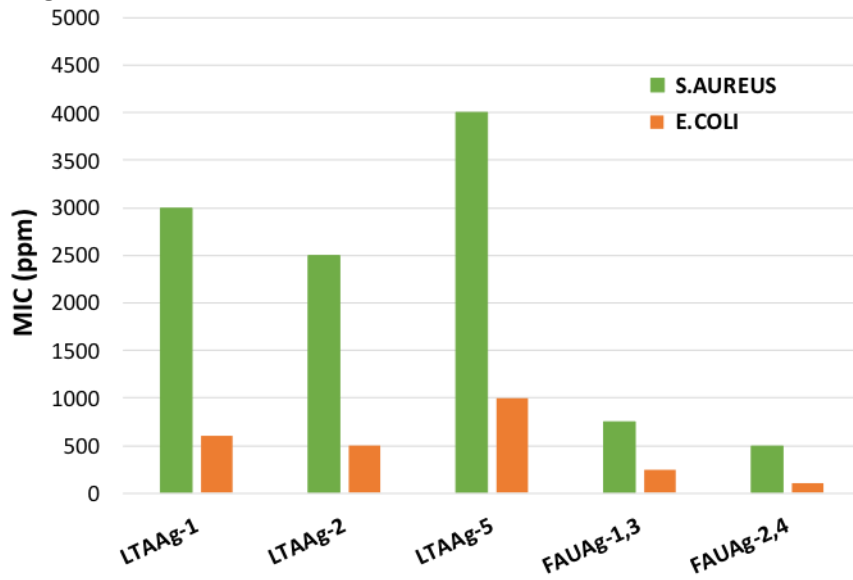
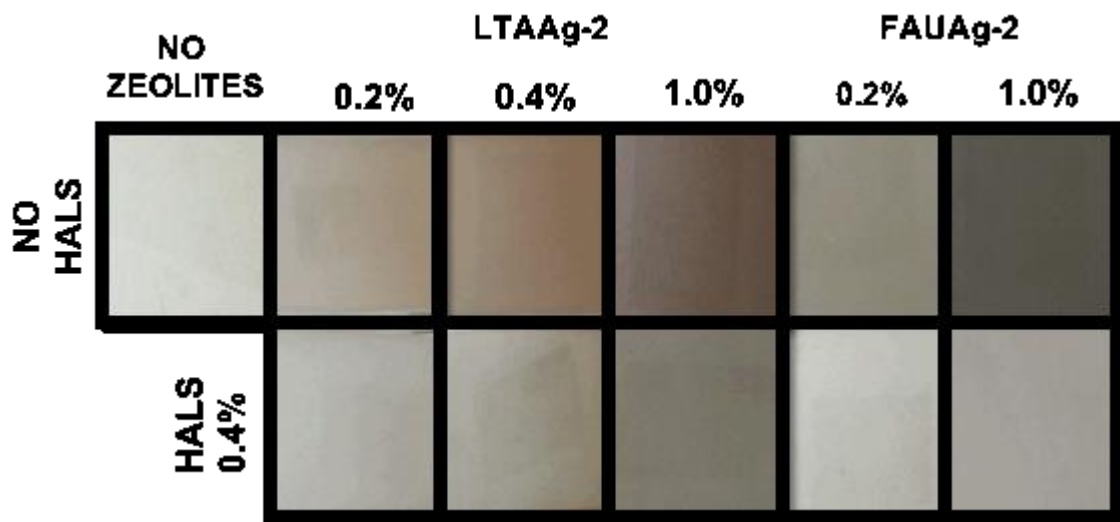


Image 2:



References: [1] Annual Epidem. Report on Communicable diseases in Europe, Stockholm (2008).

[2] S. Chen, J. Popovich N. Iannuzo, S. Haydel, D. Seo, Applied Materials Interfaces, 9 (2017) 39271

[3] P. Lalueza, M. Monzon, M. Arruebo, J. Santamaria, Mater. Res. Bull., 46 (2011) 2070

[4] J. Cerrillo, A. Palomares, F. Rey, S. Valencia, L. Palou, M.B. Pérez-Gago, Microporous and Mesoporous Materials, 254 (2017) 69

## ***Ion Exchange and Other Applications / Zeolites / Inorganic materials***

FEZA21-PO-187

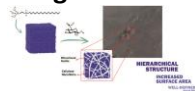
### **Macro-meso-microporous materials formed by hierarchical zeolite A impregnation in Bacterial cellulose aerogels**

R. A. Bessa<sup>1,2,\*</sup>, A. L. S. Pereira<sup>2</sup>, M. Perez-Page<sup>3</sup>, S. Holmes<sup>3</sup>, M. F. Rosa<sup>4</sup>, A. R. Loiola<sup>2</sup>, M. W. Anderson<sup>1</sup>

<sup>1</sup>Chemistry, University of Manchester, Manchester, United Kingdom, <sup>2</sup>Organic and Inorganic Chemistry, Federal University of Ceará, Fortaleza, Brazil, <sup>3</sup>Chemical Engineering and Analytical Science, University of Manchester, Manchester, United Kingdom, <sup>4</sup>Chemistry, Brazilian Agricultural Research Corporation, Fortaleza, Brazil

**Abstract Text:** In the last decade a remarkable increase of around 200% in hierarchization-related publications has been observed. Among the materials with a great impact to this characteristic, zeolites can be highlighted due to the huge industrial interest. Their chemical and physical properties (such as ionic exchange capacity, molecular sieving characteristic and acid sites for catalysis) are hindered by separation processes in a post-application step or even for problems related to mass transfer in single bed experiments.[1, 2] Many approaches can be used to obtain zeolites in a bottom-up method with a hierarchical structure, where beyond the zeolite micropores, mesopores are formed using a single molecule. Organosilanes can be used for a variety of zeolite structures resulting in pure phases containing both types of pore systems to a good extent.[3] Although several works report the advantages in using them to catalytic processes, they are also very promising in other applications where zeolites are largely used, as in adsorption.[4] The aim of this work is to evaluate preliminarily the synthesis of a novel material composed of bacterial cellulose, which accounts for macroporosity and acts as a support to a bimodal hierarchical zeolite A (LTA) prepared via a bottom-up approach. Hierarchical zeolite A was synthesized using the organosilane surfactant [(3-trimethoxysilyl)propyl] octadecyldimethyl-ammonium chloride-TPOAC, as described by Cho *et al.*, 2009 [5]; Bacterial cellulose (BC) suspensions were obtained from pellicles, oxidized and homogenized in a suspension. Composite cartridges were prepared by mixing 1.0 wt% of zeolite to this BC suspension, frozen with liquid N<sub>2</sub> and freeze-dried. The XRD shows zeolite A as the main phase, with suitable crystallinity, highlighting the role of TPOAC for hierarchical zeolite synthesis. As shown in the SEM, crystals have the same morphology as conventional zeolite A, with cubic habit having ca. 2 μm diameter. The most prominent characteristic is that the particles are composed of numerous domains of interconnected nanocrystals and the particle outline is more rounded than a conventional one. These characteristics are desirable towards the following step of cartridge formation as the presence of those spaces on the structure promotes a better interaction with the cellulosic matrix. In the composite cartridges, the zeolite crystals are mostly dispersed throughout cellulose sheets, which are formed by nanofibrils with big interconnected voids among them, forming a hierarchical material with 3 pore systems. Although some agglomeration can be seen, it appears as a minor effect, since it is not causing compaction or other problems related to mass transfer. The N<sub>2</sub> adsorption/desorption isotherms show both zeolite A and cellulose with low surface area (8 and 20 m<sup>2</sup> g<sup>-1</sup>, respectively, as expected for the used conditions). When the bimodal zeolite is added to the BC, a higher surface area is observed, ca. 38 m<sup>2</sup> g<sup>-1</sup>, and a hysteresis type IVa to the isotherm, characteristic of meso+macroporous materials. Thus, we have evidence of the effective interaction between the zeolite A and the bacterial cellulose, even with some agglomeration points, and the formation of the desired hierarchy with the 3 pore types. Ionic exchange experiments indicate lower exchange capacity for Ca<sup>2+</sup> for the hierarchical sample, compared to the conventional synthesis, since there is a lower cations number stabilizing the zeolite structure. Even though, around 80% removal is observed and this capacity is maintained to the composite. In summary, hierarchical zeolite A was successfully obtained via a bottom-up approach using TPOAC as surfactant and the product presented a cubic aspect formed by connected nanocrystals. When added to the cellulose, an interconnected 3-pore system is formed, being like this, a hierarchical porous material.

#### **Image 1:**



**References:** [1] Cychosz KA, Guillet-Nicolas R, Garcia-Martinez J, Thommes M. Chem Soc Rev 2017; 46, 389.  
[2] Wei Y, Parmentier TE, de Jong KP, Zecevic J. Chem Soc Rev 2015; 44, 7234.

[3] Verboekend D, Nuttens N, Locus R, Van Allstate J, Verolme P, Groen, Perez-Ramirez J, Selsa BF. Chem Soc Rev 2016; 45, 3331.

[4] Hartmann M, Machoke AG, Schwieger W. Chem Soc Rev 2016; 45 3313

[5] Cho K, Cho HS, de Menorval L-C, Ryoo R. Chem Mater 2009; 21, 5664.

## ***Ion Exchange and Other Applications / Zeolites / Inorganic materials***

FEZA21-PO-190

### **The direct alkylation of benzene with methane over Co-ZSM-5**

M. Aigner<sup>1,\*</sup>, S. van Daele<sup>2</sup>, M. Sanchez-Sanchez<sup>1</sup>, J. A. Lercher<sup>1</sup>

<sup>1</sup>Chemistry, Technical University Munich, Garching bei München, Germany, <sup>2</sup>Total Research and Technology Feluy (TRTF), Feluy, Belgium

#### **Abstract Text:**

##### **Introduction**

A major byproduct of conventional petrochemical-based plants are methane rich streams which are not commonly valorized. Due to environmental concerns, novel strategies to integrate methane into the crude oil are highly desired. In this work, we study the non-oxidative alkylation of benzene with methane as a model reaction for the direct methylation of aromatics. An outstanding activity was reported for Co-loaded ZSM-5 [1]; however, a fundamental understanding of the prevailing reaction mechanism(s) is lacking. Here, we combine thorough sample characterization with catalytic evaluation to screen the impact of catalyst properties on activity and product selectivity.

##### **Materials and methods**

In this study, H-ZSM-5 (Si/Al=15) was exchanged with 0.0025 - 0.01 M cobalt acetate solution. The catalysts were characterized by *in-situ* IR spectroscopy, solid state <sup>27</sup>Al NMR, X-ray absorption spectroscopy, atomic absorption spectroscopy, UV-Vis spectroscopy, and thermal gravimetric analysis with differential scanning calorimetry.

##### **Results and discussion**

Image 1 shows that the normalized toluene formation rate per Co increases for ion exchanged Co-ZSM-5 catalysts with increasing Co loading. This points to a change of the Co speciation at high Co loadings, leading to the formation of a higher fraction of active sites at Co contents above 200  $\mu\text{mol}_{\text{Co}} \text{g}_{\text{cat}}^{-1}$ . Quantification of the Brønsted acidity after Co loading suggests that one  $\text{Co}^{2+}$  compensates for the negative charges of an Al pair. However, at high Co loadings we observe a ratio of covered BAS per Co slightly lower than 2, indicative of an increasing fraction of Co forming sites with a different structure. In comparison, samples prepared by impregnation showed very low rates per Co site, indicating the formation of inactive Co particles.

Based on the product distribution obtained in catalytic tests and tests performed feeding reaction intermediates, we propose a reaction network for benzene methylation with methane on Co-ZSM-5 (Image 2). Secondary reactions lead to the formation of xylenes and higher alkylated products. The main byproduct, biphenyl, is formed directly from benzene in a parallel route. Competition of benzene methylation and biphenyl formation for the active Co sites drives the selectivity of the process.

Image 1:

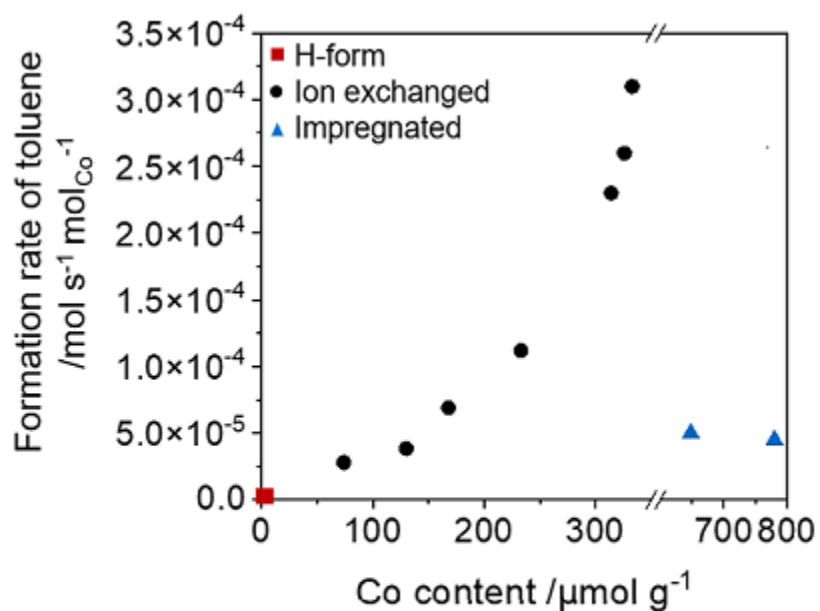


Image 1: Formation rate of toluene per Co in dependency of the Co content in the alkylation of benzene with methane. Reaction at 550 °C and 1 atm, WHSV = 0.6 h<sup>-1</sup>, methane:benzene = 80.

Image 2:

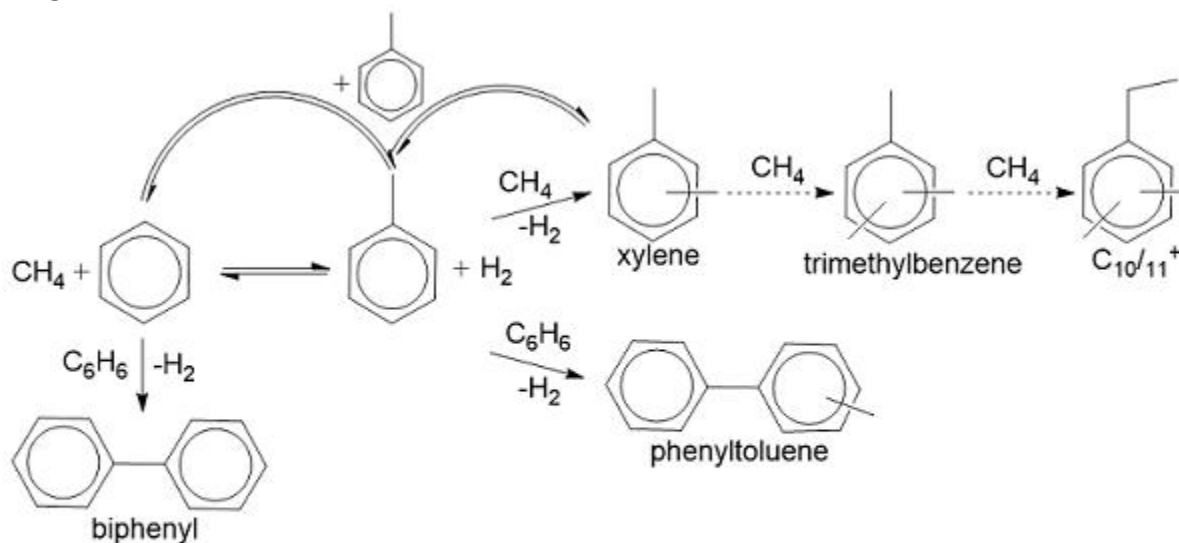


Image 2: Reaction network of benzene with methane over Co-ZSM-5. Minority routes are displayed with dashed arrows.

**References:** [1] K. Nakamura, A. Okuda, K. Ohta, H. Matsubara, K. Okumura, K. Yamamoto, R. Itagaki, S. Suganuma, E. Tsuji, N. Katada, ChemCatChem 2018, 10, 3806-3812.

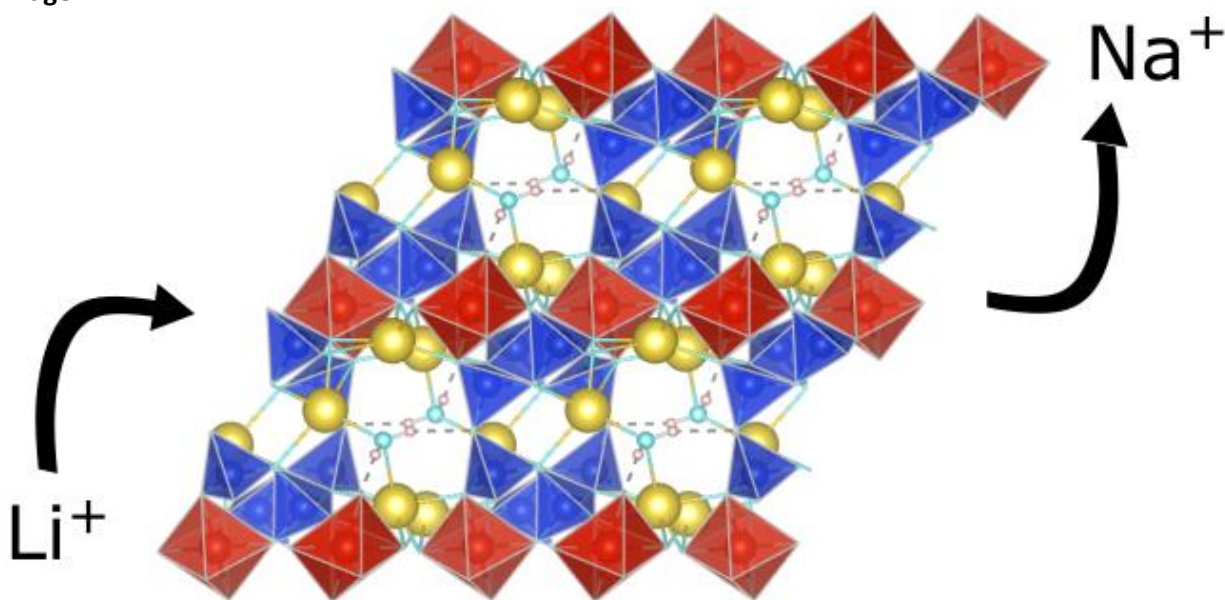
**Dehydration and lithium ion-exchange of the open framework vanadium silicate VSH-16Na**

R. M. Danisi<sup>1,\*</sup>, F. Schilling<sup>1</sup>

<sup>1</sup>Institute of Applied Geosciences, Karlsruhe Institute of Technology, Karlsruhe, Germany

**Abstract Text:** Microporous VSH-16Na of  $\text{Na}_3\text{V}(\text{Si}_4\text{O}_{11})\cdot\text{H}_2\text{O}$  composition was synthesized under mild hydrothermal conditions and studied by single-crystal X-ray diffraction. Its vanadosilicate framework contains unbranched silicate double chains along the [100] direction connected by  $[\text{V}^{3+}\text{O}_6]$  octahedra to form an open framework structure with eight-membered ring channels. The compound is triclinic with space group  $P-1$ , however the framework topology suggests higher symmetry reduced by the arrangement of the extraframework components. After removal of the  $\text{H}_2\text{O}$  molecule at 733 K, the anhydrous structure adopted monoclinic symmetry (space group  $C2/c$ ) with  $a = 15.9201(13)$   $b = 8.7274(7)$   $c = 7.4821(6)$   $\beta = 95.909(3)^\circ$ ,  $V = 1034.05(14)$   $\text{\AA}^3$ . The dehydration is irreversible due to the adjustment of the Na positions upon removal of the  $\text{H}_2\text{O}$  molecule. In particular, the Na2 site displays positional disorder at two sub-sites, ca. 1.7  $\text{\AA}$  apart. After  $\text{Li}^+$  ion exchange, the resulting structure with unit-cell parameters  $a = 16.638(5)$   $b = 8.028(3)$   $c = 7.382(2)$   $\beta = 90.183(8)^\circ$ ,  $V = 986.0(6)$   $\text{\AA}^3$  (space group  $C2/c$ ) closely simulates orthorhombic symmetry. Although the substitution of  $\text{Na}^+$  by  $\text{Li}^+$  was accompanied by hydration, the unit-cell volume decreased by  $\sim 5\%$  compared to the dehydrated Na-bearing framework. The Li-exchanged structure is apparently alkali-deficient; however, we infer the presence of hydronium  $\text{H}_3\text{O}^+$  ions at the OWa sites to counterbalance the deficit of positive charge. Framework distortions upon Li-exchange and hydration adjust the effective pore size and micropore volume. Based on the X-ray diffraction data, we suggest the following Li-exchange mechanism with electroneutrality maintained throughout the process:  $3\text{Na}^+ + \text{H}_2\text{O} \rightarrow 2\text{Li}^+ + (\text{H}_3\text{O})^+ + \text{H}_2\text{O}$  [1].

**Image 1:**



**References:** [1] R.M. Danisi, F.R. Schilling, Dehydration and lithium ion-exchange of the open framework vanadium silicate VSH-16Na, *Microporous Mesoporous Mater.* (2021) 111064. <https://doi.org/https://doi.org/10.1016/j.micromeso.2021.111064>.

**Conversion of Alum Sludge and Waste Glass into Zeolite LTA for Municipal Water Softening**

A. Rozhkovskaya\*, J. Rajapakse, G. J. Millar

**Abstract Text:** Sodium exchanged low silica zeolite LTA, is one of the most widely used synthetic zeolites today. Commercially, the major market is water softening due to high cation exchange capacity and particular selectivity towards calcium ion [1]. Currently, zeolite LTA is produced from reagents such as sodium metasilicate and sodium aluminate. However, the process is not environmentally friendly and generates chemical wastes [2, 3]. The worldwide increase in zeolite LTA consumption makes it important to find alternative low-cost raw materials for synthesis to replace expensive commercial chemicals and to improve the technological process [4].

A large volume of studies has been published, investigating various solid residues with similar to zeolite chemical composition [1]. However, using abundant and widely available wastes, such as Alum Sludge (or water treatment sludge) and Waste Glass as sources of alumina and silica for zeolite production is of particular advantage due to produced material can be used locally at water treatment plant reducing both raw water hardness and water treatment costs.

This study optimized a synthesis of high quality zeolite LTA from alum sludge and waste glass, addressed the process engineering issues associated with manufacturing and examined ion-exchange performance of the material as softening effectiveness for naturally hard river water.

Dewatered alum sludge (AS) was collected from the Mount Crosby West Bank water treatment plant, Queensland, Australia. Waste glass was separated from municipal solid wastes produced in Queensland. Zeolite LTA was made via alkaline fusion pre-activation of alum sludge and waste glass at 700°C for 2 h; followed by hydrothermal treatment at 80°C for 5 hours. Despite similar values of crystallinity of around 80%, increase in SiO<sub>2</sub>/Al<sub>2</sub>O<sub>3</sub> ratio of the feed mixture from 1 to 2.3 doubled the yield of zeolite LTA to 67% (Image 1). Thus, yield has to be taken into account when making synthetic zeolites from wastes, as consideration of only the crystalline content might be misleading. Consequently, a feed mixture of composition 9.2Na<sub>2</sub>O:Al<sub>2</sub>O<sub>3</sub>:2.3SiO<sub>2</sub>:276H<sub>2</sub>O was adopted for subsequent tests. Once synthesis was optimized, the performance of zeolite LTA made from waste materials as a water softener was studied using pure calcium chloride solution and simulated hard river water of similar calcium concentration (*ca.* 99 mg Ca<sup>2+</sup>/L). Equilibrium isotherm studies were conducted using the constant concentration method as this has been demonstrated to be more precise compared to the constant sorbent mass approach [5]. Equilibrium isotherm profiles for both the simple calcium chloride solution and river water were compared (Image 2). It was found that calcium uptake on zeolite LTA was reduced by 10% when treating simulated river water (65.5 mg Ca<sup>2+</sup>/g) due to competitive ion-exchange. Further investigation of removal efficiencies of competing ions revealed that magnesium and potassium ions were also removed from the river water and the selectivity series was K<sup>+</sup> < Mg<sup>2+</sup> < Ca<sup>2+</sup>. Regeneration of calcium loaded zeolite LTA was also studied in four loading/regeneration cycles. It was demonstrated that a NaCl solution with a molarity of at least 2M and a dose of 200 mL/g was required for complete calcium recovery. However, upon multiple loading/regeneration cycles the degree of softening eventually diminished which suggested an improved regeneration procedure may be considered.

Overall, these results suggest that alum sludge produced by drinking water treatment plants along with waste glass could be successfully converted into high quality zeolite LTA for efficient water softening. The outlined technology proposed a feasible and scalable approach to recycling of wastes, producing a commodity, which could be successfully used locally by the water treatment plant as a water softener. Thus, providing significant environmental and economic benefits for the water treatment industry.

**Image 1:**

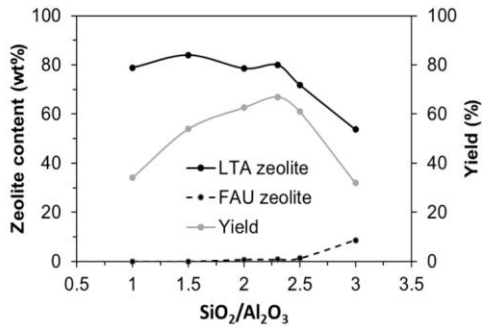
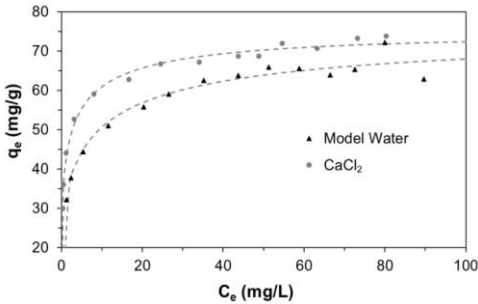


Image 2:



**References: 1.**

1. Collins, F., et al., A critical review of waste resources, synthesis, and applications for Zeolite LTA. *Microporous and Mesoporous Materials*, 2020. 291: p. 109667.
2. Zhang, X., et al., Studies on room-temperature synthesis of zeolite NaA. *Materials Research Bulletin*, 2014. 52: p. 96-102.
3. Qian, T. and J. Li, Synthesis of Na-A zeolite from coal gangue with the in-situ crystallization technique. *Advanced Powder Technology*, 2015. 26(1): p. 98-104.
4. Shoumkova, A. and V. Stoyanova, SEM–EDX and XRD characterization of zeolite NaA, synthesized from rice husk and aluminium scrap by different procedures for preparation of the initial hydrogel. *Journal of Porous Materials*, 2012. 20(1): p. 249-255.
5. Millar, G.J., S.J. Couperthwaite, and C.W. Leung, An examination of isotherm generation: Impact of bottle-point method upon potassium ion exchange with strong acid cation resin. *Separation and Purification Technology*, 2015. 141: p. 366-377.

**Role of aluminium in interzeolite conversion synthesised MFI and CHA: towards generic principles of acid site genesis and distributions [1]**

J. Devos<sup>1</sup>, S. Robijns<sup>1,\*</sup>, I. Khalil<sup>1</sup>, M. Dusselier<sup>1</sup>

<sup>1</sup>Center for Sustainable Catalysis and Engineering (CSCE), KU Leuven, Leuven, Belgium

**Abstract Text:** *Little is known on the genesis of acid sites and their origin during hydrothermal zeolite synthesis. More and more recent findings suggest that zeolite catalysts are influenced by synergistic effects derived from acid site proximity, in particular, or Al distribution, in general.*

*In this work, for the first time, we uncover some generic synthesis factors and mechanisms key to the output acid site distribution. An extensive study of five crystallization systems yielding ZSM-5 (MFI) and SSZ-13 (CHA) was performed, focusing on interzeolite conversion (IZC) strategies. Aluminum was identified as key component during all aspects of synthesis: (FAU) dissolution, nucleation, assembly and maturation.*

## **INTRODUCTION**

Acid site distributions tuned by the underlying synthesis are, since recently, explored by the zeolite catalysis community.<sup>[1-3]</sup> Nonetheless, a rational understanding of the creation of acid site arrangements during synthesis is lacking due to the complex nature of the crystallization process, the numerous possible proximate Al and acid sites (even in the symmetric CHA framework<sup>[4]</sup>), and the lack of systematic and comparable syntheses. During a single-parameter IZC investigation within one SDA-zeolite system ([TMAda]), we linked the synthesis output (CHA, Si/Al = 40) to reaction performance of a Fe-CHA redox system (methane partial oxidation), hence, demonstrating the application of the divalent cation capacity (DCC) probe used as structural proxy for local acid duo's (pairs) and highlighting the importance of synthesis time to stir the latter.<sup>[2]</sup>

Here, we try to identify key synthesis variables and mechanisms with a pivotal role on the genesis of acid site distributions during synthesis, using DCC as structural parameter for acid site (and Al) proximity, in line with the earlier work.<sup>[2]</sup> The latter is done for at least five SDA-zeolite system (mainly IZC based).

## **EXPERIMENTAL**

High silica SSZ-13 (CHA) and ZSM-5 (MFI) materials were synthesized using IZC protocols (from FAU, Si/Al = 40). The investigated SDA-zeolite systems were synthesized at equimolar compositions yielding CHA ([TMAda] & [TMAda;Na]) or MFI ([TPA] & [TPA;Na]) at constant charge density (Na+OSDA/Al). The synthesis output is investigated in time and the material output is characterized via elemental analysis, P-XRD, DR-UV-VIS, N<sub>2</sub>-physisorption, (D)TGA, TEM-EDX and (Pyridine) FT-IR. The synthesis series were also subjected to aqueous Co<sup>II</sup>-exchange of the calcined zeolite (cfr. ref [3]) to probe DCC.

## **RESULTS AND DISCUSSION**

Interzeolite conversion (IZC)<sup>[5]</sup> propels fast nucleation (~1 hour after heating) in any SDA-zeolite system at the investigated conditions, which is multiple times faster than its amorphous counterparts. Most SDA-zeolite systems crystallize extremely fast (after nucleation) and are defined as Al-“loving” crystallizing environments. One notable exception had much slower assembly than amorphous counterparts (Al-averse [TPA], Image 1). These findings allow us to build a model for IZC, stressing the pivotal role of Al. By analyzing divalent cation capacity (DCC) in the investigated SDA-zeolite system, remarkable system-specific acid site mobility was found thorough the crystallization processes (Image 2), hereby stressing the importance of SDA-zeolite flexibility and synthesis time (maturation).

## CONCLUSION

Based on the distinct crystallization behaviors of the various investigated SDA-zeolite systems and the direct probing of local Al (acid sites) via DCC analysis, this study yielded new insights regarding the importance of charge balancing during zeolite assembly, the pivotal (generic) role of Al during IZC (Image 1, blue), the importance of prolonged synthesis on acid site distributions (Image 1, pink) and some key insights on the genesis (and evolution) on acid site arrangements during synthesis (Image 2).

Image 1:

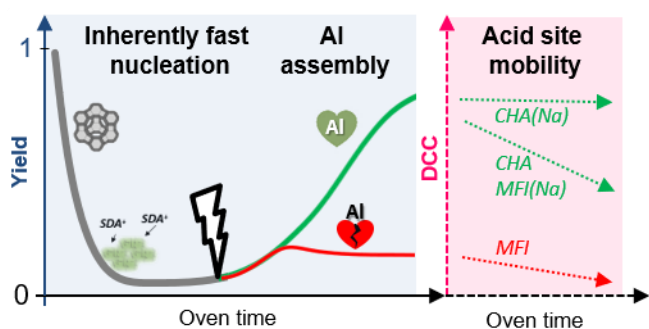
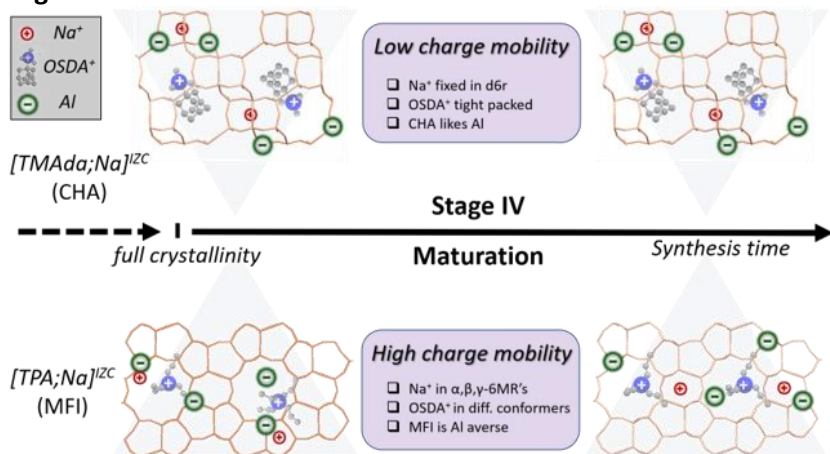


Image 2:



**References:** [1] Devos et al., (2021). Chem. Mater. 34 (7), 2229

[2] Devos et al., (2020). Chem. Mater. 33 (1), 273

[3] Dědeček et al., (2019). ChemSusChem 12 (3), 556

[4] Li et al., (2018). J. Phys. Chem. C 122 (41), 23564

[5] Dusselier et al., (2018). Chem. Rev. 118 (11), 5265

**Synthesis of hierarchical zeolite LTA and application in toxic metals adsorption**

A. M. M. França<sup>1</sup>, R. A. Bessa<sup>2,3,\*</sup>, M. V. M. Nascimento<sup>1</sup>, E. S. Oliveira<sup>3</sup>, A. R. Loiola<sup>3</sup>, R. F. Nascimento<sup>1</sup>

<sup>1</sup>Analytical Chemistry and Physical Chemistry, Federal University of Ceará, Fortaleza, Brazil, <sup>2</sup>Chemistry, University of Manchester, Manchester, United Kingdom, <sup>3</sup>Organic and Inorganic Chemistry, Federal University of Ceará, Fortaleza, Brazil

**Abstract Text:** Zeolites are crystalline microporous materials with considerable technological interest in chemical process industries. Generally, these materials are produced in the form of fine powders, limiting several applications, due to the unpacking phenomenon. Therefore, the use of hierarchical zeolites has gained enormous attention once in this configuration zeolites show superior mechanical strength, as well as increasing mass transfer rate, facilitating the access of analytes to the adsorption pore. The aim of the present study is to synthesize a hierarchically structured zeolite and to evaluate its adsorptive capacity in the adsorption of toxic metals in aqueous medium. Hierarchical zeolite was produced by *in situ* growth of zeolite LTA crystals over glass fibers ( $\text{Al}_2\text{O}_3\text{-SiO}_2$ ). The ideal synthesis condition was obtained by studying the reaction time (2, 4 and 6h) of this fiber with  $\text{NaOH } 4.0 \text{ mol L}^{-1}$  at  $110^\circ\text{C}$  in a Teflon-lined stainless steel autoclave. The reaction time was selected using characterization techniques such as powder X-ray diffraction (XRD), Fourier transform infrared spectroscopy (FTIR) and scanning electron microscopy (SEM). The adsorption test was performed using the best synthetic batch sample for 24 h at 200 rpm, in which 25 mL of a  $100 \text{ mg L}^{-1}$  multicomponent solution of  $\text{Cu}^{2+}$ ,  $\text{Pb}^{2+}$ , and  $\text{Cd}^{2+}$  at pH 5.0 was added in a 125 mL Erlenmeyer flask containing 0.3 g of the sample. The test was performed in duplicate. According to XRD measurements, zeolite LTA formation was found as a single crystalline phase, free of impurities, in the samples with 4 h and 6 h reaction time, named as FB4 and FB6, respectively. For the same samples, in infrared spectra, the characteristic bands for zeolite LTA were found at  $464 \text{ cm}^{-1}$ ,  $558 \text{ cm}^{-1}$  and  $665 \text{ cm}^{-1}$ . The precursor fiber material (FBSA sample) presented smooth surface, with a homogenous morphology, as observed in SEM. After 2h of reaction (sample FB2), a surface roughness could be observed, indicating the beginning of its surface dissolution. Uniform formation of LTA zeolite on  $\text{Al}_2\text{O}_3\text{-SiO}_2$  glass fibers was observed after 4 h of reaction, where the dissolution rate of Si and Al from the fibers was similar to the zeolite crystallization on their surface. That sample was chosen for the initial adsorption tests. With 6 h of reaction time, zeolite was still observed. However, due to the longer reaction time, part of the zeolite formed on the fiber surface detached. The adsorption tests showed that FB4 sample presents good efficiency in the adsorption of  $\text{Cu}^{2+}$ ,  $\text{Pb}^{2+}$ , and  $\text{Cd}^{2+}$ , having the following adsorption capacities:  $3.63 \text{ mg g}^{-1}$ ,  $5.64 \text{ mg g}^{-1}$  and  $2.76 \text{ mg g}^{-1}$ , respectively. Therefore, it is suggested that this material can be applied in both batch and fixed bed adsorption studies, since its fibrous properties can help to minimize problems related to column compaction.

**Image 1:**

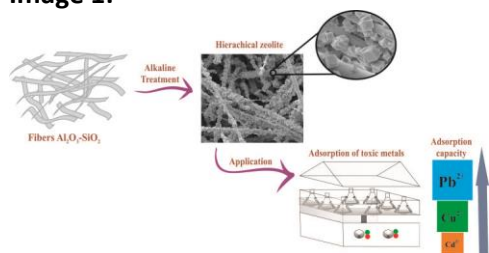
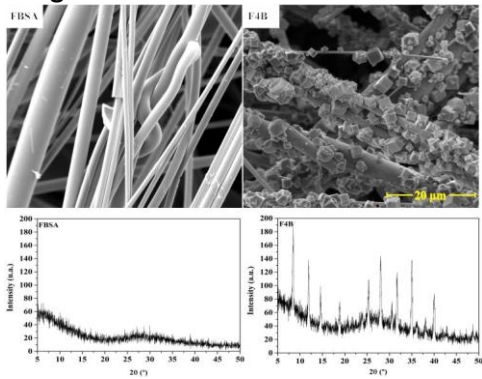


**Image 2:**



**References:** OKADA, K. et al. In-situ coating of zeolite Na-A on Al<sub>2</sub>O<sub>3</sub>-SiO<sub>2</sub> glass fibers. *Journal of Porous Materials*, v. 5, n. 2, p. 163-168, 1998. ISSN 1380-2224.

OKADA, K. et al. In situ zeolite Na-X coating on glass fibers by soft solution process. *Microporous and mesoporous materials*, v. 37, n. 1-2, p. 99-105, 2000. ISSN 1387-1811.

GAO, X. et al. Fabrication of stainless steel hollow fiber supported NaA zeolite membrane by self-assembly of submicron seeds. *Separation and Purification Technology*, v. 234, p. 116121, 2020. ISSN 1383-5866.

**Zeolite K-F from Waste Container Glass**

N. J. Coleman<sup>1,\*</sup>, V. K. Elmes<sup>1</sup>

<sup>1</sup>School of Science, University of Greenwich, Kent, United Kingdom

**Abstract Text:**

**Introduction**

Poor collection infrastructure and colour mismatch restrict regional demand for coloured waste container glass that can be recycled as new bottles and jars [1,2]. For example, green and amber soda-lime-silica glasses are widely distributed as bottled alcoholic beverages; however, their effective recovery from the waste stream and subsequent recycling are limited to regions with established wine- and beer-making industries [1]. In this study, waste amber container glass was evaluated as a feedstock for the hydrothermal synthesis of zeolite K-F ( $K_2Al_2Si_3O_{10}$ ). Current interest in the facile and economical synthesis of zeolite K-F from municipal and industrial wastes arises from its applications in soil fertilisation and conditioning [3].

**Experimental**

3.0 g of ground amber glass ( $< 125 \mu m$ ), 0.45 g of waste aluminium foil and  $15 \text{ cm}^3$  of  $4M \text{ KOH}_{(aq)}$  were heated at  $100 \text{ }^\circ\text{C}$  for 1, 3 or 10 days in a sealed PTFE autoclave. The products (*viz.* K-1, K-3 and K-10, respectively) were recovered by filtration, washed with deionised water to pH  $\sim 8$ , dried in air at  $40 \text{ }^\circ\text{C}$  and analysed by powder X-ray diffraction analysis (XRD) and scanning electron microscopy (SEM). Uptake of  $Zn^{2+}$  and  $Pb^{2+}$  were determined by exposure of 0.1 g of K-10 product to  $200 \text{ cm}^3$  of 0.5 mM single metal nitrate solution for 24 h [2]. Solutions were analysed by inductively coupled plasma spectroscopy (ICP). All preparations and analyses were carried out in triplicate.

**Results & Discussion**

Under the selected reaction conditions, the initial dissolution of the glass and development of the principal zeolite K-F and minor katoite phases were slow, with only 5% crystallinity having been achieved within the first 24 h (Fig. 1). The reaction rate then markedly increased to give products of 60% and 78% crystallinity at 3 and 10 days, respectively. The final product, K-10, was found to comprise 64% zeolite K-F, 14% katoite and 22% amorphous material. The total yield of solid product increased from 2.1 g to 6.5 g between 1 and 10 days.

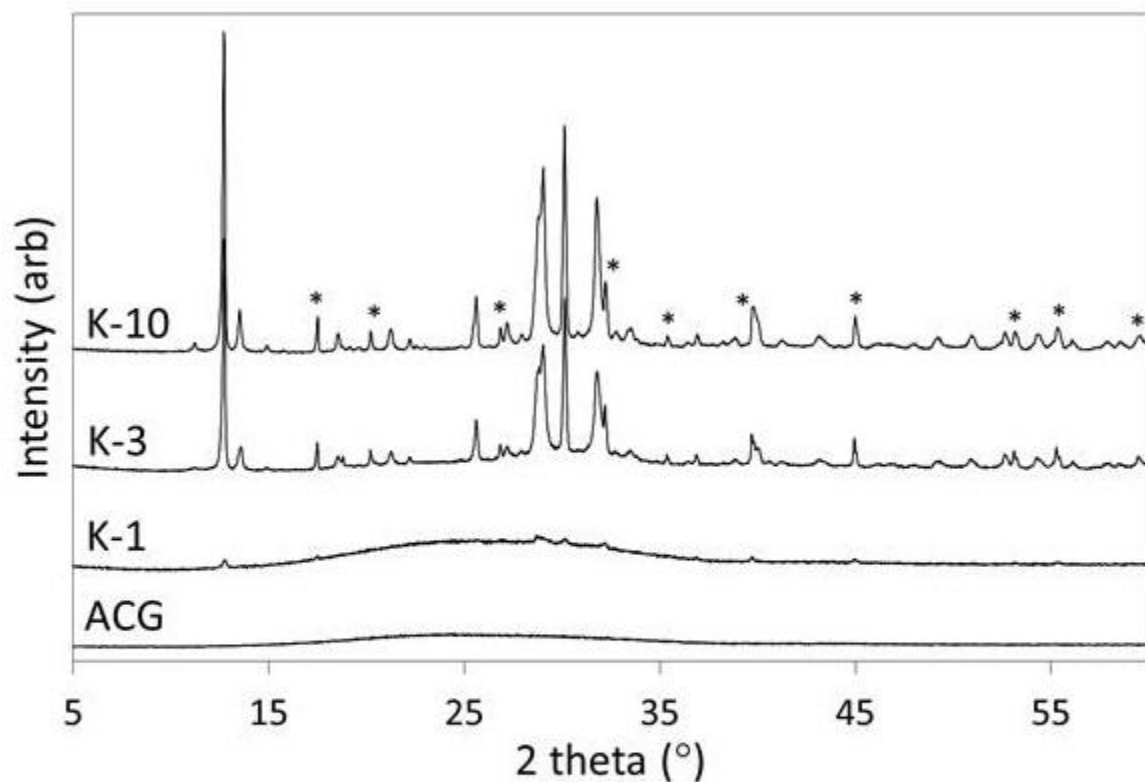
Initial 1-day hydration products appeared as textured distorted spherical bundles of a calcium aluminosilicate gel precursor which were distributed across, but did not wholly cover, the surface of the glass (Fig. 2). Within 3 days, sub-micron tetragonal crystals of zeolite K-F were seen to entirely populate the surfaces of the glass particles among which were dispersed occasional hexagonal plates of katoite and some remaining distorted spheres. As the reaction progressed, crystalline products incompletely filled the lacunae created by the continuing dissolution of the glass to produce porous hierarchical structures comprising tetragonal K-F crystals between 2 and  $5 \mu m$  in length.

Despite the incomplete conversion of amber glass into crystalline zeolite K-F, the uptake capacities of the 10-day product for  $Pb^{2+}$  ( $4.5 \text{ meq g}^{-1}$ ) and  $Zn^{2+}$  ( $4.1 \text{ meq g}^{-1}$ ) ions compared favourably with those of many other zeolites and waste-derived inorganic sorbents reported in the literature [4].

**Conclusions**

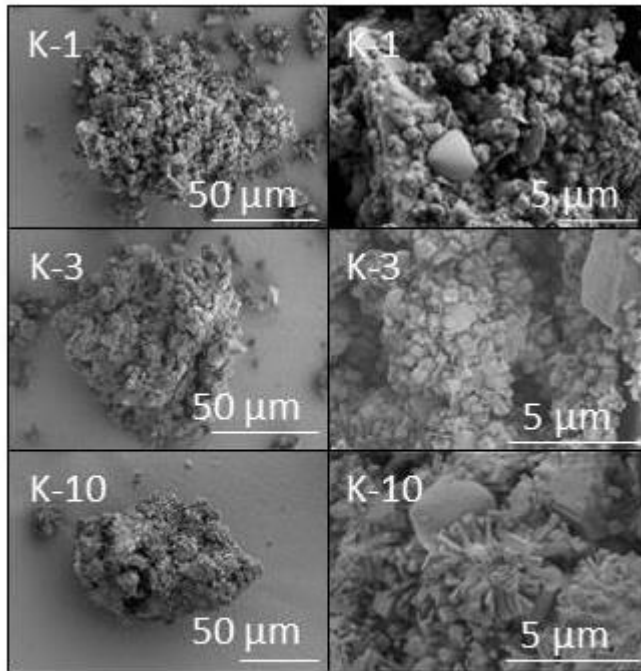
This study has confirmed that an impure zeolite K-F product can be prepared by one-pot hydrothermal synthesis from a mixture of amber container glass and aluminium waste ( $Al:Si = 1$ ) at  $100 \text{ }^\circ\text{C}$  in  $4 \text{ M KOH}_{(aq)}$ . Waste coloured container glass is a particularly attractive feedstock for the facile one-pot synthesis of zeolites as, unlike many industrial silicate-bearing wastes, it does not require pre-treatment for activation or removal of hazardous components.

Image 1:



**Fig. 1.** XRD patterns of amber container glass (ACG) and zeolite K-F products K-1, K-3 and K-10 (asterisks denote katoite phase)

**Image 2:**



**Fig. 2.** SEM images of zeolite K-F products K-1, K-3 and K-10

**References:**

1. V.K. Elmes et al., *Ceram. Int.* 44 (2018) 17069
2. N.J. Coleman, *Int. J. Environ. Waste Manage.* 8 (2011) 366
3. T. Wajima & K. Munakata, *Chem. Eng. J.* 207-208 (2012) 906
4. S. De Gisi et al., *Sustain. Mater. Technol.* 9 (2016) 10

## ***New Synthetic Methods and Post-Synthetic Modification***

FEZA21-PO-200

### **Managing the properties of microporous silicoaluminophosphates SAPO-11 and SAPO-34**

I. Shamanaeva<sup>1,\*</sup>, Z. Yu<sup>2,3</sup>, D. Sladkovskiy<sup>4</sup>, E. Parkhomchuk<sup>1</sup>

<sup>1</sup>Boreskov Institute of Catalysis SB RAS, Novosibirsk, Russian Federation, <sup>2</sup>Heilongjiang University, Harbin, China,

<sup>3</sup>Novosibirsk State University, Novosibirsk, <sup>4</sup>St. Petersburg State Technological Institute, Saint-Petersburg, Russian Federation

**Abstract Text:** SAPO-11 and SAPO-34 with AEL and CHA structure, respectively, are the most popular and used molecular sieves of the silicoaluminophosphates (SAPOs) family. Catalytic and adsorption properties of the certain SAPOs are determined by the size, morphology, texture and acidity of crystals, which, in turn, depend on the way of material preparation. On this basis, the development of synthetic methods to control these ones has long been pursued in order to fine-tune the properties of the SAPOs crystals. SAPO-11 and SAPO-34 structures are usually obtained by hydrothermal synthesis (HTS) in aqueous medium at 200°C for 24 and 48 hours, respectively [1]. SAPO-11 typically represents spherical aggregates of 5-20 micrometers consisting of small slab-like crystallites (Image 1,a) and SAPO-34 crystals usually are cubic morphology with crystal sizes similar to SAPO-11 (Image 1,d).

We have been using two approaches to obtain both SAPO-11 and SAPO-34 precursor mixtures as well as we have been varying molar compositions and HTS conditions (temperature and duration). One of the approaches was ordinary stirring on a magnetic stirrer, another one was ultrasonic (US) pre-treatment of precursor suspensions before HTS. Crystals of SAPO-11 were synthesized in different media (water, water-ethanol mixture and ethanol (EtOH)) and the molar composition varied in the following range: (0.1-0.2)SiO<sub>2</sub>:1Al<sub>2</sub>O<sub>3</sub>:1P<sub>2</sub>O<sub>5</sub>:1DPA:(0.05-50)H<sub>2</sub>O:(0-60)EtOH. We changed the temperature of HTS from 200°C to 100°C and altered its duration from 2 to 160 hours for SAPO-11 synthesized in different media as well. Since silicon may be introduced into aluminophosphate-CHA structure more easily in the case of SAPO-34 crystals, its molar composition varied more significantly: (0.2-0.8)SiO<sub>2</sub>:1Al<sub>2</sub>O<sub>3</sub>:1P<sub>2</sub>O<sub>5</sub>:(1-3)TEAOH (MOR):(50-150)H<sub>2</sub>O.

As a result, US treatment allowed us to obtain the SAPO-34 phase with a higher crystallinity, improved texture and acidity comparing with crystals synthesized by conventional mixing. In addition, in the case of SAPO-11, improved mixing facilitated a reduction of the synthesis time from 24 to 1 hour [2].

Template type, its amount [3] and water content strongly influenced the phase purity, crystal size, mesopore size and acidity of SAPO-34 crystals.

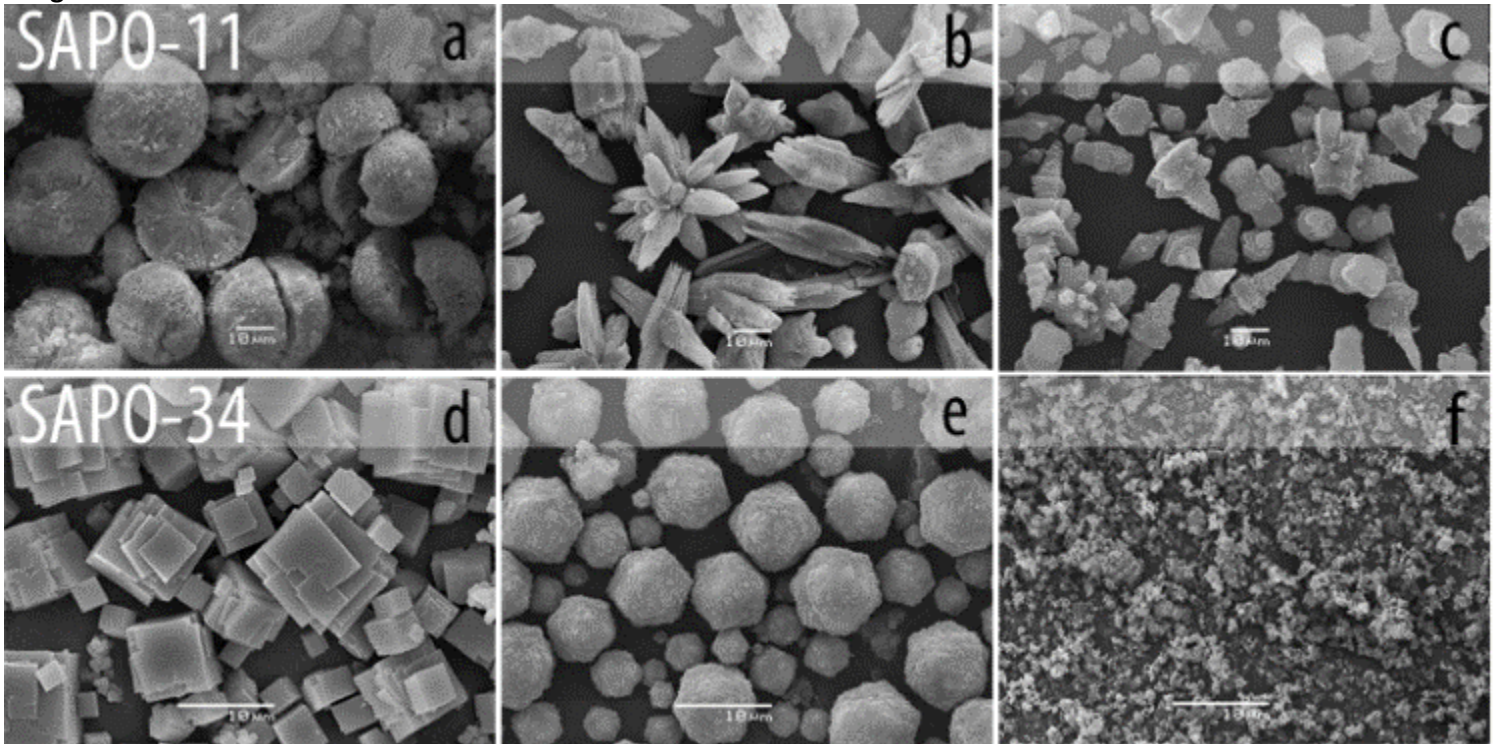
Considering the effect of solvent type on SAPO-11 crystal properties, some surprising changes in the crystal morphology and porosity were observed when the reaction medium type gradually changed from water to ethanol. We adjusted the HTS conditions to produce the pure SAPO-11 phase in ethanol medium with novel previously unobservable screw-like morphology (Image 1,c) [4]. SAPO-11 crystals also were obtained at a lower temperature (150°C) in a water medium by the one-stage method, which also affected the texture properties of the molecular sieve.

To sum up, our group has carried out plenty of experiments on the synthesis of SAPO-11 and SAPO-34 crystals to find out dependencies of synthesis conditions and properties of produced materials. Crystal sizes and morphologies of both types were significantly changed (Image 1), and properties of SAPO-34 varied in the following ranges:  $S_{\text{BET}} = 516 - 790 \text{ m}^2/\text{g}$ ,  $V_{\text{total}} = 0.25 - 0.33 \text{ cm}^3/\text{g}$ ,  $V_{\text{micro}} = 0.18 - 0.27 \text{ cm}^3/\text{g}$ , total acidity was 0.8 - 1.7 mmol/g; these ones for SAPO-11 were:  $S_{\text{BET}} = 154 - 292 \text{ m}^2/\text{g}$ ,  $V_{\text{total}} = 0.13 - 0.29 \text{ cm}^3/\text{g}$ ,  $V_{\text{micro}} = 0.04 - 0.12 \text{ cm}^3/\text{g}$ , total acidity was 0.10 - 0.49 mmol/g.

A comparative analysis of catalytic properties of most of the synthesized SAPO-34 and SAPO-11 samples was carried out for the methanol-to-olefins process and will be shown in the presentation.

The reported study was funded by RFBR, project number 20-33-90254

Image 1:



**References:** 1. Lok B.M., et.al. Patent 4440871. 1984.

2. Shamanaeva I.A., et.al. Influence of the Precursor Preparation Procedure on the Physicochemical Properties of Silicoaluminophosphate SAPO-11//Petroleum chemistry. 2019. V. 59. № 8. P. 854

3. Shamanaeva I.A., et.al. Role of SAPO-34 texture and acidity in the conversion of methanol-to-olefins //Petroleum chemistry. 2019. Accepted to press

4. Tiuliukova I.A., et.al. Screw-like morphology of silicoaluminophosphate-11 (SAPO-11) crystallized in ethanol medium //Materials Letters. 2018.V.228.P.61

## ***New Synthetic Methods and Post-Synthetic Modification***

FEZA21-PO-201

### **1,3,5-trioxane as structure directing molecule for zeolites omega and ECR-1**

A. Tuel, C. Chatelard\*, D. Mathias, R. Martinez-Franco

#### **Abstract Text: Introduction**

The structure of zeolite ECR-1 (**EON** framework type) consists of a regular stacking of sheets found in zeolites mordenite and omega, respectively.<sup>1</sup> Many organic molecules have been used to synthesize zeolite omega, in particular the tetramethylammonium (TMA<sup>+</sup>) cation, which appeared to be small enough to be occluded in the *gme* cages during crystallization.<sup>2</sup> Other small molecules such as 1,4-dioxane, pyrrolidine or piperazine were also successfully applied for the crystallization of omega zeolite.<sup>3-5</sup> Despite the presence of *gme* cavities in both structures, the synthesis of ECR-1 has only been reported using traces of TMA<sup>+</sup> but molecules were not occluded in the final solid and served essentially to initiate the organic-free crystallization.<sup>1</sup>

The present work reports the synthesis of zeolites omega (**MAZ** framework type) and ECR-1 using the small 1,3,5-trioxane (or trioxane) molecule. The influence of various synthesis parameters on the formation of both zeolites are discussed. The relative proportion of omega and ECR-1 in the different solids has been monitored by X-ray diffraction and solid-state nuclear magnetic resonance.

#### **Experimental**

In a typical synthesis a gel with the composition  $10\text{SiO}_2 - 0.86\text{Al}_2\text{O}_3 - 7.5\text{Trioxane} - 2.2\text{Na}_2\text{O} - 142\text{H}_2\text{O}$  was prepared, stirred at room temperature for 3 hours, placed in an autoclave and crystallized at 115°C for 7 days under dynamic conditions (60 rpm). After crystallization, the solid was recovered by filtration, washed, dried and eventually calcined at 550°C in air for 8 hours. All syntheses were carried out following the same procedure by changing the amount of NaOH and/or NaAlO<sub>2</sub> or the temperature.

Zeolites were characterized using X-ray Diffraction (XRD), Scanning Electron Microscopy (SEM) Thermogravimetric Analysis (TGA), solid state Nuclear Magnetic Resonance (NMR) and chemical analysis by X-ray fluorescence (FX).

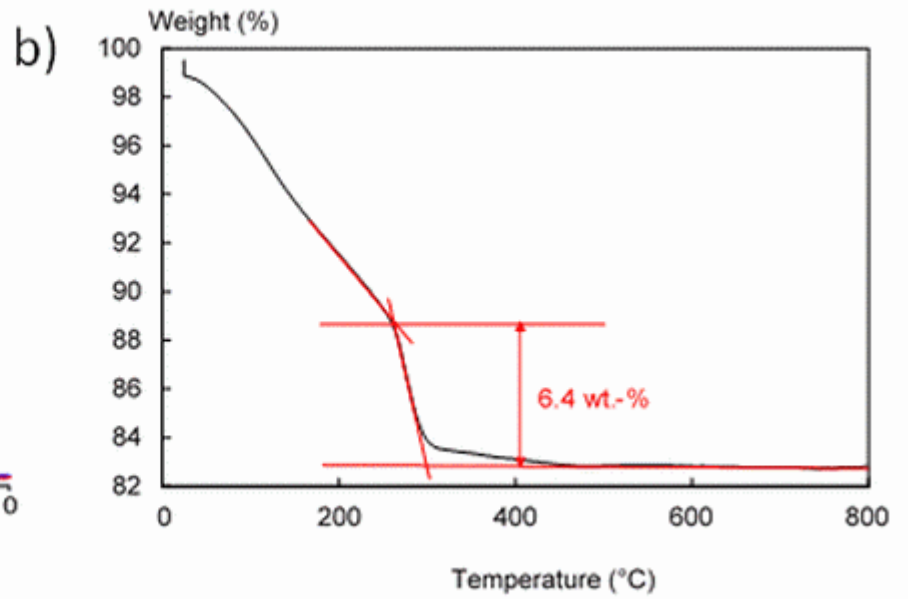
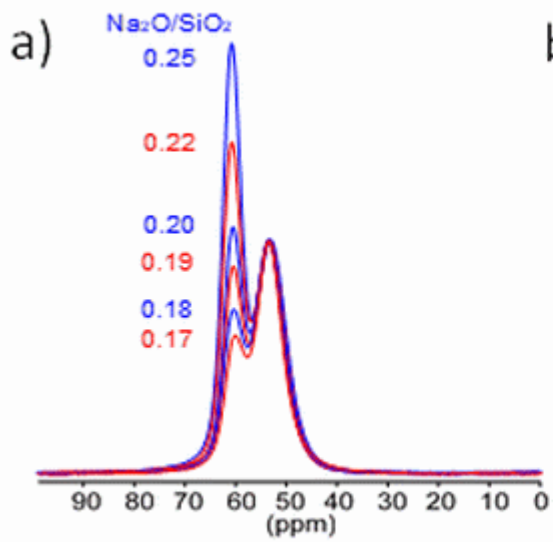
#### **Results**

Trioxane has been effectively used to synthesize both omega and ECR-1 zeolites with framework  $\text{SiO}_2/\text{Al}_2\text{O}_3$  between 7 and 8. The molecule behaves differently from 1,4-dioxane that was previously reported as structure directing molecule for zeolite omega but not for ECR-1. The nature of the zeolite formed depends mainly on the alkalinity of the precursor gel. Pure omega zeolite is obtained at high  $\text{Na}_2\text{O}/\text{SiO}_2$  ratios while ECR-1 is progressively formed when the NaOH content is decreased. The percentage of each zeolite in solids obtained at intermediate alkalinities is difficult to estimate by XRD but reliable methods based on the evolution of <sup>27</sup>Al and <sup>23</sup>Na NMR spectra have been developed and successfully applied (Figure 1a). Even though the structure of the solids was not refined, it is reasonable to assume that trioxane molecules are occluded in the *gme* cages of the structure, likely in the form of [Na<sup>+</sup>\_trioxane] complexes. A great advantage of trioxane is that zeolites omega and ECR-1 can be calcined in air at ca. 280°C, typically 300°C below temperatures necessary to remove other small 6-ring molecules such as 1,4-dioxane, pyrrolidine or piperazine (Figure 1b).

**Figure 1** Evolution of <sup>27</sup>Al NMR spectra with the Na<sub>2</sub>O content in the gel (a) and TGA of zeolite omega prepared with trioxane (b)

Modeling the trioxane molecule and its decomposition products in the zeolite are in progress to better understand how the organics can be removed at such a low temperature. Results will be presented and compared with those obtained on a zeolite synthesized in the presence of 1,4-dioxane.

Image 1:



References: 1)

- 2)
- 33-42
- 3)
- 4)
- 5)

A.F. Gualtieri et al., Chem. Mater. 18 (2006) 76-84

A. Martucci et al. Microporous Mesoporous Mater. 63 (2003)

B. De Witte et al. Microporous Mater. 10 (1997) 247-257

H. Xu et al. J Porous Mater 17 (2007) 97-101

M.K. Rubin et al. U S Patent 4,021,447(1977)

## New Synthetic Methods and Post-Synthetic Modification

FEZA21-PO-202

### High-stability methanol-to-aromatics conversion over [Ca,Ga]/H-ZSM-5

C. Liu<sup>1,\*</sup>, E. Khramenkova<sup>1</sup>, E. Sireci<sup>1</sup>, S. Ganapathy<sup>2</sup>, E. Uslamin<sup>1</sup>, F. Kapteijn<sup>1</sup>, E. Pidko<sup>1</sup>

<sup>1</sup>Chemical Engineering, <sup>2</sup>Radiation Science and Technology, Delft University of Technology, Delft, Netherlands

**Abstract Text:** To meet the increasing demand for aromatic compounds, much effort has been devoted to the methanol-to-aromatics (MTA) process. This process is particularly attractive as methanol can be obtained from a number of sustainable feedstocks including shale gas, biomass, and CO<sub>2</sub>. [1] One of the main challenges in MTA is related to the catalyst deactivation due to the formation of intra-zeolite coke species. In turn, it is believed that the coke formation is directly linked to the formation of light aromatic compounds. In this study, we demonstrate that the formation of aromatics and catalyst deactivation can be decoupled by using Ga/HZSM-5 zeolite catalyst modified by of Ca. These bimetallic catalysts combine high selectivity to light aromatics and extended MTA lifetime. We show that MTA lifetime is highly sensitive to even a low Ca concentration, going through a maximum with increasing Ca loading. The optimal loading of Ca is 0.01 wt%, corresponding to an atomic ratio of only 1:50 for Ca:Ga. The effect of metal modification on the acidic properties of the bimetallic zeolite materials was evaluated by IR spectroscopy with adsorbed pyridine and acetonitrile-d<sub>3</sub> probe molecules. The density of BAS shows a good correlation with MTA lifetime. The combined results revealed that the presence of Ca at low non-stoichiometric amounts can significantly alter the acidic properties of zeolite which might indicate a re-arrangement of extra-framework species in the micropores. Based on the following GA (generic algorithm) structure prediction and *ab initio* thermodynamic analysis, we propose that the synergy originates from Ca stabilizing Ga oxides anchoring at the extra-framework sites under the reaction conditions. When excessive water molecules are locally produced by methanol dehydration in the MFI unit cell, initial Ga oxide structures get hydrolyzed and are eventually detached from the active sites. On the contrary, the hybrid CaGa oxides remain the direct interaction to the zeolite framework with the same amount of water. The formed Ga hydroxides leaving the unit cell lost the shape selectivity causing the fast deactivation in Ga-modified HZSM-5.

Figure 1. Acid site density of BAS and LAS determined by IR with adsorbed pyridine at 160 °C.

Figure 2. Total throughput of methanol before conversion drops below 95% (bar to the left axis) and estimated carbon selectivity to different hydrocarbon groups at TOS 0.5 h (right axis). Reaction conditions: T = 450 °C, M<sub>cat</sub> = 40 mg (150-212 μm), P<sub>reactor</sub> = 1 bar, WHSV = 5.4 g<sub>MeOH</sub>/g<sub>cat</sub>·h<sup>-1</sup>, carrier gas N<sub>2</sub> = 50 mL/min. C<sub>>4</sub>: hydrocarbons with the carbon number higher than 4. Ga(2) and Ca(x)Ga(2) refer to H-ZSM-5 modified by 2 wt% of Ga and H-ZSM-5 via a sequential impregnation of Ga (2 wt%) and Ca (x wt%), respectively.

**Image 1:**

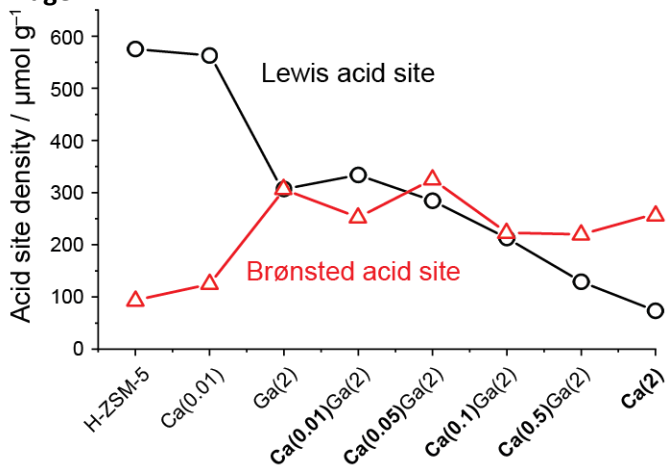
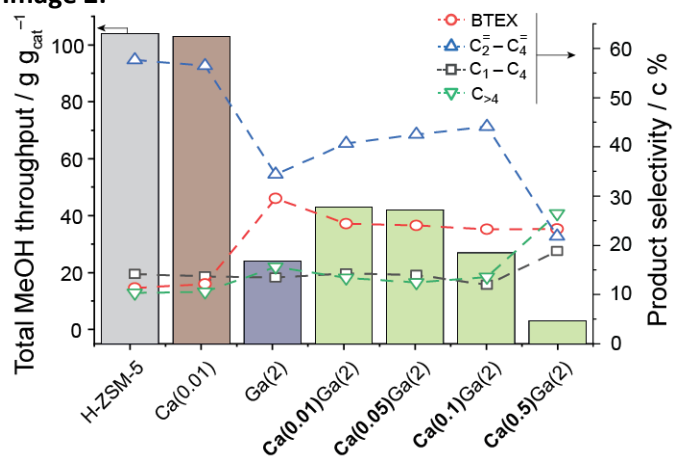


Image 2:



**References:** 1. Olah, G.A., A. Goepfert, and G.S. Prakash, Chemical recycling of carbon dioxide to methanol and dimethyl ether: from greenhouse gas to renewable, environmentally carbon neutral fuels and synthetic hydrocarbons. The Journal of organic chemistry, 2008. 74(2): p. 487-498.

## ***New Synthetic Methods and Post-Synthetic Modification***

FEZA21-PO-203

### **Pore visualization of hierarchical MOR zeolites and the catalytic performances in ethanol dehydration**

P. Iadrat\*, N. Horii<sup>1</sup>, T. Atitthep<sup>2</sup>, C. Wattanakit<sup>3</sup>

<sup>1</sup>Engineering division, System in Frontier Inc., Tachikawa-shi, Tokyo, Japan, <sup>2</sup>Frontier Research Center (FRC), <sup>3</sup>School of Energy Science and Engineering, Vidyasirimedhi Institute of Science and Technology, 555 Moo 1 Payupnai, Wangchan Rayong, Thailand

**Abstract Text:** The hierarchical zeolite is one of the most promising materials for catalytic applications. The synthesis of hierarchical zeolites has been commonly proposed by using the templating approach.<sup>1</sup> However, the cost of organic templates is expensive, and therefore it is not appropriate to use in the practical industries. Moreover, the greenhouse gases (e.g. CO<sub>2</sub>) are also emitted due to the removal of the structure-directing agent. Therefore, the template-free synthesis of zeolites is a very interesting task. The seed-assisted template-free synthesis of zeolites has been widely proposed.<sup>2</sup> However, some of them showed the dense porous structures.<sup>3</sup> Therefore, the post-synthetic treatment is required to open their structure. Interestingly, the NH<sub>4</sub>F etching is one of the promising post-synthetic treatment method because it not only enhances the external surface area and mesoporosity but also preserves the structural composition (Si/Al ratio) by the dissolution of Si and Al in the zeolite frameworks with the similar rate.<sup>4</sup>

In this contribution<sup>5</sup>, the pore-opened mordenite (MOR) zeolite with hierarchical structures has been successfully synthesized by combination of seed-assisted template-free synthesis and NH<sub>4</sub>F etching. The effect of crystallization time, seed amount, and NH<sub>4</sub>F concentration was systematically studied. It was found that the relative crystallinity increases with an increase in crystallization time and the smaller particle size is observed at larger amount of MOR seed. Moreover, although the zeolite framework can be destroyed at high concentration of NH<sub>4</sub>F but the fluoride treatment with a suitable condition (20 wt.% of NH<sub>4</sub>F) of the synthesized MOR can provide the highest external surface area and comparable micropore volume with the parent MOR, resulting in the highest hierarchy factor. Remarkably, the visualization of mesopore-architecture in three-dimensional perspectives together with the pore connectivity network of pore-opened hierarchical MOR was clearly illustrated by the electron tomography (ET) technique. Interestingly, the pore-opened zeolite exhibited the higher catalytic performance (approximately 80 % of ethylene yield) in ethanol dehydration compared to the parent one due to the additional pore-opened structure connected to the external surface of zeolite. In addition, the effect of pore connectivity network on the coke location and type obtained from ethanol conversion was also observed and it was found that almost the whole area of the pore-opened MOR crystals contributes to the reaction, whereas the untreated sample allows the reaction to proceed mainly on the outermost area of crystals. These results explicitly explain the effect of pore connectivity of pore-opened hierarchical zeolites on catalytic behaviors and coke formation in ethanol dehydration.

**References:** [1] Wannapakdee, W., Wattanakit, C., Paluka, V., Yutthalekha, T., and Limtrakul, J. *RSC Adv.* 6, 2875 (2016).

[2] Nada, M.H., and Larsen, S.C. *Microporous Mesoporous Mater.* 239, 444 (2017).

[3] Todorova, T., and Kalvachev, Y. *Bulg. Chem. Commun.* 47, 409 (2015).

[4] Qin, Z., Melinte, G., Gilson, J.-P., Jaber, M., Bozhilov, K., Boullay, P., Mintova, S., Ersen, O., and Valtchev, V. *Angew. Chem. Int. Ed.* 55, 15049 (2016).

[5] Iadrat, P., Horii, N., Atitthep, T., and Wattanakit, C. *ACS Appl. Mater. Interfaces* 13, 8294 (2021).

## ***New Synthetic Methods and Post-Synthetic Modification***

FEZA21-PO-204

### **An Intrinsic Synthesis Parameter Governing the Crystallization of Silico(zinco)aluminophosphate Molecular Sieves**

S. H. Park\*, K. C. Kemp, J. Hong, J. G. Min, S. B. Hong

**Abstract Text:** Zeolites and related microporous materials are of vital importance in the modern chemical industry, mainly owing to their diverse structures/compositions and (hydro)thermal stability. For instance, silicoaluminophosphate (SAPO) molecular sieves, one family of crystalline microporous materials, have been applied as commercial catalysts to the methanol-to-olefins conversion and lube dewaxing process. This success story would suggest that the synthesis of new zeolites of varying structures and compositions proceeds similar to that of designed metal-organic frameworks (MOFs). However, the reality is that luck and intuition have been the major players. As a result, whether or not an intrinsic synthesis factor governing the microporosity in the synthesis of zeolites and zeolite-like materials really exists has long plagued the field.

As a step forward in answering this long-standing question, we show here the existence of a simple experimental parameter ( $\text{MOH}/\text{P}_2\text{O}_5$ , where M is alkali metal ions) controlling the microporosity, as well as the phase selectivity, of the crystallization product in the organic-free synthesis of SAPO and zincoaluminophosphate (ZnAPO) molecular sieves. Using sodium SAPO and ZnAPO gels with  $\text{ca. } 3.3 \leq \text{MOH}/\text{P}_2\text{O}_5 \leq 5.3$ , we were able to obtain SAPO materials with CHA and LTA topologies, as well as a SAPO FAU/EMT intergrowth, and also ZnAPO ones with CZP and SOD topologies. However, the phases obtained were always dense or amorphous materials when the  $\text{MOH}/\text{P}_2\text{O}_5$  ratio, which we termed the 'synthesis charge density (SCDM)', becomes higher ( $> 5.3$ ) or lower ( $< 3.3$ ), respectively. Surprisingly, to the best of our best knowledge, the existence of such intrinsic parameter in the synthesis of phosphate-based molecular sieves has never been reported, even though intuitively such a factor should exist. We anticipate that combining the synthesis charge density concept with the currently available zeolite synthesis database might pave the way for the rational discovery of zeolites and zeolite-like materials with interesting applications in the fields of energy and environment.

## New Synthetic Methods and Post-Synthetic Modification

FEZA21-PO-205

### High Silicon Nanosized Beta zeolite: Efficient Synthesis, Mechanism and its Toluene Adsorption Application

J. Wang<sup>1</sup>, S. Cao<sup>1</sup>, Y. Sun<sup>1</sup>, X. Meng<sup>1</sup>, L. Meng<sup>1</sup>, S. Shang<sup>1</sup>, Y. Gong<sup>1,\*</sup>

<sup>1</sup>college of Chemical Engineering and Environment, China University of Petroleum-Beijing, Beijing, China

**Abstract Text:** Volatile organic compounds (VOCs) are destructive to the environment and human health. Adsorption has proven to be an effective technology for decades. For treating VOCs, high silicon zeolites (ZSM5, Y, Beta) have been considered as effective adsorbents for capturing diverse VOC molecules. Herein, a series of nano-sized Beta zeolites were successfully obtained by seed-assisted method (denoted as S-Beta-x, x is ratios of SiO<sub>2</sub>/Al<sub>2</sub>O<sub>3</sub> 30, 100, 200, 400, 600). In order to explore the reasons that hinder the synthesis of high-silicon Beta zeolites under normal hydrothermal method, Small-angle X-ray scattering (SAXS) was used to analyse the particle structure parameter in the precursors at aging stage, and combined the assistance of other technologies, the crystallization behaviour without and with adding seeds crystal was comparatively studied. The results showed that the seed crystals would be completely dissolved to form Beta zeolite building units during crystallization process, then a large number of crystal nuclei can be grown on the basis of structural units, which would eventually lead to the formation of nanocrystals and improving the utilization of silica materials, and the crystallization time of beta zeolite could be shortened from 4 days to 2 days. Moreover, as the SiO<sub>2</sub>/Al<sub>2</sub>O<sub>3</sub> ratios increasing, it is easier to form nano-sized zeolite and the crystal size would be getting smaller. The nano-sized high silicon Beta zeolites possess excellent hydrophobicity and larger mesopore volume. And because of that, the high silicon Beta zeolite showed excellent adsorption capacity in the evaluation of toluene adsorption, which can be improved at least by 43% than that of bulk Beta zeolite (N-Beta). Further, the moisture was introduced into the adsorption environment, nano Beta can also maintain good adsorption performance. In conclusion, as-synthesized high silicon nano-sized S-Beta zeolites prepared by seed-assisted method can be considered as an applicable VOCs adsorption material.

This work was sponsored by the National Natural Science Foundation of China (22078356, U1662116).

#### Image 1:

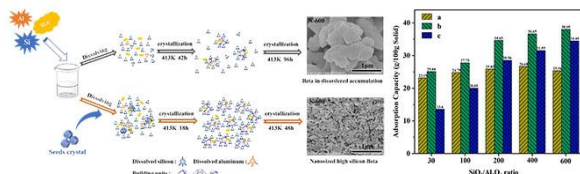


Figure 1. Schematic representation of the proposed crystallization mechanism (left) and Adsorption Capacity of toluene over (right): (a) N-Beta zeolites under dry conditions, (b) S-Beta zeolites under dry conditions, (c) S-Beta zeolites under moisture conditions.

## New Synthetic Methods and Post-Synthetic Modification

FEZA21-PO-206

### Promotive Effect of MWW Nanosheet on its Alkylation Performance

S. Cao<sup>1</sup>, J. Wang<sup>1</sup>, Y. Sun<sup>1</sup>, X. Meng<sup>1</sup>, L. Meng<sup>1</sup>, S. Shang<sup>1</sup>, Y. Gong<sup>1,\*</sup>

<sup>1</sup>college of Chemical Engineering and Environment, China University of Petroleum-Beijing, Beijing, China

**Abstract Text:** MCM-22 and MCM-49 zeolite as the main members of MWW zeolite proved to be an excellent aromatic alkylation catalyst which was quickly implemented in valuable industrial process, such as the liquid phase alkylation reaction of benzene-ethylene. The key factors to promote the performance of MWW zeolite is exposed external surface, to shorten the *c* axis, aggrandize the mesopores, etc. The morphology of MWW zeolite, particular the thickness of layers, can be regulated by dual-template synthesis, which is effective for promoting the reactivity and selectivity in the alkylation reaction of benzene. Controlling MWW nanosheet is achieved by adding gemini quaternary ammonium salts with different alkyl chains ( $C_{n6n}Br_2$ ,  $n=4, 5, 6, 7, 8, 9, 12, 18$ , such as  $C_{6-6-6}Br_2$ ,  $C_{18-6-6}Br_2$ , abbreviated as C6, C18) into the conventional system. Typically, SEM and TEM images show that these MWW nanosheets (named as C6-MCM-22 (Fig.1a-c), C18-MCM-49 (Fig.1d-f), respectively) were specifically assembled and aligned with uniformed hexagonal nanosheets in a spiral mode, therein the crystal sheets decrease to  $\sim 200$  in size nm and 5-20 nm in thickness. Distinctively, the length of hydrophobic chain can modulate the size and thickness of MCM-22 zeolite. For instance, the  $C_{6-6-6}$  possesses a shorter hydrophobic tail, C6-MCM-22 leading to a thinner MWW sheet (5-20 nm). Due to its long alkyl chain of  $C_{18-6-6}$ , C18-MCM-22 gives a thicker MWW sheet (20-50 nm). While, MCM-49 type materials give a thinner MWW sheet (5-20 nm), no matter the length of the alkyl chain. At the equivalent evaluation condition, the catalytic results for MCM-22, C6-MCM-22, C18-MCM-22, MCM-49 and C18-MCM-49 showed the thinner layered C18-MCM-49, C6-MCM-22 samples all performed better reactivity then their conventional ones (Fig.1g). C18-MCM-49 catalyst exhibits the highest conversion ( $\sim 34\%$ ) and ethylbenzene selectivity ( $\sim 95\%$ ) among these five catalysts. These results indicate MWW zeolites having thinner layer structure are critical for improving the alkylation reaction and C18-MCM-49 catalyst provides more distinctive advantage than C6-MCM-22. This can be explained that C18-MCM-49 catalyst possesses a connatural more external acid sites in microstructure, coupled with thinner layered morphology featuring larger external surface areas, and thus renders more accessible active centres. As seen, the C18-MCM-49 nanosheet stands out from MWW zeolites in terms of reactivity and selectivity, and it can be an alternative candidate in the liquid phase alkylation reaction for industrial applications.

This work was sponsored by the National Natural Science Foundation of China (22078356, U1662116).

### Image 1:

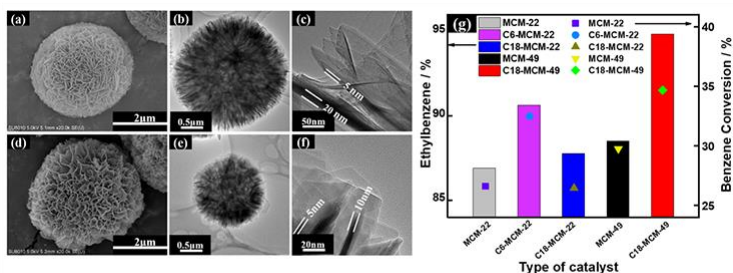


Fig. 1 SEM and TEM images of MWW type materials (a-c) C18-MCM-49, (d-f) C18-MCM-22. (g) Catalytic performance for typical MWW zeolite samples. WHSV=2 h<sup>-1</sup>, T=210 °C, P=3.4 MPa.

## ***New Synthetic Methods and Post-Synthetic Modification***

FEZA21-PO-207

### **ZSM-5 Nano-slab with reverse Al distribution and short b-axis for super MTP catalyst**

Y. Sun<sup>1</sup>, S. Cao<sup>1</sup>, J. Wang<sup>1</sup>, H. Tang<sup>1</sup>, Y. Gong<sup>1\*</sup>

<sup>1</sup>college of Chemical Engineering and Environment, China University of Petroleum-Beijing, Beijing, China

**Abstract Text:** The perfect match of the acid properties and diffusion properties ensures ZSM-5 zeolite performing excellent catalytic performance. The facile self-assembly synthesis of specific b-axis oriented ZSM-5 single crystal without twin structure in nanoscale is carried out for MTP reaction. The target thin-slab zeolite was synthesized under the synergistic effect of nano seed and neutral template within fast crystallization time of 3 hours. The structure evolution mechanism of the sol species during the crystallization process was investigated. It was found that the optimal system belongs to the solid-phase crystallization mechanism, which can avoid secondary nucleation on the surface of the aggregate. In addition, the smaller sized structure units through in situ SAXS analysis is also the key factor. The as-synthesized ZSM-5 with different seed amount (denoted as BZ-NS<sub>x</sub>, x=1, 2, 3) shows b-axis oriented slab, with 50-100 nm b-axis length and hence higher proportion of straight channels, in combination of its due to reverse Al distribution, which facilitates to improve the intrinsic molecular diffusion and inhibit coke formation at the external surface. Among them, BZ-NS<sub>3</sub> shows maximum life (297 h), corresponding to more than 1782 h with the WHSV of 1 h<sup>-1</sup> and a relatively high P/E ratio of 9.6, which stand out much higher than that of conventional ZSM-5 zeolite (nanosheet morphology NS sample and sphere morphology TZ-NS sample) in MTP reaction. In addition, the synthesis method proposed in this paper was more rapid, more efficient and lower energy consumption.

This work was sponsored by the National Natural Science Foundation of China (22078356, U1662116).

#### **Image 1:**

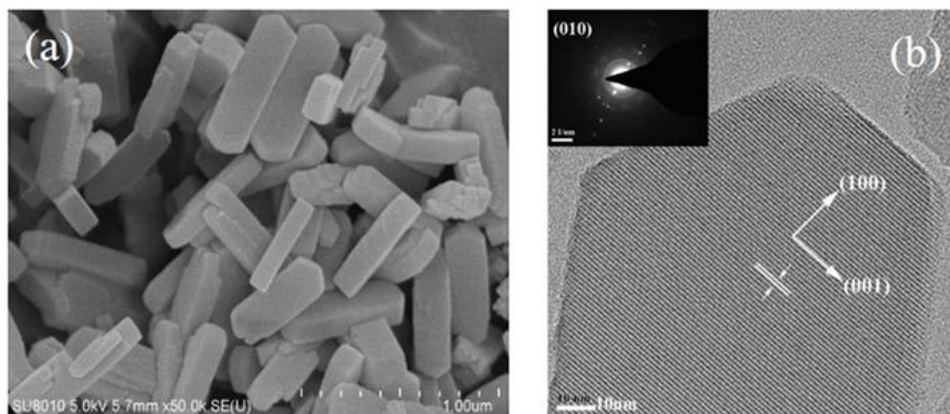


**Fig.1. SEM and TEM images of BZ-NS sample.**

Image 2:

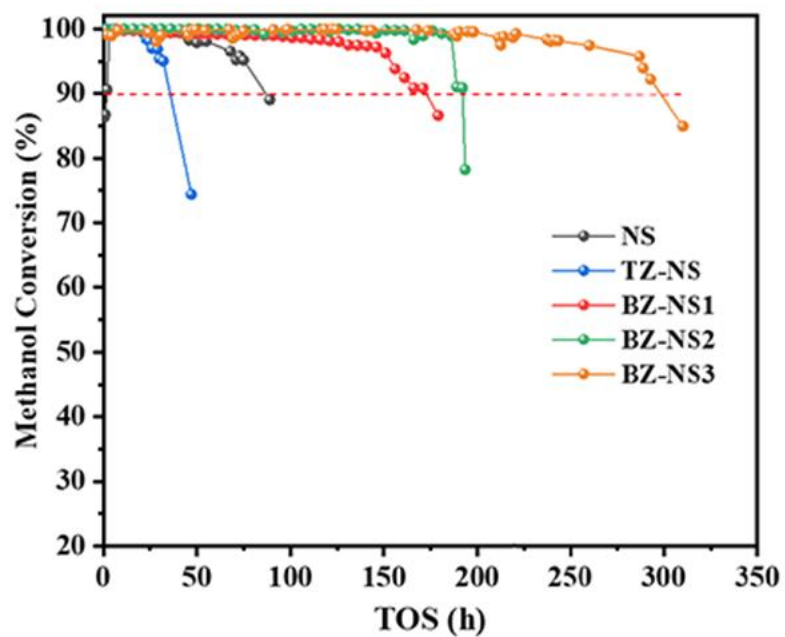


Fig. 2. Catalyst lifetime of the samples for MTP reaction,  $T = 753 \text{ K}$ ;  $\text{WHSV} = 6 \text{ h}^{-1}$ .

## ***New Synthetic Methods and Post-Synthetic Modification***

FEZA21-PO-208

### **Microwaves-assisted surfactant removal of a mesoporous material with unprecedented features from the process and material points of view**

I. Melián-Cabrera<sup>1</sup>, M.-A. López-Martínez<sup>2</sup>, L. López-Pérez<sup>2,\*</sup>, K. Djanashvili<sup>3</sup>, K. Góra-Marek<sup>4</sup>, K. A. Tarach<sup>4</sup>, M. E. María Emma Borges<sup>5</sup>

<sup>1</sup>Applied Photochemistry and Materials for Energy Group, La Laguna University, San Cristóbal de La Laguna (S/C de Tenerife), Spain, <sup>2</sup>División de Ciencias Básicas e Ingeniería, Universidad Autónoma Metropolitana-Unidad Azcapotzalco, Mexico City, Mexico, <sup>3</sup>Department of Biotechnology, Delft University of Technology, Delft, Netherlands, <sup>4</sup>Faculty of Chemistry, Jagiellonian University in Kraków, Krakow, Poland, <sup>5</sup>Department of Chemical Engineering, La Laguna University, San Cristóbal de La Laguna (S/C de Tenerife), Spain

**Abstract Text:** Ordered mesoporous materials are nano-structures that can be used in catalysis, adsorption, sensing and separation, among others [1-3]. Mesoporous materials expand the pore-size of the zeolites; and therefore, overcome typical limitations in zeolites' catalysis. This allows an unrestricted diffusion of large-in-volume molecules for catalytic applications [4]. Such a control in the pore size was obtained by a new synthetic methodology using supramolecular organic molecules as structuring directing agents (SDA) in the sol-gel process. Those SDAs can be cationic, anionic and non-ionic (neutral) surfactants. They normally lead to mesoporous materials [1,5], though macroporosity is also feasible [6,7]. A key step is the SDA removal, which is conventionally done by calcination.

Calcination consists of a thermal treatment in air of the as-synthesized mesoporous material. Typical temperatures are 500-600 °C, at which the SDA is fully decomposed, though it is known that the local temperature can be higher due to hot-spots [8]. Calcination is very detrimental in the case of unstable mesoporous materials as the structure suffers irreversible damage; mesoporous materials synthesized without any hydrothermal treatment lay in this category (i.e. rapidly synthesized but ill-polymerized mesoporous materials). Other negative aspects about calcination are the high energy consumption and the slow pace of the process, as it requires a low heating rate. Therefore, from the process and material viewpoints, it can be useful to develop a suitable SDA removal strategy for this kind of materials.

When exploring state-of-the-art literature, a few methods have been proposed for SDA removal. Microwave processing looks attractive due to the short processing time. Tian et al. [9] proposed the use of a microwaves digestion to remove the template of SBA-15, which is known to be a hydrothermally stable material in liquid water. Applying such a methodology onto an ill-polymerized MCM-41 is not a rational choice since the materials' hydrothermal stability is very different than SBA-15, and collapse of the structure would be expected.

In this work, we systematically studied different SDA removal strategies (i.e. calcination, microwaves, solvent extraction, ozonation and Fenton chemistry) onto an ill-polymerized MCM-41, and the resulting properties were evaluated in terms of product structure, texture and surface chemistry. It was found that microwave processing was effective in removing all the SDA within short processing times, and the structure was preserved (this failed for the other methods, except for calcination). Therefore, microwaves and calcination are the only ones with potential. However, microwaves have two additional benefits over calcination. Firstly, it provides a much richer surface chemistry (more types of Si-OH groups). Secondly, from the energy consumption point of view, it consumes less energy. On the negative side, microwaves lead to some alteration of the porosity (broader pores) that was associated to local hot spots leading to hydrolysis. It is worth stating that this contribution brings additional benefits to the pioneer study [9], using a more complex material. Figures 1 and 2 provide a graphical overview of the benefits of microwave processing from the material point of view, in comparison to calcination, featuring a good structural ordering (Fig. 1a and Fig. 2c), good textural features with a high pore volume and surface area (Fig. 1b) but broader pore sizes (Fig. 1c) and, finally, a much richer surface chemistry (Fig. 2a and 2b). These topics will be expanded during the conference presentation, including the process aspects that have not been yet discussed here, due to space limitation. However, the reader is referred to Lopez-Perez et al. [10] for additional insights.

Figures 1 and 2 were adapted with permission from López-Pérez et al. ACS Sustainable Chem. Eng. 2020, 8, 16814–16822. Copyright 2020, American Chemical Society.

## Image 1:

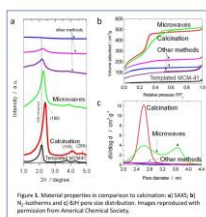
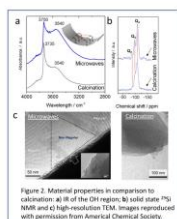


## Image 2:



**References:** [1] Zhao, D. Y.; Wan, Y.; Zhou, W. *Ordered Mesoporous Materials*; Wiley-VCH, Weinheim, 2013.

[2] Wang, Y.; Du, X.; Liu, Z.; Shi, S.; Lv, H. Dendritic fibrous nano-particles (DFNPs): rising stars of mesoporous materials, *J. Mater. Chem. A*, 2019, 7, 5111-5152. DOI: 10.1039/C8TA09815H.

[3] Wu, K. C.-W.; Jiang, X.; Yamauchi, Y. New trend on mesoporous films: precise controls of one-dimensional (1D) mesochannels toward innovative applications, *J. Mater. Chem.*, 2011, 21, 8934-8939. DOI: 10.1039/C1JM10548E.

[4] Parlett, C. M. A.; Wilson, K.; Lee, A. F. Hierarchical porous materials: catalytic applications, *Chem. Soc. Rev.*, 2013, 42, 3876-3893. DOI: 10.1039/C2CS35378D.

[5] Zhao, D. Y. in *Introduction to Zeolite Science and Practice*, Vol. 168 (Eds: Cejka, J.; van Bekkum, H.; Corma, A.; Schüth, F.) 3rd revised Ed.; Elsevier B.V.: Amsterdam, 2007, pp. 241-300.

[6] Imhof, A.; Pine, D. J. Ordered macroporous materials by emulsion templating, *Nature*, 1997, 389, 948-951. DOI: 10.1038/40105.

[7] Parlett, M. A.; Isaacs, M. A.; Beaumont, S. K.; Bingham, L. M.; Hondow, N. S.; Wilson, K.; Lee, A. F. Spatially orthogonal chemical functionalization of a hierarchical pore network for catalytic cascade reactions, *Nature Mater.* 2016, 15, 178-182. DOI: 10.1038/nmat4478.

[8] López Pérez, L.; Ortiz-Iniesta, M. J.; Heeres, H. J.; Melián-Cabrera, I. Hot-spots during the calcination of MCM-41: A SAXS comparative analysis of a soft mesophase, *Mater. Lett.* 2014, 118, 51-54. DOI: 10.1016/j.matlet.2013.11.091.

[9] Tian, B.; Liu, X.; Yu, C.; Gao, F.; Luo, Q.; Xie, S.; Tu, B.; Zhao, D. Y. Microwave assisted template removal of siliceous porous materials, *Chem. Commun.*, 2002, 1186-1187. DOI: 10.1039/B202180C.

[10] López-Pérez, L.; López-Martínez, M.A.; Djanashvili, K.; Góra-Marek, K.; Tarach, K.A.; Borges, M. E.; Melián-Cabrera, I., Process Intensification of Mesoporous Material's Synthesis by Microwave-Assisted Surfactant Removal, *ACS Sustainable Chem. Eng.* 2020, 8, 16814-16822. DOI: 10.1021/acssuschemeng.0c05438.

## ***New Synthetic Methods and Post-Synthetic Modification***

FEZA21-PO-209

### **Synthesis of robust *b*-oriented ZSM-5 zeolite membranes on coated porous ceramics in neutral fluoride media**

R. L. Riemersma\*, B. M. Weckhuysen<sup>1</sup>, E. Vogt<sup>1</sup>, A.-E. Nieuwelink<sup>1</sup>

<sup>1</sup>Inorganic Chemistry and Catalysis, Utrecht University, Utrecht, Netherlands

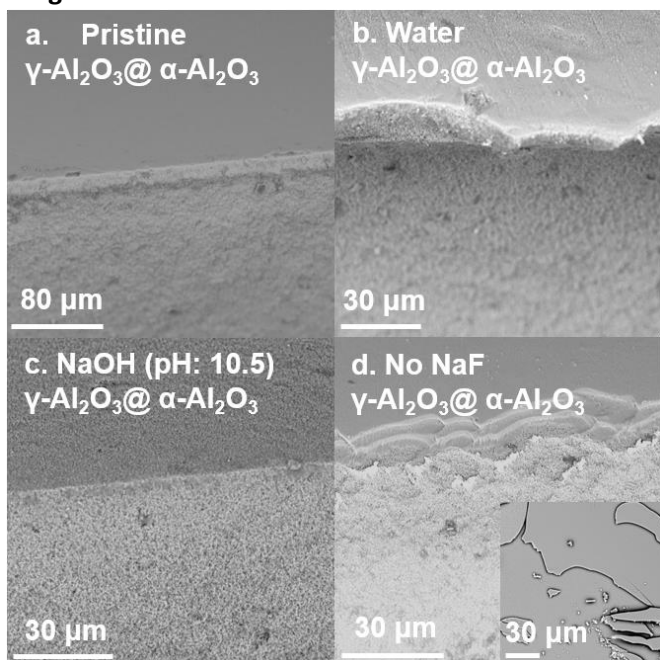
**Abstract Text:** The synthesis of *b*-oriented ZSM-5 zeolite membranes has garnered considerable attention in recent years. The combination of catalytically active ZSM-5 zeolites with the separation functionality of membranes opens up a path to promising applications in catalytic membrane reactors. Furthermore, the specifically controlled orientation means that only the straight channels of the zeolite ZSM-5 structure are accessible, enhancing molecular diffusion properties. Previous work in our group demonstrated the fabrication of ZSM-5 zeolite membranes by assembling monolayers of silicalite-1 seeds on porous ceramic supports, and growing these into *b*-oriented ZSM-5 films through the secondary growth method.<sup>[1]</sup> The porous ceramic support ensures mechanical and structural stability. They can be covered with a thin porous coating that gives several benefits; it provides a smooth surface enabling facile monolayer assembly of silicalite-1 seeds, it protects the support from leaching, and it provides a diffusion barrier during ZSM-5 zeolite film growth preventing penetration of the film into the support.

In this work, an  $\alpha$ -Al<sub>2</sub>O<sub>3</sub> support with a  $\gamma$ -Al<sub>2</sub>O<sub>3</sub> coating was used. However, the coatings suffer from delamination during secondary growth. We have investigated the cause and mechanism of delamination by treating the support in different media at hydrothermal conditions (in an autoclave) at 175°C for 24 h (Fig. 1). The  $\gamma$ -Al<sub>2</sub>O<sub>3</sub> coating of the NaOH (pH = 10.5) treated support disappeared entirely. Therefore, it was suspected that hydrolysis of the coating in the alkaline growth medium (pH = 11) was the cause. Further investigation showed that delamination became more severe as the secondary growth medium's pH moved further away from neutral. In addition, a neutral fluoride-based secondary growth method was developed that circumvents delamination and results in predominantly *b*-oriented zeolite ZSM-5 films. It was found that TPABr was essential to stimulate secondary growth, whereas the *b*-orientation could be partially brought back using (NH<sub>4</sub>)<sub>2</sub>SO<sub>4</sub>.

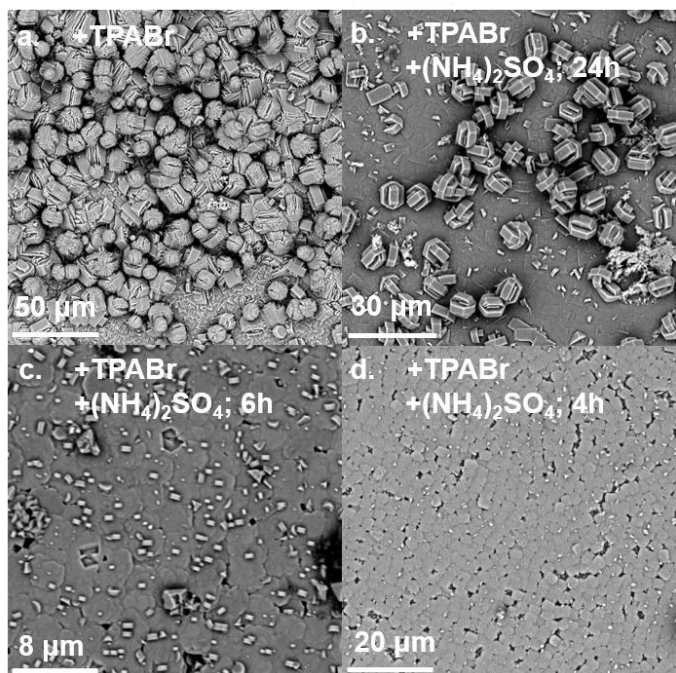
Fig. 1: Illustration of delamination. a. SEM image of pristine  $\gamma$ -Al<sub>2</sub>O<sub>3</sub> coated  $\alpha$ -Al<sub>2</sub>O<sub>3</sub>.  $\gamma$ -Al<sub>2</sub>O<sub>3</sub> coated  $\alpha$ -Al<sub>2</sub>O<sub>3</sub> treated in b. water, c. NaOH solution (in water, pH = 10.5), d. secondary growth medium without NaF.

Fig. 2: ZSM-5 zeolite film grown at different growth times on  $\gamma$ -Al<sub>2</sub>O<sub>3</sub> coated  $\alpha$ -Al<sub>2</sub>O<sub>3</sub> support in secondary growth media of various composition at pH = 8. a. TPA/Si = 0.098, t = 24h b. TPA/Si = 0.098, NH<sub>4</sub>/Si = 0.0364, t = 24h, c. TPA/Si = 0.098, NH<sub>4</sub>/Si = 0.0364, t = 6h, d. TPA/Si = 0.098, NH<sub>4</sub>/Si = 0.0364, t = 4 h.

**Image 1:**



**Image 2:**



**References:** [1] D. Fu et al., *Angew. Chem. Int. Ed.*, 2018, 57, 38; doi: 10.1002/anie.201806361.

## ***New Synthetic Methods and Post-Synthetic Modification***

FEZA21-PO-210

### **Unique roles of heteroatoms in the synthesis of zeolite catalysts**

D. Parmar<sup>1,\*</sup>, A. Mallete<sup>1</sup>, L. C. Grabow<sup>1</sup>, J. D. Rimer<sup>1</sup>

<sup>1</sup>Department of Chemical and Biomolecular Engineering, University of Houston, Houston, United States

**Abstract Text:** The incorporation of heteroatoms has opened up various new and exciting avenues for the synthesis and applications of traditional (alumino)silicate zeolites. The role of metals in zeolite synthesis ranges from adjusting catalyst acidity by isomorphous substitution of atoms like B, P, Fe, Sn and Ti, to directing crystal structure and/or acid siting within the zeolite framework. Heteroatoms in zeolites have also led to the development of bifunctional catalysts where heteroatoms typically act as primary active sites while framework aluminum and nanopores of zeolites provide Brønsted acid sites and shape selectivity, respectively. Here, we present two cases where incorporation of heteroatoms in zeolite synthesis leads to significant improvements in their physiochemical properties in unexpected ways.

The first example will highlight a facile and generalizable strategy to synthesize nano-sized zeolites using inexpensive metals as heteroatoms. The latter act as zeolite growth modifiers to reduce crystal size (<100 nm) and/or change the morphology of various framework types (e.g. MEL, MFI and MOR). We will show how these unique features lead to significant improvement in their diffusion properties and hence, their performance in different catalytic applications.

The synthesis of high silica faujasite (FAU) has been a challenge via organic-free routes. We have developed an organic-free method to generate a FAU zeolite (HOU-3) with the highest Si/Al ratio (~ 3). In this presentation, we will discuss a new method to achieve FAU with Si/Al = 3.5 via the addition of zinc oxide in the synthesis gel. In addition, we will demonstrate how this high-silica FAU material performs as a bifunctional catalyst compared to conventional zeolite Y analogues.

Overall, we will show how the judicious selection of heteroatoms can be used to tailor the properties and performance of zeolite catalysts, leading to significant improvements in zeolite properties that extend beyond those obtained by conventional zeolite syntheses.

**Design synthesis of (extra)-large pore zeolite by interlayer expansion**

H. Xu\*, B. Yang<sup>1</sup>, J. Jiang<sup>1</sup>, H. Wu<sup>1</sup>, P. Wu<sup>1</sup>

<sup>1</sup>School of Chemistry and Molecular Engineering, East China Normal University, Shanghai, China

**Abstract Text: 1. Introduction**

(Extra)-large pore zeolites, with the pores larger than 12-member rings (R), have showed great potential in processing bulky substrates. The interlayer expansion of layered zeolites, with hydrogen bonded frameworks continuously extended in two dimensions, provide an important strategy to design synthesis of (extra)-large pore zeolite *via* top-down post-modification.<sup>1,2</sup> Normally, the monomer silane could introduce two additional Si atoms, while dimeric silane introduces four into interlayer space. In the present study, bulky silanes, including dimeric silane of 1,2-dichlorotetramethyldisilane (ClMe<sub>2</sub>Si-SiMe<sub>2</sub>Cl, DCTMDS) and single 4R shaped silane of 1,3,5,7-tetramethylcyclotetrasiloxane (TMCS) were used to achieve the silylation of FER-type layered zeolites. For the PREFER layered zeolite synthesized with large amines as SDAs, these bulky silanes could be directly inserted into the interlayer space, while a structural deconstruction-reconstruction strategy was needed in the silylation of PLS-3 layered zeolite with FER topology but narrower interlayer space.<sup>3</sup>

**2. Experimental**

The PREFER zeolite was silylated with diethoxydimethylsilane (DEDMS), DCTMDS and TMCS in 1M HNO<sub>3</sub> solution with the liquid/solid mass ratio of 30 and the silane amount of 2 mmol per gram zeolite. The layered PLS-3 was firstly treated in HCl/Ethanol solution at 443 K for 40 min to give ECNU-8 sub-zeolite. By immersing ECNU-8 zeolite in 4-amion-2,2,6,6-tetramethylpiperidine solution for 20 h, an analogy of PREFER was prepared and named as ECNU-9(P). Finally, ECNU-9 zeolite was synthesized by the structural expansion of ECNU-9(P) with TMCS silane in HCl/Ethanol. Ti active sites were introduced into ECNU-9 by post-treating in H<sub>2</sub>TiF<sub>6</sub> aqueous solutions.

**3. Results and discussion**

A direct calcination burned off the organic species incorporated in PREFER, and induced a topotactic transformation of 2D precursor to 3D crystalline material with interlayer 10R and 8R pores along [001] and [010], respectively (Figure 1A, a and b). The silylation with different silanes lead the 200 reflection shift to lower angles compared to 3D FER, indicating increased interlayer space. The interlayer expanded FER(DCTMDS) and FER(TMCS) showed very similar XRD patterns (Figure 1A, d and e) with the 200 reflection appearing at lower position than FER(DEDMS). The HRTEM, Ar adsorption, structural refinement all confirmed that the FER(DCTMDS) and FER(TMCS) possessed 14R and 12R pores. However, the detailed structure viewed along [001] direction was different as shown in Figure 2A.

PLS-3 layered zeolite, synthesized with smaller SDA than PREFER, showed nanosized particle size, which would exhibited much higher activity than micro-sized PREFER related materials. However, the direct insertion of S4R shaped TMCS failed to give interlayer expanded structure analogous to FER(TMCS) but produced the structure similar to FER(DEDMS), suggesting that the interlayer space of PLS-4 is too small to introduce bulky silanes. A deconstruction-reconstruction strategy was performed (Figure 2B). The layered PLS-3 precursor was firstly disassembled into a sub-zeolite ECNU-8 composed of FER-type nanosheets (Figure 1Bb), which were then reorganized with the help of a classical bulky SDA for PREFER synthesis (Figure 1Bc). With enough expanded interlayer space, the TMCS silane molecules are introduced as linkers to interconnect the up-down layers, creating new 14R and 12R pores (Figure 1Be). With open pore system and less diffusion constrains, Ti-incorporated ECNU-9 showed superior catalytic performance for bulky substrates.

**4. Conclusion**

Interlayer expansion of layered zeolite with bulky silanes is an effective way to design synthesis (extra)-large pore zeolite. For layered zeolite with smaller interlayer space, the structural deconstruction-reconstruction method could increase the interlayer space without ruining the framework crystallinity, which is potentially expanded to other layered precursors.

**Image 1:**

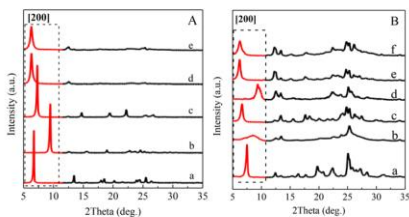


Figure 1. XRD pattern of (A) PREFER(a), 3D FER (b), PREFER silylated with monomer silane (c), C1Me<sub>2</sub>Si-SiMe<sub>2</sub>Cl (d) and TMCS (d) in calcined form; (B) PLS-3 (a), ECNU-8 (b), ECNU-9(P) (c), ECNU-9(P)-cat823 (d), ECNU-9 (e), and ECNU-9-cat823 (f)

## Image 2:

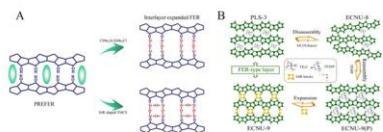


Figure 2. Schematic description of the structural changes in the silylation of FER-type PREFER and PLS-3 layered zeolite

- References:** 1. P. Wu, J. Ruan, L. Wang, L. Wu, Y. Wang, Y. Liu, W. Fan, M. He, O. Terasaki, T. Tatsumi, *J. Am. Chem. Soc.*, 2008, 130, 8178–8187.  
 2. H. Xu, L. Fu, M. He, P. Wu, *Micropor. Mesopor. Mater.*, 2014, 189, 41-48.  
 3. B. Yang, J. Jiang, H. Xu, H. Wu, M. He, P. Wu, *Angew. Chem. Int. Ed.*, 2018, 57, 9515-9519.

## ***New Synthetic Methods and Post-Synthetic Modification | Zeolites/Inorganic materials***

FEZA21-PO-212

### **One shot synthesis of hierarchical MFI-type zeolite beads**

K. Moukahhal<sup>1</sup>, B. Lebeau<sup>1</sup>, L. Josien<sup>1</sup>, H. Nouali<sup>1</sup>, J. Toufaily<sup>2</sup>, T. Hamieh<sup>2</sup>, A. Galarneau<sup>3</sup>, J. Daou<sup>1,\*</sup>

<sup>1</sup>University of Haute Alsace, CNRS, Institut of Material Science of Mulhouse UMR 7361, Mulhouse, France, <sup>2</sup>Lebanese University, Laboratory of Materials, Catalysis, Environment and Analytical Methods Faculty of Sciences, Section I, Beyrouth, Lebanon, <sup>3</sup>Institut Charles Gerhardt Montpellier, UMR 5253 CNRS, CNRS, Montpellier, France

**Abstract Text:** Due to the multiple applications of zeolites, such as molecular sieving, ion exchange, adsorption and catalysis, increasing attention has been paid worldwide to the preparation of zeolite in suitable form for industrial applications. Zeolite beads are often preferable for continuous flow-based applications due to limitation of large pressure losses and clogging effects and for easy handling. However, despite their excellent properties, the conventional zeolite crystals are micron-size that often lead to low adsorption capacities and relatively slow diffusion kinetics. To overcome this problem, the ideal solution is to reduce the size of the crystals constituting the beads beyond the nanoscale and create additional mesoporosity inside or between the crystals to improve the diffusion and increase the capacity of adsorption of small molecules such as volatile organic compounds (VOCs) [1]. Most shaping processes require several steps: adding binders or macrotemplates, sieving... Among these methods, pseudomorphic transformation seems to be a promising alternative. To our knowledge, it is the only method to directly obtain zeolite beads in a single step without using sacrificial binders or macrotemplates. It consists in changing the nature of the material without modifying its macroscopic morphology by dissolving the initial phase which serves as raw material, followed by a simultaneous precipitation of the targeted phase [2].

In this work, the concept of pseudomorphic transformation has been applied to transform spheres of amorphous mesoporous silica with different sizes (20, 50 and 75  $\mu\text{m}$ ) but having similar pore sizes (6-8 nm) into MFI-type hierarchized beads composed of ZSM-5 nanosheets [2]. Well-crystallized 20  $\mu\text{m}$  ZSM-5 nanosheets beads similar in size and shape to the original mesoporous amorphous silica beads were obtained after a hydrothermal treatment at 150  $^{\circ}\text{C}$  for 5 days in a tumbling oven and 2 days in static conditions at 120  $^{\circ}\text{C}$ . The influence of the bead size on the pseudomorphic transformation was studied in order to prepare well-crystallized ZSM-5 nanosheets beads of 50 and 75  $\mu\text{m}$ . Results showed that the required time of static treatment at 120 $^{\circ}\text{C}$  increases when the size of the parent silica spheres increases.

**References:** [1] I. Kabalan, G. Rioland, H. Nouali, B. Lebeau, S. Rigolet, M.-B. Fadlallah, J. Toufaily, T. Hamiyeh, T.J. Daou, *RSC Adv.* 2014, 4, 37353.

[2] K. Moukahhal, T.J. Daou, L. Josien, H. Nouali, J. Toufaily, T. Hamieh, A. Galarneau, B. Lebeau, *Microporous and Mesoporous Materials*, 2019, 288, 109565.

## ***New Synthetic Methods and Post-Synthetic Modification | Zeolites/Inorganic materials***

FEZA21-PO-213

### **Zeolite pellets as a major solution for molecular decontamination in space**

M. Diboune<sup>1</sup>, G. Rioland<sup>2</sup>, H. Nouali<sup>3</sup>, D. Faye<sup>2</sup>, J. Patarin<sup>3</sup>, J. Daou<sup>3,\*</sup>

<sup>1</sup>University of Haute Alsace, French Space Agency (CNES), Mulhouse, <sup>2</sup>CNES, French Space Agency (CNES), Toulouse,

<sup>3</sup>University of Haute Alsace, CNRS, Institut of Material Science of Mulhouse UMR 7361, Mulhouse, France

**Abstract Text:** Space industries are really concerned by a major issue: molecular contamination. Indeed, once satellites are in orbit, molecules contained in paints, adhesives or glues can outgas and form films or droplets on the surface of mirrors, lenses, solar cells or thermal detectors. The National Aeronautic and Space Administration (NASA) and the French Space Agency (CNES) have investigated the chemical nature of these molecules; hydrocarbons and plasticizers were identified as the most important part of the outgassed molecules [1]. Those molecules can deposit on the surface of on-boarded equipment like optics and damage them. After testing several porous materials as molecular adsorbents to fix the molecular contamination issue, zeolites have been designed as the ideal candidates thanks to their great adsorption capacities, and especially their ability to trap the volatile organic compounds at very low concentration in the atmosphere. Synthetic zeolites are generally obtained as powders leading to non-bonded particles. In space application, zeolite have to be shaped to avoid particulate contamination. Nonetheless, it is necessary to introduce additives to increase the mechanical properties of the shaped zeolites. Usually, very large amounts of binders, such as clays, silica based compounds or aluminum base compounds are used to link zeolite crystals together in order to produce bodies with high mechanical resistance and optimal dimensions. Hence, methods that allow the preparation of zeolite pellets with a small amount of binder and a high mechanical resistance are highly desired.

In this work, two hydrophilic (LTA and FAU) and two hydrophobic zeolites (MFI and \*BEA) have been chosen to make zeolite pellets using the less possible binder amount (5 wt. % of methylcellulose (MC) or sodium metasilicate (Na<sub>2</sub>SiO<sub>3</sub>)) without affecting a lot the adsorption properties. The adsorption properties of these zeolite pellets were then studied using 2 VOCs (n-hexane and cyclohexane). These 2 molecules were chosen to simulate pollutants potentially present in satellites [2,3]. The influence of the amount of binder and the compression load on the ultimate compressive strengths of pellets were investigated. It was shown that the optimum amount of binder is 5 wt. %: above this amount, the mechanical resistance does not increase. If the compression load increases (from 2 to 8 tons), the mechanical resistance of the pellet increases as well (from 35 MPa to 171 MPa). Nitrogen sorption-desorption has also been carried out to evaluate the influence of the presence of binder and the compression load on the adsorption capacities of zeolite pellet. If the compression load is too important, the micropore volume is lower of 10 %. The presence of binder does not affects the adsorption capacities. Nitrogen sorption-desorption revealed a small loss of micropore volume (10 %) with a compression load of 6 tons (0.24 cm<sup>3</sup>.g<sup>-1</sup> instead of 0.27 cm<sup>3</sup>.g<sup>-1</sup> for the mixture of FAU and \*BEA-types zeolites powders), which can be attributed to a partial amorphization. Adsorption kinetics of n-hexane, and cyclohexane showed that the optimum pellets can adsorb volatile organic compounds. For example, FAU-\*BEA-type zeolite powder mixture (50 wt. % of each zeolite) adsorb 130 mg of n-hexane per g of anhydrous zeolite whereas the pellets made with 5 wt. % of MC or Na<sub>2</sub>SiO<sub>3</sub> adsorb about 118 mg of n-hexane per g of anhydrous zeolite. These results are coherent with the ones obtained with the cyclohexane and nitrogen adsorption where a small loss of the adsorption capacities was observed.

Zeolitic pellets are the ideal candidates for molecular decontamination in space. Indeed, their great mechanical resistance and high adsorption capacities make them unavoidable to trap pollutants and to protect sensible devices. These pellets were already used for molecular decontamination in Curiosity robot (Chemcam part) that have been sent to Mars planet by NASA.

**References:** 1- J.L. Perry, NASA Technical Memorandum, 108497, 4-9 (1995).

2- G. Rioland, T.J. Daou, D. Faye, J. Patarin, Microporous Mesoporous Mater., 221, 167-174 (2016).

3- G. Rioland, H. Nouali, T.J. Daou, D. Faye, J. Patarin, Adsorption, 23, 395-403 (2017).

## ***New Synthetic Methods and Post-Synthetic Modification | Zeolites/Inorganic materials***

FEZA21-PO-214

### **Ab initio investigation of the respective stability of silicogermanates and their (Alumino)silicates counterparts**

E. EL HAYEK<sup>1,2,\*</sup>, B. Harbuzaru<sup>1</sup>, J. Martens<sup>2</sup>, C. Chizallet<sup>1</sup>

<sup>1</sup>Catalysis, Biocatalyse and Separation Division, IFP Energies nouvelles, Lyon, France, <sup>2</sup>Center for Surface Chemistry and Catalysis, KU Leuven, Leuven, Belgium

**Abstract Text:** The introduction of Germanium into the synthesis medium of zeolites has played a special role for about twenty years in the discovery of new zeolite structures. Ge allowed the formation of many open structures with large pores, e.g. the IM-12 zeolite (structural type UTL)<sup>[1]</sup> having pore openings with 12 and 14 tetrahedral atoms. However, the interest of germanium is counterbalanced by two major drawbacks which lie in the ease of hydrolysis of the Ge-O bond, and the absence of acid sites. Therefore, these zeolites are unstable in the presence of ambient air humidity after calcination and are deficient of active sites, which limit their use as adsorbents or catalysts. The stabilization of Ge-containing zeolites has been explored experimentally by post-treatment steps through the direct substitution of Ge for another structural element such as aluminum (e.g. ITQ-17 zeolite)<sup>[2]</sup>. Periodic density functional theory (DFT) calculations show that for ITQ-44 (IRR), the Ge→Si and {Si or Ge}→{Al and H} substitutions are thermodynamically favorable reactions<sup>[3]</sup>.

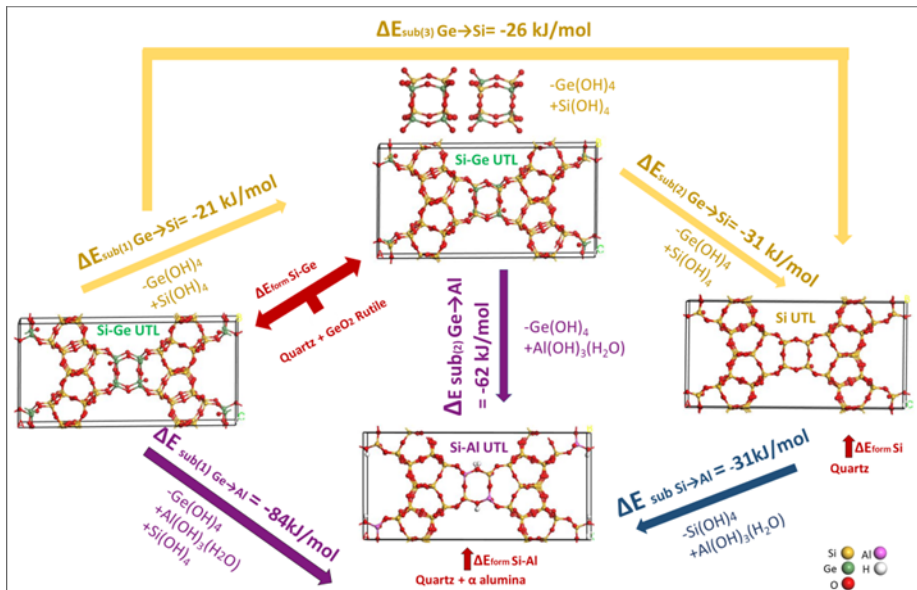
In the presented work, we aim to quantify systematically the respective stability of all silicogermanates known in the literature, with respect to their silicate and aluminosilicates counterparts, accounting for the framework relaxation effect. The ultimate goal is to pave the way for experimental Ge→Si and {Si or Ge}→{Al and H} substitutions on well-chosen frameworks, to obtain stable and active zeolitic solids (Figure 1). Periodic DFT calculations (VASP code, PAW, PBE-dDsC functional) include a relaxation of the cell parameters (energy cut-off: 800 eV) during the systematic search for the stability of the substituted networks. The stability, substitution energies and free energies are quantified with respect to several sets of references (pure Si, Ge or Al inorganic solids, molecular chlorides or hydroxides).

The results show that it is favorable to obtain a pure silicic or aluminosilicate UTL structure even if it is not possible to date to synthesize this solid without Ge. Thus to understand the geometric effect on zeolites' stability, the same investigation has been carried on all the silicogermanates attributed by the international zeolite association (24 structures). Here we show, that thermodynamically all the silicogermanate structures can exist either in aluminosilicate or silicic forms. Also, substituting Ge→Al is preferential compared to Si→Al substitution (Figure 1).

On the other hand, it is seen that an inverse relationship between the stability of the silicic structures and the number of double four ring (d4r) units in the framework exist. Meanwhile a proportional correlation is revealed between the framework density and the stability of the structures. In addition, the effect of the Ge distribution was studied. It is seen that the substitution is nearly independent of the Ge position inside the d4r. Furthermore, the substitution is not strongly affected by the d4r distribution between the different structures.

Besides, ongoing experimental works, prove the successful stabilization of silicogermanates through the proposed treatments giving zeolites with promising catalytic activity.

**Image 1:**



- References:** [1] J.L Paillaud, B. Harbuzaru, J. Patarin and N. Bats, Science, 304, 990, (2004).  
 [2] F.Gao, M. Jaber, K. Bozhilov, A. Vicente, C. Fernandez and V. Vatchev, J. Am. Chem. Soc.,131, 16580 (2009).  
 [3] St.P. Petkov, H.A. Aleksandrov, V. Valtchev and G.N. Vayssilov, Chem. Mater., 24, 2509 (2012).

## ***New Synthetic Methods and Post-Synthetic Modification | Zeolites/Inorganic materials***

FEZA21-PO-215

### **Mechanochemically Assisted Hydrolysis in the ADOR Process**

D. N. Rainer<sup>1,\*</sup>, C. M. Rice<sup>1</sup>, S. E. Ashbrook<sup>1</sup>, R. E. Morris<sup>1,2</sup>

<sup>1</sup>School of Chemistry, University of St Andrews, St Andrews, United Kingdom, <sup>2</sup>Department of Physical and Macromolecular Chemistry, Charles University, Prague, Czech Republic

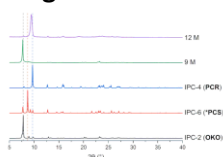
**Abstract Text:** The ADOR (Assembly-Disassembly-Organization-Reassembly) process has been shown to be a successful methodology producing zeolites inaccessible through conventional hydrothermal procedures.<sup>1,2</sup> It revolves around the lability of Ge–O bonds towards hydrolysis, relative to Si–O, enabling controlled breakdown of the framework of a parent zeolite phase into its layered precursor analogue. Subsequent rearrangement, potentially aided by additives, and condensation leads to daughter materials exhibiting new frameworks.

Mechanochemical methods such as ball milling have great potential to improve chemical synthesis procedures in terms of efficiency and reduction of waste material. Applications in zeolite chemistry have already led to improvements in areas such as reaction time and required amounts of solvent.<sup>3,4</sup>

In an effort to increase the value of the ADOR process, especially in regard to eventual industrial applications, the usage of ball milling during the disassembly step of zeolite **UTL** was investigated. Both water and hydrochloric acid in different concentrations were used as hydrolysis agents, using increased zeolite/liquid ratios compared to previously published studies. Generally, partly disassembled and organized materials IPC-2P/IPC-6P were obtained, which act as direct precursors to their reassembled counterparts IPC-2 (**OKO**)<sup>5</sup> and IPC-6 (**\*PCS**)<sup>6</sup>. PXRD patterns of as made products are indifferent to the acid concentration, however, reassembled materials vary significantly. Noteworthy products of acid treated samples are obtained using 9 M and 12 M HCl resulting in **OKO** and **PCR**-type frameworks, respectively (see Image 1). Experiments employing water as reagent also lead to materials with **OKO** framework.

The required volume of water for hydrolysis was also shown to be reducible to 100  $\mu$ l for 500 mg of parent zeolite. This allows for a cost-efficient reaction with <sup>17</sup>O enriched water (40%). The produced material was enriched with this NMR-active oxygen isotope demonstrating the possibility for a fast and feasible enrichment procedure with the presented methodology.

#### **Image 1:**



**References:** [1] W.J. Roth, P. Nachtigall, R.E. Morris, P.S. Wheatley, V.R. Seymour, S.E. Ashbrook, P. Chlubná, L. Grajcar, M. Položij, A. Zukal, O. Shvets and J. Čejka, *Nat. Chem.* 5, 628–633 (2013).

[2] P. Eliášová, M. Opanasenko, P.S. Wheatley, M. Shamzhy, M. Mazur, P. Nachtigall, W.J. Roth, R.E. Morris and J. Čejka, *Chem. Soc. Rev.* 44, 7177–7206 (2015).

[3] R.E. Morris and S.L. James, *Angew. Chem. Int. Ed.* 52(8), 2163–2165 (2013).

[4] G. Majano, L. Bochart, S. Mitchell, V. Valtchev and J. Pérez-Ramírez, *Microporous Mesoporous Mater.* 194, 106–114 (2014).

[5] M. Mazur, M. Kubů, P.S. Wheatley and P. Eliášová, *Catal Today* 243, 23–31 (2016).

[6] S.A. Morris, G.P.M. Bignami, Y. Tian, M. Navarro, D.S. Firth, J. Čejka, P.S. Wheatley, D.M. Dawson, W.A. Slawinski, D.S. Wragg, R.E. Morris and S.E. Ashbrook, *Nat. Chem.* 9, 1012–1018 (2017).

## ***New Synthetic Methods and Post-Synthetic Modification | Zeolites/Inorganic materials***

FEZA21-PO-216

### **Desilicated MWW zeolites synthesized from rice-based waste materials**

A. J. Schwanke<sup>1</sup>, J. F. Gomes, A. Sachse<sup>2</sup>, J. R. Gregorio<sup>1</sup>, K. Bernardo-Gusmao<sup>1,\*</sup>

<sup>1</sup>Instituto de Química, UFRGS, Porto Alegre, Brazil, <sup>2</sup> Institut de Chimie des Milieux et Materiaux de Poitiers, Université de Poitiers, Poitiers, France

#### **Abstract Text:**

Zeolites are crystalline microporous materials extensively used in adsorption, separation and catalysis<sup>1-3</sup>. A sustainable and cost-efficient approach to obtain desilicated MWW-type zeolites was developed through the use of silica from rice husk ash, which is the largest agro-industrial waste product in the world<sup>4</sup>. The effect of the leaching procedure of the rice husk silica and concentration of OH<sup>-</sup> ions were evaluated to obtain MWW zeolites with optimal conditions, which is after desilicated by post synthetic modification<sup>5</sup>. The obtained materials were characterized by Powder X-ray diffraction (XRD); Nitrogen adsorption and desorption isotherms at -196 °C; Inductively coupled plasma optical emission spectrometry (ICP-OES); Field-emission scanning electron microscopy (FESEM); Transmission electron microscopy (TEM); Fourier transform infrared (FTIR) spectroscopy with adsorption-desorption of pyridine; <sup>29</sup>Si and <sup>27</sup>Al nuclear magnetic resonance (NMR). The results show the leaching of silica from rice husk ash is not a necessary condition to obtain MCM-22 with high crystallinity. The optimal materials were named R-MCM-22 (Si/Al=19), R-MCM-22 (Si/Al=10) and desilicated D-R-MCM-22 (Si/Al=7). Therefore, an environmentally benign synthesis (without the use of HCl as strong acid, high temperature, and large water volume for neutralizing the acidic pH) was disclosed through using calcined rice husk directly as the silica source. We have demonstrated that silica extracted from rice husk ash plays a key role during the synthesis of MCM-22 zeolites and the presence of cations has a further important impact when used as a silica source decreasing the crystallization time. These cations also influenced the synthesis of MCM-49 which its 3D structure was not obtained by direct synthesis and confirming that the cations may influencing the formation of 2D MCM-22 precursor. The procedure to achieve desilicated materials featured a hierarchically MWW zeolite with intracrystalline mesopores ranging from 2 – 5 nm as shown in **Image 1** [*N<sub>2</sub> adsorption and desorption isotherms at -196 °C (a) and NLDFT pore size distribution (b) of R-MCM-22 (Si/Al=19), R-MCM-22 (Si/Al=10) and desilicated D-R-MCM-22 (Si/Al=7) samples*].

The impact of texture and acidity on the catalytic cracking of LDPE due to their branched polyethylene chains (with diameters of 0.49 nm) can be considered a suitable probe reaction for the diffusion limited reactions, as shown in **Image 2** [*LDPE conversion versus temperature (a) and correlation between the catalytic activity (T<sub>50</sub>, temperature at 50% conversion) during pyrolysis tests (b) over the acidic R-MCM-22 (Si/Al=19), R-MCM-22 (Si/Al=10) and desilicated D-R-MCM-22 (Si/Al=7). Heating rate 20 °C min<sup>-1</sup>*].

The uncatalyzed pyrolysis herein shows that 50% of LDPE was decomposed at 446 °C, i.e. T<sub>50</sub> = 446 °C. T<sub>50</sub> was reduced to ca. 428 °C when R-MCM-22 (Si/Al=10) was used as catalyst, which was shifted by ca. 18 °C to lower temperature. The R-MCM-22 (Si/Al=19) presents T<sub>50</sub> = 421 °C and desilicated D-R-MCM-22 (Si/Al=7) presents T<sub>50</sub> = 403 °C and indicate a decrease of T<sub>50</sub> by 43 °C, which can be attributed to the increase of external surface area and the presence of intracrystalline mesopores after desilication.

Image 1:

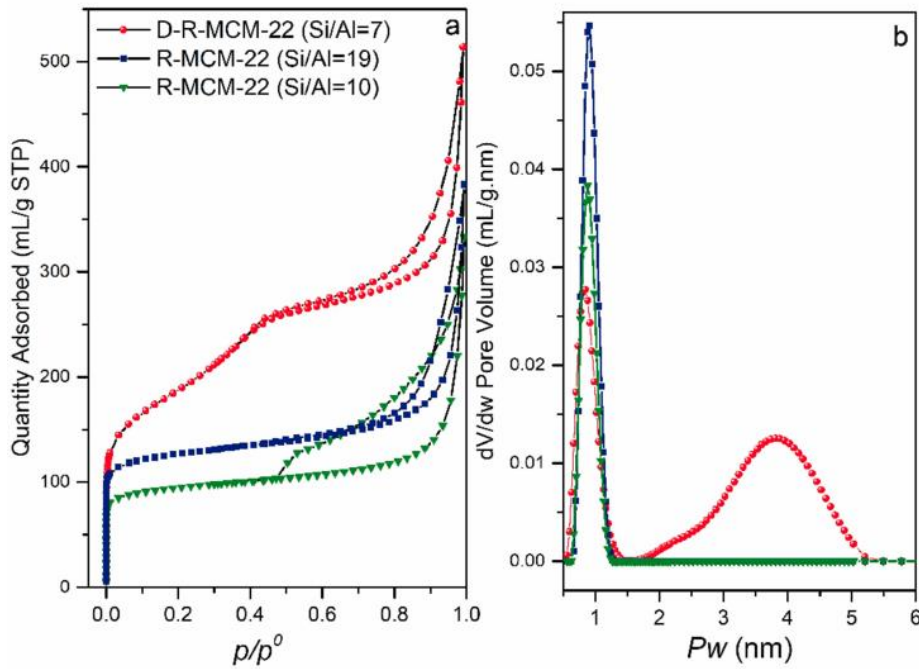
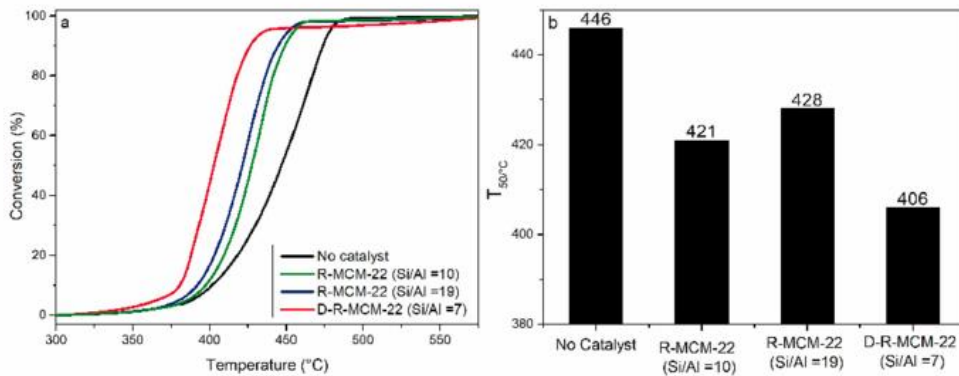


Image 2:



**References:** (1) Li, C.; Moliner, M.; Corma, A., Building Zeolites from Precrystallized Units: Nanoscale Architecture. *Angew. Chem. Int. Ed.* 2018, 57, (47), 15330-15353.

(2) Li, Y.; Cao, H.; Yu, J., Toward a New Era of Designed Synthesis of Nanoporous Zeolitic Materials. *ACS Nano* 2018, 12, (5), 4096-4104.

(3) Dusselier, M.; Davis, M. E., Small-Pore Zeolites: Synthesis and Catalysis. *Chem. Rev.* 2018, 118, (11), 5265-5329.

(4) Pode, R., Potential applications of rice husk ash waste from rice husk biomass power plant. *Renewable and Sustainable Energy Reviews* 2016, 53, 1468-1485.

(5) Gomes, J. F.; Sachse, A.; Gregório, J. R.; Bernardo-Gusmão, K.; Schwanke, A. J., Sustainable Synthesis of Hierarchical MWW Zeolites Using Silica from an Agro-industrial Waste, Rice Husk Ash. *Crystal Growth & Design* 2020, 20, (1), 178-188.

**Formation pathway of AEI zeolites as a basis for a streamlined synthesis**

N. Tsunoji<sup>1,\*</sup>, D. Shimono<sup>1</sup>, K. Tsuchiya<sup>1</sup>, M. Sadakane<sup>1</sup>, T. Sano<sup>1</sup>

<sup>1</sup>Graduate school of engineering, department of applied chemistry, Hiroshima University, Higashi-hiroshima, Japan

**Abstract Text:** In the past decade or so, small-pore zeolites with eight-membered tetrahedral (T)-atom-oxygen rings (8MRs) have received much attention.<sup>1</sup> CHA zeolites are well-known candidates to be applied commercially in light olefin production (especially for methanol-to-olefin, MTO) and exhaust cleaning (the selective catalytic reduction of NO<sub>x</sub> by ammonia, NH<sub>3</sub>-SCR). In contrast, the catalytic merit of another small-pore zeolite, AEI, has been reported in recent year, where their catalytic selectivity and durability were superior to the industrial standard CHA zeolite.<sup>2,3</sup> Correspondingly, in the past several years, the synthesis of AEI zeolite has progressed remarkably. Various synthesis systems focusing on the control of their framework composition and crystal size, decrease of synthesis cost, one-pot phosphorus modification, and crystallization behavior have been reported.<sup>4</sup> However, existing AEI zeolite synthesis recipes involve the use of FAU zeolite as alumina or as a specific silica/alumina source. This unavoidable starting material causes indirect and multistep synthesis requirements and complicate the entire synthesis system and crystallization phenomenon, thus hindering further development of the synthesis system.

Herein, we investigated the formation process of AEI zeolite using a combination of analysis methods, including X-ray diffractometry, nuclear magnetic resonance, and electrospray-ionization mass spectrometry, and developed a rational synthesis method without the use of a specific silica/alumina source (FAU zeolite).<sup>5</sup> First, the synthesis condition was optimized by selecting a variety of synthesis components: FAU zeolites with different Al contents, colloidal silica, sodium aluminate, and three types of organic structure-directing agents (OSDAs, *N,N*-dimethyl-3,5-dimethylpiperidinium (DMDMP), *N,N*-diethyl-2,6-dimethylpiperidinium (DEDMP), and tetraethylphosphonium (TEP) hydroxides).

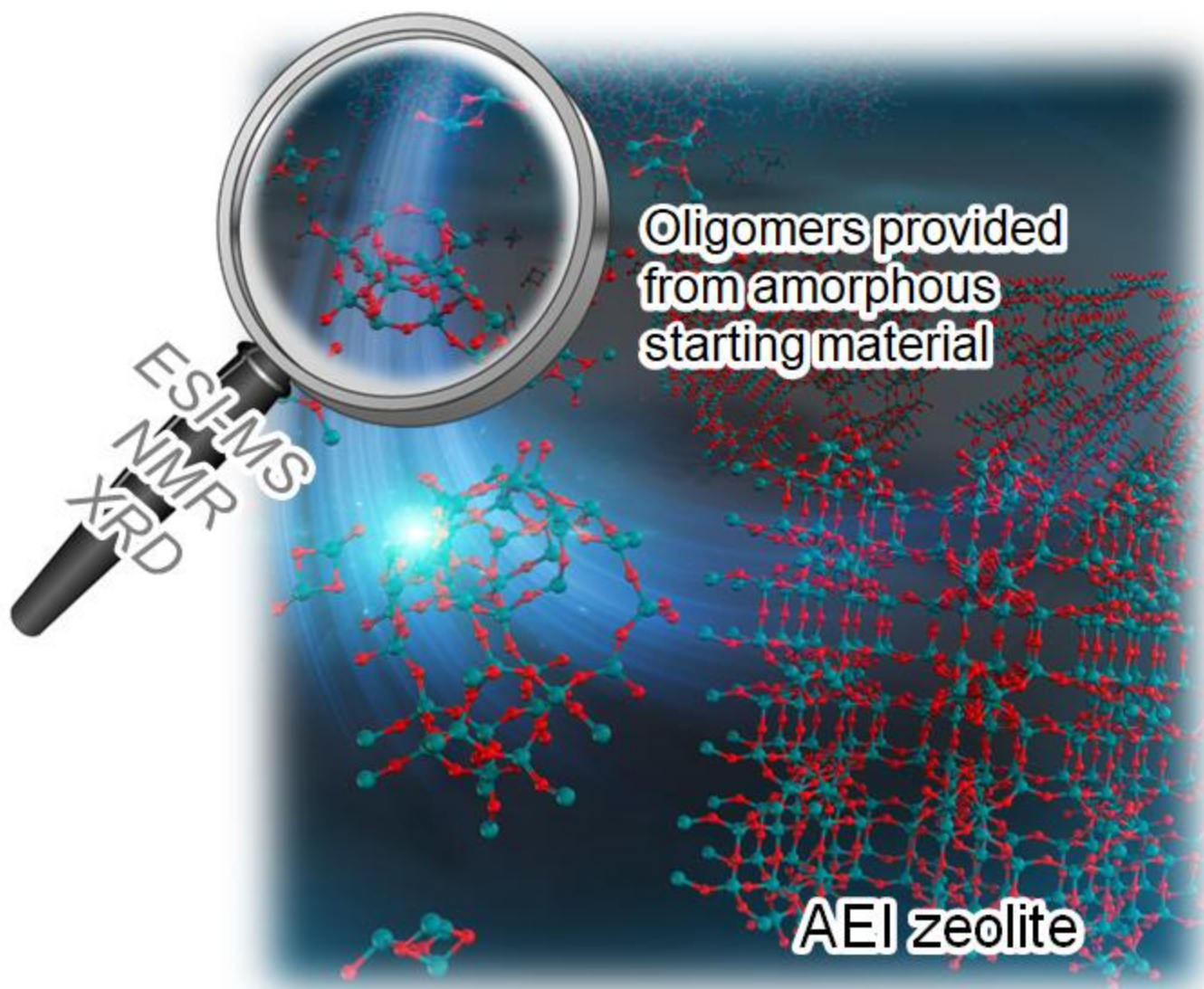
AEI zeolite preintroduced into the synthesis system (seed crystal) effectively functions to improve the product phase selectivity, which enabled crystal growth of AEI zeolite from an easily available amorphous silica/alumina source.

Stepwise gel preparation (SGP)<sup>6</sup> through divided compositional control using an amorphous starting material gave a higher compatibility on the AEI zeolite synthesis compared with the conventional gel preparation method (mixing all synthesis components in one step). SGP method provided AEI zeolite in the presence of two types of OSDAs (DMDMP and DEDMP).

A selected synthesis component (SGP with DMDMP) and further optimized synthesis condition formed AEI zeolite without even using AEI seed. Although the seed-free system contained a trace amount of impurity, the obtained product could be used as seed crystal for providing pure-phased AEI zeolite. In a series of the above synthesis experiments, there was no necessity of starting zeolite, achieving starting-zeolite-free AEI zeolite synthesis. Finally, in the both synthesis system in the presence and absence of seed crystal, we investigated liquid phase aluminosilicate oligomer during the induction period of the AEI zeolite formation. For the first time, oligomer species that can contribute to AEI zeolite crystal growth and nucleation were proposed, respectively.

Furthermore, we also investigated the NH<sub>3</sub>-SCR performance of Cu-loaded AEI zeolite catalysts prepared from different starting silica/alumina sources (FAU zeolites, SGP, and CGP materials). Higher catalytic activity and durability could be attained by the SGP synthesis strategy owing to the superior crystallinity of the zeolite framework with fewer structural defects compared with other samples. This comprehensive study including synthesis, analysis, and catalytic application would help rationally build zeolite synthesis and function design, particularly in a case that strongly depends on the starting material.

**Image 1:**



- References:** 1. M. Dusselier and M. E. Davis, *Chem. Rev.*, 2018, 118, 5265.  
2. M. Moliner, C. Franch, E. Palomares, M. Grill and A. Corma, *Chem. Commun.*, 2012, 48, 8264.  
3. M. Dusselier, M. A. Deimund, J. E. Schmidt and M. E. Davis, *ACS Catal.*, 2015, 5, 6078.  
4. Y. Kakiuchi, T. Tanigawa, N. Tsunoji, Y. Takamitsu, M. Sadakane and T. Sano, *Appl. Catal. A-Gen.*, 2019, 575, 204.  
5. N. Tsunoji, D. Shimono, K. Tsuchiya, M. Sadakane and T. Sano, *Chem. Mater.*, DOI: 10.1021/acs.chemmater.9b02227.  
6. Y. Joichi, D. Shimono, N. Tsunoji, Y. Takamitsu, M. Sadakane and T. Sano, *Cryst. Growth Des.*, 2018, 18, 5652.

**Extremely Stable Zeolites Developed via Liquid-Mediated Self-Defect-Healing**

K. Iyoki<sup>1,\*</sup>, K. Kikumasa<sup>1</sup>, T. Onishi<sup>1</sup>, Y. Yonezawa<sup>1</sup>, A. Chokkalingam<sup>1</sup>, T. Okubo<sup>1</sup>, T. Wakihara<sup>1</sup>

<sup>1</sup>Department of Chemical System Engineering, The University of Tokyo, Tokyo, Japan

**Abstract Text:** The successful application of zeolites in diverse fields largely relies on their high stability compared with other porous materials. However, the property requirements for zeolites have become stringent due to their diverse and demanding applications. Aluminosilicate zeolites are utilized for adsorptive and catalytic applications, wherein they are sometimes exposed to high-temperature steaming conditions (~1000 °C). Zeolites are exposed to severe steaming conditions in regenerators to remove coke, and over 400,000 t/y of catalysts are discarded due to degradation during the FCC process<sup>[1]</sup>. Recently, zeolites have been used in exhaust gas treatment processes, such as the selective catalytic reduction of NO<sub>x</sub>, catalytic oxidation for diesel engines, and hydrocarbon trapping<sup>[2]</sup>, wherein they degrade due to interactions with high-temperature (>800 °C) steam. In automotive applications, degradation is often severe because zeolites are continuously exposed to steam without replacement. Therefore, the development of highly stable zeolites has become an important issue. As the degradation of high-silica zeolites originates from the defect sites in their frameworks, feasible defect-healing methods are highly demanded. Herein, we propose a method for healing defects to create extremely stable high-silica zeolites. High-silica (SiO<sub>2</sub>/Al<sub>2</sub>O<sub>3</sub> > 240) zeolites with \*BEA-, MFI-, and MOR-type topologies could be stabilized by significantly reducing the defect sites via a liquid-mediated treatment without using additional silylating agents, in which a fluoride anion, hydroxide anion, and pore filler cation were used cooperatively. Upon exposure to extremely high-temperature (900–1150 °C) steam, the stabilized zeolites retain their crystallinity and micropore volume, whereas the parent commercial zeolites degrade completely (Image 1(a)). Both the parent and treated samples showed similar morphologies in SEM images, indicating that no significant dissolution and/or precipitation of silicate species occurred during the treatment. Interestingly, well-faceted voids with diameters of approximately 50 nm were clearly observed through-out the sliced, treated samples (Image 1(b)). The presence of intra-particle voids was also confirmed by nitrogen adsorption-desorption isotherms (Image 1(c)). The parent ZSM-5 shows a typical type-I isotherm with-out hysteresis loops, while the treated ZSM-5 shows two hysteresis loops at low ( $P/P_0 \sim 0.2$ ) and high ( $P/P_0 > 0.5$ ) relative pressure regions. Low-pressure hysteresis can be explained by several models such as phase change of the zeolite framework, adsorb-ate-adsorbent interactions, and pressure-induced swelling processes<sup>[3]</sup>. High-pressure hysteresis is attributed to cavitation due to inkbottle-shaped cavities covered with small pore openings (<4 nm) indicating the presence of intra-particle voids. In the <sup>29</sup>Si MAS NMR spectra (Image 1(d)), broad signals were observed in both Q<sup>3</sup> and Q<sup>4</sup> regions in the spectrum of the parent sample, which indicated the presence of a significant amount of defects, with an enhancement of the Q<sup>3</sup> signal in the CP MAS spectrum. Conversely, the Q<sup>3</sup> signal was hardly detected for the treated sample, even in the CP MAS spectrum. The Q<sup>4</sup> signals in the DD MAS spectrum were clearly separated corresponding to different T-atom sites. A self-defect-healing mechanism for the decrease in the number of defect sites and the formation of intra-particle voids is proposed based on the above-mentioned results, as illustrated in Image 2. The proposed self-defect-healing method provides new insights into the migration of species through porous bodies and significantly advances the practical applicability of zeolites in severe environments.

**Image 1:**

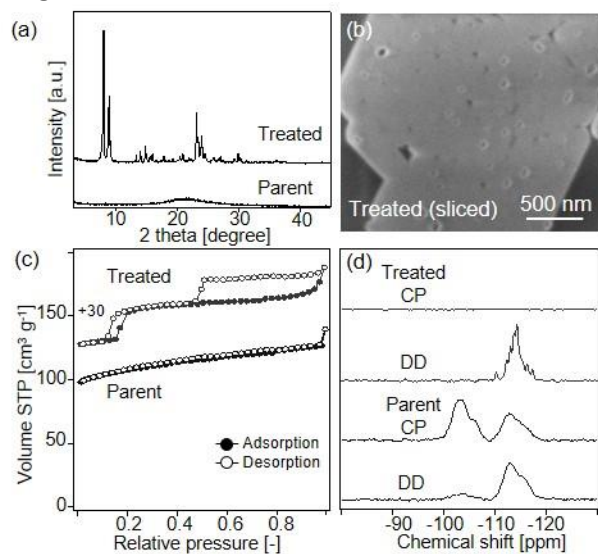
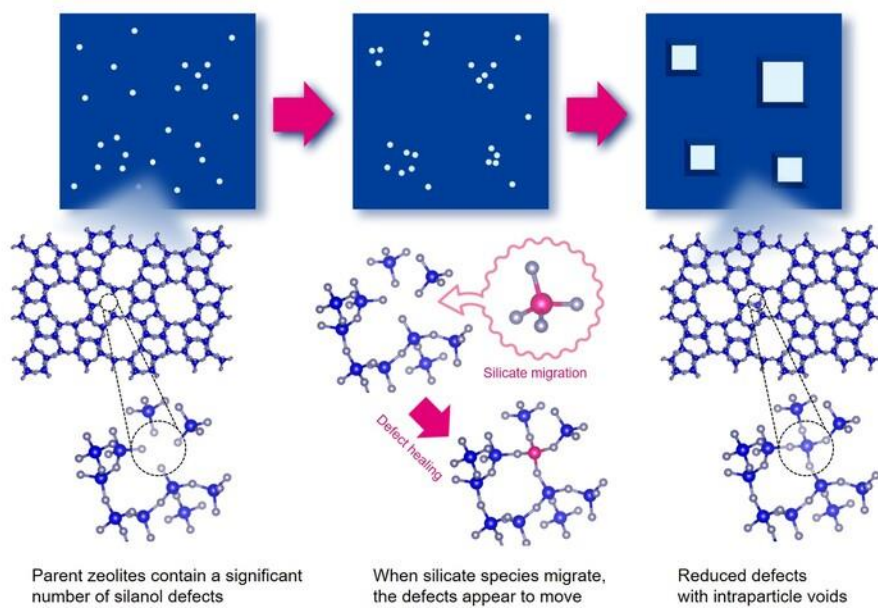


**Image 2:**



- References:** [1] H. S. Cerqueira, et al., *J. Mol. Catal. A: Chem.* 292, (2008) 1–13.  
[2] A. M. Beale, et al., *Chem. Soc. Rev.* 44, (2015) 7371–7405.  
[3] A. M. Silvestre-Albero, et al., *J. Phys. Chem. C* 116, (2012) 16652–16655.

## **New Synthetic Methods and Post-Synthetic Modification | Zeolites/Inorganic materials**

FEZA21-PO-219

### **Synthesis-structure-activity relations in Fe-CHA for C-H activation: interzeolite conversion allowing Al-distribution control [1]**

J. Devos<sup>1,\*</sup>, M. Bols<sup>1</sup>, D. Plessers<sup>1</sup>, C. Van Goethem<sup>2</sup>, J. W. Seo<sup>3</sup>, S.-J. Hwang<sup>4</sup>, B. Sels<sup>1</sup>, M. Dusselier<sup>1</sup>

<sup>1</sup>Center for Sustainable Catalysis and Engineering (CSCE), <sup>2</sup>Centre for Membrane Separations, Adsorption, Catalysis, and Spectroscopy for Sustainable Solutions, <sup>3</sup>Department of Materials Engineering, KU Leuven, Leuven, Belgium, <sup>4</sup>Division of Chemistry and Chemical Engineering, CALTECH, Pasadena, United States

#### **Abstract Text:**

*Little is known about the mechanisms and dynamics that are responsible for the creation of structurally relevant Al arrangements in zeolite synthesis. Here, we uncover new strategies to create Al hosts in small-pore zeolites suitable for divalent cation catalysis. Specifically, SSZ-13 synthesis protocols allow synthesis with a high and controlled divalent cation capacity (DCC). These hosts are perfect for  $\alpha$ -Fe, the active site for methane partial oxidation (MPO) using  $N_2O$ . Using DCC we can now steer SSZ-13 to be more active for this important catalytic challenge reaction (MPO). Additionally, this study offers pieces to a puzzle that could lead to systematic understanding of Al incorporation at the atomic length scale during synthesis.*

#### **INTRODUCTION**

The unique nature of the active site for MPO ( $\alpha$ -Fe<sup>[2]</sup>), the highly symmetric CHA framework and the ease of FAU-to-CHA interzeolite conversion syntheses (IZC)<sup>[3]</sup> provides a unique opportunity to link zeolite synthesis and reaction performance of a challenging redox system. MPO is one of the holy grails of catalysis with transition-metal ion containing zeolites under investigation.<sup>[3-4]</sup> The zeolite host and its aluminium distribution play a crucial role to active site formation and operation. 8MR-zeolites are suitable hosts due to stability and cage structures,<sup>[3,5]</sup> but few Al arrangements are able to accommodate active sites.<sup>[3]</sup> Since synthetic variation can affect the latter, we set out to discover synthesis-structure-activity relations (image 1) for SSZ-13.<sup>[1]</sup>

#### **EXPERIMENTAL**

SSZ-13 (CHA) was made following IZC conversion protocols (FAU-to-CHA IZC; <100 syntheses). Aqueous Co<sup>II</sup>-exchange of the calcined zeolite (cfr. [6]) was used to probe DCC, a proxy for internal Al-distribution and pairing. Fe cations were exchanged as in [2]. Methane oxidation was performed after one activation cycle and followed by methanol extraction. Additionally, for a high Si FAU-to-CHA IZC protocol, structural evolution was followed in time from 15 minutes to 12 days. Characterization of the materials includes elemental analysis, P-XRD, DR-UV-VIS, N<sub>2</sub>-physisorption, TGA and TEM-EDX.<sup>[1]</sup>

#### **RESULTS**

An exhaustive investigation with single-parameter variations and the resulting Al arrangements probed by Co<sup>2+</sup> uncovered remarkable effects demonstrating the importance of often-neglected synthesis parameters on the DCC of the resulting zeolite. These parameters include synthesis time, temperature and compositional factors, such as dilution. Using IZC, control over DCC was established over a wide range (Co/Al = 0.04–0.35), yielding reliable synthesis–structure relations. Using DCC as a probe for Al arrangements capable of hosting Fe<sup>II</sup>, a structure–activity relation for methanol productivity was demonstrated. Fe<sup>II</sup>-redox zeolites were made with productivities surpassing the maximum productivity possible with random Al distributions. On top, the standard conditions are fast (<3h to obtain ~100% crystalline materials) and yield high DCC values (Co/Al=0.23(±0.01)). Temporal investigation of this IZC showed four distinct phases (image 2), allowing us to paint a new Al-distribution genesis hypothesis.<sup>[1]</sup>

#### **CONCLUSION**

Here, we present new synthesis-structure-activity relations for methanol synthesis in CHA using IZC. The divalent cation capacity (DCC) is a useful numerical structural descriptor bridging the consequences of zeolite synthesis with reactivity and is therefore a useful tool to engineer more active TMI-zeolite catalysts. Seemingly, kinetically fast IZC syntheses can produce metastable DCC-rich zeolites, likely linked to the occurrence of atypical modes of assembly and influenced by incongruent dissolution of the starting zeolite.

Image 1:

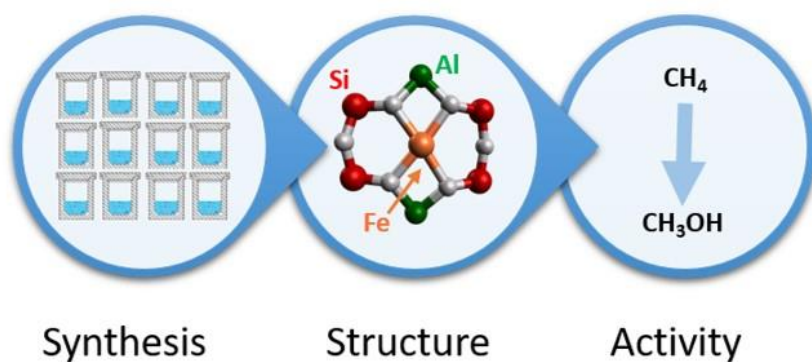
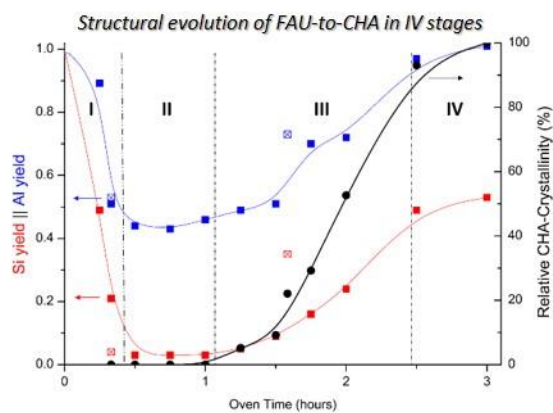


Image 2:



#### References:

- [1] Devos et al., (2020). Chem. Mater. 1 , 273
- [2] Bols et al., (2018). JACS 38 , 12021
- [3] Dusselier et al., (2018). Chem. Rev. 11, 5265
- [4] Snyder et al., (2018). Chem. Rev. 5, 2718
- [5] Wulfers et al., (2015). Chem. Commun., 21 , 4447
- [6] Dědeček et al., (2019). ChemSusChem 3 , 556

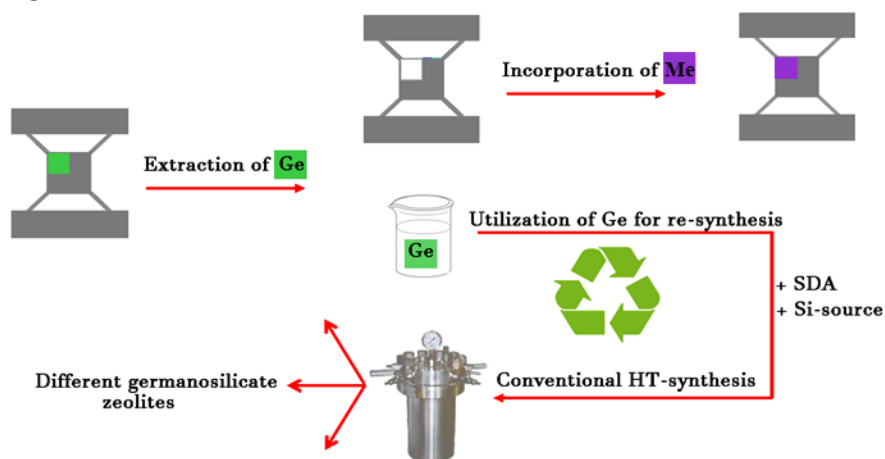
**Improving Application Potential of Germanosilicate Zeolites: Post-synthesis Tailoring the Active Sites Coupled with Ge Recycling**

J. Zhang\*, Q. Yue, M. Opanasenko, M. Shamzhy

**Abstract Text:** For 2 recent decades germanosilicate zeolites have deservedly gained much attention not only from fundamental but also from an applied point of view. Indeed, the most of extra-large pore zeolites being of high interest for oil industry and synthesis of specialty chemicals were prepared as germanosilicates.<sup>1</sup> Moreover, germanosilicate zeolites characterized by the unidirectional location of Ge-enriched D4R units were recently discovered as perfect precursors for engineering novel nanoporous materials via ADOR synthesis protocol.<sup>2</sup> However, despite being highly attractive for purposeful catalytic applications, both germanosilicate and ADORable zeolites suffer from the high cost of Ge limiting their practical use. Recent investigations indicated that low hydrolytic stability of Si–O–Ge and Ge–O–Ge bonds can be exploited for regulation of acidic and catalytic properties of germanosilicate zeolites by the post-synthesis isomorphous substitution of Ge for T<sup>III</sup> and T<sup>IV</sup> elements.<sup>3</sup> However, despite its obvious advantages, post-synthesis method still produced expensive zeolites since Ge was substituted without any recycling treatment.

In this contribution, we propose 2 step post-synthesis approach (i.e. 1) leaching and subsequent recycling of Ge, 2) incorporation of three- or four- valent elements generating catalytically active Bronsted and/or Lewis acid sites into de-germanated zeolite is proposed and optimized.) as a method for cost efficient production of the catalysts based on germanosilicate zeolites (Scheme 1). Our results indicate that tailoring the active sites by post-synthesis of germanosilicate zeolites can be used to design new effective catalysts.

**Image 1:**



**References:** [1] Jiang, J.; Yu, J.; Corma, A. *Angew. Chem. Int. Ed.* 2010, 49, 3120-3145

[2] Eliasova, P.; Opanasenko, M.; Wheatley, P. S.; Shamzhy, M.; Mazur, M.; Nachtigall, P.; Roth, W. J.; Morris, R. E.; Cejka, J. *Chem. Soc. Rev.* 2015, 44, 7177-7206

[3] Shamzhy, M.; Opanasenko, M.; Concepción, P.; Martínez, A. *Chem. Soc. Rev.* 2019, 48, 1095-1149

**Seed-assisted synthesis of hierarchical zeolite ZSM-5 in the absence of organic templates**

D. O. Shestakova<sup>1,2,\*</sup>, K. A. Sashkina<sup>1,2</sup>, E. V. Parkhomchuk<sup>1,2</sup>

<sup>1</sup>Novosibirsk State University, <sup>2</sup>Boreskov Institute of Catalysis SB RAS, Novosibirsk, Russian Federation

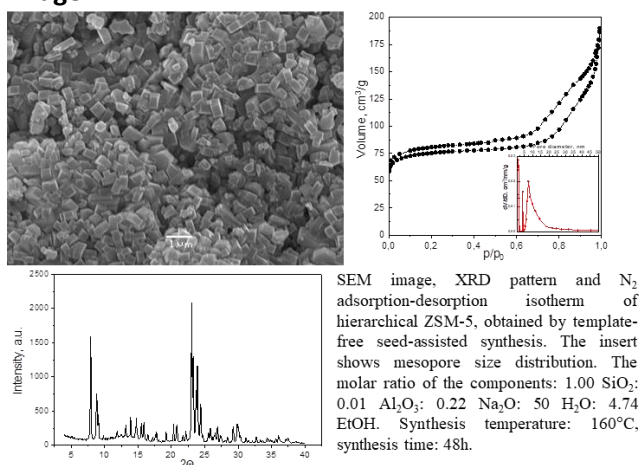
**Abstract Text:** Due to the unique physicochemical properties, zeolite-based catalysts are widely used in the refining industry. However, conventional zeolites with only microporous systems (0.25-2 nm) have diffusion limitations resulting in the rapid deactivation of catalysts in a number of petrochemical processes, such as cracking, isomerization and alkylation. In the last two decades, it was shown that creation of hierarchical porosity, i.e. introduction of additional meso / macropores into the structure of zeolite, leads to higher efficiency and stability of hierarchical zeolite-based catalysts over conventional ones [1].

Because of widespread use of zeolites in industry, there is a constant development of synthetic methods using commercially available reagents. Most known syntheses of hierarchical zeolites require expensive organic templates (usually quaternary ammonium compounds), which is economically unacceptable. Therefore, seed-assisted synthesis of zeolites in the absence of organic templates was proposed as one of the possible solutions [2]. The basic action of seed crystals is to provide surface for nucleation or nucleus, which results in reduction of synthesis time and suppression of impurity phases' appearance.

In the present study, we vary conditions of template-free seed-assisted synthesis such as temperature (120-200 °C) and time (12-72 h) of the hydrothermal treatment, alkali content, amount (0 – 20 wt.%) and size (100 – 1000 nm) of seeds added and aluminum and silicon sources to find out the influence of these factors on crystallinity, morphology and texture of hierarchical zeolite ZSM-5. The molar ratio in the reaction gel was as follows: 1,00 SiO<sub>2</sub> : 0,01 Al<sub>2</sub>O<sub>3</sub> : x Na<sub>2</sub>O : 50 H<sub>2</sub>O : 4,74 EtOH, where x = 0,15-0,45. As a result of this work, optimal synthetic conditions to achieve highly crystalline hierarchical zeolite ZSM-5 were determined (Image 1). The presence of meso- and macropores in well-crystallized samples of ZSM-5 has been established by low-temperature nitrogen adsorption, indicating the formation of hierarchical pore structure [3]. Catalytic activity of synthesized samples was tested in the hexane cracking reaction and compared with that one of nano- and microsized ZSM-5, obtained earlier [4].

**Acknowledgments:** The research was funded by RFBR and Novosibirsk region, project number 20-43-543036.

**Image 1:**



**References:** 1. Pérez-Ramírez J. et al. // Chem. Soc. Rev. 2008. Vol. 37, № 11. P. 2530.

2. Cundy C.S., Cox P.A. // Microporous Mesoporous Mater. 2005. Vol. 82, № 1–2. P. 1–78.

3. Shestakova D.O., Sashkina K.A., Parkhomchuk E. V. // Pet. Chem. Pleiades Publishing, 2019. Vol. 59, № 8. P. 838–844.

4. Parkhomchuk E. V et al. // Pet. Chem. Pleiades Publishing, 2019. Vol. 59, № 3. P. 338–348.

**Investigation of Structural Features of Ordered Mesoporous Carbons and Composites on their Powder X-ray Diffraction Pattern**

B. Schwind<sup>1</sup>, M. Tiemann<sup>1</sup>, C. Weinberger\*

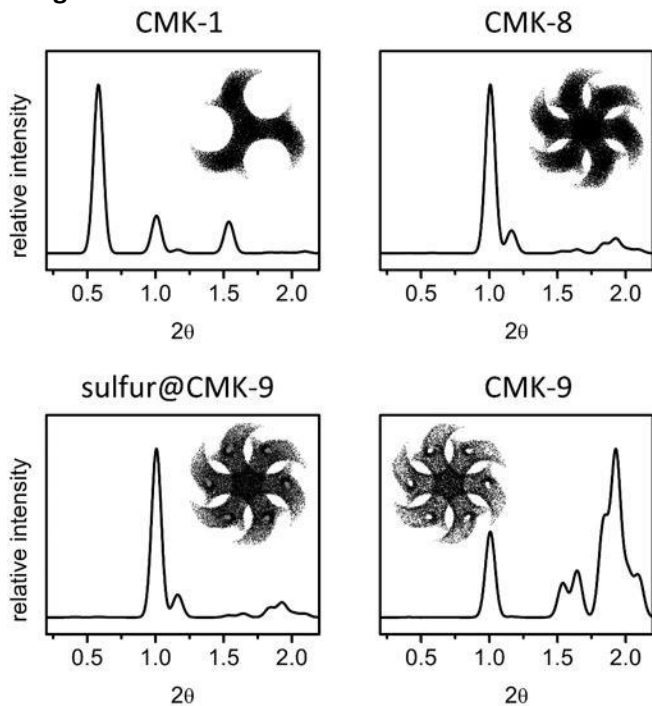
<sup>1</sup>Faculty of Science, Department of Chemistry, Paderborn University, Paderborn, Germany

**Abstract Text:** Powder X-ray diffraction is an essential tool for the characterization of periodically ordered mesoporous carbon materials. Features of the nanostructure can be deduced from the (relative) intensities of low-angle reflections in the diffraction patterns (see figure).<sup>[1]</sup> Ordered mesoporous CMK-1 carbon (space group  $I4_132$ ) consists of a single gyroid structure that can be described by a nodal surface approximation.<sup>[2]</sup> It exhibits a dominant 110 reflection over the entire range of possible carbon wall thickness.

CMK-8, on the other hand, consists of two gyroids (inverse structure of KIT-6 silica; space group  $Ia-3d$ ) that are connected with each other. It exhibits a dominating 211 reflection. When these gyroids are hollow the structure is called CMK-9 carbon.<sup>[3,4]</sup>

Both the geometry and the carbon wall thickness of the (hollow) carbon gyroids have a significant influence on the X-ray diffraction patterns. This has been investigated for hexagonally ordered mesoporous carbon materials (*i.e.* CMK-3 and CMK-5 carbon),<sup>[5,6]</sup> but no such studies exist for carbon materials with cubic symmetry (*i.e.* CMK-1/-8/-9). In case of CMK-9 carbon the structure consists of two different pore systems. Here, the carbon wall thickness has a much stronger impact on the diffraction pattern than in case of the previously discussed CMK-1 and CMK-8 carbon materials. Furthermore, novel sulfur@CMK-9 carbon composite materials were modeled and synthesized. The amount of infiltrated sulfur significantly changes the relative intensity of the diffraction peaks. In contrast to the hexagonal analogues (*i.e.* sulfur@CMK-5 carbon composites) the diffraction patterns change, especially for low sulfur content. This study compares simulated carbon (composite) structures with experimental results.<sup>[7]</sup>

**Image 1:**



- References:** [1] L. A. Solovyov, Chem. Soc. Rev. 42 (2013) 3708-3720.
- [2] A. H. Schoen, NASA Technical Note TD-5541 (1970).
- [3] F. Kleitz, S. Hei, H. Choi, R. Ryoo, Chem. Commun. (2003) 2136-2137.
- [4] L. A. Solovyov, V. I. Zaikovskii, A. N. Shmakov, O. V. Belousov, R. Ryoo, J. Phys. Chem. B 106 (2002) 12198-12202.
- [5] Schmidt, Microporous Mesoporous Mater. 117 (2009) 372-379.
- [6] C. Weinberger, M. Hartmann, S. Ren, T. Sandberg, J.-H. Smått, M. Tiemann, Microporous Mesoporous Mater. 266 (2018) 24-31.
- [7] C. Weinberger, B. Schwind, S. Ren, B. Draphoen, J.-H. Smått, M. Tiemann, (2020) submitted.

## ***New Synthetic Methods and Post-Synthetic Modification | Zeolites/Inorganic materials***

FEZA21-PO-230

### **Room-Temperature, OSDA-Free Synthesis of Linde Q (BPH) Nanosheets**

E. Clatworthy<sup>1,\*</sup>, M. Debost<sup>1</sup>, A. Vicente<sup>1</sup>, S. Gascoin<sup>2</sup>, N. Barrier<sup>2</sup>, P. Boullay<sup>2</sup>, J.-P. Gilson<sup>1</sup>, N. Nesterenko<sup>3</sup>, S. Mintova<sup>1</sup>

<sup>1</sup>Laboratoire Catalyse et Spectrochimie, <sup>2</sup>Laboratoire de Cristallographie et Science des Matériaux, Normandie Université, ENSICAEN, UNICAEN, CNRS, Caen, France, <sup>3</sup>Total Research & Technology, Total, Feluy, Belgium

**Abstract Text:** The development of affordable and energy-efficient materials for the chemicals and petrochemicals industry is highly desirable as this sector is the largest industrial consumer of energy and the third largest direct emitter of greenhouse gases.<sup>1-2</sup> For the past half-century zeolites have been a key component in refinement and petrochemistry operations, such as fluid catalytic cracking, and continue to be a subject of intense research. Specifically, the development of nano-dimensional zeolites has attracted significant interest over the last decade due to their properties such as high specific surface area and reduced diffusion path length for guest molecules. However, the use of organic structure-directing agents (OSDAs) to achieve nano-dimensional zeolites is undesirable due to their relatively high cost. Here we report on the room-temperature, OSDA-free synthesis of Linde Q zeolite (beryllophosphate-H, BPH structure) nanosheets containing a combination of Cs<sup>+</sup>, K<sup>+</sup>, and Na<sup>+</sup>. Following the patent by Union Carbide (Breck *et al.* 1961), Linde Q has received little research attention due to its low thermal stability (structural collapse above 160 °C in air).<sup>3-4</sup> However, using variable-temperature X-Ray diffraction (XRD), we observe that the nanosheets retain up to 60% of their crystallinity at 350 °C under vacuum. In addition to XRD, the nanosheets were characterised by a combination of techniques including transmission electron microscopy (TEM), thermogravimetric analysis (TGA), inductively coupled Plasma mass spectrometry (ICP), N<sub>2</sub> and CO<sub>2</sub> adsorption, nuclear magnetic resonance (NMR) and infrared (IR) spectroscopy. The Linde Q nanosheets are highly stable in aqueous colloidal suspension; the nanosheets are approximately 7–11 nm thick and 90–130 nm wide (Fig. 1A, B, C). N<sub>2</sub> adsorption analysis further demonstrates the improved thermal stability of the nanosheets under vacuum (pre-treatment at 350 °C) whereas conventional Linde Q underwent structural collapse. CO<sub>2</sub> adsorption analysis shows that the Linde Q nanosheets possess considerable CO<sub>2</sub> adsorption capacity (Fig. 1D), and TGA employing multiple cycles of heating and CO<sub>2</sub> flow reveal an initial equilibration in the CO<sub>2</sub> capacity of the nanosheets followed by stable reproducible behavior. These results indicate potential application in gas separation using membrane technology.

### Image 1:

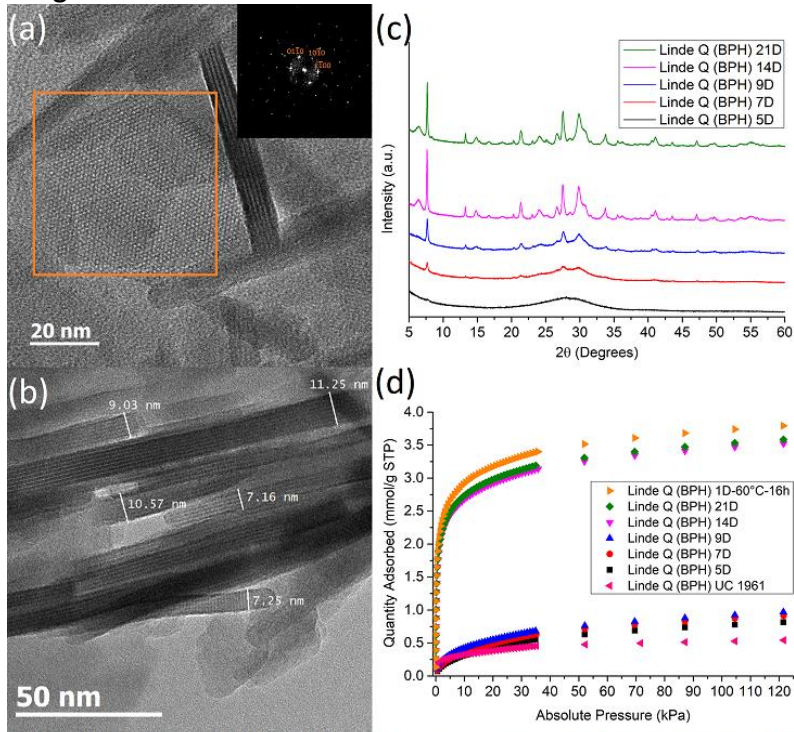


**Figure 1.** (a, b) High-resolution TEM images of Linde Q nanosheets after 14 days of stirring at room temperature. (c). XRD pattern of Linde Q nanosheets prepared at room temperature with different stirring time periods. (d). CO<sub>2</sub> adsorption isotherms of Linde Q nanosheets prepared at room temperature with different stirring time periods, or mild hydrothermal treatment.

**References:** 1. Tracking Clean Energy Progress 2017. International Energy Agency: Paris, France, 2017.

2. Fishedick, M.; Roy, J.; Abdel-Aziz, A.; Acquaye, A.; Allwood, J.; Ceron, J.-P.; Geng, Y.; Kheshgi, H.; Lanza, A.; Percayk, D., Industry. In Climate Change 2014: Mitigation of Climate Change. IPCC Working Group III Contribution to AR5., Cambridge University Press: 2014.

3. Breck, D. W.; Acara, N. A. Crystalline Zeolite Q. US2991151A, 1961.

4. Andries, K.; De Wit, B.; Grobet, P.; Bosmans, H., The synthesis and properties of synthetic zeolite Linde Q. Zeolites 1991, 11 (2), 116-123.

## ***New Synthetic Methods and Post-Synthetic Modification | Zeolites/Inorganic materials***

FEZA21-PO-233

### **Al-ITQ-34: A three-dimensional medium pore zeolite of high potential as catalyst**

M. P. Cumplido Comeche\*, M. J. Díaz Cabañas<sup>1</sup>

<sup>1</sup>Instituto de Tecnología Química (UPV-CSIC), Instituto de Tecnología Química (UPV-CSIC), Valencia, Spain

**Abstract Text:** The zeolite ITQ-34, with the ITR IZA code, has a three-dimensional channel system delimited by 10 x 10 x 9 rings and a medium pore size in all directions. It is one of the few zeolites synthesized using an alkyl phosphonium, propane-1,3-bis(trimethylphosphonium) hydroxide, as a structure directing agent (SDA) instead of an alkyl ammonium as usual <sup>[1]</sup>.

ITQ-34 was first synthesized as a germanosilicate in fluoride medium. Therefore, the incorporation of Al as well as the reduction of Ge in the zeolitic framework has a great interest in order to be used as acid catalyst in chemical processes. However, when zeolites synthesized with a phosphonium SDA are calcined, sometimes the P remains in the zeolitic material, which occludes its cavities and reduce the acidic strength of the zeolite <sup>[2]</sup>.

In this work, a new synthetic method have been developed to incorporate as much Al as possible in the ITQ-34 structure framework. Furthermore, innovative post-synthetic modification methods were used to reduce the dealumination of the zeolite during the SDA removing and to increase the Si/Ge ratio by the replacement of Ge by Al in the zeolite framework.

**References:** [1]A. Corma, M. J. Diaz-Cabanias, J. L. Jorda, F. Rey, G. Sastre, K. G. Strohmaier, Journal of the American Chemical Society 2008, 130, 16482-16483.

[2]R. Simancas, J. L. Jordá, F. Rey, A. Corma, A. Cantín, I. Peral, C. Popescu, Journal of the American Chemical Society 2014, 136, 3342-3345.

**Additive-free Synthesis of Hierarchical Zeolites by Utilizing Aluminosilicate Gel Memory**

M. Khaleel<sup>1,2,3,\*</sup>, D. K. Dumbre<sup>1</sup>

<sup>1</sup>Chemical Engineering Department, <sup>2</sup>Research and Innovation Center on CO<sub>2</sub> and H<sub>2</sub> (RICH), <sup>3</sup>Center for Catalysis and Separation (CeCaS), Khalifa University of Science and Technology, Abu Dhabi, United Arab Emirates

**Abstract Text:** Efforts to overcome diffusional limitation in microporous zeolites have been directed towards the design of hierarchical zeolite structures. Interest in these materials stems from the higher reaction rates, improved selectivity, resistance to deactivation, and novel adsorption behavior that they exhibit in comparison to the typical zeolites that only have micropores.

Faujasite is one of the most widely used catalysts, mainly in fluid catalytic cracking (FCC) of heavy petroleum, where coking is significant. Hierarchical Faujasite has been prepared by post synthetic treatment, or by using soft-templates or hard templates, adding extra cost and complexity to the synthesis. House-of-card assembly of Faujasite sheets by repetitive branching has been previously reported using either organosilane surfactants<sup>1</sup> or lithium or zinc salts<sup>2</sup>. Previous work by Khaleel et. al.<sup>3</sup> showed that FAU/EMT intergrowth is responsible for the repetitive branching leading to the development of house-of-card assembly of zeolite X nanosheets. Thus, being able to control the intergrowth of crystal phases in particles will allow control of mesopore size by controlling sheet thickness and branching frequency. Both FAU and EMT can nucleate from inorganic sols containing only sodium ions. Hence, the development of a house-of-card assembly of Faujasite sheets from sodium aluminosilicate sol is in principle possible, thus avoiding the extra cost of additives. House-of-card assembly of Faujasite nanosheets was synthesized solely from inorganic sodium aluminosilicate solution following earlier findings by Khaleel et. al.<sup>4</sup> demonstrating the use of pre- and post-nucleation trajectories for the synthesis of high FAU content Faujasite nanocrystals (Fig. 1). In this work, the effect of combining different synthesis trajectories on the branching of FAU/EMT materials, and hence on mesopore size, was studied. The synthesized materials were characterized using XRD, SEM, TEM, nitrogen physisorption, and carbon dioxide adsorption. Results show that branching in Faujasite can be enhanced by first mixing the sol at compositions that favor micron size crystal formation and then—after a certain time—adjusting the composition to favor FAU/EMT intergrowth (Fig.1).<sup>5</sup> House-of-card assembly of Faujasite nanosheets, synthesized from a combination of trajectories, shows smaller pores with a narrower size distribution, and high external surface area while retaining high micropore volume, compared to samples from direct syntheses.

The effect of the hierarchical morphology of different zeolite X samples on the catalytic properties was also investigated to understand the effect of the high external surface area and the active sites located at the external surface on the catalytic performance and material stability. Reactions with different probe molecules were tested.

Following the same approach, LTA, another important zeolite in industry, has been synthesized as nanocrystals (around 200 nm) from sodium aluminosilicate sols, thereby avoiding the large amount of organic additives that are usually needed to reduce crystal size (Fig. 2). The performance of the nanosized LTA samples for gas drying was compared to micron sized LTA crystals.

The results of this work demonstrate that the pool of accessible zeolite morphologies can be expanded beyond those possible from direct synthesis, by utilizing the gel memory effect to combine different synthesis trajectories. This allowed us to prepare the House-of-card Faujasite morphology and nanosized LTA crystals from sodium aluminosilicate sols, initially only possible with additives, with a proper choice of starting and ending compositions. While the structure of the initial gel has an effect on the nucleation trajectory and hence on the crystal size, the final composition determines the crystallization kinetics and the resulting crystal phase.

**Image 1:**

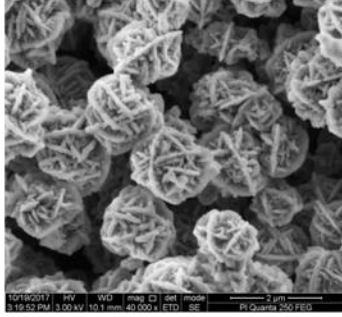


**Figure 1.** Hierarchical house-of-card Faujasite synthesized from inorganic sodium aluminosilicate sols.

**Image 2:**

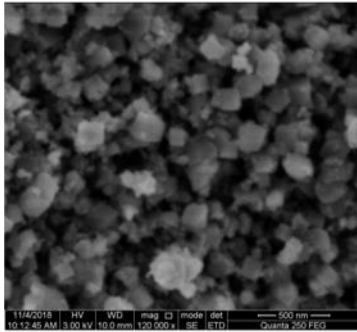


**Figure 2.** Nano-sized LTA synthesized from inorganic sodium aluminosilicate sols.

- References:** 1.A. Inayat, I. Knoke, E. Spiecker, W. Schwieger, *Angew. Chemie Int. Ed.* 51 (8), 1962–1965 (2012).  
2.A. Inayat, C. Schneider, W. Schwieger, *Chem. Commun.* 51 (2), 279–281 (2015).  
3.M. Khaleel, A. J. Wagner, K. A. Mkhoyan, M. Tsapatsis, *Angew. Chemie - Int. Ed.* 53 (36), 9456–9461 (2014).  
4.M. Khaleel, W. Xu, D. A. Lesch, M. Tsapatsis, *Chem. Mater.* 28 (12), 4204–4213 (2016).  
5.Gaber, S.; Gaber, D.; Ismail, I.; Alhassan, S.; Khaleel, M. *CrystEngComm* 2019, 21 (11), 1685–1690.

## ***New Synthetic Methods and Post-Synthetic Modification | Zeolites/Inorganic materials***

FEZA21-PO-242

### **2D-to-3D zeolite transformation for shape-selective catalysis: electron microscopy studies**

M. Mazur<sup>1,\*</sup>, Y. Zhang<sup>1</sup>, M. Kubu<sup>1</sup>, J. Cejka<sup>1</sup>

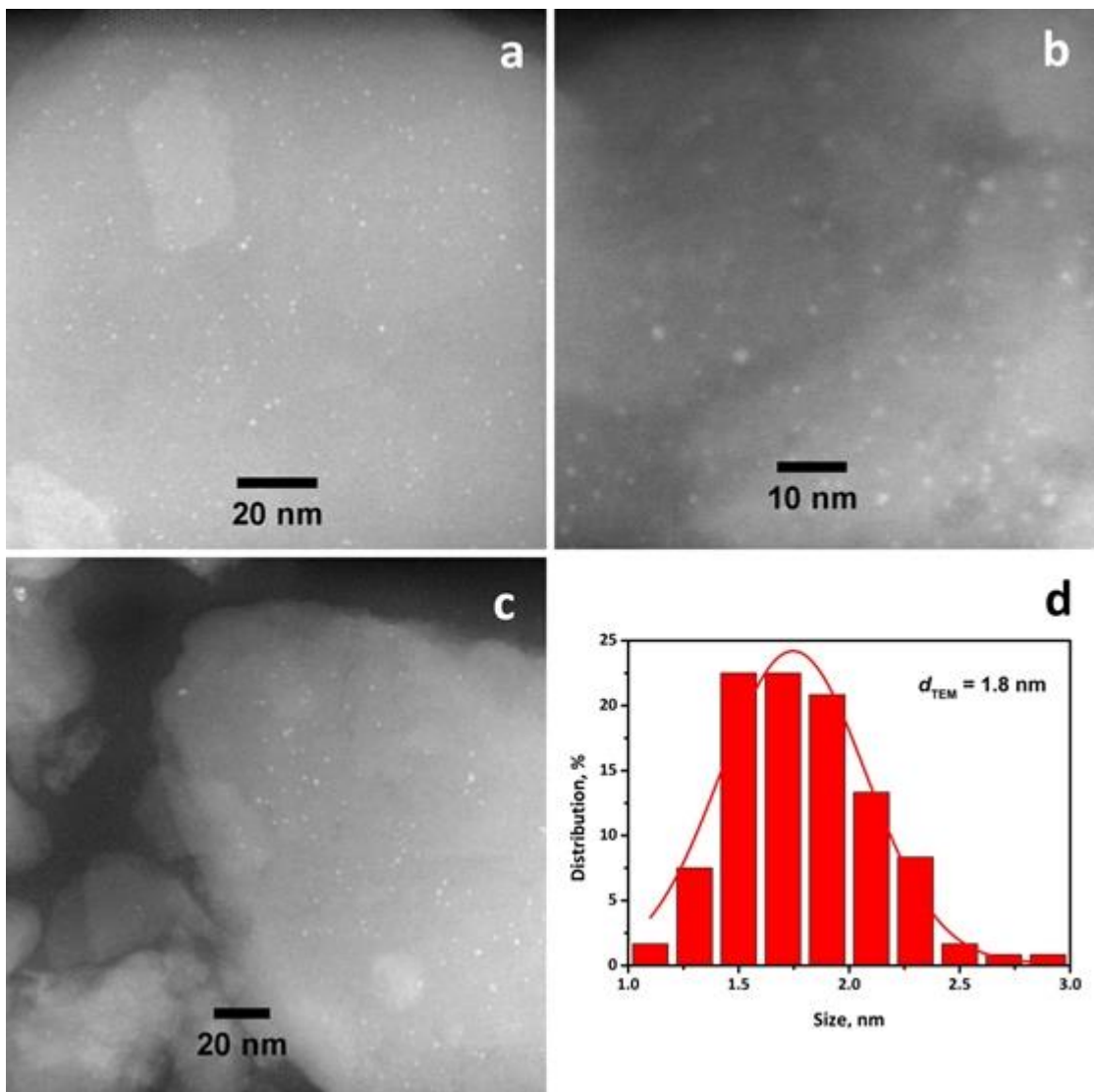
<sup>1</sup>Faculty of Science, Charles University, Prague, Czech Republic

**Abstract Text:** Encapsulation of metal nanoparticles within zeolite matrix can provide the shape selectivity of zeolite channels. Layered zeolite precursors are the materials that blend the advances of layered solids with the properties of zeolites [1]. One of the methods for synthesis of metal nanoparticles in the zeolite system uses two dimensional (2D) zeolites. It is a two-step procedure based on the introduction of metal source in between layers and consecutive transformation of them to three dimensional (3D) zeolites [2,3].

Herein we present, synthetic way of introduction of various metal nanoparticles (Pt, Pd, Rh) into MCM-22P during the swelling of lamellar zeolitic precursor followed by calcination. This results in encapsulation of metal clusters within the 3D framework of **MWW** zeolite. To design the size of metal species we used a series of surfactants with different carbon chain lengths ( $C_{12}$ ,  $C_{14}$ ,  $C_{16}$ ,  $C_{18}$ ) as swelling agents [4]. The size, distribution and location of the metal clusters were characterised by electron microscopy methods, mostly scanning transmission electron microscopy (STEM). Catalytic properties of synthesised materials were investigated in the shape-selective hydrogenation of nitroarenes to anilines. Moreover, we extended this method to other zeolite precursors like layered ZSM-5 and IPC-1P. *Via* ADOR process, we encapsulated various metal nanoparticles into IPC-2 and IPC-4 materials [5]. All synthesized materials were investigated by PXRD, sorption, ICP-OES, SEM, and TEM methods.

**Fig.1** STEM images (a,b,c) and nanoparticles size distribution (d) of Pd@MCM-22.

**Image 1:**



- References:** [1] W.J. Roth, B. Gil, W. Makowski, B. Marszalek, P. Eliasova., *Chem. Soc. Rev.*, 45, 2016, 3400-3438.  
 [2] Z. Zhao, Y. Li, U. Müller, W. Zhang., *ChemCatChem.*, 10, 10, 2018, 22554-2259.  
 [3] Liu, L.; Díaz, U.; Arenal, R.; Agostini, P.; Corma, A., *Nat. Mater.*, 16, 2017, 132-138.  
 [4] Y. Zhang, M. Kubů, M. Mazur, J. Čejka, *Catal. Today.*, 324, 2019, 135-143.  
 [5] Y. Zhang, M. Kubů, M. Mazur, J. Čejka, *Microporous Mesoporous Mater.*, 279, 2019, 364-370.

**Synthesis of Zeolite-A from fly ash and zeolite-glass composites for nuclear waste immobilisation**

M. Kumar<sup>1,\*</sup>, H. Jena, V. Jayaraman, N. Sivaraman, B. K. Panigrahi

<sup>1</sup>Homibaba National Institute, Kalpakkam, India

**Abstract Text:** The nuclear waste produced in the pyrochemical reprocessing of metallic fuel is in chloride form<sup>1</sup>. Zeolites can be used as ceramic waste form (matrices) for nuclear waste containment<sup>2</sup>. Zeolites are crystalline, microporous aluminosilicates comprised of Si and Al tetrahedral networks connected through bridging oxygen. Zeolites have been widely used in decontamination processes of Fukushima-Daiichi, Chernobyl and Three Mile Island nuclear disaster sites. Zeolite-4A was synthesised from calcined flyash via fusion followed by hydrothermal synthesis. Flyash and sodium carbonate were taken in 1:1.0-1.5 ratios and heated at various temperatures (500-800 C) to ascertain the formation of the fused product. Sodium aluminate solution was prepared by adding 100 mg of Al powder to 10 ml of 3M NaOH. Then, the sodium aluminate solution was added to the fused product and treated under hydrothermal reaction in an autoclave at 80 C/3h. Zeolite-4A samples were loaded with simulated EBR-2 waste composition (10- 25wt %). The loaded zeolite was bonded with aluminium borosilicate glass by heating the mixture at 900 C. Fig.1 illustrates the XRD pattern and SEM image (given in the inset) of 20wt% simulated EBR-II waste<sup>3</sup> loaded zeolite. The waste loading into the zeolite-A at 600 C didn't affect the framework structure of zeolite-A. The waste salt uptake into the zeolite-A is found to be up to 20 wt%. Scanning electron microscope (SEM) image (in inset) showed the unchanged morphology after loading the salt. However, on heating the 20wt% salt loaded zeolite and aluminium borosilicate glass at 900 C in 1:1 ratio for glass bonding; the crystalline phase of zeolite-A is transformed to sodalite as shown in Fig.2. Transformation of zeolite-A to sodalite phase was observed in all the cases of different proportions of glass bonding to salt loaded zeolite-A. But when pristine zeolite-A bonded with glass, sodalite phase is less significant in the composite. Morphology of 20wt% salt loaded zeolite-A with aluminium borosilicate glass in 1:1 ratio, revealed the sufficient coverage of glass around the zeolite-A surface. Loading capacities of simulated pyro processed salt waste into zeolite-A has been determined and found to be 20wt% in zeolite-A at 600 C without change of phase. Salt loaded zeolite-A and glass bonded zeolite-A composite, both transformed to thermodynamically stable sodalite phase on heating at 900 C/3h. The present study reports on loading capacities of zeolite-A and its glass bonded composites, and phase transformations on heat treatment at higher temperatures.

**Image 1:**

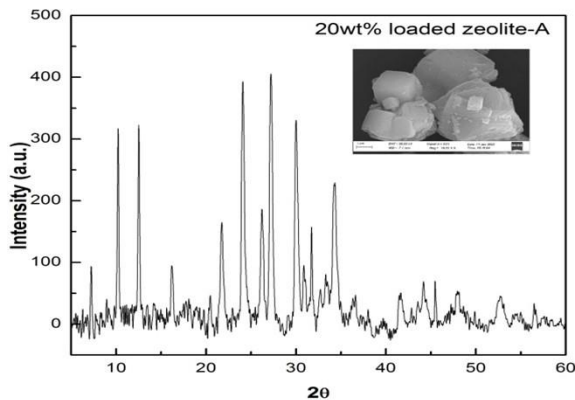
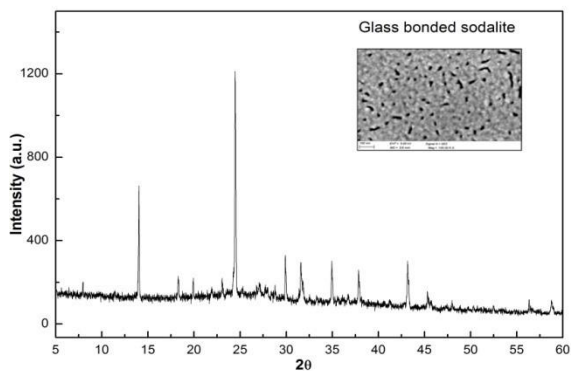


**Image 2:**



**References:** Acknowledgements: Authors are very much thankful to the Director, IGCAR, Director, MC&MFCG, Associate Director, FMCG for support and encouragement. Mr Pradyumna Parida are duly acknowledged for acquiring the SEM images.

References: (1) G. Leturcq (2005), Immobilization of fission products arising from pyrometallurgical reprocessing in chloride media, J. Nucl. Mater. Vol347, page no. 1-11, <http://doi:10.1016/j.jnucmat.2005.06.026>

(2) I N Donald (2009), Book on Waste Immobilization in Glass and Ceramic based Hosts, Wiley publishers, ISBN: 978-1-444-31937-8

(3) Lewis, M. A. (1995), Effect of different glasses in glass bonded zeolite, Document no. ANL-CMT/CP-4676, URL, [http://inis.iaea.org/search/search.aspx?orig\\_q=RN:26067438](http://inis.iaea.org/search/search.aspx?orig_q=RN:26067438)

**Hydroisomerization of Renewable and Fossil n-Alkanes over Bifunctional Dealuminated Pt/H-ZSM-5 Catalysts**

F. Schmutzler<sup>1,\*</sup>, J. Titus<sup>1</sup>, D. Poppitz<sup>1</sup>, J. Freiding<sup>2</sup>, R. Rakoczy<sup>2</sup>, A. Reitzmann<sup>2</sup>, R. Gläser<sup>1</sup>

<sup>1</sup>Institute of Chemical Technology, Universität Leipzig, Leipzig, <sup>2</sup>Clariant Produkte (Deutschland) GmbH, Bruckmühl/Heufeld, Germany

**Abstract Text:**

**Introduction**

The hydroisomerization (HI) reaction is used to upgrade fossil and renewable hydrocarbon feedstocks into transportation fuels. Renewable feedstocks like hydrogenated vegetable oils (HVO, chain length C<sub>15</sub>-C<sub>22</sub>) may serve as an alternative to fossil resources [1]. HI is commonly carried out over bifunctional catalysts, e.g., noble metals on acidic zeolites. In presence of high acid site density, undesired cracking products are formed. Therefore, the Al-content of the zeolite and, thus, the acid site density can be post-synthetically reduced by dealumination leading to decreased readsorption of isomerization products and undesired consecutive reactions [2]. Further, dealumination can change the textural properties of zeolites, leading to higher fractions of sterically demanding branched isomers [3]. This work investigates the hydroisomerization of two n-alkane mixtures with different chain lengths, a fossil C<sub>10</sub>-C<sub>13</sub> mixture and a biomass-derived C<sub>15</sub>-C<sub>22</sub> mixture (HVO), over Pt/H-ZSM-5 catalysts before and after dealumination by hydrothermal treatment and acid leaching of preshaped binder-containing zeolite pellets. The effect of zeolite dealumination on the catalytic activity and selectivity for the conversion of both feedstocks was studied.

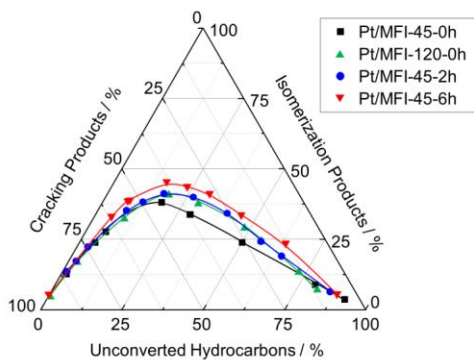
**Experimental Part**

Dealumination was performed by hydrothermal treatment of the parent zeolite pellets (60 wt.% zeolite ( $n_{Si}/n_{Al} = 45$ ) with 40 wt.% Al<sub>2</sub>O<sub>3</sub>-binder, Clariant) at 823 K for 2 h or 6 h. After hydrothermal treatment, a treatment with aqueous acid (0.6 M HCl solution, 2 h at 383 K) was applied to remove extra-framework aluminum species. In addition to the Al-rich ZSM-5 zeolite, a less acidic untreated pelletized zeolite ZSM-5 with  $n_{Si}/n_{Al} = 120$  (MFI-120-0h) was used. The zeolite pellets were labeled according to their  $n_{Si}/n_{Al}$ -ratio and the duration of hydrothermal treatment, e.g., MFI-45-xh. Prior to the catalytic experiments the pellets were impregnated with 0.8 wt.% Pt. Hydroisomerization experiments were carried out in a plug-flow trickle-bed reactor with 20 g catalyst and a WHSV = 3 h<sup>-1</sup>. The liquid n-alkane feeds were introduced into the reactor after mixing with a gaseous hydrogen flow of 30 L h<sup>-1</sup> at a total pressure of 4 MPa. The reaction temperature was varied in the range of 493 – 593 K to obtain conversions in the range of 10 – 100%.

**Results and Discussion**

Via dealumination, the acid site density of the zeolite was reduced from 467 μmol g<sup>-1</sup> for the parent MFI-45-0h to 42 μmol g<sup>-1</sup> for MFI-45-2h and 27 μmol g<sup>-1</sup> for MFI-45-6h, respectively. The HI activity of the catalysts decreases with decreasing acid site density, making higher reaction temperatures necessary to achieve comparable conversion. This typically leads to a lower yield of isomers due to an enhanced cracking activity. Even though dealumination causes a lower activity, the selectivity for (multi-)branched isomers increases, while the selectivity for cracking products decreases from MFI-45-0h to MFI-45-6h as shown in Image 1 for the C<sub>10</sub>-C<sub>13</sub> n-alkane mixture. When comparing catalysts with similar acid site density (MFI-45-2h and MFI-120-0h), a higher ratio of multi- to mono-branched C<sub>10</sub>-C<sub>13</sub> isomerization products was achieved for the dealuminated MFI-45-2h. Therefore, it can be assumed that the dealumination results in a higher availability of space in the vicinity of the active sites of the zeolite. This leads to a higher yield of bulkier multi-branched C<sub>10</sub>-C<sub>13</sub> isomers as well as mono-branched C<sub>15</sub>-C<sub>22</sub> isomers compared to the untreated catalysts. The dealumination of zeolite pellets in the presence of a binder, therefore, provides a route to make medium-pore zeolites attractive tunable catalyst components for the hydroisomerization of long-chain hydrocarbons.

**Image 1:**



## References:

- [1] I. Kubičková, D. Kubička, *Waste Biomass Valorization* 1 (2010) 293–308.
- [2] G. Wang, Q. Liu, W. Su, X. Li, Z. Jiang, X. Fang, C. Han, C. Li, *Appl. Catal., A* 335 (2008) 20-27.
- [3] P. Sazama, Z. Sobalik, J. Dedecek, I. Jakubec, V. Parvulescu, Z. Bastl, J. Rathousky, H. Jirglova, *Angew. Chem., Int. Ed.* 52 (2013) 2038–2041.

**Synthesis of nanosized chabazite using alkali-metal cations as SDA: a record of dynamic exchange of alkali-metal cations over hydrothermal treatment time**

S. Ghosvand<sup>1,\*</sup>, E. Clatworthy<sup>1</sup>, V. Ruaux<sup>1</sup>, S. Mintova<sup>1</sup>

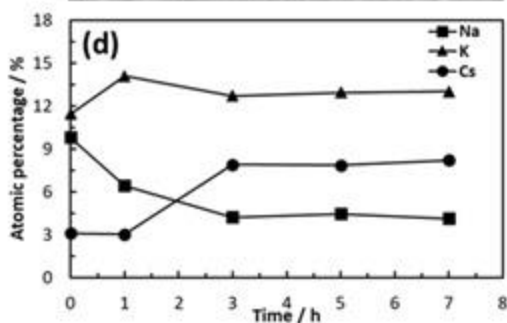
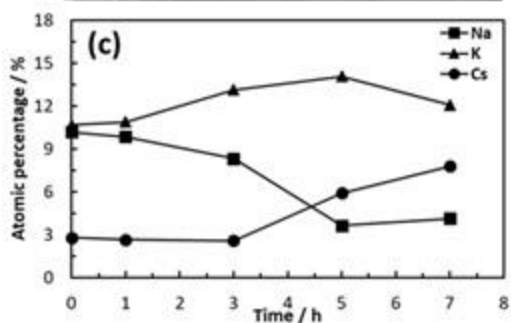
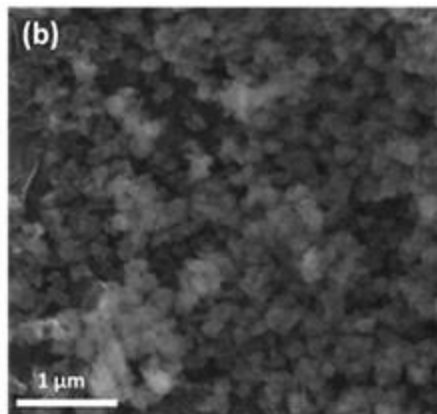
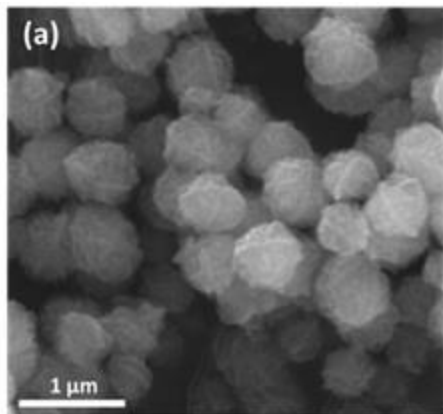
<sup>1</sup>Laboratoire Catalyse & Spectrochimie (LCS), Ensicaen, Caen, France

**Abstract Text:** Zeolites have immense importance in industrial applications such as separation and catalysis because of their thermally stable crystalline structures and molecular-sized pore networks ( $\approx 0.3$  to  $1.5$  nm)<sup>1,2</sup>. Typically, the synthesis of high silica or nano-sized zeolites involves using organic structural directing agents which increases the cost of manufacturing, and are often non-environmentally friendly<sup>3</sup>. Nanosized zeolites were also synthesized using alkali-metal cations as structure directing agents (SDAs) which reduces the budgetary and environmental cost by eliminating the use of expensive organic templates<sup>3</sup>. Recently nano-sized chabazite zeolite (nano-CHA) was synthesized in our group using alkali-metal cations as SDAs<sup>4</sup>. However, the role of the alkali-metal cations during the synthesis requires further investigation.

In this work we focus on the effect of aging time at room-temperature on the formation of nanosized CHA zeolite. The change in the cation composition of the recovered solid material during the hydrothermal (HT) treatment at  $90$  °C was evaluated. Here, a mixture of  $\text{Na}^+$ ,  $\text{K}^+$ , and  $\text{Cs}^+$  cations were used to direct the formation of the CHA structure. Prolongation of the aging time at room-temperature (from 4 days (K04) to 17 days (K17)) resulted in smaller nanosized crystals of CHA (from  $500$  nm to  $50$  nm) and faster crystallization during the HT treatment ( $7$  h to  $3$  h). Crystal sizes were investigated by SEM, and crystal formation by XRD measurements. Finally, changes in the cation composition of the recovered solid materials were followed by ICP-MS. The results highlighted that the  $\text{Na}^+$  content plays a critical role in the early stages of nucleation and at the beginning of the HT treatment by facilitating the dissolution of silica species. The  $\text{K}^+$  content increases slightly during the HT treatment leading to the formation of CHA nanocrystals: the role of  $\text{K}^+$  is to facilitate the formation of the CHA structural building units such as *t-cha* and *d6r*. Finally, the  $\text{Cs}^+$  content increases during the HT treatment simultaneously with a decrease in the  $\text{Na}^+$  cation content, reaching a maximum when fully crystalline nano-CHA zeolite is formed which suggests that  $\text{Cs}^+$  stabilizes the structure.

*Image 1. SEM images of chabazite nanocrystals (a) sample K04 and (b) sample K17 synthesized under HT treatment at  $90$  °C for 7 and 3 hours, respectively, and the cation contents of (c) K04 and (d) K17 over 7 hours of HT treatment measured by ICP-MS.*

**Image 1:**



- References:** 1. Cheung, O. & Hedin, N. Zeolites and related sorbents with narrow pores for CO<sub>2</sub> separation from flue gas. *RSC Adv.* 4, 14480–14494 (2014).
2. Shang, J. et al. Determination of Composition Range for “Molecular Trapdoor” Effect in Chabazite Zeolite. *J. Phys. Chem. C* 117, 12841–12847 (2013).
3. Ng, E.-P., Chateigner, D., Bein, T., Valtchev, V. & Mintova, S. Capturing Ultrasmall EMT Zeolite from Template-Free Systems. *Science* 335, 70–73 (2012).
4. Debost, M. et al. Synthesis of discrete CHA zeolite nanocrystals without organic templates for selective CO<sub>2</sub> capture. *Angew. Chem.* (2020).

## ***New Synthetic Methods and Post-Synthetic Modification | Zeolites/Inorganic materials***

FEZA21-PO-247

### **Synthesis of self-standing FAU-X porous monoliths by geopolymer gel conversion**

A. Campanile<sup>1,\*</sup>, B. Liguori<sup>1</sup>, D. Caputo<sup>1</sup>, C. Ferone<sup>2</sup>, L. Gigli<sup>3</sup>, P. Aprea<sup>1</sup>

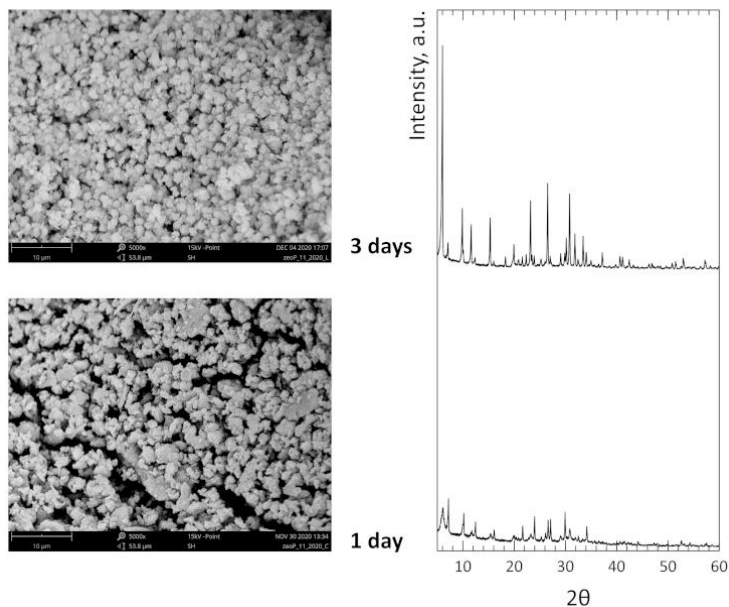
<sup>1</sup>Department of Chemical, Materials and Production Engineering (DICMaPI), University of Naples Federico II,

<sup>2</sup>Department of Engineering, University of Naples Parthenope, Naples, <sup>3</sup>Elettra Synchrotron Light Source, Trieste, Italy

#### **Abstract Text:**

FAU-X zeolite has been extensively used for long, either in standard industrial processes or in emerging fields, such as removal of hydrogen sulfide from biogas and CO<sub>2</sub> capture [1]. Since the zeolite is generally synthesised as micronic powder (0.5–5 μm), shaping it has become necessary for most industrial processes. Different methods have been developed to achieve this technological goal, by using porous ceramic binders, polymer foams, or permeable bags [2]. Pelletization and extrusion are the most frequently used methods to shape powdery zeolites, but they require a binder that can partially obstruct the active sites of zeolite [3-4]. Recently, additive manufacturing (AM) approach has been also tested to obtain binder-less shaped zeolite monoliths [5]. Geopolymers can be considered the amorphous counterpart or precursors of crystalline zeolites, therefore it is possible to promote the nucleation of a zeolite inside a geopolymeric matrix by tuning pH, temperature, pressure, and time of the geopolymerization reaction. Recently, a one-step procedure is successfully carried out realizing geopolymerization and crystallization under mild operating conditions [6]. An open cellular porosity was also induced by in-situ inorganic foaming process. It has been demonstrated that this route leads to the crystallization of two distinct zeolites, Na-A [LTA] and 13X [FAU], obtaining a hierarchical porous monolith containing macro-, meso- and micro-pores [6]. However, the possibility to drive the synthesis toward a monophasic zeolitic sample represents a challenge to improve the technological performances of these monoliths. Previous results [6] demonstrated that the nucleation started after one day and, without any control, the growth of both phases completed after 3 days of curing time. Starting from these findings, in this paper a two-step geopolymer conversion process to obtain a self-standing FAU-X monolith has been set up. Firstly, a metakaolin-based geopolymer precursor was obtained, inducing the formation of macropores by silicon-promoted foaming. Then, the porous geopolymer precursors, containing nanometer-sized crystalline structures resembling the nuclei around which zeolites crystallize [7], have been converted into FAU-X monoliths by means of an alkaline treatment at different temperatures and times. The influence of NaOH concentration (0.1 to 2 M), treatment temperature (40 to 80 °C) and time (24 to 72 h) on the FAU-X crystallization was studied. The crystallization kinetics of FAU-X inside the geopolymer slurry was investigated by means of X-ray diffraction quantitative phase analysis (XRD-QPA) and scanning electron microscopy (SEM). As revealed from such analysis, the highest yield in terms of zeolite content and FAU-X / LTA ratio (about 9 / 1) was obtained performing the synthesis process with a 0.5 M NaOH solution at 60°C for 72 hours.

**Image 1:**



### References:

- [1] Fan, X. and Jiao, Y. (2020). Porous Materials for Catalysis: Toward Sustainable Synthesis and Applications of Zeolites. In *Sustainable Nanoscale Engineering* (pp. 115-137). Elsevier.
- [2] Bingre, R., Louis, B., Nguyen, P. (2018). An overview on zeolite shaping technology and solutions to overcome diffusion limitations. *Catalysts*, 8(4), 163
- [3] Aranzabal, A. et al. Optimization of process parameters on the extrusion of honeycomb shaped monolith of H-ZSM-5 zeolite. *Chem. Eng. J.* 162, (2010).
- [4] Li, Y. Y., Perera, S. P., Crittenden, B. D. & Bridgwater, J. The effect of the binder on the manufacture of a 5A zeolite monolith. *Powder Technol.* 116, (2001).
- [5] Lawson, S. et al. Binderless zeolite monoliths production with sacrificial biopolymers. *Chem. Eng. J.* 407, (2021).
- [6] Liguori, B., Aprea, P., Roviello, G., & Ferone, C. (2019). Self-supporting zeolites by Geopolymer Gel Conversion (GGC). *Microporous and Mesoporous Materials*, 286, 125-132.
- [7] Provis, J. L., Lukey, G. C., van Deventer, J. S. (2005). Do geopolymers actually contain nanocrystalline zeolites? A reexamination of existing results. *Chemistry of materials*, 17(12), 3075-3085.

**Magnetic Chabazite Zeolite: An Ecofriendly Synthesis**

C. R. F. Alves<sup>1,\*</sup>, A. D. L. Freitas<sup>1</sup>, T. G. Martins<sup>1</sup>, S. N. C. Oliveira<sup>1</sup>, S. D. A. Soares<sup>1</sup>, A. R. Loiola<sup>1</sup>

<sup>1</sup>Organic and Inorganic Chemistry Department, Federal University of Ceará, Fortaleza, Brazil

**Abstract Text:** Energy generation is one of the biggest challenges for modern society. In this context, mineral coal, the most abundant fossil fuel on Earth, with reserves estimated at one trillion tons, plays an important role. However, its use involves some major disadvantages, including the generation of high amounts of fly ash. In contrast, fly ash has the potential to be used as the main sources of new materials, which is not only desirable but also needed considering the possibility of converting a residue that is harmful into a useful material. Fly ash appears as micrometric spherical particles, resulted from the fused aluminosilicate minerals being carried by the combustion gases. Their major mineral constituents include kaolinite, illite, and quartz, which can be applied as raw materials for the zeolite synthesis. Scientific community have shown interest in zeolitic materials for their potential applications in different areas, for example, in the treatment of effluents and soil, in agriculture, in animal and veterinary production, and even in medicine. Many other applications may emerge for environmental protection and the production of renewable fuels derived from biomass. Bearing this in mind, there is a continuous search for new zeolitic structures with well-defined properties and reengineering of existing structures, particularly magnetic zeolites. This work proposes the synthesis of chabazite (CHA) zeolite from coal fly ash (FA) and the incorporation of magnetic oxides, extracted from the FA, in the zeolite structure producing a magnetic composite. For that, FA underwent a prior physical-chemical separation treatment to remove potentially interfering materials in the syntheses of zeolites. The synthesis of CHA zeolite was carried via hydrothermal route based on the methodology described by Bourgogne[1]. The formation of zeolitic phases (ZC and ZCM) was confirmed via X-ray diffractometry (XRD) (Fig. 1a), as well as the presence of the preserved zeolitic phases in the samples of the prepared composites[2]. Scanning electron microscopy (SEM) analyses of the NMF samples show the characteristic spherical shape (Fig. 1b), while the MF samples, also spherical, have their surfaces covered by iron oxides particles (Fig. 1c). The SEM images of the synthesized zeolite (ZC – Fig. 1d-e) and the magnetic composite (ZCM – Fig. 1f-g) show the pseudo-hexagonal shape characteristic of chabazite zeolite, indicating the magnetic particles do not affect the zeolite crystal habit. N<sub>2</sub> adsorption isotherms for ZC and ZCM isotherms are presented in Fig. 2a. Specific BET surface area was calculated for the samples of ZC and ZCM, with respective values of 296.67 m<sup>2</sup> g<sup>-1</sup> and 1,230.58 m<sup>2</sup> g<sup>-1</sup>. Fig. 2b presents the pore size distribution for ZC and ZCM indicating uniform width of pore. The zeolites proposed in this work were efficiently synthesized and maintained their crystalline phases in their respective composites, with magnetic responses, giving them the potential for use in applications such as adsorption in gaseous systems and metal ions in aqueous solutions, having the advantage of the high adsorption capacity characteristic of zeolites, combined to the magnetic responses from the iron oxides present in the composites, in a single, simple, and compact process, giving a purpose to an industrial by-product.

**Image 1:**

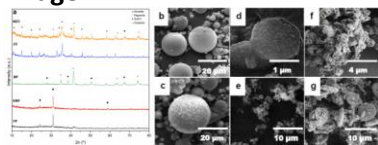
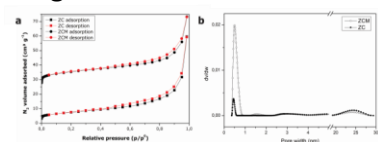


**Image 2:**



**References:** [1] Bourgogne, J.-L Guth, R. Wey, *Verified Syntheses of Zeolitic Materials*, 123 (2001)

[2] X. Xiong, et. al, *Journal of Materials Chemistry A*, Vol 5, Ed: 19, 9076-9080 (2017).

**Alkaline treatment for self-defect-healing of silicalite-1 membrane**

M. Sakai<sup>1</sup>, H. Hori<sup>2,\*</sup>, M. Matsukata<sup>1,2,3</sup>

<sup>1</sup>Research Organization for Nano & Life Innovation, <sup>2</sup>Applied Chemistry, <sup>3</sup>Advanced Research Institute for Science and Engineering, Waseda University, Tokyo, Japan

**Abstract Text:** Reducing intercrystalline defects is essential to obtain a zeolite membrane with good molecular sieving ability. Various post-treatment methods such as silylation and carbon modification have previously been reported to improve the separation performance of membrane [1,2]. Alkaline treatment with surfactant has been reported to produce a hierarchical zeolite [3]. The addition of surfactant like cetyltrimethylammonium bromide (CTAB) allows the formation of uniform mesopores without disrupting crystal structure. Such alkaline treatment with surfactant is used to enhance the catalytic properties of zeolites. In this study, we adopt the alkali treatment to silicalite-1 membrane and investigated the effect of this treatment method on the permselectivity of silicalite-1 membrane.

Silicalite-1 membrane was prepared by a secondary growth method. Seed crystals were loaded on the outer surface of  $\alpha$ -alumina support by a dip-coating technique, and the seeded support was hydrothermally treated to produce silicalite-1 membrane. The obtained silicalite-1 membrane was subjected to the alkaline treatment. Silicalite-1 membrane was immersed in an aqueous solution containing 0.1 M NaOH and 0.05 M CTAB at 358 K for given periods. The membrane was then washed with boiling water and calcined at 673 K. *n*-Hexane(*n*-Hex)/2,3-dimethylbutane(2,3-DMB) permeation separation test was performed to evaluate the molecular sieving property of membranes. Changes in the ratio of non-zeolitic pathway were evaluated by the nano-permporometry. Various characterizations such as XRD and N<sub>2</sub> adsorption were also performed.

When the alkali treatment was performed up to 15 min, the permeance of 2,3-DMB decreased and the separation factor remarkably increased from 86.5 to 559. The results of nano-permporometry suggested that the non-zeolitic pathways on silicalite-1 membrane were occluded in the early stage of the alkaline treatment, resulting in the enhancement of separation performance. In contrast, the permeance of 2,3-DMB increased with decreasing separation factor after prolonged alkaline treatment for >30 min. These results indicated that large defects formed in the later stage. In addition, based on the results of XRD and N<sub>2</sub> adsorption, we confirmed that the crystallinity of membrane hardly declined up to 30 min of treatment.

While in order to study the role of CTAB in the alkali treatment post-treatments with only NaOH or CTAB were carried out, respectively, the separation performance of silicalite-1 membranes treated with only NaOH and CTAB was not improved. These results indicated the concerted effect of NaOH and CTAB is necessary to improve separation performance.

References

- [1] M. Nomura, T. Yamaguchi, S. Nakao, *Ind. Eng. Chem. Res.*, 36 (1997) 4217-4223.
- [2] Y. Yan, M. E. Davis, G. R. Gavalas, *J. Membr. Sci.*, 123 (1997) 95-103.
- [3] J. Garcia-Martinez, M. Johnson, J. Valla, K. Li, J. Y. Ying, *Catal. Sci. Technol.*, 2 (2012) 987–994.

**Core-shell ZSM5/Sil-1 composites: application in dehydration reactions.**

G. Ferrarelli<sup>1,\*</sup>, A. Aloise<sup>2</sup>, F. Dalena<sup>2</sup>, G. Giorgianni<sup>2</sup>, G. Giordano<sup>2</sup>, M. Migliori<sup>2</sup>

<sup>1</sup>Department of Chemical, Biological, Pharmaceutical and Environmental Sciences, UNIME, UNIME, Messina,

<sup>2</sup>Department of Environmental Engineering, , University of Calabria, Rende, CS, Italy

**Abstract Text: INTRODUCTION**

Acidity control is still one of the most relevant research topics for zeolites applications in heterogeneous industrial catalysis. Growing interest in renovating towards approach with the aim of changing surface acidity has been developed. The strategy consists in depositing a shell layer of an inert material, typically Silicalite-1, around the crystals of an acid zeolite, with the purpose of passivating zeolites surface acidity [2],[3]. Core-shell synthesis generally consists in two phases: core synthesis and epitaxial growth of Silicalite-1 over the starting catalyst. The technique of passivating with Silicalite-1 zeolites surface acidity has been used for various applications such as the alkylation of toluene to enhance the selectivity to para-xylene [2], methanol to hydrocarbon reaction [3],[4], biomass catalytic pyrolysis [4]. However, the Silicalite-1 layer coated on a zeolitic core is an useful approach to avoid the contact between Redox and Acid functions in the synthesis of hybrid catalysts that is one of the most frequent catalyst deactivation causes [5],[6]. To study the effect of Silicalite-1 deposition over a zeolitic core, we report on core-shell synthesis (using ZSM-5 cores with Si/Al ratio equal to 11 and 25 respectively) and application on methanol dehydration reaction.

**MATERIALS AND METHODS**

ZSM-5 zeolites with a Si/Al ratio in the synthesis gel equal to 11 and 25 was prepared following the procedure published elsewhere [7] and it was used as core for the following Silicalite-1 layer deposition.

The Silicalite-1 synthesis gel had the following molar ratios:  $2\text{SiO}_2 - 0.5\text{TPAOH} - 8\text{EtOH} - 120\text{H}_2\text{O}$ . 5 g of H-ZSM-5 crystals previously obtained were immersed into the precursor solution. The crystallization was carried out under hydrothermal conditions at 180°C for 24 h in a stainless-steel vessel using a tumbling oven. The products were rinsed repeatedly by deionized water and dried at 363 K overnight. The procedure was repeated twice to increase the Silicalite-1 layer thickness. Samples obtained were named ZSM-5\_N\_X, where N indicated the core Si/Al ratio (11 or 25) and x indicated the presence of the double-Silicalite-1 layer. Samples were studied by X-ray diffraction (XRD), N<sub>2</sub> adsorption isotherms, transmission electron microscopy (TEM), atomic absorption spectroscopy (AAS), thermogravimetric analysis (TGA), temperature-programmed desorption of ammonia and infrared spectroscopy (FR-IR). Parent zeolite and core-shell catalysts were tested for the reaction of methanol dehydration to DME in an atmospheric system at 160-240°C.

**RESULTS AND DISCUSSION**

X-ray patterns demonstrated the samples crystallinity (Figure 1). Atomic absorption results and TEM images confirmed the growth of a thin Silicalite-1 layer over the starting cores. Porosimetric data showed an increase in external surface area of the coated samples compared to that of the parent zeolites one. NH<sub>3</sub>-TPD and IR results showed a lower acid content for core-shell catalysts. Furthermore, a weak decreasing of the catalytic activity was observed using core-shell samples (Figure 2) in agreement with the decreased acidity.

**CONCLUSION**

In this work core-shell catalysts have been synthesized by growing a layer of Silicalite-1 over a H-ZSM-5 zeolite core through the epitaxial growth technique. The obtained samples showed a lower acidity than the parent zeolites supporting the hypothesis of a good happened passivation process and promising results were obtained in catalytic test for the DME production from methanol.

Image 1:

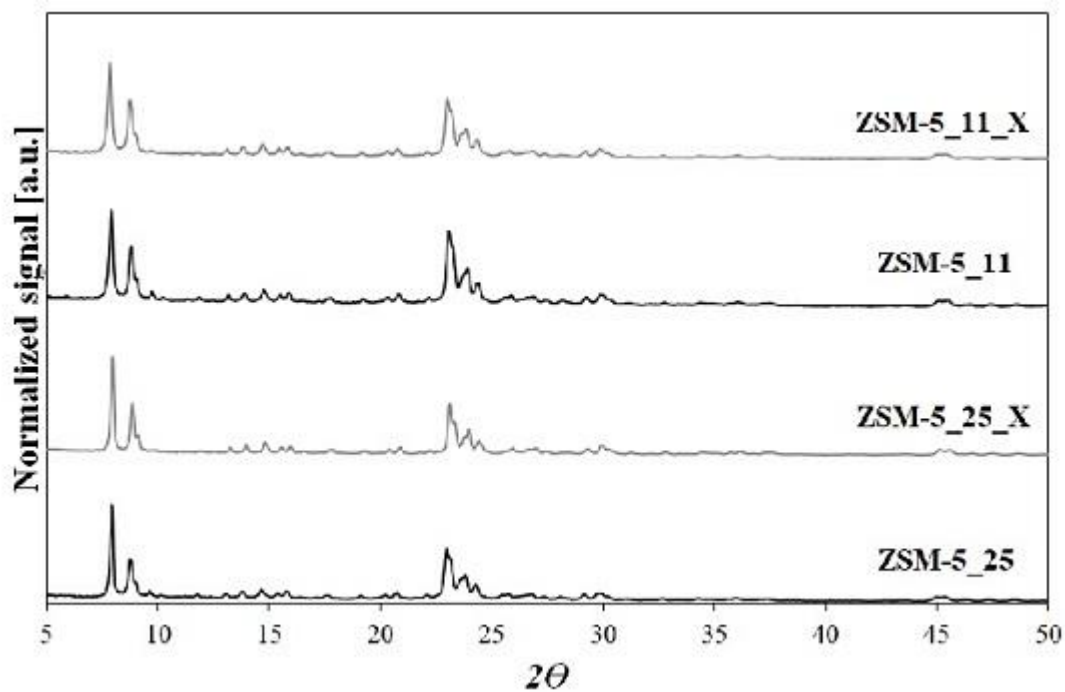
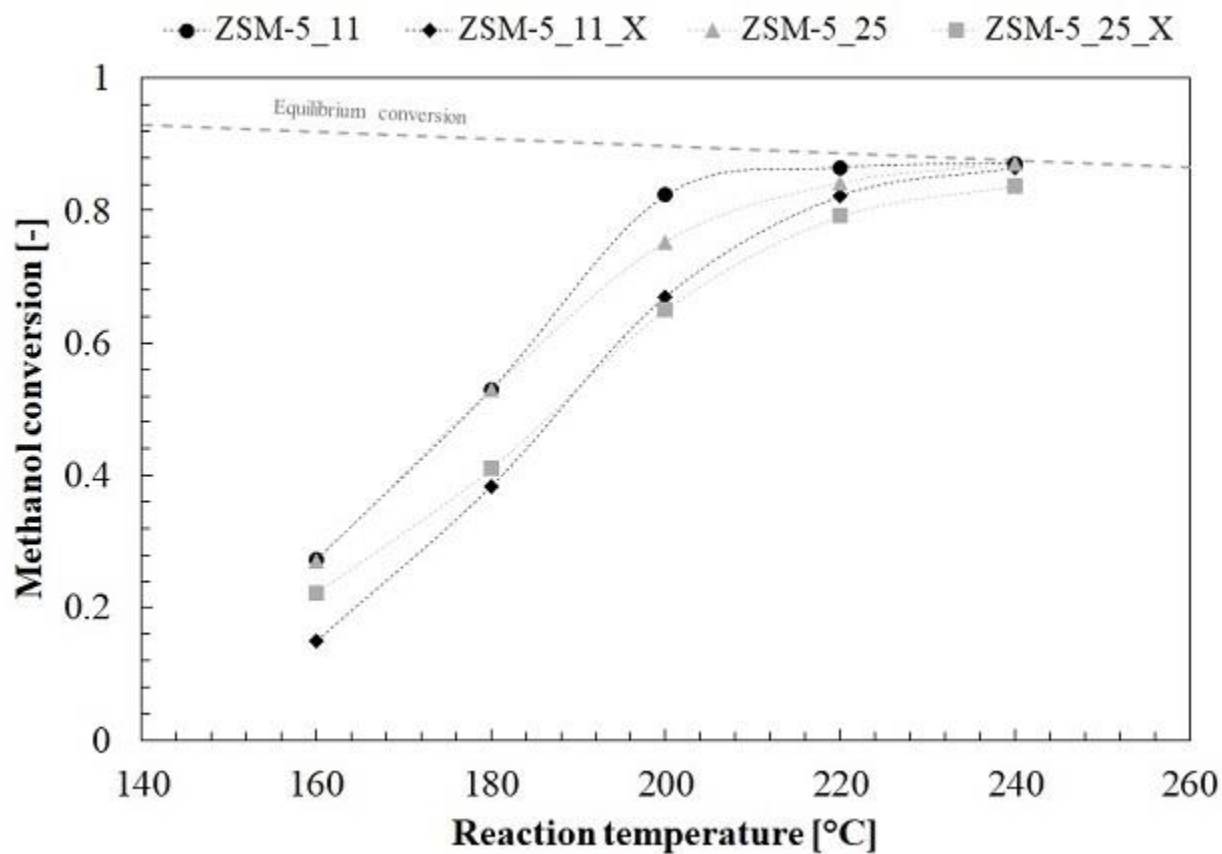


Image 2:



**References:** [1]

- E. Catizzone, M. Migliori, A. Aloise, R. Lamberti, G. Giordano, Hierarchical low si/al ratio ferrierite zeolite by sequential postsynthesis treatment: Catalytic assessment in dehydration reaction of methanol, *J. Chem.* 2019 (2019). <https://doi.org/10.1155/2019/3084356>.
- [2] D. Van Vu, M. Miyamoto, N. Nishiyama, S. Ichikawa, Y. Egashira, K. Ueyama, Catalytic activities and structures of silicalite-1/H-ZSM-5 zeolite composites, *Microporous Mesoporous Mater.* 115 (2008) 106–112. <https://doi.org/10.1016/j.micromeso.2007.12.034>.
- [3] F. Goodarzi, I.P. Herrero, G.N. Kalantzopoulos, S. Svelle, A. Lazzarini, P. Beato, U. Olsbye, S. Kegnæs, Synthesis of mesoporous ZSM-5 zeolite encapsulated in an ultrathin protective shell of silicalite-1 for MTH conversion, *Microporous Mesoporous Mater.* 292 (2020) 109730. <https://doi.org/10.1016/j.micromeso.2019.109730>.
- [4] M. Li, Y. Hu, Y. Fang, T. Tan, Coating mesoporous ZSM-5 by thin microporous Silicalite-1 shell: Formation of core/shell structure, improved hydrothermal stability and outstanding catalytic performance, *Catal. Today.* 339 (2020) 312–320. <https://doi.org/10.1016/j.cattod.2019.02.041>.
- [5] Z. Jin, S. Liu, L. Qin, Z. Liu, Y. Wang, Z. Xie, X. Wang, Methane dehydroaromatization by Mo-supported MFI-type zeolite with core-shell structure, *Appl. Catal. A Gen.* 453 (2013) 295–301. <https://doi.org/10.1016/j.apcata.2012.12.043>.
- [6] I. Miletto, E. Catizzone, G. Bonura, C. Ivaldi, M. Migliori, E. Gianotti, L. Marchese, F. Frusteri, G. Giordano, In situ FT-IR characterization of CuZnZr/ferrierite hybrid catalysts for one-pot CO<sub>2</sub>-to-DME conversion, *Materials (Basel).* 11 (2018). <https://doi.org/10.3390/ma11112275>.
- [7] M. Migliori, A. Aloise, G. Giordano, Methanol to dimethylether on H-MFI catalyst: The influence of the Si/Al ratio on kinetic parameters, *Catal. Today.* 227 (2014) 138–143. <https://doi.org/10.1016/j.cattod.2013.09.033>.

**Computational Study of the Formation of Sn-BEA for Liquid Phase Catalysis**

O. T. Beynon<sup>1,\*</sup>, A. J. Logsdail<sup>1</sup>, A. Owens<sup>2</sup>

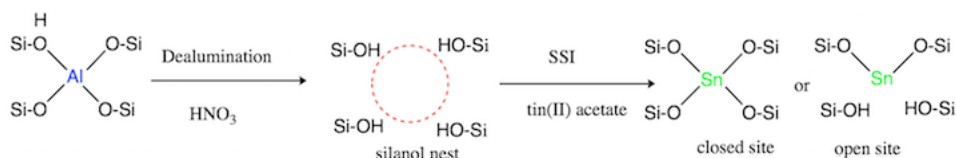
<sup>1</sup>School of Chemistry, <sup>2</sup>School of Medicine, Cardiff University, Cardiff, United Kingdom

**Abstract Text:** Lewis acidic zeolites have gained much interest recently, owing to their ability to efficiently catalyse several important reactions. The substitution of Lewis-acid heteroatoms into zeolitic framework induces increased catalytic activity compared to purely siliceous zeolites and Brønsted-acidic aluminosilicates. Zeolite Tin-BETA (Sn-β) is a tin-containing zeolite of the BEA-type framework, which has shown remarkable activity and selectivity for numerous catalytic reactions, such as the Baeyer-Villiger oxidation (BVO) and the Meerwein-Ponndorf-Verley reduction (MPV reduction). [1] In the BVO, Sn-β can utilise hydrogen peroxide as a green-oxidant, compared to conventional oxidants such as mCPBA. Sn-β has shown increased activity over analogous Lewis-acid zeolites such as Ti-β. This increased catalytic ability highlights the potential importance for green and sustainable chemistry; however, conclusive understanding of the Sn active site remains elusive.

Conventional methods of zeolite synthesis, such as hydrothermal synthesis, pose a problem as the procedure requires strong acids, such as HF, as mineralising agents, which is both environmentally harmful and industrially inappropriate, due to its acidic nature. New methods of synthesis, such as solid-state incorporation (SSI) [1], have successfully inserted Sn into the BEA framework, without impairing the activity of the catalyst for the BVO and MPV reactions. SSI also demonstrates higher metal loading and decreased synthesis time compared to hydrothermal synthesis, which addresses some of the key limitations for industrial applications. In this method (Figure 1), complete dealumination of the framework occurs, forming silanol nests in the previous Al sites. The solid tin(II) acetate precursor is added, forming Sn sites in the vacant tetrahedral (T-sites) within the framework. The solvent free nature of this method makes it highly scalable and is environmentally beneficial.

Though there have been several experimental studies, the exact mechanism of insertion remains elusive. Therefore, my research is a computational investigation into the formation of these tin sites within the dealuminated framework, extending on work conducted by experimental collaborators [2]. The inserted tin can exist in both Sn(II) and Sn(IV) oxidation states, which manifest as an open or closed site, respectively (Figure 1) and exhibit different catalytic activity. Current efforts are focused on modelling the T2 and T9 sites, which have been reported to be the most stable sites for substitution. [3], [4] Extra-framework tin species are also of interest, as these oligomeric tin species, Sn<sub>x</sub>O<sub>y</sub>, are produced at higher loadings and block the pores, reducing catalytic activity. Thus, gaining insights into tin insertion can lead to an optimisation of synthetic procedure, and the catalytic performance, potentially leading to successful industrial applications.

**Image 1:**



**References:** [1] Hammond C, et al., *Angew. Chem. Int.*, (2012) 51, 11736–11739; [2] Hammond C, et al., *ChemCatChem* (2015) 7, 3322–3331; [3] Shetty S, et al., *Chem. Eur. J* (2006) 12, 518–523; [4] Valencia B, et al., *J. Phys. Chem. C* (2016), 120, 2176–2186

**Phosphorus modification into various small-pore zeolites for improvement of catalytic durability in ethanol conversion and NH<sub>3</sub>-SCR reactions**

N. Tsunoji<sup>1,\*</sup>, Y. Kakiuchi<sup>1</sup>, M. Sadakane<sup>1</sup>, T. Sano<sup>1</sup>

<sup>1</sup>Graduate school of engineering, department of applied chemistry, Hiroshima University, Higashi-hiroshima, Japan

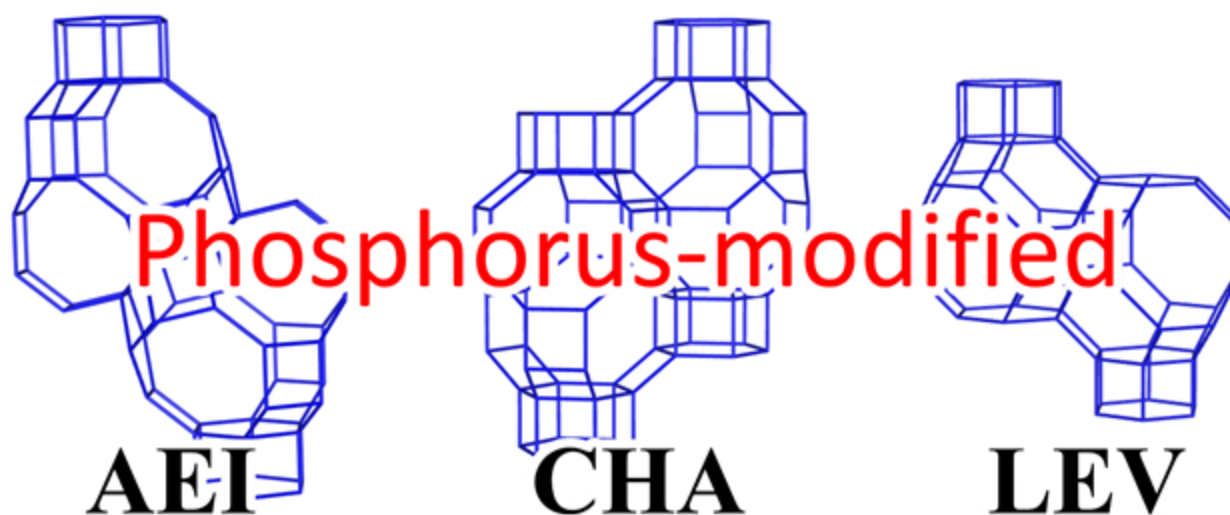
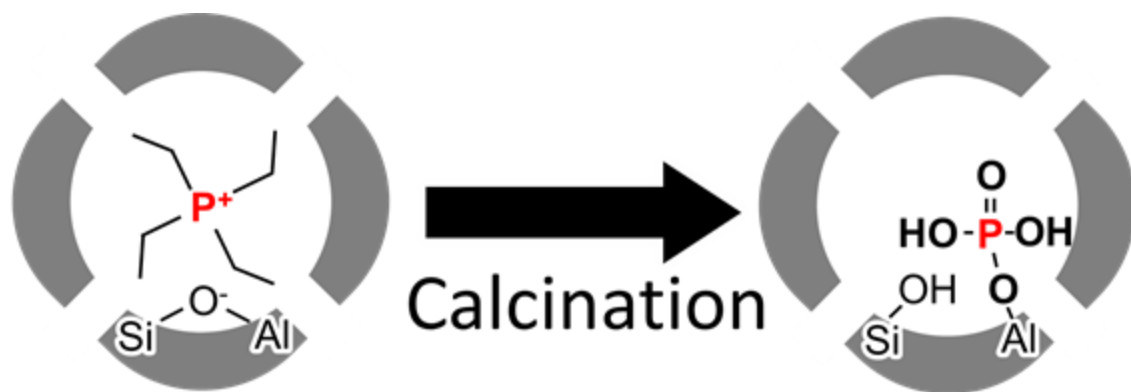
**Abstract Text:** Small-pore zeolites with 8-membered ring (8-MR) windows, such as CHA, AEI, and LEV have received a considerable amount of attention, recently. They are typically used as industrial catalysts for the selective catalytic reduction of NO<sub>x</sub> by ammonia (NH<sub>3</sub>-SCR), for emission purification and light olefin production using alcohol; especially from methanol (methanol to olefin, MTO) and ethanol (ethanol to olefin, ETO), due to their useful framework structures and pore systems. In contrast, given that these processes are conducted at high reaction temperatures in the presence of steam, thermal and hydrothermal resistances of the small-pore zeolites are essential for maintaining their high catalytic activity and selectivity during the catalytic system. In addition, further enhancement of the thermal/hydrothermal stability ensures a high catalytic efficiency at high reaction temperatures, and their application in a wide range of fields.

We have investigated zeolite synthesis from zeolite as a starting material<sup>1</sup>, hydrothermal conversion of zeolite or interzeolite conversion (IZC), as an alternative method for obtaining highly-stable zeolite materials<sup>2,3</sup>. This method can provide highly crystalline zeolite without structural defects. This is probably due to the locally ordered specific aluminosilicate formed by the hydrothermal decomposition of the zeolite starting material that was effectively construct the framework of the formed zeolite. Recently, by using phosphonium-containing OSDA (P-OSDA) during the hydrothermal conversion, a phosphorus modified small-pore zeolite with a high thermal/hydrothermal stability was successfully synthesized<sup>4,5</sup>. It is common knowledge that the impregnation of phosphorus compounds such as H<sub>3</sub>PO<sub>4</sub> is highly effective for the enhancement of the thermal/hydrothermal stability of zeolites, given that the presence of highly condensed polyphosphate species bound to the framework Al suppresses the crystal structure collapse caused by dealumination. In contrast, the post-modification has not been achieved in small-pore zeolites due to the limited diffusion of such phosphorus species into the small pores. Therefore, the phosphorus modification using alkylphosphonium would be additional tool to further improve and tune catalytic durability of zeolite.

In this study, phosphorus modified small-pore zeolites with different phosphorus modification degrees and framework structures (CHA, AEI, and LEV) were prepared by using various combination of alkylammonium and alkylphosphonium. The catalytic performances in NH<sub>3</sub>-SCR reaction and alcohol conversion reaction of ethanol to olefin (ETO) were investigated<sup>6</sup>. The catalytic performances of small-pore zeolites synthesized using different starting materials; namely, amorphous silica or zeolite material (zeolite hydrothermal conversion), were also evaluated and compared.

The thermal stabilities of the zeolites were strongly dependent on the framework topologies and degrees of phosphorus modification. Moreover, the phosphorus modification on small-pore zeolites was very useful for preparing a highly durable catalyst. An increase in the degree of phosphorus modification resulted in an increase in the catalytic durability and thermal stability by the suppression of the dealumination of zeolite framework. However, in the case of the catalyst for NH<sub>3</sub>-SCR, an optimized degree of phosphorus modification was required for showing high NO conversion even after severe hydrothermal treatment. By changing the combination of the OSDA, the method of phosphorus modification in this study would be applied to a wide variety of zeolite syntheses and can be used to improve the thermal and hydrothermal stabilities. Thus, the method will serve as a suitable alternative for the synthesis of zeolite material with high durability, for new application fields that require high catalytic efficiency.

**Image 1:**



Highly stable catalyst in  
**NH<sub>3</sub>-SCR** and **ETO** process

- References:** 1. T. Sano, M. Itakura and M. Sadakane, *J. Jpn. Pet. Inst.*, 2013, 56, 183.  
 2. T. Takata, N. Tsunoji, Y. Takamitsu, M. Sadakane and T. Sano, *Microporous Mesoporous Mater.*, 2016, 225, 524.  
 3. N. Funase, T. Tanigawa, Y. Yamasaki, N. Tsunoji, M. Sadakane and T. Sano, *J. Mater. Chem. A*, 2017, 5, 19245.  
 4. T. Sonoda, T. Maruo, Y. Yamasaki, N. Tsunoji, Y. Takamitsu, M. Sadakane and T. Sano, *J. Mater. Chem. A*, 2015, 3, 857.  
 5. Y. Yamasaki, N. Tsunoji, Y. Takamitsu, M. Sadakane and T. Sano, *Microporous Mesoporous Mater.*, 2016, 223, 129.  
 6. Y. Kakiuchi, T. Tanigawa, N. Tsunoji, Y. Takamitsu, M. Sadakane and T. Sano, *Appl. Catal. A-Gen.*, 2019, 575, 204.

**Cross-shaped gismondine-type zeolite from Philippine bentonite**

H. S. O. Cosinero<sup>1,\*</sup>, M. T. Conato<sup>2</sup>

<sup>1</sup>Materials Science and Engineering, <sup>2</sup>Institute of Chemistry, College of Science, University of the Philippines Diliman, Quezon City, Philippines

**Abstract Text:** The Philippines is home to many volcanic structures which makes it abundant in natural clay materials. This study utilized natural Philippine bentonite, locally used in commercial cosmetics, as raw material for gismondine-type zeolite synthesis. The initial silicon-aluminum ratio was adjusted to 1.18 and was mixed with 3M NaOH and heated to 300°C for 1h. The incubation time was 92h, after that, the sample was crystallized at 90°C for 24h. Successful synthesis of gismondine-type zeolite was confirmed through X-ray diffraction analysis and Fourier transform infrared spectroscopy. The scanning electron micrograph showed cross-shaped morphology with average particle size of  $8.97 \pm 3.2 \mu\text{m}$ . Gismondine-type zeolites are known for their adsorption application.

**Image 1:**

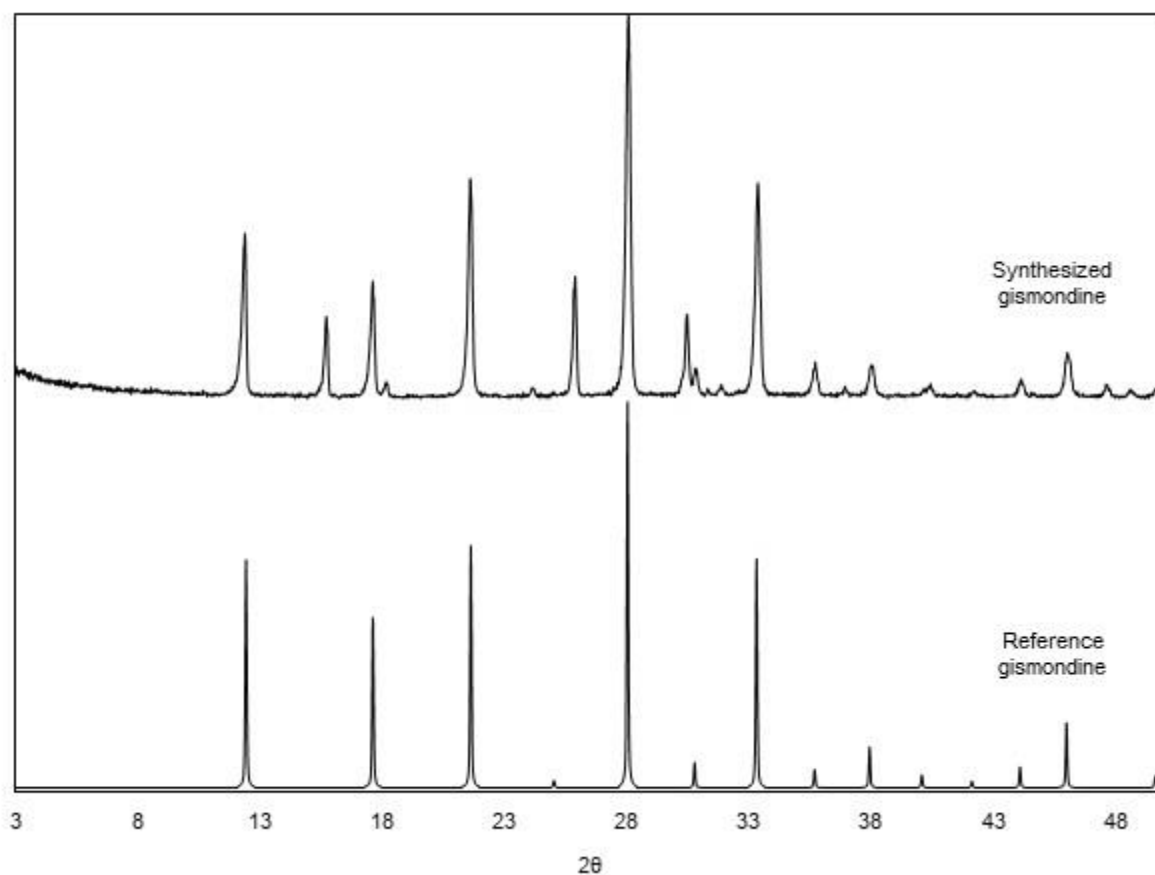
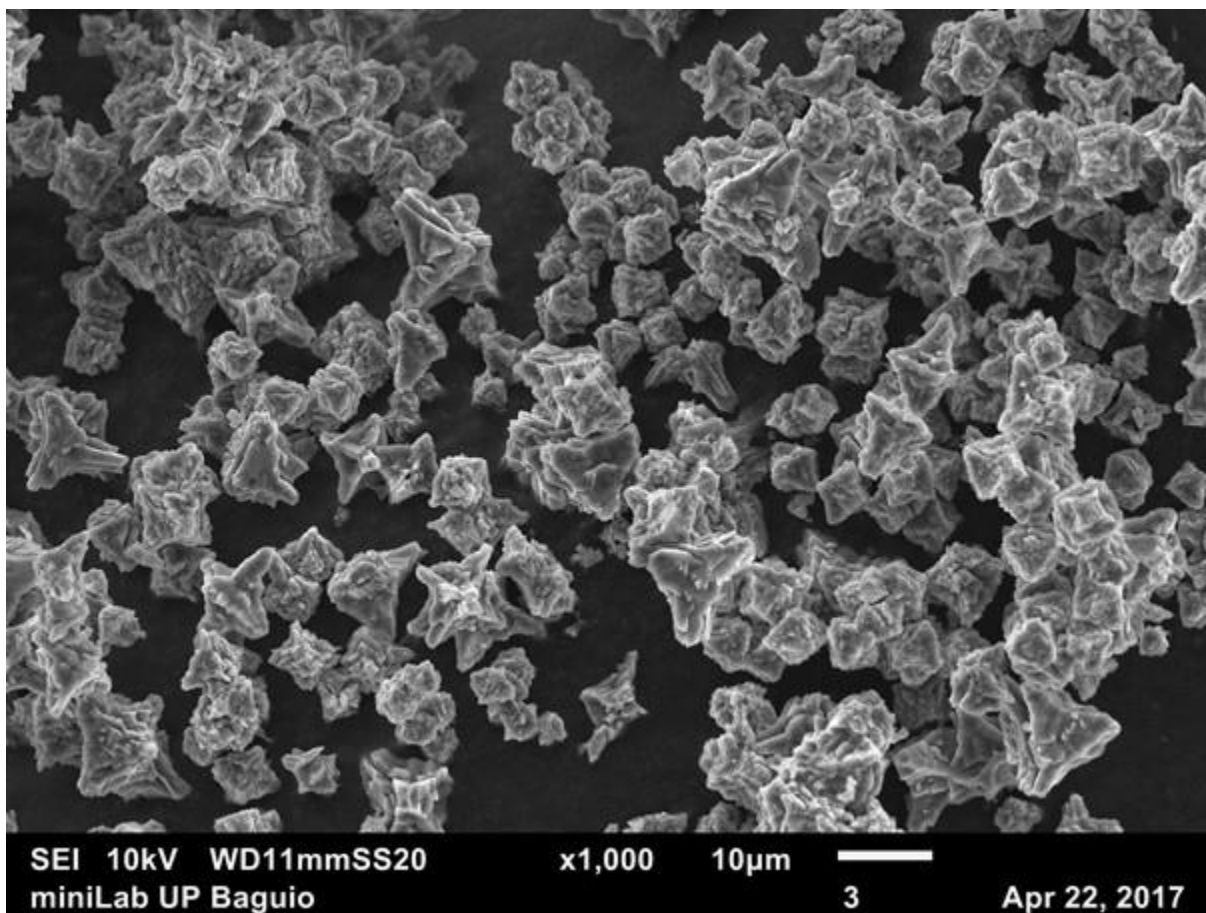


**Image 2:**



- References:** 1. H. Faghihian and N. Godazandeha, "Synthesis of nano crystalline zeolite Y from bentonite," *Journal of Porous Materials*, vol. 16, pp. 331-335, 2009.
2. T. Aldahri, J. Behin, H. Kazemian and S. Rohani, "Synthesis of zeolite Na-P from coal fly ash by thermo-sonochemical treatment," *Fuel*, vol. 182, pp. 494-501, 2016.
3. E. A. Hildebrando, C. G. B. Andrade, C. A. d. R. Junior, R. S. Angelica, F. R. V. Diaz and R. d. F. Neves, "Synthesis and Characterization of Zeolite NaP Using Kaolin Waste as a Source of Silicon and Aluminum," *Materials Research*, 2014.
4. C. R. Reyes, C. D. Williams and C. Roberts, "Synthesis and Characterization of SOD-, CAN-, and JBW-type structures by hydrothermal reaction of kaolinite at 200C," *DYNA*, vol. 78, no. 166, pp. 38-47, 2011.
5. C. A. Rios, C. D. Williams and M. A. Fullen, "Nucleation and growth history of zeolite LTA synthesized from kaolinite by two different methods," *Applied Clay Science*, vol. 42, pp. 446-454, 2009.
6. P. Sharma, J.S. Song, M.H. Han and C.H. Cho, "GIS-NaP1 zeolite microspheres as potential water adsorption material: Influence of initial silica concentration on adsorptive and physical/topological properties," *Scientific Reports*, vol. 6, 22734, 2016.

**Hydrothermal synthesis and characterization of cancrinite-type zeolites**

J. E. L. Camacho<sup>1,\*</sup>, M. T. Conato<sup>2</sup>

<sup>1</sup>Materials Science and Engineering, <sup>2</sup>Institute of Chemistry, College of Science, University of the Philippines Diliman, Quezon City, Philippines

**Abstract Text:** Cancrinite is a porous aluminosilicate mineral that offers numerous applications such as removal of heavy metals and catalysis. It can be synthesized using kaolin, giving an economic advantage as compared to synthesis using commercial reagents. In this study, a carbonate cancrinite-type zeolite derived from kaolin was synthesized via hydrothermal method at 200°C at different hydroxide concentrations and crystallization time. Samples were analyzed using different characterizations such as XRD, SEM, and FTIR. The XRD patterns reveal that the hydroxide concentration plays a significant role in the transformation of kaolin to cancrinite. In general, relatively high hydroxide concentrations are favorable in cancrinite zeolite formation. Crystallization time is also a key factor in formation of the zeolite. Cancrinite formation is mostly observed at a minimum crystallization time of 36 hours at hydroxide-carbonate ratios of 4:1 and 8:1. A crystalline intermediate phase other than cancrinite is detected at low hydroxide concentrations and shorter crystallization time.

**Image 1:**

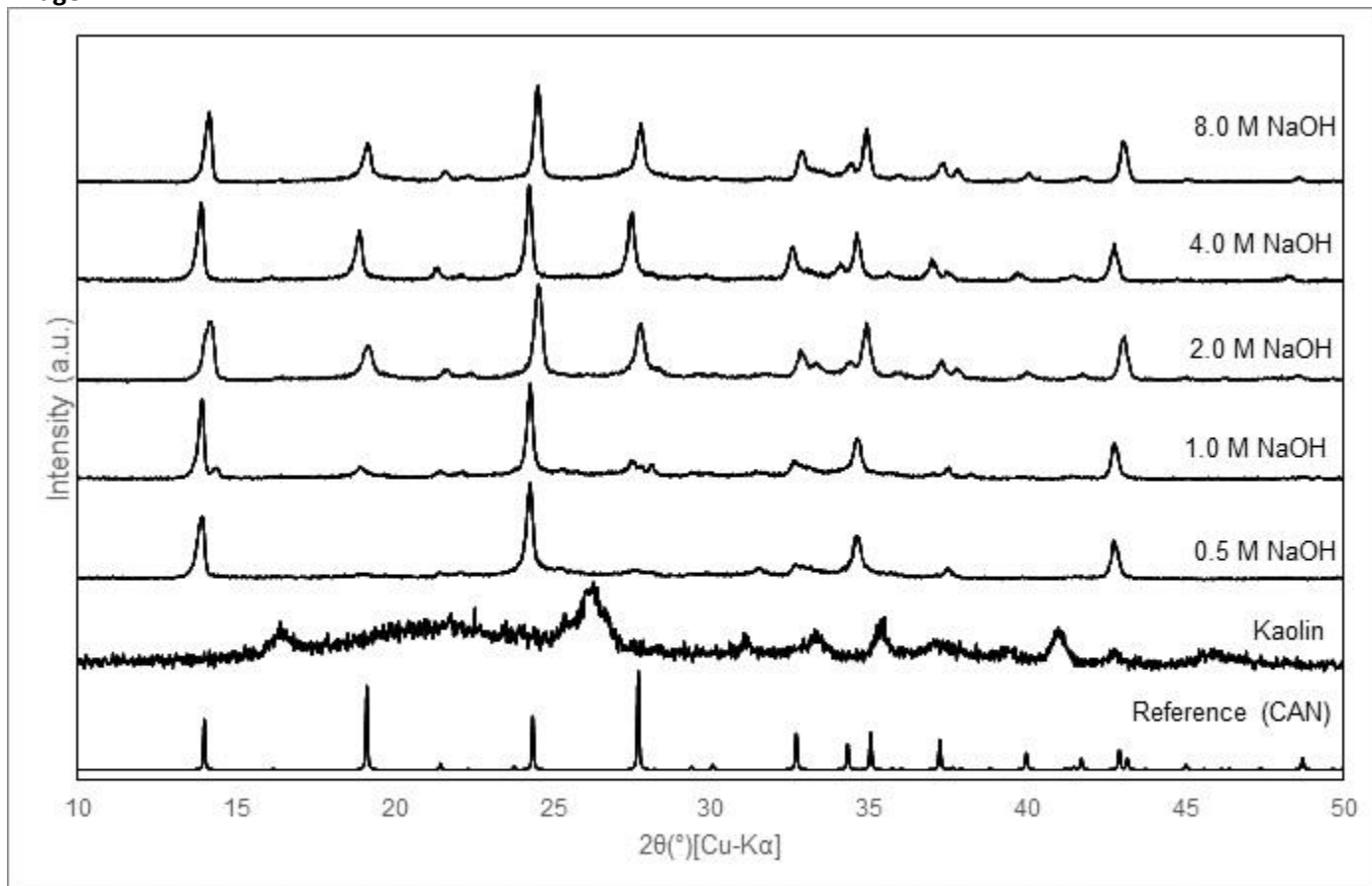


**Figure 1:** XRD patterns of precursor (kaolin), and zeolite synthesized for 48 hours at different hydroxide concentrations (0.5-8.0 M). Reference pattern obtained from International Zeolite Association.

**Image 2:**

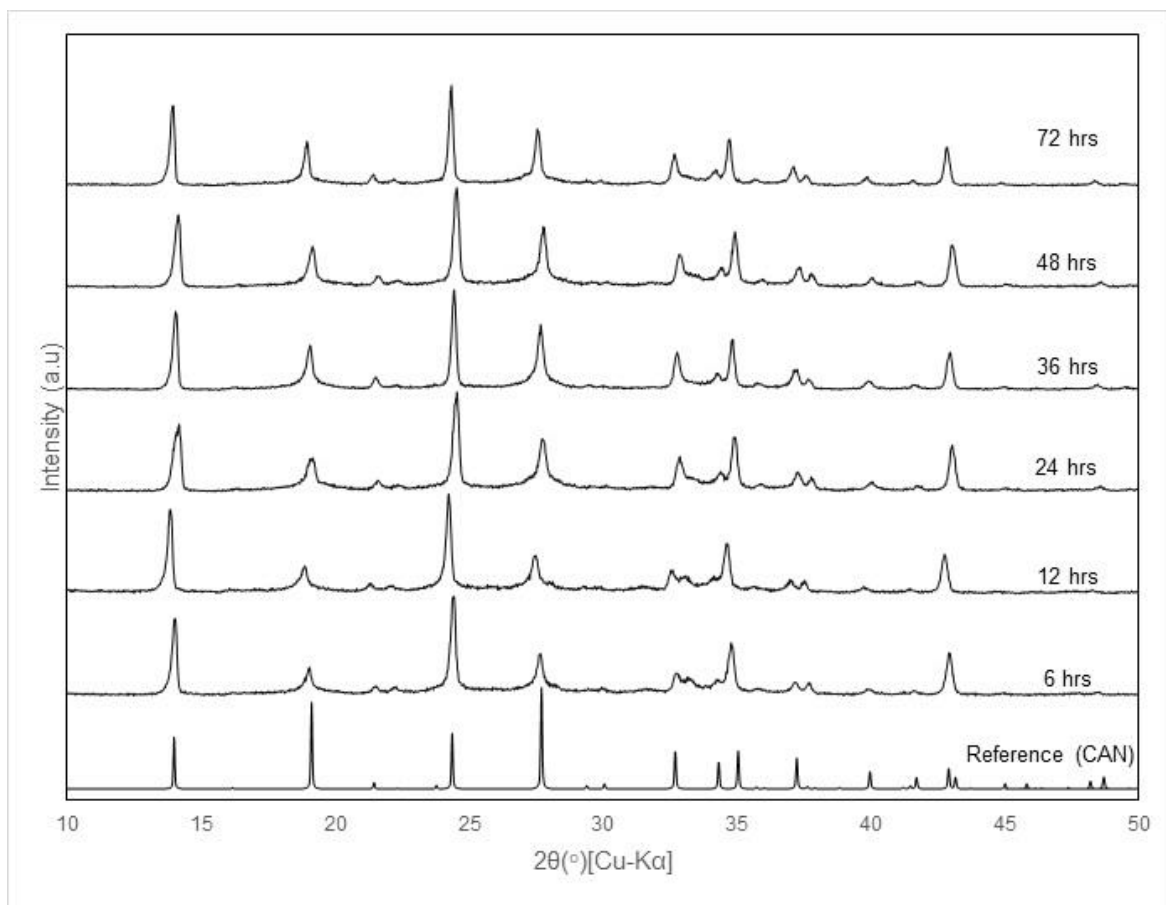


**Figure 2.** XRD pattern of 8.0 M NaOH/ 1.0 M Na<sub>2</sub>CO<sub>3</sub> in different crystallization times (6-72 hrs). Reference pattern of CAN was obtained from International Zeolite Association.

- References:** (1) Hermeler, G.; Hoffmann, W.; Buhl, J.-Ch. "The Influence of Carbonate on the Synthesis of an Intermediate Phase between Sodalite and Cancrinite." *Catal. Today* 1991, 8, 415–426.
- (2) Buhl, J. C. "Synthesis and Characterization of the Basic and Non-Basic Members of the Cancrinite-Natrodavnye Family." *Thermochim. Acta* 1991, 178 (C), 19–31.
- (3) Reyesa, C. A. R.; Williams, C.; Alarcón, O. M. C. "Nucleation and Growth Process of Sodalite and Cancrinite from Kaolinite-Rich Clay under Low-Temperature Hydrothermal Conditions." *Mater. Res.* 2013, 16, 424–428.
- (4) Hackbarth, K.; Gesing, T. M.; Fechtelkord, M.; Stief, F.; Buhl, J. "Synthesis and Crystal Structure of Carbonate Cancrinite Grown under Low-Temp." *Microporous Mesoporous Mater.* 1999, 30, 347–358.
- (5) Lindner, G.-G.; Massa, W.; Reinen, D. "Structure and Properties of Hydrothermally Synthesized Cancrinite." *J. Solid State Chem.* 1995, 117, 386–391.
- (6) Hassan, I.; Antao, S. M.; Parise, J. B. "Cancrinite: Crystal Structure, Phase Transitions, and Dehydration Behavior with Temperature." *Am. Mineral.* 2006, 91 (7), 1117–1124.
- (7) Cancrinite synthesis. Synthesis Commission, International Zeolite Assoc. (<http://www.iza-online.org/synthesis/>). Accessed last January 18, 2019.
- (8) Grader, C.; Buhl, J.-Ch. "The Intermediate Phase Between Sodalite and Cancrinite: Synthesis of Nano-crystals in the Presence of Na<sub>2</sub>CO<sub>3</sub>/TEA and its Thermal and Hydrothermal Stability
- (9) Cisneros, V.; Ocanto, F.; Linares, C.F. "Ca<sup>2+</sup>, Mg<sup>2+</sup> or Fe<sup>2+</sup> Ion-Exchanged Cancrinite-Type Zeolites as Possible Hypoglycemic Agents" *Rev. latinoam. quím [online]*. 2011 (39), n.1-2, pp.55-61. ISSN 0370-5943.

(10) Abdul – Moneim, M.; Abdelmoneim, A. A.; Geies, A. ; Farghaly, S.O. "Synthesis, Characterization and Application of Cancrinite in Ground Water Treatment from Wadi El-Assiuti Area, Assiut, Egypt." Ass. Univ. Bull. Environ. Res. 2018, 21 (1), 23 – 40.

(11) S. Cheng, G. Zhang, M. Javed, W. Gao, B. Mazonde, Y. Zhang, C. Lu, R. Yang, C. Xing, "Solvent-Free Synthesis of 1D Cancrinite Zeolite for Unexpectedly Improved Gasoline Selectivity:.. ChemistrySelect 2018, 3, 2115.

**Impact of sulphonic species on vanadium properties in SBA-15 material**

A. Nurwita<sup>1,\*</sup>, M. Trejda<sup>1</sup>, P. Decyk<sup>1</sup>, M. Ziolk<sup>1</sup>

<sup>1</sup>Zakład Katalizy Heterogenicznej, Uniwersytet im. Adama Mickiewicza w Poznaniu, Wydział Chemii, Poznań, Poland

**Abstract Text:**

**Introduction**

Multi-step transformation of different chemicals can be simplified by the application of bi-functional catalysts, in which two different single active sites are responsible for two consecutive chemical reactions. For instance two step production of acrylic acid from glycerol, which involve dehydration to acrolein and its oxidation, can be performed by the application of catalyst having both acidic and redox sites. These sites should be separated from each other thus the support for active centres should have rather large surface area. A well developed pore system should enhance the diffusion of reactants as well. In this context the aim of our study was the design of bifunctional catalyst which could be applied for the abovementioned process. For that purpose we have applied SBA-15 mesoporous silica that was modified with 3-(trihydroxysilyl)-1-propanesulfonic acid and vanadium species as dehydration and redox centers, respectively.

**Experimental**

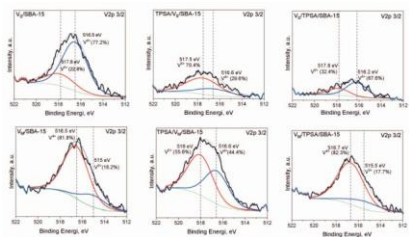
SBA-15 support was synthesised using standard hydrothermal procedure. Vanadium species (assumed value - 2 wt%) were incorporated by wetness impregnation using vanadyl sulfate ( $V_S$ ) or ammonium metavanadate ( $V_M$ ) precursor and materials were calcined. Next 3-(trihydroxysilyl)-1-propanesulfonic acid (TPSA) was grafted on the vanadium containing samples keeping the molar ratio of Si/TPSA = 10. Alternative modification procedure was also applied, i.e. vanadium species were incorporated after grafting of TPSA on SBA-15 samples. TPSA/SBA-15 materials were modified by the wetness impregnation with vanadium species and finally calcined. Materials obtained were characterized using following techniques: X-ray diffraction (XRD),  $N_2$  adsorption/desorption, IPC, X-ray photoelectron spectroscopy (XPS), electron spin resonance (ESR), UV-Vis spectroscopy and FTIR spectroscopy followed by pyridine adsorption.

**Results and discussion**

Two series of V/SBA-15 catalysts basing on different vanadium precursor (vanadyl sulfate or ammonium metavanadate) were obtained. Both XRD and  $N_2$  adsorption/desorption techniques confirmed the well preserved mesoporous structure of SBA-15 material with surface area in the range 457-687  $m^2g^{-1}$  after modification of the support. The XRD patterns did not point on the presence of crystalline vanadium(V) oxide suggesting good dispersion of metal species. These data were in-line with UV-Vis measurements results showing mainly isolated or dimeric vanadium species for dehydrated samples. Such kind of species was also confirmed by ESR technique. The state of vanadium was also examined by X-ray photoelectron spectroscopy. The difference in oxidation state of vanadium was found to be depended on the modification procedure applied for catalysts preparation. Much larger fraction of  $V^{5+}$  was detected when TPSA species were incorporated in the second step, i.e. after impregnation of SBA-15 with vanadium species (Fig. 1). This founding was independent on the kind of metal precursor. Pyridine adsorption followed by FTIR pointed on the presence of both Lewis and Brønsted acid sites on SBA-15 surface modified with vanadium species. The origin of the latter sites for TPSA free samples could be explained by the acidic proton of OH groups in the framework of hydroxylated  $(SiO)_2(OH)V=O$  species as described in [1]. The detailed results of material characterization and the impact of TPSA species on vanadium containing SBA-15 will be presented and discussed in details.

**Acknowledgements:** We are grateful to the National Science Center in Poland (Project no. project no. 2018/29/B/ST5/00137), the National Centre for Research and Development and European Union (Project no POWR.03.02.00-00-I020/17) for financial support.

**Image 1:**



**References:** 1. M. Trejda, M. Ziolek, Y. Millot, K. Chalupka, M. Che, S. Dzwigaj, J. Catal. 281 (2011) 169-176

**Synthesis and Characterisation of Zeolite ZSM-10 (MOZ)**

L. Price<sup>1,\*</sup>, A. Sartbaeva<sup>1</sup>

<sup>1</sup>Chemistry, University of Bath, Bath, United Kingdom

**Abstract Text:** Zeolites are a remarkably versatile class of crystalline, microporous materials, that are well-established in the fields of catalysis, ion-exchange and adsorption-separation. The success of these materials in such a wide range of industrial sectors is a direct consequence of their structures and chemistry. Discerning synthesis, structure and property relationships is, therefore, fundamental in the design and development of zeolite materials.

The aluminosilicate zeolite ZSM-10 (MOZ) has been synthesised using a low temperature method [1]. The local and average structure of this zeolite has been observed using both solid state, magic angle spinning NMR (SS MAS NMR) and powder x-ray diffraction (PXRD) as complimentary techniques, alongside field emission scanning electron microscopy (FESEM) and infrared spectroscopy (FTIR). The framework structure of MOZ has been determined from Rietveld refinement.

The synthesis conditions are critical to the formation of ZSM-10. Divalent N,N'-dimethyl-1,4 diazabicyclo[2.2.2]octane (Me<sub>2</sub>-DABCO) is required as an organic structure directing agent (OSDA). The best result is obtained after stirring for 2 days at room temperature, then heating for 10 days at 100°C under static conditions. Any small variation in temperature or ageing time produces structurally similar LTL and OFF zeolites. Furthermore, <sup>29</sup>Si SS-NMR data show that a slight decrease in batch SiO<sub>2</sub>/Al<sub>2</sub>O<sub>3</sub> ratio leads to local structural changes. PXRD data show that further decreasing the SiO<sub>2</sub>/Al<sub>2</sub>O<sub>3</sub> ratio results in mixed phases of MOZ, CHA and MER zeolites and replacement of K<sup>+</sup> with Na<sup>+</sup> leads to ANA. Having a more complete understanding of the relationships that exist between a zeolite structure and its synthesis conditions is critical in making advancements towards the rational design of novel functional materials with enhanced properties that can be tailored for specific applications.

**Image 1:**

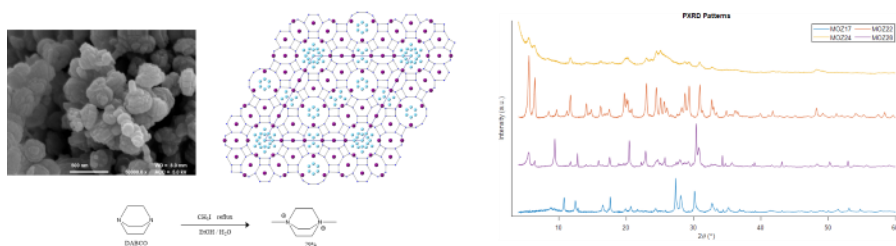
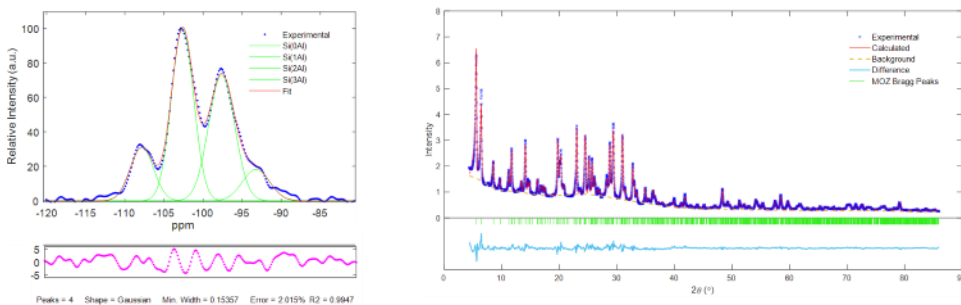


**Image 2:**



**References:** [1] Higgins, J.B. and Schmitt, K.D. "ZSM-10: synthesis and tetrahedral framework structure" *Zeolites*, 16, 236-244 (1996)

**Effect of Nickel(II) ions on properties of nanosized FAU type zeolite**

G. Medak<sup>1,\*</sup>, J. Bronic<sup>1</sup>, A. Puskaric<sup>1</sup>, F. Dalena<sup>2</sup>, M. Migliori<sup>3</sup>, G. Giordano<sup>3</sup>, T. Antonic Jelic<sup>1</sup>, I. Landripet<sup>1</sup>

<sup>1</sup>Laboratory for synthesis of new materials, Rudjer Boskovic Institute, Zagreb, Croatia, <sup>2</sup>Department of Environmental and Chemical Engineering, University of Calabria, Arcavacata di Rende (CS), <sup>3</sup>Department of Environmental and Chemical Engineering, University of Calabria, Arcavacata di Rende (CS), Italy

**Abstract Text: Introduction**

Due to its' 12-member ring cage faujasite type zeolite is one of the best catalysts for fluid catalytic cracking (FCC) and is often used as support for platinum or palladium in a hydrocracking process. Depending on the Si/Al ratio synthetic FAU is classified as X, if ratio is between 2 and 3, or Y if ratio is 3 or higher. High aluminum content in X type zeolite results in large number of Brønsted's acid sites which often leads to unwanted cyclic byproducts and formation of coke. In order to avoid this problem postsynthetic modifications to the zeolite structure are needed. One of the most promising methods to do this is wet impregnation with metal cations that increase the number of Lewis' and reduce the number of Brønsted's acid sites [1] in order to create more controlled catalytic conditions.

**Experimental**

The zeolite for post synthetic treatment (HF-AS) was isolated from a gel with following composition  $8\text{Na}_2\text{O}:0.7\text{Al}_2\text{O}_3:10\text{SiO}_2:160\text{H}_2\text{O}$  adopted from Awala and co-workers [2]. Previously prepared HF-AS was added in the water solution of nickel(II) chloride (1:50,  $0.5 \text{ mol dm}^{-3}$ ) and stirred. After 45 minutes the crystals were separated from solution and the process was repeated once more. The prepared product HF-Ni1 was then washed two times with  $40 \text{ cm}^3$  of redistilled water and then calcined at  $550^\circ\text{C}$  for 6 hours. Thus prepared product (HF-Ni1iz) was then ion exchanged with  $0.8 \text{ mol dm}^{-3}$  water solution of ammonium nitrate (1:10) for 3 hours after which it was again calcined at  $450^\circ\text{C}$  for 5 hours.

The same procedure as described above was also used for the synthesis of HF-Ni2, HF-Ni3 and HF-Ni4 with the exception that before washing the products with redistilled water they were hydrothermally treated at  $100^\circ\text{C}$  for 24, 1.5 and 3 hours respectively.

**Results and discussion**

It was observed that calcination following wet impregnation with nickel(II) ions leads to increase of intensity of (111) peak and disappearance of peaks at  $10.3^\circ$  and  $11.7^\circ$  which may indicate the migration of nickel cations from double-6 rings to supercage.

Fig.1. XRD patterns of HF-Ni3 and HF-Ni4 samples during stages in postsynthetic treatment compared to the parent sample (HF-AS).

The shift in the peak positions from  $0.2^\circ$  to  $0.4^\circ$  varying on sample was also observed (Fig.1.). The diffraction peaks of the nickel(II) oxide were not observed in any of the samples (Fig.2.). The samples were also analyzed using atomic absorption spectroscopy and vacuum FTIR.

Fig.2. XRD patterns of samples after wet impregnation with nickel(II) chloride and calcination compared to the parent sample.

**Acknowledgement**

This work was supported by Croatian Science Foundation, project IP-2016-06-2214.

Image 1:

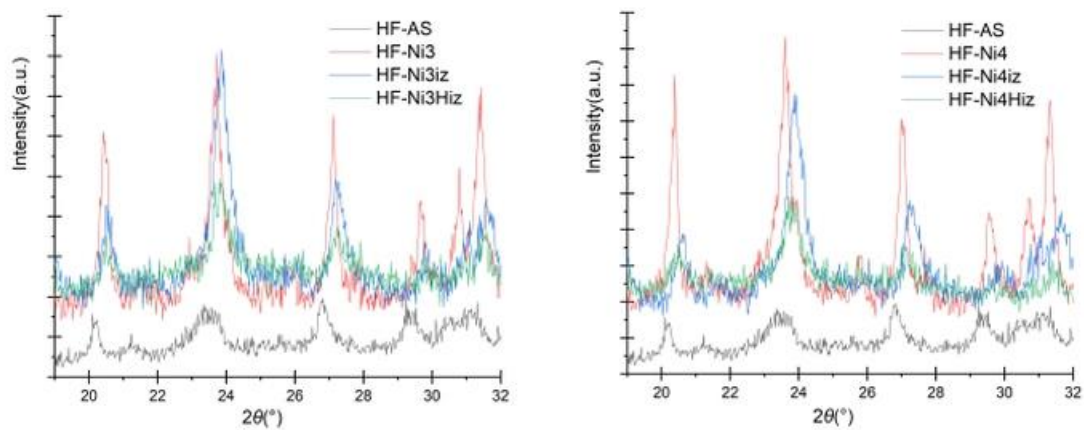
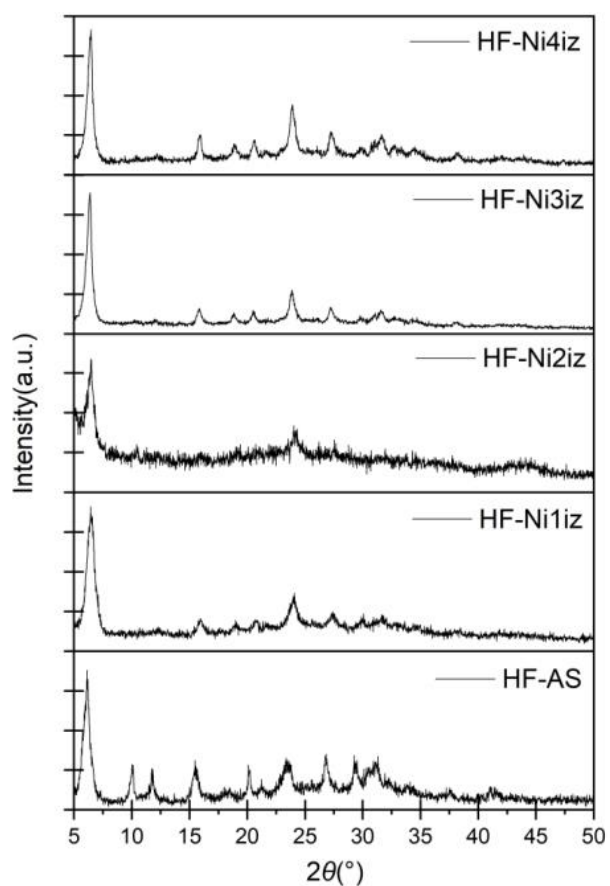


Image 2:



References: [1] G. Afreen, T. Patra, S. Upadhyayula, Mol. Catal. 2017, 441, 122-133.

[2] H. Awala, J. Gilson, R. Retoux, P. Boullay, J. Goupil, V. Valtchev and S. Mintova, Nat. Mater. 2015, 14, 447-451.

**Mechanosynthesis of microporous and layered titanosilicates**

I. Santos Vieira<sup>1,\*</sup>, Z. Lin<sup>1</sup>, J. Rocha<sup>1</sup>

<sup>1</sup>Department of Chemistry, Ciceco & University of Aveiro, Aveiro, Portugal

**Abstract Text:**

The pursuit of a sustainable society and civilization is perhaps the main challenge of our time and of future generations [1]. Waste prevention is one of the Twelve Principles of Green Chemistry, according to which it is better to prevent waste formation rather than to clean it up after. Hence, in recent years there has been a growing awareness of the importance of developing environmentally-friendly chemical processes [2].

Chemists are becoming increasingly aware of the potential of mechanical grinding or milling for the synthesis of materials. Indeed, mechanochemistry was identified by IUPAC as one of the 10 world-changing technologies. Mechanochemistry is now considered an excellent Green Chemistry method, offering, e.g., the opportunity of reducing considerably or even avoiding the use of solvents [3].

Synthetic analogues of layered and microporous titanosilicate minerals have attracted much attention in the last two decades or so, because they may have many potential applications in, for instance, catalysis, ion exchange and gas adsorption and separation. These materials are normally prepared under mild hydrothermal conditions using several titanium silicon sources, along with a large amount of water [4].

We seek to prepare layered and microporous titanosilicate via mechanochemistry, i.e., ball milling without or with only a small amount of water (liquid assisted grinding), followed by heating in an autoclave, and here we report some preliminary results of this work. Using these conditions, we have prepared small porous *sitinakite* –  $\text{Na}_2\text{Ti}_2\text{O}_3\text{SiO}_4 \cdot 2\text{H}_2\text{O}$  (no water, 6 h at 230 °C), *Ivanyukite-K* (GTS-1) –  $\text{HK}_3\text{Ti}_4\text{O}_4(\text{SiO}_4)_3 \cdot 4\text{H}_2\text{O}$  (no water, 24 h at 230 °C). A pure phase of layered *natisite* –  $\text{Na}_2\text{TiO}(\text{SiO}_4)$  and AM-2 –  $\text{K}_2\text{TiSi}_3\text{O}_9 \cdot \text{H}_2\text{O}$  were also obtained with very little water and in less than 24 h at 230 °C. ETS-10 could also be prepared in 24 h at 230 °C. The amount of water used in these experiments is over two orders of magnitude lower than in conventional hydrothermal synthesis of this kind of materials. The amount of water, time and temperature were some of the conditions studied and will be presented.

**References:**

[1] P. T. Anastas, J. B. Zimmerman Curr. Opin. Green and Sustainable Chem., 13 (2018) 150–153.

[2] Nanoscale Adv. 1 (2019) 937–947.

[3] T. Friscic, C. Mottillo, H. M. Titi, Angew. Chem. Int. Ed. 59 (2020) 1018 –1029.

[4] I. A. Perovskiy, E. V. Khramenkov, E. A. Pidko, P. V. Krivoschapkin, A. V. Vinogradov, E. F. Krivoschapkin, Chem. Eng. J. 354 (2018) 727–739.

**The influence of compositional descriptors on zeolite synthesis from hydrated silicate ionic liquids**

K. Asselman<sup>1,\*</sup>, N. Pellens<sup>1</sup>, E. Breynaert<sup>1,2</sup>, S. Pulinthanathu<sup>1</sup>, C. De Coninck<sup>1</sup>, F. Taulelle<sup>1,2,3</sup>, C. E. A. Kirschhock<sup>1</sup>

<sup>1</sup>Center for Surface Chemistry and Catalysis - Characterisation and Application Team (COK-Kat), <sup>2</sup>NMRCoRe, KU Leuven, Leuven, Belgium, <sup>3</sup>Institut Lavoisier de Versailles, University of Versailles, Versailles Cedex, France

**Abstract Text:** Of the nearly 250 known zeolite framework types, only a fraction is produced in organic-free media<sup>1</sup>. These materials are of high practical importance due to their low production costs and high ion exchange capacities. There have been many studies investigating zeolite synthesis in purely inorganic systems, the main established parameters that govern the properties of the final products like framework type, crystal size and morphology are the synthesis composition (Si/Al ratio, alkali cation, alkalinity, water content), crystallization time and temperature and the use of crystal seeds.

A novel zeolite synthesis method via hydrated silicate ionic liquids (HSILs) offers a purely inorganic pathway of synthesizing numerous zeolite frameworks<sup>2,3</sup>. By careful control of parameters like aluminate, water and alkali concentrations, gel formation is avoided over a wide compositional range and zeolites crystallize from single-phase homogeneous precursor solutions. In the studied chemical space, aluminosilicate species are in a predominantly oligomeric state and the synthesis solutions are kinetically stable at room temperature. This ensures accurate knowledge of local solution stoichiometry and eliminates factors like ingredient source or ageing time. As a result, we can investigate the influence of liquid-state solution chemistry onto zeolite phase selection, which is hindered in the presence of non-equilibrium phases like gels.

The investigated parameters in the presented study are the cation type (Na, K, Cs), cation hydration level ( $[\text{H}_2\text{O}]/[\text{MOH}]$ ) and alkalinity of the precursor mixture ( $[\text{Si} + \text{Al}]/[\text{MOH}]$ ). Ternary phase diagrams are constructed (Fig. 1) for each cation type, excluding the region below the solubility limit of the alkali hydroxide ( $[\text{H}_2\text{O}]/[\text{MOH}] \approx 3$ ) and the region where gel formation is triggered ( $[\text{Si} + \text{Al}]/[\text{MOH}] > 1$ ). The systematic variation in alkalinity and water content provides novel insights on zeolite precursor stability and the cooperative templating effect of cations and hydration water, governing the formation of the final zeolite product.

A hydrated silicate ionic liquid (HSIL) is prepared by mixing appropriate amounts of H<sub>2</sub>O, MOH and tetraethyl orthosilicate (TEOS). Complete hydrolysis of TEOS triggers spontaneous liquid-liquid phase separation in a dense bottom phase (the HSIL) containing all silica and alkali sources and some residual water, not exceeding the number of the first hydration layer of the alkali cations, and a water-ethanol phase which is readily removed by decantation. The HSIL is mixed with water, alkali hydroxide and an aluminum source to yield the desired batch compositions. After stirring overnight the mixture is transferred to polypropylene tubes and heated at 90°C for one week in a tumbling oven. The recovered solids are washed, dried and characterized via powder X-ray diffraction.

Twelve different framework types were observed for constant synthesis time and temperature. Each ternary diagram shows distinct but different phase boundaries over the explored parameter space (Fig. 2). We identify the framework composition of the formed zeolite products as a critical descriptor and show that the Si-to-Al ratio depends linearly on both batch alkalinity and water content for all cations, irrespective of the phases formed. The slope differs for the examined cations as larger cations promote framework formation with a wider range of silicon contents (Fig. 2). We rationalize these observations in terms of the complex interplay between aluminosilicate species and the charge balancing cations, which ultimately define the stability and condensation of building units in solution, and the synthesis outcome. The results of this screening provide a firm basis for future research based on zeolite formation in HSILs.

**Image 1:**

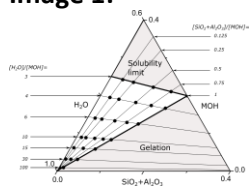
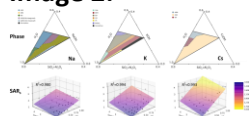


**Image 2:**



**References: 1.**

- Maldonado, M., Oleksiak, M. D., Chinta, S. & Rimer, J. D. Controlling crystal polymorphism in organic-free synthesis of na-zeolites. *J. Am. Chem. Soc.* 135, 2641–2652 (2013).
2. Haouas, M. et al. Silicate ionic liquid synthesis of zeolite merlinoite: Crystal size control from crystalline nanoaggregates to micron-sized single-crystals. *Microporous Mesoporous Mater.* 198, 35–44 (2014).
3. Van Tendeloo, L. et al. Zeolite synthesis in hydrated silicate ionic liquids. *Faraday Discuss.* 179, 437–449 (2015).

**TETRAETHYLAMMONIUM-MEDIATED ZEOLITE SYNTHESIS VIA A MULTIPLE INORGANIC CATION APPROACH**

H. Lee<sup>1,\*</sup>, J. Shin<sup>2</sup>, S. B. Hong<sup>1</sup>

<sup>1</sup>Division of Environmental Science and Engineering, POSTECH, Pohang, <sup>2</sup>Research Center for Convergent Chemical Process, Korea Research Institute of Chemical Technology, Daejeon, Korea, Republic Of

**Abstract Text:** Although the diverse and new classes of porous materials have been extensively studied in recent decades, zeolites are almost the only class whose industrial usefulness has been proved: in the \$5 billion global market for chemical catalysts, the share of zeolites amounts to about 40%. If such is the case, the development of new synthetic methods for existing zeolites, as well as for novel zeolite structures, is of technological relevance. The use of more than one type of inorganic structure-directing agents (ISDAs; alkali and/or alkaline earth cations) together with a specific organic structure-directing agent (OSDA) in zeolite synthesis has long been recognized. For instance, small-pore zeolites rho (framework type RHO) and ZK-5 (KFI) can be synthesized using quite expensive 1,4,7,10,13,16-hexaoxacyclooctadecane as an OSDA with Na<sup>+</sup>-Cs<sup>+</sup> and K<sup>+</sup>-Sr<sup>2+</sup> mixed ISDA system, respectively, although both of them were initially obtained under wholly inorganic conditions that are far from reproducible. This led us to focus our attention to the cooperative structure direction among the multiple inorganic cations in the presence of much cheaper, already known OSDAs.

We have established the reproducible synthesis procedures for small-pore zeolites rho and ZK-5 using TEA<sup>+</sup> as an OSDA via the multiple inorganic cation approach, as well as for the large-pore zeolite offretite. The results presented here show that combining the structure-directing ability of already known OSDAs with that of more than one type of ISDAs is a viable option for synthesizing zeolites that are not easy to crystallize as the pure form under wholly inorganic conditions. We expect that this synthesis strategy will also be useful for finding intermediate-silica ( $2 < \text{Si/Al} \leq 5$ ) zeolites with novel framework structures and/or compositions.

**Synthesis of FAU zeolite by a flow type-microwave reactor system**

T. Nagase<sup>1,\*</sup>, M. Miyakawa<sup>1</sup>, M. Nishioka<sup>1</sup>

<sup>1</sup>National Institute of Advanced Industrial Science and Technology, Sendai, Japan

**Abstract Text:** Synthesis of **FAU** zeolite was examined using a flow type microwave assisted reactor system (Flow-MW system)<sup>1</sup>. **LTA** and **FAU** zeolite were synthesized using a mother slurry having a composition of Na:Al:Si:H<sub>2</sub>O = 4:1:1:100 (molar ratio), which had been aged in advance at room temperature for various times. The slurry was pumped into a reaction tube of 4 mmϕ in inner diameter and heated at 140 °C for 50-120 s by running through a magnetic field inside the cylindrical cavity of 2.45 GHz MW reactor. The sample was recovered by centrifugation and washed with water. TEM images were observed for unheated sample and the PXRD pattern was measured for samples dried at 25-40 °C. The N<sub>2</sub> adsorption characteristics were measured by using the sample after pretreatment of vacuum heating at 150 °C, 24 h.

When synthesis is performed using a slurry aged for short time, the resulting crystal phase is single phase of **LTA**. **FAU** was obtained as a single phase when the slurry had been aged for more than 5 days. Even using the slurry aged for 2 h<sup>2</sup>, **FAU** had been easily co-precipitated with **LTA** in the case that the synthesis was carried out using a batch-type conventional method inside an electric oven. So, the difference in the zeolite phase synthesized by the flow MW system related to the aging time of the mother slurry, suggests that the **FAU** was more stable phase in this system and Al concentration required for crystallization of **LTA** had been reduced by the progress of nucleation.

The PXRD pattern of the obtained **FAU** sample was that of single phase, however, the peak was quite broad, and the calculated crystallite size was about 12 nm. According to a SEM image, the particle was 50-100 nm in a diameter. Moreover, by TEM, each particle was an aggregate of crystal-grains having a diameter of 20 nm or less. The small crystallite size was not owing to amorphous content, but to the crystal-grains. The specific surface area calculated from the N<sub>2</sub> adsorption curve was 510 m<sup>2</sup>/g by BET method. Since the micropore volume (P/P<sub>0</sub> = ~0.1) is 0.17 cm<sup>3</sup>/g, it is considered that the micropore in the **FAU** crystal-grain was working. The meso-macropore distribution curves calculated by the BJH method had peaks at 10.5 nm and 59.5 nm, and the pore volumes of mesopores (2-50 nm diameters) and macropores (50-190 nm diameters) were 0.38 cm<sup>3</sup>/g and 0.62 cm<sup>3</sup>/g. These were derived from the agglomeration structure which was confirmed by TEM. The mesoporous particles consisting of the crystal-grains are also recognized for **LTA** zeolite synthesized by the Flow-MW method without using organic additives<sup>2</sup>. It would be considered that zeolite nuclide could become the crystal-grain rapidly which were crystallin enough by efficient heating and was not so dissolving during the synthesis owing to short residence time. And then, the crystal grains could be remained, and were agglomerate or aligned during the growth process to become mesoporous particles<sup>2</sup>. Since in the case of **FAU** synthesis, the zeolite nuclide had been already grown during longer aging, it could be considered that the crystal grains became larger and less aligned during the agglomeration process compared to the case of **LTA**.

From the above results, since Flow MW system would have an advantage for controlling size and agglomeration process of the crystal-grains, it is possible to design a meso and macro-porous inorganic body, and furthermore, it would be expected to arrange some different types of nanomaterials in a same porous body.

**References:** (1) M. Nishioka, M. Miyakawa, H. Kataoka, H. Koda, K. Sato and T. M. Suzuki, *Nanoscale*, 3 (2011), pp. 2621-2626. DOI: 10.1039/C1NR10199D

(2) T. Nagase, M. Miyakawa, M. Nishioka, *Micropor. Mesopor. Matter.*, 306 (2020) 110375.

<https://doi.org/10.1016/j.micromeso.2020.110375>

**OPTIMIZATION OF PARAMETERS FOR THE SYNTHESIS OF HIERARCHICAL ZEOLITES BASED ON FAUJASITE**

E. Musielak\*, A. Feliczak-Guzik<sup>1</sup>, I. Nowak<sup>1</sup>

<sup>1</sup>The chemistry department, Adam Mickiewicz University in Poznań, Poznań, Poland

**Abstract Text:** Zeolites are widely used in industry due to their multidimensional structure and chemical composition. They are classified as crystalline, hydrated aluminosilicates, usually alkali elements, rare earths and other mono- or multivalent metals [1,2]. These materials exhibit a number of unique properties that have led to their applications, including catalysis. Despite their many advantages, zeolites exhibit diffusion limitations for branched molecules, and the transport of reactants of a size close to that of micropores is difficult to transport. Therefore, zeolites with a hierarchical porous structure have started to be obtained that exhibit secondary porosity, i.e., they show the presence of at least one additional pore system, mainly in the mesopore range. This arrangement is intended to facilitate the access of larger reactant molecules to the active centers of the material while maintaining the acidity and crystallinity of the starting material [3].

Faujasite-based hierarchical zeolites were synthesized based on the method described by Liu et al [4]. During the course of the synthesis the type of template used, viz: polyethylene glycol octadecyl ether (Brij S10), poloxamer (Pluronic F127), CTABr (hexadecyltrimethylammonium bromide), the amount of silicon source (TEOS) added and the aging time of the reaction mixture were modified.

All synthesized materials were characterized by several techniques: UV/Vis spectroscopy, transmission electron microscopy (TEM), Fourier transform infrared spectroscopy (FTIR), N<sub>2</sub> adsorption and X-ray diffraction (XRD).

Based on the results, the optimal parameters for the synthesis of hierarchical zeolites were developed as follows: 0.5 g of FAU-type commercial zeolite was dispersed in a mixture containing water, ethyl alcohol, template, and ammonia water and ultrasonicated for 30 min at 65°C. Then, the whole mixture was transferred to a magnetic stirrer and stirred for 4h at 65°C. The obtained product was filtered and washed with a mixture containing water and ethyl alcohol (50:50). The final material was calcined to remove the template at 550°C for 5h.

*The work was supported by grant no. POWR.03.02.00-00-1020/17 co-financed by the European Union through the European Social Fund under the Operational Program Knowledge Education Development.*

**References:** [1] G.W. Cieciszwili, T. Andronikaszwili, Zeolity naturalne, WNT, Warszawa 1990.

[2] J. Weitkamp, Solid State Ionics 2000, 131, 175.

[3] A. Feliczak-Guzik, Micropor. Mesopor. Mat. 2018, 259, 33-45.

[4] Liu X., Gao F., Xu J., Zhou L., Liu H and Hu J., Micropor. Mesopor. Mat. 2016, 222, 113.

M. Gebauer<sup>1,\*</sup>, H. Becker<sup>1</sup>, J. Titus<sup>1</sup>, R. Gläser<sup>1</sup>

<sup>1</sup>Institute of Chemical Technology, Universität Leipzig, Leipzig, Germany

**Abstract Text:**

**Introduction**

Friedel-Crafts-alkylations (FCA) are often homogeneously catalyzed by precious metals such as Pd or Au catalysts [1,2]. Asymmetric FCA products can be obtained via Brønsted acidic organocatalysts, e.g., binol-based phosphoric acids [3]. In homogeneous catalysis, catalyst recycling and separation is difficult and consumes large volumes of solvents. Organocatalysts can be applied in heterogeneously catalyzed reactions after immobilization on suitable solid supports. This study therefore aims to prepare and investigate phosphoric acids as organocatalysts supported on different mesoporous silica spheres. Ordered mesoporous silica materials like MCM-41 and SBA-15 were investigated and compared to a non-ordered silica due to their favourable properties such as mechanical and thermal stability as well as high specific surface area ( $A_{\text{BET}}$ ) and specific pore volume ( $V_p$ ). The influence of the textural properties as well as the density of silanol groups of the obtained materials was studied in the conversion of 2-(hydroxy(4-methoxyphenyl)-methyl)phenol (*o*-HBH) with 2-naphthol to triarylmethane as an FCA model reaction in a batch reactor.

**Experimental Part**

Starting from commercial silica spheres (80-90  $\mu\text{m}$ , Chromatorex MB70-75/200, denoted as SiO<sub>2</sub>), MCM-41 was synthesized via pseudomorphic transformation using trimethyloctadecylammonium bromide (C<sub>18</sub>TABr) as a structure-directing agent (SDA) [4]. The transformation was conducted in an autoclave at 393 K for 24 h, after which the solid was washed with H<sub>2</sub>O, dried at 363 K and calcined at 823 K. SBA-15 was prepared via sol-gel synthesis by adapting a literature procedure with ethanol, P-123 and tetraethoxysilane (TEOS) under acidic conditions [5]. The surface of the obtained materials (SiO<sub>2</sub>, MCM-41 and SBA-15) was phosphorylated by POCl<sub>3</sub> in anhydrous pyridine for 72 h at 298 K. The solids were filtered, washed with H<sub>2</sub>O, MeOH, acetonitrile (ACN) and dichloromethane (DCM), dried at 363 K for 24 h and calcined at 823 K. The catalytic FCA activity was studied in a mixture of 0.011 M *o*-HBH and 0.013 M 2-naphthol in DCM at 298 K in a batch reactor for 2 h using 3 mg catalyst.

**Results and Discussion**

SiO<sub>2</sub> was fully transformed into MCM-41 as confirmed via N<sub>2</sub> sorption (Image 1). Type IV hysteresis loops typical of ordered mesoporous silica are observed at  $p/p_0 = 0.3 - 0.5$ . Further, the high specific surface area (550 m<sup>2</sup> g<sup>-1</sup> to >1000 m<sup>2</sup> g<sup>-1</sup>) and pore volume (0.8 cm<sup>3</sup> g<sup>-1</sup> to 1.0 cm<sup>3</sup> g<sup>-1</sup>) prove the full transformation to MCM-41. The pore width distribution can be tuned between 2.3 and 4.7 nm by varying the alkyl chain length (C<sub>10</sub>-C<sub>22</sub> TA<sup>+</sup>) of the SDA as well as by adding a micelle expander (ammonium thiocyanate). In addition, SBA-15 with a pore width of 7.5 nm was synthesized ( $A_{\text{BET}} = 965 \text{ m}^2 \text{ g}^{-1}$ ,  $V_p = 1.7 \text{ cm}^3 \text{ g}^{-1}$ ). All materials (SiO<sub>2</sub>, MCM-41 and SBA-15) were spherically shaped. The applied phosphorylation did not affect the textural properties of the corresponding supports. TEM images (Image 2) of the SiO<sub>2</sub> (left) and the phosphorylated species (right) shows a comparable non-ordered pore structure before and after the phosphorylation.

In the model FCA reaction, a conversion of *o*-HBH of 60-70% with a triarylmethane selectivity of 30-40% was reached over the organocatalyst immobilized on all three mesoporous supports. The low selectivity is due to the side reaction of *o*-HBH dimerization, which correlates with the density of free silanol groups. During the calcination step, the silanol groups condense, increasing the conversion of *o*-HBH up to 95% with an enhanced selectivity of 60%. Consequently, catalytic activity of the immobilized phosphoric acids depends mainly on the density of free silanol groups rather than on the pore structure of the mesoporous silica supports.

Image 1:

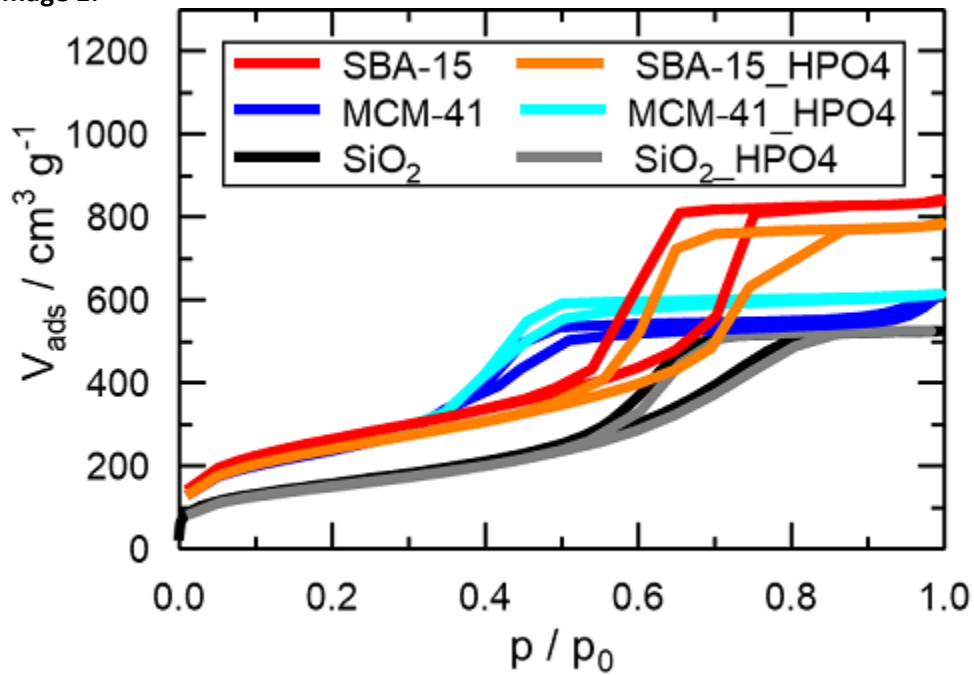
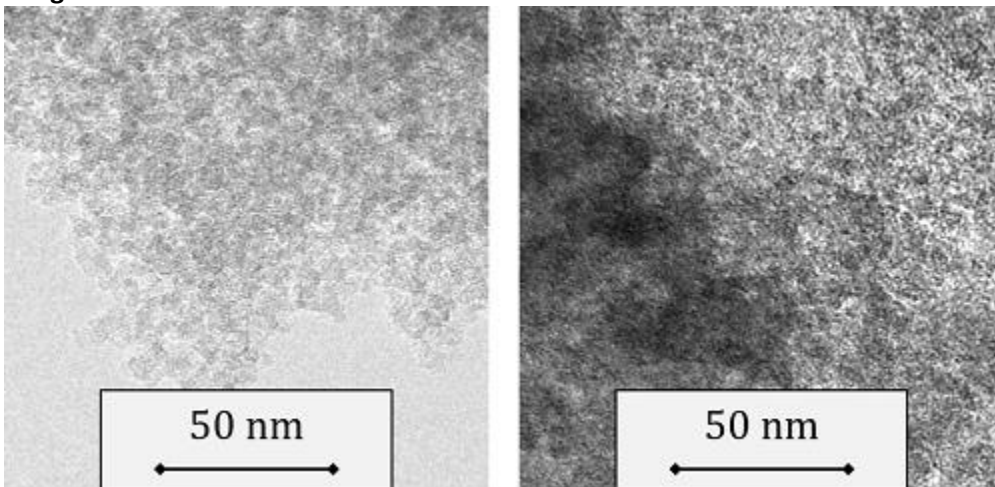


Image 2:



**References:**

- [1] J. Zhang, A. Bellomo, N. Trongsiwat, T. Jia, P. J. Carroll, S. D. Dreher, M. T. Tudge, H. Yin, J. R. Robinson, E. J. Schelter, *J. Am. Chem. Soc.* 136 (2014) 6276–6287.
- [2] S. A. Snyder, S. P. Breazzano, A. G. Ross, Y. Lin, A. L. Zografos, *J. Am. Chem. Soc.* 131 (2009) 1753–1765.
- [3] A. Moyano, R. Ríos, *Chem. Rev.* 111 (2011) 4703–4832.
- [4] D. Einicke, D. Enke, M. Dvoyashkin, R. Valiullin, R. Gläser, *Materials* 6 (2013) 3688–3709.
- [5] V. Meynen, P. Cool, E.F. Vansant, *Microporous Mesoporous Mater.* 125 (2009) 170–223.

## **Novel Materials and Structural Methods**

FEZA21-PO-271

### **Development of Hierarchical Zeolite-Templated Carbons**

T. Aumond<sup>1,\*</sup>, Y. Pouilloux<sup>1</sup>, L. Pinard<sup>1</sup>, A. Sachse<sup>1</sup>

<sup>1</sup>University of Poitiers, IC2MP, Poitiers, France

**Abstract Text:** Zeolite-templated carbons (ZTCs) have been synthesized for the first time in 1997<sup>1</sup> and are today a well-established class of microporous carbons. They feature defined textural properties that reveal very interesting in a number of fields including (electro)catalysis and adsorption,<sup>2</sup> due to their unique electronic properties in combination with very high porous volume and homogeneous micropore size distribution.<sup>3</sup> These ZTCs develop within the microporous system of a template zeolite and are hence a negative copy of their structure. In this communication we present the first achievement of ZTCs featuring hierarchical porosity.

For the development of hierarchical ZTCs, two zeolite samples featuring different mesoporous degrees and architectures were used: (i) commercial USY and (ii) surfactant templated USY<sup>4</sup> (USY<sub>ST</sub>). Two grams of the zeolite were deposited on a frit in a cylindrical quartz reactor and activated at 690 °C for 1 hour followed by ethylene CVD for 4 hours. Finally, the temperature was gradually risen to 790 °C for two hours under N<sub>2</sub> flow. Final ZTCs were obtained after HF leaching which allows to dissolve the zeolite structure.

The texture and morphology of both zeolites and ZTCs have been investigated using transmission and scanning electron microscopy. ZTC particles are of comparable size (200-600 nm) to the zeolite template crystals and feature the presence of cavities on the surface of the crystal corresponding to steamed mesopores present in USY (figure 1: (a) TEM images of USY zeolite and (b) TEM images of the resulting ZTC-USY). A wide size distribution of mesopores are further identifiable for the ZTC achieved from USY<sub>ST</sub>. The electron microscopy images moreover reveal the absence of non-templated carbon on the external surface, which is one of the major challenges when using hierarchical zeolites as template. This non-templated carbon would impede the transcription of porosity by blocking pore entrance. The shape of ZTC-USY nitrogen physisorption isotherm strongly recalls the one of the parent zeolite (figure 2a: N<sub>2</sub> physisorption isotherms at 77 K for the USY zeolite template (black) and the ZTC-USY (red)) and the resulting ZTC shows a porous volume twice as high as the parent zeolite. Mesoporosity of the resulting ZTC compares well to the one of the zeolite (0.23 and 0.24 cm<sup>3</sup> g<sup>-1</sup>, respectively) indicating that all of the mesoporosity present in the template is transcribed to the ZTC. The ZTC further presents a high microporous volume (0.29 cm<sup>3</sup> g<sup>-1</sup> for the zeolite versus 0.73 cm<sup>3</sup> g<sup>-1</sup> for the ZTC). As far as ZTC-USY<sub>ST</sub> is concerned, the shape of the isotherm differs from the one of the template zeolite (figure 2b: N<sub>2</sub> physisorption isotherms for the USY<sub>ST</sub> template (black) and the ZTC-USY<sub>ST</sub> (red)). The H<sub>2</sub> type isotherm of the ZTC-USY<sub>ST</sub> indicates the presence of occluded mesopores and a large distribution of mesopore sizes. Hence, the textural properties of the USY<sub>ST</sub> zeolite are only partially maintained. Yet, microporous volumes of ZTC-USY and ZTC-USY<sub>ST</sub> interestingly appear to be very similar (0.73 and 0.74 cm<sup>3</sup> g<sup>-1</sup> respectively).

Hierarchical ZTCs present both tailored microporosity and adjustable mesoporosity. The presence of intraparticle mesoporosity allows for reducing diffusion path length essentially, which make these materials extremely promising for developing superior gas storage devices and for achieving improved outputs in (electro)catalysis.

**Image 1:**

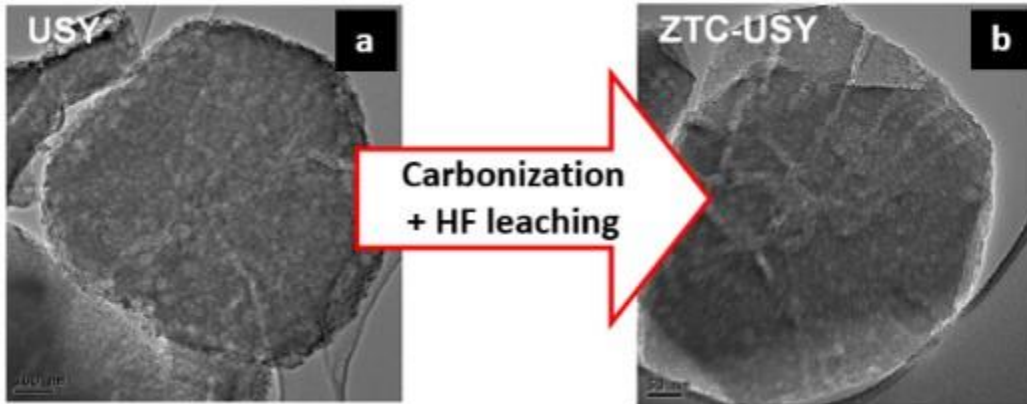
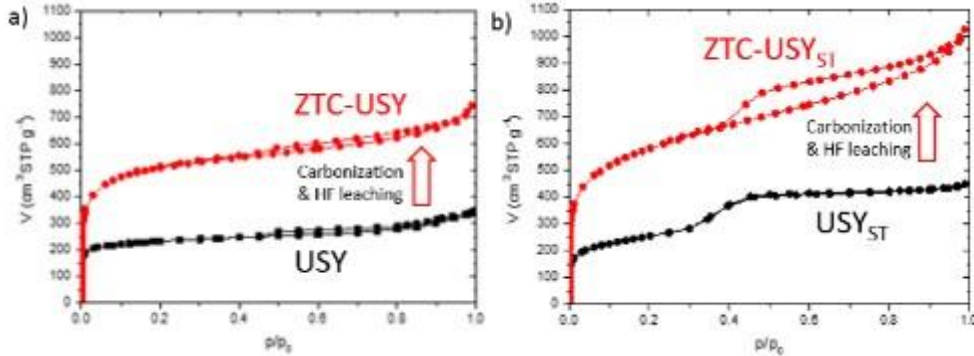


Image 2:



**References:** 1. Kyotani, T.; Nagai, T.; Inoue, S.; Tomita, A. *Chem. Mater.* 1997, 9, 609-615.

2. Wang, H. L.; Gao, Q. M.; Hu, J.; Chen, Z. *Carbon* 2009, 47, 2259-2268.

3. Nishihara, H.; Kyotani, T. *Chem. Commun.* 2018, 54, 5648-5673.

4. Sachse, A.; Grau-Atiendza, A.; Jardim, E.O.; Linares, N.; Thommes, M.; García-Martínez, J. *Cryst. Growth Des.* 2017, 17, 4289-4305.

## **Novel Materials and Structural Methods**

FEZA21-PO-273

### **C@TiO<sub>2</sub> CORE-SHELL STRUCTURES FOR ELIMINATION OF PHENOLIC COMPOUNDS FROM WATER**

K. Sidor<sup>1,\*</sup>, T. Berniak<sup>1</sup>, P. Łątka<sup>1</sup>, A. Rokicińska<sup>1</sup>, M. Michalik<sup>2</sup>, P. Kuśtrowski<sup>1</sup>

<sup>1</sup>Faculty of Chemistry, <sup>2</sup>Faculty of Geography and Geology, Jagiellonian University, Krakow, Poland

**Abstract Text:** Carbon materials are widely used in various applications (including electrochemical, catalytic and adsorption processes) due to their extraordinary high and complex specific surface area. Huge advantages of carbon based adsorbents are environmental friendliness and low production cost. The capture of different organic pollutants by adsorption on activated carbons can be additionally enhanced by combing this process with a subsequent (photo)catalytic degradation. In this work, we report the study on design, synthesis and characterization of C@TiO<sub>2</sub> core-shell composites for dual mode organic contamination removal.

The spherical core-shell structures were produced using an one-pot approach in a water-ethanol mixture by the adopted Stöber method. A spherical resorcinol-formaldehyde resin core was covered by a TiO<sub>2</sub> precursor – titanium(IV) butoxide (TBOT). The obtained materials were subsequently carbonized in inert atmosphere (flowing N<sub>2</sub>) in a wide temperature range (600 – 1000 °C). Powder X-ray diffraction (XRD) measurements revealed different graphitization degree of the carbon core and anatase-to-rutile ratio in the TiO<sub>2</sub> shell strongly depended on the carbonization temperature. A specific surface area and porosity of individual components of the C@TiO<sub>2</sub> composites were examined. The microporous carbon cores showed high specific surface area of 700 m<sup>2</sup>/g. As expected, the TiO<sub>2</sub> shell turned out to be more mesoporous (S<sub>BET</sub> ~ 100 m<sup>2</sup>/g). The C@TiO<sub>2</sub> core-shell structure with hierarchical porosity (wider channels in the shell leading to narrow pores in the carbon core) had S<sub>BET</sub> of ca. 400 m<sup>2</sup>/g.

Equilibrium adsorption capacities in the elimination of phenol and 4-nitrophenol from water phase were determined for both the carbon cores and the C@TiO<sub>2</sub> composites. Kinetics of adsorption of phenolic compounds was also investigated. It was found that the obtained results were influenced by the carbon core sphericity and aggregation, its size and carbonization temperature. The phenol adsorption on the spherical resol based carbon materials proceeded according to pseudo-second kinetics model (R<sup>2</sup> = 0.96–0.99). Furthermore, the obtained materials exhibited excellent adsorption capacities 70–150 mg/g, which exceeded the results achieved for commercial activated carbon WG-12 (Gryfskand). An effect of heteroatom addition on the adsorption phenomena was checked after surface modification. The materials were treated by oxidation in a HNO<sub>3</sub> and H<sub>2</sub>O<sub>2</sub> solution, reduction in a NH<sub>3</sub> flow and oxidation-reduction cycles. X-ray photoelectron spectroscopy (XPS) revealed incorporation of various O- and N-containing functionalities into the resol based carbon cores. Nevertheless, the appearance of heteroatoms decreased adsorption capacities of the obtained spherical carbon materials and the corresponding composites regardless of the carbonization temperature. The collected results suggest that the mechanism of phenol adsorption is strongly related to the micropore volume and graphitization of carbon matrix.

K. Sidor has been partly supported by the EU Project POWR.03.02.00-00-I004/16.

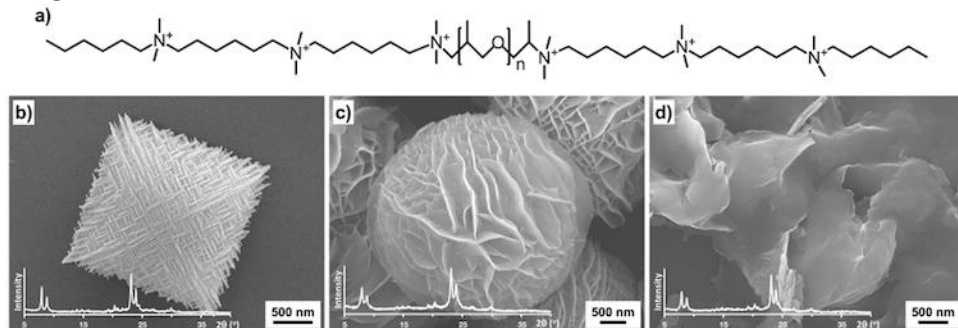
**Hierarchical Zeolites Comprising Zeolite Nanosheets with Controlled Branching and Stacking for Catalytic Applications**

C.-M. Yang<sup>1,\*</sup>, A. Chang<sup>1</sup>, T.-C. Yang<sup>1</sup>, K.-K. Chang<sup>1</sup>

<sup>1</sup>Chemistry, National Tsing Hua University, Hsinchu, Taiwan, Province of China

**Abstract Text:** Great efforts have been devoted to the preparation of zeolitic materials with hierarchical porosity for catalytic applications. A promising strategy, as pioneered by Ryoo and coworkers [1,2], is the direct synthesis of zeolite nanosheet-based materials using bifunctional structure-directing agents (SDAs). For this type of materials, a problem often encountered is a significant reduction of inter-lamellar porosity after the removal of SDAs. In this contribution, we report our recent discovery of a new type of triblock SDAs for rational control of the branching and stacking of zeolite nanosheets to result in hierarchical zeolitic materials with varied morphology. The SDAs feature two blocks of triquaternary (spaced by the  $-C_6H_{12}-$  group) ammonium groups (denoted  $N_3$ ) linked by a propylene oxide ( $PO_n$ ) segment (cf. Figure 1a). We found that the length of the  $PO_n$  linker determined the way the MFI zeolite nanosheets were arranged in the resulting materials. The triblock  $N_3-PO_3-N_3$  SDA with short linker directed the formation of hierarchical MFI octahedra comprising highly branched, orthogonally-stacked and self-pillared nanoplates, within which parallel and equally spaced MFI nanosheets were observed [3]. The morphology of the materials evolved to those with less branched nanosheets, and the material synthesized with  $N_3-PO_{68}-N_3$  was solely composed of multilamellar MFI nanosheets (cf. Figure 1b-1d for the SEM images of the materials synthesized with  $N_3-PO_6-N_3$ ,  $N_3-PO_{33}-N_3$  or  $N_3-PO_{68}-N_3$ , respectively). The correlation between the linker length and the packing, branching and stacking of zeolite nanosheet was rationalized by considering possible orientation and the occupied volume of the triblock SDAs during the growth of two-dimensional zeolite crystals. The hierarchical MFI zeolites are promising for catalytic applications. Two examples will be introduced. Owing to the presence of the silanol nests-like species at nanosheets' junctions, the hierarchical silicalite-1 materials exhibited excellent and stable activity for the vapor-phase Beckmann rearrangement of cyclic oximes with high lactam selectivity. We demonstrated the co-deposition [4] of Au and  $TiO_2$  into hierarchical silicalite-1 octahedra to form edge-attached domains of Au nanodisks and  $TiO_2$  sandwiched between adjacent zeolite nanosheets. The resulting nanocomposite showed efficient plasmonic photocatalytic activity for hydrogen production by selective alcohol photoreforming [5].

**Image 1:**



**References:**

1. M. Choi, K. Na, J. Kim, Y. Sakamoto, O. Terasaki, R. Ryoo, *Nature*, 461, 246 (2009).
2. K. Na, C. Jo, J. Kim, K. Cho, J. Jung, Y. Seo, R. J. Messinger, B. F. Chmelka, R. Ryoo, *Science*, 333, 328 (2011).
3. A. Chang, H.-M. Hsiao, T.-H. Chen, M.-W. Chu, C.-M. Yang, *Chem. Commun.*, 52, 11939 (2016).
4. S.-P. Huang, C.-Y. Lin, C.-M. Yang, *Microporous Mesoporous Mater.*, 284, 53 (2019).
5. A. Chang, W.-S. Peng, I.-T. Tsai, L.-F. Chiang, C.-M. Yang, *Appl. Catal. B: Environ.*, 255, 117773 (2019).

## **Novel Materials and Structural Methods | Zeolites/Inorganic materials**

FEZA21-PO-275

### **Asymmetric diquatery ammonium salts for the synthesis of microporous silicates and germanosilicates**

C. Isaac<sup>1</sup>, J.-L. Paillaud<sup>1,\*</sup>, T. J. Daou<sup>1</sup>, A. Ryzhikov<sup>1</sup>

<sup>1</sup>The Mulhouse Materials Science Institute (IS2M), UMR 7361, CNRS-UHA, Mulhouse, France

**Abstract Text:** Zeolites are microporous ordered solids with a framework formed by tetrahedral units TO<sub>4</sub> (T = Si, Al, Ge ...). They are widely used in various industrial applications such as catalysis, adsorption, molecular sieving, ion exchange and energetics.<sup>1,2,3</sup> The use of organic structure-directing agents (OSDA) such as quaternary ammonium ions during hydrothermal synthesis salts has speed up research and led to the discovery of many new zeolites. Structure-directing phenomenon depends on other factors such as chemical composition of the synthesis gels, nature of mineralizing agent, concentration (H<sub>2</sub>O/T ratio), and presence of heteroatoms.<sup>4</sup>

In this contribution, we present new syntheses using unusual asymmetric diquatery ammonium salts as OSDAs where several chemical parameters were taken into account. Thus, seven pyrrolidinium and piperidinium derivatives have been chosen, with different carbon chain lengths and different terminal groups linked to the second nitrogen atoms. Syntheses were performed with different gel composition in pure silica and germanosilicate media with hydroxide and/or fluoride mineralizing agent.

Among the obtained different known topologies (**AST, BEC, ITG, IWW, MFI, MEL, \*MRE, NON, -SVR, UOV**), special effort has been devoted to the structural analysis of **BEC** and **-SVR**-type structures. Thus, the Rietveld methods allowed us to localize the ordered OSDAs inside the pores. Concerning the **-SVR** topology, a comparison with the original structure of SSZ-74 was performed.<sup>5,6</sup> In addition, a new phyllosilicate has been synthesized and characterized. This new structure reveals its potential use as a precursor for original zeolitic topologies.<sup>7</sup>

#### **References:**

- 1) Weitkamp, J., Zeolites and Catalysis. Solid State Ionics 2000, 131, (1), 175-188.
- 2) Zeolites and their applications; Rashed, M. N.; Palanisamy, P., Eds.; IntechOpen, 2018.
- 3) Eroshenko, V.; Regis, R.-C.; Soulard, M.; Patarin, J. J. Am. Chem. Soc. 2001, 123, 8129.
- 4) Insights into the chemistry of organic structure-directing agents in the synthesis of zeolitic materials; Gómez-Hortigüela, L., Ed.; Springer, 2018.
- 5) Baerlocher, C.; Xie, D.; McCusker, L. B.; Hwang, S.-J.; Chan, I. Y.; Ong, K.; Burton, A. W.; Zones, S. I., Ordered silicon vacancies in the framework structure of the zeolite catalyst SSZ-74. Nature Materials 2008, 7, (8), 631-635.
- 6) Isaac, C. et al., Asymmetric diquatery ammonium salts for the synthesis of microporous silicates and germanosilicates. Microporous and Mesoporous Mater., in preparation.
- 7) Isaac, C. et al., Mu-46: a new phyllosilicate formed by a stacking of original layers made up of bre composite building units, in preparation.

**Multiple Phase Transformations During the Synthesis of Germanosilicate UOS**

Q. Yue<sup>1,\*</sup>, M. Opanasenko<sup>1</sup>

<sup>1</sup>Department of Physical and Macromolecular Chemistry, Charles University, Praha, Czech Republic

**Abstract Text:** Zeolites are an important class of crystalline microporous materials with molecular-scale pore architectures constructed by TO<sub>4</sub> tetrahedra (T=Si, Al, B, Ge, P, etc.) and played important roles in industrial applications, such as ion-exchange, catalysis, gas adsorption and separation. In general, zeolites are synthesized under hydrothermal–solvolothermal conditions, and the reaction gel contains the source of framework atoms, solvents, organic structure-directing agents (OSDAs), and mineralizers<sup>1</sup>. Although the systematic studies of the role of OSDAs in zeolite synthesis have allowed the discovery of many attractive structures<sup>2</sup>, the rational synthesis of new zeolites is still far away due to the lack of knowledge on all crystallization parameters on zeolite phase selectivity. Many parameters can influence the crystallization kinetics, such as nature of components and chemical ratio of reaction gel, crystallization temperature and time, and also the type of reactor<sup>3</sup>. This makes realization of the *ab initio* synthesis of a desired new structures difficult<sup>4</sup>. Many works have been devoted to search of OSDA molecules with proper size, shape, rigidity, polarity, and C/N ratio as well as to optimization of chemical composition of reaction mixture to synthesize new germanosilicate zeolites<sup>1</sup>. However, the *ab initio* synthesis depending on the crystallization time is far away from the expected outputs. In the present work, the growth and phase isolation of germanosilicates were realized by adjusting crystallization time without changing any other parameters. A fixed chemical composition with SiO<sub>2</sub>: GeO<sub>2</sub>: OSDA: HF: H<sub>2</sub>O = 0.5: 0.5: 0.9: 1: 8 was used for hydrothermal synthesis at 170 °C. The OSDA used was 3-ethyl-1-methyl-3H-imidazol-1-ium, which has been utilized to synthesize IM-16 previously<sup>5</sup>. *Ab initio* synthesis of germanosilicates with structures depending on the crystallization time was applied. Optimization of crystallization time allowed to separate two pure phases (**Phase 1**, i.e. **STW** and **Phase 2**) before the crystallization of final phase of IM-16. First, the **STW** is formed in a short time and possesses a hexagonal bipyramid shape of the crystals. The pure **STW** can be obtained in 4 hours. With the prolonging time, a new **Phase 2** was generated inside the **STW**. The pure **Phase 2** can be separated in 7 days. It has a spindle-shaped crystal formed by aggregation of small rods. The nanosized rod-shape **Phase 2** grows to laminar crystals with the increasing of time. Finally, a pure IM-16 (**UOS**) phase was formed in 14 days. The multiple phase transformations were revealed by the in-situ synchrotron XRD. And also, other techniques, such as powder XRD, single crystal XRD, RED, SEM, EDS *et al*, were applied to determine the phase purity and structures of obtained materials.

**Reference**

- [1] Li, J.; Corma, A.; Yu, J. *Chem. Soc. Rev.* **2015**, 44, 7112-7127.
- [2] Jiang, J.; Yu, J.; Corma, A. *Angew. Chem. Int. Ed.* **2010**, 49, 3120-3145.
- [3] Li, S.; Li, J.; Dong, M.; Fan, S.; Zhao, T.; Wang, J.; Fan, W. *Chem. Soc. Rev.* **2019**, 48, 885-907.
- [4] Wang, Z.; Yu, J.; Xu, R. *Chem. Soc. Rev.* **2012**, 4, 1729-1741.
- [5] Lorgouilloux, Y.; Dodin, M.; Paillaud, J.-L.; Caullet, P.; Michelin, L.; Josien, L.; Ersen, O.; Bats, N. *J. Solid State Chem.* **2009**, 182, 622-629.

**Confinement and condensation of amino acid molecules in 1-D mordenite channels**

M. Polisi<sup>1</sup>, M. Fabbiani<sup>2</sup>, G. Vezzalini<sup>1,\*</sup>, G. Martra<sup>2</sup>, F. Di Renzo<sup>3</sup>, S. Quartieri<sup>1</sup>, R. Arletti<sup>1</sup>

<sup>1</sup>Department of Chemical and Geological Sciences -, University of Modena and Reggio Emilia, Modena, <sup>2</sup>Dept. Chemistry, University of Torino, Torino, Italy, <sup>3</sup>Institut Charles Gerhardt, Univ Montpellier-CNRS-ENSCM, Montpellier, France

**Abstract Text:** Amide bond formation is one of the most important reactions in organic chemistry. It plays a key role in biological systems growth and development, since the amide bond is the main chemical bond connecting amino acids together giving peptides and proteins. In the recent years, the demand of improved methods for the synthesis of amide/peptide functionality is increasing, due to the expensive and wasteful approach of the current synthesis strategies, that are not “atom economical”, since great quantities of waste are generated (Constable *et al.*, 2007). The aim of this work is to induce the amino-acid condensation with a new protocol: the molecules polymerization will be obtained by applying only pressure, using zeolites pores as scaffold.

This study, from one side, will open the way to a “green” and solvent-free, peptide synthesis. On the other side, it will contribute to shed light on the possible role of zeolites in amino acids polymerization under abiotic conditions, which is a still open issue in prebiotic chemistry (Martra *et al.*, 2014; Whitesides, 2015).

Glycine, alfa-alanine and beta-alanine were selected and adsorbed in a Na-mordenite [Na-MOR: Na<sub>4</sub>Al<sub>4.3</sub>Si<sub>43.9</sub>O<sub>96</sub>·28.2H<sub>2</sub>O, s.g. *Cmc2<sub>1</sub>*, *a*=18.080(1) Å, *b* = 20.380(1) Å, *c* = 7.489(3) Å, *V* = 2759.3 (3) Å<sup>3</sup>] synthesized at the Institut Charles Gerhardt in Montpellier. Na-mordenite was chosen as porous host for this experiment because the Na cations located in the side pocket of MOR are expected to trap the water molecules possibly generated by the formation of the peptide bond during the condensation reaction.

The three obtained hybrid materials were characterized by TG analysis, elemental analysis, IR spectroscopy, XRPD and then compressed at high pressure (HP) in order to explore the possibility of using pressure to induce amino acids condensation in zeolite pores.

Glycine and beta-alanine were loaded from vapor phase at mild temperature (150-160°C) in a previously dehydrated Na-MOR powder sample. Alfa-alanine was loaded from aqueous phase and then the hybrid material was dehydrated at 150° C. The IR spectra collected on glycine and β-alanine/Na-MOR composites show the presence of a peptide bond moiety inside the composite materials already at ambient conditions. This is not observed in the alfa alanine sample, probably due to the presence of residual water molecules deriving from the different loading, that modify the amino acid leading to zwitterion form and hindering oligomerization.

XRPD and elemental analyses show that both vapour and aqueous loading lead to a partial filling of the pores, being the alanine composites the most filled: 1.4, 2.4 and 3.8 molecules for glycine, alfa-alanine and beta-alanine, respectively.

The XRPD HP structural data are available only on glycine and alfa-alanine samples. The pressure seems to only slightly modify the distribution of the molecules, sited in the 12MR channel. The shortening of the cell parameters, induced by compression, is not enough to bring them at bond distance. As a consequence, at least up to 2 GPa, peptide formation is not observed.

Since on the basis of the position of the molecules and of their steric hindrance four molecules would be allowed for each unit cell, XRPD results indicate that a further loading of the channel could be a promising perspective for peptide formation.

**References:** Constable D.J.C., Dunn P.J., Hayler J.D., Humphrey G.R., Leazar J.L., Linderman R.J., Lorenz K., Manley J., Pearlman B.A., Wells A., Zaks A. and Zhang T.Y. *Green Chemistry* 2007, 9, 411-420.

Martra, G.; Deiana, C.; Sakhno, Y.; Barberis, I.; Fabbiani, M.; Pazzi, M.; Vincenti, M. *Angew. Chem. Int. Ed.* 2014, 53, 4671.

Whitesides G.M. *Angewandte Chemie* 2015, 54, 3196.

## **Novel Materials and Structural Methods | Zeolites/Inorganic materials**

FEZA21-PO-284

### **CrystalGrower: A General Tool for Modelling Crystal Growth**

A. Hill<sup>1</sup>, M. Anderson<sup>1,2,\*</sup>, J. Gebbie-Rayet<sup>1,3</sup>, M. Trueman<sup>1</sup>, M. Attfield<sup>1</sup>, V. Blatov<sup>4,5</sup>, D. Proserpio<sup>4,6</sup>

<sup>1</sup>Chemistry, University of Manchester, Manchester, United Kingdom, <sup>2</sup>Chemistry, Curtin University, Perth, Australia,

<sup>3</sup>Computational Research, STFC, Daresbury, United Kingdom, <sup>4</sup>Chemistry, Samara University, Samara, Russian

Federation, <sup>5</sup>Chemistry, Northwestern Polytechnical University, Xi'an, China, <sup>6</sup>Chemistry, Università degli Studi di Milano, Milan, Italy

#### **Abstract Text:**

Influence over the processes of crystallisation and dissolution are crucial in many areas of industry *e.g.* optimising the performance of industrial catalysts by controlling their crystal morphology. The performance of porous material catalysts and adsorbents are directly tied to their morphologies through pore diffusion lengths and overall accessible surface area. With the improvements in microscopy techniques, particularly atomic force microscopy (AFM), researchers have the unprecedented ability to delve into the kinetic processes that underpin the foundations of crystal growth.<sup>1</sup> By understanding these procedures, eventually we hope that they can be directed with a high degree of control for any application where crystalline materials are required.

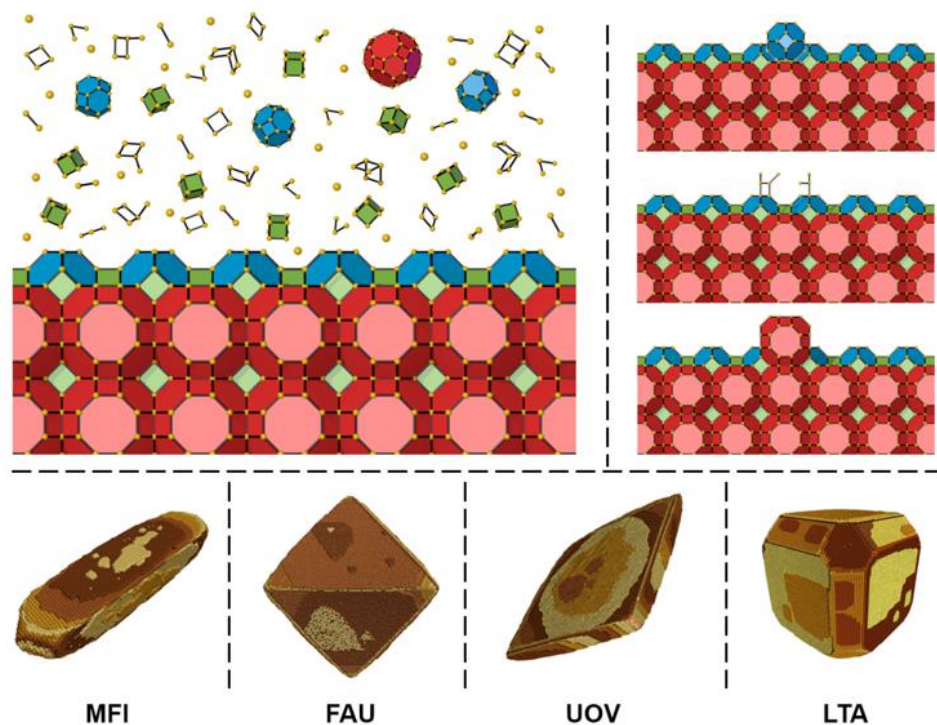
Recently, our group developed a general Monte Carlo crystal growth tool which allows the simulation of not just porous materials, but all materials with a regular crystal structure – *CrystalGrower*.<sup>2</sup> To simulate the growth of a crystal structure, it must first be broken down to sensible *units of growth* which can combine to describe the entire framework. These *units of growth* differ from the *growth units* of the crystal, as the former are rate-determining steps in the formation of the crystal (*e.g.* cages) and the latter are the exact units that assemble the crystal structure (*e.g.* monomers / dimers).

To simulate porous materials such as zeolites and zeotypes, *CrystalGrower* uses natural tiles as *units of growth*. These tiles are the lowest energy cage structures that can assemble an entire framework, composed of many connected Q<sup>4</sup>, Q<sup>3</sup> and Q<sup>2</sup> tetrahedral units. Tiles are separated into site types based on all the combinations of tetrahedral units between an isolated tile (highest energy) and a fully-condensated tile within the crystal bulk (lowest energy). By assigning energy penalties for each missing degree of condensation at a tile vertex, an energy ranking for each tile combination can be constructed. At each cycle of the program, tiles will compete to grow or dissolve, growing a crystal representative of the average of these competing processes. The solution from which the crystal is grown is also simulated as a modifiable thermodynamic driving force, resulting in a truly kinetic model. Additionally, *CrystalGrower* can be used in a predictive sense to explore which crystal morphologies should be accessible under certain energetic conditions.

*CrystalGrower* has already been used to model the growth of numerous porous material frameworks, with simulation data closely matching experimentally characterised morphology and surface topology data.<sup>2,3</sup> Until now, the software has been exclusively used by our group, but will be released publicly at FEZA 2020.

**Figure 1: Top** – A schematic showing how natural tiles are incorporated into the crystal structure from solution as rate-determining steps. Only the complete, correct tile (shown in red) will persist at the crystal surface as it is metastable, all other arrangements will eventually dissolve back into solution. **Bottom** – Examples of simulated zeolite crystals grown using *CrystalGrower*.

**Image 1:**



**References:**

- 1 - M. W. Anderson, J. R. Agger, N. Hanif and O. Terasaki, Growth models in microporous materials, *Microporous Mesoporous Mater.*, 2001, 48, 1–9.
- 2 - M. W. Anderson, J. T. Gebbie-Rayet, A. R. Hill, N. Farida, M. P. Attfield, P. Cubillas, V. A. Blatov, D. M. Proserpio, D. Akporiaye, B. Arstad and J. D. Gale, Predicting crystal growth via a unified kinetic three-dimensional partition model, *Nature*, 2017, 544, 456.
- 3 - H. S. Cho, A. R. Hill, M. Cho, K. Miyasaka, K. Jeong, M. W. Anderson, J. K. Kang and O. Terasaki, Directing the Distribution of Potassium Cations in Zeolite-LTL through Crown Ether Addition, *Cryst. Growth Des.*, 2017, 17, 4516–4521.

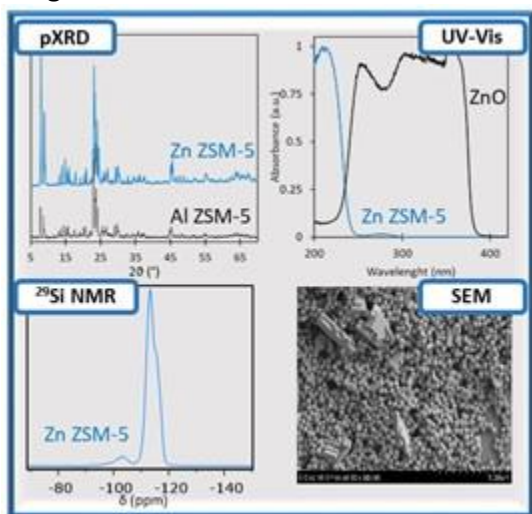
**Synthesis and Characterisation of Zincosilicate Zeotypes and their Application as Lewis-Acid Catalysts**

I. Mazzei<sup>1,\*</sup>, R. Taylor<sup>1</sup>

<sup>1</sup>Chemistry, Durham University, Durham, United Kingdom

**Abstract Text:** The direct synthesis of higher value products from natural gas represents a real challenge for modern catalysis and could bring huge energy and environmental advantages.<sup>1</sup> Zeolites containing Lewis acid sites have been widely studied for applications aimed at the upgrade of feedstock to more useful products, such as the dehydrogenation of ethanol to acetaldehyde.<sup>2</sup> However, the role that the framework metals play in these reactions remains unclear. Replacing Al<sup>III</sup> with divalent heteroatoms such as Zn<sup>II</sup> or Mg<sup>II</sup> in the framework would introduce a divalent negative charge and stabilise multi-valent extra-framework cations more effectively. This would also be extremely useful for reactions catalysed by Lewis acid sites, as it would avoid the drawbacks related to a high Al:Si ratio<sup>3, 4</sup> and support a greater number of extra-framework active sites per heteroatom in the framework. We have employed and optimised a quick and straightforward synthetic strategy for the preparation of zincosilicates with MFI topology (Zn ZSM-5).<sup>5</sup> The zincosilicates synthesised were characterised through p-XRD, EDXRF, SEM and solid-state MAS-NMR. Further characterisation techniques such as XPS, XAS and DRS UV-Vis were also employed in order to identify the coordination environment of Zn species and confirmed that the samples are free of ZnO and that the heteroatoms occupy tetrahedral framework positions. Ethanol dehydrogenation performed on Zn ZSM-5 samples showed a high (> 90%) product selectivity to acetaldehyde and high (> 70%) and stable conversion. This is due to the absence of strong Brønsted acidity in the catalysts, which prevents (i) the formation of by-products and (ii) a fast deactivation of the materials.

**Image 1:**



**References:**

1. G. A. Olah, *Angew. Chem. Int. Ed.*, 2005, 44, 2636-2639.
2. W. Yan, S. Xi, Y. Du, M. K. Schreyer, S. X. Tan, Y. Liu, A. Borgna, *ChemCatChem*, 2018, 10, 3078.
3. M. A. Deimund, J. Labinger and M. E. Davis, *ACS Catal.*, 2014, 4, 4189-4195.
4. N. Koike, K. Iyoki, B. Wang, Y. Yanaba, S. P. Elangovan, K. Itabashi, W. Chaikittisilp and T. Okubo, *Dalton Trans.*, 2018, 47, 9546-9553.
5. N. K. Mal, V. Ramaswamy, P. R. Rajamohanam and A. V. Ramaswamy, *Microporous Mater.*, 1997, 12, 331-340.

**Thermally Stable Mesoporous Tetragonal Zirconia Through Surfactant-Controlled Synthesis and Si-Stabilization**

K. L. Abel<sup>1,\*</sup>, S. Weber<sup>2</sup>, D. Poppitz<sup>1</sup>, J. Titus<sup>1</sup>, T. Sheppard<sup>2</sup>, R. Gläser<sup>1</sup>

<sup>1</sup>Institute of Chemical Technology, Leipzig University, Leipzig, <sup>2</sup>Institute for Chemical Technology and Polymer Chemistry, Karlsruhe Institute of Technology, Karlsruhe, Germany

**Abstract Text:**

Due to the strong tendency of ZrO<sub>2</sub> to crystallize, the preparation of mesoporous zirconia powders is challenging. In particular, the transition of the tetragonal (*t*) to the monoclinic (*m*) phase at elevated temperatures leads to a collapse of the mesopore structure [1]. To address this issue, the stabilization of *t*-ZrO<sub>2</sub> with Si has been established as an effective way to prevent the *t*-*m*-ZrO<sub>2</sub> transition. This strategy results in nanocrystalline *t*-ZrO<sub>2</sub> powders with high specific surface area ( $A_{\text{BET}}$ ), but only few, if any, mesopores are formed [2]. Thus, various structure-directing agents have been employed in the synthesis of mesoporous ZrO<sub>2</sub>. Unfortunately, the few reported examples of mesoporous, Si-stabilized ZrO<sub>2</sub> exhibit two major limitations. Firstly, the mesopore width is small (< 6 nm) [3]. Secondly, the dissolution from glass surfaces (e. g. from the preparation vessel) during treatment of hydrous ZrO<sub>2</sub> precipitates in alkaline media is the most commonly applied method to incorporate Si into mesoporous ZrO<sub>2</sub> [4,5]. This strategy not only offers limited practicality in terms of ambiguous Si content, but also prevents distinction between the impacts of Si incorporation and alkaline treatment, which has been reported to influence the pore structure [6]. In this study, we present an experimental procedure towards synthesis of mesoporous ZrO<sub>2</sub>, with a precise amount of Si supplied by an external source. This allows to independently investigate the effects of Si, the surfactant dodecylamine (DDA), and an alkaline treatment (NH<sub>3,aq</sub>) of the hydrogel, on both the textural properties and thermal stability of the ZrO<sub>2</sub> obtained.

**Results and Discussion**

ZrO<sub>2</sub> with 15 mol.% Si exhibits much higher  $A_{\text{BET}}$  (>150 m<sup>2</sup> g<sup>-1</sup>, Image 1) compared to pure ZrO<sub>2</sub> (<40 m<sup>2</sup> g<sup>-1</sup>), since crystallite growth is restricted to <10 nm and full stabilization of the *t*-ZrO<sub>2</sub> phase is reached. Moreover, the addition of DDA during gelation strongly increases the specific pore volume ( $V_p$ ). For example,  $V_p$  increases from 0.17 cm<sup>3</sup> g<sup>-1</sup> to 0.38 cm<sup>3</sup> g<sup>-1</sup>, if 20 mol.% DDA are used in a gelation of ZrO<sub>2</sub> with 15 mol.% Si (Image 1). As shown in Image 2, the increase of  $V_p$  due to the generation of large mesopores with a broad distribution of 4-40 nm. The ZrO<sub>2</sub> hydrogel treatment with NH<sub>3,aq</sub> increases both  $A_{\text{BET}}$  and  $V_p$  (Image 1), but retains the pore width distribution (Image 2). This may arise from unblocking of pores due to dissolution-reprecipitation processes.  $A_{\text{BET}}$  and  $V_p$  of zirconia can be enhanced even further by using a higher Si molar fraction up to 44 mol.% Si (Image 1). However, this is accompanied by broadening of the pore width distribution (Image 2). Therefore, improving thermal stability must be balanced with control over the pore system. Based on the high thermal stability, mesoporous nature and both high  $A_{\text{BET}}$  and  $V_p$ , Si-stabilized zirconia presented in this study is a promising catalyst support with potential applications in demanding chemical environments such as catalytic conversions at high temperature or in strongly acidic media.

**Image 1:**

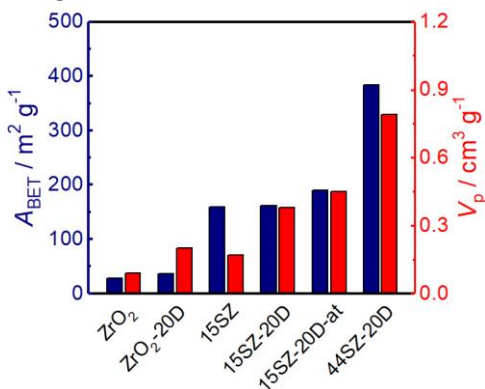
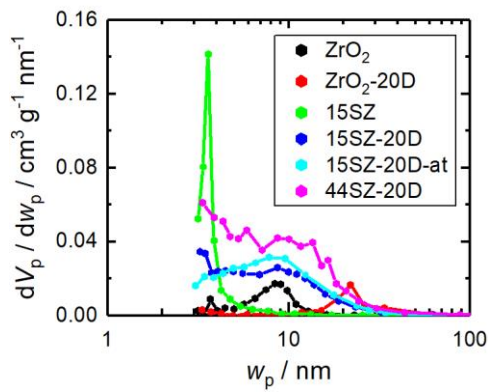


**Image 2:**



**References:**

- [1] D. A. Ward, E. I. Ko, *Chem. Mater.*, 1993, 5, 956-969.
- [2] S. Jaenicke, G. K. Chuah, V. Raju, Y. T. Nie, *Catal Surv. Asia*, 2008, 12, 153-169.
- [3] M. J. Hudson, J. A. Knowles, *J. Mater. Chem.*, 1996, 6, 89-95
- [4] K. Cassiers, T. Linssen, K. Aerts, P. Cool, O. Lebedev, G. van Tendeloo, R. van Grieken, E. F. Vansant, *J. Mater. Chem.*, 2003, 13, 3033-3039.
- [5] A. Peters, F. Nouroozi, D. Richter, M. Lutecki, R. Gläser, *ChemCatChem*, 2011, 3, 598-606.
- [6] S.-F. Yin, B.-Q. Xu, *ChemPhysChem*, 2003, 4, 277-281.

**Heterogeneous catalysis beyond the active site. Design and synthesis of active site environment for directing the reaction mechanism.**

P. Ferri Vicedo<sup>1,\*</sup>, C. Li<sup>1</sup>, C. Paris<sup>1</sup>, M. Moliner<sup>1</sup>, M. Boronat<sup>1</sup>, A. Corma<sup>1</sup>

<sup>1</sup>Instituto Universitario Mixto de Tecnología Química UPV-CSIC, Valencia, Spain

**Abstract Text:** This work combines kinetics and theoretical calculations to show the benefits of going beyond static localized and defined active sites on solid catalysts, into a system that globally and dynamically considers the active site located in an environment that involves a scaffold structure particularly suited for a target reaction. We demonstrate that such a system is able to direct the reaction through a preferred mechanism when two of them are competing. If one of the mechanisms is preferred, a catalyst can be designed and synthesized in where, besides the presence of the active sites (protons) and pore dimensions large enough to accommodate the transition state, the active site environment is optimized by building a most adequate catalyst scaffold.<sup>1,2</sup> The ab initio designed and synthesized zeolite catalyst (ITQ-27) optimizes location, density and environment of acid sites to drive the reaction through the preselected and preferred diaryl-mediated mechanism (Figure 1a), instead of the alkyl transfer pathway (Figure 1b) as demonstrated by a detailed periodic DFT study of both reaction mechanisms. This is achieved by minimizing the activation energy of the selected pathway through weak interactions, much in the way as it occurs in enzymatic catalysts. We show that ITQ-27 outperforms previously reported zeolites for the DEB-Bz transalkylation and, more specifically zeolites industrially relevant such as FAU, BEA and MOR (Figure 2).<sup>3</sup>

Following our initial hypothesis, the fact that IWV zeolite gives higher intrinsic activity and selectivity should be related with a better stabilization of the transition states involved in the diaryl-mediated reaction pathway by zeolite confinement. To check this, we performed a detailed theoretical study of the two possible mechanistic routes on the IWV and MOR zeolite structures by means of periodic DFT calculations. Brønsted acid sites were placed at the two most stable locations for Al in the IWV structure, T3 and T6, and at T4 position accessible from the 12-ring channel in MOR. The geometry of all minima and transition states involved in the alkyl-transfer and diaryl-mediated pathways of DEB-Bz transalkylation and DEB dealkylation were fully optimized without restrictions at the three sites considered, IWV-T3, IWV-T6 and MOR-T4 and using the most stable isomer of DEB, para-DEB. The DFT study shows that the IWV structure intrinsically favours the diaryl-mediated pathway in the DEB-Bz transalkylation reaction, because the topology of the bi-dimensional channel system enhances the formation of the I1+ intermediate. The activation barrier for the global process ranges from 40 to 70 kJ mol<sup>-1</sup>, depending on the route followed for the intramolecular proton transfer generating the I4+ intermediate. In contrast, the alkyl-transfer route competes with the diaryl-mediated pathway in the unidimensional channels of MOR, and the calculated activation barriers are never below 80 kJ mol<sup>-1</sup>, in agreement with the lower activity experimentally determined for MOR.

From the initial reaction rates of EB formation obtained experimentally, activation energies  $E_a$  were calculated by means of the Arrhenius plots, and Gibbs free energies  $\Delta G^\ddagger$ , enthalpies  $\Delta H^\ddagger$  and entropies  $\Delta S^\ddagger$  of activation were obtained by means of the Eyring equation. The lowest activation energies are obtained with the two IWV zeolite samples (57 kJ/mol), followed by FAU (66 kJ/mol), and MOR (74 kJ/mol). The same trend was found for the enthalpies of activation  $\Delta H^\ddagger$ , indicating that the energy involved in the rate-determining step of the mechanism is lower in IWV than in FAU, and the highest in MOR. The results obtained experimentally are close to the theoretical ones and follow the same order, indicating that the diaryl-mediated pathway is favoured in IWV zeolite due to a larger stabilization by confinement of the transition states and intermediates involved in this route, in agreement with the starting hypothesis.

**Image 1:**

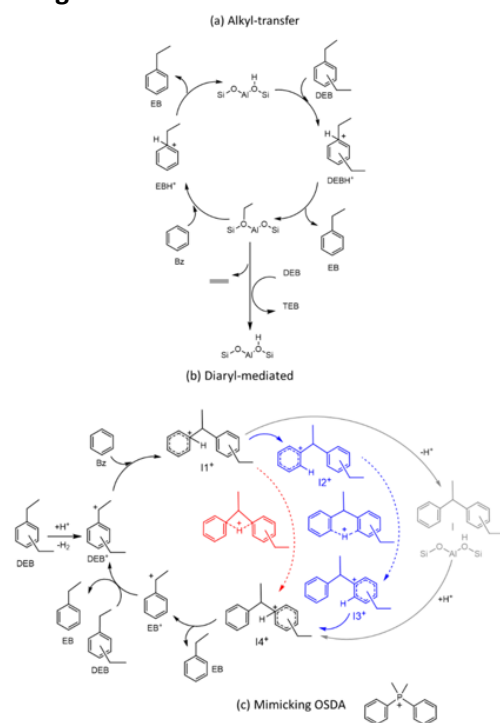
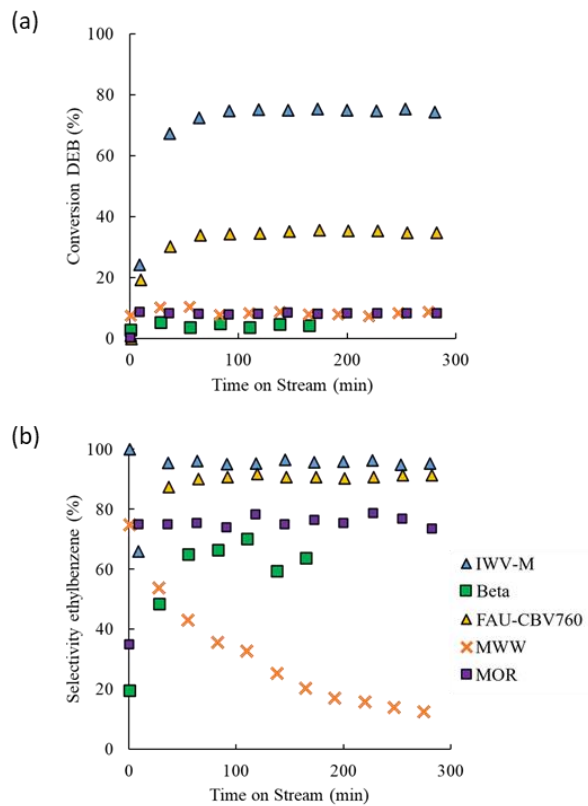


**Image 2:**



- References:** [1] Reference #1 Huang, J.; Jiang, Y.; Marthala, V. R. R.; Hunger, M. Insight into the Mechanisms of the Ethylbenzene Disproportionation: Transition State Shape Selectivity on Zeolites. *J. Am. Chem. Soc.* 2008, 130 (38), 12642–12644
- [2] Reference #2 Margarit, V. J.; Osman, M.; Al-Khattaf, S.; Martínez, C.; Boronat, M.; Corma, A. Control of the Reaction Mechanism of Alkylaromatics Transalkylation by Means of Molecular Confinement Effects Associated to Zeolite Channel Architecture. *ACS Catal.* 2019, 9 (7), 5935–5946.
- [3] Reference #3 Gerzeliev, I. M.; Khadzhiev, S. N.; Sakharova, I. E. Ethylbenzene Synthesis and Benzene Transalkylation with Diethylbenzenes on Zeolite Catalysts. *Pet. Chem.* 2011, 51 (1), 39–48

Variation of counter cations of cage germanoxanes encapsulating fluoride ions

T. Hayashi<sup>1,\*</sup>, N. Sato<sup>1</sup>, H. Wada<sup>1,2</sup>, A. Shimojima<sup>1,2</sup>, K. Kuroda<sup>1,2</sup>

<sup>1</sup>Department of Applied Chemistry, Faculty of Science and Engineering, <sup>2</sup>Kagami Memorial Research Institute for Materials Science and Technology, Waseda University, Tokyo, Japan

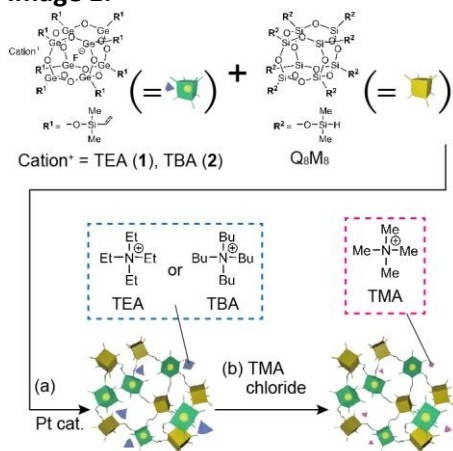
Abstract Text:

**【Introduction】** Inorganic cage compounds with a double-4-ring (D4R) structure are useful as nano-building blocks for porous materials because they are rigid and can be modified with various functional groups at the corners.<sup>1)</sup> For further functionalization, the use of the cavity in the cage structure is of interest. It is known that D4R cage siloxanes<sup>2)</sup> and germanoxanes<sup>3)</sup> can encapsulate fluoride anions inside the cages. Variation of the counter cations outside the cage is expected to be useful in controlling the nanostructures of the porous materials constructed with cage compounds and their applications. Here, we report on the cation exchange not only in the discrete cage germanoxane but also in the cross-linked porous materials. Furthermore, the difference in the porous structures due to the different cations in the porous materials was investigated.

**【Experimental】** A dimethylvinylsilylated cage germanoxane (**1**), containing a fluoride anion inside the cage and a tetraethylammonium (TEA) cation outside, was synthesized by the methods reported previously by us.<sup>4)</sup> **1** and tetrabutylammonium (TBA) bromide were stirred in toluene, forming a cage germanoxane with a TBA cation (**2**). **1** and **2** were cross-linked with a dimethylsilyl-modified cage siloxane (Q<sub>8</sub>M<sub>8</sub>) as a linker by a hydrosilylation reaction (Image 1a). The products were added to an ethanol solution of tetramethylammonium (TMA) chloride to exchange the cations (TEA or TBA) with TMA cation (Image 1b).

**【Results and discussion】** Synthesis of **1** and **2** and the formation of their cross-linked networks with Q<sub>8</sub>M<sub>8</sub> were confirmed by FT-IR and NMR analyses. The N<sub>2</sub> adsorption–desorption isotherms indicated that the cross-linked materials possessed both micropores and mesopores with broad pore size distributions. <sup>13</sup>C MAS NMR spectra confirmed that these porous solids underwent almost complete cation exchange with TMA cations. The N<sub>2</sub> adsorption–desorption measurement showed the increase in the Brunauer–Emmett–Teller (BET) area and micropore volume upon cation exchange with TMA cations. These results suggest that the exchange of the counter cations of the cage germanoxane-based porous materials is effective to tune the pore characteristics.

Image 1:



References:

- 1) R. E. Morris, *J. Mater. Chem.*, 2005, 15, 931.
- 2) A. R. Bassindale et al., *Angew. Chem. Int. Ed.*, 2003, 42, 3488.
- 3) L. A. Villaescusa et al., *Dalton Trans.*, 2004, 820.
- 4) N. Sato, T. Hayashi, et al., *Chem. Eur. J.*, 2019, 25, 7860.

**Synthesis of core – shell zeolite composites BEA@MFI**

E. Luzina<sup>1,2,\*</sup>, I. Shamanaeva<sup>1</sup>, E. Parkhomchuk<sup>1,2</sup>

<sup>1</sup>Boreskov Institute of Catalysis SB RAS, <sup>2</sup>Novosibirsk State University, Novosibirsk, Russian Federation

**Abstract Text:** Zeolites are widely used as catalysts in a number of petrochemical and refinery processes due to a high surface area and strong acid sites. However, too strong catalyst acidity often leads to side reactions and rapid catalyst deactivation by coke deposition on its active sites [1]. A core-shell zeolite composites make it possible to control the zeolite external surface acidity and diffusion of substances to active sites [2]. Thus, stability of catalysts can be increased in such processes as alkylation of isobutane with olefins, when strong acidity is required to obtain the desired products, but the catalyst lifetime is extremely short [3]. In general, a procedure of composite synthesis consists of the following steps: synthesis of micron-sized crystals of “core” zeolite with high acidity, synthesis of nano-sized crystals of “shell” zeolite with low acidity with the subsequent covering “core” crystals with “shell” crystals using polycationic agent followed by growth of the homogeneous shell under hydrothermal conditions [4].

In this work, we have been studying the synthesis conditions of core-shell zeolite composite consisting of BEA (“core”) and MFI (“shell”) structure types. We have determined the optimal synthesis conditions to produce both nano-sized Silicalite-1 and micron-sized zeolite Beta crystals, and also we have studied the conditions for covering the “core” crystals with “shell” particles and subsequent “shell” growth.

We have carried out a number of syntheses of nano-sized Silicalite-1 crystals and micron-sized zeolite Beta crystals by varying temperature and time of hydrothermal synthesis (HTS) and precursor mixture compositions. Silicalite-1 crystals of 100 nm in size is synthesized at the following conditions: molar composition is 1 SiO<sub>2</sub> : 0.244 TPAOH (Tetrapropylammonium hydroxide) : 0.045 Na<sub>2</sub>O : 11.4 H<sub>2</sub>O, HTS was carried out at 95°C for 48 hours. Zeolite Beta crystals with a size of about 500 nm are formed at the following conditions: molar composition is 1 SiO<sub>2</sub> : 0.017 Al<sub>2</sub>O<sub>3</sub> : 0.22 TEAOH (Tetraethylammonium hydroxide) : 8.7 H<sub>2</sub>O, HTS was carried out at 150°C for 168 hours. XRD patterns of Silicalite-1 and Beta zeolite are presented in Fig.1.

Poly(diallyldimethylammonium chloride) (polyDADMAC) was used for zeolite Beta surface modification, HTS of covered with Silicalite-1 nanocrystals “core” was carried out under varying conditions (T = 150-170 °C, t = 30-60 min, TPAOH/SiO<sub>2</sub> = 0.06-0.24, NaOH/SiO<sub>2</sub> = 0.04-0.09) to obtain a layer of Silicalite-1 on Beta “core”. The XRD pattern of final product of core-shell zeolite composites synthesis is shown in Fig.1, its SEM image and textural properties are shown in Fig.2.

*Acknowledgments: The research was funded by RFBR and Novosibirsk region, project number 20-43-543036*

Image 1:

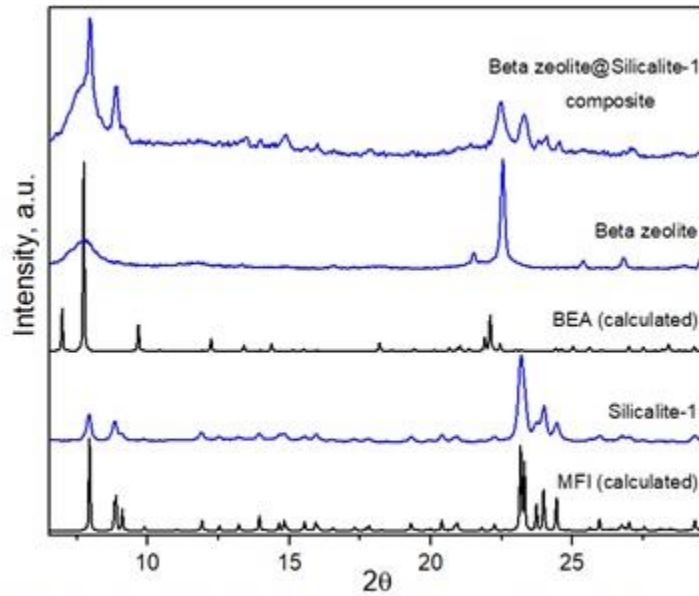
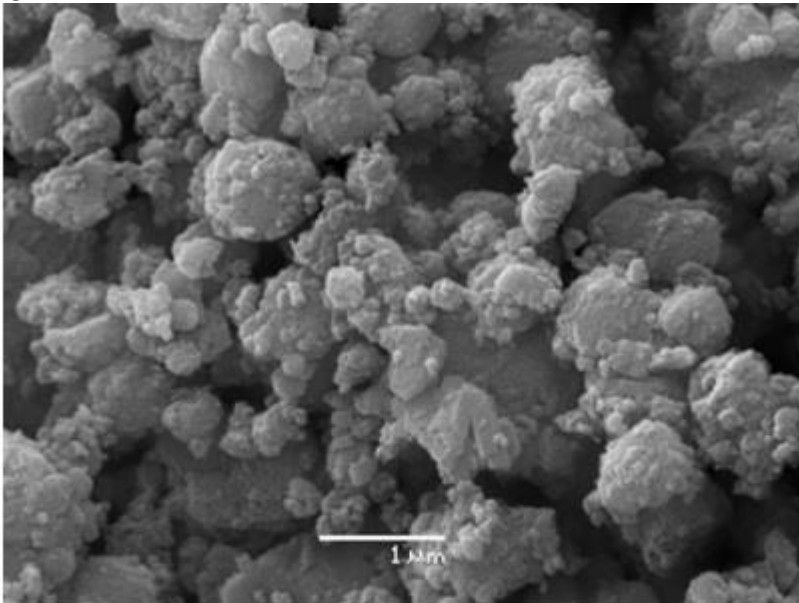


Fig. 1. XRD patterns of Silicalite-1, zeolite Beta and zeolite Beta@Silicalite-1 composite and calculated XRD patterns of MFI and BEA structures

Image 2:



Sample	$S_{BET}$ , $m^2/g$	$V_{tot}$ , $cm^3/g$	$V_{micro}$ , $cm^3/g$
Zeolite Beta	665	0.40	0.21
Silicalite-1	414	0.89	0.13
Beta@Silicalite-1 composite	590	0.44	0.15

Fig. 2. SEM image and textural properties of core-shell zeolite composite

References: [1] Dalla Costa B.O., Querini C.A. Isobutane alkylation with solid catalysts based on beta zeolite // Appl. Catal. A Gen. Elsevier B.V. — 2010. — V. 385. — № 1–2. — P. 144–152.

- [2] Zhang L. et al. Synthesis of core-shell ZSM-5@meso-SAPO-34 composite and its application in methanol to aromatics // RSC Adv. — 2015. — V. 5. — № 69. — P. 55825–55831.
- [3] Ghorbanpour A. et al. Epitaxial growth of ZSM-5@Silicalite-1: A core-shell zeolite designed with passivated surface acidity // ACS Nano. — 2015. — V. 9. — № 4. — P. 4006–4016.
- [4] Wang J. et al. Core-Shell Composite as the Racemization Catalyst in the Dynamic Kinetic Resolution of Secondary Alcohols // ChemCatChem. — 2013. — V. 5. — № 1. — P. 247–254.

***Novel Materials and Structural Methods | Zeolites/Inorganic materials***

FEZA21-PO-293

**Silver quasi-nanoparticles: bridging the gap between clusters molecular-like and plasmonic nanoparticles**

D. Fatima\*, M. ELROZ, L. mama

**Abstract Text:** we report a new strategy for preparing connected silver sub-nanoparticles with unique optical behavior via a selective photo-assisted electrochemical reduction of silver cations in FAU-type zeolite X (FAUX) cages. Bi<sup>2+</sup>/Bi<sup>3+</sup> doped zeolite nanoparticles (ZX-Bi) were prepared by one-pot hydrothermal synthesis and stabilized as colloidal water suspension. Silver nitrate-containing ZX-Bi suspension was subjected to UV irradiation resulting in the reduction of silver cations and generation of Ag<sup>&sup\_+&sub\_n</sup> clusters (Ag@ZX-Bi). The physicochemical characterization of the samples, using XRD, TG, N<sub>2</sub> sorption, NMR, HRTEM-STEM, ICP, EDX and XPS analyses, provided comprehensive information on the textural and structural properties, the chemical compositions and the metal oxidation state of the samples. Their optical behaviors have been investigated using UV-visible and photoluminescence spectroscopies. The IR-operando analysis under visible-light revealed local heating of Ag@ZX-Bi up to 400K. The theoretical calculation of the absorption, scattering, and extinction cross-sections  $s_{abs}$ ,  $s_{sca}$  and  $s_{ext}$  of different silver models performed in this study, was in agreement with the experimental data, elucidating the unique optical behavior of the silver particles. The set of analyses show that quasi-nanoparticles of Ag are formed from bridged Ag clusters (AgCLs) through zeolite channels closing for the first time the gap between clusters and plasmonic nanoparticles.

**Photoassisted electrochemical preparation of connected Silver clusters in host-zeolite channels for photocatalytic application**

D. Fatima\*, E. R. Mohamad, L. Mama, D. Fatiha, L. Louwanda, V. Valentin, L. Oleg, C. Julien

**Abstract Text:** Silver nanoclusters continue to gain a potential attention due to their arresting features including electrical, optical and catalytic properties which strongly depend on their size and shape and differ dramatically from those of larger nanosized particle. These subunits constitute a cross-link between the limits of the single atomic level and plasmonic nanoparticles. The individual behavior of these subsystems is governed by their discrete electronic energy states. A wide variety of synthesis strategies have been developed for generating well-controlled size silver clusters. Hence, it is always challenging to maintain high dispersion of ultra-small metallic clusters, as they are susceptible to agglomerate due to their high surface energy.

Undoubtedly, Zeolite can provide the unique hosting environment for the construction of metallic clusters. Recently, subnanometer silver clusters confined in zeolite are developed by El-Roz et al. [i] as a worthwhile system to investigate its optical properties and photocatalytic properties. This study presented an innovative synthesis method of well controlled preparation of sub-nanometer Silver Clusters trapped into faujasite framework in the presence of vanadate species Ag@ZX-V. This method consists in ultrafast and simple synthetic route via the UV photoexcitation of zeolitic suspension containing vanadate species in the presence of electron scavenger. Vanadate species serve as photoactive species that initiate the formation of silver clusters followed by the expansion of silver clusters by autocatalytic process. This new approach ensures a good dispersion, high abundance, uniformity, and increased stability of silver clusters into the cages of nanosized zeolite crystals.

Herein, we applied this method for preparing connected AgCLs in FAUX doped with Bi<sup>2+</sup>/Bi<sup>3+</sup> cations via an auto-electrochemical reduction of Ag cations, this process was accelerated using photo-assisted reduction. We demonstrate that the optical features are strongly related to the nature of the photo-reductive species (Figure 1). [ii] Different characterizations techniques are employed to reveal the successful encapsulation of silver clusters in the FAUX as well as their specific optical behaviors including: UV-visible, photoluminescence spectroscopies and modeling calculations to determine the absorption, scattering, and extinction cross-sections  $S_{abs}$ ,  $S_{sca}$  and  $S_{ext}$  of different silver. The different experiment demonstrate that the Ag's unique optical behavior is a consequence of the formation of interconnected silver clusters (silver quasi-nanoparticles) through the zeolite channels. The IR operando analysis of the samples in dark and under visible light confirmed the surprising plasmonic behavior of the Ag@ZX-Bi samples and registered local heating equivalent to 190°C under visible irradiation, a characteristic behavior of plasmonic nanoparticles. Therefore, to our knowledge, the gap between clusters and plasmonic nanoparticles with well-controlled and reproducible size of Ag-QNPs is bridged for the first time. The simplicity of the used method allows an easy scaling-up for different possible applications ( $\mu$ -sensors, electronic, optic, etc.).

**References:**

[i] Mohamad El-Roz, Igor Telegeiev, Natalia E. Mordvinova, Uniform Generation of Sub-nanometer Silver Clusters in Zeolite Cages Exhibiting High Photocatalytic Activity under Visible Light. ACS Appl. Mater. Interfaces, , 10, 28702–28708, (2018)

[ii] Fatima Douma, Louwanda Lakiss, Oleg I. Lebedev, Julien Cardin, Krassimir L. Kostov, Jaafar El Fallah, Valentin Valtchev and Mohamad El-Roz, Silver quasi-nanoparticles: bridging the gap between clusters molecular-like and plasmonic nanoparticles, Submitted.

**Open framework sulfur based materials from photocatalytic applications**

B. Silva Gaspar<sup>1,2,\*</sup>, R. Martinez-Franco<sup>1</sup>, A. Fécant<sup>1</sup>, U. Diaz<sup>2</sup>, A. Corma<sup>2</sup>

<sup>1</sup>IFP Energies nouvelles, Solaize, France, <sup>2</sup>Instituto de Tecnología Química, Universitat Politècnica de València-Consejo Superior de Investigaciones Científicas, Valencia, Spain

**Abstract Text:** The consequences of mankind's strong dependence on fossil fuels has is being felt, now more than ever. The production of high value-added compounds, through the photoreduction of CO<sub>2</sub>, has been seen as a viable option to mitigate the greenhouse gas effect and the upcoming energy crisis.

Metal oxides are the most studied materials as photocatalysts. However, the vast majority show high values for the optical band gap and can only absorb radiation in the UV region. Bearing in mind that only 5% of the solar spectrum is made up of UV radiation, the synthesis of materials with band gaps more adapted to solar radiation becomes essential to meet high yields of conversion. Metal chalcogenides comprise a viable alternative to metal oxides, as they have a band gap more suitable for solar radiation [1]. There are several advantages in using crystalline microporous materials as active photocatalysts. The open framework architecture is likely to reduce the electron-hole recombination rate since it reduces the average carrier path to reach the surface of the catalysts particle where the reaction occurs [2]. Recently, porous chalcogenides materials have received special attention, as they combine the presence of an open framework with semiconductivity, thus making it possible to use such materials as photocatalysis [3].

In this work we report the development of new ordered and structured sulfur-based materials. A hydrothermal synthesis under autogenous pressure, a methodology already widely used in the synthesis of microporous oxides, was used to obtain the materials under studied. Something that was taken into account when synthesizing these materials was the reagents used. Abundant, non-toxic reagents, namely a safe sulfur precursor, have been chosen, something that sometimes does not happen in this class materials (see Figure 1). The different materials obtained were characterized with various techniques (XRD, TGA-DTA, chemical and elemental analysis, FESEM, HRTEM, IR spectroscopy, DRS) which allowed conclusions to be drawn regarding the structures obtained, their thermal stability and to evaluate the interaction with UV-Vis radiation.

The synthesized materials, composed of Sn, Zn and S, can be classified as laminar materials and are stable up to a temperature of 300°C. In order to change the electronic properties of the obtained structure, these were doped with Cu. After doping it was observed the reduction of the band gap value to 1,9 eV, optimal value to use these materials in CO<sub>2</sub> photoreduction processes. It is therefore believed by the authors that the materials under study are promising photocatalysts, particularly in solar-to-fuel route, that would help to develop processes with high yields of conversion.

**Image 1:**

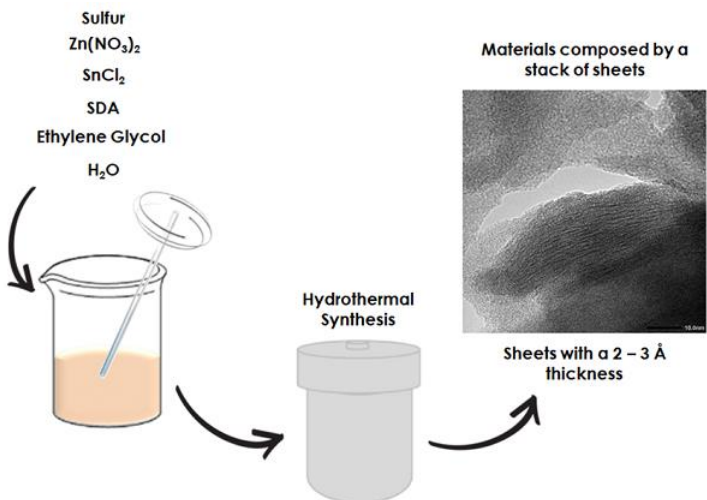


Figure 1. Synthesis procedure, based on hydrothermal synthesis, to obtain sulfur based materials composed by a stack of sheets

- References:** [1] L Nie, Q. Zhang, *Inorg. Chem. Front.*, 2017, 4, 1953-1962.  
[2] N. Zheng, X. Bu, B. Wang, P. Feng, *Angew. Chem., Int. Ed*, 2005, 44, 5299-5303.  
[3] S. Santner, J. Heine, S. Dehnen, *Angew. Chem., Int. Ed*, 2016, 55, 876-893.

**Novel Materials and Structural Methods / Zeolites / Inorganic materials / Poster**

FEZA21-PO-298

**Antibacterial properties of biodegradable polyester/Ag-zeolite composites**

S. Jevtić<sup>1</sup>, J. Đorđević<sup>2,\*</sup>, J. Dikić<sup>3</sup>, M. Nikolić<sup>1</sup>

<sup>1</sup>Department of General and Inorganic Chemistry, Faculty of Technology and Metallurgy, <sup>2</sup>Department of General and Inorganic Chemistry, Faculty of Technology and Metallurgy, <sup>3</sup>Innovation Centre of the Faculty of Technology and Metallurgy, Belgrade, Serbia

**Abstract Text:** Poly(lactic acid), PLA, as a polyester obtained from renewable resources and with biodegradable properties, is seen as a promising alternative to conventional commodity plastics. In the field of packaging application it would be of great importance to improve some functional properties of PLA, such as antibacterial activity. Within the framework of this study, PLA composites with antibacterial activity were obtained by incorporation of silver-enriched zeolite (Ag-Z) in polymer matrix. Composites with 1, 3 and 5 wt.% of Ag-Z were obtained by solution casting from chloroform. Thermal and thermo-oxidative properties were not altered in great extent by the introduction of zeolite, which could be beneficial for future melt processing. Degrees of crystallinity of the samples were calculated from melting enthalpy obtained from DSC analysis. Slight decrease of crystallinity degree of polymer matrix was observed with increase in Ag-Z content. Dynamic-mechanical analysis was used to evaluate mechanical properties and transition temperatures. Reinforcement effect of Ag-Z is observed, as judged from storage modulus increase with introduction of Ag-Z filler in polymer matrix. Glass transition temperature of composites was not affected by the presence of the filler. Antibacterial activity of all synthesized composites was investigated toward two bacterial strains, Gram-negative *Escherichia coli* DSM 498 and Gram-positive bacteria *Staphylococcus aureus* ATCC 25923. Composites showed good antibacterial activity toward examined strains which is slightly pronounced toward *E.coli*. In order to investigate the mechanism of antibacterial activity, the leached amount of silver from composites after the investigation of antibacterial activity was measured. The results show slow release of silver, indicating that the mechanism of antibacterial effect can be connected to the metal itself. According to the present results, PLA/Ag-Z composites are promising materials for food packaging.

## **Physical Properties and the Role of Defects**

FEZA21-PO-299

### **Critical hydroxyl concentration at the frontier between hydrophobic and hydrophilic zeolites**

A. Tuel, M. Lions\*, C. Daniel, B. Coasne, F. Meunier, D. Farrusseng

#### **Abstract Text: Introduction**

The properties of water confined in hydrophobic zeolite cavities remains a topic of fundamental and applied interests.<sup>1,2</sup> The estimation at which pressure water condensation (or evaporation) occurs is not obvious as zeolites often contain structural defects which nature and concentration depend on the synthesis process. These defect sites interact with water, and once the number of water molecules in the cavities is increased, water clusters are formed through hydrogen bonding.<sup>3</sup> Many types of defect sites can co-exist in all-silica zeolites, mainly internal and external silanol groups. While there is an abundant literature on the nature of defect sites, critical concentrations of these defects which may turn a particular zeolite from hydrophobic to hydrophilic has not been systematically determined.<sup>1-4</sup> The objective of this study was to estimate the critical concentration of defects beyond which all silica-zeolites become hydrophilic. A set of all-silica zeolites was prepared, characterized by <sup>29</sup>Si NMR, IR and methanol (MeOH) and water (H<sub>2</sub>O) sorption. A correlation between water uptake at low pressure and the SiOH concentration has been established and used to estimate a critical SiOH concentration beyond which the zeolite becomes hydrophilic.

#### **Experimental**

All-silica zeolites Silicalite-1(OH), Silicalite-1(F), ITQ-13(F), Beta(OH), Beta(F) and Chabazite(F) were prepared using procedures of the literature in alkaline (OH) or fluoride (F) media. They were characterized by <sup>29</sup>Si Nuclear Magnetic Resonance (NMR), X-ray diffraction (XRD), N<sub>2</sub> physisorption, diffuse Reflectance FT-IR spectroscopy (DRIFTS) and Scanning Electron Microscopy (SEM). Adsorption of probe molecules H<sub>2</sub>O and MeOH were measured at 293,15 K on a BelMax system (BelJapan).

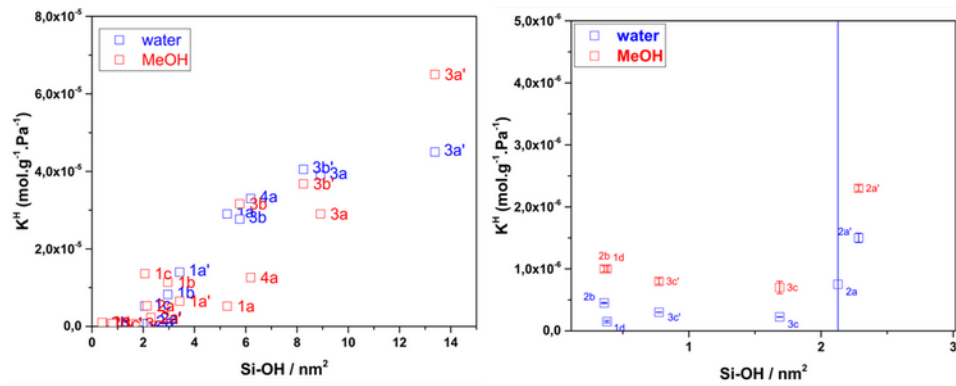
#### **Results**

All zeolites exhibit BET surface areas and pore volumes typical of highly crystalline solids. All additional characterization data by XRD, SEM, IR and <sup>29</sup>Si NMR are in line with literature results. Major differences between MeOH and H<sub>2</sub>O adsorption are observed in the low-pressure part of the isotherms: in most cases, water hardly adsorbs on hydrophobic zeolites while MeOH uptake is significant even at low pressure. The surface affinity for both adsorbates has been quantitatively characterized for all zeolites by the calculation of Henry's constants for water and methanol vapors at low pressure. In order to correlate the hydrophobic character of zeolites with a density of framework defects, the concentration of silanol groups per unit cell was estimated from i) <sup>29</sup>Si NMR spectra and ii) the intensity of the vibrations of free and H-bonded hydroxyls in DRIFTS spectra. Although NMR is sensitive to the environment of Si atoms while DRIFT is sensitive to OH vibrations, the two methods provide similar silanol concentrations. Two major trends regardless of the probe molecules can be observed by plotting Henry's constants for water and MeOH as a function of silanol concentration (Fig. 1). For concentrations < 2 SiOH/nm<sup>2</sup>, Henry's constants are very low (ca. 10<sup>-6</sup> mol.g<sup>-1</sup>.Pa<sup>-1</sup>) whereas for higher concentrations, Henry's constant markedly increases with the silanol concentration in a linear fashion. We also observe that the Henry's constants of water are systematically inferior to those of methanol when the silanol concentration is below 2 SiOH/nm<sup>2</sup> whereas the opposite trend is observed at higher concentrations. The clear cut of adsorption properties observed for silanol concentration around 2 SiOH/nm<sup>2</sup>, which seems to delimit a frontier between hydrophobic and hydrophilic solids, will be discussed and compared to other experimental and theoretical values of the literature.

**Figure 1** Henry's constants for MeOH and H<sub>2</sub>O as a function of the overall silanol density in zeolites (left) with a zoom on the region below 2 SiOH/nm<sup>2</sup> (right)

**Acknowledgments.** We thank IMPRESS and CatCall projects that have received funding from the European Union's Horizon 2020 (SPIRE GA No. 869993) and ANR (CE07-0025)

Image 1:



References: 1)

Mesoporous Mater. 35–36 (2000) 435.

2)

of Porous Solids in Handbook of Porous Solids, F. Schuth, K.S.W. Sing, J. Weitkamp (Eds), Vol. 1, WILEY-VCH Verlag GmbH (2002) pp. 395-431

3)

Mesoporous Mater. 22 (1998) 1.

4)

(1995),12588.

D.H. Olson, W.O. Haag, W.S. Borghard, Microporous

R. Gläser, J. Weitkamp, Surface Hydrophobicity or Hydrophilicity of Porous Solids in Handbook of Porous Solids, F. Schuth, K.S.W. Sing, J. Weitkamp (Eds), Vol. 1, WILEY-VCH Verlag GmbH (2002) pp. 395-431

J. Stelzer, M. Paulus, M. Hunger, J. Weitkamp, Microporous

H. Koller, R.F. Lobo, S.L. Burkett, M.E. Davis, J. Phys. Chem. 99

## Physical Properties and the Role of Defects

FEZA21-PO-300

### Pressure-mediated crystal-fluid interactions in natural erionite-K

T. Battiston\*, F. Pagliaro<sup>1</sup>, P. Lotti<sup>1</sup>, G. D. Gatta<sup>1</sup>

<sup>1</sup>Earth Science Department, University of Milan, Milano, Italy

**Abstract Text:** Investigating the behaviour at high pressure of crystalline compounds with a microporous structure, e.g. zeolites, has experienced a boosted interest in the last two decades, especially due to the  $P$ -induced intrusion of molecules and ions into the structural nano-cavities from the  $P$ -transmitting fluids [1]. Zeolites have a consolidated history of technological and industrial applications, but the understanding of these  $P$ -induced phenomena may further expand their utilizations, opening the way for new routes for tailoring functional materials. In this study, we have investigated the behaviour of the natural zeolite erionite when compressed in non-penetrating and potentially penetrating fluids: i.e. those fluids made by molecules having a kinetic diameter that may allow their  $P$ -mediated adsorption into the zeolite structural cavities.

Erionite is a zeolite with a wide chemical variability in Nature, expressed as solid solutions among three end-members: erionite-Ca, erionite-Na and erionite-K.

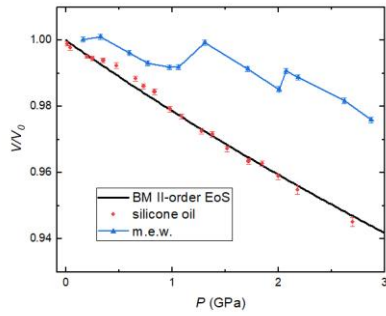
Our sample, classified as erionite-K, has an average chemical formula:  $K_{2.31}Na_{0.02}Ca_{2.15}Mg_{0.69}Ba_{0.04}Sr_{0.02}Al_{9.00}Si_{27.19}O_{72} \cdot 18.66(H_2O)$ . Erionite crystal structure is characterized by the presence of large cages (23-hedron, called "erionite-cage"), superposed along the  $c$  axis, hosting most of the extra-framework population.

We have conducted experiments by single-crystal X-ray diffraction under *in-situ* high-pressure conditions at the Xpress beamline of the Elettra Synchrotron, using an ETH-type diamond anvil cell (DAC) and ruby as  $P$ -calibrant. We have performed two  $P$ -ramps using different  $P$ -transmitting media: the first one using the non-penetrating silicone oil, up to 2.60(5) GPa, and the second one with the potentially penetrating methanol:ethanol:H<sub>2</sub>O = 16:3:1 (hereafter *mew*) mixture, up to 4.97(5) GPa. Using the EoSFit7c software, the  $P$ - $V$  data obtained by the silicone oil ramp were fitted by a II order Birch-Murnaghan equation of state, yielding the following refined isothermal bulk modulus  $K_{V0} = 44(1)$  GPa ( $\beta_{V0} = K_{V0}^{-1} = 0.0227(5)$ , where  $\beta_{V0}$  is the bulk volume compressibility).

$P$ - $V$  data from the *mew* ramp (Fig. 1) show a significant decrease in compressibility, which unambiguously suggests the (irreversible)  $P$ -induced intrusion of H<sub>2</sub>O (and possibly alcohols) molecules. The adsorption seems to occur in three different steps, approximately around 0.2, 1.2 and 2 GPa. This behaviour is somehow surprising if we consider that the magnitude of the intrusion process is comparable with that of synthetic SiO<sub>2</sub>-ferrierite [2] and AlPO<sub>4</sub>-5 [3] zeolites, but in this case has been observed in a natural sample of erionite, with structural cavities filled by extraframework population. Further experiments with different classes of potentially penetrating fluids will allow a full understanding and constraints of the  $P$ -induced adsorption phenomena in erionite.

Fig. 1: High-pressure evolution of the normalized unit-cell volume of natural erionite-K, compressed in *mew* (blue triangles) and silicone oil (red spheres). Silicone oil data are fitted by II-order Birch-Murnaghan equation of state (black line).

**Image 1:**



- References:** [1] Gatta GD, Lotti P, Tabacchi G (2018). Phys. Chem. Miner. 45, 115-138.  
[2] Lotti P, Arletti R, Gatta GD, Quartieri S, Vezzalini G, Merlini M, Dmitriev V, Hanfland M (2015) Micropor. Mesopor. Mater. 218, 42-54.  
[3] Lotti P, Gatta GD, Comboni D, Merlini M, Pastero L, Hanfland M (2016) Micropor. Mesopor. Mater. 228, 158-167.

**The distribution and inhomogeneity of Al within the framework of the catalytically relevant CHA zeolite**

I. G. Clayson<sup>1,\*</sup>, B. Slater<sup>1</sup>

<sup>1</sup>Chemistry, UCL, London, United Kingdom

**Abstract Text:** The distribution of Al defects in the aluminosilicate zeolite CHA is critical in determining the catalyst's properties where this effects: (i) catalytic effectiveness for the methanol-to-olefin process for H-CHA, both directly<sup>1</sup> or indirectly via the proton positions,<sup>2</sup> and (ii) the metal speciation with respect to Cu-CHA, utilised in NO<sub>x</sub> abatement in vehicle exhausts.<sup>3</sup> Conventionally, Lowenstein's rule, that states that Al-O-Al linkages are forbidden,<sup>4</sup> and Dempsey's rule, that the Al defects should maximise their separation,<sup>5</sup> are employed when considering Al distributions. However, previous computational work has demonstrated that the global energy minimum distribution of Al in aluminosilicate zeolites does not follow these laws rigorously and thus the thermodynamically expected distribution is non-trivial to determine.<sup>6</sup> This work aims to extend the previously reported results by considering the global minimum Al distribution as a function of the distance from the external surface as well as the most favourable H arrangement for a given Al arrangement through the use of *ab initio* computational methods in an exhaustive fashion.

Current results demonstrate that for the bulk CHA species, having the protons occupy separate 6-membered and 8-membered rings is the global minimum configuration for non-Lowensteinian Al distributions, suggesting that the H will be not only separated by a significant degree but will at a sufficiently high enough Si/Al distribution will have a substantial H population in both rings that have non-negligible separations, where this will subsequently have consequences for acid catalysis. Moreover, preliminary results demonstrate a preference for Al pairs to segregate the external surface and occupy the Q3 positions. Thus, there is an apparent thermodynamic drive for the CHA crystal to be Al-rich at the surface and relatively Si-rich in the bulk, as previously seen in other zeolites such as ZSM-5,<sup>7</sup> yielding possibly greater diversity in Al sites and ergo active sites than usually considered. On-going work, expected to be later coupled with experimental data, will hopefully explore the inhomogeneity of the framework composition across multiple topologies and the computationally under-explored external surface and the effect of hydration on the thermodynamic drive.

**References:**

- 1) E. M. Gallego, C. Li, C. Paris, N. Martín, J. Martínez-Triguero, M. Boronat, M. Moliner and A. Corma, Chem. - A Eur. J., 2018, 24, 14631–14635.
- 2) S. Bordiga, L. Regli, D. Cocina, C. Lamberti, M. Bjørgen and K. P. Lillerud, J. Phys. Chem. B, 2005, 109, 2779–2784.
- 3) C. Paolucci, A. A. Parekh, I. Khurana, J. R. Di Iorio, H. Li, J. D. Albarracin Caballero, A. J. Shih, T. Anggara, W. N. Delgass, J. T. Miller, F. H. Ribeiro, R. Gounder and W. F. Schneider, J. Am. Chem. Soc., 2016, 138, 6028–6048.
- 4) W. Lowenstein, Am. Mineral., 1954, 39, 92–96.
- 5) E. Dempsey, in Molecular Sieves, Soc. Chem. Ind. London, 1968, p. 293.
- 6) R. E. Fletcher, S. Ling and B. Slater, Chem. Sci., 2017, 8, 7483–7491.
- 7) Z. Ristanović, J. P. Hofmann, U. Deka, T. U. Schüllli, M. Rohnke, A. M. Beale and B. M. Weckhuysen, Angew. Chemie - Int. Ed., 2013, 52, 13382–13386.

**Thermodynamic stability of siliceous zeolites by tailored neural network potentials**

A. Erlebach<sup>1,\*</sup>, C. J. Heard<sup>1</sup>, P. Nachtigall<sup>1</sup>, L. Grajciar<sup>1</sup>

<sup>1</sup>Department of Physical and Macromolecular Chemistry, Charles University, Prague, Czech Republic

**Abstract Text:** The thermodynamic stability of zeolites is of fundamental importance for the design of novel zeolite frameworks.<sup>1</sup> In recent years, the ADOR synthesis protocol has enabled the discovery of novel (unfeasible) high-silica zeolites.<sup>2</sup> However, the targeted *in silico* guided optimization of zeolite synthesis is hampered due to the high computational costs of *ab initio* simulations and the limited accuracy of available empirical force fields. Therefore, this work focuses on developing *linear scaling reactive* neural network potentials (NNP)<sup>3</sup> for accurate large-scale simulations of siliceous zeolites. First, we generated an *ab initio* (DFT) dataset for zeolites, several silica polymorphs, and amorphous silica, including low-energy equilibrium structures and high-energy transition states of the potential energy surface (PES).<sup>4</sup> Next, NNP training used an active learning approach for NNP error estimation, the extension of the training set, and iterative refinement of the NNPs allowing highly accurate modeling of the PES.<sup>4,5</sup> The resulting NNPs enable large-scale simulations of zeolites retaining DFT accuracy (Figure) and providing a computational speed-up of at least three orders of magnitude. Structure optimizations at the NNP level are applied to more than 330 thousand (hypothetical) frameworks<sup>6</sup> revealing more than 20 thousand new hypothetical zeolites in the thermodynamically accessible range of zeolite synthesis.<sup>4</sup> The NNPs accurately reproduce the structure, stability, and vibrational properties of various existing silica structures in good agreement with DFT simulations and experiments. Additionally, the new NNPs facilitate rapid (free) energy calculations of zeolites under high temperatures and pressures, including phase transitions such as zeolite amorphization.<sup>7</sup> Together with the generated DFT database, the new NNPs form the basis for their future extension to facilitate realistic large-scale simulations of the structure and thermodynamic stability of complex zeolites such as water-loaded aluminosilicates under synthesis and operating conditions.

**Image 1:**

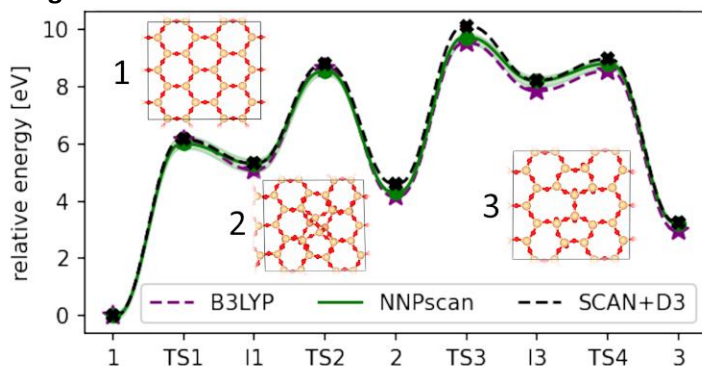


**Figure.** Stone-Wales defect formation from DFT and NNP (Ref. 4).

**References:** 1 J. L. Salcedo Perez, M. Haranczyk and N. E. R. Zimmermann, High-throughput assessment of hypothetical zeolite materials for their synthesizability and industrial deployability, *Z. Kristallogr. - Cryst. Mater.*, 2019, 234, 437–450.

2 M. Mazur, P. S. Wheatley, M. Navarro, W. J. Roth, M. Položij, A. Mayoral, P. Eliášová, P. Nachtigall, J. Čejka and R. E. Morris, Synthesis of ‘unfeasible’ zeolites, *Nature Chemistry*, 2016, 8, 58–62.

3 K. T. Schütt, H. E. Saucedo, P.-J. Kindermans, A. Tkatchenko and K.-R. Müller, SchNet – A deep learning architecture for molecules and materials, *J. Chem. Phys.*, 2018, 148, 241722.

4 A. Erlebach, P. Nachtigall and L. Grajciar, Accurate large-scale simulations of siliceous zeolites by neural network potentials, arXiv: 2102.12404 [cond-mat], 2021, <http://arxiv.org/abs/2102.12404>.

5 J. Behler, First Principles Neural Network Potentials for Reactive Simulations of Large Molecular and Condensed Systems, *Angew. Chem. Int. Ed.*, 2017, 56, 12828–12840.

6 M. W. Deem, R. Pophale, P. A. Cheeseman and D. J. Earl, Computational Discovery of New Zeolite-Like Materials, *J. Phys. Chem. C*, 2009, 113, 21353–21360.

7 L. Wondraczek, Z. Pan, T. Palenta, A. Erlebach, S. T. Misture, M. Sierka, M. Micoulaut, U. Hoppe, J. Deubener and G. N. Greaves, Kinetics of Decelerated Melting, *Adv. Sci.*, 2018, 5, 1700850.

Selection of ZnO Photoluminescence by Distributed Bragg Reflectors Based on Low- $\epsilon$  Porous Silica

L. Kothe<sup>1,\*</sup>, S. Amrehn<sup>1</sup>, M. Tiemann<sup>1</sup>, T. Wagner<sup>1</sup>

<sup>1</sup>Chemistry, Paderborn University, Paderborn, Germany

**Abstract Text:** Zinc oxide (ZnO) is a semiconductor that is widely used for optoelectronic applications. It shows photoluminescence (PL) in the UV and, based on lattice defects, radiative transitions in the visible range.<sup>[1]</sup> To minimize such defects, complex manufacturing processes are frequently used.<sup>[2]</sup> We present a simple and straightforward method of suppressing defect emission, by using a so-called distributed Bragg reflector (DBR), that serves as a wavelength-selective reflector. The DBR consists of alternating layers of high- $\epsilon$  titania (TiO<sub>2</sub>) and low- $\epsilon$  porous silica (SiO<sub>2</sub>), prepared by a spin-coating process.<sup>[3]</sup> At the top of the DBR we synthesized a thin layer of ZnO by a sol-gel method (Figure 1).<sup>[4]</sup> Reflectance and PL spectroscopy reveal that the emission from the ZnO layer is suppressed when the photonic bandgap of the DBR matches the luminescence energy and that the PL is enhanced when the luminescence energy is at the photonic band edge (Figure 2). By contrast, without the underlying DBR (after mechanically destroying the photonic structure by milling), only defect luminescence is observed (Figure 2). These findings suggest that the DBR modulates the electron recombination rate of the luminescent ZnO layer and that the ZnO layer is part of the DBR.

Image 1:

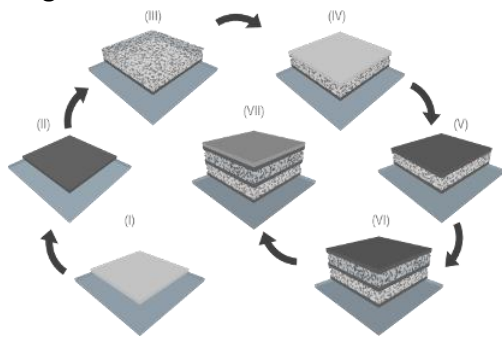
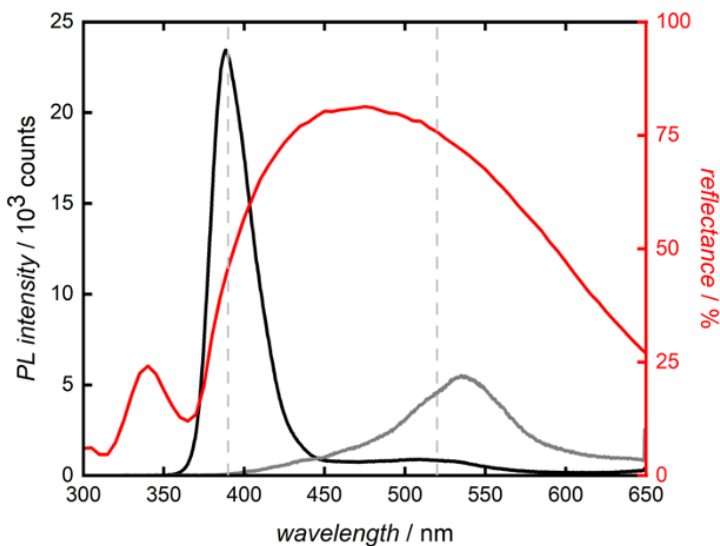


Image 2:



References: [1]

WAAG, Phys. Stat. Sol. C 4 (2007) 158–161.

[2]

J. A. VOIGT, B. E. GNADE, J. Appl. Phys. 79 (1996) 7983–7990.

A. BAKIN, A.C. MOFOR, M. AL-SULEIMAN, E. SCHLENKER, A.

K. VANHEUSDEN, W. L. WARREN, C. H. SEAGER, D. R. TALLANT,

[3]  
Chem. C 4 (2016) 4532–4537.

M. ANAYA, A. RUBINO, M. E. CALVO, H. MÍGUEZ, J. Mater.

[4]  
D. COMEDI, Mater. Sci. Semicon. Proc. 56 (2016) 59–65.

O. MARIN, M. TIRADO, N. BUDINI, E. MOSQUERA, C. FIGUEROA,

Theoretical Study of Zeolite Hydrolysis under Alkaline Conditions

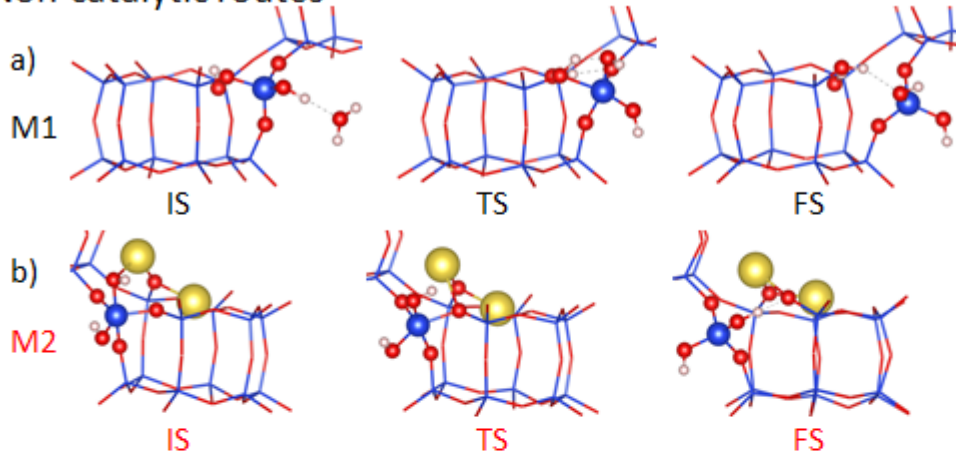
M. Jin<sup>1,\*</sup>, M. Liu, P. Nachtigall<sup>1</sup>, L. Grajciar<sup>1</sup>, C. J. Heard<sup>1</sup>

<sup>1</sup>Department of Physical and Macromolecular Chemistry, Faculty of Science, Charles University, Praha 2, Czech Republic

**Abstract Text:** Treating zeolites under alkaline conditions is an effective way to tune zeolite pore sizes by partial hydrolysis<sup>[1-3]</sup>. Zeolite hydrolysis is essential for understanding zeolite synthesis, i.e. the inverse process to desilication. However, the mechanism of alkaline hydrolysis in zeolites is poorly understood at present. The role of micropore confinement and the (micro)solvation of ions in the ever-present water are both currently unknown. Using density functional theory with a periodic model, we have investigated the hydrolysis mechanisms of silicious chabazite (CHA) under basic (NaOH/H<sub>2</sub>O) conditions with various degrees of water loading. We consider several mechanisms, as shown in Fig.1 and confirm NaOH may play a role as both a catalyst and a reactant. We determine that collectivity in the mechanism, enhanced by the presence of water, enhances the initial hydrolysis of the pristine framework and lowers reaction barriers via a cooperative mechanism. Water and NaOH concentration play an important role for the kinetics and energetics of the hydrolysis process. The cooperative desilication mechanism is general and can be extended to other zeolites. We are now investigating a related problem (the role of microsolvation for acid hydrolysis).

Image 1:

Non-catalytic routes



Catalytic route

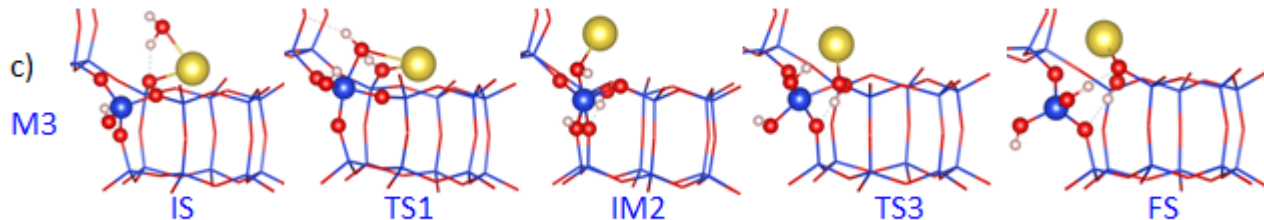


Fig.1: Structures of initial, transition and final states of the second hydrolysis step using a minimum water model, according to a) Mechanism M1 (sequential single water splitting), b) Mechanism M2 (sequential single NaOH splitting), c) Mechanism M3 (catalytic NaOH splitting/water splitting).

**References:** 1.Zhai D. et.al., Dissolution and Absorption: A Molecular Mechanism of Mesopore Formation in Alkaline Treatment of Zeolite, Chem. Mater. 2015, 27, 67-74

2. Barrer R. M. et.al., Molecular Sieve Sorbents from Clinoptilolite. *Can. J. Chem.* 1964, 42, 1481-1487.
3. Silaghi M.-C. et.al., Regioselectivity of Al-O Bond Hydrolysis during Zeolites Dealumination Unified by Brønsted-Evans-Polanyi Relationship. *ACS Catal.* 2015, 5, 11-15

**Role of silanol nest defects in siliceous zeolite hydrolytic (in)stability**

M. Liu<sup>1,\*</sup>, C. J. Heard<sup>1</sup>, L. Grajciar<sup>1</sup>, P. Nachtigall<sup>1</sup>

<sup>1</sup>Department of Physical and Macromolecular Chemistry, Faculty of Science, Charles University, Hlavova 8, 12843 , Prague 2, Czech Republic

**Abstract Text:** Zeolites as solid catalysts have widespread applications in many chemical reactions involving water, such as fluid catalytic cracking (FCC) and biomass conversion. Zeolite is fairly easy to hydrolysis under steaming or hot liquid water (HLW) conditions so that their crystalline framework can be partly or completely destroyed, thereby preventing their use in these processes. However, the zeolite instability in such conditions can be also used for improvement of zeolite properties, including the preparation of novel zeolite frameworks, modification of zeolite acidity for use as FCC catalysts, or the formation of a secondary mesoporous channel system to remove the diffusion limitations. It has been proposed that the most vital factor determining the stability of zeolites in HLW conditions is that silanol defects (Si-OH) are more hydrophilic than pristine Si-zeolites.<sup>[1]</sup> Furthermore, stability of zeolites in the aqueous solution was shown to be improved via selective removal of silica defects.<sup>[2]</sup> Hence, in order to understand the importance of silanol defects in framework lability and uncover its atomistic origins, we explored the partial hydrolysis process of CHA and MFI zeolites, under low water loading, using density functional theory.

The complete desilication is composed of four steps, moving from Q<sup>4</sup> to Q<sup>0</sup> framework silicon atom, breaking four Si-O bonds to finally remove the Si atom from the framework. We considered desilication in both pristine and defected frameworks, where defected framework contained a single silanol nest in the unit cell. We found that for pristine zeolites, the Q<sup>4</sup>->Q<sup>3</sup> step, proceeding via an equatorial mechanism<sup>[3]</sup>, has the highest apparent activation barriers (above 150 kJ/mol) representing thus the rate-limiting step of the whole desilication process (Figure 1). The significant height of the apparent activation barriers confirm the experimental findings that hydrolysis process of pristine zeolites is extremely difficult under low water conditions. However, hydrolysis of siliceous zeolites containing silanol nests appears to be easier, confirming the silanol nest defect induce instability of the zeolite framework (Fig. 1). This silanol-induced instability is partly due to the reduced hydrolysis barriers with respect to the pristine zeolite, and partly due to avoidance of the extremely challenging Q<sup>4</sup>->Q<sup>3</sup> step, since Q<sup>3</sup> silicon atoms are already present at the silicon vacancy site (Fig. 1). Reduced hydrolysis barriers for Q<sup>3</sup>->Q<sup>2</sup> step for silanol nest case appear to originate from stabilization of transition state by the existing hydrogen bond network (Fig. 2). Since we observe similar results for both CHA and MFI zeolites, these results appear to be generalizable to other siliceous zeolites as well.

Image 1:

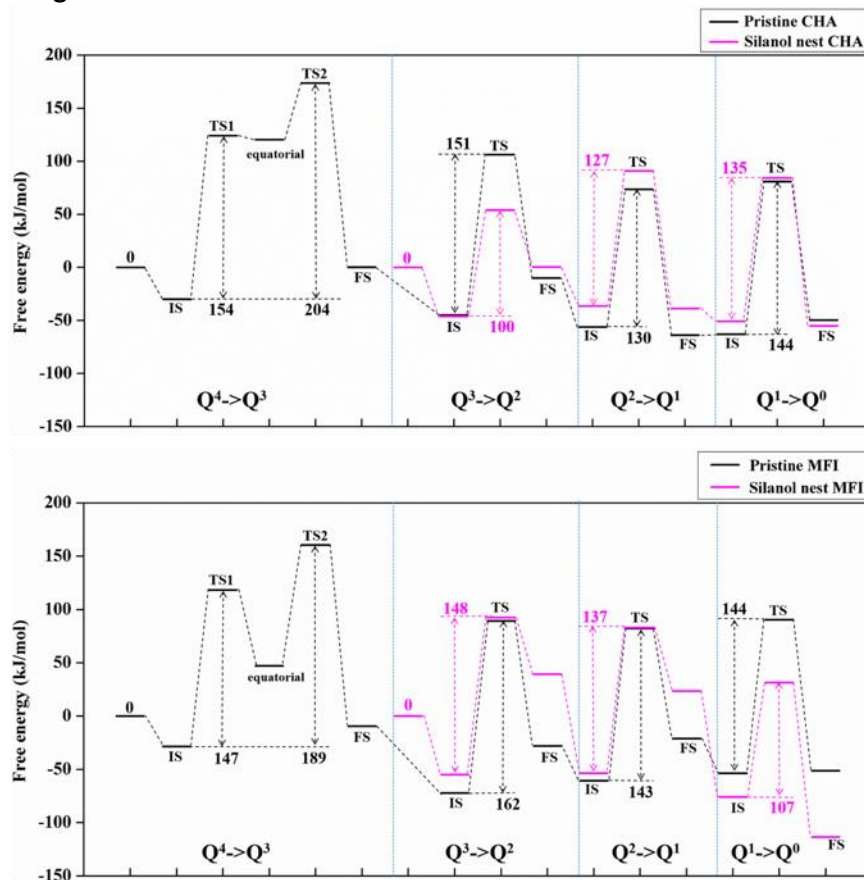


Fig 1. The minimum energy pathways of pristine Si zeolites and silanol nest zeolites.

Image 2:

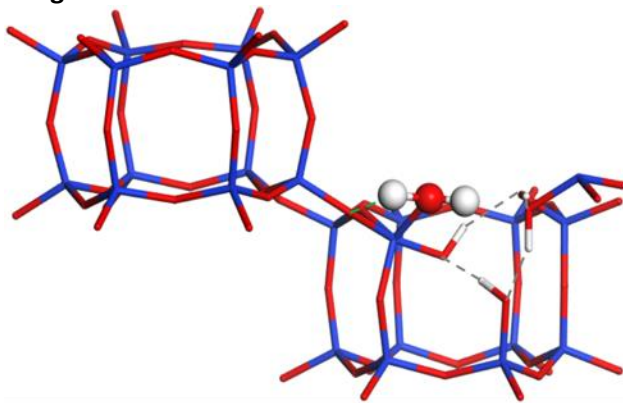


Fig 2. Transition state (TS) of hydrolysis process for silanol nest CHA.

- References:** [1]. Lu Zhang, et al., J. Am. Chem. Soc., 2015, 137, 11810–11819.  
[2]. Sebastian, et al., J. Am. Chem. Soc., 2016, 138, 4408–4415.  
[3]. Heard, C. J., Grajciar, L., et al., Advanced Materials, 2020, 32(44), 2003264.

**Effect of silanol nest and Brønsted site presence on the diffusion of water in FAU type zeolites**

A. J. Porter<sup>1,\*</sup>, A. J. O'Malley<sup>1</sup>

<sup>1</sup>Department of Chemistry, University of Bath, Bath, United Kingdom

**Abstract Text:** Zeolites are used in a wide range of applications, most of which depend on controlled molecular diffusion through the zeolite pores. Water, as a zeolite adsorbate, is of interest due to two zeolite uses: one as a molecular filter within the water purification field, and the other within catalysis where water is often a byproduct. These catalytic zeolites are often used as acid catalysts and contain Brønsted sites as their source of acidity. On top of this, silanol nest defects are relevant as they are the proposed result of the dealumination process which is routinely undertaken to increase the Si/Al ratio, and acidity, of many commercial zeolites. Understanding the diffusive properties of water confined within the zeolite pores, as a function of composition and defect presence, is pivotal to further optimise these materials for their purposes.

The diffusion of water confined within the pores of an FAU type zeolite was investigated using molecular dynamics simulation. A range of Si/Al ratios (5, 10, 15, 30, 60, 191 and purely siliceous), indicating different numbers of Brønsted sites, were used – alongside cells with and without silanol nests (1 per unit cell). The simulations were also repeated at multiple water loadings (5, 10, 20 and 40 wt%). A small difference between the two highest loadings, 20 and 40 wt% was observed. The water diffusion was quantified by calculation of the diffusion coefficient, showing a negative correlation between the number of Brønsted sites and the diffusion coefficient at all loadings – figure 1. The introduction of silanol nests increased the diffusion coefficient of water at both 5 wt% and 10 wt% water loading – also shown in figure 1.

**Image 1:**

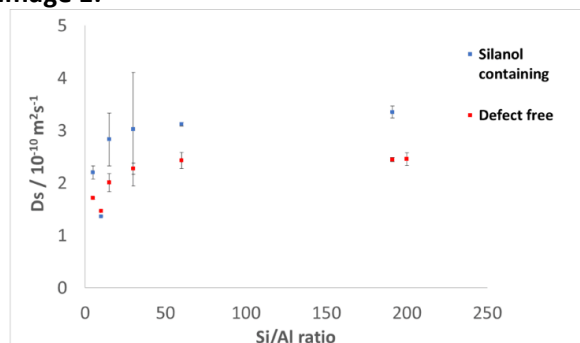


**Figure 1.** Comparison of the diffusion coefficient of water at 10 wt% loading within silanol containing and defect free cells with different Si/Al ratios – purely siliceous is indicated as a ratio of 200.

### Computational Modelling of Zeolite Surfaces to Predict Crystal Morphology

D. Turski<sup>1,\*</sup>, A. Sartbaeva<sup>1</sup>, S. Parker<sup>1</sup>

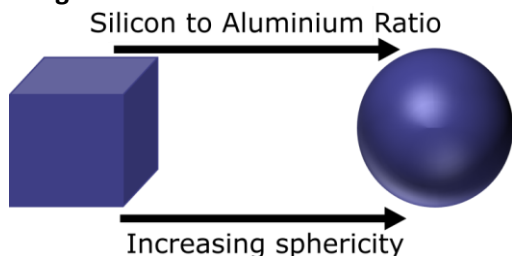
<sup>1</sup>Chemistry Department, University of Bath, Bath, United Kingdom

#### Abstract Text:

Zeolite synthesis is a notoriously challenging field of research with different recipes giving different crystal morphologies for identical framework types. Being able to predict or control the shape of the synthesized zeolite product would be beneficial from both a research and industrial standpoint.<sup>[1-2]</sup> Theoretical methods are now being utilized alongside the experimental in efforts to provide new insight into this area. One computational approach that has recently been explored is to simulate zeolite crystal surfaces and subsequently calculate surface energies.<sup>[3]</sup>

Our research focuses on simulating LTA crystal surfaces to carry out energy minimization calculations. Previous experimental results have lead us to believe that the Si to Al ratio affects the crystal morphology. The Si to Al ratio is varied between purely siliceous and 50:50 to observe whether there is any correlation between higher percentages of aluminium and increased curvature of the crystals. We use computational methods based on molecular mechanics to calculate the surface energies which are then plotted to generate Wulff constructions. These minimize the total surface energy of a crystal at equilibrium to predict the thermodynamically favoured morphology, in this case for the zeolite to adopt.

#### Image 1:



#### References:

1. O. Larlus and V. P. Valtchev, *Chemistry of Materials*, 2004, 16, 3381-3389.
2. Y. Guo, T. Sun, X. Liu, Q. Ke, X. Wei, Y. Gu and S. Wang, *Chemical Engineering Journal*, 2019, 358, 331-339.
3. Y. Chen, X. Zhang, C. Zhao, Y. Yun, P. Ren, W. Guo, J. P. Lewis, Y. Yang, Y. Li and X.-D. Wen, *The Journal of Physical Chemistry C*, 2018, 122, 24843-24850.

**T-atom defects formation in zeolite with MSE topology**

P. Petkov<sup>1,\*</sup>, I. Koleva<sup>1</sup>, S. Kolev<sup>2</sup>

<sup>1</sup>Faculty of Chemistry and Pharmacy, University of Sofia, University of Sofia, <sup>2</sup> Institute of Electronics, Bulgarian academy of sciences, Sofia, Bulgaria

**Abstract Text:** Following our previous experience in modeling T-atom defects formation in ITQ-44 zeolite framework [1] we have performed a computational study on the T-atom defect formation in the zeolite with MSE topology. It has been reported that such zeolites with Ti in the framework perform very well in the process of selective phenol oxidation [2]. The role of the Si-vacancy and Ti distribution in the framework was not clarified yet. For this reason, we have performed computational study on this material. The relative energy for the formation of Si-vacancy and substitution of Si for Ti and Al has been studied by means of density functional theory. For all non-equivalent T sites, we have calculated the relative energy for Si vacancy formation. We have found that the easiest Si vacancy can be formed in T8 followed by T3 position, while the formation of Si vacancy in T1, T2, T4, and T5 is thermodynamically unfavorable. The substitution of Si for Ti or Al was also studied. It has been found that Si will be substituted by Ti in T8, T3, and T7 positions in the MSE framework.

**Acknowledgments:** This work was supported by the program concert-JAPAN, grant number: КП-06-Д002/2 NSF - Bulgaria, (НИС-2850)

**References:** 1. P. Petkov, H. Aleksandrov, V. Valtchev, G. Vayssilov, "Framework Stability of Heteroatom-Substituted Forms of Extra-Large-Pore Ge-Silicate Molecular Sieves: The Case of ITQ-44." *Chem. Mater.*, 2012, 24 (13), pp 2509–2518  
2. M. Sasaki, Y. Sato, Y. Tsuboi, S. Inagaki, Y. Kubota, "Ti-YNU-2: a microporous titanosilicate with enhanced catalytic performance for phenol oxidation", *ACS Catal.* 2014, 4 (8), 2653–2657

## ***Stimuli Responsive Behaviour and Emerging Properties***

FEZA21-PO-313

### **High pressure intrusion of aqueous chloride salt solutions in silicalite-1 for mechanical energy storage: influence of cation nature**

A. Ryzhikov<sup>1,2,\*</sup>, A. Astafan<sup>1,2</sup>, J. T. Daou<sup>1,2</sup>, H. Nouali<sup>1,2</sup>, G. Chaplais<sup>1,2</sup>, C. Marichal-Westrich<sup>1,2</sup>

<sup>1</sup>axe Matériaux à Porosité Contrôlée (MPC), Institut de Science des Matériaux de Mulhouse (IS2M), <sup>2</sup>Université de Haute-Alsace - Université de Strasbourg, Mulhouse, France

**Abstract Text:** Heterogeneous lyophobic systems, which combine a lyophobic porous matrix and a non-wetting liquid, are one of the promising technologies to absorb and store the mechanical energy. Since pioneering works of our group, the systems based on hydrophobic pure silica zeolites (zeosils) and water have been studying for these applications [1]. Depending on the zeolite structure, framework stability and presence of defects, the “zeosil-water” system, when the pressure is released (extrusion), is able to restore, dissipate or absorb the supplied mechanical energy during the compression step (intrusion) and therefore to display a spring, shock-absorber or bumper behaviour. Later, it was found that the use of aqueous salt solutions could considerably improve the energetic performances of such systems by a strong increase of intrusion pressure [2] and even change the behavior of the system in the case of highly concentrated solutions [3]. Recently, it was discovered that the nature of anion had a drastic influence on the behavior of the systems [4]. In this work, the results concerning the influence of cation nature on high pressure intrusion-extrusion of aqueous chloride solutions in MFI-type zeosil (silicalite-1) are reported.

The intrusion-extrusion tests have been performed with the solutions of various chloride salts (LiCl, NaCl, KCl, RbCl, CsCl, CaCl<sub>2</sub>, MgCl<sub>2</sub>, ZnCl<sub>2</sub>, CuCl<sub>2</sub>, NiCl<sub>2</sub>...). The aqueous solutions have been prepared at saturation concentration and also by setting the molar H<sub>2</sub>O/cation ratio at 12 and 18 in order to better compare cations impact.

The cation nature does not have a significant influence on the behavior. All the systems demonstrate a fully reversible spring behavior except the ones with concentrated ZnCl<sub>2</sub> (H<sub>2</sub>O/cation = 3.5, 6.0) and saturated CsCl (5.0) solutions, where the intrusion is slightly irreversible in the first cycle. Moreover, the intrusion of all the solutions leads to a strong increase of intrusion pressure in comparison with the one of water. The highest intrusion pressure values are observed for the solutions with lowest H<sub>2</sub>O/cation ratios (highest concentrations). For the saturated ZnCl<sub>2</sub> solution, it exceeds 400 MPa (measurement limit) and the pressure values near 300 MPa are noticed for LiCl (2.8) and ZnCl<sub>2</sub> (3.5) ones. At fixed H<sub>2</sub>O/cation ratio of 12 and 18, the pressure varies considerably depending the cation nature with highest values obtained for MgCl<sub>2</sub> and CaCl<sub>2</sub> solutions. This study emphasizes also that the pressure increases as the ion size decreases for alkaline and alkali earth metal salts. In addition, the increase of cation charge leads to the intrusion pressure rise as well.

**References:** [1] V. Eroshenko, R. C. Regis, M. Soulard, J. Patarin, *J. Am. Chem. Soc.*, 2001, 123, 8129.

[2] L. Tzanis, H. Nouali, T. J. Daou, M. Soulard, J. Patarin, *Mater. Lett.*, 2014, 115, 229.

[3] A. Ryzhikov, I. Khay, H. Nouali, T. J. Daou, J. Patarin, *Phys. Chem. Chem. Phys.*, 2014, 16, 17893.

[4] A. Ryzhikov, H. Nouali, T. J. Daou, J. Patarin, *Phys. Chem. Chem. Phys.*, 2018, 20, 6462.

**Pressure and Hydration Effects in the Yugawaralite-Laumontite-Wairakite system**

O. Wardle<sup>1,\*</sup>, D. W. Lewis<sup>1</sup>

<sup>1</sup>Department of Chemistry, University College London, London, United Kingdom

**Abstract Text:** We will describe a series of computational studies of Yugawaralite and Wairakite and make correlations to previous studies on Laumontite.

We compare results interatomic potential (using GULP) methods with DFT approaches in being able to accurately describe structural changes during dehydration of these systems, (Image 1) comparing to the work of Atrioli *et al.*<sup>1</sup> We will show how the low-cost interatomic potential methods provide us with a means to focus the more expensive QM approach, particularly in studying the pathway to dehydration. The limitations of the potential methods will be discussed with respect to their ability to allow large deformations of pores which occur at low water content (Image 2) An investigation of the response of both minerals to pressure will also be presented. We will propose full atomistic models for the high-pressure structures of Wairakite, experimentally measured, but not solved, by Ori *et al.*<sup>2</sup> We will also probe the possibility of overhydration in Wairakite, as postulated by Chipera and Apps.<sup>3</sup> We will compare the likelihood of the formation of such a pressure-induced overhydrated structure with those already observed and modelled in other natural zeolites such as Laumontite and NAT structured materials.

We will conclude with a discussion of the relative phase stabilities of Yugawaralite, Wairakite and Laumontite.

**Image 1:**

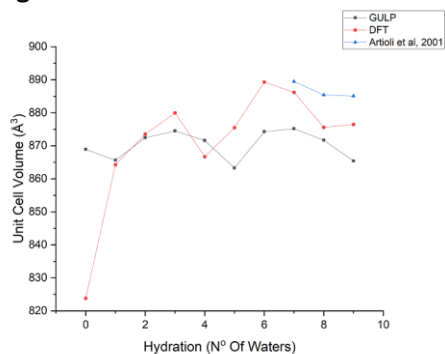
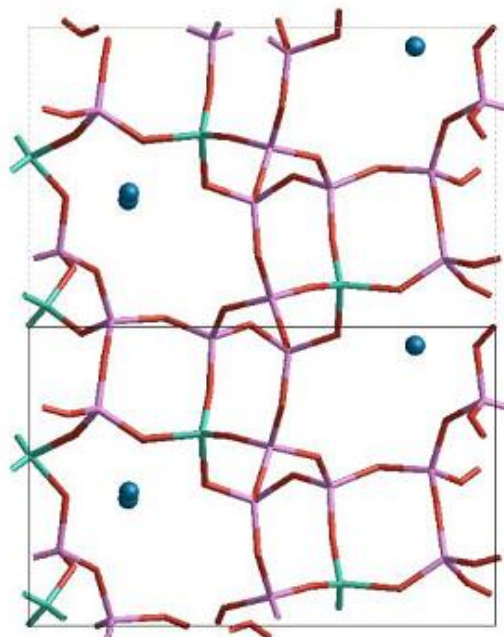
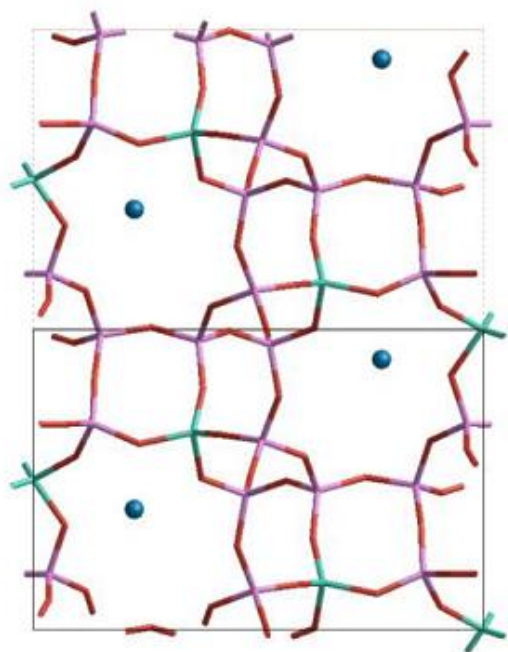


**Image 2:**

Fully dehydrated Yugawaralite (left) using interatomic potentials and (right) DFT



**References:**

1. Artioli, G., Ståhl, K., Cruciani, G., Gualtieri, A., and Hanson, J.C., *Amer. Miner.*, 86 (2001), 185–192
2. Ori, S., Quartieri, S., Vezzalini, G., Dmitriev, V., *Amer. Miner.*, 93 (2008), 53-62
3. Chipera, S.J., Apps, J.A., in *Natural Zeolites: Occurrence, Properties, Applications*, *Rev. Mineral. Geochem.* (eds. Bish, D.L., Ming, D.W.), 45 (2001), 117-162

## **Advanced Characterisation and Operando Spectroscopies**

FEZA21-PO-315

### **Using $^{17}\text{O}$ solid-state NMR spectroscopy to investigate mixed-metal MIL-53**

E. A. L. Borthwick<sup>1,\*</sup>, Z. H. Davis<sup>1</sup>, D. M. Dawson<sup>1</sup>, S. E. Ashbrook<sup>1</sup>

<sup>1</sup>School of Chemistry, University of St Andrews, St Andrews, United Kingdom

**Abstract Text:** The metal-organic framework (MOF), MIL-53 can be synthesised using a range of trivalent metals, including  $\text{Al}^{3+}$ ,  $\text{Ga}^{3+}$  and  $\text{Sc}^{3+}$ , and the linker benzene-1,4-dicarboxylic acid (BDC).<sup>1</sup> MIL-53 exhibits considerable structural flexibility during absorption and desorption of guest molecules within its pores, leading to it being termed a “breathing MOF”.<sup>2</sup> Different breathing behaviour is exhibited depending on the metal present, leading to the possibility of mixing metals to try and control this effect.

Solid-state NMR spectroscopy has already been widely used for investigating MOFs. For example, in MIL-53 (Al) the position of the carboxylate peak in the  $^{13}\text{C}$  Cross Polarisation (CP) Magic Angle Spinning (MAS) NMR spectrum can be used to determine the pore-form present. This is due to the influence of the water molecules present in the pores and the hydrogen bonding that then occurs.<sup>3</sup> By studying the hydration states *via*  $^{13}\text{C}$  CP MAS NMR the pore forms present can be observed and this can allow us to investigate the breathing behaviour of the mixed-metal samples.

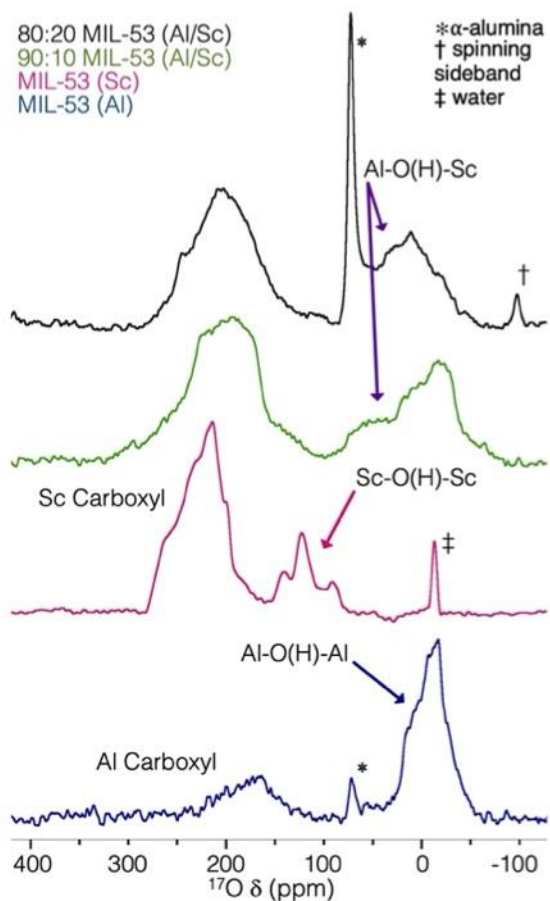
However,  $^{17}\text{O}$  NMR spectroscopy has been less commonly exploited. In principle, this provides a useful approach for studying mixed-metal materials with carboxyl and hydroxyl groups bound directly to metal centres. However, the low natural abundance of  $^{17}\text{O}$  (0.037%), requires isotopic enrichment in order to acquire NMR spectra in a reasonable timeframe.<sup>4</sup> The high cost of  $^{17}\text{O}$ -enriched reagents (1 mL of 90%  $\text{H}_2^{17}\text{O}$  (*l*) costs ~ £1900) requires the development of cost-effective and atom-efficient enrichment techniques.

In this work, a range of post-synthetic  $^{17}\text{O}$  enrichment techniques (e.g., hydrothermal, *ex situ* and *in situ* enrichment) have been explored for end-member and mixed-metal MIL-53 (Al/Sc) materials. This allows the metal cation disorder and subsequent effects on the breathing behaviour in the materials to be investigated. The various methods are compared to determine the level and selectivity of enrichment. Experimental results are compared to parameters from first-principles DFT calculations (using a suite of potential structural models) and to aid spectral assignment and interpretation.

During the hydrothermal enrichment process it was seen that both end-member and mixed-metal MIL-53 (Al/Sc) can be enriched, as shown in Figure 1.  $^{17}\text{O}$  MAS and MQMAS NMR spectra showed good levels of enrichment, approximately 7.5-10%, of all the possible oxygen sites; Al and Sc carboxylate environments, and three bridging hydroxyls sites. However, it is not possible to easily distinguish the different carboxyl sites in the MAS spectra for the sample. Further work at a higher field strength could enable this.

We show that post-synthetic hydrothermal enrichment can lead to framework breakdown giving impurities such as  $\alpha$ -alumina and the small pore MOF,  $\text{Sc}_2\text{BDC}_3$ , and so room temperature *in-situ* enrichment approaches have also been investigated. These have shown good levels of enrichment in the hydroxyl site of the MIL-53 (Sc) framework but no enrichment of the MIL-53 (Al) framework. This suggests the scandium form of MIL-53 is more labile than the aluminium form.

**Image 1:**



- References:** 1) J. P. S. Mowat, V. R. Seymour, J. M. Griffin, S. P. Thompson, A. M. Z. Slawin, D. Fairen-Jimenez, T. Düren, S. E. Ashbrook and P. A. Wright, *Dalt. Trans.*, 2012, 41, 3937–3941.  
 2) C. Serre, F. Millange, C. Thouvenot, M. Noguès, G. Marsolier, D. Louër and G. Férey, *J. Am. Chem. Soc.*, 2002, 124, 13519–13526.  
 3) T. Loiseau, C. Serre, C. Huguenard, G. Fink, F. Taulelle, M. Henry, T. Bataille and G. Férey, *Chem. – A Eur. J.*, 2004, 10, 1373–1382.  
 4) P. J. Hore, *Nuclear Magnetic Resonance*, Oxford University Press, Oxford, 2nd edn., 2015.

**Solid-State NMR Spectroscopy of Breathing Metal-Organic Frameworks**

Z. H. Davis<sup>1,\*</sup>, C. M. Rice<sup>1</sup>, G. P. M. Bignami<sup>1</sup>, D. M. Dawson<sup>1</sup>, R. E. Morris<sup>1</sup>, S. E. Ashbrook<sup>1</sup>

<sup>1</sup>School of Chemistry, University of St Andrews, St Andrews, United Kingdom

**Abstract Text:** Metal-organic frameworks (MOFs) are a class of compounds that belong to the family of microporous solids. MOFs are known for their wide range of applications (gas storage, catalysis, drug delivery *etc.*), arising from their characteristic molecular-scale pores and channels.<sup>1-3</sup> Owing to the importance of these diverse applications, there is an increasing need to understand in greater detail the structures of MOFs which, in general, consist of nodes, *i.e.*, a single or a cluster of metal cations, connected by spacers, which are typically polydentate organic ligands, forming a 3D structure.<sup>4</sup> In particular, the use of carboxylate ligands as spacers results, due to the presence of a strong M-OC bond,<sup>4</sup> in MOFs with high thermal stability, such as MIL-53. MIL-53 is known as a “breathing MOF”<sup>5</sup> because of the significant variation in pore size it displays upon interaction with guest molecules or with a variation in experimental conditions, such as temperature and pressure.

The bridging nature of the oxygen atoms present in MOFs makes <sup>17</sup>O NMR spectroscopy a potentially useful technique for investigating small changes in their structures, such as metal cation substitution and pore size. However, <sup>17</sup>O NMR is not routine, owing to its quadrupolar nature ( $I = 5/2$ ), extremely low natural abundance (0.037%) and only moderate gyromagnetic ratio. For these reasons, to allow a complete and high-resolution spectroscopic investigation of MOFs, pathways for cost-effective <sup>17</sup>O enrichment have been optimised using either a direct synthetic approach using dry gel conversion (DGC) or a post-synthetic exchange (PSE). DGC uses microlitre quantities of solvent, providing a low-cost synthetic route to enriched materials. Where the direct synthesis of a MOF is not possible *via* DGC, PSE has been employed *via* a steaming procedure.<sup>6</sup>

In this work, the effects of metal cation composition on the breathing behaviour of a mixed-metal Al, Ga-MIL-53 have been explored by analysing the structural variations in the calcined, hydrated and dehydrated forms. Additionally, investigations have been undertaken to understand any potential effects the synthesis route has on site-specific <sup>17</sup>O enrichment and the metal cation distribution in these important materials.

**References:** 1. J. Della Rocca et al., *Acc. Chem. Res.*, 2011, 44, 957.

2. L. Hamon et al., *J. Am. Chem. Soc.*, 2009, 131, 17490.

3. G. Zi et al., *Carbohydr. Polym.*, 2015, 115, 146.

4. P. Wright, *Microporous Framework Solids*, RSC Publishing, Cambridge, 2008.

5. C. Serre et al., *J. Am. Chem. Soc.*, 2002, 124, 13519.

6. G. Bignami et al., *Chem. Sci.*, 2018, 9, 850.

**Adsorption of H<sub>2</sub>O and D<sub>2</sub>O on porous aluminium terephthalate metal organic frameworks**

M. Mihaylov, K. Chakarova, E. Ivanova, N. Drenchev, K. Hadjiivanov\*

**Abstract Text:** Water is always present in “as-prepared” metal-organic frameworks (MOFs) and therefore affects the properties of the non-activated materials. Detailed knowledge of water adsorption on different MOFs is also important for their application in humidity control and adsorption heat pumps as well as for gas separation and purification. Concerning the stability of MOFs, the weakest point is the metal-ligand bond, where hydrolysis by H<sub>2</sub>O can cause a structure collapse.

Being a strong Lewis base, water is preferably adsorbed on acid sites, open metal sites or hydroxyl groups, where it is coordinated *via* its oxygen atom. However, additional stabilization could occur as a result of bonding of one or two H-atoms with basic sites.

One of the most suitable techniques for studying gas-solid interaction is IR spectroscopy. Preliminary IR experiments on H<sub>2</sub>O adsorption on nanoporous aluminium terephthalates, MIL-53(Al) and NH<sub>2</sub>-MIL-53(Al), indicated adsorbed water is located on the structural OH groups. The adsorption is weak and the principal part of H<sub>2</sub>O is removed by evacuation at room temperature. The spectra of the water containing samples are complicated because of the superimposition of the different bands arising from H-bonded hydroxyl groups, including those of water. To overcome the complications in the interpretation of results, we performed a comparative H<sub>2</sub>O and D<sub>2</sub>O adsorption study.

Dehydrated MIL-53(Al) sample contains isolated structural  $\mu_2$ -OH groups monitored by an IR band at 3708 cm<sup>-1</sup>. Successive adsorption of small doses of H<sub>2</sub>O causes decrease of the intensity of this band and a parallel development of bands at 3622, 3547 and 3468 cm<sup>-1</sup>.

Separate experiments indicated that H/D exchange of the structural hydroxyls with D<sub>2</sub>O does not occur at ambient temperature. Adsorption of D<sub>2</sub>O on MIL-53(Al) leads to appearance of an intense and broad band at 3467 cm<sup>-1</sup> (observed also after H<sub>2</sub>O adsorption) and a weak band at 3584 cm<sup>-1</sup> assigned to OH modes of adsorbed HOD molecules present in our adsorbate (Fig. 1). The results unambiguously demonstrate that the band at 3468 cm<sup>-1</sup> is due to the perturbed OH vibrations of the structural hydroxyls, while the bands at 3622 and 3547 cm<sup>-1</sup> characterize the  $\nu_3$  and  $\nu_1$  O-H modes, respectively, of adsorbed H<sub>2</sub>O molecules.

Similar results were obtained with NH<sub>2</sub>-MIL-53(Al). In this case, however, the hydroxyls H-bonded to amino groups (3683 cm<sup>-1</sup>) interacted more weakly with adsorbed water because of the pre-existing H-bond.

Acknowledgements: This work was supported by the Bulgarian National Research Program EPLUS (approved by DCM # 577/17.08.2018).

Image 1:

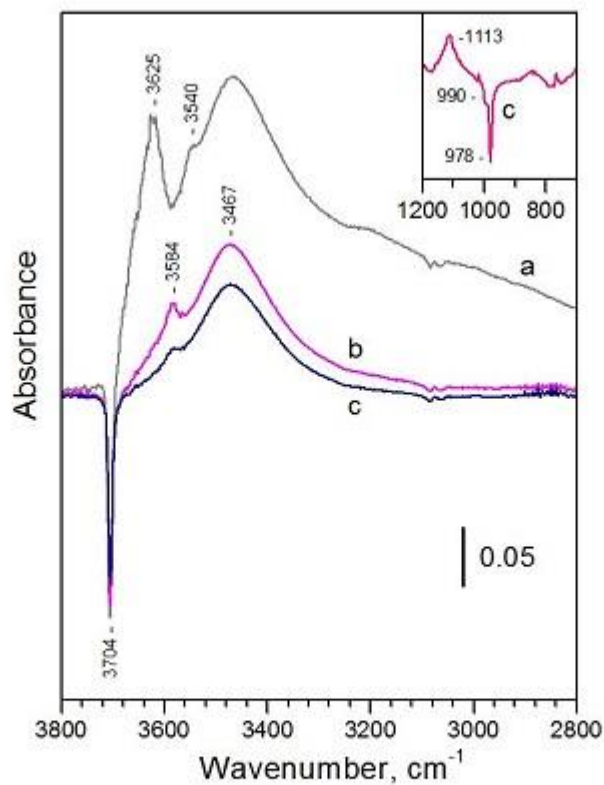


**Figure 1.** Comparison between the IR spectra registered after contacting MIL-53(Al) sample with  $\text{H}_2\text{O}$  (a) or  $\text{D}_2\text{O}$  (b, c) at 4 mBar equilibrium pressure. Spectrum c corresponds to a more deuterated sample as compared to the sample giving spectrum b.

**Abstract Text: Molecular Simulations of Biocompatible Metal Organic Framework Membranes for Uremic Toxin Separation**

**Abstract**

Metal organic frameworks (MOFs) have recently gained importance for gas and liquid separation processes due to their large surface areas, tunable pore sizes and high chemical stabilities. The accumulation of urea and creatinine which are small and water-soluble uremic toxins in the blood causes renal failure in patients. Efficient removal of these uremic toxins from the body is important to decrease the risk of mortality. In this study, membrane-based uremic toxin separation performances of 60 bio-compatible metal organic frameworks (bio-MOFs) have been investigated using atomically-detailed simulations. Maximum adsorption capacity was determined using Monte Carlo (MC) simulations. The transport of uremic toxins within the pores of bio-MOFs was then examined using equilibrium molecular dynamics (EMD) simulations at infinite dilution and 1 bar, 310 K. Our results show that self-diffusivities of creatinine, urea, and water computed at 1 bar are much lower than those of computed at infinite dilution which was attributed to strong adsorbate-adsorbate interactions occurred at 1 bar. The top-performing 15 MOFs among 60 bio-MOFs having high selectivity towards urea ( $>40$ ) and creatinine ( $>10^3$ ) in the presence of water were identified and performed molecular simulations for binary and ternary mixtures of urea, water, and creatinine at 1 bar, 310 K. We found that diffusion selectivity ( $S_{diff}$ ) for urea-water binary mixture is higher than single component at 1 bar whereas membrane selectivity ( $S_{mem}$ ) and adsorption selectivity ( $S_{ads}$ ) at single component are higher than binary mixture. Bio-MOF-11 exhibited high membrane selectivity for urea-water and creatinine-water separation. We also performed flexible molecular dynamics simulations to examine the effect of MOF's flexibility on the predicted membrane performance. Our results will be highly useful to develop novel MOF membranes for uremic toxin separations.

**Computational Investigations of Metal Organic Frameworks for Adsorption-based Uremic Toxin Separation**

T. Yıldız<sup>1,\*</sup>, I. Erucar<sup>2</sup>

<sup>1</sup>Mechanical Engineering, <sup>2</sup>Natural and Mathematical Sciences, Ozyegin University, İstanbul, Turkey

**Abstract Text: Computational Investigations of Metal Organic Frameworks for Adsorption-based Uremic Toxin Separation**

**Abstract**

Polymeric membranes are used for the separation of uremic toxins in current treatments of hemodialysis. However, they show poor performance (<40 mg/g) for removing uremic toxins. As an alternative to membranes, adsorption-based separation methods can be used to remove uremic toxins from the blood. Recently, metal organic frameworks (MOFs) have been tested for the separation of uremic toxins and a high amount of uremic toxins from solutions could be adsorbed within the pores of MOFs. In this study, we aimed to identify adsorption-based uremic toxin separation performances of 1525 bio-compatible MOFs (bio-MOFs) with the help of atomically detailed simulations. We then computed the saturated urea, creatinine, and water adsorption in these MOFs by performing grand canonical Monte Carlo simulations (GCMC) at 310 K and 1 bar. Adsorption selectivities for urea/water, creatinine/water and creatinine/urea separations were calculated at infinite dilution and 1 bar, 310 K. We also performed binary and ternary mixture GCMC simulations to examine the co-adsorption of uremic toxins within the pores of MOFs in detail. Results showed that 6 bio-MOFs outperform traditional adsorbents such as zeolites, activated carbons and polymers in terms of creatinine uptake. Our results will be highly useful for the development of high-performance MOF adsorbents for uremic toxin separation.

## Catalytic Properties/MOFs/Organic materials

FEZA21-PO-323

### Linker Functionalisation in UiO-66 and its Effect on Geometry and Surface-Chemistry Control of Pd Nanoclusters

J. King<sup>1,\*</sup>, P. Á. Szilágyi<sup>1</sup>, M. Addicoat<sup>2</sup>, M. Hirsher<sup>3</sup>, L. Zhang<sup>3</sup>, S. Doszczeczko<sup>1</sup>, H. Luo<sup>4</sup>, O. Sambalova<sup>5</sup>, F. Rohman<sup>6</sup>, A. Borgschulte<sup>7</sup>, O. Phillips<sup>8</sup>

<sup>1</sup>School of Engineering and Material Science, Queen Mary University of London, London, <sup>2</sup>School of Science and Technology, Nottingham Trent University, Nottingham, United Kingdom, <sup>3</sup>Modern Magnetic Systems, Max Planck Institute for Intelligent Systems, Stuttgart, Germany, <sup>4</sup>Chemical Engineering, Imperial College London, London, United Kingdom, <sup>5</sup>Advanced Analytical Technologies, Empa Materials Science and Technology, Dübendorf, Switzerland, <sup>6</sup>Center Facility for Electron Microscopy, RWTH Aachen University, Aachen, Germany, <sup>7</sup>Advanced Analytical Technologies, Empa Materials Science and Technology, Dübendorf, Switzerland, <sup>8</sup>Faculty of Engineering and Science, University of Greenwich, London, United Kingdom

**Abstract Text:** Metal-organic frameworks (MOFs) boast highly regular textural properties, with an abundance of relevant inorganic and organic building blocks that give way to numerous well-defined pore geometries<sup>1</sup>. These pores offer suitable environments for the confinement of metal nanoclusters (NCs), producing materials capable of acting as catalysts for a wide variety of reactions<sup>2</sup>. The anchoring of the NCs in the pores increases the cyclability of the catalyst with the added benefit of increased activity due to strong host-guest interactions between the NCs in the pores and the framework<sup>3</sup>.

In this presentation, our recent work on the embedding of Pd NCs into a series of functionalised UiO-66 MOFs, such as -Br, -Cl, -NH<sub>2</sub>, -OH, etc., will be discussed. Previously, some of us have been able to put forward a way to predict the success of embedding Pd nanoclusters in the pores of MOFs using a model based on the adsorption enthalpy of Pd single atoms and dimers<sup>4</sup>. The work described here expands on this, by evaluating a new set of Pd-laden UiO-66 analogues to enhance the computational model for the success of embedding. We also set out to further probe strong host-guest interactions between the NCs and the frameworks and attempted to look at how this can affect the catalytic activity of the nanoclusters.

The new set of frameworks tested were chosen on the basis of different computed descriptors, such as the overall adsorption enthalpy and the enthalpy of Pd dimerisation, suggesting various degrees of embedment to occur. We then used a range of microscopy and spectroscopy techniques to experimentally verify the veracity of the predictions, which were found to be in good agreement. Finally, we compared the composite catalysts' activity for hydrogen activation reaction in a case where identical particle sizes were obtained through successful embedment but different degrees of Pd surface oxidation were observed.

#### Image 1:

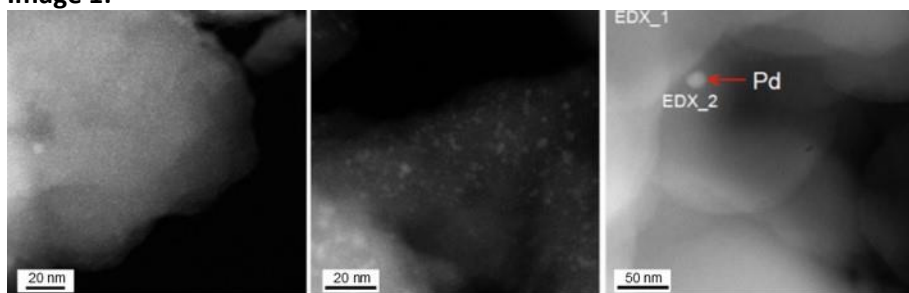


**Image 1** HAADF-STEM micrographs of Pd<sub>2</sub>-Br-UiO-66, Pd/(Cl)<sub>2</sub>-UiO-66, and Pd/(OH)<sub>2</sub>-UiO-66 (left to right).

**References:** 1 H.-C. Zhou, J. R. Long and O. M. Yaghi, *Chem. Rev.*, 2012, 112, 673–674.

2 Q. Yang, Q. Xu and H.-L. Jiang, *Chem. Soc. Rev.*, 2017, 46, 4774–4808.

3 Y. Tong, G. Xue, H. Wang, M. Liu, J. Wang, C. Hao, X. Zhang, D. Wang, X. Shi, W. Liu, G. Li and Z. Tang, *Nanoscale*, 2018, 10, 16425–16430.

4 D. E. Coupry, J. Butson, P. S. Petkov, M. Saunders, K. O'Donnell, H. Kim, C. Buckley, M. Addicoat, T. Heine and P. Á. Szilágyi, *Chem. Commun.*, 2016, 52, 5175–5178.

**Synthesis and photocatalytic oxidation reaction on ruthenium-complex incorporated in titanium-based metal-organic framework**

Y. Kondo<sup>1,\*</sup>, Y. Kuwahara<sup>1,2,3</sup>, K. Mori<sup>1,2</sup>, H. Yamashita<sup>1,2</sup>

<sup>1</sup>Graduate School of Engineering, Osaka University, Osaka, <sup>2</sup>Elements Strategy Initiative for Catalysts & Batteries, Kyoto University, Kyoto, <sup>3</sup>PRESTO, Japan Science and Technology Agency, Saitama, Japan

**Abstract Text:** Metal-organic frameworks (MOFs) are a kind of porous materials constructed of metal oxide clusters and organic linkers. Their porosity, high surface area, modularity have a great potential for catalyst materials. In addition, the well-defined cavities of MOFs provide an ideal platform for the encapsulation of metal complexes and nanoparticles. Ruthenium tris-2,2'-bipyridine complex ( $[\text{Ru}(\text{bpy})_3]^{2+}$ ) is a typical molecular photocatalyst but it is difficult to be recovered.[1] Amine-functionalized titanium based MOF (MIL-125-NH<sub>2</sub>) composed of Ti<sub>8</sub>O<sub>8</sub>(OH)<sub>4</sub> clusters and 2-aminothrephthalate linkers is known to be also a visible-light responsive photocatalyst, and its cavity is larger than the size of the  $[\text{Ru}(\text{bpy})_3]^{2+}$  complex.[2] However, the incorporation of  $[\text{Ru}(\text{bpy})_3]^{2+}$  complex into a photoactive MOF, such as MIL-125-NH<sub>2</sub>, has never been examined.

In this work, we synthesized MIL-125-NH<sub>2</sub> incorporating of the  $[\text{Ru}(\text{bpy})_3]^{2+}$  complex ( $\text{Ru}(\text{bpy})_3@$ MIL-125-NH<sub>2</sub>) by solvothermal method (Fig. 1).[3] The BET surface area of  $\text{Ru}(\text{bpy})_3@$ MIL-125-NH<sub>2</sub> (1020 m<sup>2</sup>/g) was smaller than that of the pristine MIL-125-NH<sub>2</sub> (1498 m<sup>2</sup>/g). The  $[\text{Ru}(\text{bpy})_3]^{2+}$  complexes were contained while maintaining the complex structure as evidenced by Ru K-edge FT-EXAFS spectra. The phosphorescence emission due to the <sup>3</sup>MLCT state of the  $[\text{Ru}(\text{bpy})_3]^{2+}$  complex of  $\text{Ru}(\text{bpy})_3@$ MIL-125-NH<sub>2</sub> under visible-light irradiation was blue-shifted from that of the  $[\text{Ru}(\text{bpy})_3]^{2+}$  complex impregnated onto fumed silica. This shift is considered to be the result of the so-called rigidchromism, which is due to the distorted conformation of the complex encapsulated inside a small cavity.[4] The  $[\text{Ru}(\text{bpy})_3]^{2+}$  complexes in  $\text{Ru}(\text{bpy})_3@$ MIL-125-NH<sub>2</sub> were not leached after stirring in the acetonitrile solution for 7 hours. These results indicate the  $[\text{Ru}(\text{bpy})_3]^{2+}$  complexes were successfully incorporated into the cavities of MIL-125-NH<sub>2</sub>.  $\text{Ru}(\text{bpy})_3@$ MIL-125-NH<sub>2</sub> was applied to the photocatalytic aerobic benzyl alcohol oxidation under visible-light ( $\lambda > 450$  nm) irradiation. Benzaldehyde was formed as an oxidation product under visible-light irradiation utilizing the pristine MIL-125-NH<sub>2</sub>. The catalytic activity was much enhanced utilizing  $\text{Ru}(\text{bpy})_3@$ MIL-125-NH<sub>2</sub>. On the other hand, the photocatalytic activity of the physical mixture of  $[\text{Ru}(\text{bpy})_3]^{2+}$  complex and MIL-125-NH<sub>2</sub> was slightly increased in the photocatalytic activity than the pristine MIL-125-NH<sub>2</sub>. These results show the incorporation of  $[\text{Ru}(\text{bpy})_3]^{2+}$  complexes into the cavities of MIL-125-NH<sub>2</sub> is indispensable to enhance the photocatalytic activity.

**Image 1:**

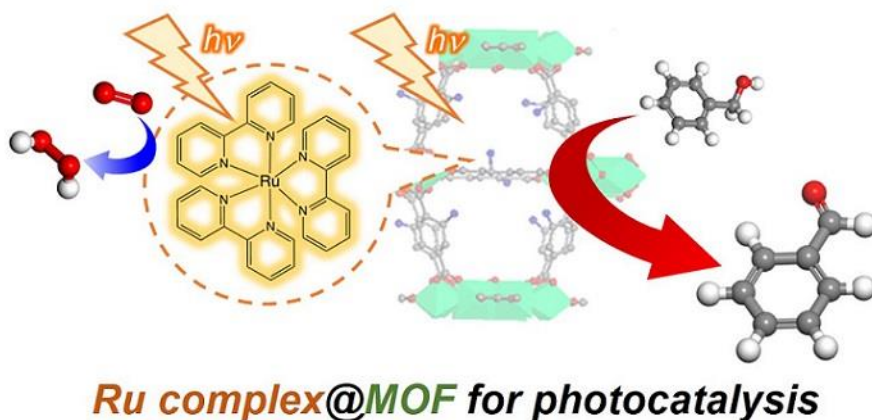


Fig. 1 Photocatalytic aerobic benzyl alcohol oxidation utilizing  $[\text{Ru}(\text{bpy})_3]^{2+}$  complex incorporated into MIL-125-NH<sub>2</sub>.

- References:** [1] Y. Isaka, S. Kato, D. Hong, T. Suenobu, Y. Yamada, S. Fukuzumi, *J. Mater. Chem. A* 3 (2014) 12404-12404.
- [2] Y. Isaka, Y. Kondo, Y. Kawase, Y. Kuwahara, K. Mori, H. Yamashita, *Chem. Commun.* 54 (2018) 9270-9273.
- [3] Y. Isaka, Y. Kondo, Y. Kuwahara, K. Mori, H. Yamashita, *Catal. Sci. Technol.* 9 (2019) 1511-1517.
- [4] K. Mori, M. Kawashima, K. Kagohara, H. Yamashita, *J. Phys. Chem. C* 112 (2008) 19449–19455.

**Metal Organic Frameworks for the catalytic degradation of Chemical Warfare Agents**

C. G. Elliott<sup>1,\*</sup>, R. E. Morris<sup>1,2</sup>

<sup>1</sup>Department of Chemistry, University of St Andrews, St Andrews, United Kingdom, <sup>2</sup>Department of Physical and Macromolecular Chemistry, Charles University, Prague, Czech Republic

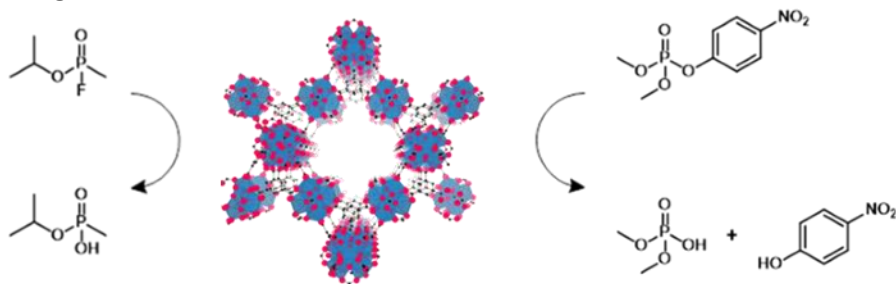
**Abstract Text:**

Since the Chemical Weapons Convention in 1997 there has been a necessity to develop methods that efficiently and safely destroy chemical warfare agent (CWA) stockpiles, as well as technologies that would be suitable to protect against these chemicals in the rare case of an attack. This has been further intensified due to use of CWAs by terror organisations; the 1995 sarin attack on the Tokyo subway left 12 dead and 5,000 injured.<sup>1</sup> Current protection devices use impregnated activated carbon due to its high porosity and ease of use, however they also exhibit low adsorption capacities, short lifetimes, and little adaptability.

Metal-organic frameworks (MOFs) have been identified as promising materials for sorption applications due to their incredibly high surface area and the ability to tailor chemical and physical properties.<sup>2</sup> Attention has therefore turned to these materials for the capture and catalytic destruction of CWAs. Among these, Zr-MOFs such as UiO-66, have emerged as excellent catalysts for the hydrolysis of nerve agents and simulants due to the Lewis-acidic nature of the Zr nodes.<sup>3</sup> However, there are limitations to these materials, such as small pore size which prevents the nerve agent from entering the internal structure, and blocking of the catalytic sites by linkers.

Our investigations focus on developing Zr-MOFs for the catalytic hydrolysis of CWAs through linker design and doping of the primary Zr framework with other Lewis acidic metals. A series of mixed metal MOFs have been synthesised. Here we present the characterisation of these materials using a variety of techniques; PXRD, SEM, EDS and DLS. The synthesised materials are subsequently tested for their suitability as catalysts in the hydrolysis of the nerve agent simulant dimethyl 4-nitrophenylphosphate (DMNP).

**Image 1:**



**References:**

1. P. Zurer, Chem. Eng. News Arch., 1998, 76, 7.
2. R. B. Getman, Y.-S. Bae, C. E. Wilmer and R. Q. Snurr, Chem. Rev., 2012, 112, 703–723.
3. M. Kalaj, J. M. Palomba, K. C. Bentz and S. M. Cohen, Chem. Commun., 2019, 55, 5367–5370.

**Modifying the Properties of Photoactive Metal-organic Frameworks (MOFs)**

K. J. Everden\*, R. Walton<sup>1</sup>, V. Degirmenci<sup>2</sup>

<sup>1</sup>Chemistry, <sup>2</sup>Engineering, University of Warwick, Coventry, United Kingdom

**Abstract Text:** Metal-organic frameworks (MOFs) are highly crystalline materials with large surface areas and porosities. MOFs have been used in the field of catalysis for many years, however their use in photocatalysis has gained progressively more interest due to the need to develop new photoactive materials for applications such as water splitting and carbon dioxide conversion, of relevance to environmental and energy concerns.<sup>1</sup> By partial substitution of metals and/or linkers in MOFs, it is possible to tune the band gaps of the materials, extending their activity to the visible region in addition to the UV region. Compared to the reference inorganic semiconductor, TiO<sub>2</sub>, it is possible to obtain smaller band gaps with Ti MOFs due to possible ligand functionalisation/metal exchange. Additionally, Ti MOFs can avoid the fast electron-hole recombination that can occur in TiO<sub>2</sub>.

MUV-10 is a highly stable and chemically robust MOF recently reported in the literature.<sup>2</sup> It is comprised of Ti and Ca or Mn, and utilises trimesate (BTC) as the organic linker (Figure 1). MUV-10(Ca) is shown to absorb UV light whilst MUV-10(Mn) is able to additionally absorb visible light. Through a combination of metal and linker substitution, we have further modified the band gap of this highly stable material, enabling it to harvest an even greater proportion of the visible spectrum.

Herein we report the synthesis of a variety of titanium containing MOFs and their suitability for photocatalysis. Partial substitution of titanium with tin and the utilisation of alternative linkers such as 2-aminoterephthalic acid and 5-aminoisophthalic acid in materials are assessed as ways of adjusting the band gap. These MOFs have been tested for CO<sub>2</sub> conversion, yielding products including formic acid and methanol, which are of value to a range of other chemical reactions.

**References:** [1] Y. Fu, D. Sun, Y. Chen, R. Huang, Z. Ding, X. Fu and Z. Li, *Angew. Chemie - Int. Ed.*, 2012, 51, 3364-3367  
[2] J. Castells-Gil, N. M. Padial, N. Almora-Barrios, J. Albero, A. R. Ruiz-Salvador, J. González-Platas, H. García and C. Martí-Gastaldo, *Angew. Chemie - Int. Ed.*, 2018, 57, 8453-8457

**Catalytic Properties/MOFs/Organic materials/Poster**

FEZA21-PO-329

**Water-Stable Metal-Organic Frameworks as Heterogeneous Catalysts for Conversion of Biomass-Derived Sugars**

T. Chamberlain<sup>1,\*</sup>, R. I. Walton<sup>2</sup>, V. Degirmenci<sup>1</sup>

<sup>1</sup>School of Engineering, <sup>2</sup>Department of Chemistry, University of Warwick, Coventry, United Kingdom

**Abstract Text:** Heterogeneous catalysts are desired for the conversion of biomass derived glucose, but the current benchmark catalysts require extended, multi-step syntheses using environmentally hazardous solvents. Metal-organic frameworks (MOFs) are well known for their high porosity tuneable structures, but they are largely considered to be unstable compared to other porous solids such as zeolites, especially under hydrothermal conditions.

Herein, we describe the water based synthesis of a variety of hydrothermally stable MOFs and investigate their stability towards oxidising aqueous conditions. Their potential use as heterogeneous redox catalysts in the oxidation of HMF into the useful monomer 2,5-furan dicarboxylic (FDCA) acid in water is then evaluated. We use a combination of <sup>1</sup>H NMR and HPLC to quantify conversion and yields of products as well as to analyse for the formation of side products.

MIL-100 (Fe) is a well-known water stable MOF, synthesised under relatively mild hydrothermal conditions. It contains trimers of Fe(III) connected by trimesate forming two distinct cage structures, a small cage (25 Å) and a large cage (29 Å). The high density of catalytic sites in MIL-100 (Fe) leads to excellent conversion of HMF and high yields of the desired products.

UiO-66 and Yb<sub>6</sub> are zirconium and ytterbium based MOFs respectively. Due to their hydrothermal and tuneable structures, efforts are made to dope their structures with redox active metals such as iron and vanadium. The MOFs are fully characterized by a combination of powder XRD, TGA and SEM, and their activity as redox active catalysts is evaluated.

**Direct methylation of benzene with Co catalysts**

M. Aigner<sup>1,\*</sup>, S. Van Daele<sup>2</sup>, R. Bermejo de Val<sup>3</sup>, J. A. Lercher<sup>4</sup>

<sup>1</sup>Chemistry, Technische Universität München, München, Germany, <sup>2</sup>Total Research and Technology Feluy (TRTF, Feluy, Belgium, <sup>3</sup>Chemistry, Technische Universität München, München, Germany, <sup>4</sup>Pacific Northwest National Laboratory, Institute for Integrated Catalysis, Richland, WA, United States

**Abstract Text:** Introduction Petrochemical-based plants produce associated gas that is mostly flared. This gas contains valuable methane, limited to oxidation reactions.[1] The goal is to integrate methane directly into crude oil to inhibit the formation of greenhouse gases, such as CH<sub>4</sub> and CO<sub>x</sub>. Therein, alkylation of methane on benzene is used as a model reaction to study the direct methylation of aromatics.

Materials and methods In this study, H-ZSM-5 (Si/Al=15), H-MCM-22 (Si/Al=11), H-MOR (Si/Al=10), and LaX (Si/Al=2) were exchanged with a 0.01 M cobalt acetate solution. ZrO<sub>2</sub> and Al<sub>2</sub>O<sub>3</sub> were impregnated with Co-Acetate solutions to get comparable Co contents as for the zeolites. AAS (Atomic adsorption spectroscopy) was used to determine the Co loadings of the different samples. Pyridine was adsorbed in the Infrared (IR) to quantify the coverage of Brønsted acid sites (BAS) by the Co cation.

Results and discussions Table 1 shows the different zeolite frameworks and amorphous supports loaded with Cobalt. Cobalt was chosen, since previous studies, reported by Nakamura et al.,[2] already show Cobalt to be the most active metal for the direct methylation of benzene. The importance of the specific shape-selective environment provided by the MFI topology is strongly suggested by the lack of activity for the other supports. This structure provides the highest activity for the non-oxidative formation of toluene. The latter is accompanied with the formation of C<sub>8</sub> to C<sub>14</sub> and even larger aromatic molecules. Next, the impact of the Co loading on H-ZSM-5 was tested. Figure 1 shows the BAS coverage of the different samples, and their corresponding toluene formation rate as a function of the Co/Al ratio. The coverage of BAS increases with increasing Co/Al until a plateau of ~60% is reached at 0.2. Nevertheless, the formation rate of toluene significantly enhances with higher Co/Al, even when the BAS coverage levels off. This indicates that a different Co species is formed after the specific BAS coverage of ~60%, which is in agreement with Matsubara et al.[3] We suggest that the single Co<sup>2+</sup> sites present at low metal loadings act as the active species, while inactive CoO clusters were built starting from a Co/Al ratio > 0.2. A possible reaction network for the secondary products is illustrated in Figure 2. The direct methylation of benzene leads to the formation of toluene. However, secondary reactions with methane result in the formation of xylenes, trimethylbenzene or higher alkylated products. In addition, further condensation of toluene and benzene into biphenyls, 9-H-fluorene and derivatives are suggested. The detection of such sterically hindered products suggests a key role of the external surface in their generation.

**Image 1:**

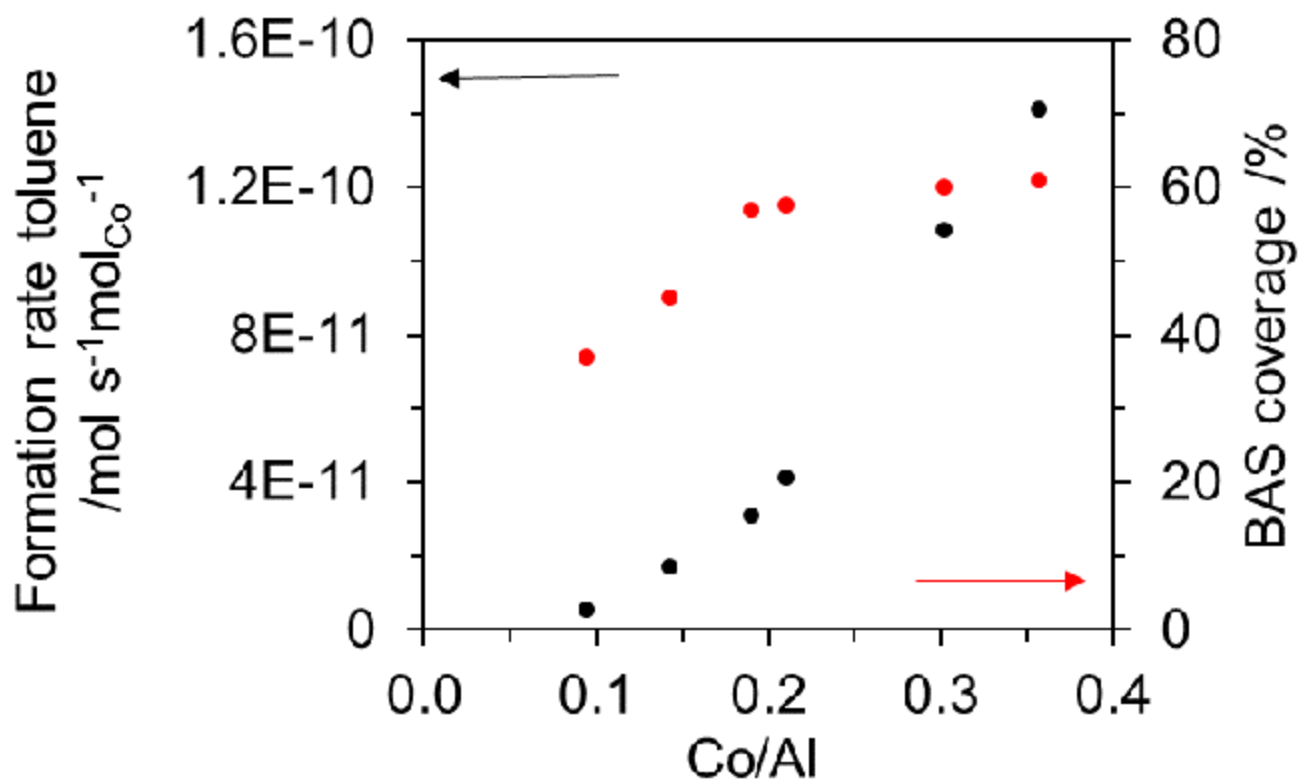
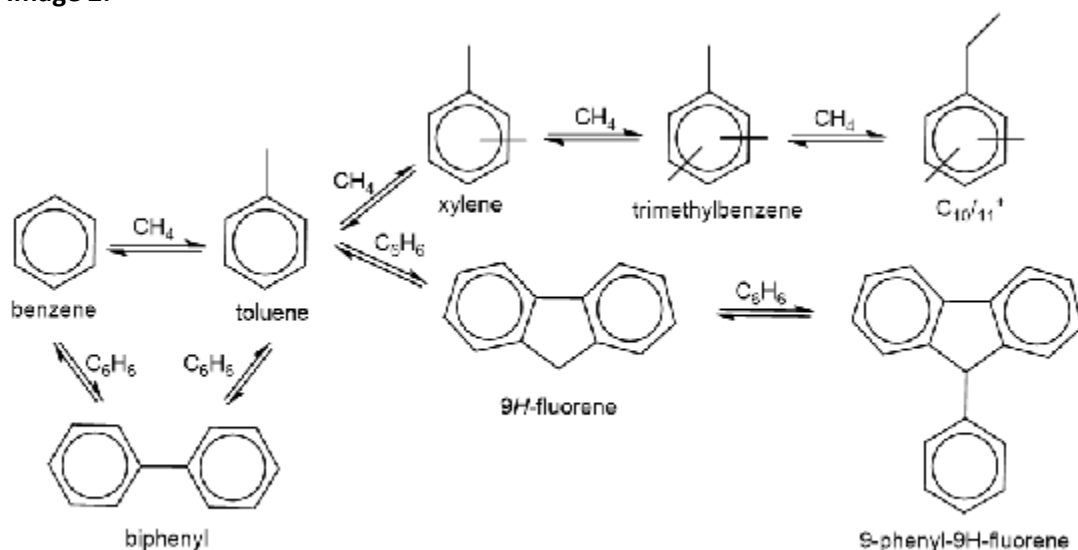


Image 2:



#### References:

Reference

- [1] L. G. Pinaeva, A. S. Noskov, V. N. Parmon, *Catalysis in Industry* 2017, 9, 283-298.
- [2] K. Nakamura, A. Okuda, K. Ohta, H. Matsubara, K. Okumura, K. Yamamoto, R. Itagaki, S. Suganuma, E. Tsuji, N. Katada, *ChemCatChem* 2018, 10, 3806-3812.
- [3] H. Matsubara, E. Tsuji, Y. Moriwaki, K. Okumura, K. Yamamoto, K. Nakamura, S. Suganuma, N. Katada, *Catalysis Letters* 2019, 149, 2627-2635.

A. K. Rajagopalan\*, C. Petit<sup>1</sup>

<sup>1</sup>Department of Chemical Engineering, Imperial College London, London, United Kingdom

**Abstract Text:** Gas sensors are used extensively in indoor, industrial, medical and automotive sectors. Gas sensing devices can be broadly classified into two groups, i.e. sensors whose sensing mechanism depends on electrical variation or sensors whose sensing mechanism depends on change of a given property (e.g. luminescence or mass change). Irrespective of the sensing mechanism, a good sensor should exhibit excellent selectivity, sensitivity, reusability, response time and stability. Metal-organic frameworks (MOFs) have shown great promise in gas sensing applications due to their tunable chemical and structural features. These features could lead to a high selectivity toward a target gas. MOFs also perform well at both ambient and elevated pressure and temperature conditions.<sup>1</sup> These features might be difficult to encounter in commercial polymeric or metal oxide sensors.

Irrespective of their favorable features, a single MOF cannot detect multiple gases in a mixture. Therefore, an electronic nose or sensor array, composed of several materials has to be constructed. Subsequently, the composition of the gas mixture can be resolved by analyzing the response of all the constituent materials in the array. Screening MOFs that can be coated on a sensor array is challenging due to the many candidate materials. Recent studies propose methodologies to screen materials and to quantify the performance of a sensor array.<sup>2,3</sup> These studies assume sensing at equilibrium, based on estimating the gas composition by monitoring the change in mass of the material due to gas sorption. However, kinetic characteristics also dictate the gas sorption. More specifically, the amount of gas adsorbed will determine the sensitivity and the rate at which the gas is adsorbed will determine the sensor response time.

The overarching goal of this work is three fold. First, to highlight the impact of equilibrium characteristics on array performance and to propose a graphical approach to rapidly screen materials for a gravimetric sensor. Second, to highlight the need to incorporate the gas sorption kinetic characteristics and engineering variables to realistically gauge array performance. Third, to characterize multicomponent equilibrium and kinetics of candidate MOFs for a given gas sensing application. To address the first and the second goal, we have developed a computational test bench that incorporates a mathematical model of the array to simulate its response when exposed to a gas mixture. Our detailed model incorporates both equilibrium and kinetic characteristics of the materials in the array. We also coupled the model to an optimization routine that estimates the gas composition of the mixture. For these studies, we used hypothetical materials that exhibit adsorption behavior similar to MOFs to have a generic framework. To address the third goal, we built an experimental test bench, inspired by the zero length column chromatographic technique,<sup>4</sup> to simultaneously estimate the equilibrium and kinetics of target gases on MOFs. The studies performed here led to several key learnings: (1) one can exploit the shape of the sensor response as a function of gas composition to rapidly screen materials for gravimetric sensor arrays; (2) one should incorporate both equilibrium and kinetics to accurately estimate gas compositions in a dynamic system; and (3) one should engineer the array by accounting for the gas flow rate, size of the device, and kinetics of the materials to be used.

To conclude, this work stresses the importance of utilizing a detailed sensor model, which is often not considered, to better reflect reality, both for material screening and for gas composition estimation purposes.

**References:** (1) Zhou, H.-C.; Long, J. R.; Yaghi, O. M. *Chem. Rev.* 2012, 112 (2), 673–674.1.

(2) Gustafson, J. A.; Wilmer, C. E. *ACS Sensors* 2019, 4 (6), 1586–1593.

(3) Sousa, R.; Simon, C. M. *ACS Sensors* 2020, 5 (12), 4035–4047.

(4) Brandani, S.; Mangano, E. *Adsorption* 2020, 1, 3.

## ***Gas Adsorption, Separation and Storage***

FEZA21-PO-334

### **Pyrrole/thiophene graphene, graphyne and graphdiyne composites as sensors for toxic chemical warfare agents: A density functional theory approach**

H. Sajid\*

**Abstract Text:** Pyrrole@graphene or thiophene@graphene composites and their optoelectronic applications are well-known, however, the behaviour of their graphdiyne and graphyne analogues are less well explored. In this study, sensor applications of nanocomposites of graphene (Gp), graphyne (Gy) and graphdiyne (Gd) with monomer and dimer of pyrrole (Py) and thiophene (Thy) have been explored by means of density functional theory (DFT) calculations. Six models, namely, nPy@Gp, nThy@Gp, nPy@Gy, nThy@Gy, nPy@Gd and nThy@Gd are evaluated against two different toxic gaseous analytes. Chemical interactions of the nanocomposites with phosgene and thiophosgene analytes are analysed via structural geometries, interaction energies and electronic properties. Global minima for each system were determined using a stochastic geometry search employing Grimme's GFN1-xTB method followed by Density Functional Theory calculations using the GGA-PBE functional. The interaction energy results reveal that the graphyne nanocomposites are highly sensitive towards phosgene and thiophosgene compared to their graphene and graphdiyne equivalents. This result is also supported by the electronic parameters including density of state, band structure, QTAIM charge transfer and nonequilibrium Green's function analysis which show clear improvement in the behaviour of the graphyne nanocomposites upon complexation with the chosen analytes. The data presented here suggest that nPy@Gy or nThy@Gy composites can effectively be used for the rational design of toxic chemical gas sensors.

**Gas Adsorption, Separation and Storage**

FEZA21-PO-335

**Novel Green Synthesis of Polypyrrole and Application in CO<sub>2</sub> Capture and Storage**

Z. Wang\*, L. Liu, G. Li

**Abstract Text: Novel Green Synthesis of Polypyrrole and Application in CO<sub>2</sub> Capture and Storage**

*Zhe Wang<sup>1</sup>, Liying Liu<sup>1,\*</sup>, Gang Li<sup>2,\*</sup>*

*(<sup>1</sup> State Environmental Protection Key Laboratory of Eco-Industry, Northeastern University, Shenyang, 110819, China; <sup>2</sup> Department of Chemical Engineering, The University of Melbourne, VIC3010, Australia)*

*Corresponding authors: Liying Liu, liuly@smm.neu.edu.cn; Gang Li, li.g@unimelb.edu.au*

The CO<sub>2</sub> generated during fossil fuel combustion is documented as the main cause of global warming. It is of great importance to choose a high-quality adsorbent for carbon capture and reduction. Carbon capture and storage (CCS) is widely considered to be a meaningful technology even from an industrial viewpoint, where the adsorbent plays an important role in CCS technology. When choosing a specific capture method, not only the cost but also its environmental impact should be considered.

Polypyrrole (PPy) is a conductive polymer obtained by polymerization with five-membered heterocyclic of carbon-nitrogen, which has been widely applied in various fields, such as capacitor, catalysis, adsorption, and biomedicine. The extensive research is mainly attributed to its air biocompatibility and high electrical conductivity, more importantly, it has an excellent properties of air stability and environmental benign. The polymerization approaches to synthesize PPy may be classified into two categories, electrochemical and chemical oxidation. The chemical polymerization of PPy refers to the oxidation and polymerization of pyrrole monomer by oxidizing agent in a certain medium, which is easy to operate and suitable for mass production.

In this paper, a novel green synthesis of PPy had been mentioned. HCl and H<sub>2</sub>O<sub>2</sub> reagent have been used to play the role in acidic solvent and oxidant, respectively. In addition, iron ions were added as catalysts or dopants to facilitate the synthesis efficiency by accelerating the rate of polymerization. The filtrate after the reaction was recovered to provide acidic environment and oxidizing agent for the next reaction. This green and sustainable system is appropriate for industrial mass production. The synthesized PPy has a homogeneous spherical morphology with an adsorption capacity of 1.2 mmol/g at 273 K.

**Development of pressure and temperature swing adsorption (PVSA, TVSA) screening tools for metal organic framework in the context of post-combustion and industrial CO<sub>2</sub> capture**

D. Danaci<sup>1,2,\*</sup>, M. Bui<sup>3,4</sup>, W. Arts<sup>1</sup>, N. MacDowell<sup>3,4</sup>, C. Petit<sup>1,2</sup>

<sup>1</sup>Chemical Engineering, <sup>2</sup>Barrer Centre, <sup>3</sup>Centre for Environmental Policy, <sup>4</sup>Centre for Process Systems Engineering, Imperial College London, London, United Kingdom

**Abstract Text:** Metal-organic frameworks (MOFs) have received significant attention by the research community for CO<sub>2</sub> capture. Yet, today there is no confirmed suitable MOFs for cyclic post combustion and industrial CO<sub>2</sub> capture processes. This is unsurprising given the large number of MOF structures, their limited production at scale and the absence of suitable and accessible assessment of MOFs in an actual adsorption process.

In this work, we aim to develop screening tools for MOFs for post-combustion and industrial CO<sub>2</sub> capture while at the same time identifying the MOF properties and process conditions that yield better performance. Our approach could better direct research efforts and expedite the development process. To achieve this, we first developed a simplified pressure-vacuum swing adsorption (PVSA) model with integrated process economics [1]. The PVSA model is based on a one bed, three-step equilibrium cycle which reflects the non-isothermal nature of adsorption while still allowing rapid solutions [2]. While temperature swing adsorption (TSA) would traditionally have been disregarded for this style of application due to prohibitively long cycle times, rapid TSA technologies are gaining popularity and they may enable the deployment of TSA to these very large-scale applications. Therefore, an analogous study was carried out for TSA for which we developed a simplified equilibrium temperature-vacuum swing adsorption (TVSA) model. For both the PVSA and TSA/TVSA studies, we used the separation performance results to size and cost the process equipment required to process flue gas of a given flow rate. In addition to the traditional metrics of purity, recovery, working capacity, and specific energy, the cost of capture allows the identification of trade-offs not otherwise seen.

We focused our study on 22 MOFs for which we could find CO<sub>2</sub> and N<sub>2</sub> isotherms at, at least, three temperatures. We estimated other required inputs such as density, porosity, and heat capacity by their respective methods. While the adsorption cycle used may not reflect the greatest attainable performance for each MOF, it does allow for rapid evaluation of the adsorbent-process ensemble. We benchmarked the performances against those of common adsorbents, i.e. zeolite and activated carbon.

Our screening tool allowed us to determine the ideal MOF isotherms for a set of post-combustion and industrial flue gases. For the PVSA case, we found that improving selectivity by reducing N<sub>2</sub> adsorption, and improving CO<sub>2</sub> working capacity by having moderate enthalpies of adsorption yield the greatest process improvements both technically and economically. For TSA, there are a much wider range of isotherms which yield good performance. This is due to the fact that adsorbents which perform well for PVSA are those that do not show significant thermal effects, whereas for TSA, thermal effects are desired to take advantage of the temperature driving force. MOFs that displayed poor performance for PVSA such as Ni- and Mg-MOF-74, and HKUST-1, showed significantly improved separation performance in TSA due to their higher enthalpies of adsorption. For PVSA, the capture costs are dominated by process capital costs which are primarily comprised of vacuum requirements and adsorbent inventory due to low working capacities. Preliminary work on the process economics for the TSA/TVSA case show that higher working capacities can be obtained which would lead to lower adsorbent inventories.

Overall, our work presents a screening tool to evaluate the performance of published MOFs for post-combustion and industrial carbon capture applications in PVSA, TSA, and TVSA processes. We propose ideal MOF isotherms for a selection of CO<sub>2</sub> capture scenarios. Finally, we highlight areas to focus adsorbent development on considering both separation performance and process cost.

**References:** [1] – D. Danaci et al., *Mol. Syst. Des. Eng.*, 2020, Advance Article

[2] – B.J. Maring, P.A. Webley, *Int. J. Greenh. Gas. Con.*, 15, 16-31, 2013

## ***Gas Adsorption, Separation and Storage | MOFs/Organic materials***

FEZA21-PO-339

### **Unique Magnetic Responses in RE-DOBDC MOFs with NO<sub>x</sub> Adsorption**

S. Henkelis<sup>1,\*</sup>, D. Huber<sup>2</sup>, T. Nenoff<sup>3</sup>

<sup>1</sup>Nanoscale Sciences Department, <sup>2</sup>Center for Integrated Nanotechnologies, <sup>3</sup>Material, Physical, and Chemical Sciences Center, Sandia National Laboratories, Albuquerque, United States

**Abstract Text:** The burning of fossil fuels has produced the energy that the nation depends on for over a century and remains the biggest contributor to our energy needs. Flue gas streams generated from burning fossil fuels contain ppm levels of NO<sub>x</sub> and SO<sub>x</sub> and are a significant environmental concern. Porous adsorbents such as metal-organic frameworks (MOFs) remain a promising mechanism to selectively adsorb NO<sub>x</sub> from flue streams. The magnetic properties of MOFs such as RE-DOBDC, and their magnetic response with adsorption of acid gases, makes them ideal candidates for use in detecting ppm levels of acid gases from harsh environments.

Here, the magnetic susceptibility of RE-DOBDC (rare earth, Y, Eu, Tb, Yb; DOBDC – 2,5-dihydroxyterephthalic acid) MOFs has been investigated pre- and post-NO<sub>x</sub> loading. RE-DOBDC samples were synthesized, activated and subsequently loaded with humid NO<sub>x</sub>. Humid NO<sub>x</sub> was generated by acidifying a solution of sodium nitrite in an adsorption chamber and maintained at 50 ppm NO<sub>2</sub> and 60% RH. Each MOF was characterized by powder X-ray diffraction and the magnetic characteristics probed using a VersaLab Vibrating Sample Magnetometer (VSM). Lanthanide-containing RE-DOBDC (Eu, Tb, Yb) are paramagnetic with a reduction in paramagnetism upon adsorption of NO<sub>x</sub>. Y-DOBDC exhibited a diamagnetic moment with a slight reduction upon adsorption of NO<sub>x</sub>. The magnetic susceptibility of the MOF is determined by the framework metal center and electronic population of the orbitals contributes to determining the extent of magnetism and change with NO<sub>x</sub> (electron acceptor) adsorption. Eu-DOBDC results in the largest mass magnetization change upon adsorption of NO<sub>x</sub> due to more available unpaired electrons. The unique change in magnetic susceptibility with NO<sub>x</sub> adsorption allows for the potential use as a magnetic sensor for NO<sub>x</sub>.

\* This work was supported as part of UNCAGE-ME, an Energy Frontier Research Center funded by the U.S. Department of Energy, Office of Science, Basic Energy Sciences under Award #DE-SC0012577. SNL is managed and operated by NTESS under DOE NNSA contract DE-NA0003525

**Thin film synthesis of hybrid ultramicroporous materials for gas separation and sensing - A comparative approach**

B. Tokay\*, J. Warfsman, N. Champness

**Abstract Text:**

A new class of metal-organic frameworks (MOFs), known as hybrid ultramicroporous (HUMs) materials with high CO<sub>2</sub> adsorption capacities [1], have been recently introduced to solve the problems related to water stability, using strong interactions based on tight fitting. They have pore apertures, which are often less than 0.5 nm [2] (e.g., ZIF-8= 0.9 nm [3]; HKUST-1: 1.0-1.5 nm [4]).

From the existing HUMs, TIFSIX-3-Ni (for simplification; TIFSIX from now on) is one of the most promising candidate that has one of the highest CO<sub>2</sub> capacities (40 cm<sup>3</sup> g<sup>-1</sup> at 2 mbar CO<sub>2</sub> pressure) [5]. The structure of the silicon derivate SIFSIX-3-Ni (due to the lack of crystal data for TIFSIX in literature) is shown in Fig 1, a structure whose crystal parameters are close to those reported for TIFSIX [6]. In the cubic structure the nickel cation is surrounded by 4 pyrazine groups through Ni-N bonds. Since pyrazine is a linear molecule, a cubic cell is formed. The two remaining octahedral positions around nickel are occupied with by TiF<sub>6</sub><sup>2-</sup> anions, separating the layers composed of nickel and pyrazine. The different pyrazine motifs are stacked in a coplanar manner and the framework is stabilized by hydrogen bonds between the hydrogen of the pyrazine and fluorine anionic pillars (highlighted as pale red bonds in Fig 1).

Powder form of TIFSIX has been investigated for gas separation and purification [7] whilst TIFSIX film synthesis procedure has not studied yet. The transfer of powder synthesis to membrane synthesis is often challenging. Powder synthesis typically seeks to determine properties such as morphology or particle size. However, additional properties such as film thickness and roughness have to be considered in order to create high quality films. Furthermore, the formation of films and membranes of MOFs is highly dependent on the specific structure to be studied, the nature of the substrate and the interaction between the two [8], [9] [10].

The thin-film synthesis of the hybrid ultramicroporous material (HUM) TIFSIX-3-Ni on glass substrates are reported by employing several methods including dip-coating, seeding and secondary growth, vapour-assisted conversion, rapid thermal deposition and in-situ coating. Using the in-situ approach with DMF as solvent, we were able to grow homogeneous TIFSIX-3-Ni films at relatively low temperatures and reduced reaction times.

Herein, we present the thin-film formation of TIFSIX by a straightforward in-situ synthesis without a need of surface modification on a glass support. In this study, we show the first example of preparation of TIFSIX films on glass substrates using various film synthesis strategies including dip-coating, seeding and secondary growth, vapour-assisted conversion, rapid thermal deposition and in-situ coating. Amongst employed methods, only seeding and secondary growth and in-situ coating methods resulted in the formation of a few micron thick TIFSIX films on glass substrates. We then report a fabrication methodology based on seeding and secondary growth for TIFSIX films on ceramic tubular substrates for CO<sub>2</sub>/CH<sub>4</sub> separations. The choice of tubular supports allows for the high surface area to volume ratios required for industrial separations.

**References:**

1. O. Cheung and N. Hedin, RSC Adv., 2014, 4, 14480–14494.
2. L.-Y. Lin and H. Bai, Micro. Meso. Mat., 2010, 136, 25–32.
3. M. M. Maroto-Valer, Z. Tang and Y. Zhang, Fuel Process. Technol., 2005, 86, 1487–1502.
4. S. Choi, J. H. Drese and C. W. Jones, ChemSusChem, 2009, 2, 796–854.

- 5 M. Kandiah, M. H. Nilsen, S. Usseglio, S. Jakobsen, U. Olsbye, M. Tilset, C. Larabi, E. A. Quadrelli, F. Bonino and K. P. Lillerud, *Chem. Mater.*, 2010, 22, 6632–6640.
- 6 X. Y. Chen, V.-T. Hoang, D. Rodrigue and S. Kaliaguine, *RSC Adv.*, 2013, 3, 24266–24279.
- 7 H. S. Scott, A. Bajpai, K.-J. Chen, T. Pham, B. Space, J. J. Perry and M. J. Zaworotko, *Chem. Commun.*, 2015, 51, 14832–14835.
- 8 A. Cadiou, K. Adil, P. M. Bhatt, Y. Belmabkhout and M. Eddaoudi, *Science*, 2016, 353, 137–140.
- 9 L. T. Ngyen, K. K. LE and N. T. PHAN, *Chinese J. Catal.*, 2012, 33, 688–696.
- 10 A. R. Millward and O. M. Yaghi, *J. Am. Chem. Soc.*, 2005, 127, 17998–17999.

## **Gas Adsorption, Separation and Storage | MOFs/Organic materials**

FEZA21-PO-341

### **Complex Gas Dynamics of Humid SO<sub>x</sub> in Rare Earth DOBDC Metal-Organic Frameworks**

D. Vogel<sup>1,\*</sup>, S. Henkelis<sup>1</sup>, T. Nenoff<sup>2</sup>, J. Rimsza<sup>3</sup>

<sup>1</sup>Nanoscale Sciences Department, <sup>2</sup>Material, Physical, and Chemical Sciences, <sup>3</sup>Geochemistry Department, Sandia National Laboratories, Albuquerque, United States

**Abstract Text:** Designing porous materials for chemical separation and sensing that are stable in the harsh acid gas environments of industrial flue streams is an ongoing and pressing challenge. A series of synthesized rare earth 2,5-dihydroxyterephthalic acid (RE-DOBDC; RE=Y, Eu, Tb, Yb) metal-organic frameworks (MOFs) have been previously investigated for NO<sub>x</sub> adsorption and acid gas stability in humid NO<sub>x</sub>, indicating a unique optical response to NO<sub>x</sub> and material stability. Currently SO<sub>x</sub> adsorption following exposure to a humid SO<sub>x</sub> gas stream is being tested and characterized. The RE-DOBDC MOF series exhibits consistent crystallinity in humid SO<sub>x</sub> with no sign of degradation, indicating possible application for SO<sub>x</sub> separation. A humid SO<sub>x</sub> stream was generated by bubbling air through an acidified 4.8 mM solution of sodium sulfite, flowing SO<sub>2</sub> over the MOF sample. IR studies confirmed the presence of S-species in Y- and Yb-DOBDC, whereas Eu-, and Tb-DOBDC remain unchanged.

A series of density functional theory and *ab initio* molecular dynamic (AIMD) studies have been undertaken to further identify the fundamental structure-property relationships that control humid SO<sub>x</sub> and RE-DOBDC MOF interactions and compare with previous NO<sub>x</sub> calculations. Calculated ground state electronic structure energies provide relative binding energies for competing H<sub>2</sub>O and SO<sub>2</sub> gases and competitive binding at metal sites. To investigate the complexity of simultaneous gas-gas and gas-framework interactions AIMD trajectories have been calculated for homogeneous (SO<sub>2</sub>, H<sub>2</sub>O) and mixed gas (SO<sub>2</sub> + H<sub>2</sub>O) environments. The AIMD calculations highlight competitive adsorption mechanisms, the possible formation of gas reaction species, and MOF framework modification facilitated by humid SO<sub>x</sub>.

This work was supported as part of UNCAGE-ME, and Energy Frontier Research Center funded by the U.S. Department of Energy, Office of Science, Basic Energy Sciences under Award #DE-SC0012577. SNL is managed and operated by NTESS under DOE NNSA contract DE-NA0003525.

**Puzzled by features of an adsorption isotherm? Try molecular simulations!**

G. Donval<sup>1,\*</sup>, T. Düren<sup>1</sup>

<sup>1</sup>Centre for Advanced Separations Engineering, Chemical Engineering, University of Bath, Bath, United Kingdom

**Abstract Text:** Adsorption mechanisms of microporous solids can be complex and challenging to understand. Yet complex adsorption phenomena are often key to superior material performance such as higher storage densities and better selectivity. Often the location of guest molecules is required to understand adsorption performance.

There are very few experimental techniques able to provide a precise mapping of guest molecules within the pores. For example, neutron diffraction or high-pressure crystallography are expensive, time consuming and lack general availability. A number of models based solely on experimental isotherms have been developed to alleviate those problems. Most of them however rely on simplified assumptions, e.g. specific pore geometry (or pore model) in methods for determining pore size distribution such as *HK*, *BJH* and *DFT* or specific isotherm types for textural analysis in techniques such as hysteresis scanning.

This kind of insight can also be obtained from molecular simulation, including grand canonical Monte Carlo (GCMC) simulations, which additionally provides detailed information about host-guest interactions. In contrast to high pressure crystallography and neutron diffraction experiments, GCMC calculations can be performed on a normal computer within a few hours with freely available tools making them accessible to everybody. Yet the lack of advanced tooling so far has hindered the analysis of GCMC data to its full extent, most notably to calculate quantitative guest mapping in pores and shed light into puzzling features of measured isotherms.

In this contribution, we will present the freely available tools we developed and will demonstrate their use on a series of MOFs and COFs (though they can be applied to any sort of porous materials, even amorphous structures). We will visualise how isotherm features are linked to adsorption mechanisms and will show how this advanced analysis and quantification allows us to univocally identify the proper *BET* region in not only simulated but also experimental isotherms.

**Shaping, characterization and measurement of adsorption properties of ZIF-8**

A. Pereira<sup>1,\*</sup>, M. J. Regufe<sup>1</sup>, A. E. Rodrigues<sup>1</sup>, A. M. Ribeiro<sup>1</sup>, A. Ferreira<sup>1</sup>

<sup>1</sup>Chemical Engineering, FEUP, Porto, Portugal

**Abstract Text:** Nowadays, the chemical industry is dependent on processes like separation, purification, and storage of gases. One of the techniques employed in this type of processes is adsorption. However, in the industry, the adsorbent powders must be converted into hierarchical porous structures in order to guarantee a low-pressure drop and a high packing density, thermal conductivity, and mechanical strength [1], increasing, this way, the efficiency of the process. Taking this into account, ZIF-8 powder (Basolite® Z1200) was shaped into pellets and monoliths, using extrusion and direct ink writing (DIW), respectively. For the pellets, alumina and carboxymethyl cellulose were used as binders. Carboxymethyl cellulose was the binder employed in the monolith. Pellets with 5, 10 and 15 %wt of alumina and 5 and 10 %wt of carboxymethyl cellulose were prepared. Posteriorly, the pellets were thermally treated. Prior to the printing of the monoliths, the rheological behavior of the adsorbent inks was evaluated to understand if these ones had the rheological properties required, like a pseudoplastic behavior, to be printed. Since both inks displayed the desired rheological features, monoliths with 5 and 10 %wt of carboxymethyl cellulose were synthesized. These structured materials were morphologically and chemically characterized through SEM/EDS analysis, x-ray diffraction, N<sub>2</sub> adsorption isotherms at 77 K, CO<sub>2</sub> adsorption isotherms at 273 K and mercury porosimetry. These characterizations allowed to understand the effect of the type and of the amount of binder in the shaped materials when compared to the pristine powder. For all the materials, was observed that neither the thermal treatment nor the shaping process has no impact on the crystalline structure of the final structured material. The binder has impact on the textural properties of the materials and, surprisingly, the pellets with 10 %wt of alumina had a similar volume of pores and Langmuir surface area than the pellets with 5 %wt of alumina. Besides the tests mentioned previously, radial crushing strength tests were also performed on the pellets in order to study the effect of the shaping and the amount of binder on the mechanical stability of the material. It was proved that the mechanical strength of the materials increases with the binder amount. Gathering the information from the morphological and chemical characterizations and of the mechanical strength tests, it was possible to identify which were the materials with the best set of properties. For those materials, the adsorption equilibrium isotherms for CH<sub>4</sub> and N<sub>2</sub> were measured at 303 K up to 4 bar. The Langmuir adsorption model was used to fit the experimental data. The CH<sub>4</sub>/N<sub>2</sub> selectivity values of the shaped materials up to 6 bar were evaluated and compared with the ones obtained for the pristine powder with the purpose of comprehending the effect of the shaping. Some of the materials demonstrated the potential to be used in large scale applications.

**Nanoporous organic frameworks for selective VOC adsorption**

H. Krafczyk<sup>1,\*</sup>, M. Rose<sup>1</sup>

<sup>1</sup>Chemistry, Ernst-Berl Institute, Technical University Darmstadt, Darmstadt, Germany

**Abstract Text:**

Volatile organic compounds (VOC) are a hazardous class of air pollutants which are heavily emitted by industrial processes. Hence, VOC must be removed from waste and flue gas streams. Due to their low boiling point and high vapor pressure adsorption based processes are highly suitable for VOC separation from flue gas streams. Compared to other separation methods adsorption has the advantage of high efficiency, and its nondestructive nature allows to recover valuable VOC from waste streams. Activated carbon is widely used as adsorbent for VOC separation due to its high specific surface area and adsorption capacity. Nevertheless, in order to use adsorption based separation over a wide range of VOC efficiently, the selectivity of the adsorbent material needs to be enhanced and specifically tunable for the respective separation problems.<sup>[1]</sup>

Hyper cross linked polymers (HCP) exhibit a variety of tunable structures and functional groups while maintaining a high specific surface area. They are typically formed by a Friedel-Crafts alkylation where aromatic building blocks are connected either by an intramolecular cross-linking reaction or via external linker molecules using stoichiometric amounts of FeCl<sub>3</sub> as catalyst. To avoid residual traces of metal in the HCP, the metal-free Brønsted acid trifluoromethanesulfonic acid was used as an alternative catalyst during the synthesis as recently introduced in literature.<sup>[2]</sup> By varying functional groups of the monomers, the pore size and polarity of the HCP can be specifically adjusted to the respective adsorption/separation problem. Besides connecting bis(chloromethyl)-biphenyl (BCMBP) via internal cross-linking, benzene (Bz) and fluorobenzene (FBz) building blocks were externally crosslinked using dimethoxymethane as linker molecule. To vary the HCP's polarity, the ratio of Bz and FBz as building blocks was varied. The physisorption properties of the HCPs were investigated especially for benzene and cyclohexane (Ch) as model substances for the separation of aliphatic and aromatic molecules. Ch and Bz are particularly hard to separate due their similarity in physical properties and kinetic ratios which complicates size exclusion adsorption processes.<sup>[3]</sup> Hence, separation must be controlled via the different interactions between the adsorbent and the adsorptives.

For all HCPs the Bz sorption isotherms show a significantly higher uptake over the entire relative pressure range compared to the Ch isotherms (see figure 1). This indicates a pronounced selectivity towards the adsorption of aromatic over aliphatic molecules, which is supported by the isosteric heat of adsorption as an indicator for the interaction strength of the adsorptives with the HCP. The isosteric heat of adsorption was calculated from Bz and Ch sorption isotherms at three different temperatures. Both components show the maximum adsorption enthalpy at low loadings which is significantly higher for Bz than for Ch. With increasing loading, the heat of adsorption decreases until the condensation enthalpy of the respective fluid is reached (see figure 2).<sup>[4]</sup> Furthermore, the separation selectivity of the externally linked Bz/FBz-HCP decreases with increasing FBz content but always exceeds the BCMBP-HCP's selectivity. Overall, the high potential of nanoporous polymers for the adsorption of aromatic and aliphatic model components is proven. The results indicate a specific selectivity towards the adsorption of aromatics which also allows selective separation of aliphatic and aromatic molecules with very similar thermophysical properties.

Image 1:

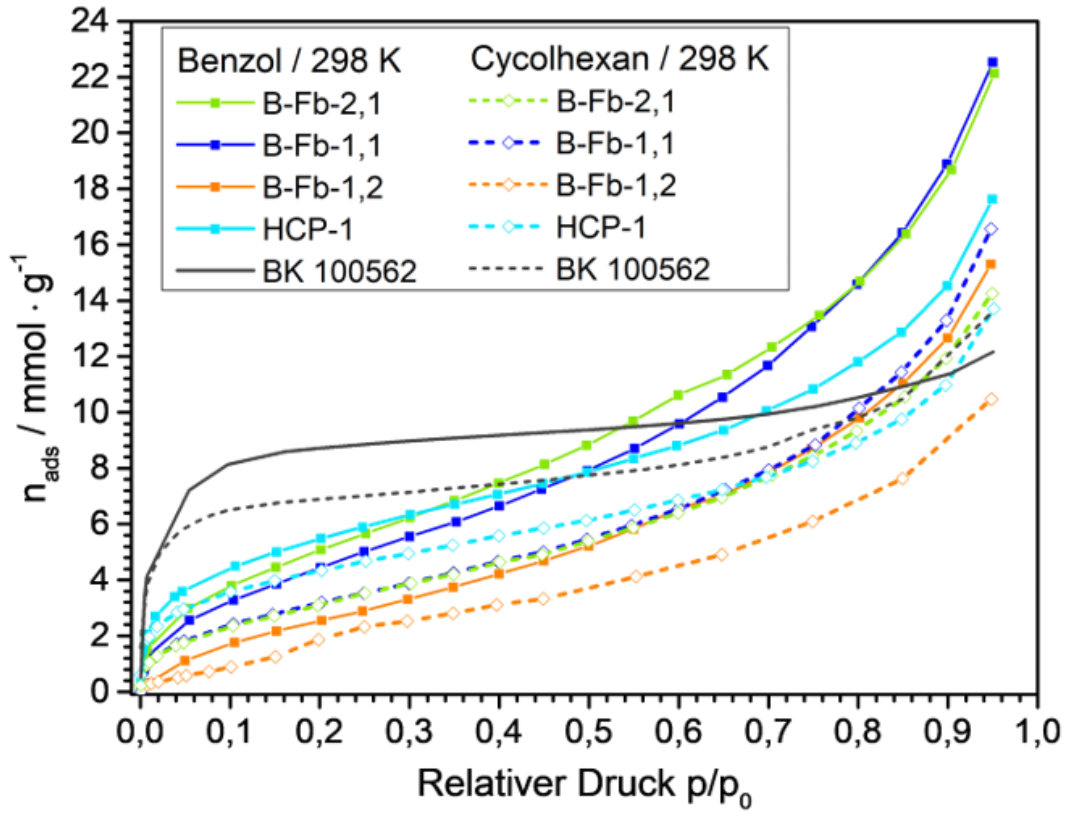
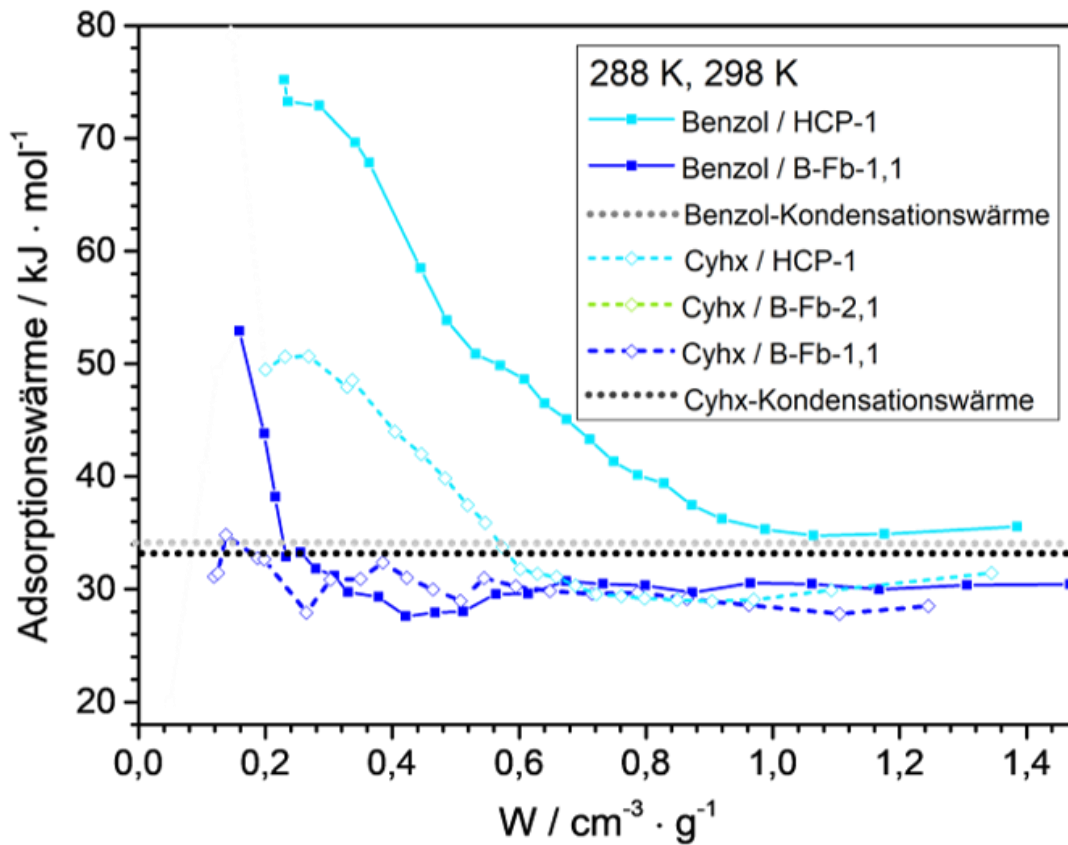


Image 2:



References:

- [1] G. Wang et al., J. Environ. Sci. 2015, 30, 65-73.
- [2] K. Schute, M. Rose, ChemSusChem 2015, 8, 3419-3423.
- [3] G. Wang et al., RSC Advances 2013, 3, 20523-20531.
- [4] S. Grätz, H. Krafczyk et al., Beilstein J. Org. Chem. 2019, 15, 1154-1161.

**Development of Crystalline Porous Organic Salts.**

M. O'Shaughnessy<sup>1,\*</sup>, M. Little<sup>1</sup>, R. Clowes<sup>1</sup>, A. Cooper<sup>1</sup>

<sup>1</sup>Department of Chemistry, University of Liverpool, Liverpool, United Kingdom

**Abstract Text:** Porous materials are useful for applications in areas such as gas storage, separations and catalysis. A class of porous material is porous molecular solids where the molecular subunits are held together using weak intermolecular interactions<sup>1</sup>. These materials have unique advantages over other classes of porous materials such as solution processability and characterisation, simple purification and ease of regeneration by recrystallization<sup>2</sup>. Crystalline porous organic salts (CPOSSs) are another less studied class of porous materials utilising intermolecular interactions, in this case strong charge assisted hydrogen bonds between an acid and a base<sup>3, 4</sup>. The charge assisted hydrogen bonded gives CPOSSs an advantage over other porous molecular solids as most involve the use of hydrogen bonds which have bond strengths between 5 kJ to 50 kJ mol<sup>-1</sup> while charge assisted hydrogen bonds have strengths in the range of 20-140 kJ mol<sup>-1</sup> which in principle should make the materials more stable. In addition, there is the scope to use a diverse library of CPOSSs components and develop reticular chemistry concepts used in the design of MOFs to design and synthesis CPOSSs with tuneable properties. The use of charged components leads to a number of complications in the formation of these materials including: the high probability of forming a solvate over a co-crystal and, when a co-crystal is formed, activation can be difficult due to the interaction of the solvent with the framework. To address these challenges, we have focused on developing a high throughput method to quickly screen a vast number of solvent conditions for the crystallisations along with HT powder diffraction analysis to quickly identify different structures. Using tetrakis(4-aminophenyl)methane and tetrakis(4-sulfophenyl)methane which are both symmetrical and have tetrahedral struts with S<sub>4</sub> point groups we have employed high throughput methods to screen crystallisation conditions. Taking this approach, we have found that, whilst crystallisation solvent can direct crystallisation outcomes, they can be important for stabilizing extended packing in CPOSSs structures. We have discovered a CPOSSs which was shown by single crystal X-ray diffraction to contain 2 dimensional channels (Figure 1). We have further investigated the role of a modulator to control the formation of the CPOSS.

**Image 1:**

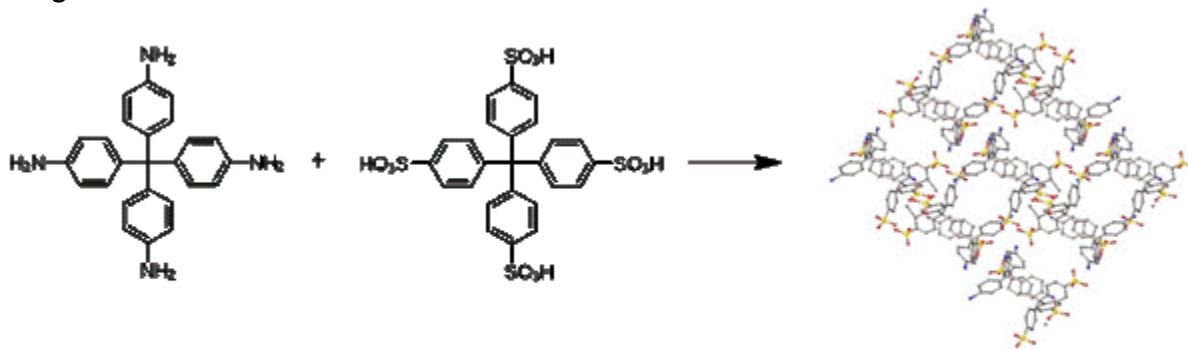


Figure 1. Schematic Representation of tetrakis(4-aminophenyl)methane and tetrakis(4-sulfophenyl)methane crystallising to form a porous network.

**References:**

1. A. I. Cooper, ACS Central Science, 2017, 3, 544-553.
2. T. Miyano, N. Okada, R. Nishida, A. Yamamoto, I. Hisaki and N. Tohnai, Chemistry-a European Journal, 2016, 22, 15430-15436.
3. A. Yamamoto, S. Uehara, T. Hamada, M. Miyata, I. Hisaki and N. Tohnai, Crystal Growth & Design, 2012, 12, 4600-4606.
4. G. Xing, I. Bassanetti, S. Bracco, M. Negroni, C. Bezuidenhout, T. Ben, P. Sozzani and A. Comotti, Chemical Science, 2019, DOI: 10.1039/C8SC04376K.

## Industry Discussion Session

FEZA21-PO-351

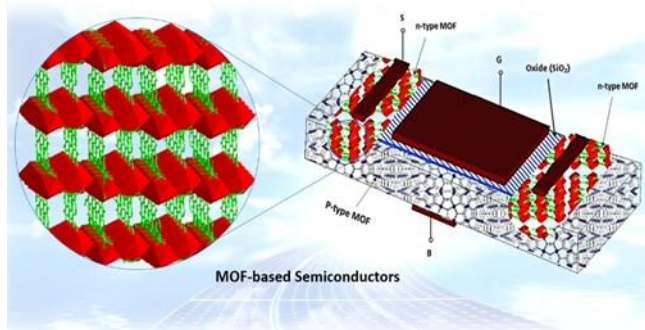
### A Journey towards Applications of Semiconductor Metal–Organic Frameworks in Microelectronic Industry

M. Usman<sup>1,\*</sup>

<sup>1</sup>Chemistry, Academia Sinica, Taipei, Taiwan, Province of China

**Abstract Text:** Metal–organic frameworks (MOFs) have emerged as a promising class of materials with a wide spectrum of useful applications in gas absorption, catalysis, biomedical and sensing etc. Their unique properties arising from the self-assembly of metal ions/clusters with electron-donating organic linkers, enable ordered frameworks with tunable functionalities, uniform pore sizes, post-synthesis modification, rich coordination chemistry and fascinating topologies are prompting us to further explore their semiconducting properties. MOFs with advantageous properties of both inorganic and organic components, promise to serve as the next generation of the semiconducting materials with the potential to be extremely stable, cheap, and mechanically flexible (Fig. 1). I have investigated fundamental dielectric, semiconducting and optical properties of various MOFs and summarized the initial theoretical and experimental research. A discuss will be presented about current journey from fundamental properties towards device designing using MOF as an active component. This study presents a significant and encouraging step towards a new research direction focused on potential applications of MOFs in the semiconductor industry.

#### Image 1:



#### References:

1. M. Usman, K. P. Bera, G. Haider, S. Batjargal, M. Hayashi, G. H. Lee, S. M. Peng, Y. F. Chen, K. L. Lu, Single-Molecule Based Electroluminescent Device as Future White Light Source. *ACS Appl. Mater. Interfaces*, 2019, 11, 4084–4092.
2. M. Usman, S. Mendiratta, K. L. Lu, Semiconductor Metal–Organic Frameworks and their Bandgap Investigation, *Adv. Mater.* 2017, 29, 1605071.
3. M. Usman, K. L. Lu, Metal–Organic Frameworks: Future of Low-k Materials, *NPG Asia Mater.*, 2016, 8, e333.
4. M. Usman, G. Haider, S. Mendiratta, T. T. Luo, Y. F. Chen, K. L. Lu, Continuous Broadband Emission from a Metal–Organic Framework as a Human-Friendly White Light Source, *J. Mater. Chem. C*, 2016, 4, 4728–4732.

## ***Ion Exchange and Other Applications***

FEZA21-PO-352

### **Porous polymer adsorbents for biorefinery downstream applications**

I. Moritz\*, M. Rose

**Abstract Text:** Hydrophobic adsorbents for future process innovations are, inter alia, hypercrosslinked polymers (HCP) [1] with specific surface areas up to 2000 m<sup>2</sup> g<sup>-1</sup>. Liquid phase adsorption offers a promising approach for cost and energy efficient downstream purification in bio refineries. Aqueous reaction and fermentation mixtures with low thermal stability remain their main challenge for polar product streams.

HCPs offer high capacities and selectivities for adsorption processes of biogenic platform chemicals [2-4]. Herein, we spotlight the separation of carboxylic acids obtained from glucose by fermentation. Batch experiments were performed with HCP as well as common reference adsorbents. The uptakes for HCP, resulting from excess adsorption, are in the range of 160 mg g<sup>-1</sup> for lactic acid, 380 mg g<sup>-1</sup> for citric acid and up to 520 mg g<sup>-1</sup> for itaconic acid with negligible glucose uptake. Polarity changes due to pH variation are used amongst others for selective product desorption.

Because of the high capacity and selectivity of itaconic acid on HCP, the system was further investigated regarding a potential technical application. A continuous fixed-bed column setup was applied to identify ideal parameters for future process design. Furthermore, shaping of the powdered adsorbents plays an important role in the continuous adsorption process due to the resulting pressure drop, and transport limitations. Moreover, the choice of monomer allows to functionalize the accessible surface of the resulting polymer to create specific atomic interactions. They enable a selective adsorption of the desired compound. Finally, we end up with an outlook on other separations challenges and want to discuss possible limitations in adsorbent design [5].

**References:** [1] a) S. Xu, Y. Luo and B. Tan, *Macromol. Rapid Commun.* 2013, 34, 471–484 b) Liangxiao Tan and Bien Tan, *Chem. Soc. Rev.*, 2017, 46, 3322

[2] L. Rübenach, J. Lins, E. Koh, M. Rose, *ChemSusChem* 2019, 12, 3627

[3] K. Schute, C. Detoni, A. Kann, O. Jung, R. Palkovits, M. Rose, *ACS Sustainable Chem. Eng.* 2016, 4, 5921–5928.

[4] C. Detoni, C. H. Gierlich, M. Rose and R. Palkovits, *ACS Sustainable Chem. Eng.* 2014, 2, 2407–2415.

[5] I. Moritz, M. Rose, Manuscript in preparation.

**A New Approach to Pest Control: Metal-Organic Frameworks for Alarm Ant Pheromone Delivery**

J. Paul-Taylor<sup>1,2,\*</sup>, D. Rixson<sup>2</sup>, G. Shearer<sup>2</sup>, C. Marsh<sup>2</sup>, J. Spencer<sup>3</sup>, W. Hughes<sup>4</sup>, T. Düren<sup>5</sup>, A. Burrows<sup>2</sup>

<sup>1</sup>Centre for Sustainable and Circular Technologies, <sup>2</sup>Chemistry, University of Bath, Bath, <sup>3</sup>Chemistry, <sup>4</sup>School of Life Sciences, University of Sussex, Brighton, <sup>5</sup>Chemical Engineering, University of Bath, Bath, United Kingdom

**Abstract Text:** With a growing population and over 1 billion undernourished people globally the sustainable production of food is one of the key challenges facing society. Pest species are a particular problem,<sup>1</sup> an example of which is the leaf-cutting ant which annually causes \$8 billion of damage to Eucalyptus forestry in Brazil alone.<sup>2</sup> Pesticides are currently used to tackle such problems, but the strategy of widespread spraying directly on target crops requires large amounts of pesticide, affects more species than necessary, and results in environmental contamination and health concerns from pesticide residues on the resulting produce.

One alternative strategy is to use semiochemicals e.g. pheromones to attract pests towards an insecticide bait trap, thus exterminating pests in a targeted manner without direct contact between the pesticide and crop.<sup>3</sup> However, pheromones are too volatile for practical use in agricultural pest control, thus necessitating a means to reduce the rate at which they evaporate. One way this can be done is to adsorb them into porous materials. To this end, metal-organic frameworks (MOFs) are particularly attractive due to the relative ease with which their properties (e.g. porosity and functionality) can be tuned, thus allowing one to tailor the affinity between the pheromone and framework. The concept behind using semiochemical-loaded MOFs for this agricultural pest control application is illustrated in Image 1.

In this contribution, we report our initial findings from a combined experimental and computational investigation on the adsorption and release of ant alarm pheromones into and from a selection of MOFs including tests for the biological effect on leaf-cutting ants. For this, we began by postulating that the interaction between the pheromones and the MOF would be maximised by the presence of a hydrogen bond donor (to interact with the carbonyl group) or an alkyl group (to provide a hydrophobic pore environment for the hydrocarbon chain) on the framework and proceeded to prepare a series of IRMOFs with organic linkers whose functionality met these criteria. After attempts to adsorb the pheromone 3-octanone onto the series of samples, quantification via <sup>1</sup>H NMR convincingly showed that the functionalised materials retained the pheromone far more effectively than the unfunctionalised framework (IRMOF-1).

The results also showed that the samples with alkyl groups retained far more of the pheromone than the material with only hydrogen bond donor groups (the amine group in IRMOF-3) despite their lower surface areas. This suggests that a hydrophobic pore environment is more important than the interaction between the amine and carbonyl group for the interaction between the framework and 3-octanone. Molecular dynamics simulations were conducted to gain more insight into the interactions involved, and the results showed that the dispersion interactions are more than five times larger than the electrostatic interaction from the amine group, thus explaining the observed behaviour when alkyl chains are present.

Release of the pheromone was studied by regularly recording <sup>1</sup>H NMR spectra on three pheromone-loaded MOFs left open to the air for nine weeks. The results, shown in Image 2, show that both the unfunctionalised materials and amine functionalised material released nearly all the guest 3-octanone within the first week. In contrast, the material containing alkyl groups (IRMOF-NHPr) released it at a steady rate for over 61 days. This suggests that the alkyl chain is key for releasing 3-octanone over a length of time suitable for this application. Finally, to assess whether pheromone-loaded MOFs have a biological impact, samples were tested in field trials together with control experiments using a more conventional bait set up. Crucially, these studies demonstrated that leaf-cutting ants show the normal behavioural responses to the released pheromone after inclusion in the MOF, including being attracted to the source.

**Image 1:**

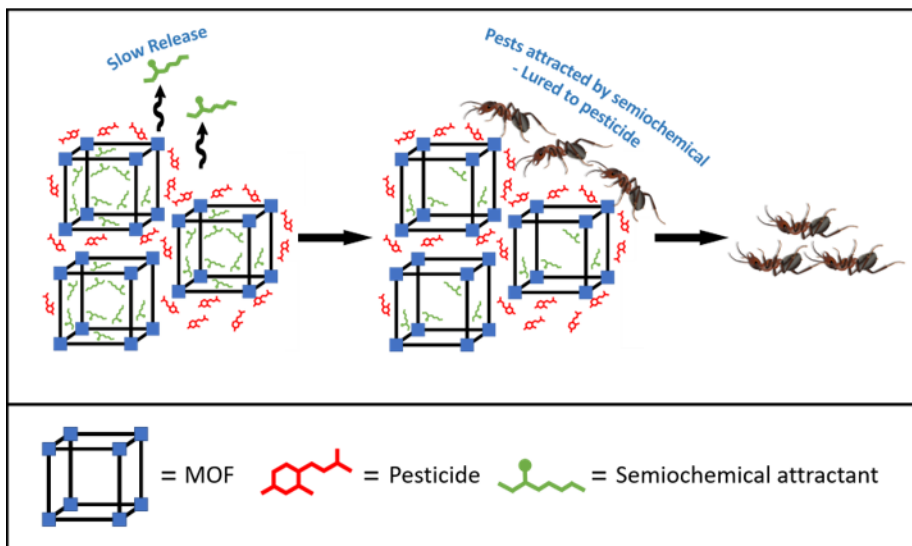
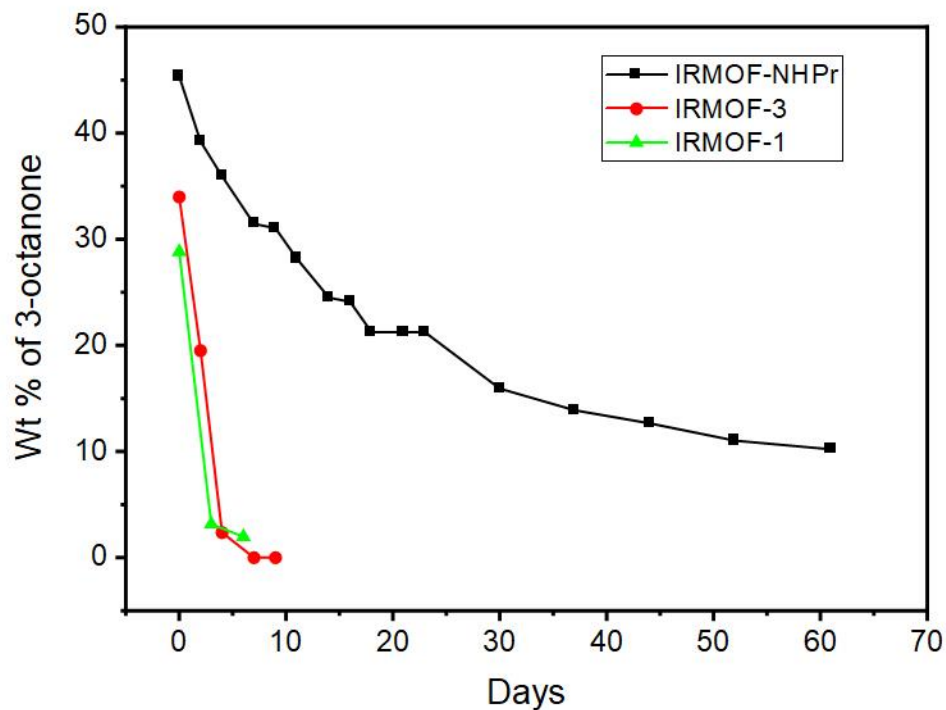


Image 2:



- References:** 1. H. C. J. Godfray, J. R. Beddington, I. R. Crute, L. Haddad, D. Lawrence, J. F. Muir, J. Pretty, S. Robinson, S. M. Thomas and C. Toulmin, *Science*, 2010, 327, 812-818.
2. T. M. C. Della Lucia, L. C. Gandrab and R. N. C. Guedes, *Pest Man. Sci.*, 2014, 70, 14-23.
3. P. Witzgall, P. Kirsch, A. Cork, *J. Chem. Ecol.*, 2010, 36, 80-100.

## ***Ion Exchange and Other Applications | MOFs/Organic materials | Poster***

FEZA21-PO-356

### **Capture of Phosphate Anions from Waste Water using Metal-Organic Frameworks**

B. Knight<sup>1,\*</sup>, C. Marsh<sup>1</sup>, J. Bagnall<sup>2</sup>, T. Düren<sup>3</sup>, A. Burrows<sup>1</sup>

<sup>1</sup>Chemistry, University of Bath, <sup>2</sup>Environment and Technology, Wessex Water, <sup>3</sup>Chemical Engineering, University of Bath, Bath, United Kingdom

#### **Abstract Text:**

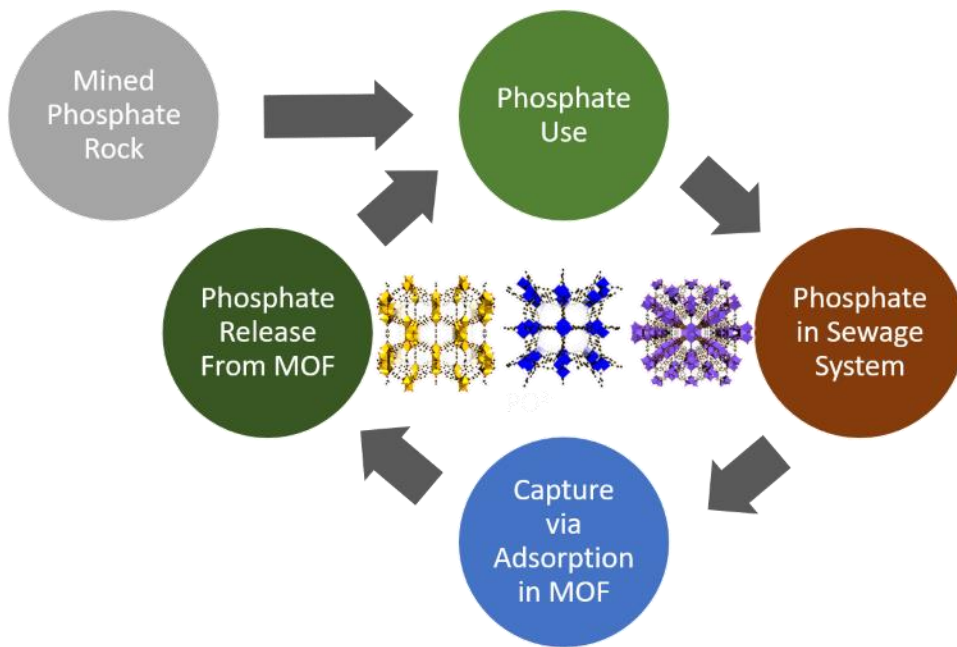
Phosphates are used in the agriculture sector, such as in fertilizers and pesticides, home use, including detergents and toothpaste, and industrial use, for instance corrosion inhibition and flame retardants.<sup>1</sup> Most of the phosphate applied as fertilizer is lost to water ways, with only 16% entering human food.<sup>2</sup> Water companies are required to reduce the amount of phosphate as part of their sewage treatment works, as it causes eutrophication which leads to the death of aquatic environments.<sup>3</sup>

Phosphorus is a finite resource found as minerals, primarily phosphates, in sedimentary rock. High quality deposits are only located in a few regions of the world; Morocco and the Western Sahara have an estimated 70 % of the remaining world phosphate reserves.<sup>1,4</sup> High quality easy to mine reserves are being depleted first – the lower quality reserves have a higher percentage of impurities and are harder to mine. Therefore, the cost of the extracting phosphorus is set to increase.<sup>1</sup>

Considering the future availability of phosphorus and the detrimental effect excess phosphorus has on the environment, it makes environmental and economic sense to develop ways to capture and reuse phosphate from sewage systems. From the potential capture methods, pollutant adsorption presents several benefits including, ease of operation, simple design, potential to remove phosphorus at low concentration, little waste production and the reusability of the adsorption material.<sup>3</sup> MOFs have been shown to be effective adsorbents in wastewater for the removal of a range of water contaminants, such as pharmaceuticals, personal care products and dyes.<sup>5</sup>

Initial work is focused on understanding how different structural features of known MOFs affect the adsorption and release of phosphate. This includes investigating the role of -OH groups on both the ligand, such as in UiO-66 ( $Zr_6O_4(OH)_4(bdc-X)_6$ ), where bdc = benzenedicarboxylate and X = OH, COOH, and the metal nodes as with the MIL-125 ( $Ti_8O_8(OH)_4(bdc)_6$ ) series. We are also exploring the role of the metal in isostructural MOFs such as the MFM-300 series [ $M_2(OH)_2(C_{16}O_8H_4)$ ], where  $C_{16}O_8H_4$  = biphenyl-3,3',5,5'-tetracarboxylic acid. The experimental work will be undertaken alongside molecular simulation, in order to enhance the understanding of how phosphate interacts with the MOFs and what factors affect the amount of phosphate adsorbed.

#### **Image 1:**



- References:** (1) E. Desmidt, K. Ghyselbrecht, Y. Zhang, L. Pinoy, B. Van der Bruggen, W. Verstraete, K. Rabaey B. Meesschaert, Global Phosphorus Scarcity and Full-Scale P-Recovery Techniques: A Review, *Crit. Rev. Env. Sci. Tec.*, 2015, 45:4, 336-384
- (2) B.K. Mayer, L. A. Baker, T. H. Boyer, P. Drechsel, M. Gifford, M.A. Hanjra, P. parameswaran, J. Stoltzfus, P. Westerhoff, B. E. Rittmann., Total value of phosphorus recovery, *Environ. Sci. Technol.*, 2016, 50, 6606-6620
- (3) P. Loganathan , S. Vigneswaran , J. Kandasamy, N. S. Bolan, Removal and Recovery of Phosphate From Water Using Sorption, *Crit. Rev. Env. Sci. Tec.*, 2014, 44:8, 847-907,
- (4) S. Daneshgar, A. Callegari, A. G. Capodaglio, D. Vaccari., The Potential Phosphorus Crisis: Resource Conservation and Possible Escape Technologies: A Review, *Resources*, 2018, 7,37
- (5) S. Dhaka, R. Kumar, A. Deep, M. B. Kurade, S. Ji, B. Jeon, *Coord. Chem. Rev.*, 2019, 380, 330–352

**Metal-Organic Framework Composites for Pertechnetate Testing and Remediation**

T. S. Crickmore<sup>1,\*</sup>, A. B. Cundy<sup>2</sup>, P. Warwick<sup>2</sup>, D. Bradshaw<sup>1</sup>

<sup>1</sup>Department of Chemistry, <sup>2</sup>GAU Radioanalytical, University of Southampton, Southampton, United Kingdom

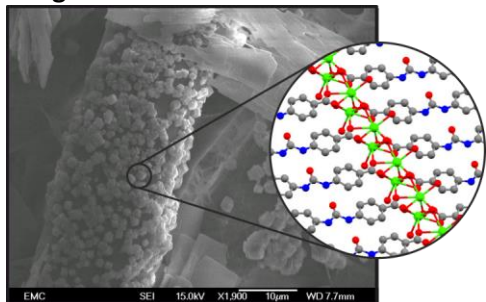
**Abstract Text:**

Nuclear energy has provided a reliable baseload to the UK national grid for over 50 years. The nuclear fission of uranium-235 fuel however produces a variety of high concentration radionuclides, such as technetium-235, which require careful disposal and handling. Technetium most commonly exists as the highly soluble, unreactive and hence mobile pertechnetate ( $\text{TcO}_4^-$ ) anion. When these properties are combined with technetium's extremely long half-life of over 200,000 years, it is clear that any releases into the environment pose a great threat. There is therefore a demand for novel materials that can selectively remove pertechnetate from contaminated groundwater.<sup>1</sup> Additionally, the development of quick and simple analytical methods to confirm the presence of radionuclides, such as  $\text{TcO}_4^-$ , in groundwater are also of utmost importance to allow for effective clean-up. Metal-organic frameworks (MOFs) have been demonstrated as potential materials for the remediation of a vast range of anions, including pertechnetate.<sup>2,3</sup> The potential porosity, chemical and physical stabilities as well as the structural diversity of these material classes make them so attractive to work with. The processing of MOFs into application specific composites is however essential for their upscale and use in many industrial applications. Highly sustainable biopolymers such as alginate, gelatin and cellulose have been incorporated with MOFs into composite hydrogels, aerogels and even fibres.<sup>4</sup> Biopolymer scaffolds carry the benefits of being non-toxic, cheap and easily processable.

Our work explores the synthesis and processing of both novel and existing MOFs (including  $\text{Ca}(\text{BDC})(\text{H}_2\text{O})_3$  (BDC = terephthalic acid) and  $\text{UiO-66-NH}_2$ )<sup>5</sup> into various bio composites. We have tailored our composites towards two different pertechnetate remediation scenarios: (1) quick spot analytical testing of potentially contaminated water samples, and (2) selective remediation of pertechnetate. Each requires a different strategy for optimal effectiveness and hence a different composite configuration. For analytical use we have deposited MOFs on non-functionalised cellulose paper to explore MOF@cellulose composites for dip stick testing of radionuclide contaminated water samples, and for pertechnetate remediation MOF@alginate composite beads have been synthesised to improve material handling and recycling.

All composite materials have been fully characterised by scanning electron microscopy, powder X-ray diffraction and thermogravimetric analysis. Our presented preliminary uptake data will guide further development and materials optimisation.

**Image 1:**



- References:** 1. J. Li, X. Dai, L. Zhu, C. Xu, D. Zhang, M. A. Silver, P. Li, L. Chen, Y. Li, D. Zuo, H. Zhang, C. Xiao, J. Chen, J. Diwu, O. K. Farha, T. E. Albrecht-Schmitt, Z. Chai and S. Wang, *Nat. Commun.*, 2018, 9, 3007.  
2. R. J. Drout, K. Otake, A. J. Howarth, T. Islamoglu, L. Zhu, C. Xiao, S. Wang and O. K. Farha, *Chem. Mater.*, 2018, 30, 1277.

3. H. Fei, M. R. Bresler and S. R. J. Oliver, *J. Am. Chem. Soc.*, 2011, 133, 11110.
4. A. Garai, W. Shepherd, J. Huo and D. Bradshaw, *J. Mater. Chem. B*, 2013, 1, 3678.
5. T. Hashem, A. H. Ibrahim, C. Wöll and M. H. Alkordi, *ACS Appl. Nano Mater.*, 2019, 2, 5804.

## ***New Synthetic Methods and Post-Synthetic Modification***

FEZA21-PO-360

### **Green Solvents based ZIF-90 Synthesis and its Use in Mixed Metal Framework Synthesis**

A. Škrjanc<sup>1,2,\*</sup>, C. Byrne<sup>1</sup>, N. Zabukovec Logar<sup>1,2</sup>

<sup>1</sup>Department of Inorganic Chemistry and Technology, National Institute of Chemistry, Ljubljana, <sup>2</sup>Graduate School, University of Nova Gorica, Nova Gorica, Slovenia

**Abstract Text:** Zeolitic imidazolate frameworks (ZIFs) have so far shown very promising results as functional materials for gas storage, separation, and catalysis applications. From the wide array of known ZIFs, ZIF-8 and ZIF-90, built from Zn-ions that are connected through 2-methylimidazolate or 2-carboxaldehyde imidazolate linkers into three-dimensional framework structures, make up more than half of all articles on ZIFs in the last 10 years. Their potential use in large-scale applications as functional materials also poses the question of atom economy in their synthesis, as well as its environmental impact. Implementation of greener solvents is one of the first approaches in reducing the environmental impact of ZIF synthesis. While some ZIFs have already been synthesised in green solvents like methanol or water, ZIF-90 nanoparticle synthesis still largely relies on *N,N*-dimethylformamide (DMF) as a solvent.

Here we present the use of green solvents as an alternative to dimethylformamide (DMF) in the synthesis of ZIF-90. We tested two bio-based aprotic dipolar solvents Cyrene<sup>TM</sup> and  $\gamma$ -valerolactone (GVL) to replace DMF in the synthesis. By using XRD, SEM, TG, and N<sub>2</sub>-physisorption analyses, we show that DMF can be successfully replaced by the two green solvents in the synthesis at room temperature with a high product yield. When doing the solvent substitution tests all other reagent concentrations were kept the same. While the Cyrene<sup>TM</sup> - based product shows reduced porosity after activation, the use of GVL in the synthesis resulted in materials with preserved crystallinity and porosity after activation (up to 1136 m<sup>2</sup>/g), without prior solvent exchange and a short treatment at 200 °C. The primary particles of 30 nm to 60 nm were detected in all products, which further formed agglomerates of different sizes and interparticle mesoporosity, depending on the type and molar ratios of solvents used.

Possible substitution of DMF with GVL was further checked in the synthesis procedure for mixed metal (MM) ZIF-90 synthesis. MM ZIFs have so far shown increased catalytic activity and stability, which could as such present an interesting field of framework modification. With the starting molar ratio of second metal (Cu, Co and Ni) to Zn in metal precursor solution of 0.25, we successfully prepared MM ZIF-90 products with a consistent ratio of approximately 0.14 second metal to Zn for all three frameworks and BET surface areas of around 950 m<sup>2</sup>/g.

## ***New Synthetic Methods and Post-Synthetic Modification | MOFs/Organic materials***

FEZA21-PO-363

### **Using Aerosol Assisted Chemical Vapour Deposition for the Synthesis of Metal Organic Framework Thin Films**

I. Doig<sup>1,\*</sup>, G. Hyett<sup>1</sup>, D. Bradshaw<sup>1</sup>, A. Kulak<sup>2</sup>

<sup>1</sup>Chemistry, University of Southampton, Southampton, <sup>2</sup>Chemistry, University of Leeds, Leeds, United Kingdom

#### **Abstract Text:**

Metal organic frameworks (MOFs) are highly porous materials, and consist of a metal node bridged by organic linker molecules.<sup>1</sup> Their high surface area and versatile structures<sup>2</sup> makes them highly desirable in a large number of industrial processes such as catalysis and gas separation. As MOF applications are becoming more diverse, the need for an industry suited synthetic method for MOF thin films is becoming ever more pressing. Currently many methods used for the synthesis of MOF thin films are modifications of the solvothermal synthesis, and as such are not well suited for large scale synthesis. This project focuses on the use of aerosol assisted chemical vapour deposition (AACVD), a well-established, scalable technique for the synthesis of MOF thin films.

AACVD is a variant of CVD, in which the precursors are transported via aerosol droplets. The precursors are dissolved in a suitable solvent, one that has a low vapor pressure, low viscosity and an appropriately high surface tension to endure the formation of an aerosol. The aerosol is formed using a piezoelectric humidifier, and carried into the reactor using a carrier gas. AACVD permits flexible reaction conditions, since it is carried out at low or atmospheric pressure in an open environment.<sup>3</sup>

In this project it has been demonstrated that AACVD can offer a simple and scalable synthetic route to adherent and crystalline MOF thin films. The quality of the films were judged by their crystallinity, purity, adherence and coverage of the substrate, which was optimised by changing the reaction conditions. The conditions were designed to limit MOF formation before entering the reactor, by modifying the precursor ratio and reactor temperature. Thin film thickness could be controlled by altering the quantity of precursors and run time of the reactor. Zinc oxide was deposited onto glass substrate prior to the MOF deposition to investigate the effect on the MOFs adherence, and was shown to greatly increase the adherence.

The deposition was carried out on a number of different substrate materials including the coverage of porous membranes, demonstrating its potential for the preparation of gas separation systems. A range of MOF thin films have been successfully synthesised using this technique demonstrating the versatility of the method. The film's adherence and coverage demonstrated makes these films promising for applications such as separation and catalysis.

#### **Image 1:**

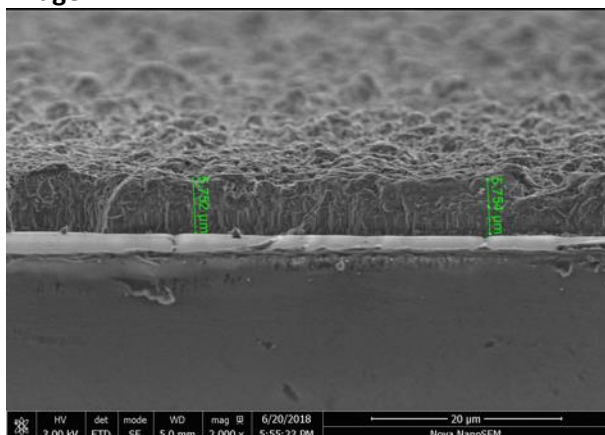
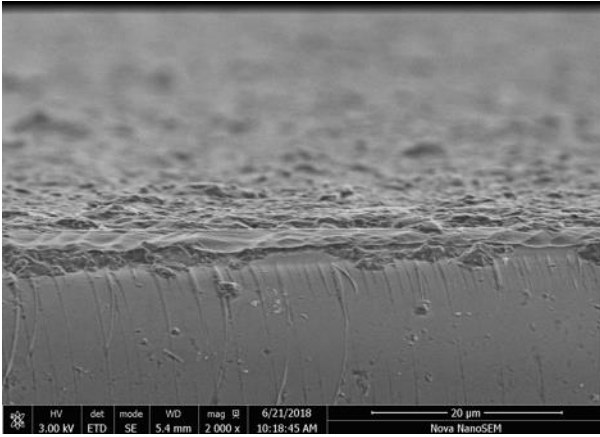


#### **Image 2:**



- References:** 1. R. B. Getman, Y.-S. Bae, C. E. Wilmer and R. Q. Snurr, *Chem. Rev.*, 2012, 112, 703–723.  
2. P. Z. Moghadam, A. Li, S. B. Wiggin, A. Tao, A. G. P. Maloney, P. A. Wood, S. C. Ward and D. Fairen-Jimenez, *Chem. Mater.*, 2017, 29, 2618–2625.  
3. X. Hou and K.-L. Choy, *Chem. Vap. Depos.*, 2006, 12, 583–596.

**Porous nickel-alumina derived from metal-organic framework : a new approach to achieve active and stable catalysts in methane dry reforming and carbon dioxide methanation.**

J. Reboul<sup>1,\*</sup>, L. Karam<sup>2</sup>, K. Jabbour<sup>2,2</sup>, N. El Hassan<sup>2</sup>, P. Massiani<sup>1</sup>

<sup>1</sup>Laboratoire de Réactivité de Surface, Sorbonne University, Paris, France, <sup>2</sup>Department of Chemical Engineering, University of Balamand, Amioûn, Lebanon

**Abstract Text:** Because of its lower cost, nickel tends to replace noble metals in the formulation of catalysts for methane dry reforming (DRM), a reaction that transforms CO<sub>2</sub> and CH<sub>4</sub> (two greenhouse gases, environmental issue) into CO and H<sub>2</sub> (syngas, a key mixture for the further production of sustainable energy). In this contribution, we will present a new strategy of synthesizing porous aluminum oxides materials containing 5 wt% Ni and high surface area that allow confining the nickel active phase inside the pores or in the oxide matrix. This leads to highly stable catalysts resistant both to Ni sintering and to carbon nanotubes formation which are two major drawbacks of existing DRM catalysts. The innovative route of preparation, differing from the usual impregnation of preformed metal oxide supports, is using an aluminum-based MOF as alumina precursor submitted to a thermal treatment after being impregnated with a nickel cations precursor.

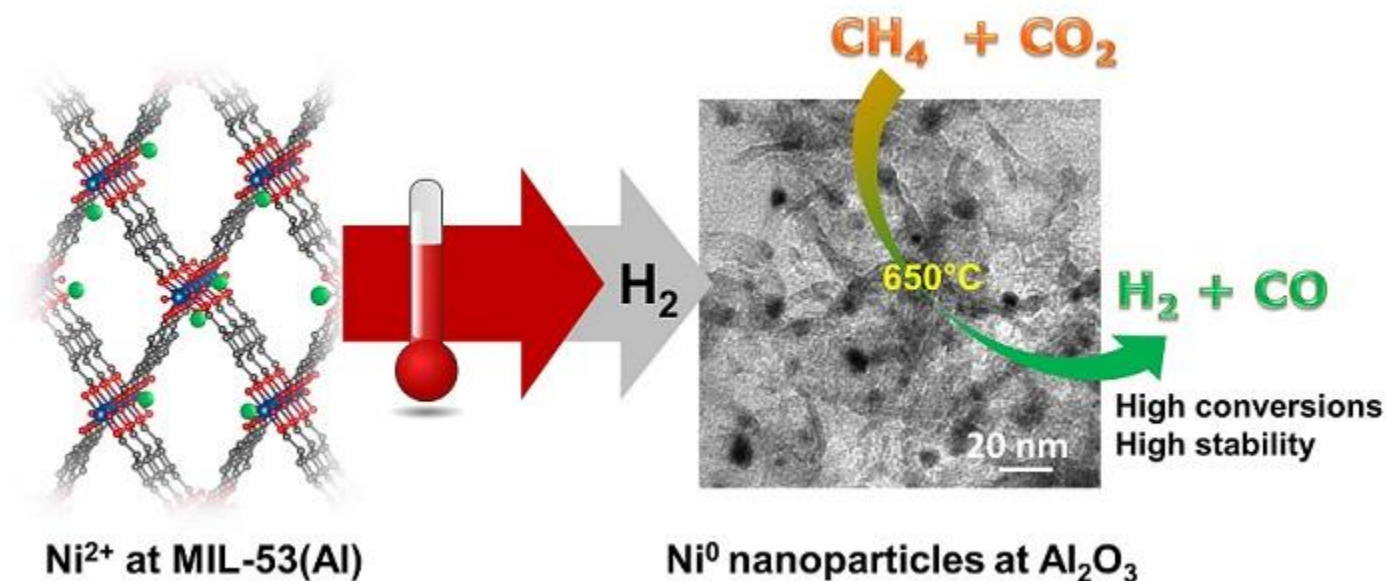
The structure, porous characteristics, morphologies and reducibility of the obtained Ni-alumina material will be discussed (XRD, N<sub>2</sub> physisorption, electron microscopy and TPR). Its catalytic behaviors will be tested and compared to those of a conventional Ni-impregnated catalyst and to a nickel-based ordered mesoporous catalyst recently described by our group and whose original "one-pot" synthesis and characteristics will be briefly introduced in this presentation. A special attention will be paid to catalytic stability during long term DRM tests carried out at the high temperatures (650-800°C) imposed by the thermodynamic of the reaction.

After reduction, the new MOF-derived catalyst contain small nickel nanoparticles homogeneously dispersed in the alumina support matrixes that appears as interwoven alumina sheets (Figure 1). This morphology agrees with the N<sub>2</sub> physisorption isotherms of the sample obtained after calcination that reveal porous characteristics of lamellar materials with intergranular macroporosity. The high reduction temperature during TPR (800-900°C) analysis of the calcined material reveals an intimate mixing between the nickel phase and the oxide support. It leads to an unusual stability of the nickel nanoparticles formed after reduction, with the absence of both Ni sintering and of related carbon deposit generation after test, in spite of the harsh conditions of the DRM reaction.

The catalytic performances are excellent, both in terms of conversion and selectivity to DRM, and much higher than those of the nickel alumina catalyst prepared by conventional impregnation. The origin of the nickel stability in this new catalyst will be discussed, notably by considering the formation of an intermediate nickel aluminate phase that appears to be at the origin of the nickel active nanoparticle stability.

Finally a greener approach of the catalyst synthesis will be also described based on the use of recycled sources of the MOF organic linker.

Image 1:



**References:** Leila Karam, Julien Reboul, Nissrine El Hassan, Jaysen Nelayah, Pascale Massiani *Molecules* 2019, 24(22), 4107.

Leila Karam, Julien Reboul, Sandra Casale, Pascale Massiani, Nissrine El Hassan *ChemCatChem* 2020,12,19012.

***New Synthetic Methods and Post-Synthetic Modification | MOFs/Organic materials***

FEZA21-PO-366

**Synthesis of New Hybrid NHC-Based Pd Catalysts for Suzuki-Miyaura Reactions**

C. Segarra<sup>1,\*</sup>, M. C. Hernández-Soto<sup>1</sup>, A. Erigoni<sup>1</sup>, U. Díaz<sup>1</sup>, F. Rey<sup>1</sup>

<sup>1</sup>Universitat Politècnica de València, Instituto de Tecnología Química, Valencia, Spain

**Abstract Text:**

In the last years the design of new hybrid organic-inorganic catalysts based on organocatalysts incorporated into inorganic supports is becoming an area of growing interest due to their specific physical and chemical properties. The use of these hybrid catalysts allows the combination of increased flexibility, functionality and efficiency from homogeneous catalysts, with the thermal and mechanic stability advantages of inorganic solids, leading to 'green catalytic processes', with higher selectivity and conversion and easy catalyst recovery.<sup>1-3</sup>

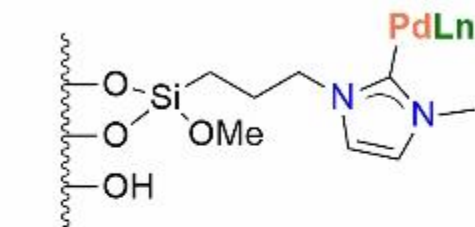
This work has been developed under the proposed objectives from MULTI2HYCAT project, and focuses on the synthesis and characterization of a new class of organometallic hybrid materials, besides the catalytic activity of these materials has been evaluated in model reactions.

Specifically, Palladium hybrid catalysts, based on silyl-derivatives of *classical* and *abnormal* NHCs have been successfully achieved through post synthetic grafting on the surface of pure silica MCM-41. Different characterization techniques were implemented to study the properties of the materials, such as solid-state NMR, elemental analysis, X-ray diffraction (XRD), N<sub>2</sub> physisorption analysis, XPS spectroscopy and ICP-AES analysis. Finally, the catalytic activity and recyclability of these compounds was demonstrated for cross-coupling reactions such as Suzuki-Miyaura reaction under mild conditions.

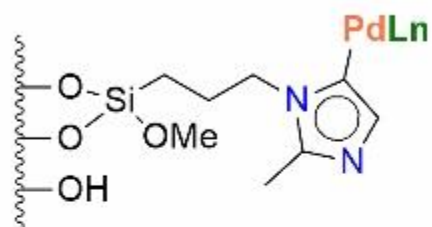
The authors are grateful for financial support from the European Union by the MULTY2HYCAT EUHorizon 2020 funded project under grant agreement no. 720783.

Image 1:

### Hybrid Pd-NHC Catalysts

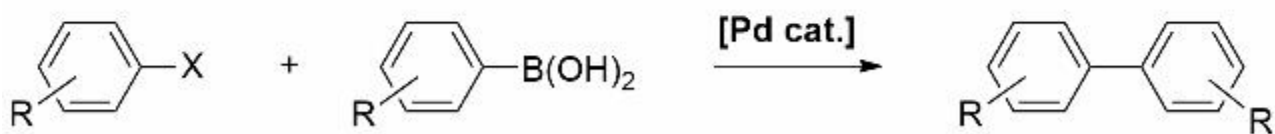


MCM-41



MCM-41

### Suzuki-Miyaura Reaction



X = Cl, Br, I  
R = H, Me, OMe

#### References:

1. Diaz, U.; Brunel, D.; Corma, A. Catalysis using multifunctional organosiliceous hybrid materials. *Chem. Soc. Rev.* 2013, 42, 4083–4097.
2. Ranganath, K. V. S.; Onitsuka, S.; Kumarc, A. K.; Inanaga, J. Recent progress of N-heterocyclic carbenes in heterogeneous catalysis. *Catal. Sci. Technol.* 2013, 3, 2161–2181.
3. Zhong, R.; Lindhorst, A. C.; Groche, F. G.; Kühn, E. F. Immobilization of N-Heterocyclic Carbene Compounds: A Synthetic Perspective. *Chem. Rev.* 2017, 117, 1970–2058.

**Dynamic Covalent Exchange on Metal-Organic Framework Nanoparticles**

A. K. Edward<sup>1,\*</sup>, E. R. Kay<sup>1</sup>, R. E. Morris<sup>1,2</sup>

<sup>1</sup>School of Chemistry, University of St Andrews, St Andrews, United Kingdom, <sup>2</sup>Department of Physical and Macromolecular Chemistry, Faculty of Sciences, Charles University, Prague, Czech Republic

**Abstract Text:**

Metal-organic frameworks (MOFs) are highly porous, complex 3D structures with flexibility in their chemical nature, which have become an immensely prevalent area of materials science over the past few decades.<sup>1,2</sup> On reducing the particle size of these materials to the nanoscale, MOF nanoparticles (MOF NPs) can also incorporate the inherent benefits of nanomaterials, such as their controllable outer surface properties and high external surface-area-to-volume ratio.<sup>1</sup> This affords the opportunity to tune the architecture of the MOF NPs by selectively utilising properties from both the MOF- and nano-fields. In particular, this is useful in controlling the outer surface modification of MOF NPs providing access to a range of applications. With the ability to incorporate different chemical entities either directly through the diverse chemical building units, or post-synthetically by covalent modification of the linker and/or coordination to the metal, MOF NPs have the ability to introduce many functional groups into their structure.<sup>2</sup>

One such functionalisation is the introduction of 'gated' or 'switchable' behaviour and involves the controlled opening/closing mechanism of MOF pores by some external or chemical stimulus. This enables the ability to control the loading and release of cargoes into and out of the pores of the MOF. Previous approaches to this have seen a focus on using 'capping' units which can be removed by external triggers such as competitive ion binding, temperature or pH changes or in using functional groups which switch between molecular states upon application of a stimulus.<sup>3,4</sup> One scarcely researched area in MOF NPs is the introduction of dynamic covalent chemistry (DCvC), such as those introduced onto the surface of monolayer-stabilised gold nanoparticles.<sup>5</sup>

In this work, we aim to incorporate the concept of DCvC onto the surface of MOF NPs, with the goal of controlling access to the internal pore surface of the MOF. We have first synthesised MOF NPs of UiO-66 with reactive capping units, which should allow the introduction of DCvC functionality. We then carried out extensive dynamic light scattering studies of these materials to investigate their colloidal stability in various solvents.

**References:**

1. P. Hirschle, T. Preiß, F. Auras, A. Pick, J. Völkner, D. Valdepérez, G. Witte, W. J. Parak, J. O. Rädler and S. Wuttke, *CrystEngComm*, 2016, 18, 4359-4368.
2. S. Wang, C. M. McGuirk, A. d'Aquino, J. A. Mason and C. A. Mirkin, *Adv. Mater.*, 2018, 30, 1800202.
3. F. Bigdeli, C. T. Lollar, A. Morsali and H.-C. Zhou, *Angew. Chem. Int. Ed.*, 2019, 58, 2-20.
4. L.-L. Tan, N. Song, S. X.-A. Zhang, H. Li, B. Wang and Y. -W. Yang, *J. Mater. Chem. B.*, 2016, 4, 135-140.
5. E. R. Kay, *Chem. Eur. J.*, 2016, 22, 10706-10716.

## Novel Materials and Structural Methods

FEZA21-PO-368

### Preparation of Metal-Organic Framework Hybrid Ceramics

L. N. Mchugh<sup>1,\*</sup>, M. F. Thorne<sup>1</sup>, G. Divitini<sup>1</sup>, G. Robertson<sup>1</sup>, T. D. Bennett<sup>1</sup>

<sup>1</sup>Department of Materials Science & Metallurgy, University of Cambridge, Cambridge, United Kingdom

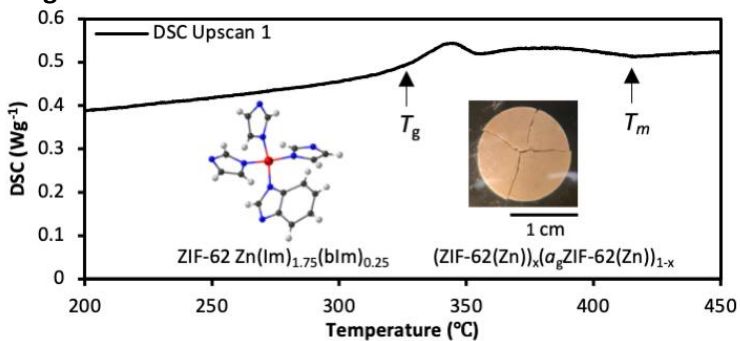
**Abstract Text:** Metal-organic framework crystal-glass composite (MOF-CGC) materials are composed of a crystalline MOF dispersed within a MOF-glass ( $a_g$ MOF) matrix.<sup>1</sup> Previous studies have illustrated the incorporation of MOFs of a different chemical composition into  $a_g$ ZIF-62(Zn),<sup>2</sup> though here we demonstrate the synthesis of novel systems, where crystalline ZIF-62(Zn) is incorporated within an  $a_g$ ZIF-62(Zn) matrix and which we have termed 'hybrid ceramics'.<sup>3</sup> Hybrid ceramics are analogous to traditional inorganic ceramics and may be distinguished from conventional MOF-CGCs by the interfacial compatibility observed between the glassy and crystalline phases within the materials.

ZIF-62(Zn) [Zn(Im)<sub>1.75</sub>(blm)<sub>0.25</sub>] was chosen as the source MOF due to its well-documented thermal properties and glass-forming ability.<sup>4</sup> Mechanochemically synthesised crystalline ZIF-62(Zn) and pre-formed  $a_g$ ZIF-62(Zn) were combined together in the desired ratios, before being pelletised and heated to above the glass transition temperature ( $T_g$ ) of ZIF-62(Zn), to form hybrid ceramics of composition: (ZIF-62(Zn))<sub>x</sub>( $a_g$ ZIF-62(Zn))<sub>1-x</sub>.

DSC scans (Image 1) showed that the ceramics displayed both a  $T_g$  and a melting point ( $T_m$ ) on the first upscans, indicating that the materials contained both glassy and crystalline components and powder X-ray diffraction demonstrated that Bragg scattering from the crystalline phase remained present within the ceramics. SEM suggested good interfacial compatibility between the crystalline and glassy phases in the ceramics and this was further investigated by SEM/EDX using a mixed-metal (ZIF-62(Co))<sub>x</sub>( $a_g$ ZIF-62(Zn))<sub>1-x</sub> ceramic.

The results provide exciting prospects for future research, where other crystalline ZIF phases may be encapsulated within their corresponding glasses. Due to the relative rarity of DSC in MOF literature, many more glass-forming MOFs that have not yet been investigated may be available to synthesise further hybrid ceramics.

**Image 1:**



**References:** (1) J. Hou et al., Nat. Commun., 2019, 10, 2580.

(2) C.W. Ashling et al., J. Am. Chem. Soc., 2019, 141, 15641-15648.

(3) L.N. McHugh et al., manuscript in preparation, 2021.

(4) A. Qiao et al., Sci. Adv., 2018, 4, eaao6827.

## ***Novel Materials and Structural Methods***

FEZA21-PO-369

### **Predicting the packing behaviour of porous organic cages**

E. H. Wolpert<sup>1,\*</sup>, K. E. Jelfs<sup>1</sup>

<sup>1</sup>Department of Chemistry, Imperial College London, London, United Kingdom

**Abstract Text:** Porous organic cages are a subset of porous materials which are made up of covalently bonded organic molecules forming cages with intrinsic porosity. Unlike extended framework materials, such as metal organic frameworks which are connected through covalent or coordination bonds, the assembly of porous organic cages is defined by weak dispersion forces. Therefore, the connectivity between the cages can be easily manipulated by varying the chemical functionality or solvent [1]. This leads to a variety of porous organic cage solids which, depending on the packing behaviour, may contain only intrinsic cavities or have extrinsic pores between the cages resulting in one, two, or, three dimensional pore networks [2]. Consequently, the packing behaviour of the porous organic cages can have a vast effect on the properties of the material [3]. It has been suggested that in principle, different cages can be combined to produce structures with specific properties [4]. However, the challenge in reliably predicting the packing behaviour of molecular crystals, due to the lack of strong bonding networks, results in difficulty in targeted design [4].

Although crystal structure prediction can accurately determine crystal energy landscapes, it is computationally expensive to apply to multiple molecular combinations [5]. Here we aim to determine the packing behaviour of porous organic cages through coarse graining. We start by creating a coarse grained Hamiltonian containing the dominant intermolecular interactions between the cages, informed by force field models. We then aim to employ Monte Carlo simulations using our model in conjunction with hard particle Monte Carlo simulations [6] to determine the thermodynamic phase behaviour of the packing of the cages. This work focuses on the well-studied porous organic cage CC3 [1] as a proof-of-concept example to determine the extent to which we can use coarse graining to analyse the packing behaviour of other, less well-studied porous organic cages.

**References:** 1. T. Tozawa, J. Jones, S. Swamy, et al. *Nature Mater* 8, 973–978 (2009)

2. Y. Liu, G. Zhu, W. You, et al. *J. Phys. Chem. C* 123, 3, 1720–1729 (2019)

3. M. E. Briggs and A. I. Cooper *Chem. Mater.* 29, 1, 149–157 (2017)

4. J. Jones, T. Hasell, X. Wu, et al. *Nature* 474, 367–371 (2011)

5. T. Hasell, S. Y. Chong, K. E. Jelfs, et al. *J. Am. Chem. Soc.* 134, 1, 588–598 (2012)

6. J. A. Anderson, M. E. Irrgang, and S. C. Glotzer. *Computer Physics Communications* 204, 21-30 (2016)

## **Novel Materials and Structural Methods**

FEZA21-PO-370

### **Developing multivariate metal organic frameworks under non-conventional synthesis**

E. Ezzatpour Ghadim<sup>1,\*</sup>, R. I. Walton<sup>1</sup>, R. Jalali Kashtiban<sup>2</sup>

<sup>1</sup>Chemistry, <sup>2</sup>Physics, university of Warwick, Coventry, United Kingdom

**Abstract Text:** Multivariate (MTV) metal organic frameworks (MOFs) containing multiple metals and ligands in ordered arrangements, allow the controllable one-pot synthesis of hierarchical MOFs, MOF-on-MOF and core-shell structures.<sup>1</sup> This notable synthetic achievement not only develops the impact of tunability to form multicomponent MOFs, but also provides a facile route to complex three-dimensional functional systems.<sup>2</sup> The UiO-n family is an important candidate to be used in MTV MOFs, because of its noted thermal and chemical stability, and the versatile range of ligands and metals possible for its construction.<sup>3</sup> In this work, one-pot MTV-MOFs with the UiO-66 structure were synthesised using a microwave reactor in a short periods of time. Ce-BDC-NDC-Zr-UiO-66 and Ce-BDC-ABDC-Zr-UiO-66 (BDC: 1,4-benzenedicarboxylate, NDC: 1,4-naphthalenedicarboxylate, ABDC: 2-amino-1,4-benzenedicarboxylate) were synthesised in 50% DMF, 25% water, and 25% acetic acid, at 120 °C in merely 15 min

Multi-length scale characterisation using HR-TEM (high resolution-transmission electron microscopy), SEM (scanning electron microscopy), EDX (energy-Dispersive X-ray), PXRD (Powder X-ray diffraction), FT-IR (Fourier- transform infrared), and SAXS (small-angle X-ray scattering) show that multiple metals and linkers are homogenously distributed through the crystal structure with no phase impurities. In addition, PXRD, TEM and SAXS clearly shows that these MTV MOFs are nanocrystalline with crystallite size between 10 and 20 nm, and EDX (elemental analysis and mapping) shows that there is an almost equal molar ratio of cerium and zirconium. The hydrothermal stability was studied, and it is shown that Ce-BDC-ABDC-Zr-UiO-66 is stable at in 120 °C for 24 hours in water. The XRD and SEM showed that there are no changes in crystallinity and morphology of particles after hydrothermal treatment.

#### **References:**

1. Feng, L.; Wang, K.-Y.; Day, G. S.; Zhou, H.-C., The chemistry of multi-component and hierarchical framework compounds. *Chemical Society Reviews* 2019, 48 (18), 4823-4853.
2. Feng, L.; Yuan, S.; Li, J.-L.; Wang, K.-Y.; Day, G. S.; Zhang, P.; Wang, Y.; Zhou, H.-C., Uncovering Two Principles of Multivariate Hierarchical Metal–Organic Framework Synthesis via Retrosynthetic Design. *ACS Central Science* 2018, 4 (12), 1719-1726.
3. Winarta, J.; Shan, B.; McIntyre, S. M.; Ye, L.; Wang, C.; Liu, J.; Mu, B., A Decade of UiO-66 Research: A Historic Review of Dynamic Structure, Synthesis Mechanisms, and Characterization Techniques of an Archetypal Metal–Organic Framework. *Crystal Growth & Design* 2020, 20 (2), 1347-1362.

***Novel Materials and Structural Methods***

FEZA21-PO-371

**Structure Exploration of Molecule Docking in Functionalized UiO-66.**

M. Nurhuda\*, M. Addicoat<sup>1</sup>

<sup>1</sup>Chemistry, Nottingham Trent University, Nottingham, United Kingdom

**Abstract Text:** Metal–organic frameworks (MOFs) have been highlighted as ideal candidates for the 3D support of drug molecules. The linkers are often functionalized with the rationale being to fine-tune the physical and chemical properties of the MOF, allowing control over host-guest interactions necessary for selectivity and providing additional adsorption sites.

The structure of the molecule@MOF composite, arises from a delicate balance of interactions between the molecule with the MOF and the conformational isomerism of the MOF itself. We have developed a computational model to explore the structure of functionalised UiO-66, X-UiO-66, which can identify ideal environments for drug molecule docking. We investigated the binding interaction of the molecules in both the tetrahedral and octahedral pores of X-UiO-66 by constructing all the possible arrangement of the functional groups followed by DFTB calculations. Preliminary results show that drug molecules are likely to bind in the region of the linker functional groups, with especially favourable configurations being possible where the spatial arrangement of linker functional groups allows for the molecule to bridge between the linkers or/and with the metal oxide node.

## **Novel Materials and Structural Methods**

FEZA21-PO-372

### **Synthesis and optimization of porous bioMOF**

T. K. Tajnšek<sup>1,\*</sup>, M. Mazaj<sup>1</sup>, N. Zabukovec Logar<sup>1,2</sup>

<sup>1</sup>Department of Inorganic Chemistry and Technology, National Institute of Chemistry, Ljubljana, <sup>2</sup>University of Nova Gorica, Nova Gorica, Slovenia

**Abstract Text:** Metal-organic frameworks (MOFs) with their specific properties and possibility of tuning the structure represent excellent candidates for use in biomedical field. Their advantage lies in large pore surfaces and volumes as well as the possibility of using bio-friendly or bioactive constituents. So-called bioMOFs are representatives of MOFs which are constructed from at least one biomolecule (metal, small bioactive molecule in metal clusters and/or linker) and are intended for bio-application (usually in the field of medicine; most commonly drug delivery). When designing a bioMOF for biomedical application, we should adhere to some guidelines for an improved toxicological profile of the material. Such as, (i) choosing an endogenous / nontoxic metal, (ii) GRAS (generally recognised as safe) linker and (iii) nontoxic solvents.

Design and synthesis of bioNICS-1 (bioMOF of National Institute of Chemistry Slovenia – 1) considers all these guidelines. Zinc (Zn) was chosen as an endogenous metal with an agreeable recommended daily intake (RDI) and LD<sub>50</sub> value, and ascorbic acid (Vitamin C) was chosen as a GRAS and active linker. With these building blocks, we have synthesised a bioNICS-1 material. Synthesis was done in ethanol using solvothermal method.

Synthesis protocol was further optimized in three separate ways. Optimization of (i) synthesis parameters to improve the yield of the synthesis, (ii) input reactant ratio and addition of specific modulators for production of larger crystals and (iii) differing of the heating source (conventional, microwave and ultrasound) to produce nano-crystals. With optimization strategies, synthesis yield was increased. Larger crystals were prepared for structural analysis with the use of a proper species and amount of modulator. Synthesis protocol was adjusted to different heating sources, resulting in production of nano-crystals of bioNICS-1 material.

BioNICS-1 was further activated in ethanol and structurally characterized, resolving the crystal structure of a new material.

#### **References:** 1.

Cai, H., Huang, Y.-L. & Li, D. Biological metal-organic frameworks: Structures, host-guest chemistry and bio-applications. *Coord. Chem. Rev.* 378, 207–221 (2019).

2.

Simon-Yarza, T., Mielcarek, A., Couvreur, P. & Serre, C.

Nanoparticles of Metal-Organic Frameworks: On the Road to In Vivo Efficacy in Biomedicine. *Advanced Materials* vol. 30 1707365 (2018).

## Isorecticular Expansion in Phosphonate Metal Organic Frameworks for Multiple Applications

P. Tholen<sup>1,\*</sup>, G. Yücesan<sup>1</sup>

<sup>1</sup>Institut für Lebensmitteltechnologie und Lebensmittelchemie, TU Berlin, Berlin, Germany

**Abstract Text:** Phosphonate metal organic frameworks (phosphonate-MOFs) constitute a very tiny fraction of the MOFs reported in the literature<sup>1</sup>. Due to the presence of two negative charges on the phosphonate metal binding group and a strong phosphorus-carbon bond, phosphonate-MOFs are an exceptionally stable platform to construct MOFs<sup>1,2</sup>. To date, only a few random isorecticular expansions are reported with phosphonate-MOFs<sup>3-6</sup>. This study focuses on the synthesis of longer tethered phosphonate MOFs with tetrahedral linkers, namely tetra(4-phosphonatophenyl)methane and tetra(4-phosphonatophenyl)silane and their analogs with expanded tethers, namely tetra(4'-phosphonato-1,1'-biphenyl)methane and -silane as well as tetra(4''-phosphonato-[1,1':4'-1''-terphenyl])methane and -silane (see image 1). The linkers have been synthesized using the combination of Arbuzov and Suzuki Cross Coupling reactions<sup>7</sup> and we have used hydrothermal reactions at varying temperatures to obtain the corresponding phosphonate-MOFs (schematics see image 2). Further analysis of the MOFs have been performed by single crystal X-ray diffraction or powder XRD, TGA, BET and UV-Vis.

We would like to thank the DFG for funding our work with grant number DFG YU 267/2-1.

### Image 1:

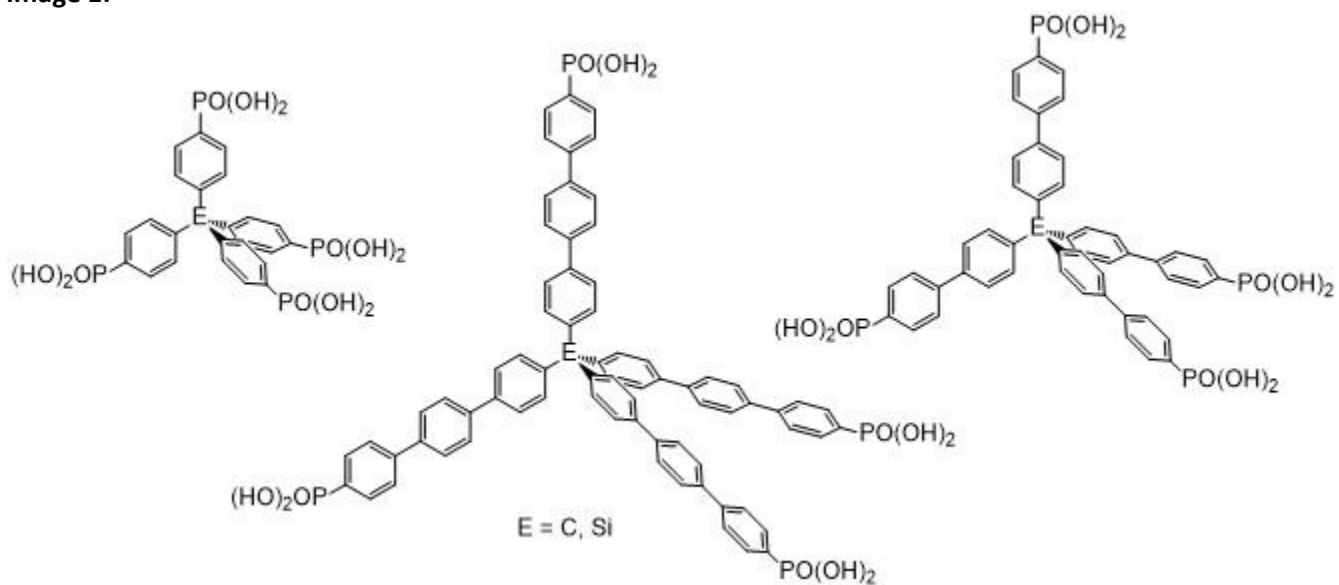
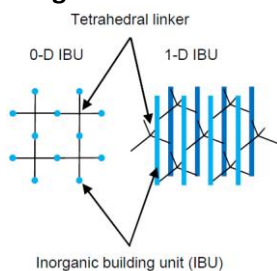


### Image 2:



**References:** 1) G. Yücesan, Y. Zorlu, M. Stricker, J. Beckmann, *Coordination Chemistry Reviews* 2018, 369, 105-122.  
2) S. J. Shearan, N. Stock, F. Emmerling, J. Demel, P. A. Wright, K. D. Demadis, M. Vassaki, F. Costantino, R. Vivani, S. Sallard, I. Ruiz Salcedo, A. Cabeza, M. Taddei, *Crystals* 2019, 9, 5, 270.

- 3) A. Schütrumpf, A. Bulut, N. Hermer, Y. Zorlu, E. Kirpi, N. Stock, A. Ö. Yazaydın, G. Yücesan, J. Beckmann, *ChemistrySelect* 2017, 2, 3035-3038.
- 4) A. Schütrumpf, E. Kirpi, A. Bulut, F. L. Morel, M. Ranocchiari, E. Lork, Y. Zorlu, S. Grabowsky, G. Yücesan, J. Beckmann, *Cryst. Growth Des.* 2015, 15, 4925-4931.
- 5) A. Bulut, Y. Zorlu, E. Kirpi, A. Çetinkaya, M. Wörle, J. Beckmann, G. Yücesan, *Cryst. Growth Des.* 2015, 15, 5665-5669.
- 6) C.-Y. Gao, J. Ai, H.-R. Tian, D. Wu, Z.-M. Sun, *Chem. Commun.* 2017, 53, 1293-1296.
- 7) A. Schütrumpf, A. Duthie, E. Lork, G. Yücesan, J. Beckmann, *Z. Allgem. Anorg. Chem.* 2018, 644, 19, 1134-1142.

## ***Novel Materials and Structural Methods | MOFs/Organic materials***

FEZA21-PO-376

### **High-throughput computational design and discovery of conductive materials in the CSD MOF subset**

F. Zanca<sup>1,\*</sup>, S. Chong<sup>2</sup>, B. Monserrat<sup>3</sup>, D. Fairen-Jimenez<sup>4</sup>, P. Z. Moghadam

<sup>1</sup>Chemical and biological engineering, University of Sheffield, Sheffield, United Kingdom, <sup>2</sup>Department of Chemical and Biomolecular Engineering, Korea Advanced Institute of Science and Technology (KAIST), Daejeon, Korea, Republic Of,

<sup>3</sup>Cavendish Laboratory, <sup>4</sup>Department of Chemical Engineering & Biotechnology, University of Cambridge, Cambridge, United Kingdom

**Abstract Text:** MOFs are innovative porous materials, and have been widely studied for the past 15 years for applications in different fields such as gas storage, gas separation and catalysis. Here, we aim to study electrical conductivity in MOFs, a less explored property that can be investigated for e.g. energy storage and sensing application. Due to their high porosity and surface area, MOFs are poor electrical conductors. In order to characterise and identify promising conductive structures, we performed high-throughput screening of the existing ca. 90,000 structures in the CSD MOF subset<sup>1</sup>— characterising the band gap and examining the presence or absence of metallic behavior. The first set of selection criteria was developed based on the nature of MOFs' surface chemistry with a focus on the type of the secondary building unit and the ligand. We focused on MOFs containing open shell metals, metal clusters and highly conjugated linkers that can facilitate through-linker charge transfer between metals. The second set of criteria involved the presence of linkers containing metal-S, -N or -O coordination, redox-active linkers,  $\pi$ - $\pi$  stacking, and mixed valence metals. For the ca. 1000 structures shortlisted, we then performed DFT calculations to derive useful insights into structure-conductivity relationships in MOFs, identify top-performing conductive MOFs, and to delineate key chemical and physical features in MOFs that influence their conductive properties. The results guide MOF researchers to assess and design conductive structures for electronics, energy storage and sensing applications.

#### **References:**

[1] Peyman Z. Moghadam, Aurelia Li, Seth B. Wiggin, Andi Tao, Andrew G. P. Maloney, Peter A. Wood, Suzanna C. Ward, and David Fairen-Jimenez. (2017) *Chemistry of Materials*, 29 (7), 2618–2625

**Novel nickel MOF as highly stable heterogeneous catalyst for reductive amination**

G. Orcajo\*, H. Montes-Andrés, P. Leo, A. Muñoz, A. Rodríguez-Diéguez, C. Martos, F. Martínez, G. Calleja

**Abstract Text:** Metal-Organic Framework (MOF) materials have attracted much attention in the last two decades due to their unique properties such as topological diversity and tunable porosity and composition [1]. Traditionally, MOF materials have been extensively studied for gas adsorption; however, at present time they are being also studied for catalytic applications due to the observed activity of the metallic clusters and the functionalized organic linkers, providing redox, acidic and basic catalytic sites [2]. MOF materials can adsorb H<sub>2</sub> through mostly physisorption mechanism, so they might be potential catalysts for hydrogenation reactions. The high density of well-distributed active sites in the crystalline network and the large surface area of these materials can promote a remarkable catalytic activity in hydrogenation reactions for the production of essential intermediates and chemicals in the pharmaceutical, fragrance, food, dye, and agrochemical industries [3].

In this work, a new 3D MOF material URJC-4 (from Universidad Rey Juan Carlos), based on Ni and a tetracarboxylic acid as organic ligand has been synthesized. The material was characterized by PXRD, FT-IR, argon adsorption/desorption isotherms at 87 K and TGA analyses for evaluating its crystalline structure, porosity and thermal stability. Finally, URJC-4 material was tested as a catalyst in the reductive amination of different carbonyl molecules.

**Synthesis of tetracarboxylic acid organic ligand (5,5'-(etine-1,2-diyl)diisophthalic acid, H<sub>4</sub>EBTC).** As H<sub>4</sub>EBTC is not commercially available, it was prepared following a synthetic route in five steps, based on the Sonogashira C-C coupling reaction [4].

**Synthesis of URJC-4 material.** A mixture of H<sub>4</sub>EBTC and nickel(II) nitrate hexahydrate was dissolved in N,N dimethylformamide and subjected to solvothermal conditions.

**Catalytic reductive amination tests of carbonyl compounds.** Several types of carbonyl substrates were mixed with primary amines in toluene under magnetic stirring for 12h. After this time, TLC (silica TLC plates) determined the development of the reaction. The crude, absorbed on silica gel, was purified by flash chromatography on silica gel in order to obtain the targeted products from the reaction.

**Results and discussion**

**Crystal Structure of URJC-4 material.** URJC-4 crystallizes in the monoclinic and  $P2^1/c$  space group, showing the following unit cell parameters:  $a = 19,1972(8) \text{ \AA}$ ,  $b = 38,1664(17) \text{ \AA}$ ,  $c = 47,308(2) \text{ \AA}$ ,  $\alpha = \gamma = 90^\circ$ ,  $\beta = 90,105^\circ$ . As shown in Figure 1a, the experimental PXRD pattern of the novel material matches quite well with the simulated one from crystallographic data, indicating a high purity of the crystalline phase in the bulk sample (Figure 1a). The Ar adsorption/desorption isotherms at 87 K (Figure 1b) displayed a type I isotherm, characteristic of microporous materials, with a BET specific surface area of 829 m<sup>2</sup>/g and a pore volume of 0.3 cm<sup>3</sup>/g at P/P<sub>0</sub> of 0.998.

**Figure 1** (a) XRD patterns (experimental and simulated from single-crystal data) and (b) Ar adsorption–desorption isotherm at 87 K of URJC-4 material.

**Catalytic Activity of URJC-4 material.** Preliminary results have shown catalytic activity with different amines at room temperature, using toluene as solvent (Table 1). Besides, URJC-4 catalyst could be easily recovered, maintaining its crystalline structure after all reaction cycles. These results show the potential of URJC-4 as a catalyst in hydrogenation reactions.

**Table 1.** Reductive amination reactions between carbonyl substrates and primary amines at room temperature with URJC-4 as catalyst.

**Image 1:**

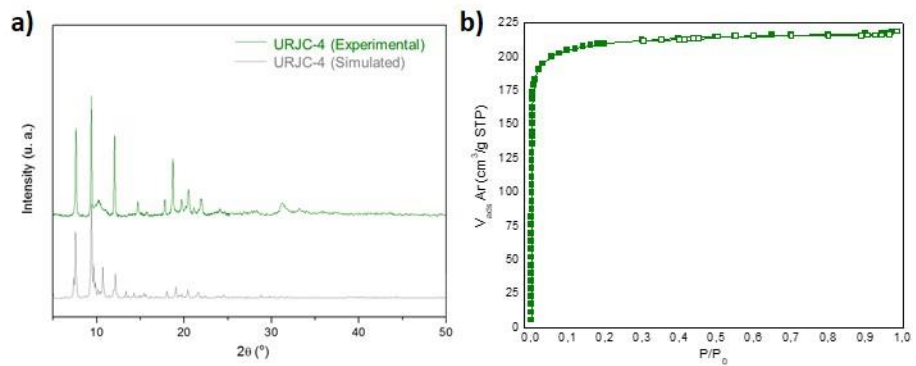
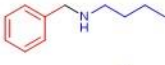
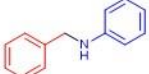
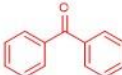
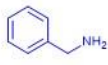
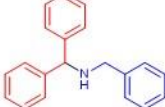


Image 2:



Entry	Sustrate A	Sustrate B	Product	Isolated Yield (%)
1				94
2				90
3				85

**References:** [1] Chem. Soc. Rev. 2016, 45, 2327–2367. [2] Chem. Rev., 2012, 112, 1126–1162. [3] Chinese Journal of Catalysis, 2017, 38, 1108–1126. [4] Sci. China Mater. 2017, 60, 1269–1271.

Redox-active metal organic frameworks constructed using novel rylene-diimides

J. O. Ogar<sup>1,\*</sup>, N. R. Champness<sup>1</sup>

<sup>1</sup>Chemistry, University of Nottingham, Nottingham, United Kingdom

**Abstract Text:** Two rylene diimide ligands, – N,N'-bis(2,6-diisopropyl-4-(pyridin-4-yl)phenyl)-1,4,5,8-naphthalenetetracarboxydiimide (DPPNDI) and N,N'-bis(2,6-diisopropyl-4-(pyridin-4-yl)phenyl)-3,4:9,10-perylenetetracarboxydiimide (DPPNDI), are used to prepare four metal-organic-framework (MOF) materials. Each of the MOFs contains a redox-active functionalised naphthalenediimide (NDI) or perylenediimide (PDI) – which acts as a pillar – in combination with a bridging carboxylate linker; all of which are coordinated to either a Co<sup>2+</sup> or Ni<sup>2+</sup> cation. The MOFs, made by solvothermal methods, were characterised using single crystal x-ray diffraction (SCXRD), powder x-ray diffraction (PXRD), thermogravimetric analysis (TGA) and cyclic voltammetry. The frameworks containing DPPNDI are all doubly interpenetrated whereas the one obtained from DPPNDI exhibits four-fold interpenetration. In terms of dimensionality, all the materials are 3-dimensional (3D) and possess the M<sub>2</sub>(μ<sub>2</sub>-O<sub>2</sub>CR)<sub>4</sub> paddle-wheel secondary building units (SBUs). These materials, due to the presence of the redox-active ligands, hold great potential for the entrapment of electron-rich species and the ability to respond to electronic stimuli through the reduction of the rylene diimide ligand.

Image 1:

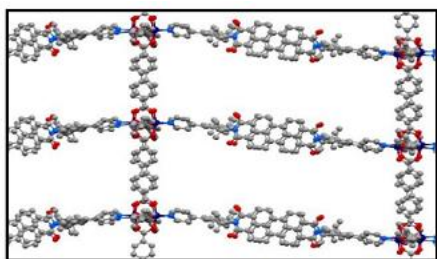


Fig. 1 Crystal structure of Co (II) DPPNDI MOF

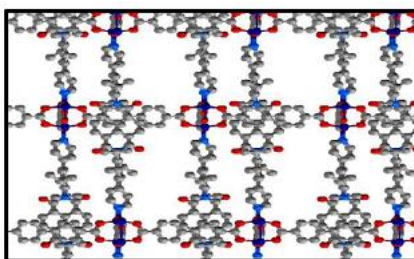


Fig. 2 Co (II) DPPNDI MOF Crystal structure

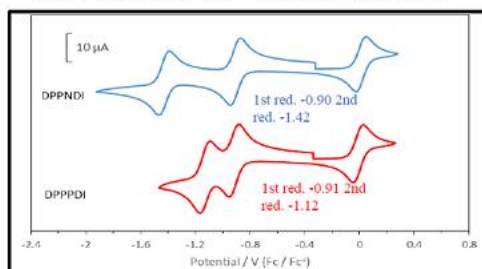


Fig. 3 Cyclic Voltammetry

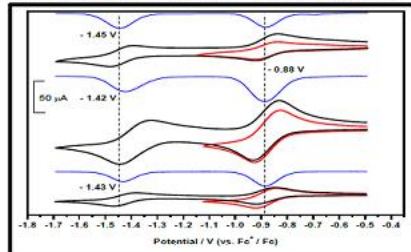


Fig. 4 Cyclic Voltammogram of the MOFs

**How MOF/Polymer Interfacial void shape/size affect the gas permeability of Mixed Matrix Membranes?**

A. Ozcan<sup>1,\*</sup>, D. Fan, R. Semino, S. Datta, M. Eddaoudi, G. Maurin

<sup>1</sup>Chemistry, Montpellier University, Montpellier, France

**Abstract Text:** Mixed matrix membranes (MMMs) incorporating Metal-organic frameworks (MOF) into polymeric matrices show promising properties for several industrial applications, such as gas separation, water desalination, and pervaporation, among others. Especially in the field of gas separation, MMMs have attracted a great attention owing to their potential for merging the processability of polymers and the excellent selectivity of MOF materials. Therefore, understanding gas transport through the MMMs is of significant importance in MOF-based materials. Here, we choose AIFVIVE-1-Ni, a MOF with a one-dimensional channel, as the filler in the polymer matrix and use our previously developed computational methods to construct a series of MOF/Polymer interfaces with the selection of both rigid and more flexible polymers.. Subsequently, we performed Grand Canonical Monte Carlo and our recently proposed concentration gradient-driven molecular dynamics (CGD-MD) simulations to assess the thermodynamic and dynamic adsorption properties of these MMMs. Our simulations showed that the distinct characteristic of polymer backbones result in different interfacial void regions. We evidenced that not only the size but also the shape of the interfacial voids region have eminent effects on the gas transport properties of the MMMs with respect to a selected range of molecules, e.g. CO<sub>2</sub>, N<sub>2</sub> and CH<sub>4</sub>. Our results constitute an important step toward the rational design of MMMs with the optimal interfacial void size/shape to achieve the highest performance for the separation of industrially relevant gas separations.

**References:** 1] Ozcan, A., Semino, R., Maurin, G., & Yazaydin, A. O. *Chem. Mater.*, 32(2020), 1288-1296; [2] Semino, R., Ramsahye, N. A., Ghoufi, A., & Maurin, G. *ACS applied materials & interfaces*, 8 (2016), 809-819.

**Illuminating ZIF-7 Metal-Organic Nanosheets by Guest@MOF dye confinement**

D. A. Sherman<sup>1,\*</sup>, J.-C. Tan<sup>1</sup>

<sup>1</sup>Engineering Science, University of Oxford, Oxford, United Kingdom

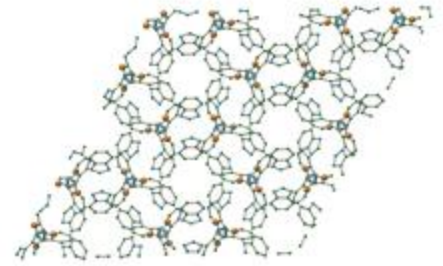
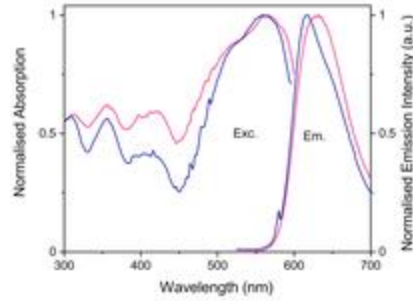
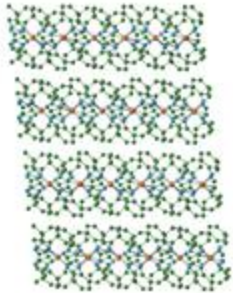
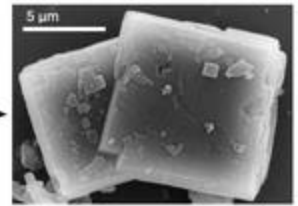
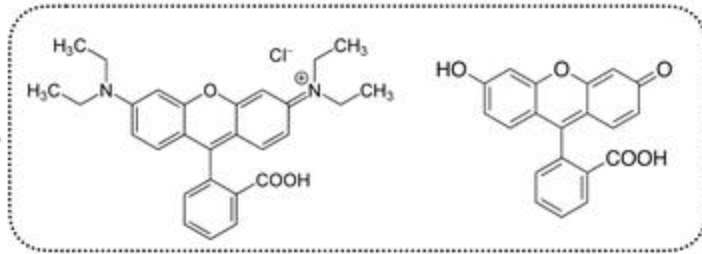
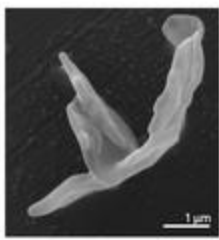
**Abstract Text:** Encapsulating dyes in a single open-framework material such as Metal-Organic Frameworks (MOFs) or Zeolitic-Imidazolate Frameworks (ZIFs) has produced many multifunctional luminescent materials that are optimisable for noninvasive sensors and optoelectronics [1]. However, effective integration of such materials into optical microscale systems or filtering and separation processes requires control of morphology to minimize thickness while maximising in-plane dimensions. Such control has been developed in select studies that synthesise Metal-Organic Nanosheets (MONs) of nanometre thickness and micron-scaled plane dimensions [2]. These, though, typically achieve nanosheet morphologies through top-down exfoliation of a bulk layered material. Few successfully utilize bottom-up techniques to directly synthesise MONs.

Here, we report the confinement of fluorophores, fluorescein and rhodamine B (RhB), in zinc based ZIF-7-III nanosheet materials, producing two novel Guest@MOF luminescent materials: RhB@ZIF-7-NS and Fluorescein@ZIF-7-NS. A prototype white-light emitting ZIF-7 nanosheet material is also reported, synthesised via a dual-guest-approach employing both fluorescein and RhB.

These materials maintain the luminescence of the guest molecules while enhancing the chemical stability and structural robustness of the dye. The nanosheets were synthesised by the first, to our knowledge, application of Guest@MOF to ZIF nanosheets along with an adapted bottom-up synthesis utilizing salt template confinement in a single room-temperature reaction [3]. Encapsulation of the dye guest molecules in the parent sodalite topology ZIF-7-I materials (Fluorescein@ZIF-7 and RhB@ZIF-7) provided a bulk comparison to the isolated nanosheets. AFM and nano-FTIR were employed to characterise the surface topology and composition of the luminescent materials, while SEM techniques imaged morphology. The photophysical properties of the materials were probed under various conditions to test structural robustness and long-term material stability. Together, the work illustrates an improvement in the technological viability of MOFs as luminescent materials.

Image 1. Top: ZIF-7-III nanosheet (left) fluorescent guests - rhodamine B (left) and fluorescein (right) (centre) and ZIF-7-I (right). Bottom: ZIF-7-III (left), excitation and emission spectra of ZIF-7-III nanosheets (dark) and ZIF-7-I (light) and ZIF-7-I (right).

**Image 1:**



- References:** [1] A. Chaudhari, J.C. Tan, *Adv. Opt. Mat.* 8 (2020) 1901912;  
[2] J. Duan, Y. Li, Y. Pan, N. Behera, W. Jin, *Coord. Chem. Rev.* 395 (2019) 25;  
[3] L. Huang, X. Zhang, Y. Han, Q. Wang, Y. Fang, S. Dong, *J. Mater. Chem. A* 5 (2017) 18610.

## ***Novel Materials and Structural Methods | MOFs/Organic materials***

FEZA21-PO-381

### **Topological characterisation of MOFs in the Cambridge Structural Database (CSD)**

L. T. Glasby<sup>1,\*</sup>, J. Cole<sup>2</sup>, P. Z. Moghadam<sup>1</sup>

<sup>1</sup>Chemical and Biological Engineering, University of Sheffield, Sheffield, <sup>2</sup>Cambridge Crystallographic Data Centre, Cambridge, United Kingdom

**Abstract Text:** Development of metal-organic frameworks (MOFs) created a unique class of crystalline materials based upon the assembly of molecular clusters, as opposed to individual single atom constructions. These molecular clusters, often termed secondary building units (SBUs) can be assembled using organic linkers to create aesthetic periodic structures. The connectivity network, or topology, of these SBUs can be instrumental in the search for new materials. The topology is a subjective property which can be best described by simplifying the atomic bonds of these structures to map out a simple graph. Graph theory allows for the simplification of these structures into fundamental unit cells which enables the comparison of two very different, but identically connected materials. These simplified graphs are collected in an open-source online database, the Reticular Chemistry Structure Resource (RCSR). The programme Systre is used in conjunction with the RCSR to allocate distinct three-letter network identifiers to a fundamental unit cell. There are several deconstruction programmes which allow a researcher to simplify their chosen material, and have a topology assigned automatically without any extensive knowledge of the subject, however there are limitations to the use of these software and it is easy to return unsuitable results. In some cases, certain representations are actually complex representations of other types of nets themselves, additionally there can be information loss due to oversimplification of certain branches. Notably, cluster type topologies should be discarded when searching for representations of periodic structures, as correct bond assignment is essential when searching for topological networks.

The CSD contains approximately 80,000 MOFs, which importantly have well defined bond assignments. This means that the CSD provides the perfect platform for structure simplification, and subsequent topological assignment by enabling a researcher to bypass any errors produced by their choice of automatic bond assignment software. Development of new tools to return topology of MOF structures has the potential to significantly increase the rate of successful topological assignment.

**Highly conducting Wurster-type redox-active covalent organic frameworks**

J. M. Rotter<sup>1</sup>, R. Guntermann<sup>1,\*</sup>, M. Auth<sup>2</sup>, A. Mähringer<sup>1</sup>, A. Sperlich<sup>2</sup>, V. Dyakonov<sup>2</sup>, D. D. Medina<sup>1</sup>, T. Bein<sup>1</sup>

<sup>1</sup>Department of Chemistry, Ludwig-Maximilian University of Munich, 81377 Munich, <sup>2</sup>Experimental Physics VI, Julius-Maximilian University of Würzburg, 97074 Würzburg, Germany

**Abstract Text:** Covalent organic frameworks (COFs) are a versatile platform combining attractive properties such as crystallinity, porosity, and chemical and structural modularity which are valuable for various applications. For the incorporation of COFs into optoelectronic or charge storage devices, efficient charge carrier transport, intrinsic conductivity and redox activity are often essential.<sup>[1]</sup> Here, we report the synthesis of WTA and WBDT, two imine-linked COFs featuring a redox-active Wurster-type motif based on the corrugated *N,N,N',N'*-tetraphenyl-1,4-phenylenediamine tetragonal node. By condensing this unit with either terephthalaldehyde (TA) or benzodithiophene (BDT), COFs featuring a dual-pore structure were obtained as highly crystalline materials with large specific surface areas. In addition, the estimated high conduction band energies of both COFs render them suitable candidates for oxidative doping. The incorporation of a benzodithiophene linear building block allowed for high intrinsic conductivity. Furthermore, different dopants such as F<sub>4</sub>TCNQ, antimony pentachloride and iodine were studied, and the conductivity of the resulting organic salts was evaluated. By using the strong organic acceptor F<sub>4</sub>TCNQ, long-term stable electrical conductivities as high as 3.67 S m<sup>-1</sup> were achieved. Expanding the design strategies for electrically conducting COFs to highly non-planar systems and achieving high and stable electrical conductivities widens the scope of applications for new COFs in optoelectronics and can ultimately promote the implementation of COFs in organic electronics.<sup>[2]</sup> Furthermore, the redox-active Wurster-type motif provides a promising basis for pseudocapacitive energy storage.

**References:**

- [1] N. Keller, T. Bein, Optoelectronic processes in covalent organic frameworks, *Chem. Soc. Rev.* 2021, 50, 1813-1845.
- [2] J. M. Rotter, R. Guntermann, M. Auth, A. Mähringer, A. Sperlich, V. Dyakonov, D. D. Medina, T. Bein, Highly conducting Wurster-type twisted covalent organic frameworks, *Chemical Science* 2020, 11, 1284.

**Ionic Liquid@Metal–Organic Framework Composites – The Influence of Macroporosity**

J. Tuffnell\*, T. Bennett<sup>1</sup>, S. Dutton<sup>2</sup>

<sup>1</sup>Department of Materials Science and Metallurgy, <sup>2</sup>Department of Physics, University of Cambridge, Cambridge, United Kingdom

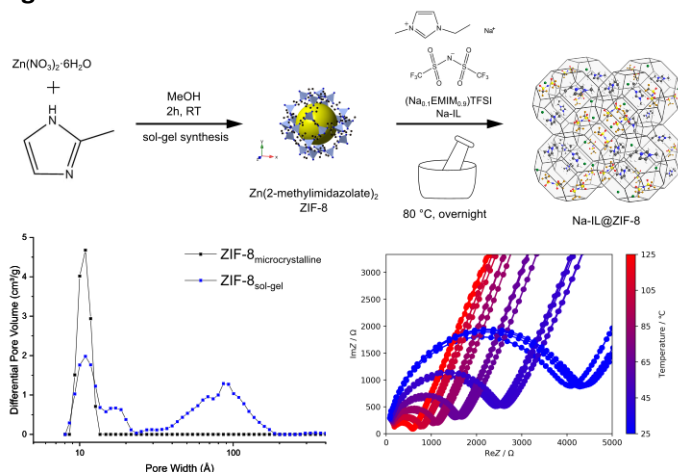
**Abstract Text:** Composites formed from Ionic liquids (ILs) incorporated within Metal–Organic Frameworks (MOFs) are part of a growing field and have shown promise for applications in gas separation, gas storage, catalysis and ionic conductivity with superior performance over the pristine MOF.<sup>1</sup> The huge variation in the chemical composition of both the IL and MOF components allow an extremely high degree of tuneability of their interaction and thus the overall properties of the composite material.

In particular, we are interested in their application as ionic conductors for solid electrolytes in batteries which can be achieved by dissolving an alkali metal ion salt into an IL and then incorporating it into a MOF. The negligible volatility and non-flammability of the alkali metal ion containing ILs alleviate many of the safety concerns when compared with traditional organic electrolytes whilst maintaining high ionic conductivities required for operation.<sup>2,3</sup> As the IL is incorporated into the MOF pores, a pseudo solid state material is obtained and the rigidity of the framework may also help to prevent dendrite formation during cycling of a battery with a solid metal electrode.

From the perspective of the MOF, characteristics such as the pore size, pore shape, open metal centres, the identity of the metal ions, surface area and structural flexibility all influence the ionic conductivity properties. In particular, the pores have shown to be essential to achieve high ionic conductivities. A comparison of activated HKUST-1 infiltrated with lithium perchlorate in propylene carbonate and activated HKUST-1 which had first been treated with pyridine to bind to the open metal centres before being infiltrated with the lithium perchlorate led to a 100x reduction in the room temperature ionic conductivity as well as a significantly higher activation energy for ion conduction.<sup>4</sup> In the latter, conduction is inhibited through the pores and the lithium can only conduct through interparticle voids. Even subtle changes in pore size from UiO-66 (pore diameters of 0.75 and 1.2 nm) to UiO-67 (pore diameters of 1.2 and 2.3 nm) show an increase in room temperature ionic conductivity from 0.18 to 0.65 mS cm<sup>-1</sup> respectively when infiltrated with lithium perchlorate in propylene carbonate.<sup>4</sup>

The poster discusses our recent work comparing the structure and ionic conductivity properties of a sodium ion containing IL@MOF composite formed from a microcrystalline MOF powder compared to that of a monolithic MOF with hierarchical porosity containing both micro- and mesopores.<sup>5</sup>

**Image 1:**



**References: 1.**  
2842–2863.

F. P. Kinik, A. Uzun and S. Keskin, ChemSusChem, 2017, 10,

2. M. J. Marczewski, B. Stanje, I. Hanzu, M. Wilkening and P. Johansson, *Phys. Chem. Chem. Phys.*, 2014, 16, 12341–12349.
3. D. Monti, E. Jónsson, M. R. Palacín and P. Johansson, *J. Power Sources*, 2014, 245, 630–636.
4. L. Shen, H. Bin Wu, F. Liu, J. L. Brosmer, G. Shen, X. Wang, J. I. Zink, Q. Xiao, M. Cai, G. Wang, Y. Lu and B. Dunn, *Adv. Mater.*, 2018, 30, 1707476.
5. B. Bueken, N. Van Velthoven, T. Willhammar, T. Stassin, I. Stassen, D. A. Keen, G. V. Baron, J. F. M. Denayer, R. Ameloot, S. Bals, D. De Vos and T. D. Bennett, *Chem. Sci.*, 2017, 8, 3939–3948.

**Effect of Unwanted Guest Molecules on the Stacking Configuration of Covalent Organic Frameworks: A Periodic Energy Decomposition Analysis**

D. A. Wonanke\*, M. A. Addicoat

**Abstract Text:**

A detailed understanding of the precise stacking configuration of covalent organic frameworks, COF, is critical to fully understand their various applications. Unfortunately, most COFs form powder crystals whose atomic characterisations are possible only through powder X-ray diffraction (PXRD) analysis. Consequently, this analysis is often coupled with computational simulations, wherein computed PXRD patterns for different stacking configurations are compared with experimental patterns to predict the precise stacking configuration. This task is often challenging firstly because, computation of these systems mostly relies on the use of semi-empirical methods that need to be adequately parametrised for the system being studied and secondly because some of these compounds possess guest molecules, which are not often taken into account during computation.

COF-1 is an extreme case in which the presence of a guest molecule plays a critical role in predicting the precise stacking configuration.<sup>1</sup> Using this as a case study, we mapped out a full PES for the stacking configuration in the guest free and guest containing systems using the GFN-xTB semi-empirical method followed by a periodic energy decomposition analysis using first-principle density functional theory, DFT, at the PBE-D3/TZ2P level of theory.

Herein, we show that the presence of the guest molecule leads to multiple low energy stacking configurations with significantly different lateral offsets, which greatly eludes the precise stacking configuration. Moreover, we show that GFN-xTB accurately accounts for dispersion correction but fails to precisely predict DFT low energy configurations. Finally, we show that the electrostatic-dispersion model suggested Hunter and Sanders accurately describe stacking in 2D COFs as oppose to the newly suggested Pauli-dispersion model.<sup>2,3</sup>

**References:**

- 1) P. Cote, H. M. El-Kaderi, H. Furukawa, J. R. Hunt, O. M. Yaghi, 2007, 129, 12914-12915.
- 2) C. A. Hunter, J. K. M. Sanders, Journal of the American Chemical Society 1990, 112, 5525–5534.
- 3) K. Carter-Fenk, J. M. Herbert, Chemical Science 2020, 6758–6765.

***Physical Properties and the Role of Defects***

FEZA21-PO-386

**Amorphization of metal-organic frameworks under non-hydrostatic pressure**

G. Robertson\*

**Abstract Text:** Metal-organic frameworks (MOFs) have a range of responses to pressure, including phase changes and reversible/irreversible amorphization, which vary widely under different conditions. This work documents the response of some prototypical MOFs to non-hydrostatic pressure. It considers what this shows about the framework's structural development under different pressure states, and possible amorphization mechanisms.

**Density functional theory modelling of the acidic behaviour of UiO-66**

M. Hutereau<sup>1,\*</sup>, B. Slater<sup>1</sup>

<sup>1</sup>Department of chemistry, University College London, London, United Kingdom

**Abstract Text:** Metal-organic frameworks (MOFs) are a growing class of highly porous materials comprising inorganic metal clusters connected by organic linker ligands, forming three-dimensional nets. They have garnered much interest due to their potential in a range of applications, such as drug delivery, gas storage, and as heterogeneous catalysts.<sup>1-6</sup> UiO-66 (University of Oslo) is a highly stable MOF which has been widely studied due to its exceptional thermal and chemical stabilities, as well as its unique defect behaviour.<sup>7</sup> It is known that in this framework, linker vacancies may be created as a result of the synthetic conditions used,<sup>8</sup> leading to increase porosity and metal clusters that are less coordinatively saturated. The material has been found to be active as both a Bronsted and a Lewis acid catalyst, though in its standard form, performance is poor.<sup>9,10</sup> Activity of the Lewis acid type is known to benefit greatly from increased defectivity, while little is known about Bronsted acidity in relation to linker disorder. In order to systematically tune the acidic behaviour of UiO-66, it is necessary to understand the influence of defects, as found by Liu *et al.* in a recent study.<sup>11</sup>

Density functional theory (DFT) can be used to probe the Bronsted and Lewis acidities of the framework. Using ammonia as a probe molecule, the probe binding energy can be used as a proxy measure of Bronsted acidity. Calculations were run using different defect distributions and termination mechanisms to evaluate the importance of these two factors, representing the largest analysis of its type on MOFs. The results reveal the importance of considering dispersion interactions in ammonia binding and further yield novel insight into the choice of capping species' for this purpose. Probing Lewis acidity requires the use of *ab initio* molecular dynamics, because even with defects, Zr atoms remain 8-fold coordinated, meaning unsaturated sites must first be created. In an unprecedented study, the approach of a prototype Lewis base reactant towards a defective metal node was modelled using umbrella sampling. This revealed that a defect provides alternative species that decoordinate more easily than the linkers, thereby explaining why catalytic activity concordantly increases. Further work is still under-way to establish the importance of the choice of capping species and the defect distribution in this regard, using a similar procedure to the one described previously.

**References:** 1. Orellana-Tavra, C. ; Baxter, E. F.; Tian, T.; Bennett, T. D.; Slater, N. K. H.; Cheetham, A. K.; and Fairen-Jimenez, D. , Chem. Commun., 2015, 51, 13878–13881.

2. Della Rocca, J.; Liu, D.; and Lin, W., Acc. Chem. Res., 2011, 44, 957–968.

3. Sumida, K.; Rogow, D. L.; Mason, J. A.; McDonald, T. M.; Bloch, E. D.; Herm, Z. R.; Bae T.-H.; and Long, J. R., Chem. Rev., 2012, 112, 724–781.

4. Ma, S.; and Zhou, H. C., Chem. Commun., 2010, 46, 44–53.

5. Yoon, M.; Srirambalaji, R.; and Kim, K., Chem. Rev., 2012, 112, 1196–1231.

6. Lee, J.; Farha, O.K.; Roberts, J.; Scheidt, K.A.; Nguyen, S.T.; and Hupp, J.T., Chem. Soc. Rev., 2009, 38, 1450–1459.

7. Wu, H.; Chua, Y.S.; Krungleviciute, V.; Tyagi, M.; Chen, P.; Yildirim, T.; and Zhou, W., J. Am. Chem. Soc., 2013, 135, 10525–10532.

8. Shearer, G.C.; Chavan, S.; Bordiga, S.; Svelle, S.; Olsbye, U.; and Lillerud, K.P., Chem. Mater., 2016, 28, 3749–3761.

9. Bakuru, V.R.; Churipard, S.R.; Maradur, S.P.; and Kalidindi, S.B., Dalt. Trans., 2019, 48, 843–847.

10. Vermoortele, F.; Bueken, B.; Le Bars, G.; Van De Voorde, B.; Vandichel, M.; Houthoofd, K.; Vimont, A.; Daturi, M.; Waroquier, M.; Van Speybroeck, V.; Kirschhock, C.; and De Vos, D.E., J. Am. Chem. Soc., 2013, 135, 11465–11468.

11. Liu, L.; Chen, Z.; Wang, J.; Zhang, D.; Zhu, Y.; Ling, S.; Huang, K.W.; Belmabkhout, Y.; Adil, K.; Zhang, Y.; Slater, B.; Eddaoudi, M.; and Han, Y., Nat. Chem., 2019, 11, 622–628.

## ***Stimuli Responsive Behaviour and Emerging Properties***

FEZA21-PO-389

### **Electrical regulation of CO<sub>2</sub> adsorption in metal-organic framework MIL-53**

K. Chen<sup>1,\*</sup>, R. Singh<sup>1</sup>, G. Li<sup>1</sup>, P. Webley<sup>2</sup>

<sup>1</sup>Chemical Engineering, The University of Melbourne, Parkville, VIC, <sup>2</sup>Chemical Engineering, Monash University, Clayton, VIC, Australia

**Abstract Text:** Active regulation of pore accessibility in microporous material by external stimuli has aroused great attention in recent years, including the use of heat, pressure, and light. In this work, we tried to apply an electric field to regulate gas adsorption in microporous materials. Through experimental study, we show that the CO<sub>2</sub> adsorption capacity of MIL-53 (Al) significantly reduced while that of NH<sub>2</sub>-MIL-53 (Al) was slightly enhanced by a direct current E-field of  $2.86 \times 10^5$  V/m. The E-field can instantly regulate the CO<sub>2</sub> adsorption in MIL-53 (Al), which was confirmed by the instantaneously decreased CO<sub>2</sub> uptake when powering on in situ during adsorption measurement. The ab initio density functional theory calculation indicated that the decrease of CO<sub>2</sub> uptake upon E-field application in MIL-53 (Al) resulted from the reduced charge rearrangement between the CO<sub>2</sub> molecule and the framework, which weakened the host-guest interaction and reduced the binding energy of CO<sub>2</sub>. This effect was only found in the narrow pore state MIL-53 (Al), rather than the large pore configuration. Our results demonstrated the feasibility to regulate the admission of small molecules in microporous materials by E-field.

***Stimuli Responsive Behaviour and Emerging Properties | MOFs/Organic materials***

FEZA21-PO-391

**Revisiting gate opening mechanism: phonon and adsorption simulations perspective**

F. Formalik<sup>1,\*</sup>, B. Mazur<sup>1</sup>, M. Fischer<sup>2</sup>, B. Kuchta<sup>1</sup>, L. Firlej<sup>1</sup>

<sup>1</sup>Department of Micro, Nano and Bioprocess Engineering, Wrocław University of Science and Technology, Wrocław, Poland, <sup>2</sup>Crystallography Group, University of Bremen, Bremen, Germany

**Abstract Text:** Subclass of metal-organic framework (MOFs) – flexible MOFs are prone to undergo different structural changes when exposed to external stimuli such as pressure, temperature, and adsorption. Despite of variety of computational and experimental studies devoted to this class of materials, still there is no generalized model of the microscopic mechanism explaining experimentally observed transformations. One of the reasons is a very intricate nature of involved phenomena, such as sublattice displacement, linker rotation and buckling or change of the angles between the linkers.

We propose a comprehensive methodology based on phonon formalism, Density Functional Theory (DFT), and Grand Canonical Monte Carlo (GCMC) adsorption calculations to revisit and get more valuable insight into the mechanism of the structural transformations in group of flexible ZIF materials with sodalite topology. We performed DFT calculations of low-frequency phonons and analyzed their potential contribution to the gate opening mechanism. For the first time, analysis of phonon-driven deformations of ZIFs was coupled with calculations of quantities describing adsorption process such as pore limiting diameter (PLD) and void fraction (VF) explicit adsorption simulations, and grand thermodynamic potential of adsorption.

**References:** [1] F. Formalik, M. Fischer, J. Rogacka, L. Firlej, B. Kuchta, *Microporous Mesoporous Mater.* 304 (2020) 109132, [10.1016/j.micromeso.2018.09.033](https://doi.org/10.1016/j.micromeso.2018.09.033)

[2] F. Formalik, B. Mazur, M. Fischer, L. Firlej, B. Kuchta, *J. Phys. Chem. C* in press (2021), [10.1021/acs.jpcc.1c01342](https://doi.org/10.1021/acs.jpcc.1c01342)

## ***Advanced Characterisation and Operando Spectroscopies***

FEZA21-PO-392

### **Advancing the Thermoporometry Characterization Approach in Mesoporous Solids**

H. R. N. B. Enniful<sup>1,\*</sup>, D. Schneider<sup>1</sup>, R. Kohns<sup>2</sup>, D. Enke<sup>2</sup>, R. Valiullin<sup>1</sup>

<sup>1</sup>Felix Bloch Institute for Solid State Physics, <sup>2</sup>Institute of Chemical Technology, Leipzig University, Leipzig, Germany

**Abstract Text:** Mesoporous solids, widely used in industrial applications exhibit structural disorder which impacts the fluid properties confined within the solids. Hence, understanding fluid phase behaviour in pores is fundamental to their optimization for various applications. Gas sorption and thermoporometry employ fluid phase transitions as markers to reveal pore morphology. While gas sorption analysis has been advanced in understanding gas-liquid phase equilibria in pores, thermoporometry, which utilizes the liquid-solid phase equilibria is yet to be exploited.

In this work, in an analogy to the advanced gas sorption analysis [1, 2], we present a novel kernel-based approach to thermoporometry characterization. This allows us to incorporate a variation of the non-frozen layer thickness with curvature and the effects of thermodynamic fluctuations on phase transitions into a recently developed theoretical framework [3]. The model considers complexities arising from coupled pore systems and allows for the analysis of pore networks beyond the simple collection of independent pores conventionally assumed in the literature [4]. By applying this approach to NMR cryoporometry of water in MCM-41 and SBA-15 materials, we validate the approach and reveal disorder respectively.

#### **References:**

1. Enniful, H.R.N.B., Schneider D., Enke D., and Valiullin R., Impact of Geometrical Disorder on Phase Equilibria of Fluids and Solids Confined in Mesoporous Materials. *Langmuir*, 2021. 37(12): p. 3521-3537.
2. Enniful, H.R.N.B., D. Schneider, A. Hoppe, S. König, M. Fröba, D. Enke, and R. Valiullin, Comparative Gas Sorption and Cryoporometry Study of Mesoporous Glass Structure: Application of the Serially Connected Pore Model. *Frontiers in Chemistry*, 2019. 7(230)
3. Enniful, H.R.N.B., Schneider D., Kohns R., Enke D., and Valiullin R., A novel approach for advanced thermoporometry characterization of mesoporous solids: Transition kernels and the serially connected pore model. *Microporous Mesoporous Mater.* 2020, 309, 110534
4. Schneider, D. and Valiullin R., Capillary Condensation and Evaporation in Irregular Channels: Sorption Isotherm for Serially Connected Pore Model. *The Journal of Physical Chemistry C*, 2019. 123(26): p. 16239-16249.

**Elucidation of Nitrogen Adsorption Behaviour of AlMepO- $\alpha$  by In-situ Powder X-ray Diffraction Study**

K. Maeda<sup>1,\*</sup>, H. Minta, A. Kondo, S. Kawaguchi<sup>2</sup>

<sup>1</sup>Department of Applied Chemistry, Tokyo University of Agriculture and Technology, Koganei, Tokyo, <sup>2</sup>SPring-8, Japan  
Synchrotron Radiation Research Institute, Sayo-cho, Hyogo, Japan

**Abstract Text:**

Much attention is focused on flexible MOFs and related porous materials because of stimuli-responsive adsorption behaviour. Although many flexible MOFs showing non-traditional behaviour such as breathing and gate adsorption are known nowadays, it is still rare for zeolitic inorganic 3D frameworks showing such nitrogen adsorption behaviours. We reported two polymorphs of microporous aluminium methylphosphonate (AlMepO), AlMepO- $\alpha$  and - $\beta$  with the framework composition  $\text{Al}_2(\text{O}_3\text{PCH}_3)_3$  [1,2]. Both polymorphs have ALPO-like 3D inorganic frameworks with methyl-lined one-dimensional channels. AlMepO- $\alpha$  gives a  $\text{N}_2$  adsorption isotherm with two adsorption steps at low pressure, while AlMepO- $\beta$  gives typical Type-I isotherm [3]. This study aims at elucidation of the adsorption behaviour of AlMepO- $\alpha$  by using in-situ high-resolution X-ray diffraction.

The in-situ XRD measurement was executed at BL02B2, SPring-8, Japan. After degassing AlMepO- $\alpha$  in a glass capillary at 723 K, the sample was cooled to 94 K, which is the lowest temperature attainable by the  $\text{N}_2$  cryostreams, and XRD data were measured by increasing  $\text{N}_2$  gas pressure up to 100 kPa.

After degassing at 723 K, no apparent phase transition is observed down to 94 K under vacuum to retain the trigonal form, though temperature-dependent lattice contraction is observed. Introduction of  $\text{N}_2$  gas up to  $P = 13.2$  kPa at 94 K retain the single trigonal phase (denoted as *np* form), which is indexed with space group *P31c* while varying the lattice constants. The Rietveld refinement reveals nitrogen molecules in the channels. Another new phase appeared at  $P = 17.8$  kPa is indexed also with a slightly larger trigonal unit cell with the same space group *P31c* (denoted as *lp* form). Increasing the gas pressure results in increase of *lp* form and decrease of *np*. The *np* to *lp* transition reasonably explains the second adsorption step around  $P/P_0 = 0.02$ - $0.03$  observed for  $\text{N}_2$  isotherm at 77 K. Although the single *lp* form was not attained in the limited synchrotron beam time, the crystal structure of both the forms (see Image 1: a) *np* and b) *lp*) were obtained in two-phase Rietveld refinement. Arising from small difference in the lattice constants and framework structure, the orientation of the methyl groups lining the channels is imperceptibly different between both the forms to slightly expand the micropore size in *lp* form. The main difference is occupancy of nitrogen molecules (*np*: 0.322(11), *lp*: 1) and orientation of the nitrogen molecules. The  $\text{N}_2$  molecules are located slantingly to the channels in *np* form, while closely packed along the channels in *lp* form. This result basically supports our previous hypothesis to explain the 2-step isotherm in Ref. 3.

The average cell  $\text{N}_2$  content, which is calculated from the molar fraction and the cell  $\text{N}_2$  content of each phase, plotted versus  $P$  shown in Image 2a should crystallographically simulate a  $\text{N}_2$  adsorption isotherm. The corresponding relative pressure ( $P/P_0$ ) by conversion using the saturation pressure at 94 K is also shown as the top axis. Image 2b shows the  $\text{N}_2$  adsorption isotherm volumetrically measured at 77 K with estimated cell  $\text{N}_2$  content as the right axis, to which the adsorbed amount is converted by assuming a pure AlMepO- $\alpha$  phase. Although many factors should perturb this crystallographically estimated adsorption isotherm, it fairly well simulates the two-step isotherm measured at 77 K.

Image 1:

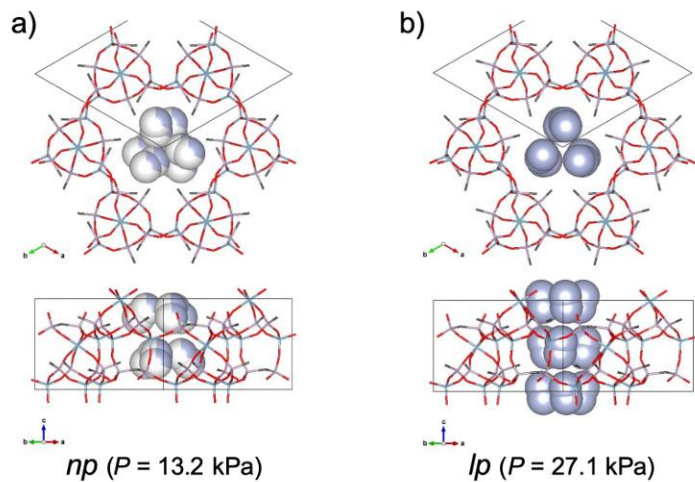
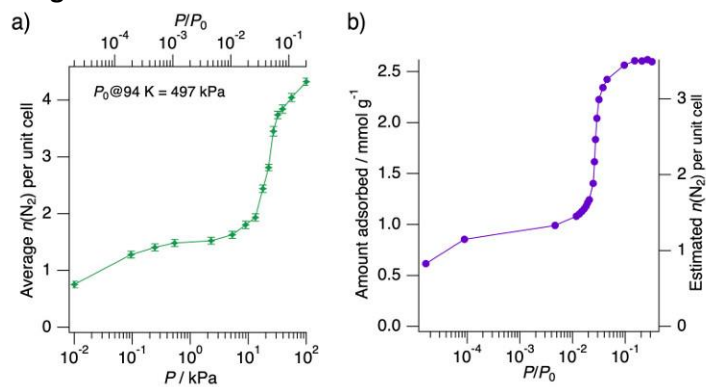


Image 2:



References:

- [1] K. Maeda et al., Angew. Chem. Int. Ed., 1995, 34, 1199.
- [2] K. Maeda et al., Angew. Chem. Int. Ed., 1994, 33, 2335.
- [3] K. Maeda et al., J. Phys. Chem. B, 1997, 101, 4402.

**Fluid Phase Equilibria in a Strongly Disordered Mesoporous Solid**

H. R. N. B. Enniful\*, D. Schneider<sup>1</sup>, A. Hoppe<sup>2</sup>, S. König<sup>3</sup>, M. Fröba<sup>3</sup>, D. Enke<sup>2</sup>, R. Valiullin<sup>1</sup>

<sup>1</sup>Felix Bloch Institute for Solid State Physics, <sup>2</sup>Institute of Chemical Technology, Leipzig University, Leipzig, <sup>3</sup>Institute of Inorganic and Applied Chemistry, Hamburg University, Hamburg, Germany

**Abstract Text:** Offering a strong balance between pore size, relatively high specific surface area, and beneficial transport properties, mesoporous solids have found immense uses in industrial applications such as catalysis, separations, adsorption and drug delivery among others. These materials may exhibit geometric disorder along varying length scales, and hence, affect fluid phase behaviour in confined spaces. Accurate characterisation of the pore structure is, therefore, a necessary step towards optimization for the above-mentioned applications.

Current characterization tools assume an independent collection of pores in such random porous solids. This way, analysis precludes interconnectivity effects arising from inter-pore coupling. Herein, we elucidate the structure of a strongly disordered mesoporous solid via analyses of both solid-liquid and gas-liquid phase equilibria in the material [1]. Utilising the serially-connected pore model which incorporates both phase nucleation and growth phenomena [2], we show that the model is able to self-consistently reproduce the boundary phase transitions and scanning behaviour in our material [3]. The, thus, derived pore size distribution proves to be a more accurate representation of the pore structure [4].

**References:**

1. Enniful, H.R.N.B., D. Schneider, A. Hoppe, S. König, M. Fröba, D. Enke, and R. Valiullin, Comparative Gas Sorption and Cryoporometry Study of Mesoporous Glass Structure: Application of the Serially Connected Pore Model. *Frontiers in Chemistry*, 2019. 7(230)
2. Schneider, D. and Valiullin R., Capillary Condensation and Evaporation in Irregular Channels: Sorption Isotherm for Serially Connected Pore Model. *The Journal of Physical Chemistry C*, 2019. 123(26): p. 16239-16249.
3. Enniful, H.R.N.B., Schneider D., Enke D., and Valiullin R., Impact of Geometrical Disorder on Phase Equilibria of Fluids and Solids Confined in Mesoporous Materials. *Langmuir*, 2021. 37(12): p. 3521-3537.
4. Enniful, H.R.N.B., Schneider D., Kohns R., Enke D., and Valiullin R., A novel approach for advanced thermoporometry characterization of mesoporous solids: Transition kernels and the serially connected pore model. *Microporous Mesoporous Mater.* 2020, 309, 110534,

**I20-EDE: The Energy Dispersive EXAFS beamline at Diamond Light Source**

L. Keenan<sup>1,\*</sup>, M. Amboage<sup>1</sup>, F. Mosselmans<sup>1</sup>, S. Hayama<sup>1</sup>, T. Kokumai<sup>1</sup>, S. Diaz-Moreno<sup>1</sup>

<sup>1</sup>Physical Science, Diamond Light Source Ltd, Didcot, United Kingdom

**Abstract Text:** The Energy Dispersive EXAFS branch of the I20 beamline, I20-EDE, is dedicated for X-ray absorption spectroscopy (XAS) measurements for material science. The beamline shares the I20 straight section of the Diamond ring with the I20-Scanning branch, which is dedicated to XAS and XES experiments. Each branch has its own wiggler source, optical elements, experimental hutch and control cabin and can therefore operate independently and simultaneously.<sup>[1, 2]</sup>

The I20-EDE source is a variable gap, hybrid wiggler, with 1.3T peak field. It delivers a continuous white beam spectrum with enough horizontal divergence to fully illuminate a 250mm long polychromator crystal. The polychromator is a long thin silicon crystal that is dynamically curved to the required ellipse, to select a bandwidth of energies focused at the sample position and diverging to a position-sensitive detector. Si(111) and Si(311) crystals are available to study absorption edges of energies between 6keV and 26keV, with dispersive bandpass of ~10% at all energies and photon flux of  $10^{12}$  ph/s at 10keV. The position-energy relation established allows for the whole absorption spectrum to be acquired in a single shot. This characteristic of the energy-dispersive configuration, together with the availability of fast detectors, gives the beamline the ability to perform time-resolved EXAFS. Processes with timescales ranging from hours all the way down to microseconds can be studied, including *in operando* heterogeneous and homogenous catalysis; electrochemical reactions; and material phase changes with temperature, or at high pressure in a Diamond Anvil Cell. Complementary techniques available include UV-vis, Raman spectroscopy and mass spectrometry. The beamline is currently accepting proposals.

**Image 1:**

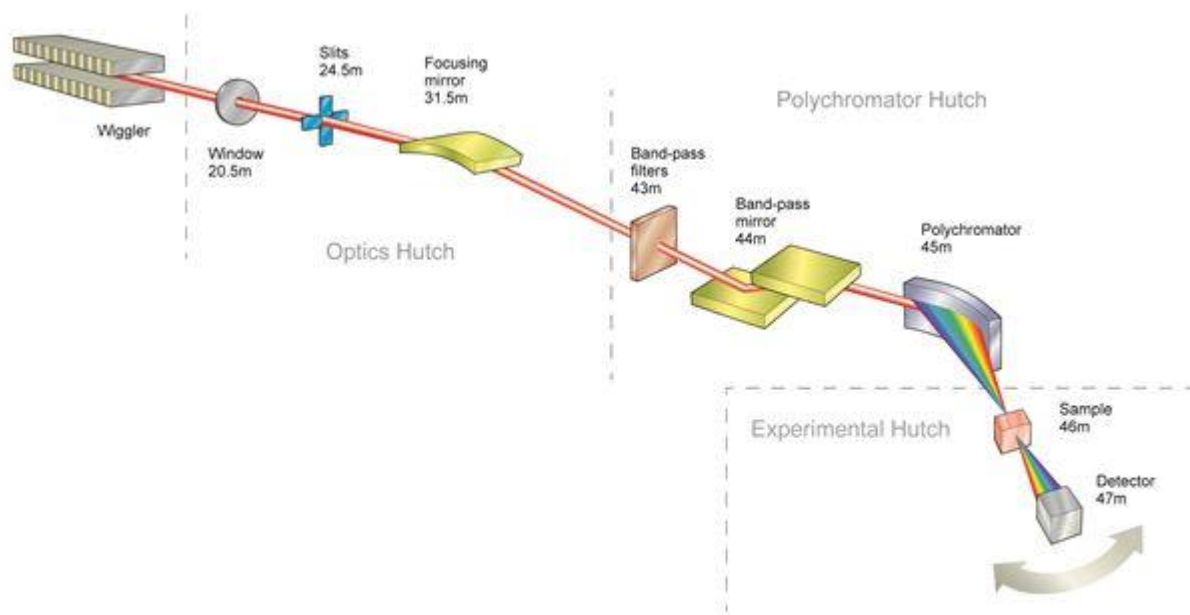


**Figure 1.** The optical components of I20-EDE extending over 47 m from source to a sample stage and detector located on a 3.5 m granite arm with 60° angular coverage.

**References:** [1] S. Diaz-Moreno et al., J. Phys.: Conf. Ser., 190, (2009), 012038

[2] S. Diaz-Moreno et al., J. Synch. Rad., 25, (2018), 998-1009

## ***Gas Adsorption, Separation and Storage***

FEZA21-PO-397

### **Basic One-Dimensional Modelica®-Model for Simulation of Gas-Phase Adsorber Dynamics**

M. Kleingries<sup>1,\*</sup>, U. C. Mueller<sup>1</sup>, A. Rettig<sup>1</sup>, S. Schneider<sup>1</sup>, R. Tamburini<sup>1</sup>

<sup>1</sup>Engineering and Architecture, Lucerne University of Applied Sciences and Arts, Horw, Switzerland

**Abstract Text:** Industrial adsorption processes are, mainly due to simultaneous heat and mass transfer, characterized by a high level of complexity. The conception of such processes often does not take place systematically, instead scale-up/down respectively number-up/down methods based on existing systems are used. This paper shows how Modelica® can be used to develop a transient model enabling a more systematic design of such ad- and desorption components and processes. The core of this model is a lumped-element submodel of a single adsorbent grain, where the thermodynamic equilibria and the kinetics of the ad- and desorption processes are implemented and solved on the basis of mass-, momentum and energy balances. For validation of this submodel a fixed bed adsorber, whose characteristics are described in detail in literature, was modeled and simulated. The simulation results are in good agreement with the experimental results from literature. Therefore, the model development will be continued and the extended model will be applied to further adsorber types like rotor adsorbers and moving bed adsorbers.

**Characterization of metal species in metal modified mordenite**

I. Landripet<sup>1,\*</sup>, M. Robić<sup>1</sup>, A. Puškarić<sup>1</sup>, G. Medak<sup>1</sup>, J. Bronić<sup>1</sup>

<sup>1</sup>Department of Chemistry, Division of Materials Chemistry, Laboratory for Synthesis of New Materials, Ruđer Bošković Institute, Zagreb, Croatia

**Abstract Text:** The unique physicochemical properties of the zeolites, such as their controlled acidity, adsorption capacity, ion exchange properties, and thermal stability, as well as uniform channels and cavities crystallographically ordered in size and position, determine their effectiveness in catalytic processes. Mordenite is widely used in catalysis, separation and purification because of its uniform, small pore size and high internal surface area. Despite the microporous structure, there are limitations that decrease the efficiency of the zeolite as catalysts. Such limitations can be avoided by creating mesoporous voids.

Another important issue in catalysis efficiency is the number of active sites (i.e. Lewis and Brønsted acid sites). Its number can be increased with a number of hetero T-atoms within the framework by post-synthesis treatment such as ion exchange.

Parent material was prepared by the hydrothermal synthesis in Teflon-lined autoclaves as one-pot synthesis and resulted in sodium mordenite zeolite. Mono- and bimetallic systems of Ag, Fe, and Ag–Fe were prepared by the ion exchange method in H-form mordenite.

PXRD pattern shows that the structure corresponds to the structure of mordenite. All post-synthesis treatments did not have a significant influence on the crystallinity of the samples.

Preliminary results (FE-SEM with EDS) have shown a certain amount of metals incorporated in mordenite and preserved structure after wet impregnation. AAS gives the exact concentration of metals in mordenite structure and was used to confirm impregnation of metals, but can't say anything about metal species. UV–Vis spectroscopy was applied to identify the silver and iron species. Due to the usually specific behavior of the Ag and Fe cations under the light, photostability was confirmed by exposing the samples to the radiation in the wavelength range of 200 to 1000 nm.

**References:** P. Sánchez-López, Y. Kotolevich, S. Miridonov, F. Chávez-Rivas, S. Fuentes, V. Petranovskii, *Catalysts*, 2019, 9, 58

**Copper modified ferrierite layered zeolite based materials as a catalysts for NH<sub>3</sub>-SCR process**

A. Świąś<sup>1,\*</sup>, A. Kowalczyk<sup>1</sup>, M. Rutkowska<sup>1</sup>, M. Michalik<sup>2</sup>, U. Diaz<sup>3</sup>, A. E. Palomares<sup>3</sup>, L. Chmielarz<sup>1</sup>

<sup>1</sup>Faculty of Chemistry, <sup>2</sup>Institute of Geological Sciences, Jagiellonian University, Kraków, Poland, <sup>3</sup>Instituto de Tecnología Química, Universitat Politècnica de València, Valencia, Spain

**Abstract Text:** Zeolites, due to very interesting characteristics such as well-defined porous structure, ion-exchange properties, surface acidity with various strength and density of acid sites, have found application in many field of industry, everyday life, large variety of reactions. Advantage of zeolitic materials is mechanical, thermal and hydrothermal stability. Ferrierite zeolite is characterized by layer structure based on 5-membered rings (MR) with two types of intersecting channels 8- and 10- MR. Although, pore dimensions is one of the main problem in reaction of bulky molecules due to internal diffusion limitations.[2] New approaches have been proposed to modified structure of microporous zeolites and obtain materials characterized by larger pore volume and accessibility of catalytically active sites.

Delamination process leads to formation of single zeolitic layers in a “house of cards” structure from layered zeolite precursor. Proposed procedure allow to obtain the ITQ-6 material with higher external surface area. ITQ-36 synthesis is based on incorporation of stable silica pillars into the interlayer space of 2D PREFER precursor. Both ferrierite based materials are characterized by presence of meso- and macroporosity.[2] Titanosilicate and aluminum silicate ferrierites: FER, ITQ-6 and ITQ-36 materials were synthesized with various Si/Al and Si/Ti ratios and finally modified by copper. The obtained materials were characterized with respect to structure, form and aggregation of deposited copper species, acidity and reducibility. The obtained samples were found to be active and selective in NH<sub>3</sub>-SCR process (Fig. 1, 2)

**Image 1:**

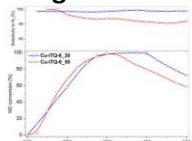
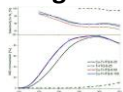


**Image 2:**



**References:** [1] L. Schreyeck, P. Caullet, J.C. Mougènel, J.L. Guth, B. Marler, J. Chem. Soc., Chem. Commun. 1995, 2187  
[2] A. Chica, U. Diaz, V. Fornes, A. Corma, Catal. Today, 2009, 179

**Functionalization of spherical MCM-41 with Cu by template-ion exchange method for the application in low-temperature NH<sub>3</sub>-SCR process**

A. Jankowska<sup>1,\*</sup>, A. Kowalczyk<sup>1</sup>, M. Rutkowska<sup>1</sup>, W. Mozgawa<sup>2</sup>, M. Michalik<sup>3</sup>, S. Liu<sup>4</sup>, L. Chmielarz<sup>1</sup>

<sup>1</sup>Faculty of Chemistry, Jagiellonian University, <sup>2</sup>Faculty of Materials Science and Ceramics, AGH University of Science and Technology, <sup>3</sup>Institute of Geological Sciences, Jagiellonian University, Kraków, Poland, <sup>4</sup>School of Materials Science and Engineering, University of Jinan, Jinan, China

**Abstract Text:** Mesoporous silicas, the representative of which is the MCM-41, constitute a group of materials characterized by intrinsic properties highly desirable from the catalysis point of view. These features include a very large specific surface area and total pore volume, as well as a strictly defined porous structure and relatively high thermal, hydrothermal and mechanical stability. [1] However, in the case of purely siliceous porous materials, a disadvantage that hinders their use in catalysis is the lack of ion-exchange properties ensuring the possibility of introducing the catalytically active phase in a highly dispersed form. An alternative, but at the same time effective method of introducing catalytically active components is the template ion exchange (TIE) method. It is based on the extraction of organic template, applied during the synthesis as a pore template, from silica materials with the use of polar solvent solutions containing metal cations. Furthermore, the degree of dispersion of the introduced catalytically active ingredients can be controlled by treating the obtained materials with complexing agents. This modified version of the template-ion exchange technique is based on the post-synthetic treatment of samples, directly after the TIE procedure, by using ammonia complexation (TIE-NH<sub>3</sub>). [2,3]

The modification of the MCM-41 material with transition metals (e.g. Cu), leads to effective catalysts for the conversion of environmentally dangerous nitrogen oxides (NO<sub>x</sub>) in the low-temperature selective catalytic reduction with NH<sub>3</sub> (NH<sub>3</sub>-SCR). [2,3] The design of catalysts for the low-temperature selective catalytic reduction of nitrogen oxide with ammonia emitted from stationary sources constitutes one of the most important issues in the field of environmental catalysis.

The main aim of the presented studies was to develop catalysts for the low-temperature NH<sub>3</sub>-SCR process basing on the modification of spherical MCM-41 with Cu. Mesoporous silica material was modified with methanolic solutions containing various copper concentrations by the TIE method and its modified version using the complexation of Cu with ammonia. The obtained materials were characterized to determine their structure (P-XRD), chemical composition (ICP-OES), texture (N<sub>2</sub>-sorption), morphology and surface composition (SEM-EDS). Moreover, aggregation of active phase (UV-vis-DRS), reducibility (H<sub>2</sub>-TPR) and surface acidity (NH<sub>3</sub>-TPD) have been also investigated.

It was shown that such catalytic systems present very interesting properties in the low-temperature selective catalytic reduction of NO with ammonia (Figure 1). The enhanced catalytic activity was observed especially in the case of the samples obtained as a result of TIE-NH<sub>3</sub> modification. For the most active sample in this series, 60Cu-A, the NO conversion above 90%, was obtained in the range of 225–300°C (Figure 1B). In the case of the TIE method, copper was introduced in the form of highly dispersed copper species as well as CuO nanorods, while for the samples modified by using post-synthetic ammonia complexation Cu was introduced in the highly dispersed form deposited inside the porous system. The morphology (SEM micrographs) of the most active samples, 60Cu and 60Cu-A, was presented in Figure 2A and 2B, respectively. The improved catalytic activity of the samples obtained as a result of the TIE-NH<sub>3</sub> method could be related presence of a well-dispersed monomeric Cu active phase, which was found to be more active compared to more aggregated copper oxide species.

**Acknowledgements:** The studies were carried out in the frame of project 2018/31/B/ST5/00143 from the National Science Centre (Poland). AJ has been partly supported by the EU Project POWR.03.02.00-00-I004/16.

**Image 1:**

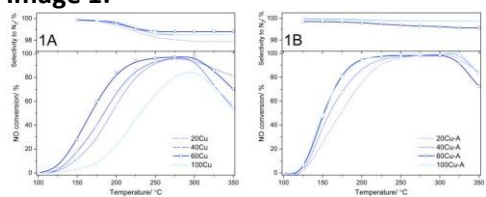
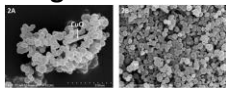


**Image 2:**



**References:** [1] L. Gao, Z. Shi, U.J. Etim, P. Wu, D. Han, W. Xing, S. Mintova, P. Bai, Z. Yan, *Microporous Mesoporous Mater.* 227 (2019) 17–28.

[2] A. Kowalczyk, A. Święs, B. Gil, M. Rutkowska, Z. Piwowarska, A. Borchuch, M. Michalik, L. Chmielarz, *Appl. Catal. B Environ.* 237 (2018) 927–937.

[3] A. Jankowska, A. Chłopek, A. Kowalczyk, M. Rutkowska, W. Mozgawa, M. Michalik, S. Liu, L. Chmielarz, *Microporous Mesoporous Mater.*, 315 (2021) 110920.

**Mesopore Enrichment of a Microporous Zeolitic Scaffold for Improved Latent Heat Storage**

H. Bildirir<sup>1,\*</sup>, C. Erdinc Tas<sup>2</sup>, B. Alkan Tas<sup>2</sup>, E. Ertas<sup>3</sup>, H. U. Unal<sup>1</sup>

<sup>1</sup>TÜBİTAK Marmara Research Centre, Kocaeli, <sup>2</sup>Sabancı University, Istanbul, <sup>3</sup>TÜBİTAK Marmara Research Centre, Kocaeli, Turkey

**Abstract Text:** Latent heat storage systems help to keep the temperature of an environment constant via phase change of the active material (phase change material (PCM)) adsorbed through the shape stabilizers.[1] PCMs store and release thermal energy as enthalpy of fusion when going liquid from the solid form or vice versa. Thus, the thermal properties and the amount of PCM involved to the process are important factors for latent heat storage systems. On the other hand, shape stabilizers play a crucial role in the latent heat storage process since they are the hosts to those PCMs.[2] The characteristics of a good shape stabilizer are their ability to keep the PCMs stationary after melting (no leak) and a suitable thermal conductivity for the corresponding application. Porous materials have been the preferred scaffolds as shape stabilizers thanks to their large accessible surface area allowing a high PCM uptake.[3] Given that, the pore-size of the porous scaffold is more important than the size of surface area. This is because microporous materials might suffer from steric hindrance for bulky PCMs and macroporous materials have higher tendency for leakage due to poor capillary forces. Therefore, mesopore rich hierarchical porosity is desired since they provide optimum storage capacity (good enough surface areas) and adequate capillary forces (less tendency for PCM leakage). In this work, we employ post-synthetic modification on a microporous ZSM-5 to yield mesopore rich hierarchical porosity along its structure.[4] Moreover, we loaded two different PCMs demonstrating low and high molecular weights (lauric acid (LA) and polyethylene glycol 4000 (PEG)) to check the response of the scaffold against small and large PCMs. We observed nearly double uptake for both PCMs after the modification, hence better latent heat storage properties. Moreover, the produced system showed a constant performance after 500 heating-cooling cycles proving the stability of the final PCM/ZSM composite. Furthermore, it is worth noting that we investigated the pore-size phenomena on the same framework structure to neglects the side effects from the skeleton of the scaffold such as thermal conductivity, which makes this study particularly intriguing for the field.

**References:** References

- |     |  |
|-----|--|
| [1] | Z. Rao, S. Wang, Z. Zhang, <i>Renew. Sustain. Energy Rev.</i> 2012, 16, 3136–3145.   |
| [2] | X. Huang, X. Chen, A. Li, D. Atinafu, H. Gao, W. Dong, G. Wang, <i>Chem. Eng. J.</i> 2019, 356, 641–661.                   |
| [3] | D. Feng, Y. Feng, L. Qiu, P. Li, Y. Zang, H. Zou, Z. Yu, X. Zhang, <i>Renew. Sustain. Energy Rev.</i> 2019, 109, 578–605.  |
| [4] | C. E. Tas, O. Karaoglu, B. A. Tas, E. Ertas, H. Unal, H. Bildirir, <i>Sol. Energy Mater. Sol. Cells</i> 2020, 216, 110677. |

## Catalytic Properties

FEZA21-PO-405

### Design of Cu-Zn bimetallic MFI zeolite based catalysts for deNOx SCR process - modeling of reaction mechanism

I. Kurzydym<sup>1,\*</sup>, I. Czekaj<sup>1</sup>

<sup>1</sup>Department of Organic Chemistry and Technology, Cracow University of Technology, Cracow, Poland

**Abstract Text:** Nitrogen oxides (NOx) emission has become a primary concern among the air pollutants emitted from various sources: automotive, energetics and heavy industry. Furthermore, NOx have a negative influence on health and human life, and due to the solar radiation react and form the so-called photochemical smog [1]. Current regulations require a significant reduction in emissions of these harmful oxides. The most promising and effective method allowing the fulfillment of these conditions is the SCR deNOx reaction with the participation of ammonia as a reducing agent. Over the literature reports, the metal modified zeolites have revealed the high activity in deNOx reaction [2,3]. Ab initio calculations within the density functional theory were used in our recent research in the line to understand different path of deNOx reaction on bimetallic nanoparticles inside MFI zeolite. The exchange and correlation functional is approximated by a Perdew-Burke-Ernzerhof (PBE) approach. Cluster model of MFI zeolite structure ( $\text{Al}_2\text{Si}_{18}\text{O}_{53}\text{H}_{26}$ ) has been used with bimetallic M1-O-M2 (M1,2 = Cu and Zn) nanoparticles adsorbed above aluminium centers in the zeolite frame. The M1-O-M2 dimers have been considered according to previous studies of bimetallic complexes [4].

Fig. 1. Structure used to calculations - MFI zeolite with bimetallic dimer ( $\text{Al}_2\text{Si}_{18}\text{O}_{53}\text{H}_{26}$ \_CuOZn).

Coadsorption of NO and NH<sub>3</sub> on Cu-Zn bimetallic nanoparticles bound in MFI cluster was investigated. Several configurations, electronic structure (charges, bond orders) were analyzed. Based on these studies, a scheme for the mechanism of the deNOx process was proposed. The main objective of this work was to find a more favorable and efficient catalyst for the deNOx process.

*This work was supported in part by the PL-Grid Infrastructure (using supercomputer Prometheus at Cyfronet Cracow).*

#### Image 1:



**References:** [1] J. Bosch, F. Janssen, Catal. Today. 2 (1988) 369–379. [2] T. J. Wang, S. W. Baek, H. J. Kwon, Y. J. Kim, I.-S. Nam, M.-S. Cha, G. K. Yeo, Ind. Eng. Chem. Res. 50 (2011) 2850-2864. [3] I.Czekaj, S. Brandenberger, O. Kröcher, Micropor. Mesopor. Materials 169 (2013) 97-102. [4] Y. J. Kim, H. J. Kwon, I. Heo, I.-S. Nam, B. K. Cho, J. W. Choung, M.-S. Cha, G. K. Yeo, Applied Catalysis B: Environmental, 126 (2012) 9– 21.

**Using iDPC-STEM to study the atomic resolution structures of zeolites**

M. Tang<sup>1,\*</sup>, K. P. de Jong<sup>1</sup>

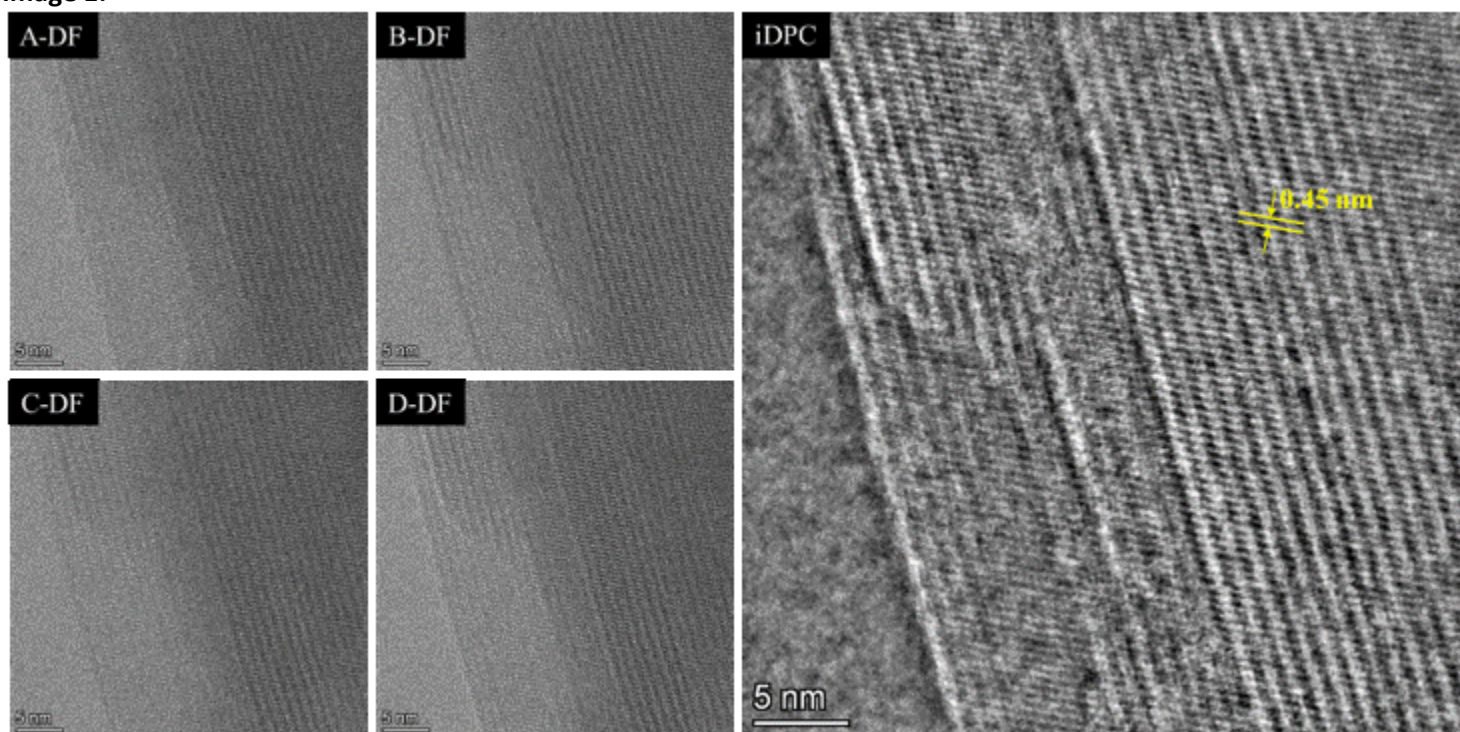
<sup>1</sup>Materials Chemistry Catalysis, Debye Institute for Nanomaterials Science, Utrecht University, Utrecht, Netherlands

**Abstract Text:** Transmission electron microscopy (TEM) has the necessary resolution and flexibility to characterize catalysts at magnifications spanning 5 orders of magnitude, from the micrometer level to atomic level via imaging, electron diffraction, and spectroscopy. It can provide detailed local structural information about the catalysts, e.g., compositions of the surfaces, atomic surface structures, and crystal structures.<sup>[1]</sup> However, the high-energy electrons can cause damage by modulating the structures of the materials. This has become a significant problem for beam-sensitive materials, including metal–organic frameworks, covalent–organic frameworks, organic–inorganic hybrid materials, 2D materials, and zeolites. With the application of spherical aberration (Cs) corrector, high angle annular dark field scanning transmission electron microscopy (HAADF-STEM) has proved to be an excellent approach for obtaining high resolution images for these beam sensitive materials.<sup>[2]</sup> In recent years, integrated differential phase-contrast scanning transmission electron microscopy (iDPC-STEM),<sup>[3]</sup> is widely used to directly probe guest molecules in zeolites, owing to its sufficient and interpretable image contrast for both heavy and light elements under low-dose conditions.<sup>[4]</sup> In this work, by using iDPC-STEM, we studied the atomic structures of H-ZSM-22 catalysts.

Figure 1 shows the DF-STEM images from the four segmented STEM detectors A-D and the Integrated Differential Phase Contrast (iDPC) STEM image of the H-ZSM-22 catalyst. From the iDPC-STEM image, we can see two dimensional fringes which clearly show the micropores of zeolites. The distance between the smaller fringes is 0.45 nm, which is consistent well with the size of the H-ZSM-22 pores (0.45 X 0.55 nm).<sup>[5]</sup> Because the micropore channels with 10-membered-ring (10-MR) openings normally run parallel to the long axis of the crystal, it's challenging to directly observe the 10-membered-ring for H-ZSM-22 unless the crystals are cut using ultramicrotomy or cyro-FIB.

iDPC-STEM is the best technique in TEM to study the atomic structures of zeolite-based catalysts owing to its sufficient and interpretable image contrast for both heavy and light elements under low-dose conditions, which may help to make a big step forward in the zeolite field.

Image 1:



**References:** [1] Min Tang, Wentao Yuan, Yang Ou, Guanxing Li, Ruiyang You, Songda Li, Hangsheng Yang, Ze Zhang, Yong Wang, *ACS Catal.* 2020, 10, 14419–14450.

[2] Alvaro Mayoral, Jung Gi Min, Suk Bong Hong, *Microporous and Mesoporous Materials*, 2016, 236, 129–133.

[3] Ivan Lazić, Eric G.T. Bosch, Sorin Lazar, Maarten Wirix, Emrah Yücelen, *Microsc. Microanal.*, 2016, 22 (Suppl 3).

[4] Boyuan Shen, Xiao Chen, Dali Cai, Hao Xiong, Xin Liu, Changgong Meng, Yu Han, Fei Wei, *Adv. Mater.*, 2020, 32, 1906103.

[5] M. Schreier, S. Teren, L. Belcher, J. R. Regalbuto, J. T. Miller, *Nanotechnology*, 2005, 16, 582–591.